

NASA Technical Memorandum 104593

AD-A274 627



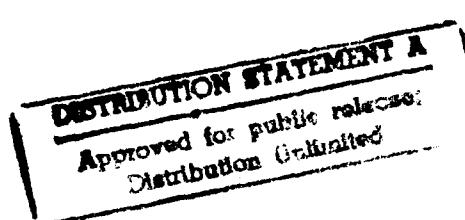
(2)

**A Synoptic-Scale Overview of the TOGA
COARE Intensive Observing Period
November 1992 - February 1993 Based on
Analyses From U. S. Operational Global
Data Assimilation Systems**

M. Fiorino, S. J. Lord, W. K-M Lau,
P. A. Phoebus, and C. G. Strey

DTIC
ELECTED
JAN 12 1994
S P D
B

November 1993



23290 94-01055

413638



94 1 10 033



**Best
Available
Copy**

NASA Technical Memorandum 104593

**A Synoptic-Scale Overview of the TOGA
COARE Intensive Observing Period
November 1992 - February 1993 Based on
Analyses From U. S. Operational Global
Data Assimilation Systems**

M. Fiorino

*Universities Space Research Association
Columbia, Maryland*

S. J. Lord

*National Meteorological Center
Camp Springs, Maryland*

W. K.-M. Lau

*Goddard Space Flight Center
Greenbelt, Maryland*

P. A. Phoebus

*Naval Research Laboratory
Monterey, California*

C. G. Strey

*Fleet Numerical Oceanography Center
Monterey, California*



National Aeronautics and
Space Administration

Scientific and Technical
Information Branch

1993

Acknowledgements

The assembly of the large Navy data set used in this study would not have been possible without the generous support of Captain R.J. Plante, USN, Commanding Officer of Fleet Numerical Oceanography Center and his staff. In particular, we thank Mr. Charles J. Mauck for adaptation and maintenance of the data exchange software on the FNOC system and for providing the tropical cyclone track data from the operational archives of the Joint Typhoon Warning Center, Guam. We also gratefully acknowledge Dr. John Janowiak of the Climate Analysis Center for providing preliminary GPI precipitation estimates during the IOP. These data were our only independent means of validation during the real-time data collection and established the realism of the large amplitude intraseasonal oscillation seen in the analyzed winds fields. Finally, we are deeply indebted to Mr. Brian Doty of the University of Maryland for use of the Grid Analysis and Display System (GrADS). All data analysis and graphics were preformed wholly within GrADS. This atlas could not have been put together expeditiously without GrADS and its scripting language. The participation of P. Phoebus was made possible through the support of Office of Naval Research under program element 0602704N. NRL Contribution No. NRL/PU/7531--93-0013.

DTIC QUALITY INSPECTED 8

Accession For	
NTIS GRA&I	<input checked="" type="checkbox"/>
DTIC TAB	<input type="checkbox"/>
Unannounced	<input type="checkbox"/>
Justification	
By _____	
Distribution/	
Availability Codes	
Dist	Avail and/or Special
A'	

Table of Contents

Section	Page
1 Introduction	1
2 The Operational Global Data Assimilation Systems of FNOA and NMC	3
3 Data and Processing	5
3.1 Calculation of Velocity Potential on a Limited-Area Grid	5
3.2 Model Precipitation	7
3.3 Surface Winds	7
3.4 MRF Sea Level Pressure	8
3.5 GPI Pentad Precipitation	8
3.6 Climatology	8
3.7 Data Availability	9
4 Major Events During the TOGA COARE IOP	11
5 Structure of the Atlas	13
6 Time Series of Area-Averaged Quantities in the Intensive Flux Array	17
7 Time-pressure Cross Sections in the Intensive Flux Array	21
8 Time-Latitude Hovmoeller Diagrams	27
8.1 Surface winds	27
8.2 Velocity Potential at 200 mb and 850 mb	31
8.3 Tropical Cyclones	41
8.4 Precipitation	45
8.5 Ocean Mixed Layer Depth and SST	57
9 Seasonal (NDJF) Means	61
10 Monthly Means	73
10.1 November 1992	73
10.2 December 1992	85
10.3 January 1993	97
10.4 February 1993	109
11 NOGAPS and MRF Pentads for December 1992 - February 1993	121
12 00 UTC Synoptic Charts for 1 -31 December 1992	191
13 00 UTC Synoptic Charts for 1 -31 January 1993	225
14 00 UTC Synoptic Charts for 1 -28 February 1993	259

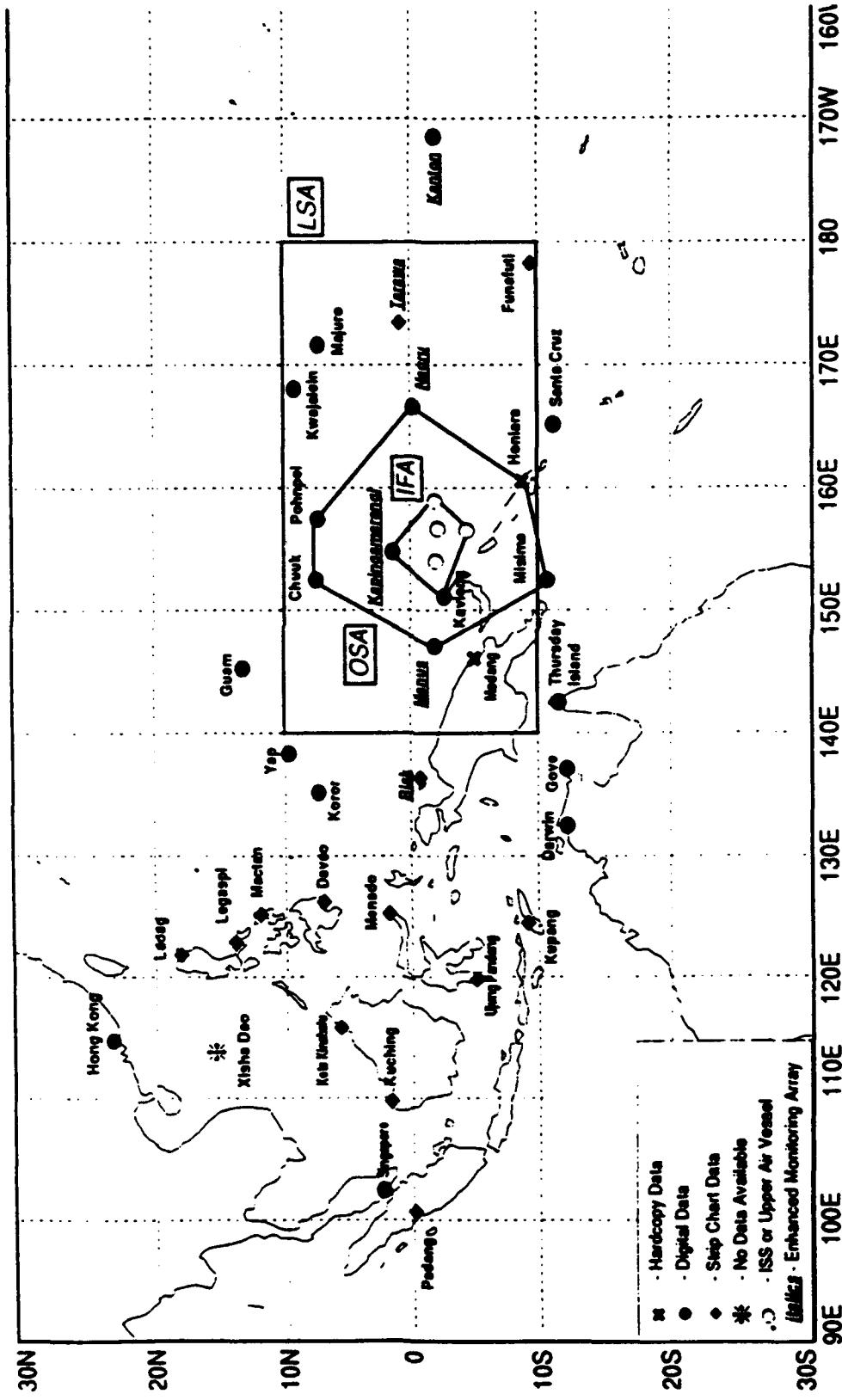
1 Introduction

One of the principal limitations to meeting the Tropical Ocean Global Atmosphere (TOGA) program objective of predicting the variability of the coupled ocean-atmosphere system on intraseasonal and interannual time scales has been an incomplete physical understanding of the mechanism of coupling in the tropics (see Webster and Lukas 1992 for an excellent description of TOGA and COARE). This lack of understanding is partly a consequence of insufficient observations in the region where the air-ocean coupling is thought to be critical over a wide range of time scales -- the so-called "warm pool" region of the tropical western Pacific. To fill this data void, an international field program, the Coupled Ocean Atmosphere Response Experiment (COARE), was organized to collect both atmospheric and oceanographic observations, particularly at the air-sea interface. The TOGA COARE program recently culminated in a four-month intensive observing period (IOP) during the period 1 November 1992 through 28 February 1993.

Although conventional observational platforms were either expanded (e.g., deployment of rawinsonde soundings systems to remote islands) or enhanced (e.g., increased frequency of satellite data collection) during the TOGA COARE IOP, most of the observational resources were concentrated in small $\sim 5 \times 10^{\circ}$ area called the Intensive Flux Array (IFA). Fig. 1, taken from the TOGA COARE International Program Office IOP summary (TCIPO 1993), illustrates the geographic structure of the telescoping TOGA COARE observational grids. Given that most of the ocean-atmosphere flux measurements were localized to the IFA, we expect that future analysis of the TOGA COARE data sets will be similarly focused on the IFA. However, these analyses will be incomplete without a proper accounting for the multiscale nature of the ocean-atmosphere coupling. Thus, the purpose of this atlas is to fill that gap by providing a description of the synoptic scales at periods ranging from one day to one month as resolved by the real-time global data assimilation systems of the two major U.S. operational numerical weather prediction (NWP) centers.

We anticipate two uses for our atlas: 1) background information for the TOGA COARE research community (e.g., tropical cyclone and westerly wind burst events); and 2) a baseline for future reanalyses of the TOGA COARE IOP where a more complete set of TOGA COARE observations will be used in the data assimilation process. The characteristics of the operational data assimilation systems and data processing aspects are first reviewed and then an overview of the major events during the IOP is given. The bulk of the atlas consists of charts arranged according to spatial and temporal scales. Each chart section is prefaced by some scientific comments and an index to the plots.

Figure 1. TOGA COARE Grid Areas. LSA = Large Scale Array; OSA=Outer Sounding Array; IFA= Intensive Flux Array.



2 The Operational Global Data Assimilation Systems of FNOC and NMC

The global data assimilation systems of the U.S. Navy Fleet Numerical Oceanography Center (FNOC) and the National Meteorological Center (NMC) are constantly evolving with improvements and/or corrections to the software made at times on a weekly basis.

Fortunately, there were no major changes to the systems during the TOGA COARE IOP so that the analyses are internally consistent in time. However, significant changes have occurred since the IOP at NMC. Thus, these data are one of a kind, but representative of the state-of-the-art in operational data assimilation in the U.S during the IOP and will serve as a baseline for future reanalysis of the TOGA COARE data.

Table 1 gives a summary of the features of the FNOC and NMC systems of significance to TOGA COARE. Although the assimilation systems have different properties, the resulting analyses exhibited a good degree of correspondence because of similarities in the input observational data and in modeling technology. However, there were notable differences possibly related to: 1) the treatment of cumulus convection; 2) land and ocean surface parameterizations; and 3) the inclusion of oceanic surface wind speeds derived from Special Sensor Microwave/Imager (SSM/I) data. These differences were largest at small space and time scales (e.g., the IFA) and especially in precipitation and upper tropospheric divergence patterns.

Table 1. Properties of the operational data assimilation systems during the TOGA COARE IOP.

Property	NOGAPS	MRF
GCM Resolution	T79/L18 ($\Delta x \sim 167\text{km}$)	T126/L18 ($\Delta x \sim 106\text{km}$)
Cumulus Parameterization	Arakawa-Schubert with down drafts	Kuo
Analysis	Multivariate OI	Statistical Spectral Interpolation
Initialization	Nonlinear Normal Mode	none
Update frequency	6 h	6 h
Use of SSM/I wind speeds	yes	no (during IOP)
Synthetic TC Observations	yes Phoebeus and Goerss (1992)	yes
Daily SST Forcing	yes	yes
References	Hogan and Rosmond (1991) Goerss and Phoebeus (1992)	Kanamitsu et al. (1991) Derber et al. (1991)

3 Data and Processing

The data used in this atlas come from the "real time" analyses executed +3 h after synoptic time that provide the initial conditions for 00 and 12 UTC global model forecast runs. A later "post-time" analysis (+9 h) is made at both centers where time-late observations are incorporated into the analysis for future data assimilation cycles and forecast runs. At NMC, the two "real-time" Medium Range Forecast (MRF) global model integrations are referred to as the "aviation" runs because they support the aviation community. Since we have used analyses from the aviation run of the MRF, both systems had essentially the same access to the observational data and our data set is thus representative of operations. However, we expect that future reanalyses using the full set of TOGA COARE observations will be more accurate.

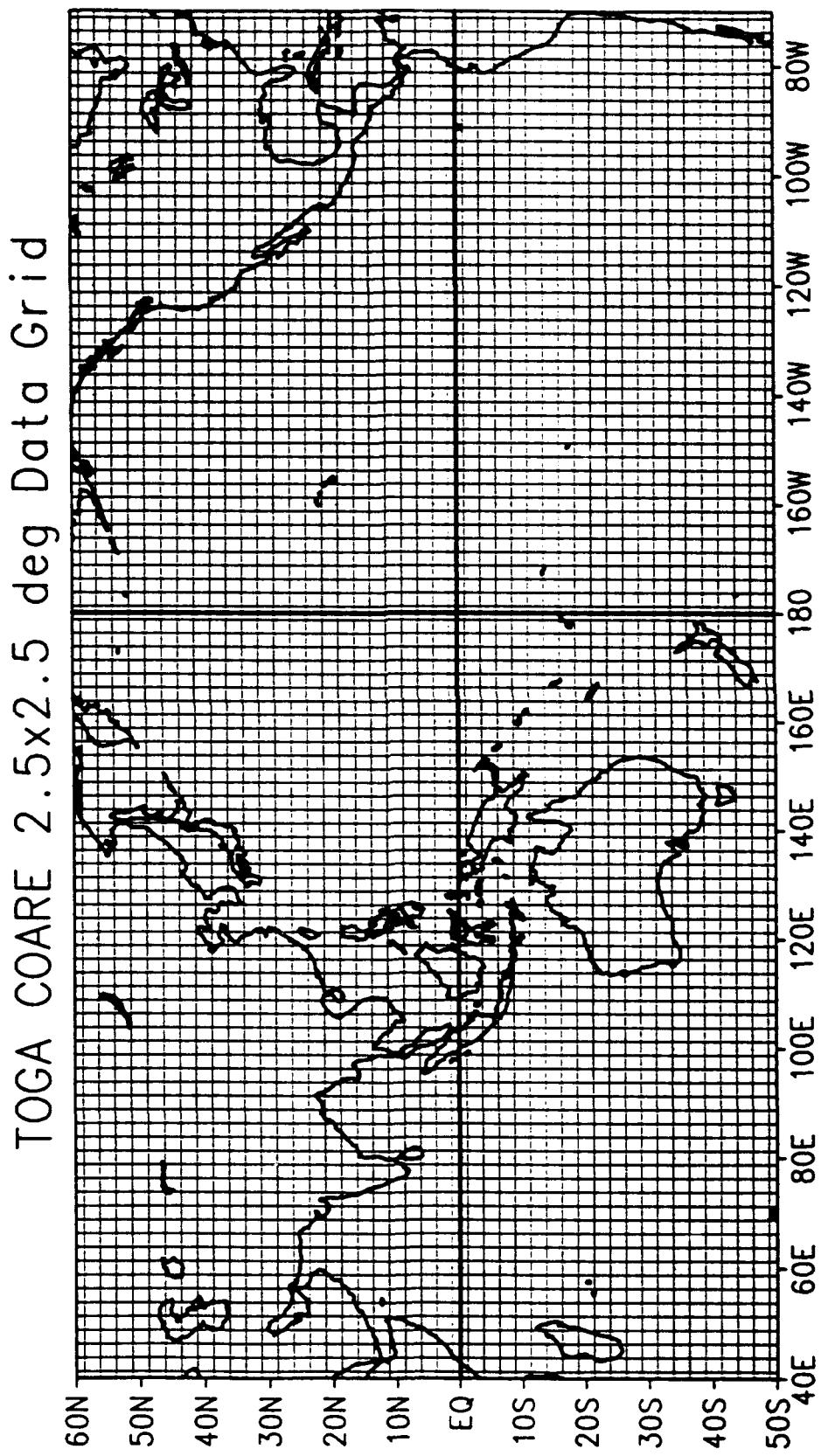
The analyses were interpolated to a common $2.5 \times 2.5^\circ$ grid encompassing the entire Pacific and Indian Oceans as shown in Fig. 2. The data came directly from the analysis procedure; the winds and mass were not initialized. The choice of a relatively coarse grid was motivated by two factors: 1) operations at FNOC; and 2) the exchange of grid fields between NWP centers typically uses this resolution. We archived wind components, temperature, geopotential height and moisture data at all mandatory pressure levels between 1000 and 100 mb. Additionally, some surface parameters, such as sea-level pressure, surface winds and temperature, and precipitation were saved. A complete listing of our data holding is available from the first author; see section 3.7 for more details. Only the wind and precipitation fields are used in this atlas; a second atlas for thermodynamic quantities is under consideration.

3.1 Calculation of Velocity Potential on a Limited-Area Grid

The low frequency, 30-60 day oscillation was a prominent feature of the TOGA COARE IOP and is the focal point of this atlas. This tropical wave or intraseasonal oscillation (ISO) is a global-scale, eastward-moving disturbance in the equatorial winds with a strong signal in the 200 mb velocity potential (Slingo and Madden 1991). The ISO is a dominate feature of the equatorial wind spectrum and is also associated with 5-10 day periods of sustained westerly winds on the equator called westerly winds bursts (Lau et al. 1989).

To calculate the velocity potential from the 200 mb wind field in a limited area, we chose the method of Tarbell et al. (1981) for specification of the lateral boundary conditions. This scheme is general, preserves net divergence in the area and recovers the large-scale structure of the velocity potential near the boundaries. Tests comparing solutions using the Tarbell et al. method with solutions using zero velocity potential at the boundary showed that while the fields were very similar in the interior (i.e., domination by the forcing function), the general scheme gave smooth variation and realistic continuity of interior features outward toward the boundaries.

Figure 2. The TOGA COARE Analyses Data Grid



3.2 Model Precipitation

Precipitation is the most important component of the hydrologic cycle in the warm pool region because rain provides a large flux of fresh water to the ocean. This flux in turn modifies the salinity structure of upper ocean and the ocean response to wind forcing and internal wave propagation. Furthermore, theories of the ISO suggest that the atmospheric diabatic forcing implied by rainfall is critical to the phase speed and propagation characteristics of these disturbance (e.g., Lau et al. 1989). Thus, it is desirable to have estimates of precipitation that are dynamically consistent with the wind when studying the ISO in a data assimilation system. Unfortunately, precipitation is not directly analyzed, which forces us to use a proxy. In this study we choose the accumulated precipitation during the 0-12 h model forecast. While this rainfall is produced solely by the model, it represents a partial response of the model physics to the analyzed flow field and has been found to correspond well to observed precipitation at other NWP centers (e.g., Sato, Japan Meteorological Agency, personal communication).

3.3 Surface Winds

Surface winds are not explicitly analyzed at FNOC or NMC from observational data. Rather, these winds are diagnosed from winds at the model levels using some boundary layer parameterization. Additionally, the height above the surface where the "surface" winds are considered valid can depend on the requirements of an application program. During the IOP (2 December 1992), FNOC changed this height from 10 m to 19.5 m ("mast level") to better support naval operations, while at NMC the 10 m winds were not readily available. As a proxy for the MRF surface winds, we used the MRF lowest layer sigma level winds valid at approximately 70 m. The only unbiased way to intercompare such a wind field would be to run the NMC and FNOC sigma level model winds through the same boundary layer parameterization. Thus, a close and quantitative intercomparison of the "surface" winds should not be made. However, no gross biases were found.

3.4 MRF Sea Level Pressure

Sea level pressure (SLP) analyses were not readily available from the NMC archives. As a proxy, we hydrostatically estimated SLP from the MRF 1000 mb heights and temperatures. A comparison with NOGAPS analyses over the ocean showed a close correspondence; however, substantial differences were found over high terrain as might be expected. Thus, intercomparison of SLP between NOGAPS and the MRF should be restricted to oceanic regions.

3.5 GPI Pentad Precipitation

In addition to the two sets of analyses, we were kindly provided preliminary GPI satellite precipitation estimates by Dr. J. Janowiak of the Climate Analysis Center, NMC. These data consist of five-day averages of precipitation rate on a $2.5 \times 2.5^\circ$ grid extending from 0 to 360° in longitude and approximately 40S to 40N in latitude. These GPI estimates are considered preliminary because only IR data from polar orbiting satellites (see Janowiak 1992 for further information on GPI) are used, but were available in near real time. The "final" GPI data use both geostationary and polar orbiting IR data. While these estimates may be timely there are two caveats regarding their quality: 1) unrealistic precipitation over land (e.g., the Himalayas); and 2) a potential over-estimation of the rain rate. However, the GPI data can resolve rain versus no rain areas and are an independent source of data to validate the gross features of the model simulated rainfall. Additionally, the data have sufficient temporal resolution to resolve the ISO (Janowiak 1992).

3.6 Climatology

The multiscale nature of the ocean-atmosphere coupling in the warm pool region requires an understanding of the large-scale/low-frequency (e.g., seasonal cycle) variability. The low frequencies can be represented by monthly and seasonal averages and anomalies about some mean or climate state. We have used a five-year average (1985-89) of the uninitialized analyses of the European Centre for Medium range Weather Forecasts (ECMWF) as an independent estimate of climatology (Schubert et al. 1992)

For precipitation, we formed a climatology by merging two monthly-mean data sets covering the 1979-89 period. Over land, we used an analysis of station data prepared by Schemm et al. (1992) and over the ocean the Microwave Sounding Unit (MSU) precipitation estimates of Spencer (1993). Comparisons of this climatology with others standards (e.g., Legates and Willmott 1990) showed reasonable agreement, but we used the merged climatology as it was based on more recent data.

3.7 Data Availability

The data used in this atlas are available at NASA GSFC. Copies of the atlas and a complete listing of our data holdings and information on data access may be obtained by contacting:

Dr. M. Fiorino
W/NMC2 WWB Room 204
Washington, DC 20233
301-763-8005
email: fiorino@climate.gsfc.nasa.gov

or,

Dr. R. Chinman
Data Manager
TOGA COARE International Project Office
UCAR P.O. Box 3000
Boulder, CA 80307-3000
303-497-8686
email: chinman@ncar.ucar.edu

4 Major Events During the TOGA COARE IOP

The major synoptic events during the TOGA COARE IOP were tropical cyclones (TC), westerly winds bursts and the ISO. These events are first overviewed to provide the reader with a basic road map to the IOP.

Table 2 summarizes tropical cyclone (TC) activity during 1 November 1992 - 28 February 1993. The data for the western North Pacific and North Indian Ocean come from the official Joint Typhoon Warning Center (JTWC) post analysis best track whereas the positions in 1993 are taken from the operational JTWC "working" best track. The use of working best track data does not affect our characterization of TC activity.

The western North Pacific basin was unusually active during the IOP with 6 typhoon-strength (> 65 kts) cyclones. Additionally, three of the storms formed east of the dateline. An eastward shift in tropical cyclone activity is typical of El Nino years (Phoebus and Kindle 1993).

Four weak TCs occurred in the North Indian Ocean with none reaching typhoon strength. While these cyclones were weak, they remained close to the equator and thus may be important to equatorial ocean forcing.

While the ISO is a global scale phenomena, it reaches its greatest amplitude as it propagates eastward through the Indian Ocean and western Pacific. The only northern-southern hemisphere TC pair occurred with the passage of the first ISO of the IOP through the Indian Ocean. This ISO was associated with the onset of the Australian monsoon (Davidson et al. 1993) and had a similar beginning as the ISO studied by Sui and Lau (1992).

Twelve cyclones occurred in the southern hemisphere, but few provided significant wind forcing on the equatorial ocean. As in the northern hemisphere, many systems formed near the dateline.

Time series of surface winds in the IFA show two periods of strong westerlies from approximately 16 December 1992 → 1 January 1993 and 22 January 1993 → 1 February 1993. These are the two westerly wind bursts (WWBs) that were associated with the passage of ISO disturbances as reflected in the velocity potential anomalies. However, the structure of the two WWB-ISO sets (subsequently referred to 1 and 2) were substantially different. The amplitude of ISO1 was weaker than ISO2 as seen the 200 mb velocity potential anomaly, yet WWB1 was stronger and persisted for a longer time in the central Pacific than WWB2. Two southern hemisphere TCs occurred during WWB1, but were noticeably absent during WWB2. Only one northern-southern hemisphere TC couplet occurred as ISO1 passed through the Indian Ocean.

5 Structure of the Atlas

All data analysis calculations (e.g., area-averaging) and plots and were produced by the Grid Analysis and Display System (GrADS, Doty and Kinter 1992). The name of the GrADS script file that produced the graphic is given in the plot subtitle. Readers interested in using GrADS and/or the scripts should contact the first author through email (fiorino@climate.gsfc.nasa.gov).

The atlas is organized to develop a multiscale understanding of specific events in the IFA. We first examine the smallest space and time scales through time series in the IFA and then consider nearby synoptic scales through time-longitude Hovmoeller diagrams of many variables including oceanographic quantities. The seasonal (NDJF) means of wind, sea-level pressure and precipitation and associated anomalies are then given, followed by individual monthly means of the same quantities. The last two sections of the atlas contain pentads from both FNOC and NMC of winds, precipitation and the GPI rainfall rate over a large horizontal domain, and daily synoptic charts of SLP and surface winds.

The NOGAPS data were transferred to NASA via a procedure executed in near real-time at FNOC. While this system was very reliable after an initial shakedown period in early November 1992, some data were not received due to network and/or workstation down time. The blanks in the plots indicate these missing data.

The following acronyms are used in the plots:

- | | | |
|--------|---|---|
| MRF | - | Analyes from the aviation run of the MRF model of NMC |
| NOGAPS | - | Navy Operational Global Atmospheric Prediction System of FNOC |
| OTIS | - | Ocean Thermal Interpolation System of FNOC (Clancy and Sadler 1992). This is the primary ocean analysis system of FNOC and provides sea surface temperature (SST) to NOGAPS. |
| TOPS | - | Thermodynamic Ocean Prediction System (Clancy and Sadler 1992) of FNOC. TOPS is a synoptic mixed-layer model that, together with OTIS, completes the global ocean data assimilation system of FNOC. |

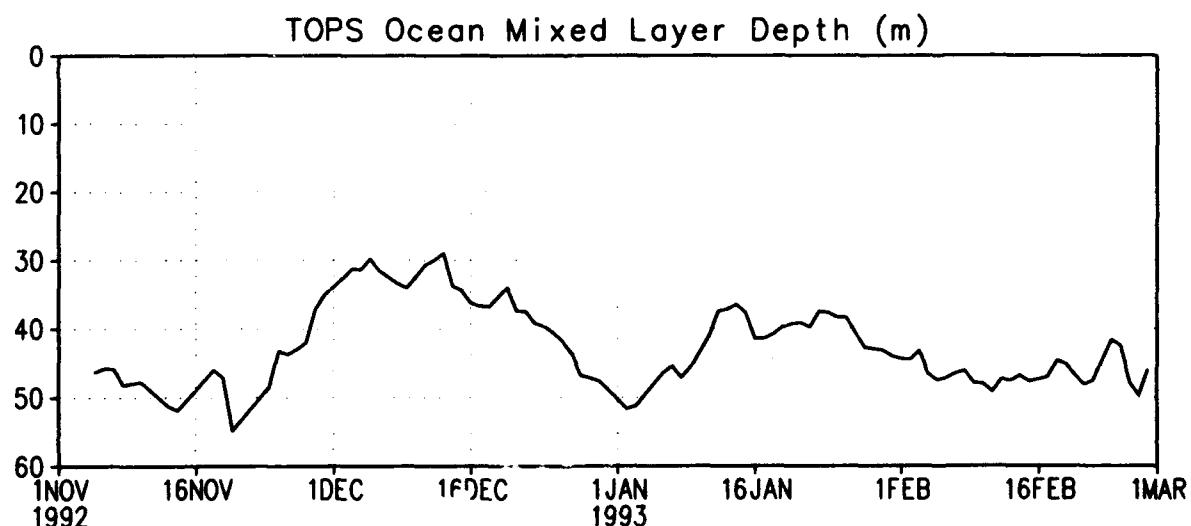
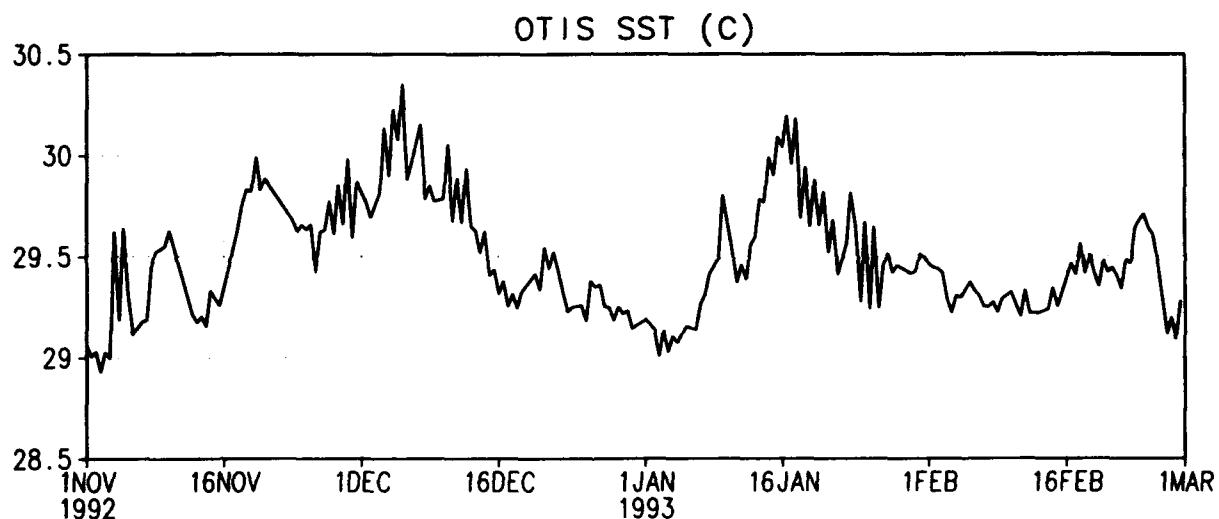
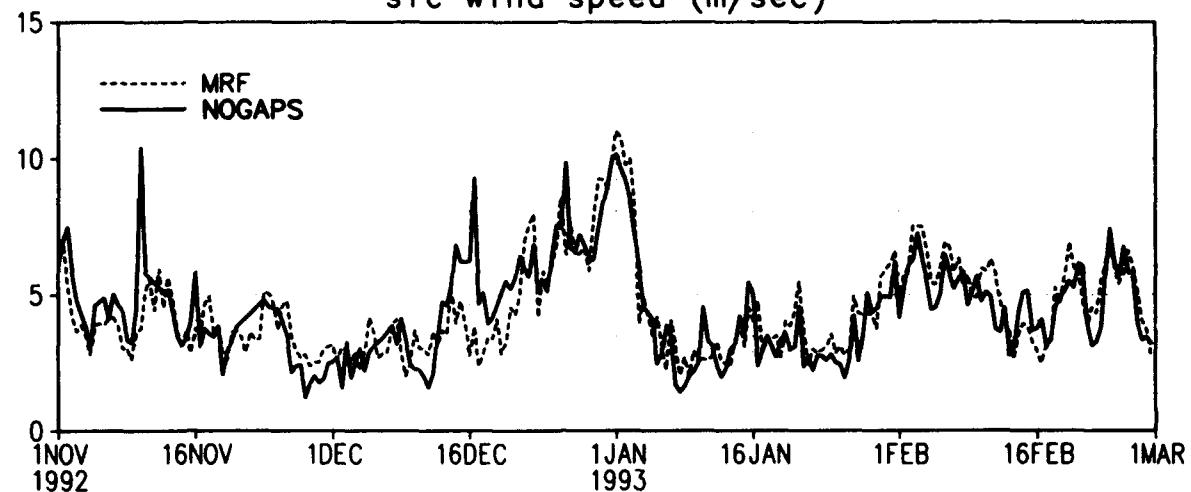
References

- Clancy, R.M. and W.D. Sadler, 1992: The Fleet Numerical Oceanography Center suite of oceanographic models and products. *Wea. Forecasting*, **7**, 307-327.
- Davidson, N.E., K. Puri and J. McBride, 1993: Real time tropical analysis and prediction during TOGA-COARE: preliminary diagnosis from the BMRC limited area system. Proceedings, 20th Conference on Hurricanes and Tropical Meteorology, 10-14 May 1993, San Antonio, TX, American Meteorological Society, 547-550.
- Derber, J.C., D.F. Parrish and S.J. Lord, 1991: The new global operational analysis system at the national meteorological center. *Wea. Forecasting*, **6**, 538-547.
- Doty, B. and J. Kinter, 1992: The grid analysis and display system (GrADS): a practical tool for earth science visualization. Preprints, Eight International Conference on Interactive Information and Processing Systems for Meteorology, Oceanography, and Hydrology. 5-11 January, 1992, Atlanta GA, American Meteorological Society, 115-116.
- Fiorino, M., J.S. Goerss, J.J. Jensen and E.J. Harrison, Jr., 1993: An evaluation of real-time tropical cyclone forecast skill of the Navy Operational Global Atmospheric Prediction System in the western North Pacific. *Wea. Forecasting*, **8**, 1-24.
- Goerss, J.S. and P.A. Phoebus, 1992: The Navy's operational atmospheric analysis. *Wea. Forecasting*, **7**, 307-327.
- Hogan, T.F. and T.E. Rosmond, 1991: The description of the Navy Operational Global Atmospheric Prediction System's spectral forecast model. *Mon. Wea. Rev.*, **119**, 1786-1814.
- Johnson, R.H., J.F. Bresch, P.E. Ciesielski and W.A. Gallus, Jr., 1993: The TOGA-COARE atmospheric sounding array: its performance and preliminary scientific results. Proceedings, 20th Conference on Hurricanes and Tropical Meteorology, 10-14 May 1993, San Antonio, TX, American Meteorological Society, 1-4.
- Kanamitsu, M., J.C. Alpert, K.A. Campana, P.M. Caplan, D.G. Deaven, M. Iredell, B. Katz, H.-L. Pan, J. Sela and G.H. White, 1991: Recent changes implemented into the global forecast system at NMC. *Wea. Forecasting*, **7**, 307-327.
- Kindle, J.C. and P.A. Phoebus, 1993: Events proceeding the 1991-92 El Nino. Part 2: The ocean response to operational westerly winds bursts. Submitted to *J. Geo. Res.*
- Lau, K.-M., L. Peng, C.H. Sui and T. Nakazawa, 1989: Dynamics of super cloud clusters, westerly winds bursts, 30-60 day oscillations and ENSO: a unified view. *J. Meteorol. Soc. Japan*, **67**, 205-219.

6 Time Series of Area-Averaged Quantities in the IFA

This plot shows time series surface wind speed in the $5 \times 10^{\circ}$ area surrounding the IFA (5S-EQ, 150E-160E), SST from OTIS and ocean mixed layer depth from TOPS. Note the physically realistic response of the ocean as the winds increase during the two westerly wind bursts -- the mixed layer deepens and the surface temperature decreases.

Sfc Air/Ocean Parameters in IFA (150E-160E, 5S-EQ)
unsmoothed ; /d2/toga_coare/apps/ts.gs
sfc wind speed (m/sec)

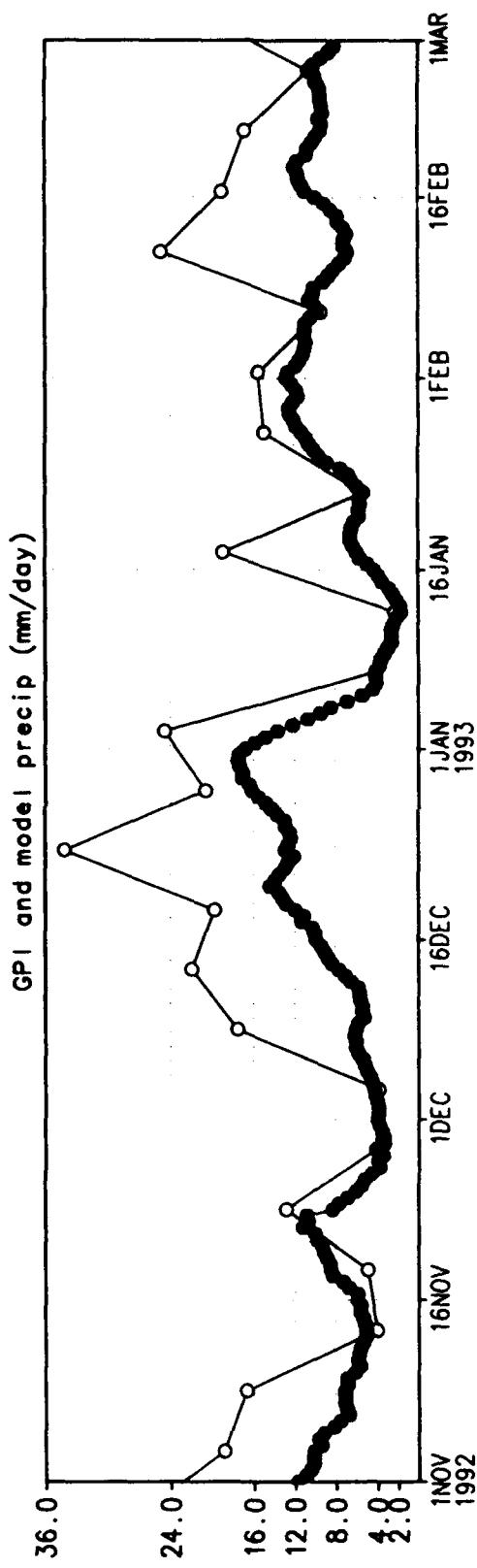
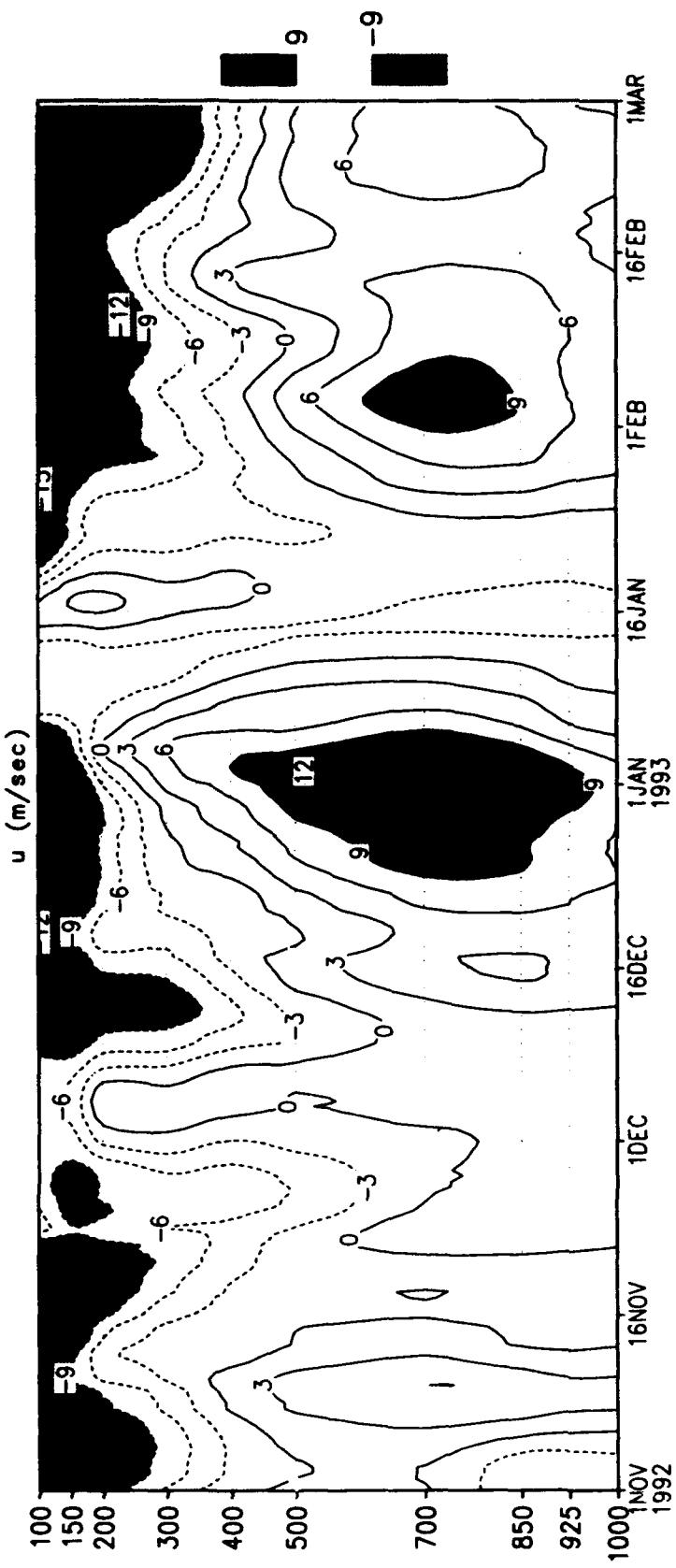


7 Time-pressure Cross Sections in the IFA

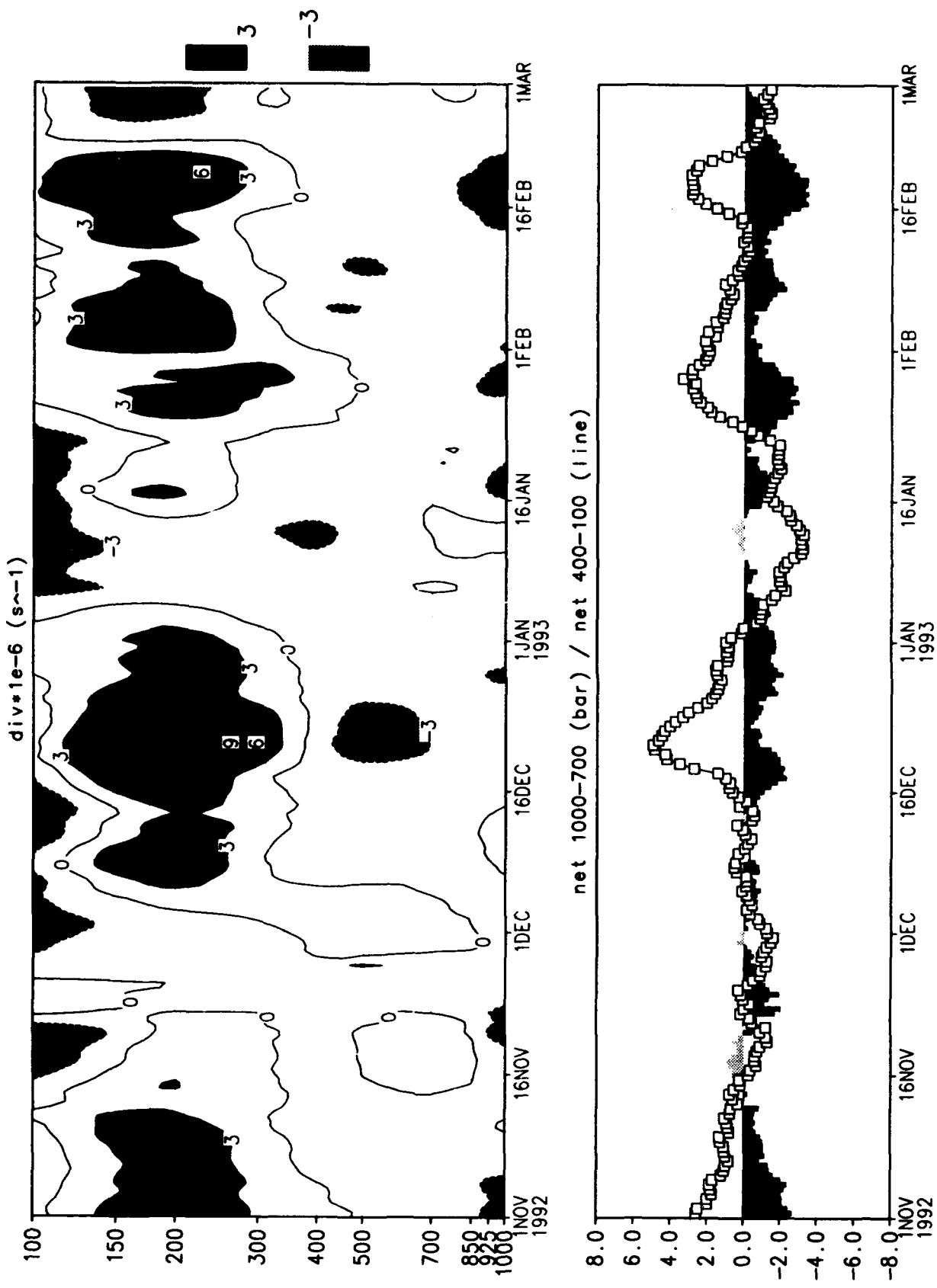
The vertical structure of the WWBs is illustrated using time-pressure (height) cross sections of precipitation, the u component of the wind and divergence in the same horizontal area as the time series. The GPI pentad precipitation is also given as an independent source of validation data. The WWBs clearly stand out in both the MRF and NOGAPS analyses and reach a maximum amplitude around 700 mb. This evolution is very similar to that depicted by the TOGA COARE rawinsonde network (Johnson et al. 1993). Many of these rawinsonde reports did not reach the NWP centers in time to be included in the operational analyses and it is encouraging to see the basic structure of the WWB was recovered and were similar in the two systems. However, note that divergence peaks at 200 mb in NOGAPS, but at a considerably higher level in the MRF and that the precipitation from the MRF shows a 15-d oscillation in the net lower and upper tropospheric divergence whereas NOGAPS more clearly resolves the slower 40-d oscillation of the ISO.

Chart	Description
1	-
2	-
3	-
4	-
	u component and precipitation in the IFA for NOGAPS
	Divergence and net upper and lower tropospheric divergence in the IFA for NOGAPS
	u component and precipitation in the IFA for MRF
	Divergence and net upper and lower tropospheric divergence in the IFA for MRF

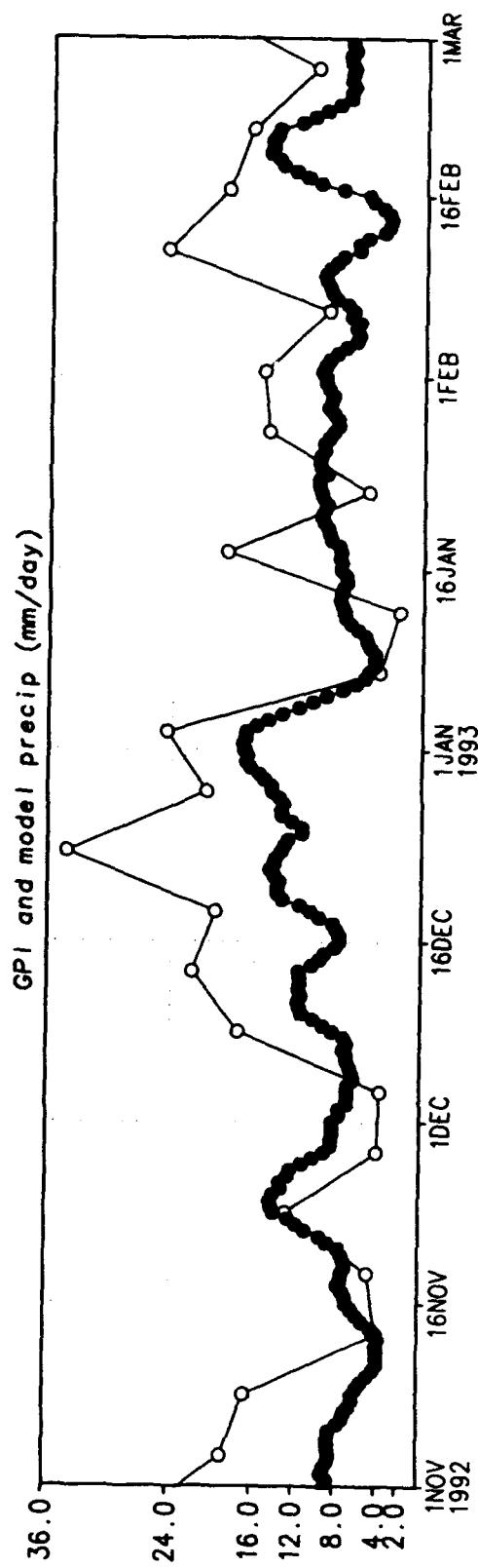
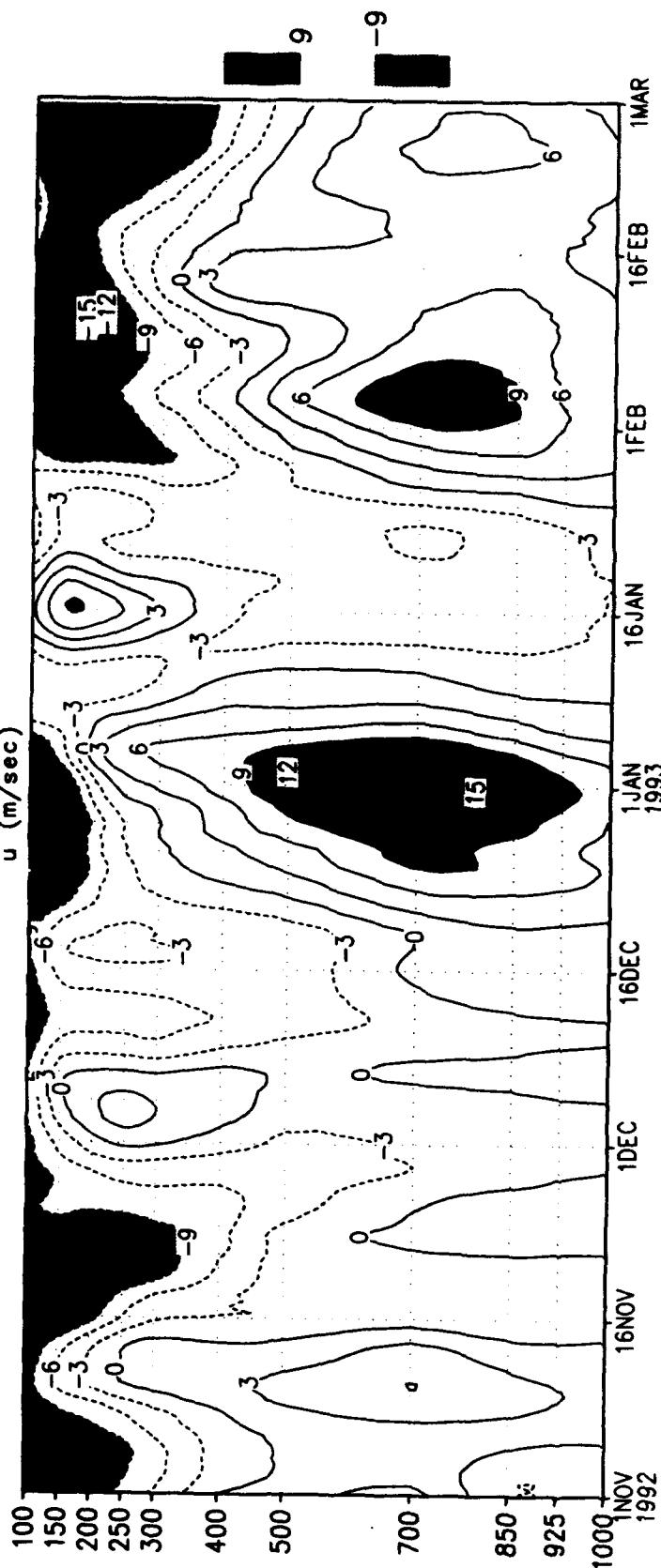
U and Precip in IFA for NOGAPS 150E–160E; 5S–EQ
5-day running mean /d2/toga_coarse/app/ifa.g8



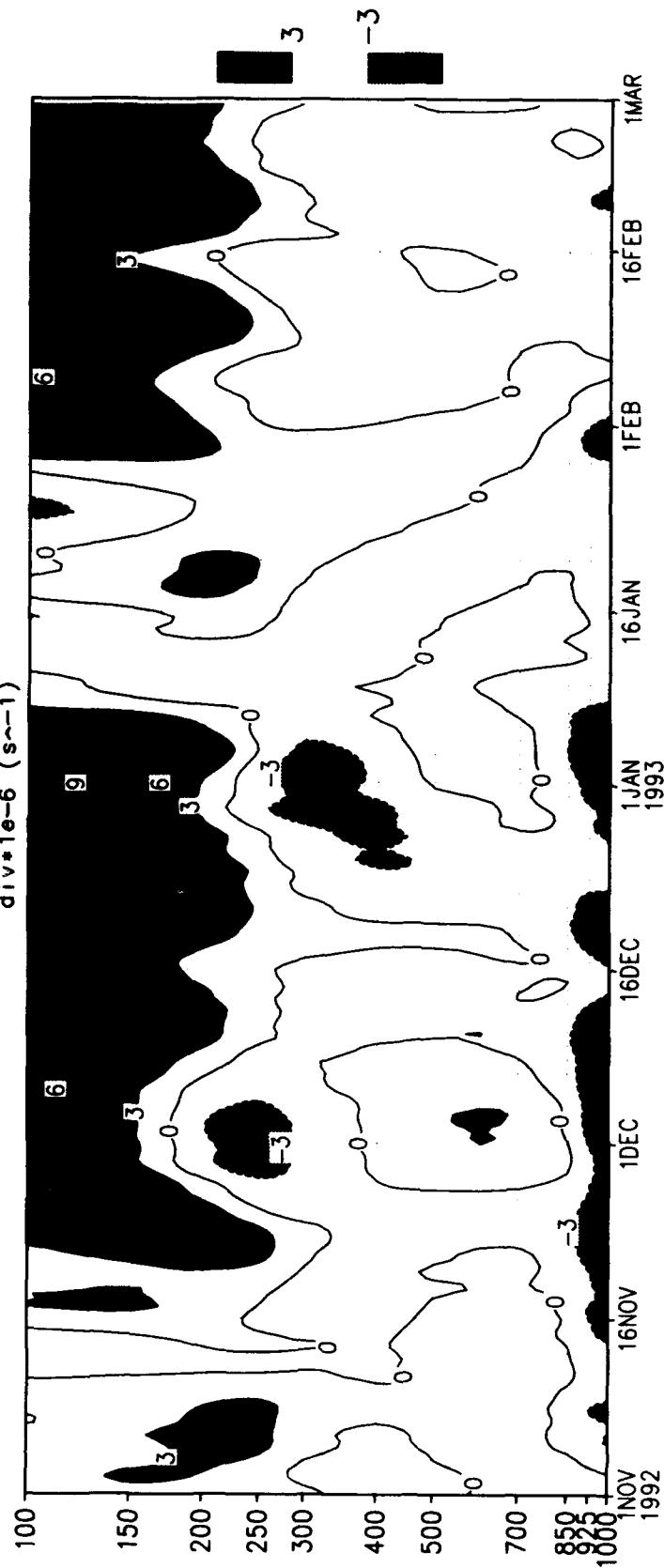
Divergence in IFA for NOGAPS 150E–160E; 5S–EQ
 5-day running mean /d2/toga_coare/apps/ifa.qs



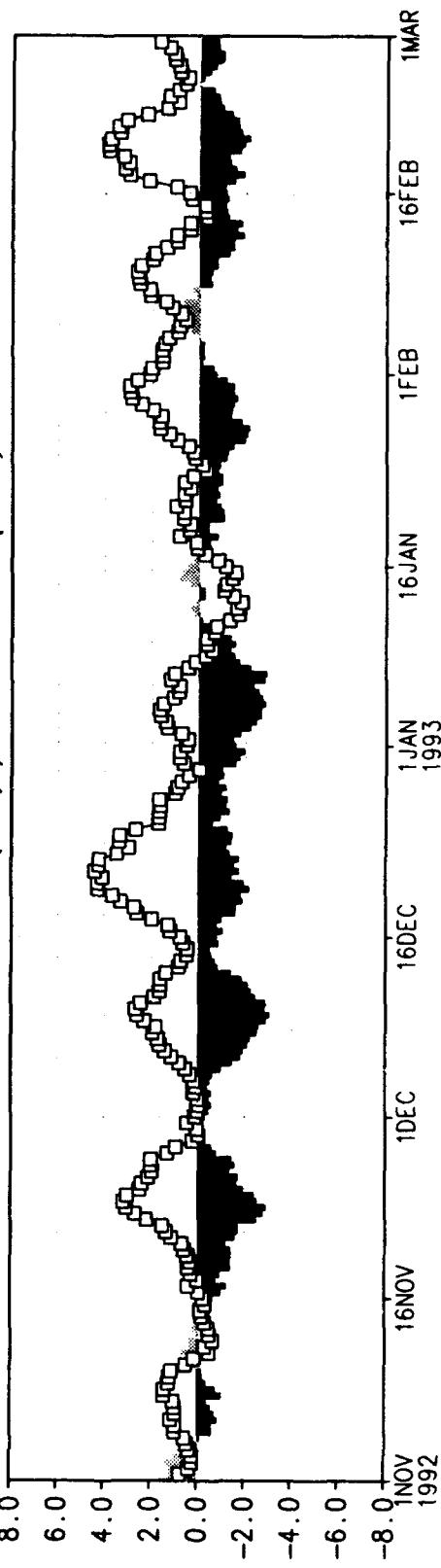
U and Precip in IFA for MRF 150E–160E; 5S–EQ
5-day running mean /d2/toga_coarse/apps/ifa_gs



Divergence in IFA for MRF 150E–160E; 5S–EQ
 5-day running mean /d2/toga_coar.e/appes/ifa.gs
 $\text{div} * 10^{-6}$ (s^{-1})



net 1000–700 (bar) / net 400–100 (line)



8 Time-Latitude Hovmoeller Diagrams

A larger scale view of the IFA events seen in the time series is made by plotting latitudinal averages as a function of longitude and time (Hovmoeller diagrams). All the following Hovmoeller charts are plotted in the same way with time running from top to bottom and longitude from 40E to 140W. The only exception is the ocean parameters where we expanded the longitudinal domain to cover the entire Pacific ocean along the equator.

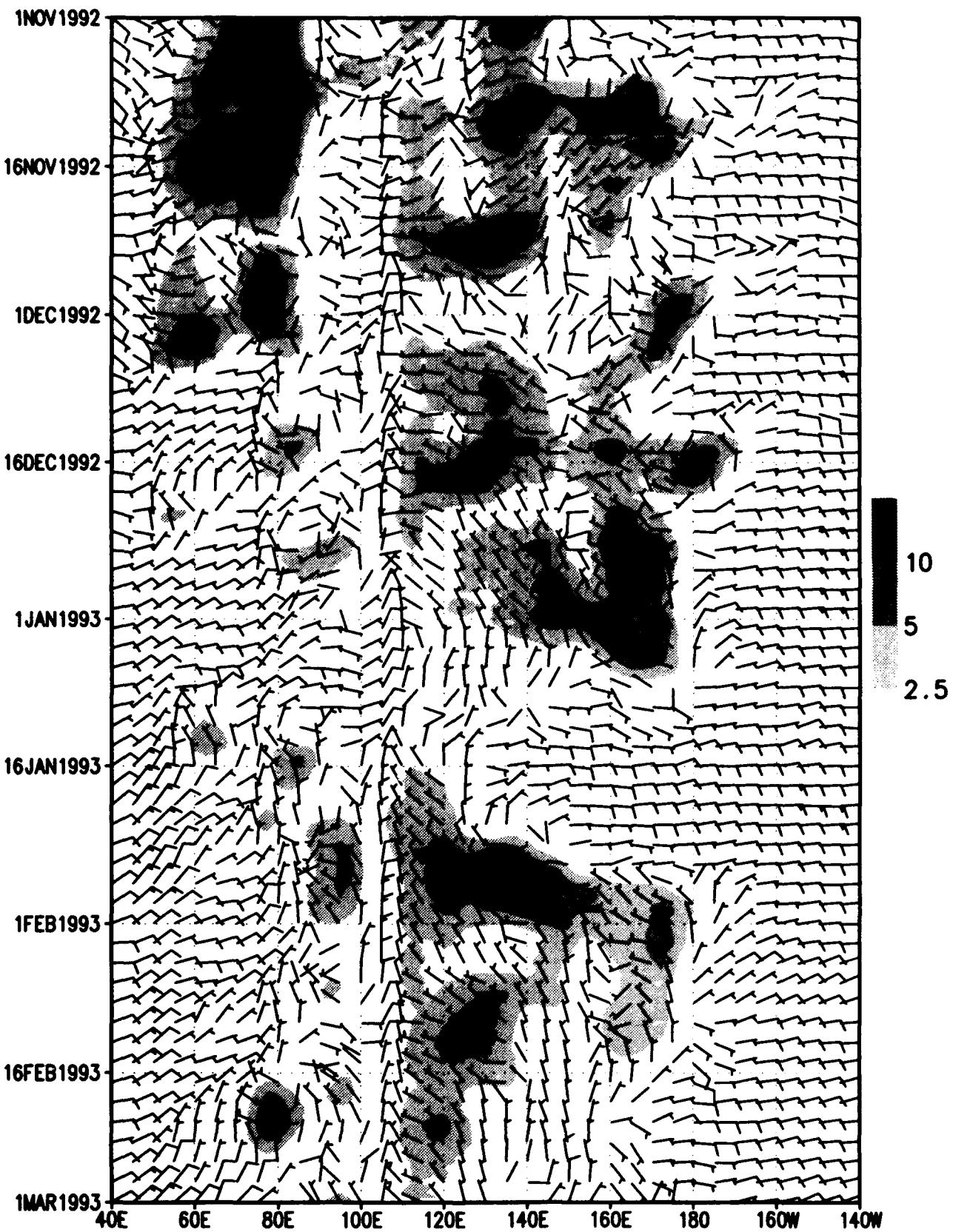
Two latitude bands were considered: 1) 5S-5N; and 2) 10S-5S. The southern band was used to examine the Australian monsoon and because the ISO signal in the precipitaiton and velocity potential was stronger here than along the equator.

8.1 Surface Winds

The five-day running means of the surface winds averaged from 5S-5N clearly show the two WWBs as emphasized through shading of positive u wind (westerlies) according to the shading bar. The winds are in knots vice m/sec because most ship and maritime stations report in this unit and because wind barbs were designed for knots. While evidence of the two WWBs centered at ~160E on 1 January 1993 (WWB1) and on 1 February 1993 (WWB2) are seen in the plots, there are substantial differences between NOGAPS and the MRF. The most obvious difference is in the magnitude of the westerly winds. This is somewhat surprising given that the MRF winds are valid at a higher level (~70 m) than from NOGAPS (19.5 m). More significantly to ocean forcing, the NOGAPS WWBs last longer (~16 d of westerly winds ~165E in WWB1) and cover a large area (110E-180E for WWB2) . Also note the strong NOGAPS westerlies in the Indian Ocean during November 1992 .

Chart	Description
1	-
2	-
	5S-5N ave for NOGAPS; 5-d running mean
	5S-5N ave for MRF; 5-d running mean

NOGAPS 5S-5N ave sfc wind (kts) ; u>0 shaded
5-d running mean ; /d2/toga_coare/apps/huv.gs



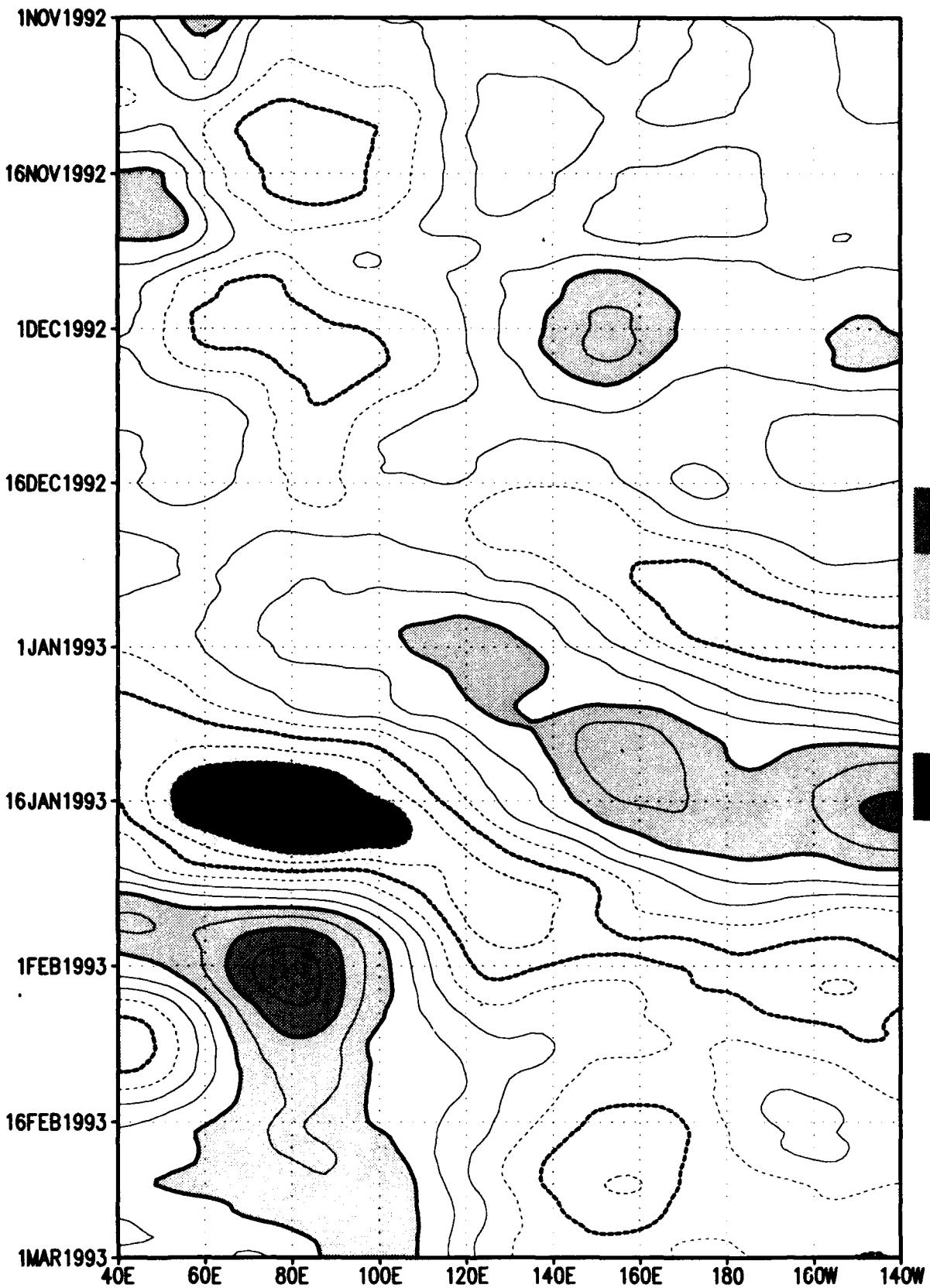
8.2 Velocity Potential at 200 mb and 850 mb

The time-pressure cross sections showed that the ISO signal in divergence peaked around 200 mb. We next show 10-d running means of the 200 mb velocity potential (χ) anomalies. The anomaly is defined as the difference of the smoothed χ from the four-month average from the same model.

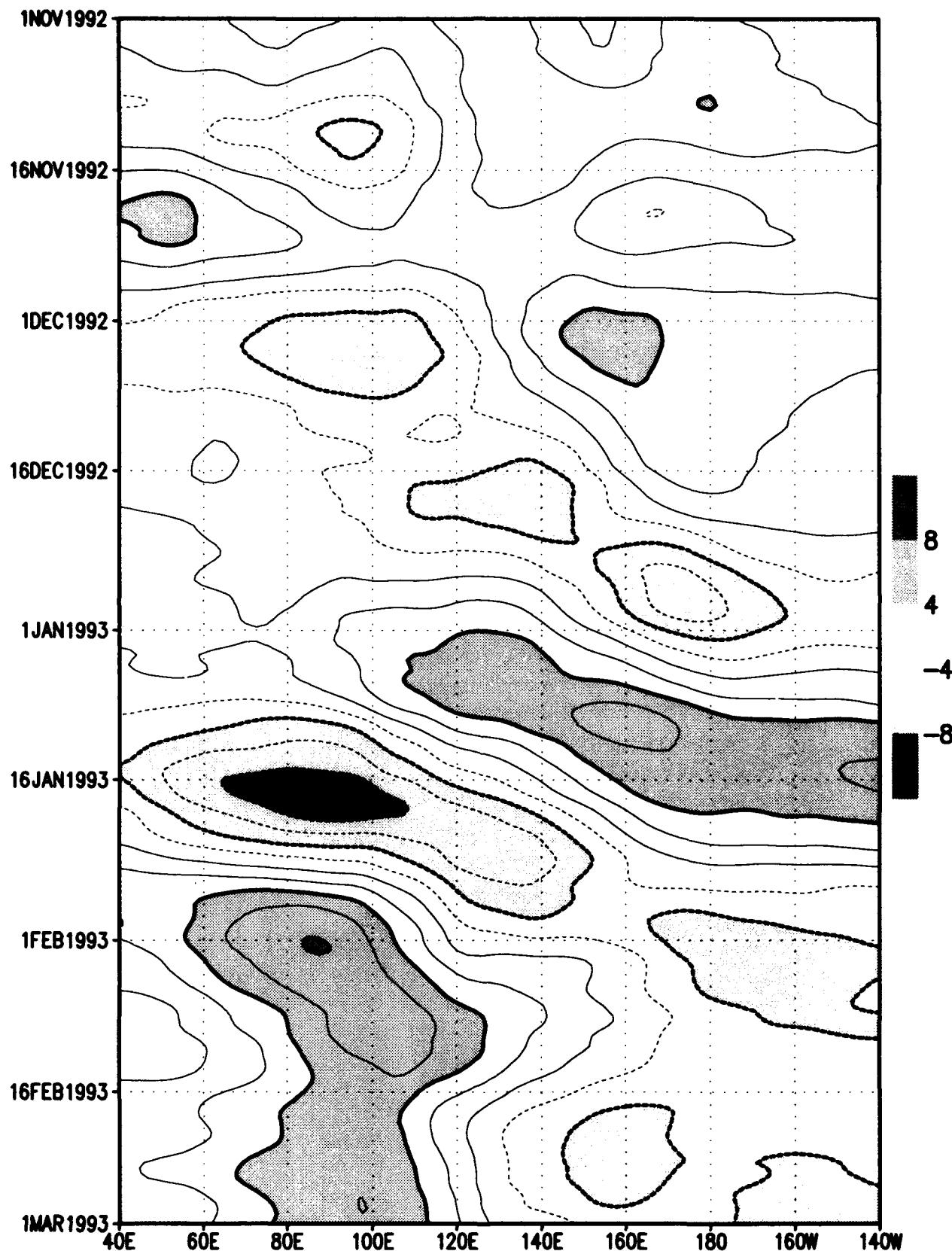
In the equatorial band, the ISO signal is indistinct prior to December but is very strong by the second ISO (ISO2) in mid January. The first ISO (ISO1) starting around 1 December at 40E is better resolved in the MRF whereas NOGAPS shows a break around 120E. Conversely, ISO2 is more continuous in NOGAPS with a larger negative-positive switch in the Indian Ocean. Part of the difference may be related to the different precipitation characteristics of the model. Averaging in the 10S-5S band showed a strong signal and the remaining plots are restricted to this band. The higher frequencies are illustrated by using a 1-d vice 10-d time smoother in an attempt to distinguish eastward from westward propagating features found in the conceptual model of Lau et al. (1989). Finally, the 10-d running mean of 850 mb velocity potential is given for completeness. χ at this level is weaker in amplitude and has an out-of-phase relationship with χ at 200 mb.

Chart	Description
1	- 5S-5N 200 mb velocity potential for NOGAPS; 10-d running mean
2	- 5S-5N 200 mb velocity potential for MRF; 10-d running mean
3	- 10S-5S 200 mb velocity potential for NOGAPS; 10-d running mean
4	- 10S-5S 200 mb velocity potential for MRF; 10-d running mean
5	- 10S-5S 200 mb velocity potential for NOGAPS; 1-d running mean
6	- 10S-5S 200 mb velocity potential for MRF; 1-d running mean
7	- 10S-5S 850 mb velocity potential for NOGAPS; 10-d running mean
8	- 10S-5S 850 mb velocity potential for MRF; 10-d running mean

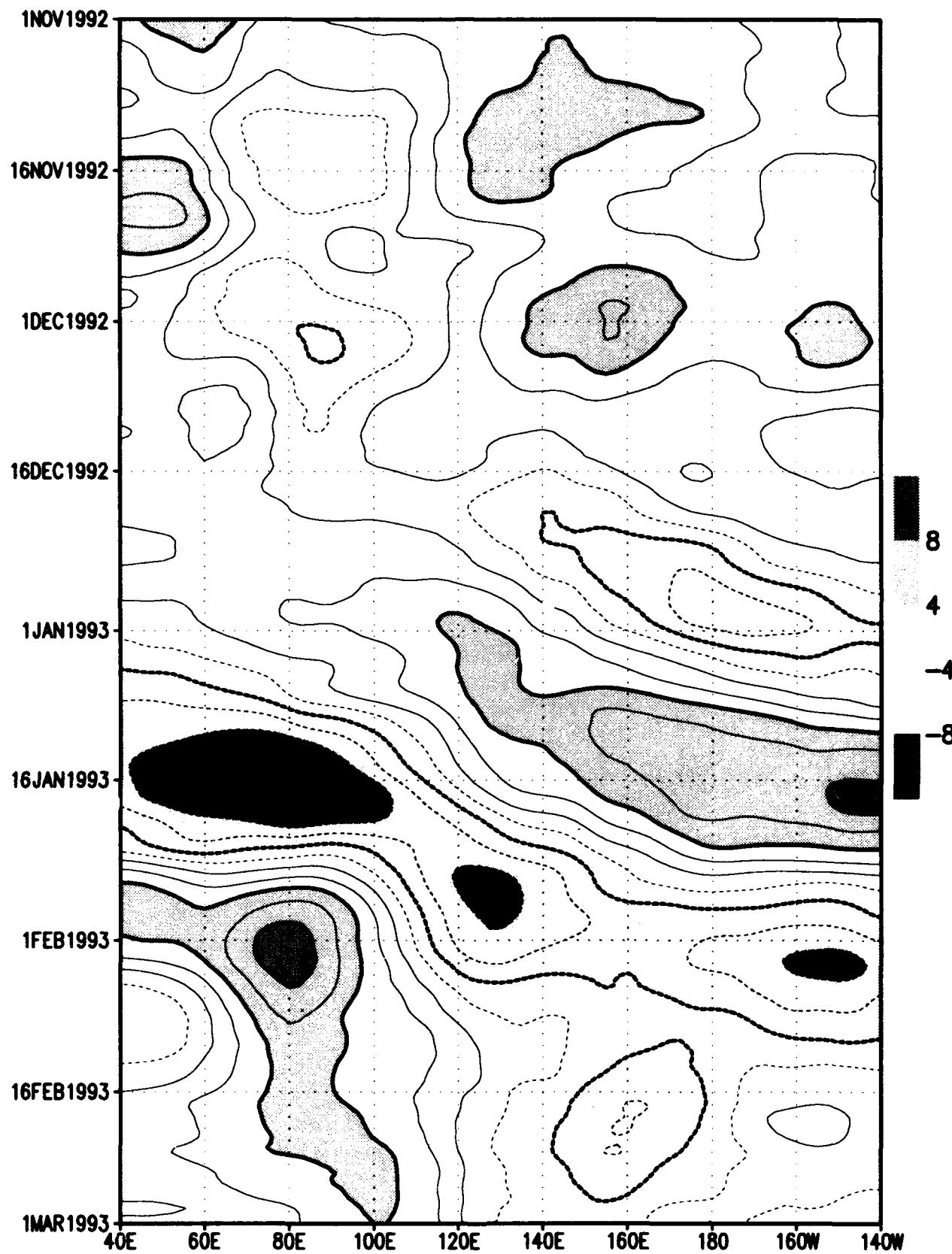
NOGAPS 200 mb chi anom ($1e6 \text{ m}^2/\text{s}$) 5S-5N
10-d running mean ; /d2/toga_coare/apps/hchi.gs



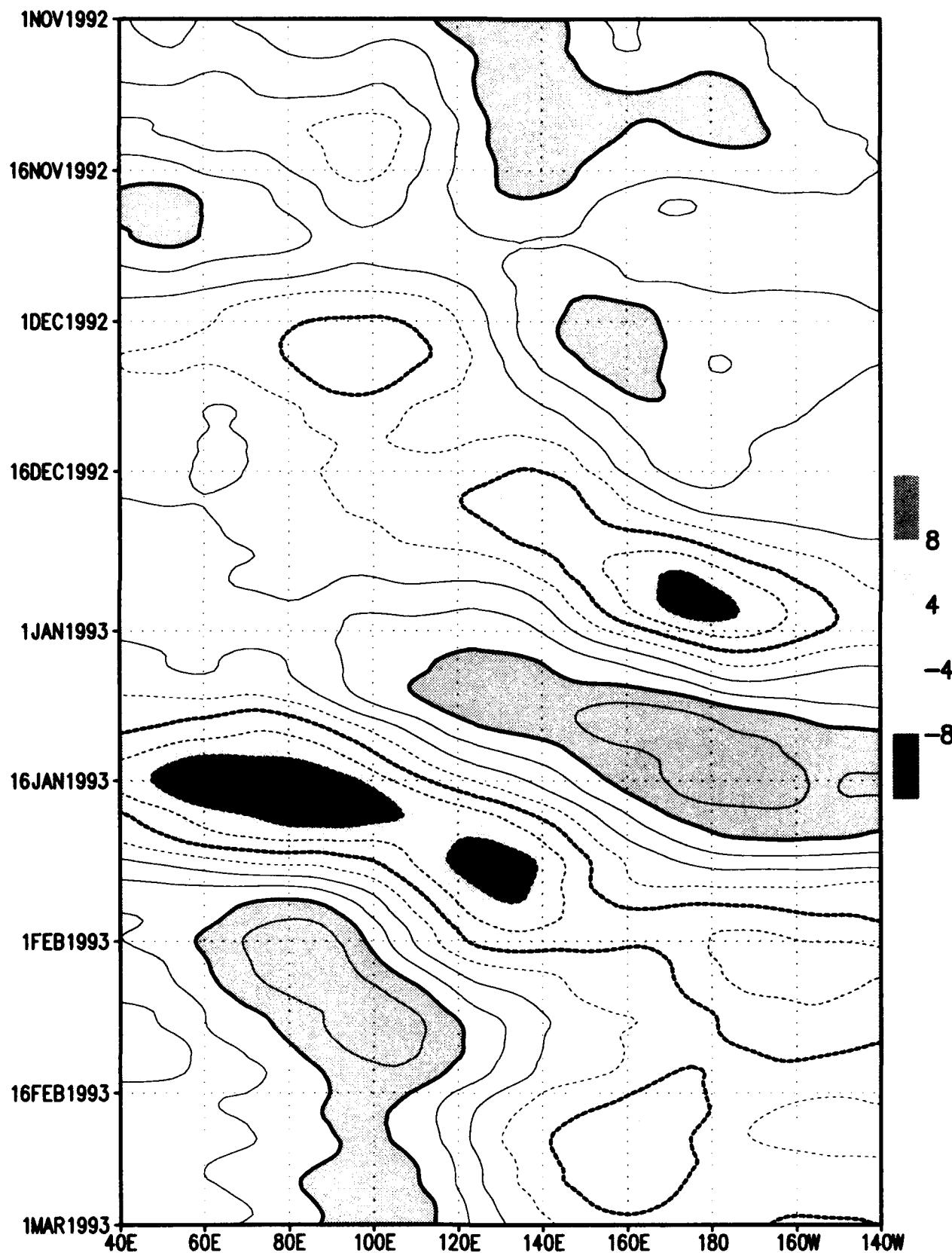
MRF 200 mb chi anom ($1e6 m**2/s$) 5S-5N
10-d running mean ; /d2/toga_coare/apps/hchi.gs



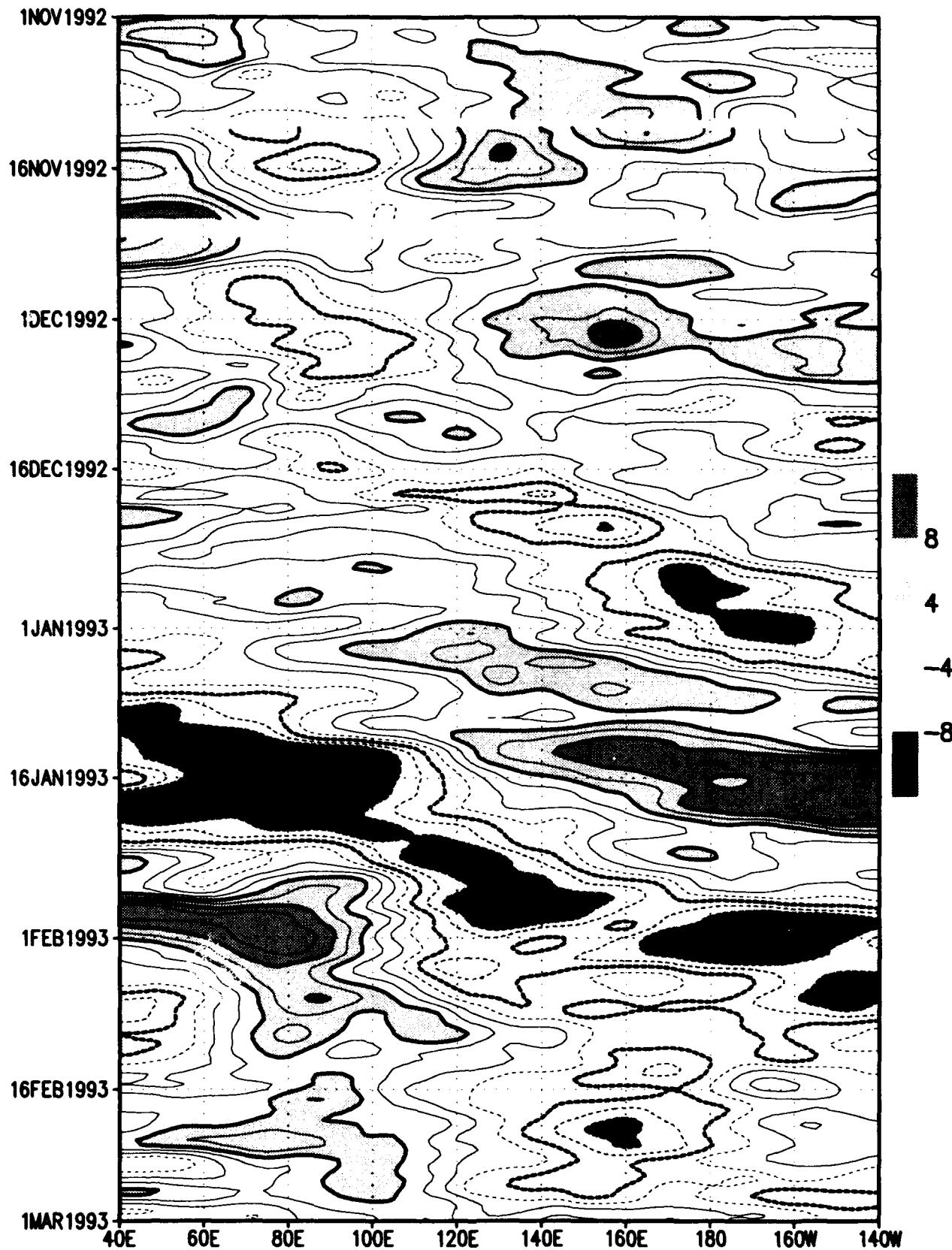
NOGAPS 200 mb chi anom ($1e6 \text{ m}^{2}/\text{s}$) 10S-5S**
10-d running mean ; /d2/toga_coare/apps/hchi.gs



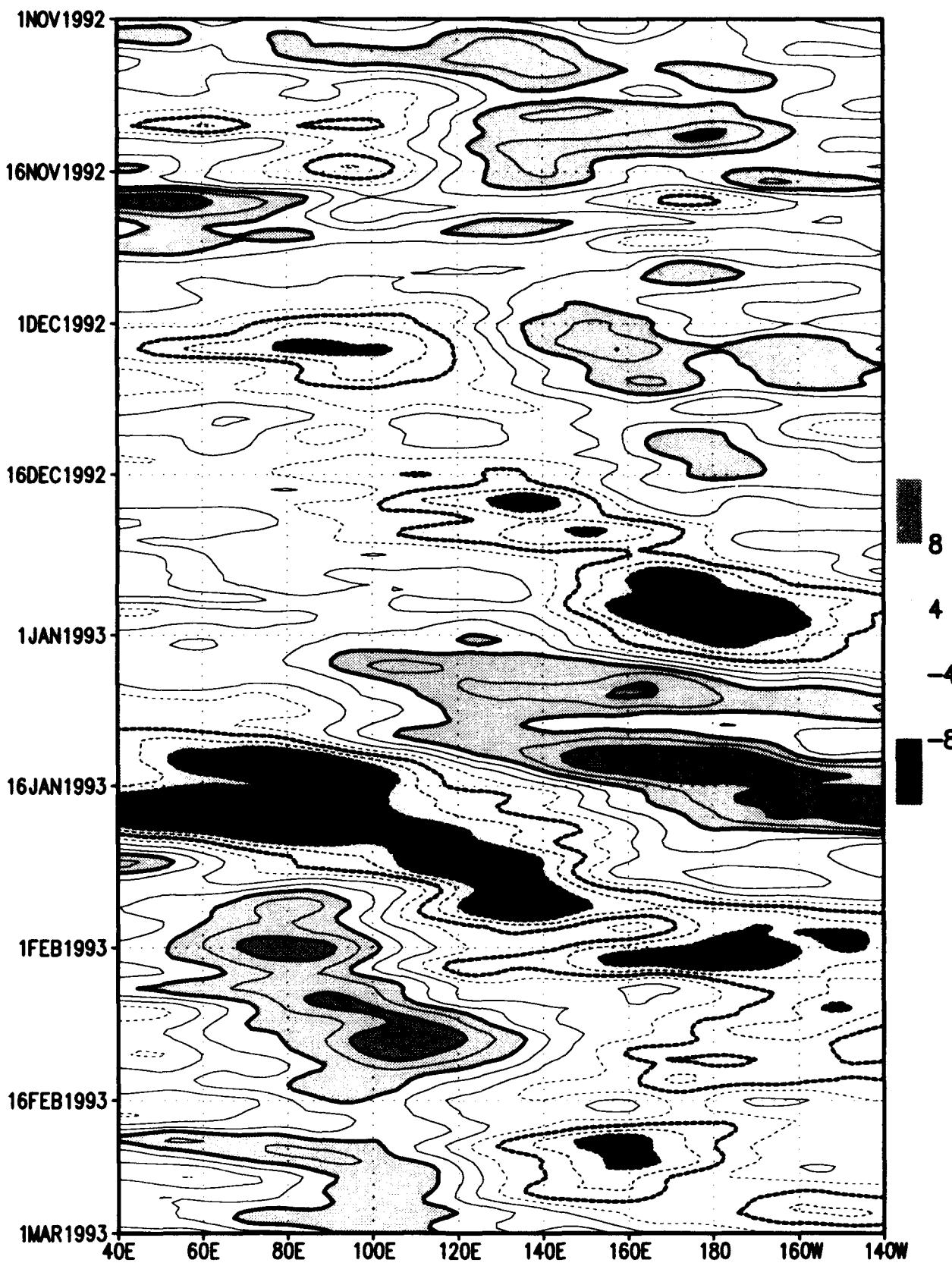
MRF 200 mb chi anom ($1e6 \text{ m}^{**2}/\text{s}$) 10S–5S
10-d running mean ; /d2/toga_coare/apps/hchi.gs



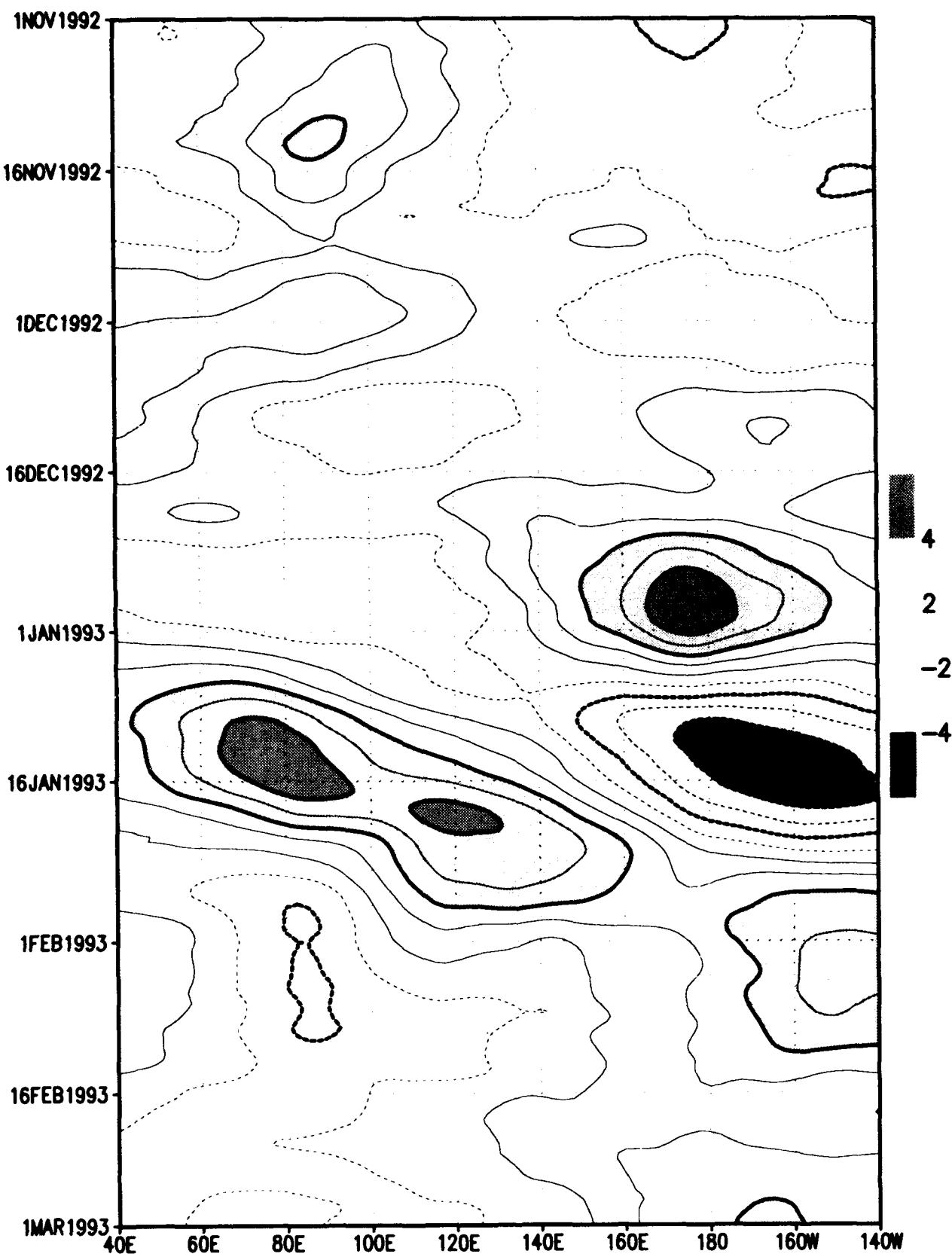
NOGAPS 200 mb chi anom ($1e6 \text{ m}^{**2}/\text{s}$) 10S-5S
1-d running mean : /d2/toga_coare/apps/hchi.gs



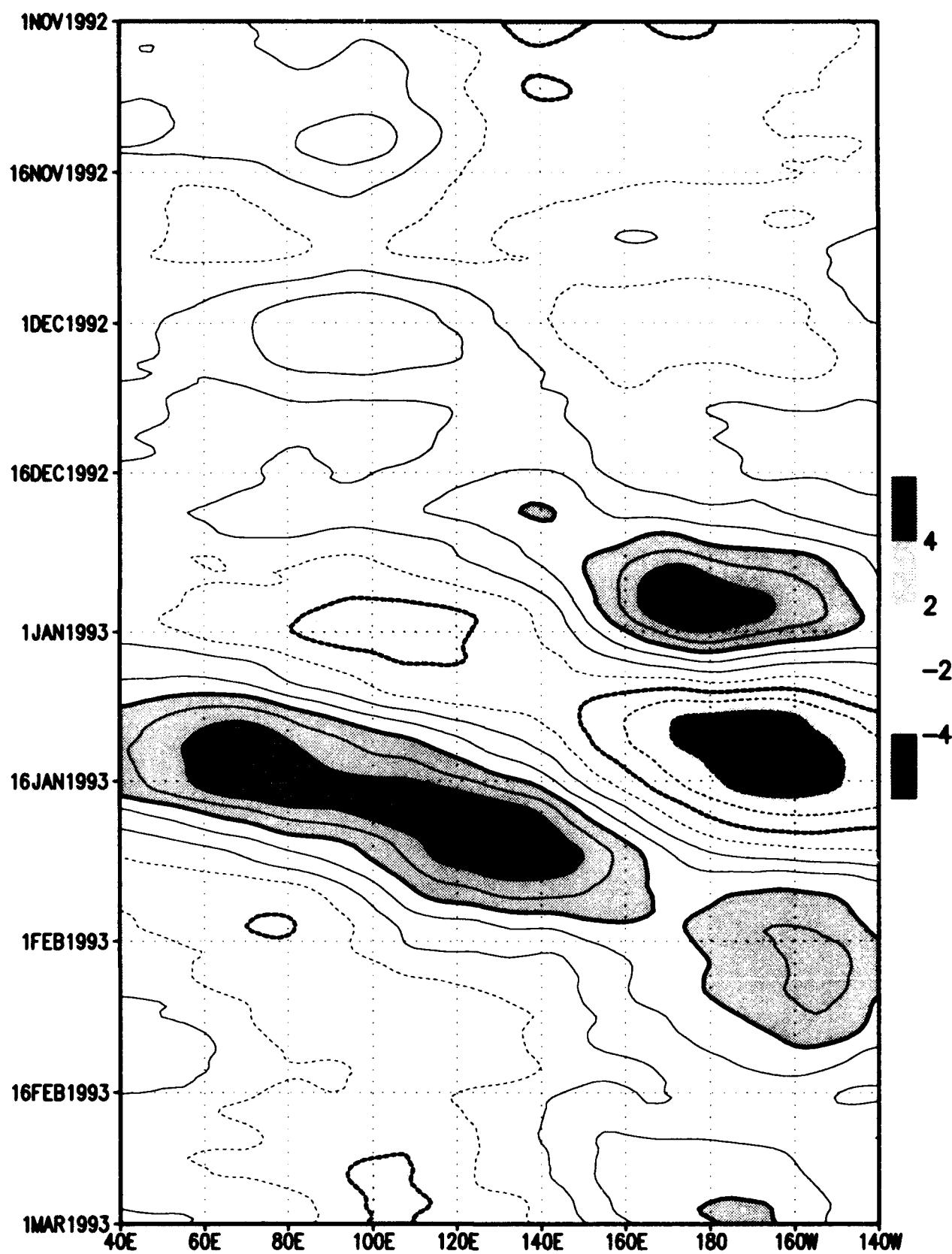
MRF 200 mb chi anom ($1e6\text{ m}^{**2}/\text{s}$) 10S–5S
1-d running mean ; /d2/toga_coare/apps/hchi.gs



NOGAPS 850 mb chi anom ($1e6 m^{**2}/s$) 10S-5S
10-d running mean ; /d2/toga_coare/apps/hchi.gs



MRF 850 mb chi anom ($1e6 \text{ m}^{**2}/\text{s}$) 10S-5S
10-d running mean : /d2/toga_coare/apps/hchi.gs



8.3 Tropical Cyclones

Synthetic or bogus tropical cyclone soundings were added to the observational data base at both centers better represent the storm circulation on scales resolved by the model. The scheme is described by Fiorino et al. (1993) for NOGAPS and by Lord (1991) for the MRF. Tropical cyclones may have an important role in the WWB and the associated forcing on the ocean (Phoebeus and Kindle 1993 and Kindle and Phoebeus 1993). Thus, it is important to know strength and location of the TCs and how they may have contributed to the two WWBs.

We take a novel approach to displaying TC position/intensity data in a Hovmoeller diagram. The hurricane symbol is plotted at the observed longitude but distance from the equator (latitude) is indicated through size. The smaller the symbol the further away the storm is from the equator to suggest less influence on the equatorial flow. Hemisphere is indicated by the line thickness of the symbol (thick = northern hemisphere; light = southern hemisphere) and intensity is indicated by the traditional tropical storm (open) and hurricane symbols (closed). Circles represent tropical depressions.

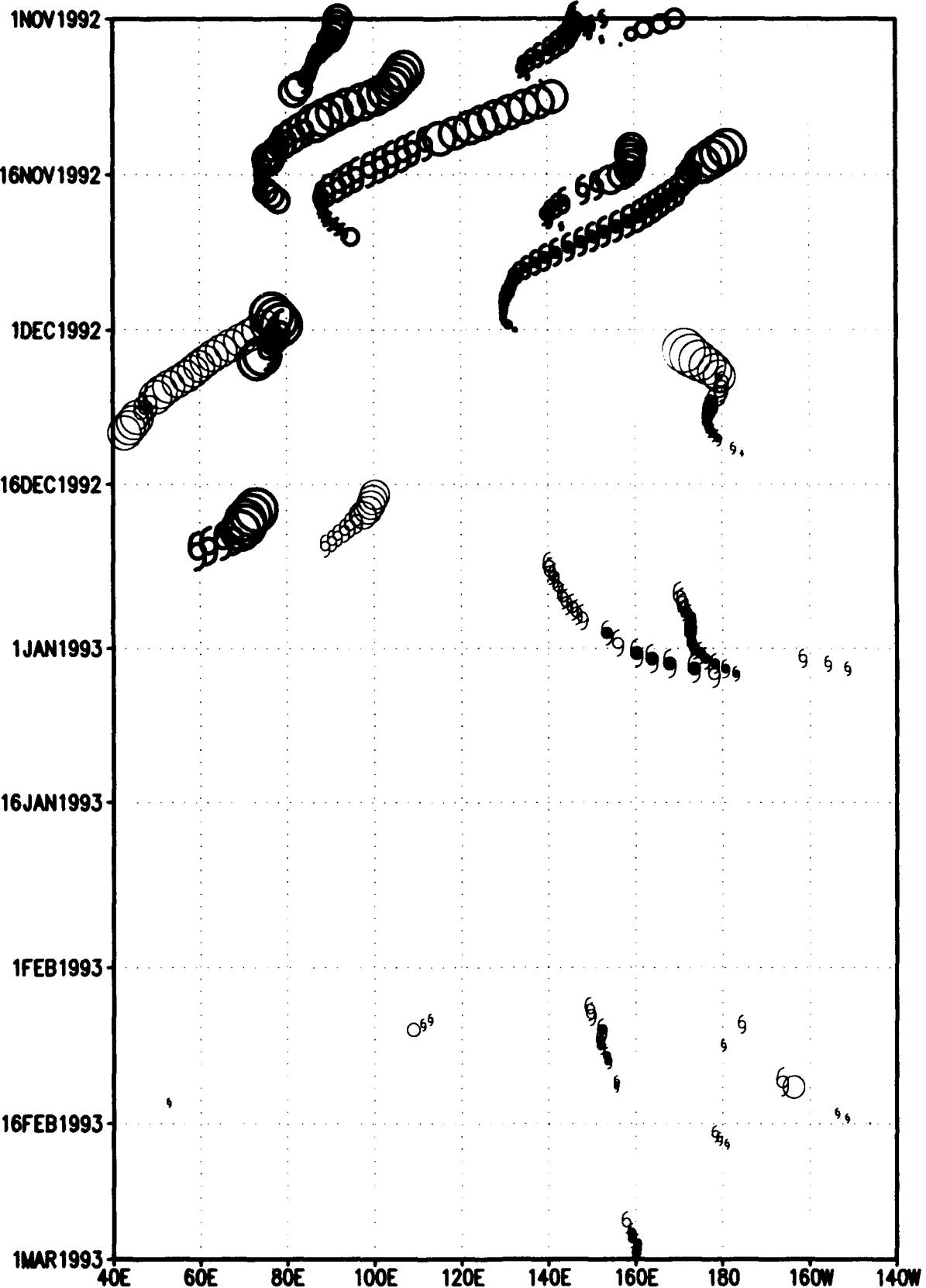
The plot shows a great deal of activity in the northern hemisphere near the equator and west of 140E before 1 December 1992. The only northern/southern hemisphere couplet forms around 1 December 92 at 80E. Most activity in the southern hemisphere was concentrated around 160E with a few storms east of the dateline.

Note the two southern hemisphere cyclones in the vicinity of WWB1. The length and strength of this WWB may have been aided by these cyclones and illustrates how the higher frequencies (e.g., TCs) may have made a important contribution to the first ISO-WWB event.

Chart	Description
1 -	TC Position and Intensity

Tropical Cyclone Positions 30S–30N at 00 & 12Z

thick sym = NHM, size inv prop to lat; script = /d2/toga_coare/apps/htcp.gs
circle = TD, open hurr sym = TS, closed hurr sym = TY



8.4 Precipitation

The two ISOs are clearly seen in the GPI pentad precipitation in the 5S-5N band as eastward propagating areas of rainfall (left-to-right and top-to-bottom on the chart). ISO2 starting around 5 January 1993 at 60E, is more distinct with greater precipitation in the Indian Ocean than ISO1. In contrast, the ISO signal in 12-h precipitation from the models averaged with a 5-day running mean is weaker and less distinct. NOGAPS shows a lack of rain in the 100E-140E whereas the MRF lacks rain between 120-140E. However, the MRF rains more over the far western Pacific Ocean (e.g., note the persistent rain from 1 November 1992 - 16 December 1992 in the 100E-140E band). This characteristic is seen in the seasonal-averaged charts as a pronounced and reversed tropical land mass bias; little rain in NOGAPS and too much rain in the MRF. ISO2, while still weak in the models, is better depicted by NOGAPS.

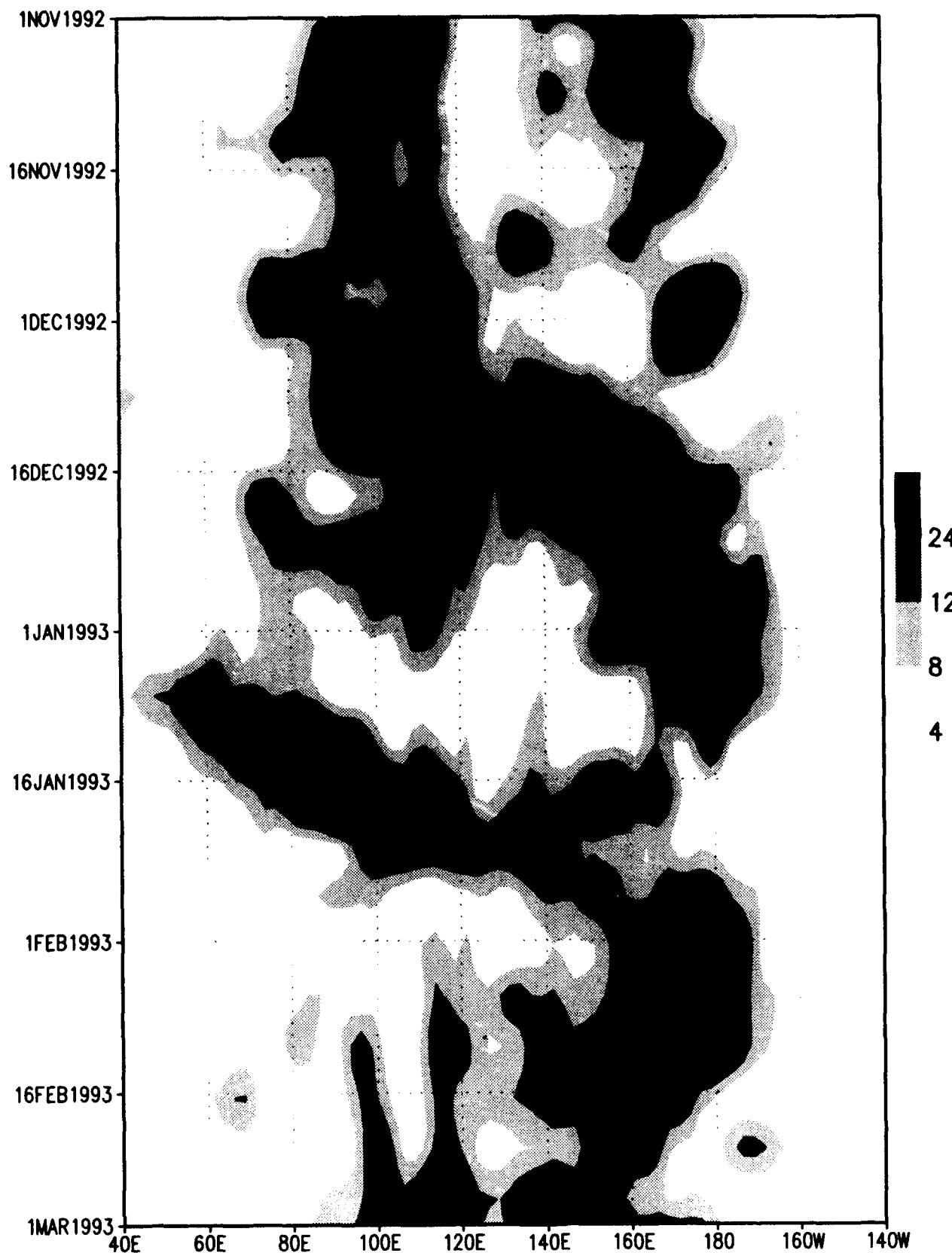
Moving the latitudinal averaging southward to 10S-5S resolves an even stronger ISO signal and a clearer depiction by the models, although in this band the MRF precipitation is weaker over the eastern Indian Ocean during ISO1.

The same set of 5-day average model precipitation plots is produced except that no time smoothing is performed. The idea here is to examine high frequencies and to look for the westward propagating systems which are part of the hierarchy proposed by Lau et al. (1989). NOGAPS exhibits stronger westward propagation than the MRF, especially in the 10S-5S band, which suggests different dynamical properties of the analyses at the higher frequencies. This aspect of the analyses should be considered when making detailed examinations of the data.

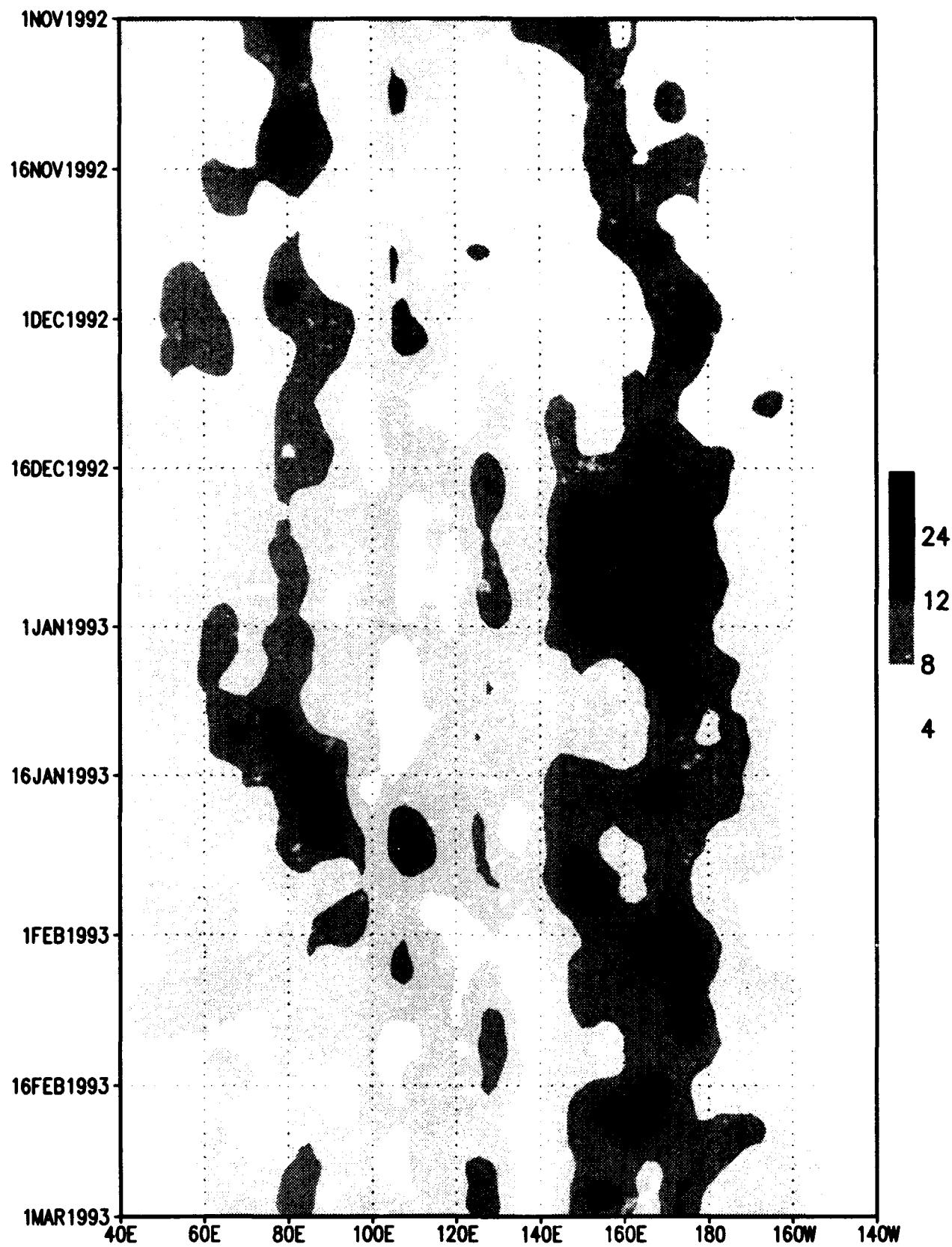
The "PP = " number in the plot title gives the average precipitation rate in mm/day in the time-space area of the chart. We generally find that NOGAPS rain rate is about 7% greater than in the MRF.

Chart	Description
1	- 5S-5N GPI pentads
2	- 5S-5N 12-h precipitation from NOGAPS; 5-d running mean
3	- 5S-5N 12-h precipitation from MRF; 5-d running mean
4	- 10S-5S GPI pentads
5	- 10S-5S 12-h precipitation from NOGAPS; 5-d running mean
6	- 10S-5S 12-h precipitation from MRF; 5-d running mean
7	- 5S-5N 12-h precipitation from NOGAPS; no time smoothing
8	- 5S-5N 12-h precipitation from MRF; no time smoothing
9	- 10S-5S 12-h precipitation from NOGAPS; no time smoothing
10	- 10S-5S 12-h precipitation from MRF; no time smoothing

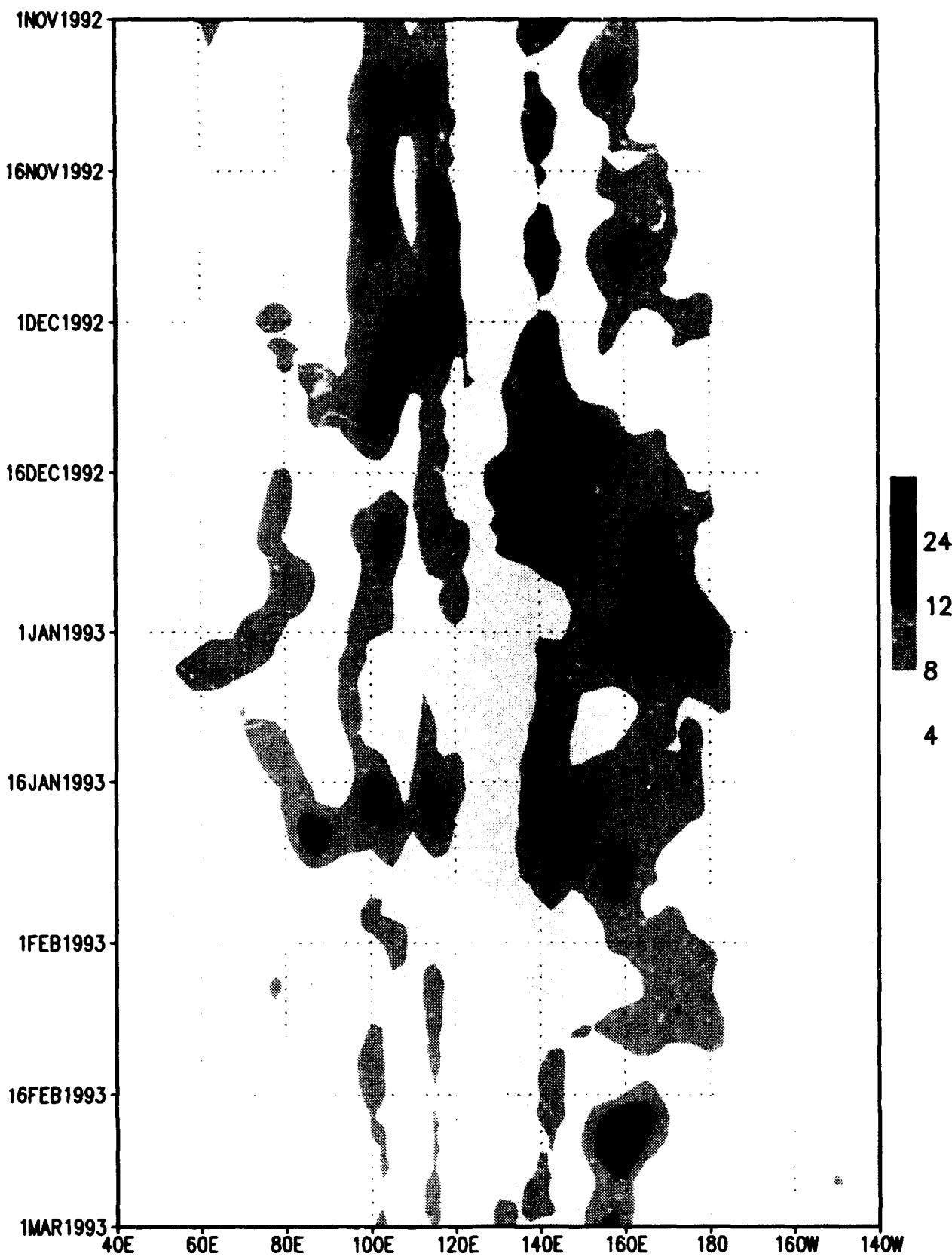
GPI prelim pentads (mm/day) 5S-5N
/d2/toga_coare/apps/hgpi.gs



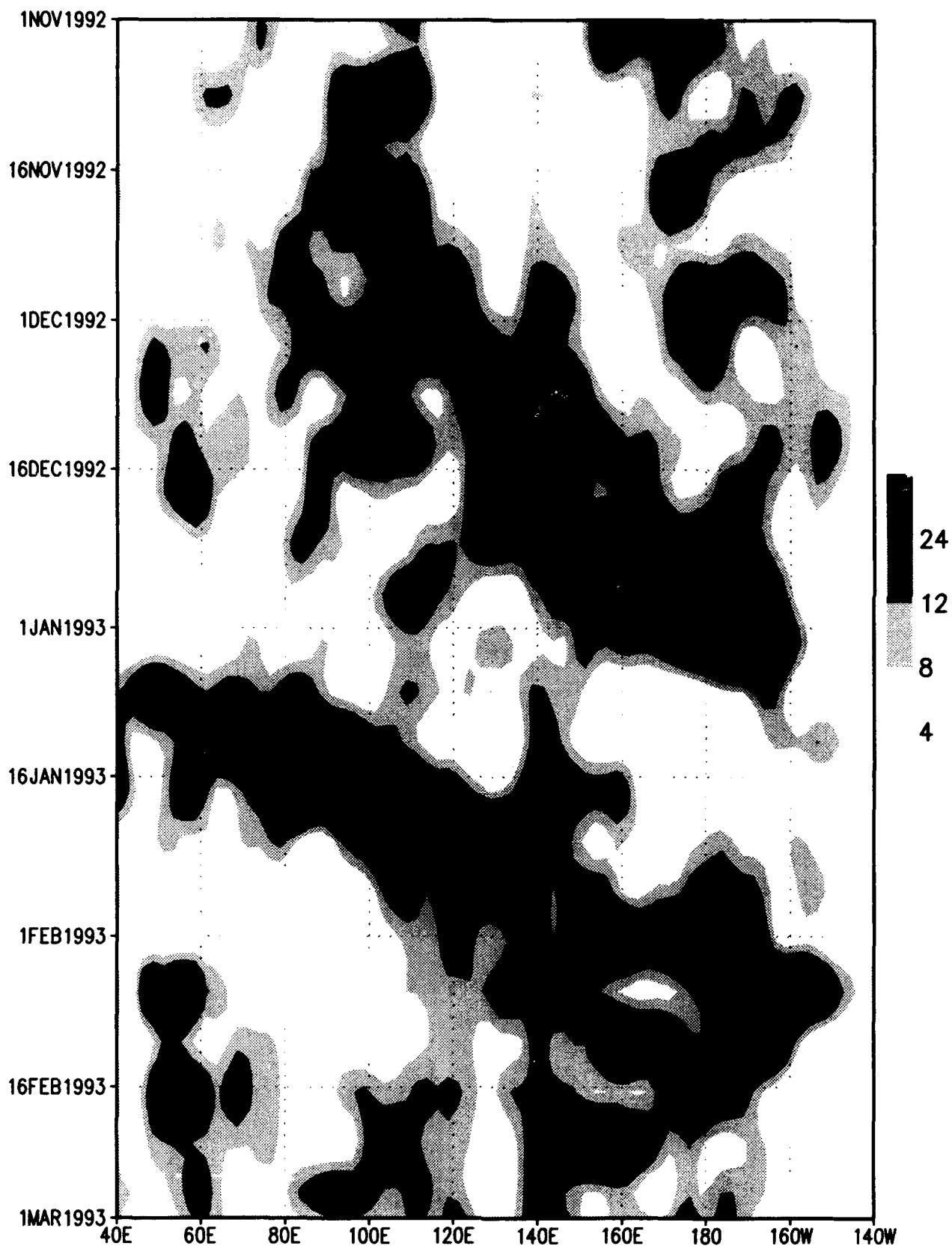
NOGAPS 12-h precip (mm/day) 5S-5N PP = 5.926
5-d running mean ; /d2/toga_coare/apps/hpp.gs



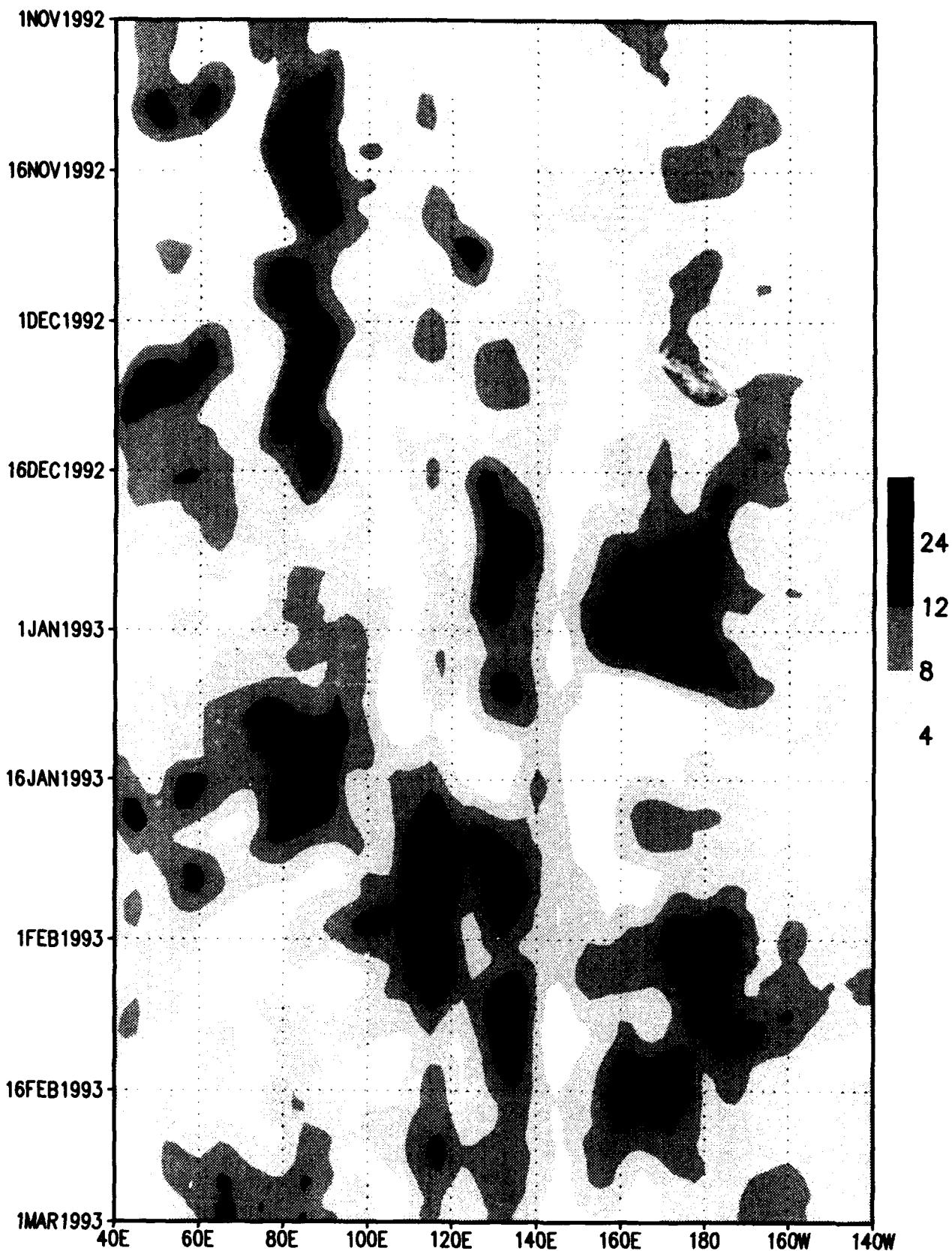
MRF 12-h precip (mm/day) 5S-5N PP = 5.467
5-d running mean ; /d2/toga_coare/apps/hpp.gs



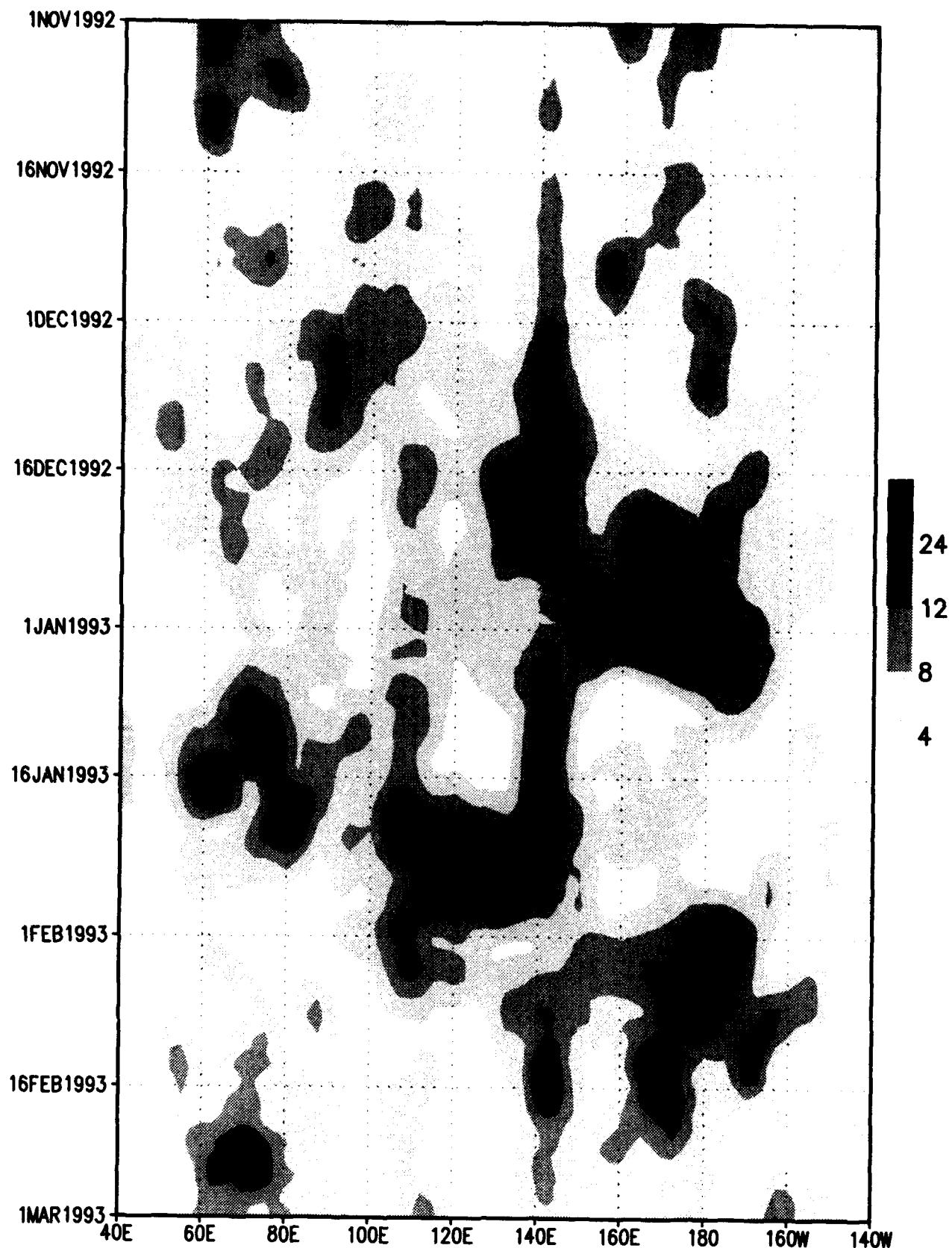
GPI prelim pentads (mm/day) 10S-5S
/d2/toga_coare/apps/hgpi.gs



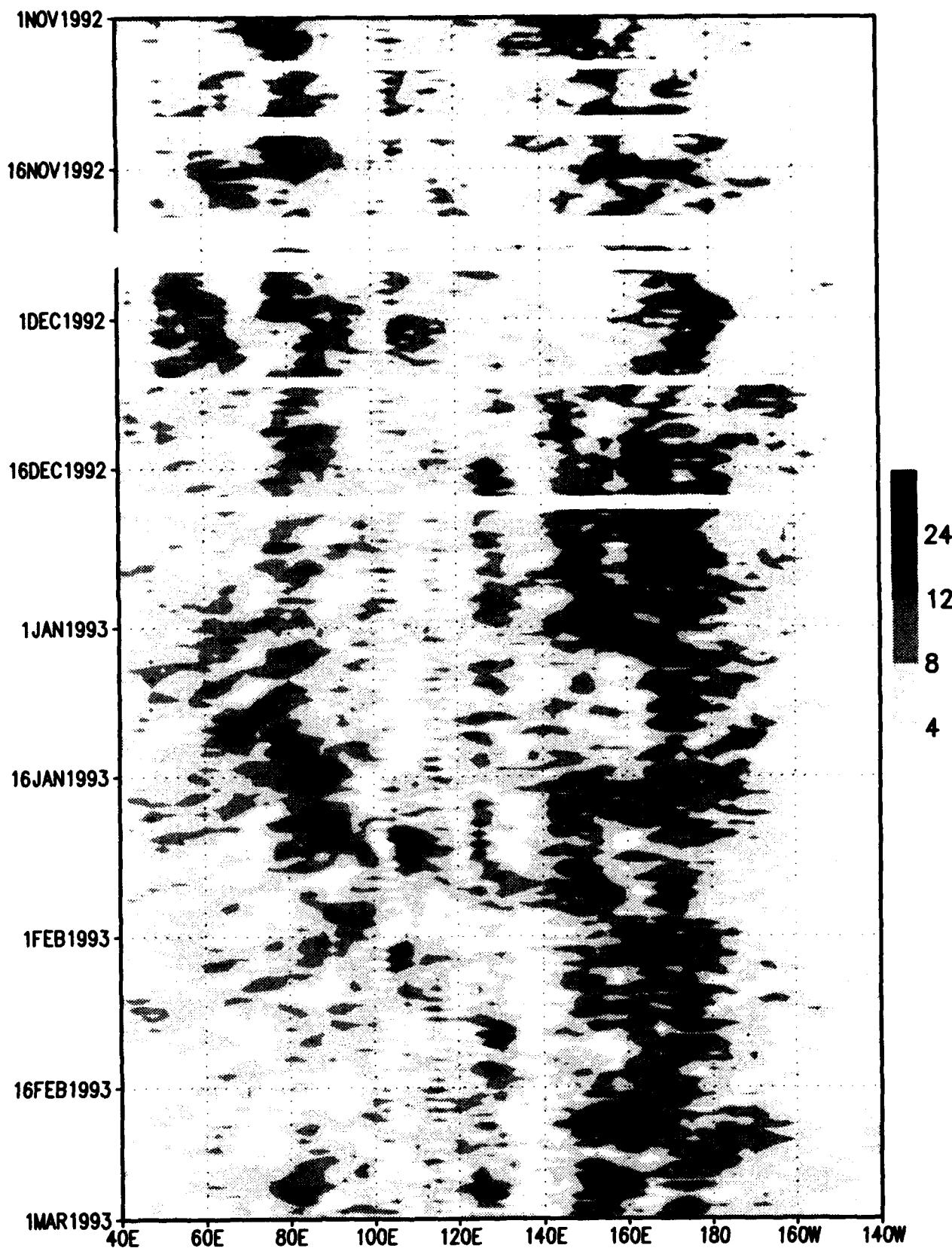
NOGAPS 12-h precip (mm/day) 10S–5S PP = 6.852
5-d running mean ; /d2/toga_coare/apps/hpp.gs



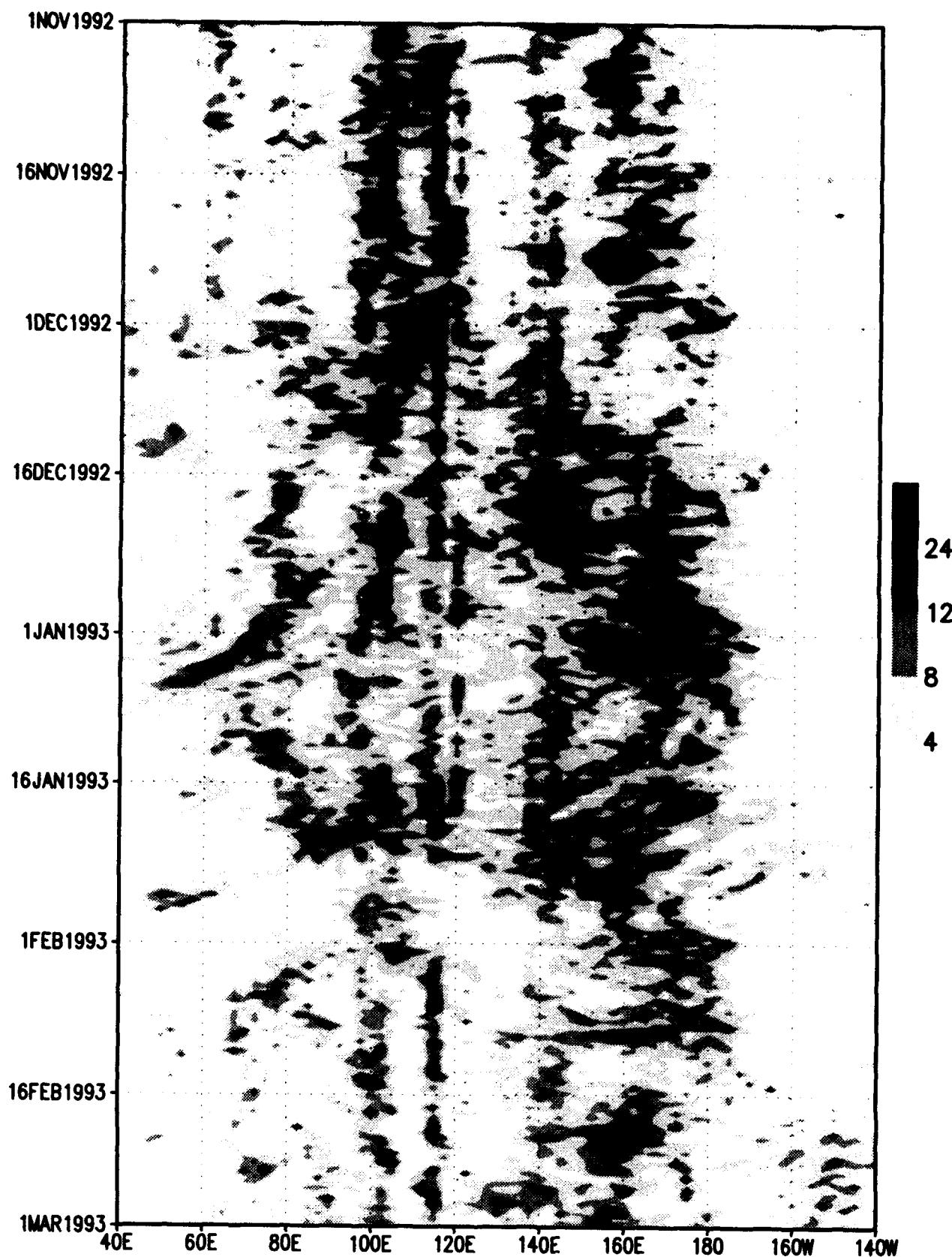
MRF 12-h precip (mm/day) 10S-5S PP = 6.365
5-d running mean : /d2/toga_coare/apps/hpp.gs



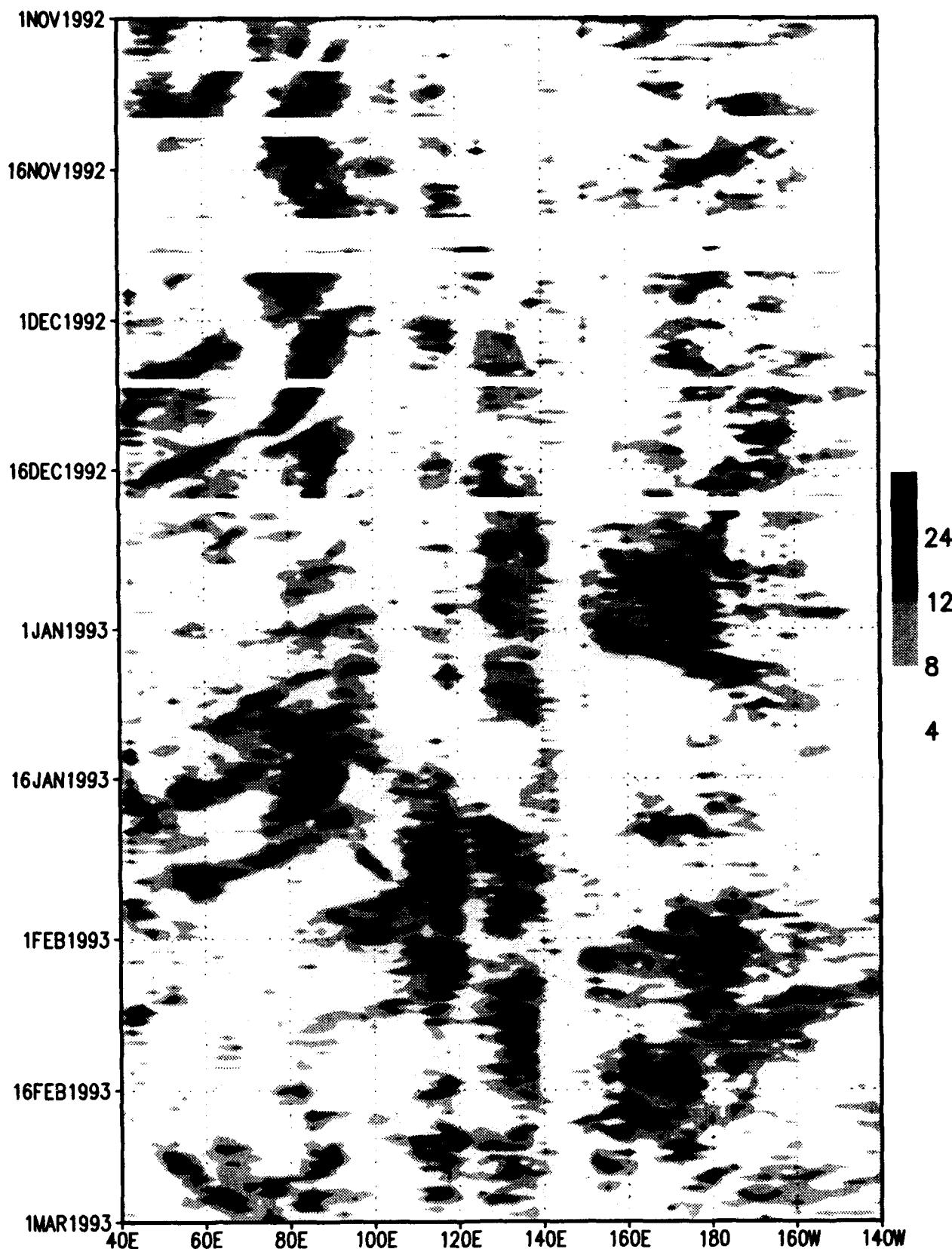
NOGAPS 12-h precip (mm/day) 5S-5N PP = 5.964
no smoothing in time ; /d2/toga_coare/apps/hpp.gs



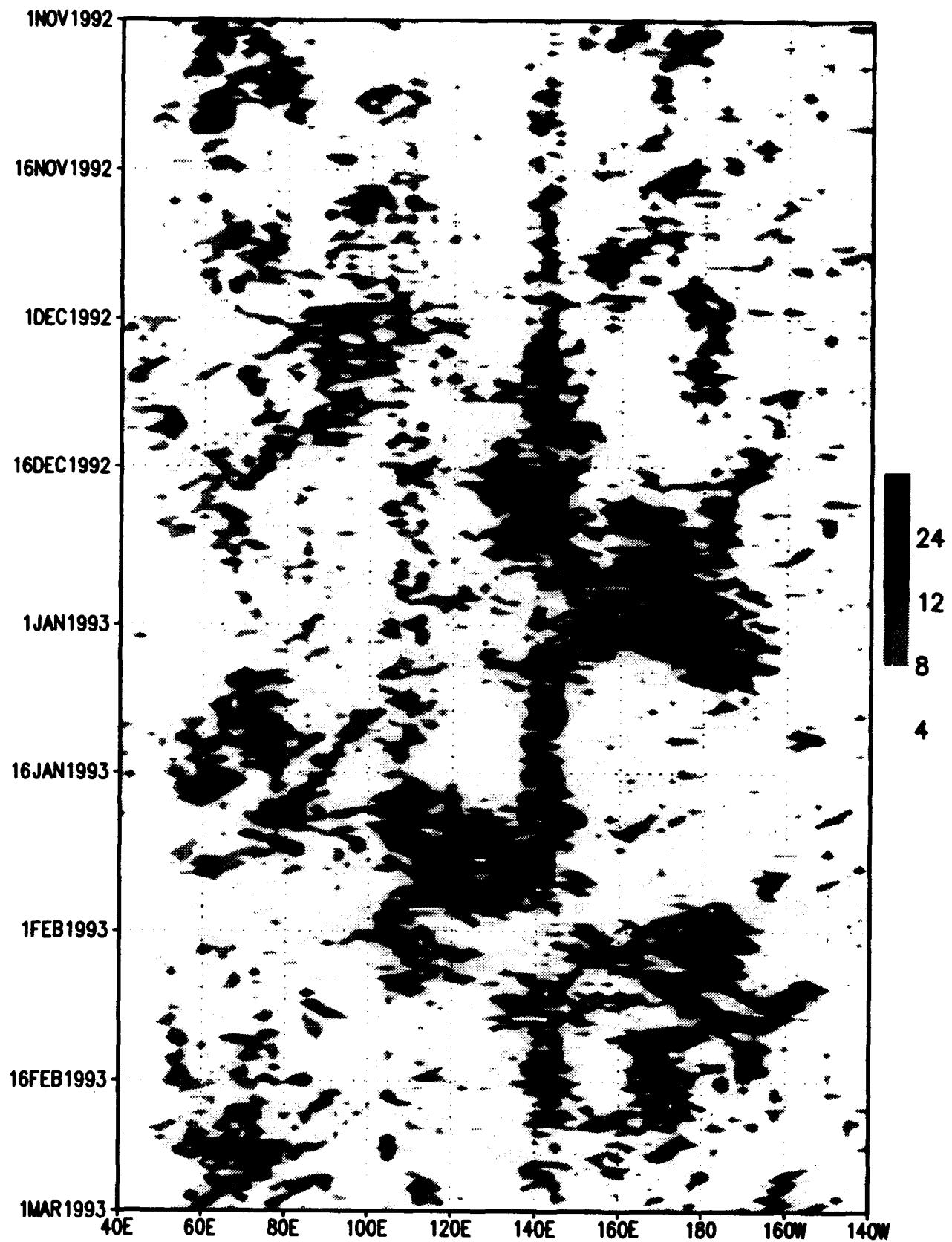
MRF 12-h precip (mm/day) 5S-5N PP = 5.468
no smoothing in time ; /d2/toga_coare/apps/hpp.gs



NOGAPS 12-h precip (mm/day) 10S-5S PP = 6.893
no smoothing in time ; /d2/toga_coare/apps/hpp.gs



MRF 12-h precip (mm/day) 10S-5S PP = 6.363
no smoothing in time ; /d2/toga_coare/apps/hpp.gs

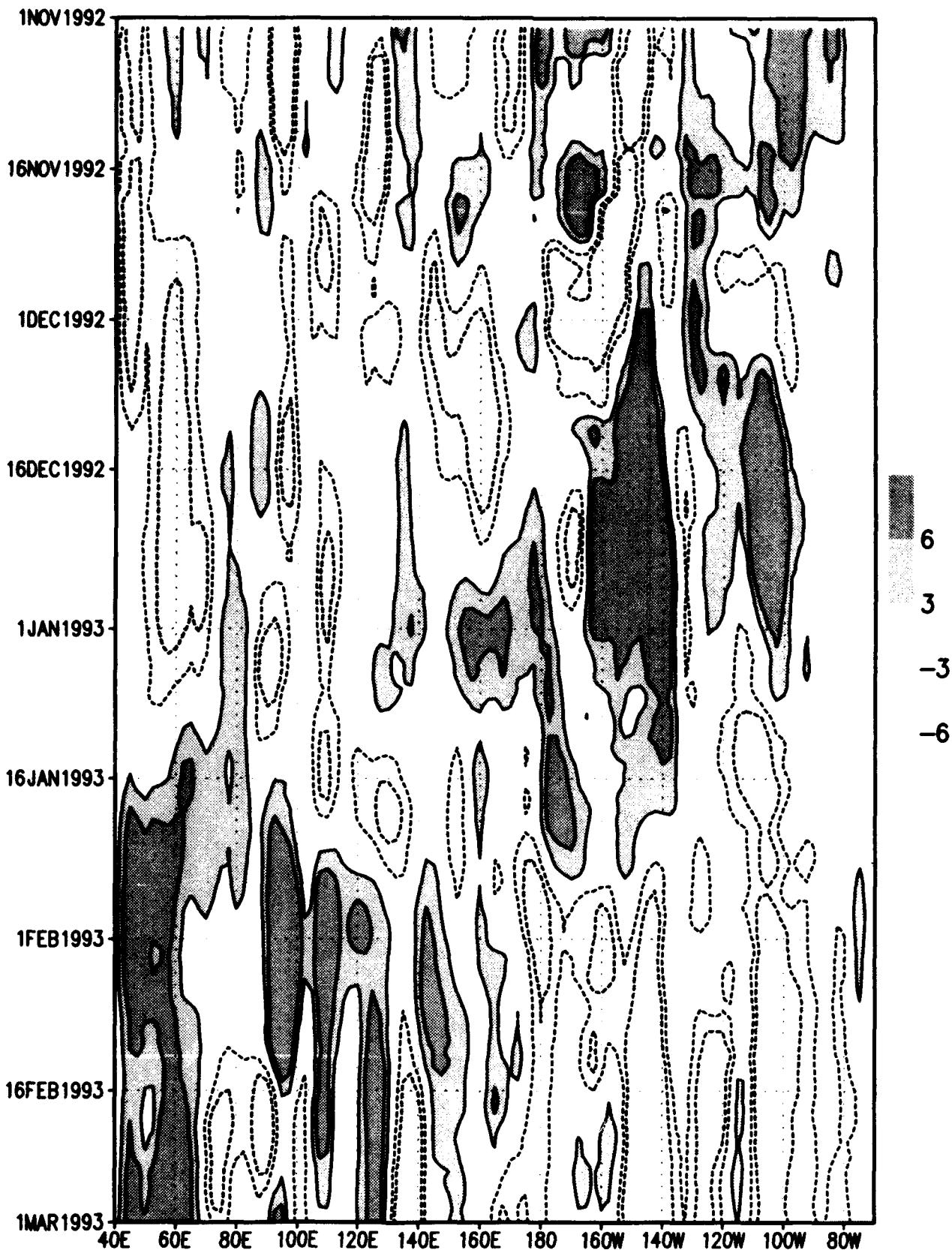


8.5 Ocean Variables

We performed that same type of analysis using the ocean mixed layer depth from TOPS and sea surface temperature (SST) from OTIS. The only difference from the previous charts is that we extended the longitude axis further eastward to cover the entire Indian Ocean and Pacific ocean at the equator and used a longer running mean of 10 d. For SST, we see a strong seasonal cycle from 140W - 80W and some suggestion of eastward propagating features associated with the ISO. An ISO type signal is more apparent in the mixed layer depth.

Chart	Description	
1	-	TOPS ocean mixed-layer depth anomaly; 10-d running mean
2	-	OTIS SST anomaly; 10-d running mean

TOPS ocean mld anomaly (m) 5S-5N
10-d running mean ; /d2/toga_coare/apps/hmld.gs



9 Seasonal (NDJF) Means

The seasonal mean state is defined as the Nov-Dec-Jan-Feb (NDJF) average and for each variable we display two charts. The first shows the average for the NOGAPS and MRF analyses and the second, the ECMWF climatology and a "pooled" anomaly formed by subtracting the NOGAPS+MRF average from the climatology. The pooled anomaly illustrates how conditions during the IOP departed from climatology rather than for NOGAPS-MRF intercomparison . We display the following variables:

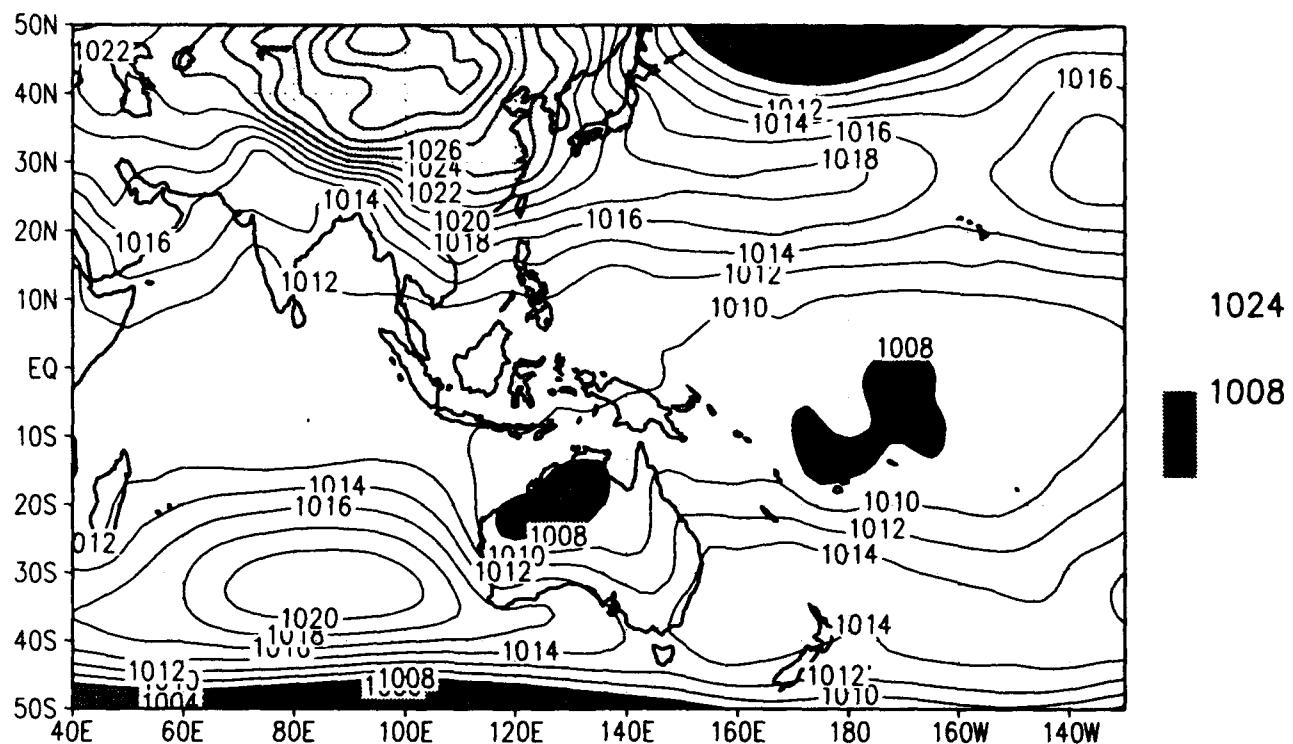
- * SLP (mb)
- * Surface wind (m/sec)
- * 850 mb wind (m/sec)
- * 200 mb wind (m/sec)
- * Precipitation (GPI instead of the anomaly) (mm/day)

As noted earlier, the difference between NOGAPS and MRF SLP over the Asian highlands is not physical, but a consequence of the conversion of 1000 mb geopotential heights and temperature. However, the pooled anomaly does show large-scale anomalies east of the dateline in the midlatitudes.

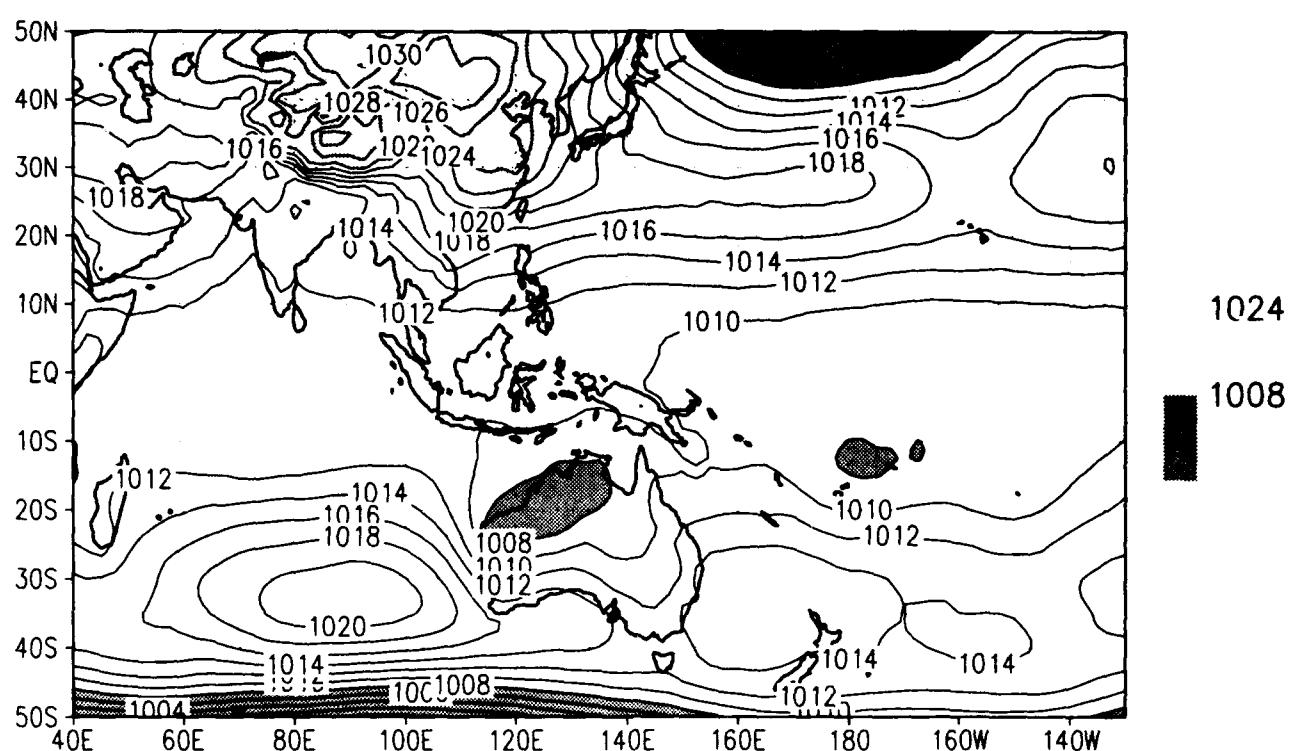
The winds in both analysis systems are more similar than dissimilar in the seasonal mean with small changes from the ECMWF climatology. We note, however, that the differences are greatest in the tropics and Indian Ocean and that the midlatitude jets in both hemisphere are weaker than the ECMWF climatology. Model precipitation, on the other hand, does exhibit more pronounced differences. The intertropical convergence zone is better resolved by NOGAPS than MRF, vis-a-vis the MSU-merged climatology and the GPI average, with pronounced disagreement over the Bay of Bengal. More significantly, the models have an opposite bias in precipitation over tropical islands (e.g., Borneo, Indonesia and New Guinea). NOGAPS is dry and the MRF is wet. These biases may have been responsible for the breaks in the ISO precipitation in the Hovmoeller diagrams. We also find that the subtropics are too rainy in both models and that the GPI "rainfall" over the Himalayas is not realistic, a likely consequence of a cold surface vice cold clouds.

Chart	Description
1	- Sea-level pressure for NOGAPS and MRF
2	- ECMWF climatological Sea-level pressure and the pooled anomaly
3	- Surface wind speed for NOGAPS and MRF
4	- ECMWF climatological surface wind and pooled anomaly
5	- 850 mb wind for NOGAPS and MRF
6	- ECMWF climatological 850 mb wind and pooled anomaly
7	- 200 mb wind for NOGAPS and MRF
8	- ECMWF climatological 200 mb wind and pooled anomaly
9	- 12-h precipitation for NOGAPS and MRF
10	- MSU merged climatological precipitation and GPI

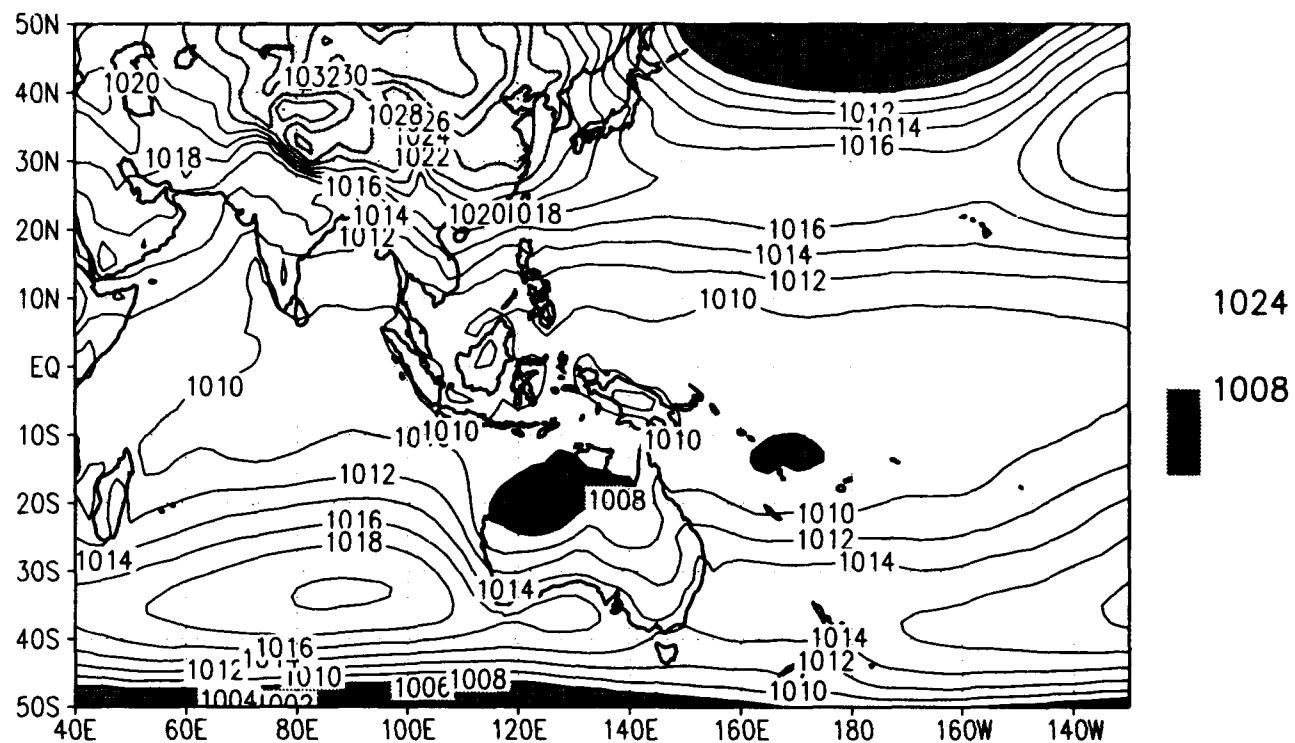
SLP climo for NDJF
 /d2/toga_coare/c.gs
 NOGAPS



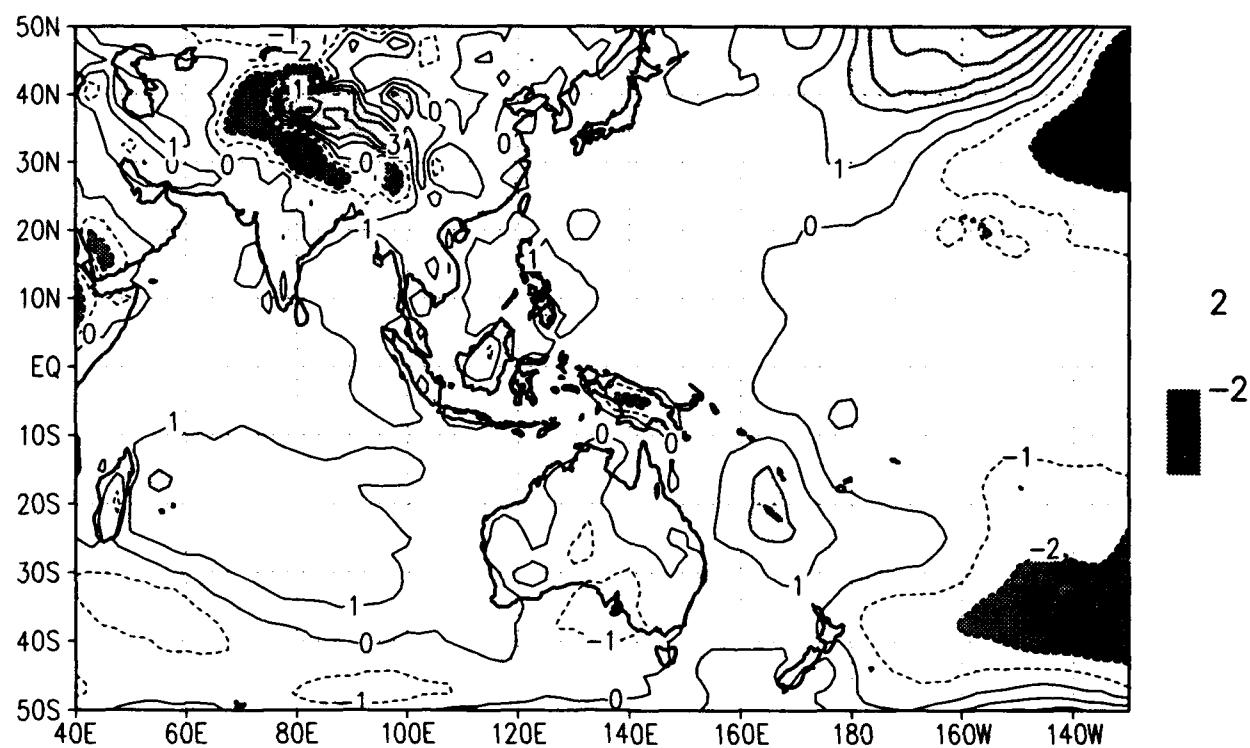
MRF



SLP climo for NDJF
 /d2/toga_coare/c.gs
 ECMWF Climatology

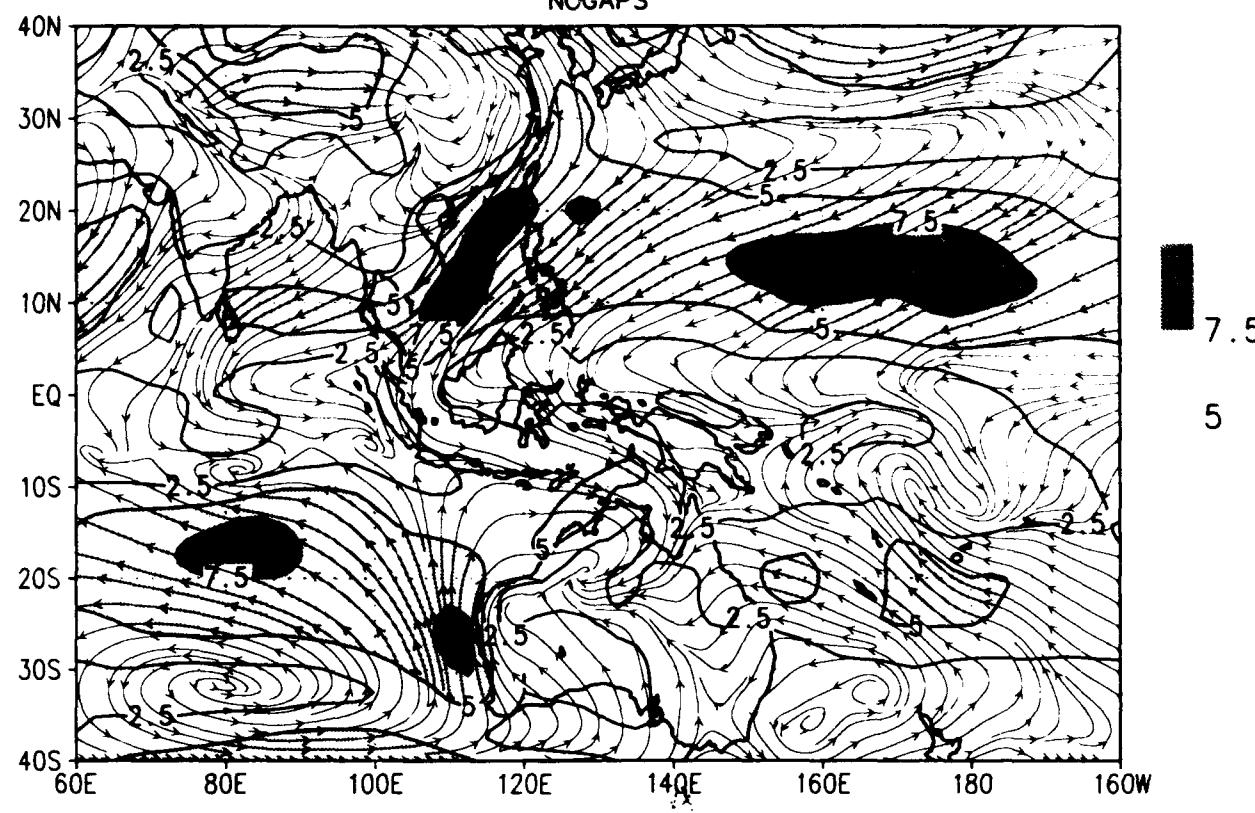


pooled anomaly

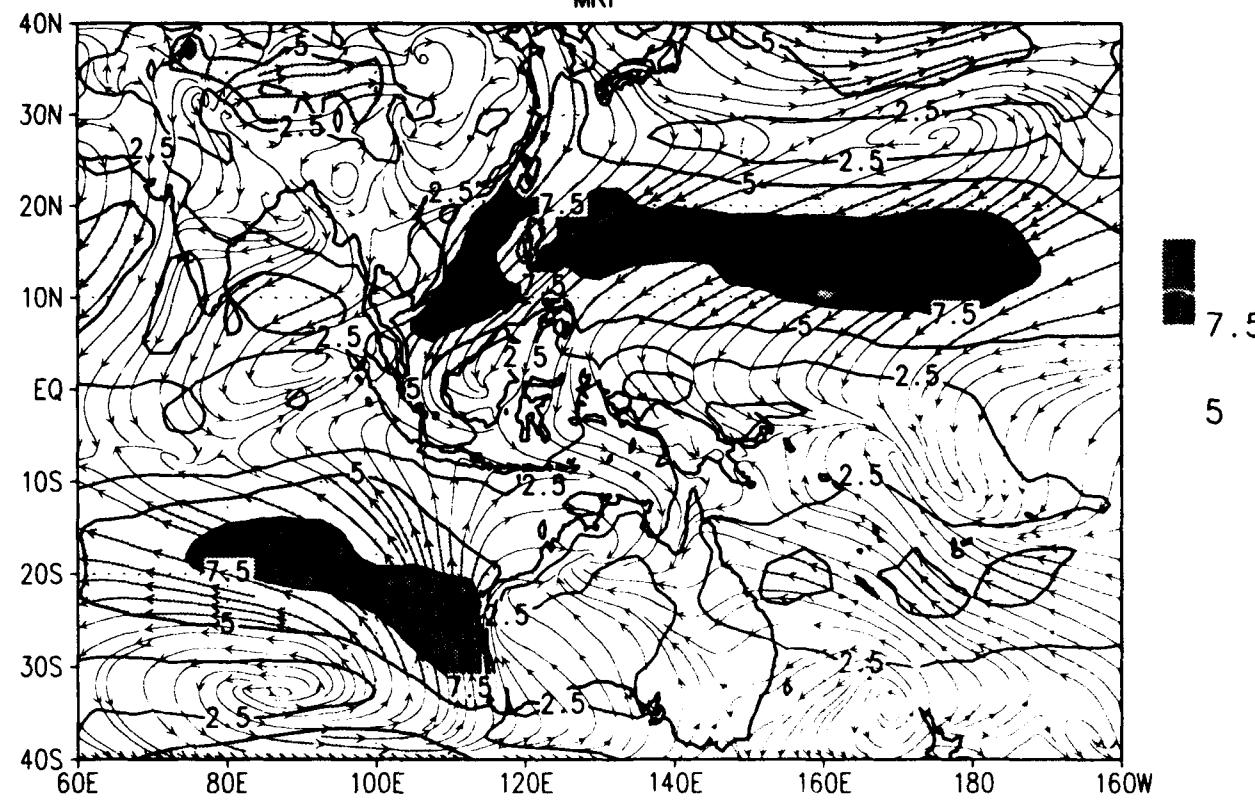


Sfc wind climo for NDJF
/d2/toga_coare/c.gs

NOGAPS

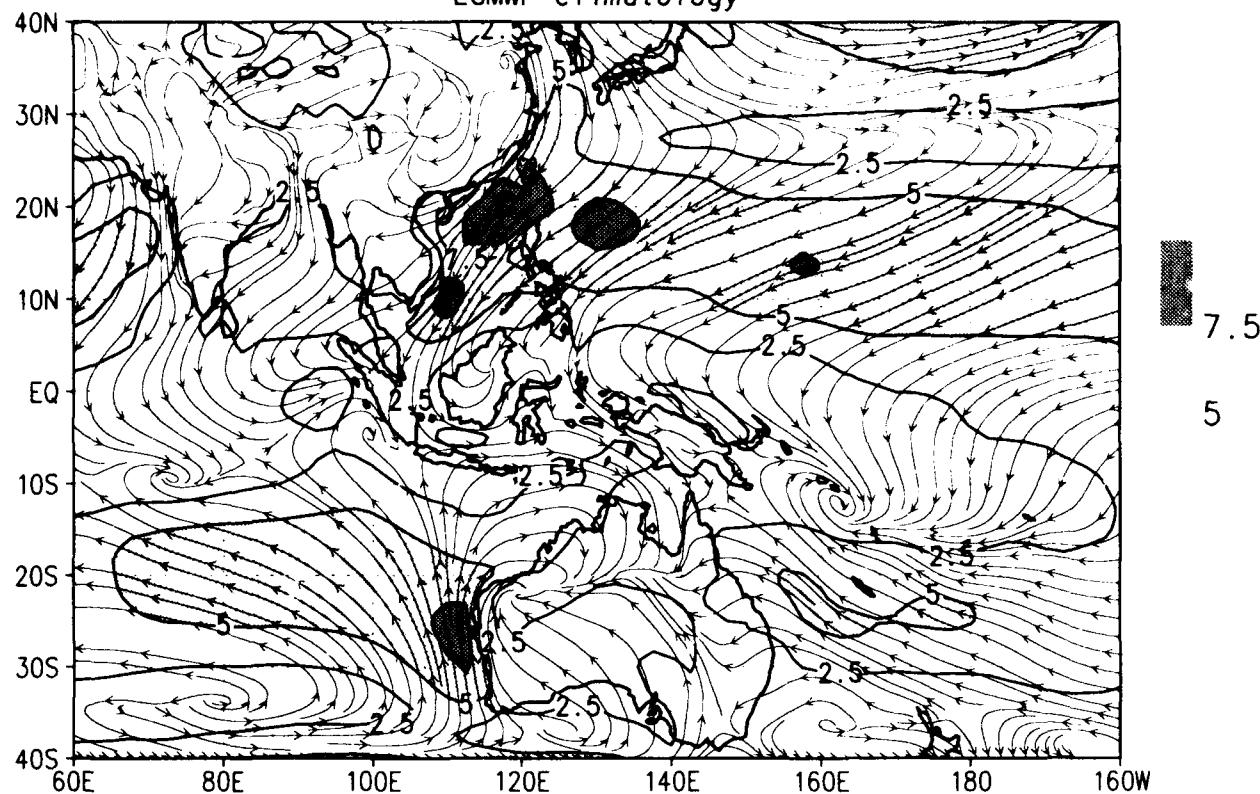


MRF

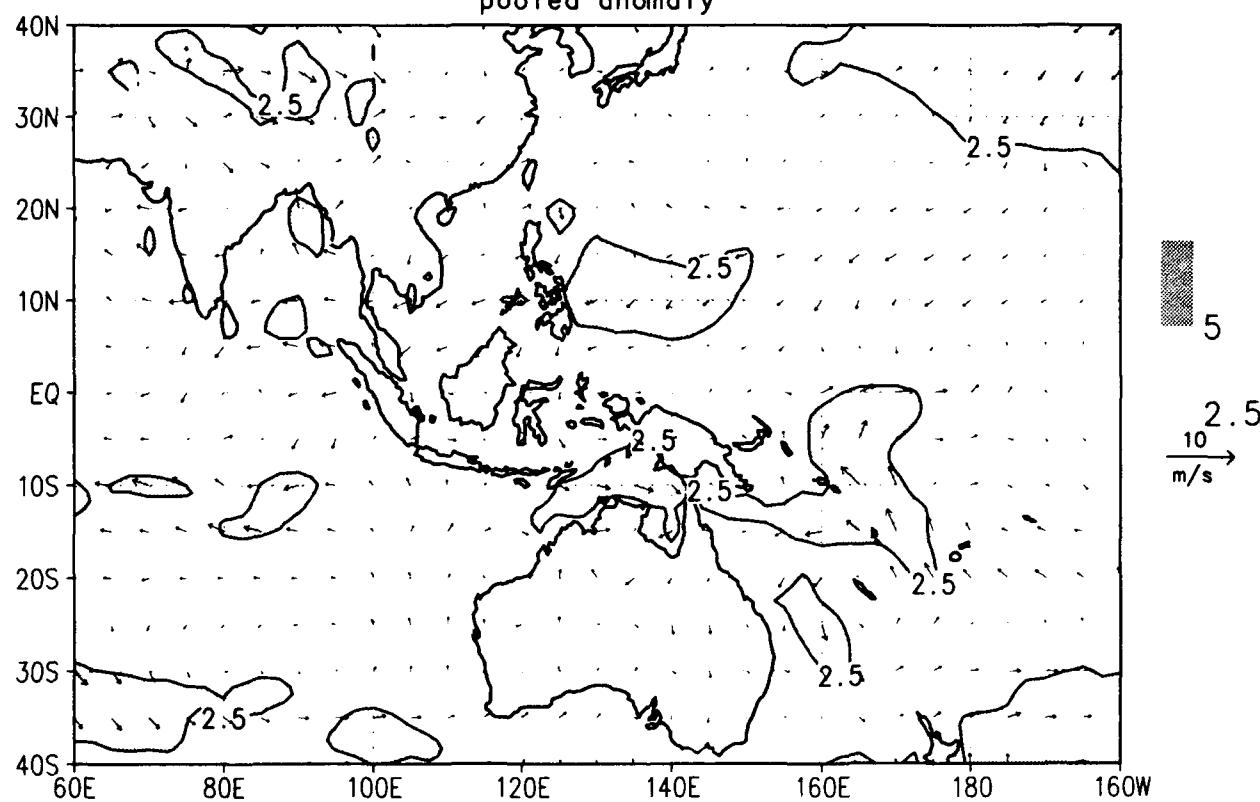


Sfc wind climo for NDJF
/d2/toga_coare/c.gs

ECMWF climatology

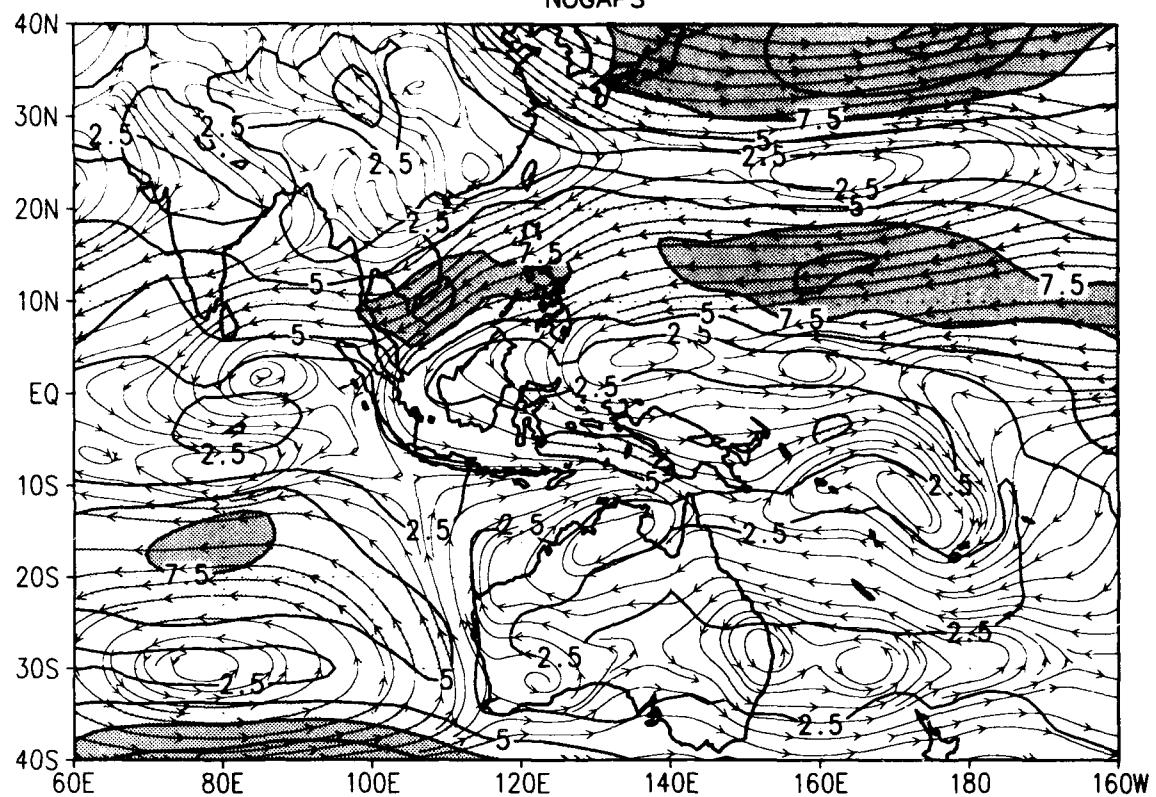


pooled anomaly



850 mb wind climo for NDJF
/d2/toga_coare/c.gs

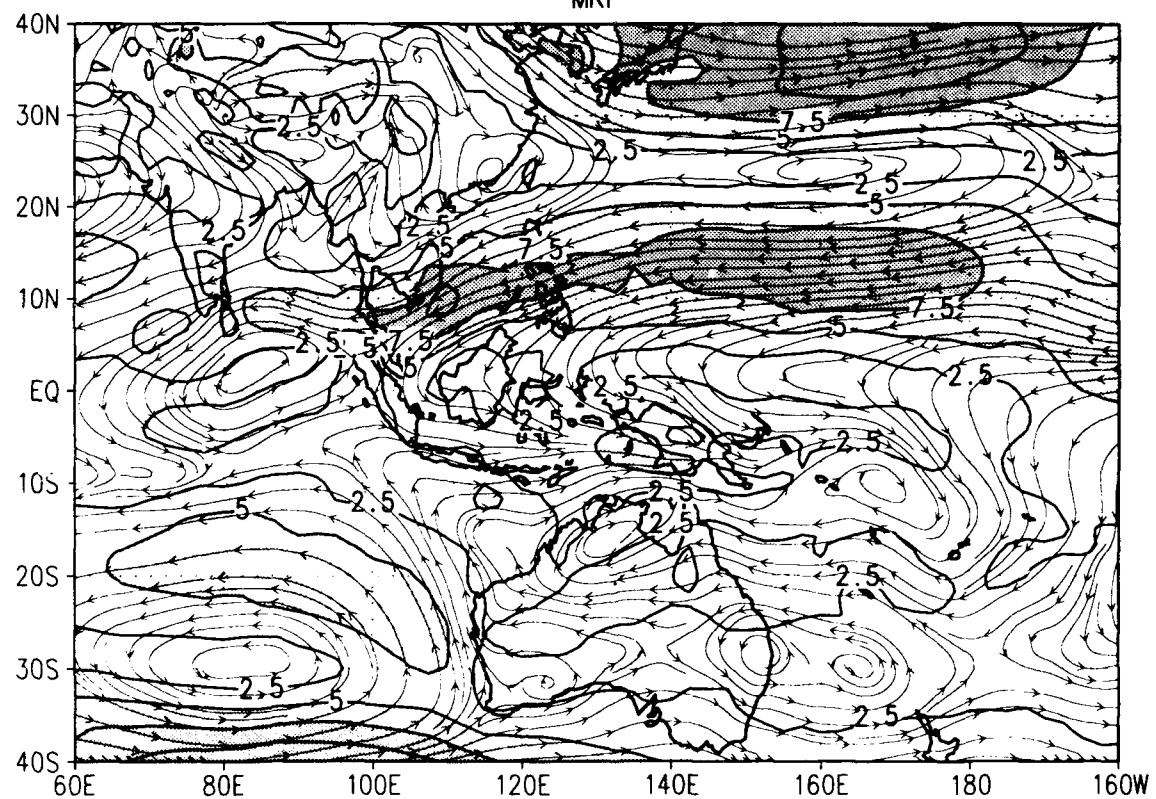
NOGAPS



7.5

5

MRF

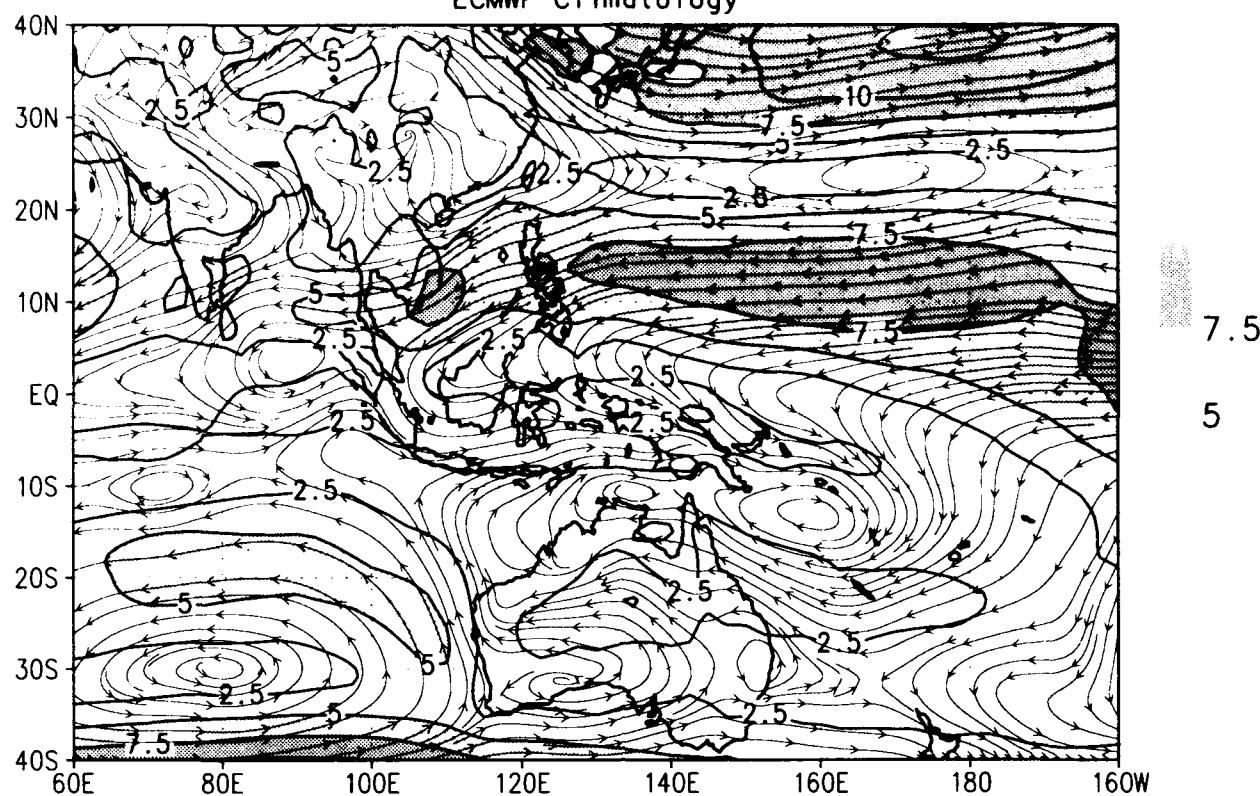


7.5

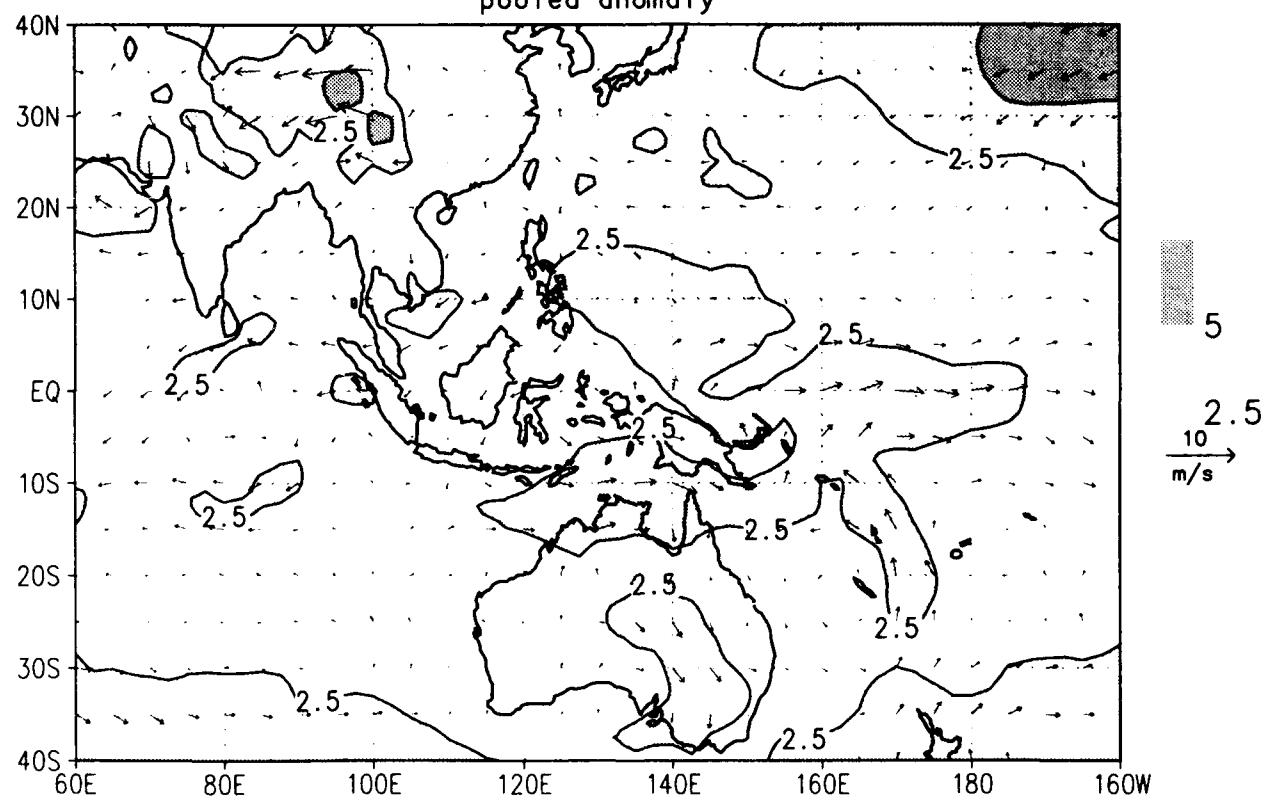
5

850 mb wind climo for NDJF
/d2/toga_coare/c.gs

ECMWF Climatology

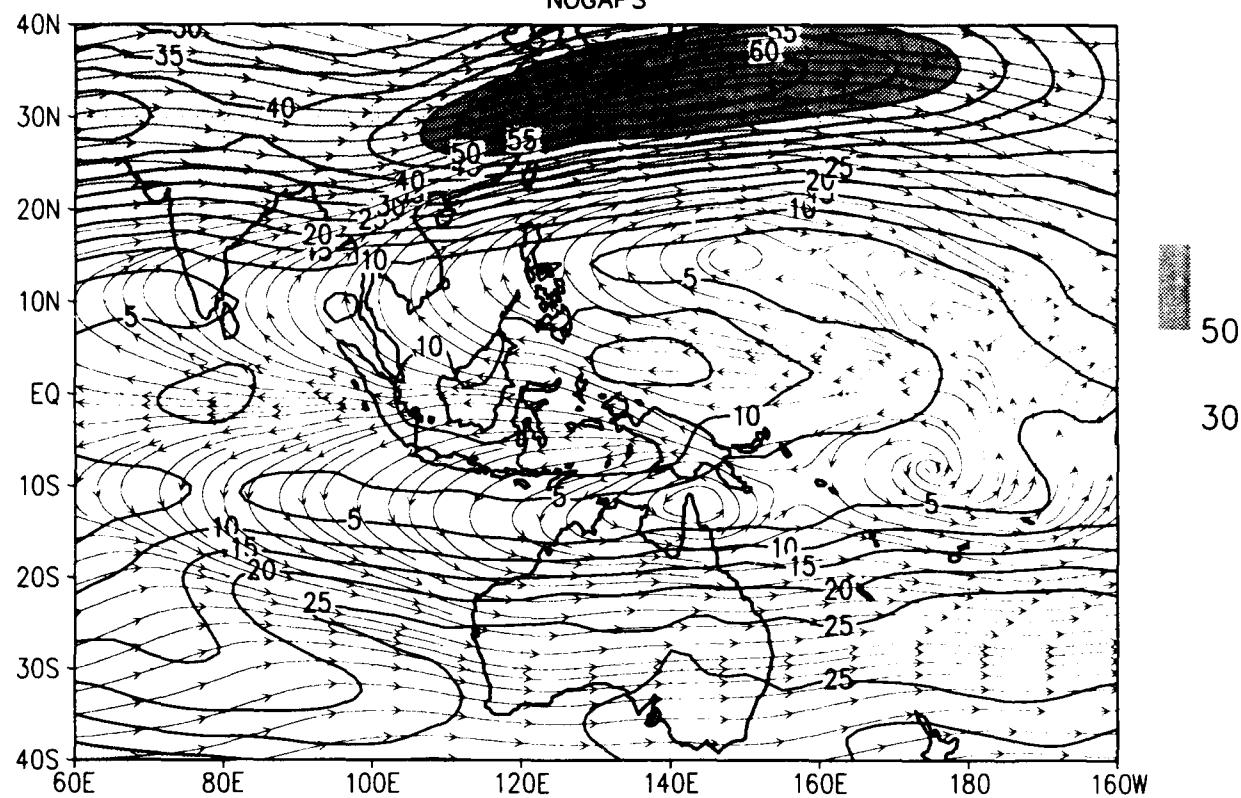


pooled anomaly

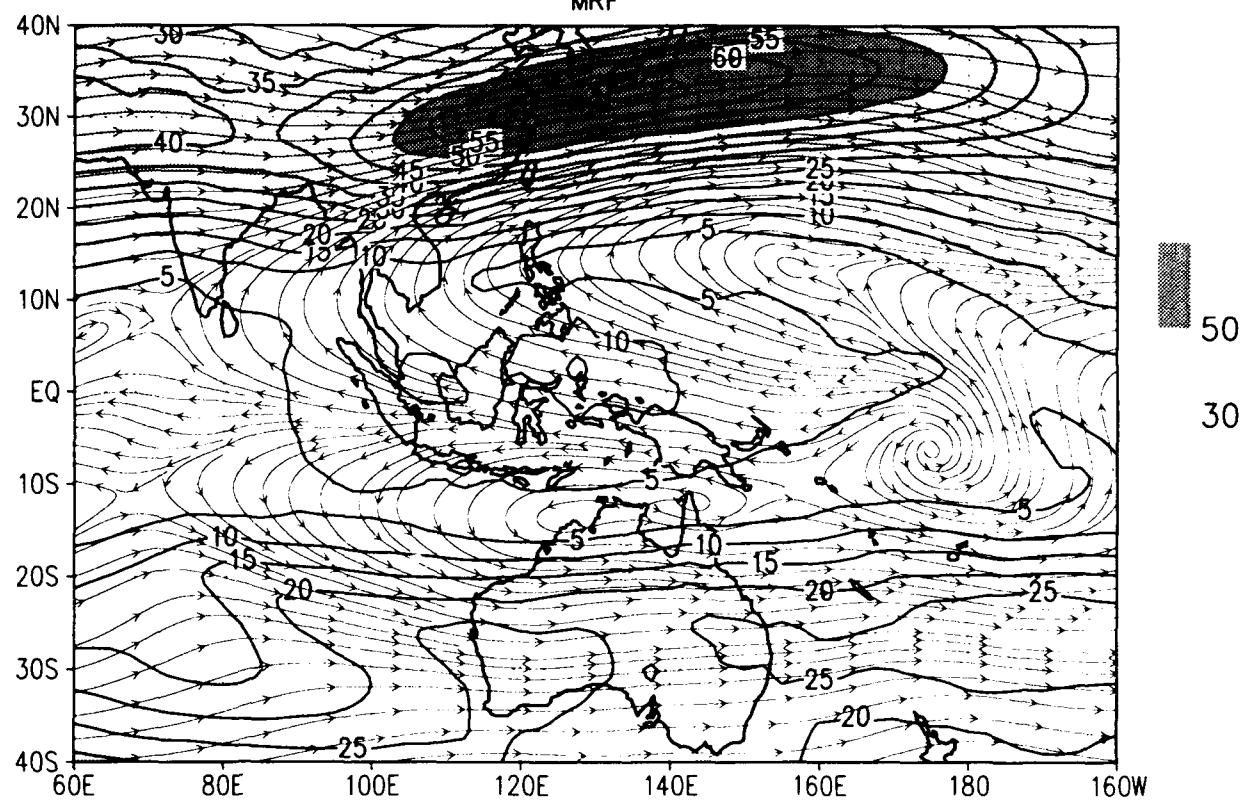


200 mb wind climo for NDJF
/d2/toga_coare/c.gs

NOGAPS

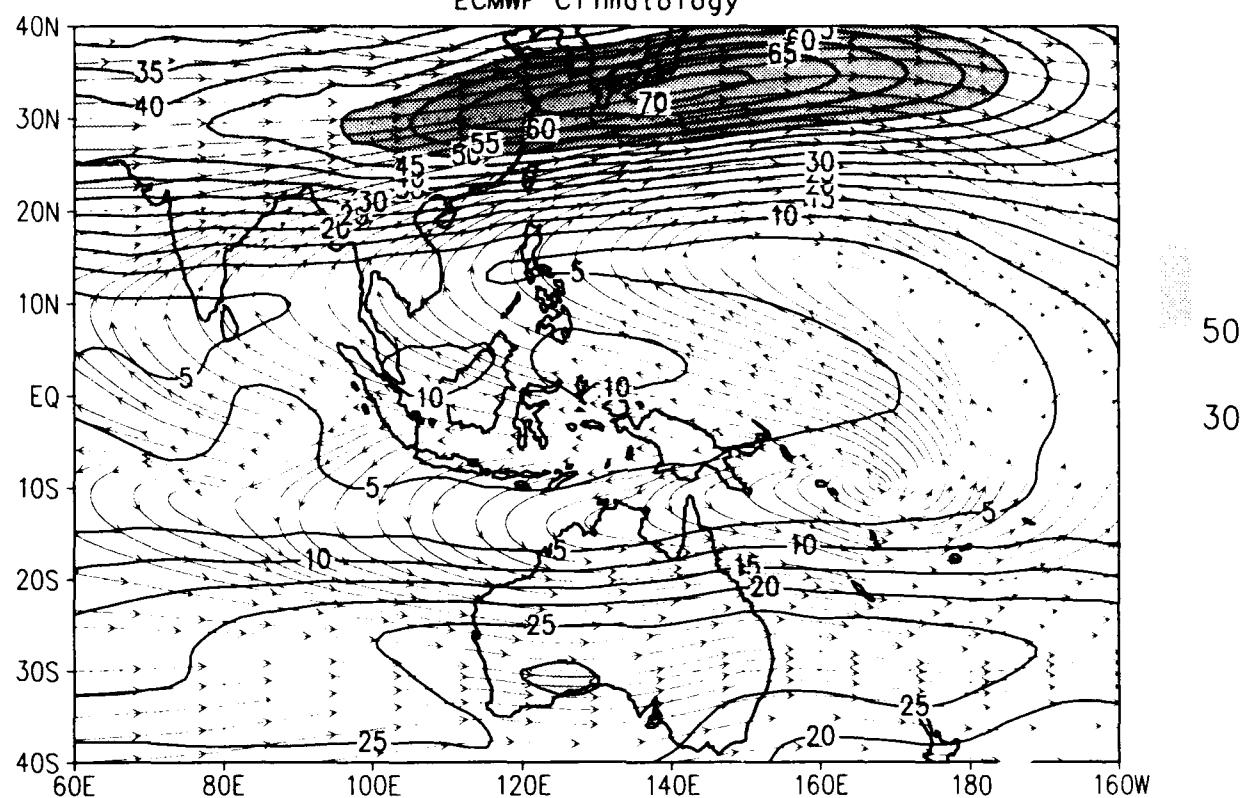


MRF

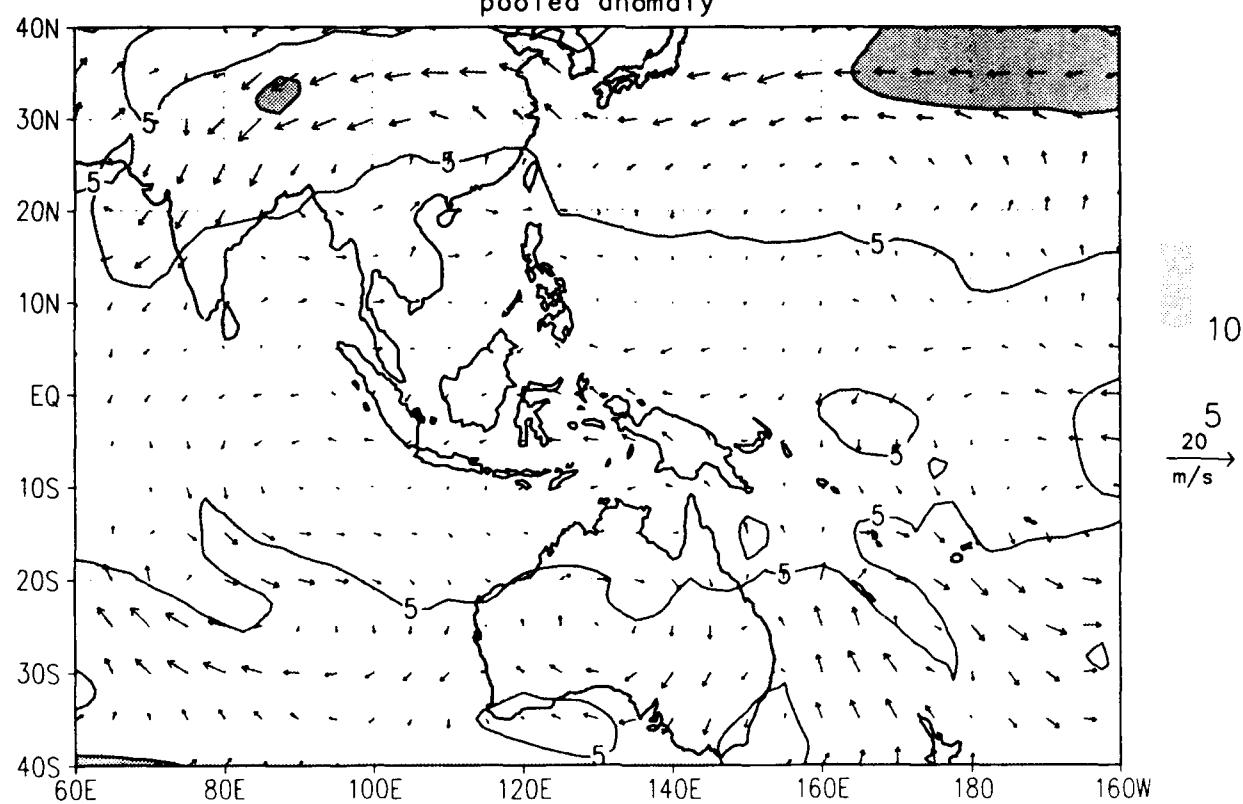


200 mb wind climo for NDJF
/d2/toga_coare/c.gs

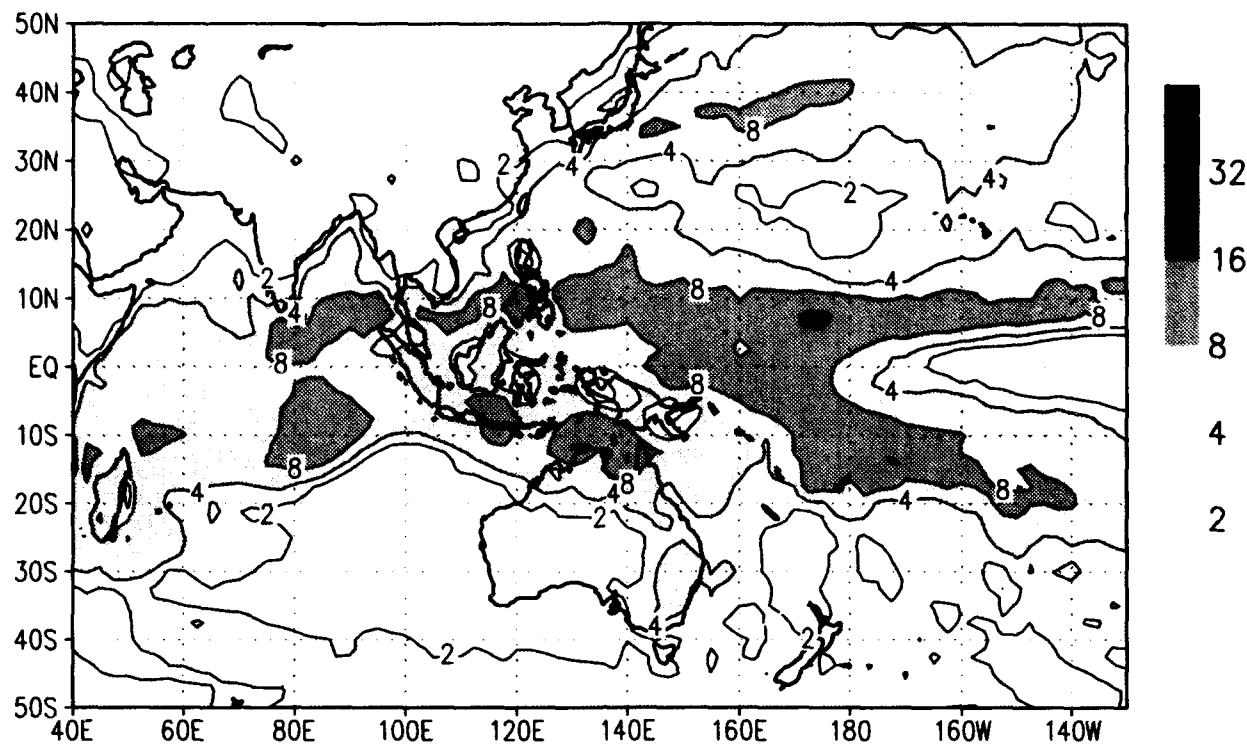
ECMWF Climatology



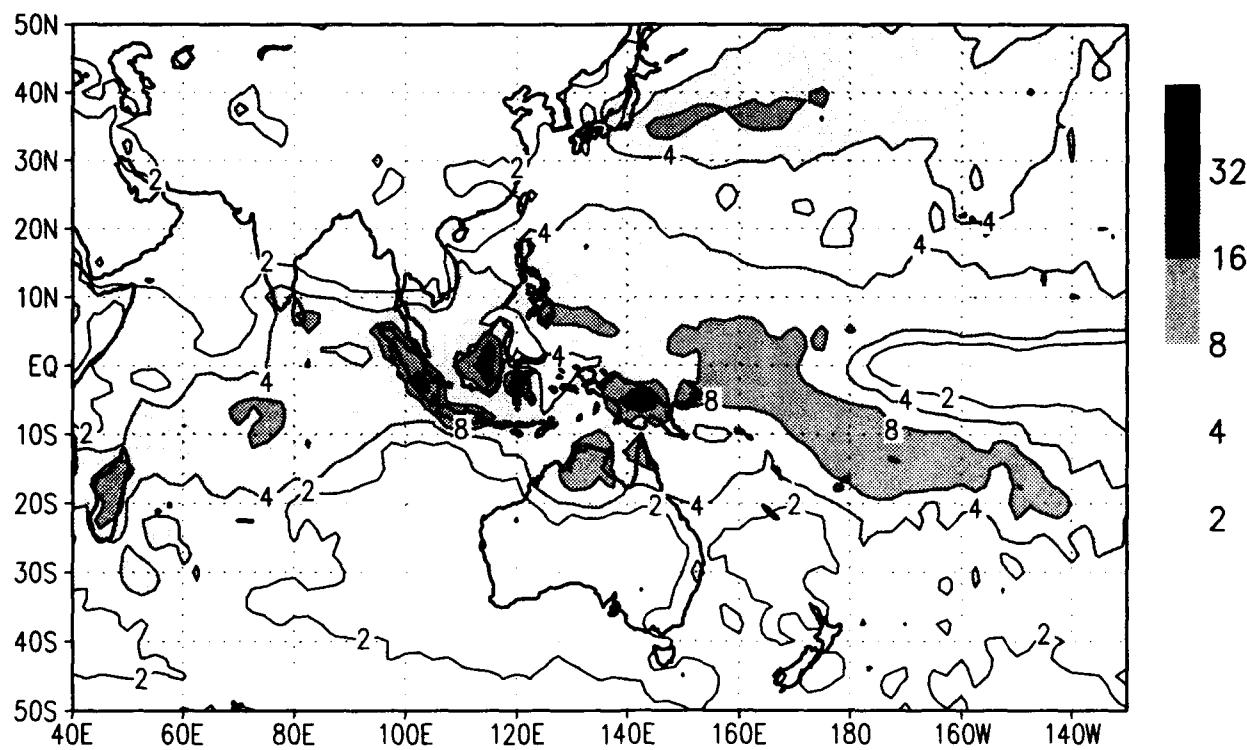
pooled anomaly



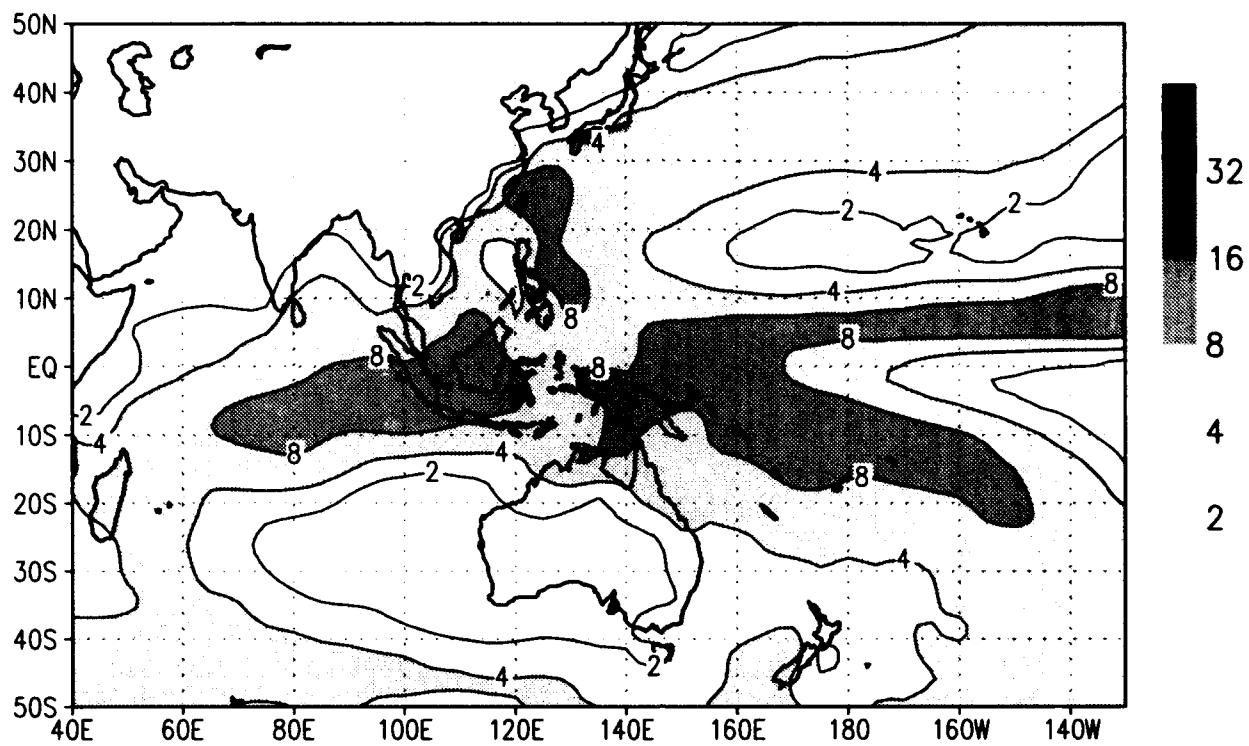
precip climo for NDJF
/d2/toga_coare/c.gs
NOGAPS



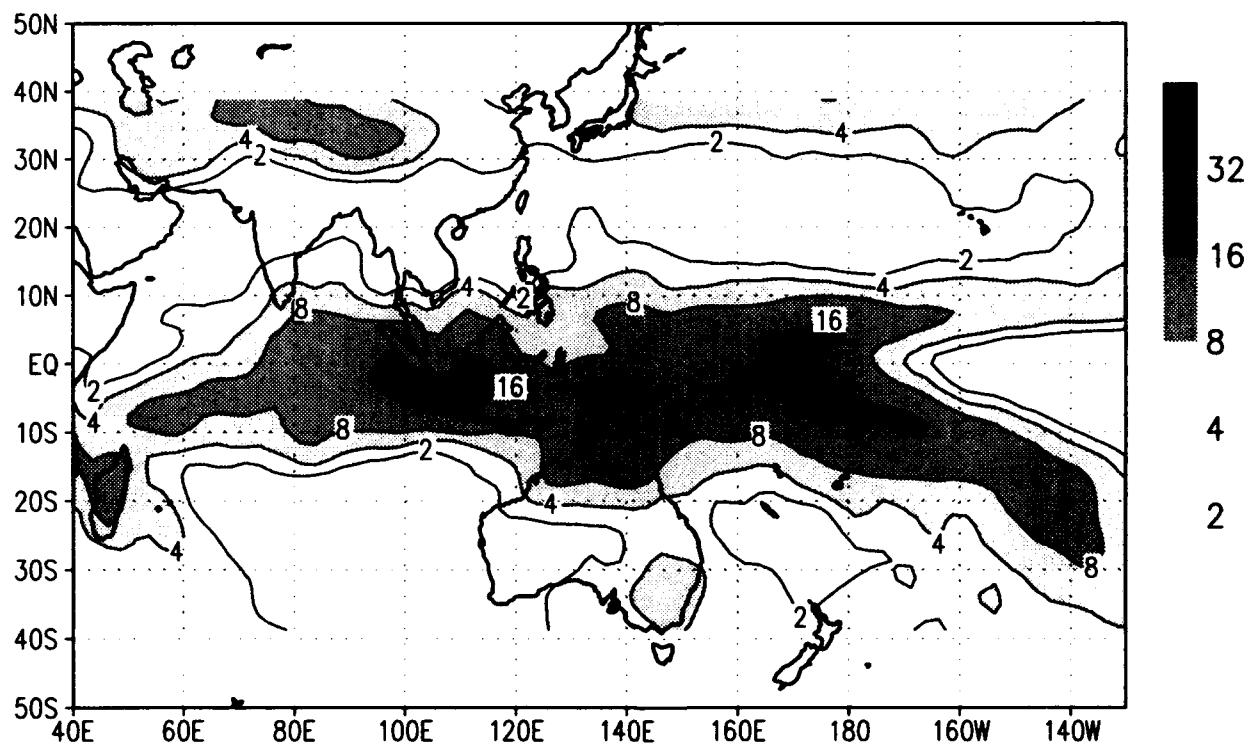
MRF



precip climo for NDJF
/d2/toga_coare/c.gs
msu_merged climo



Prelim GPI



10 Monthly Means

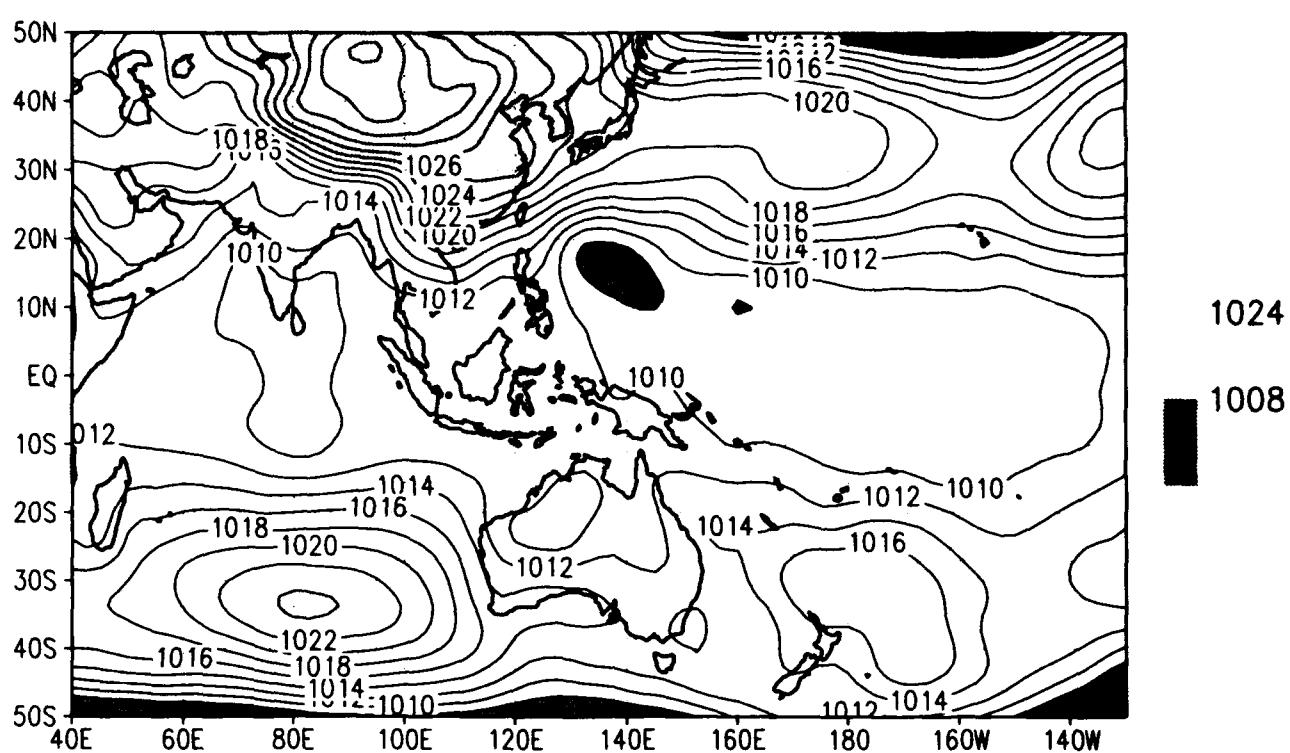
The layout of the plots in the following sections is the same as in the NDJF seasonal mean section.

10.1 January 1992

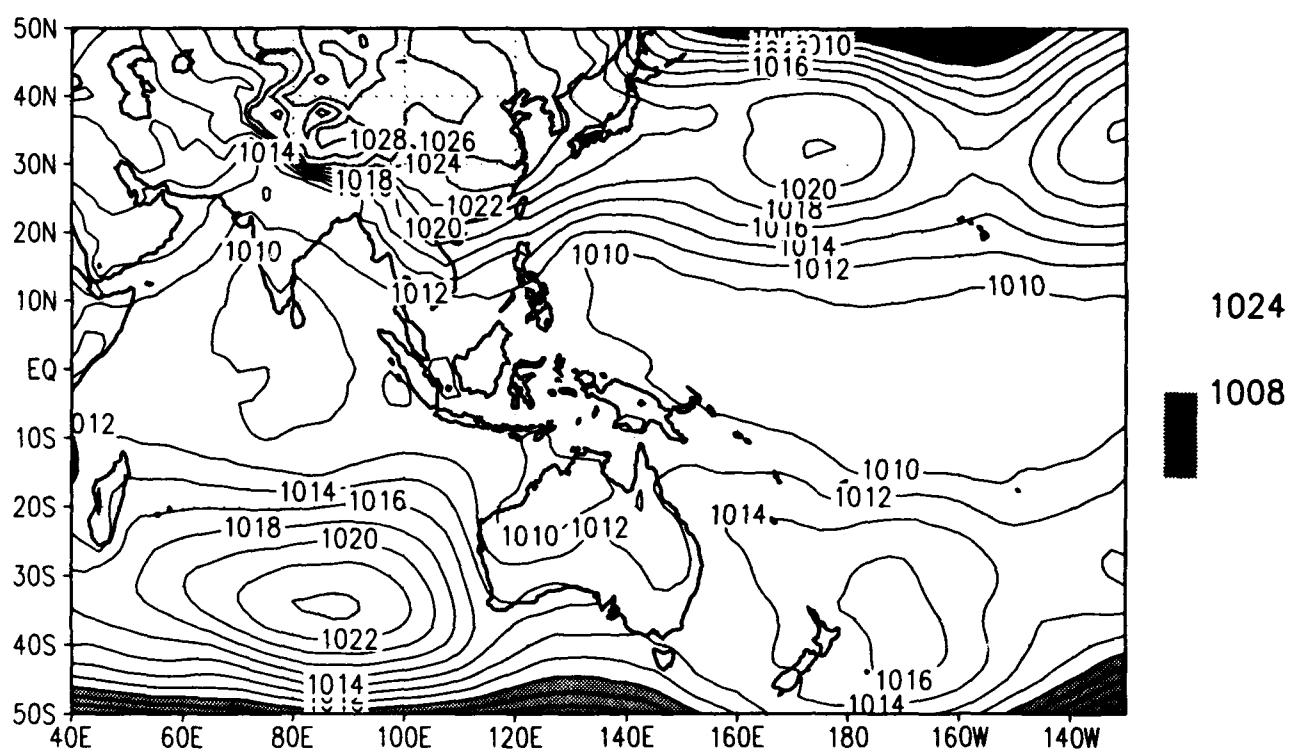
Chart	Description
1	- Sea-level pressure for NOGAPS and MRF
2	- ECMWF climatological Sea-level pressure and the pooled anomaly
3	- Surface wind speed for NOGAPS and MRF
4	- ECMWF climatological surface wind and pooled anomaly
5	- 850 mb wind for NOGAPS and MRF
6	- ECMWF climatological 850 mb wind and pooled anomaly
7	- 200 mb wind for NOGAPS and MRF
8	- ECMWF climatological 200 mb wind and pooled anomaly
9	- 12-h precipitation for NOGAPS and MRF
10	- MSU merged climatological precipitation and GPI

SLP climo for NOV 1992
/d2/toga_coare/c.gs

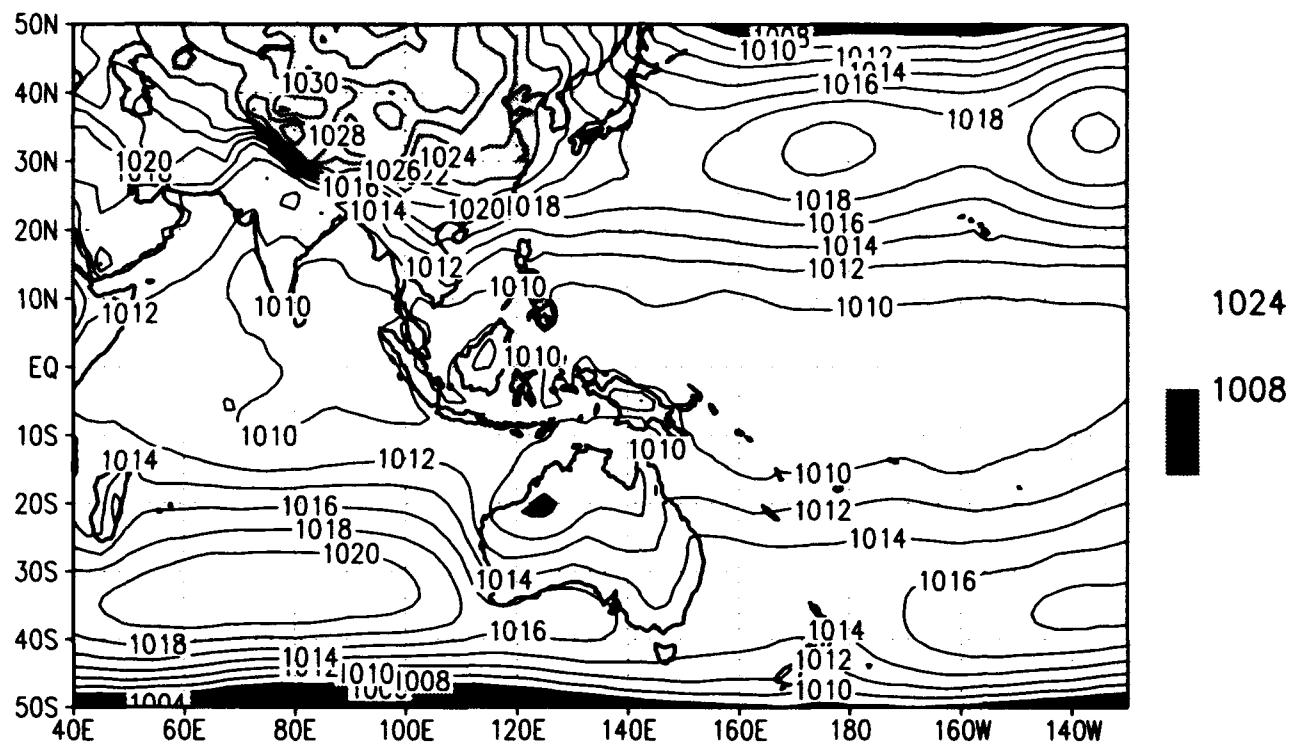
NOGAPS



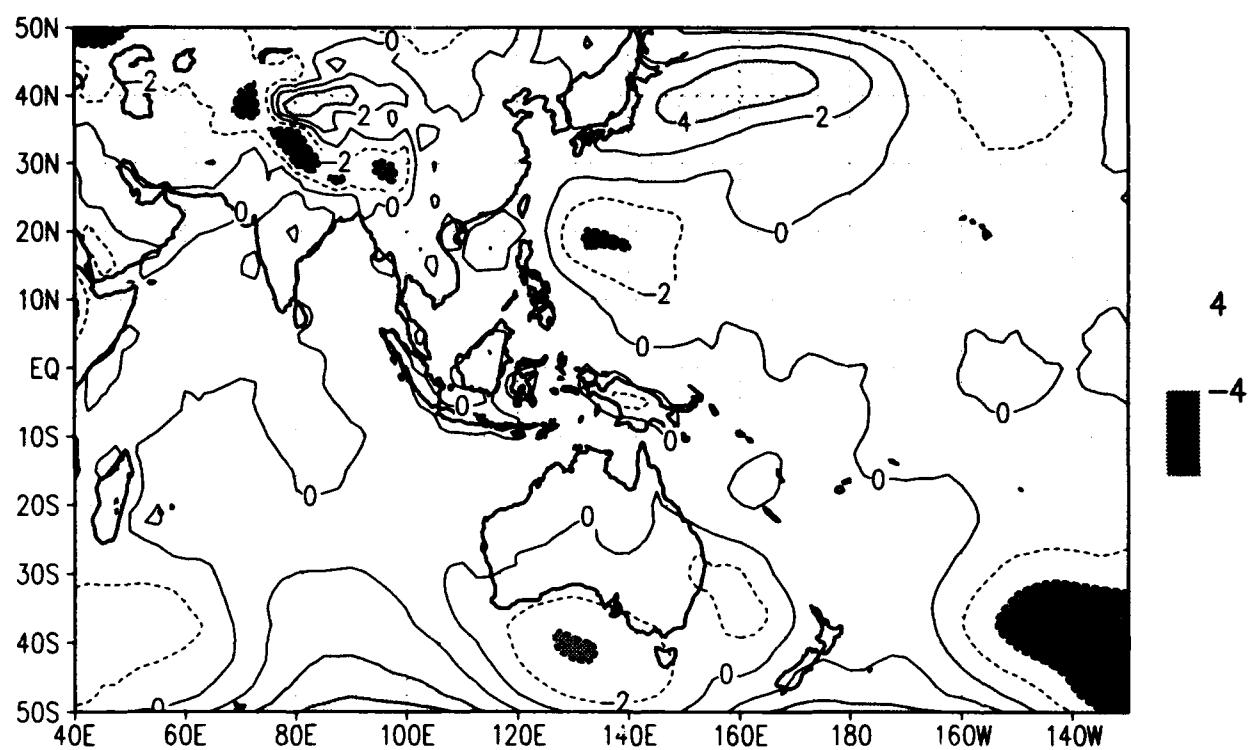
MRF



SLP climo for NOV 1992
/d2/toga_coare/c.gs
ECMWF Climatology

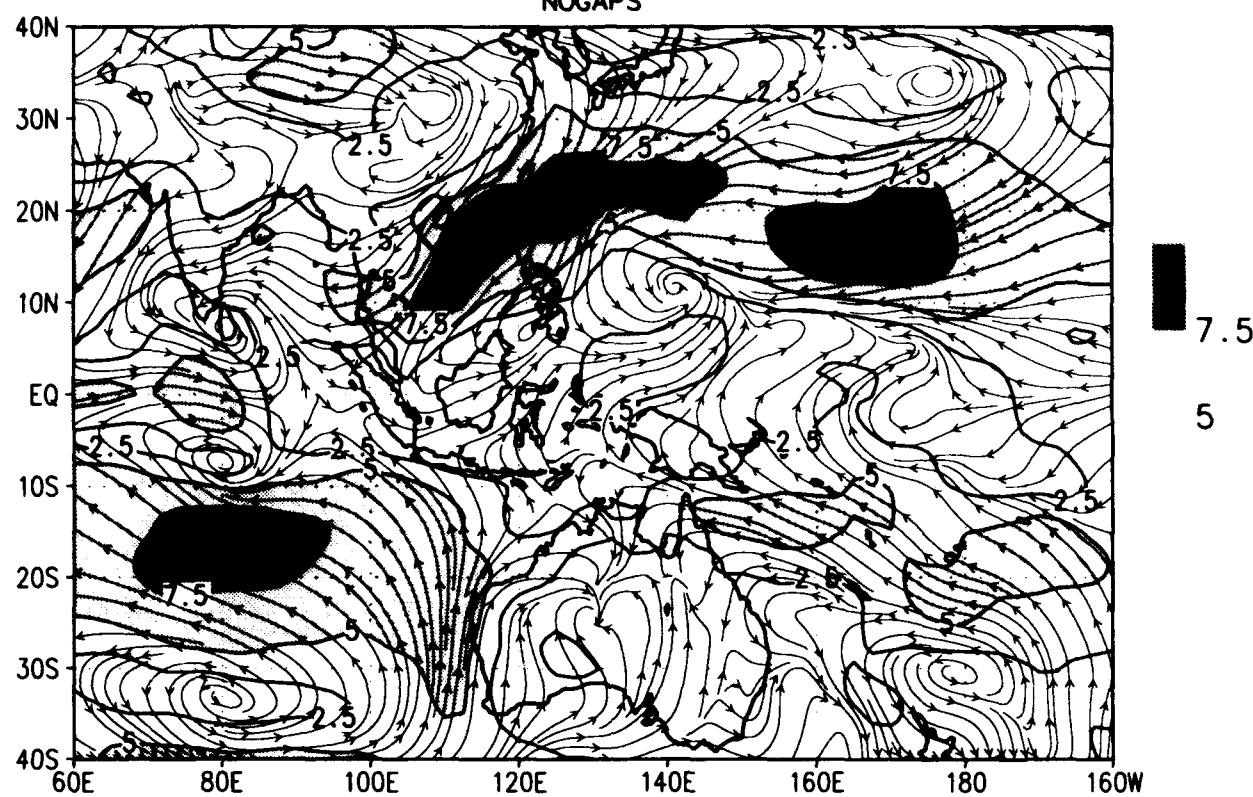


pooled anomaly

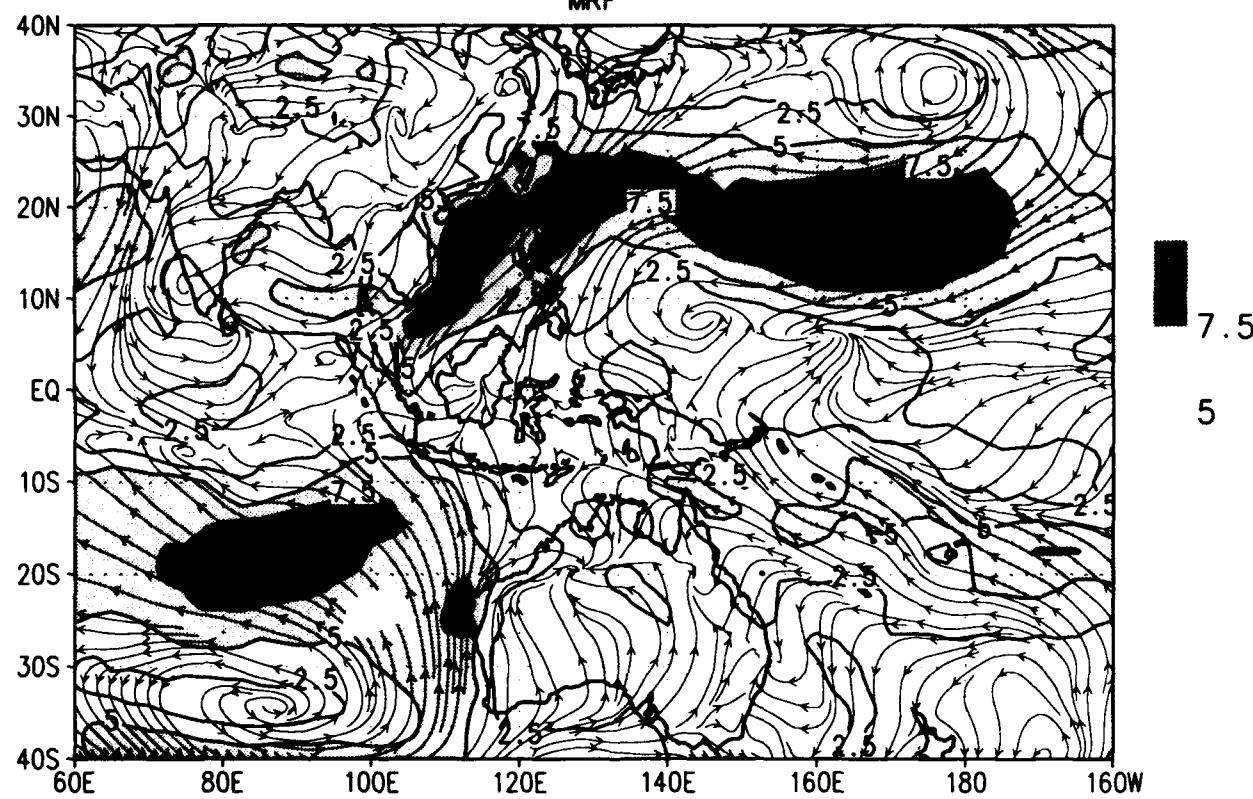


Sfc wind climo for NOV 1992
/d2/toga_coare/c.gs

NOGAPS

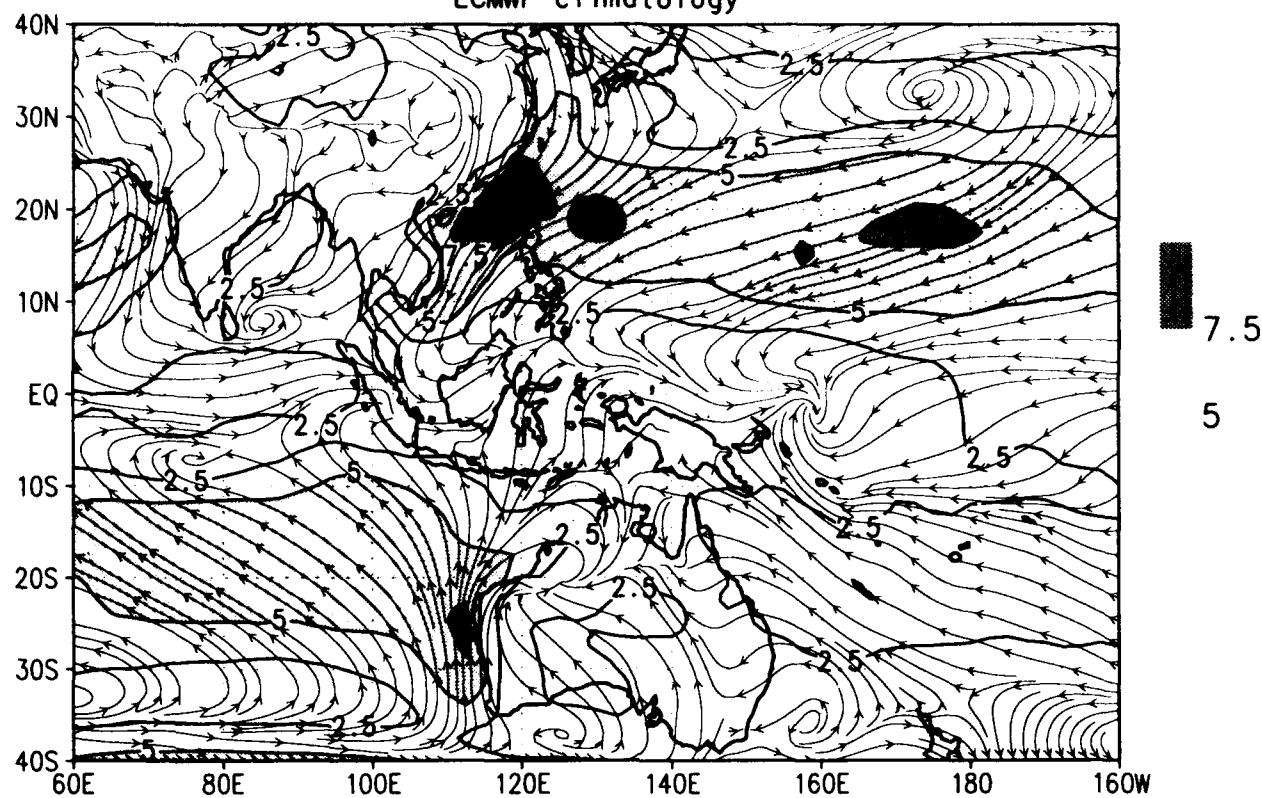


MRF

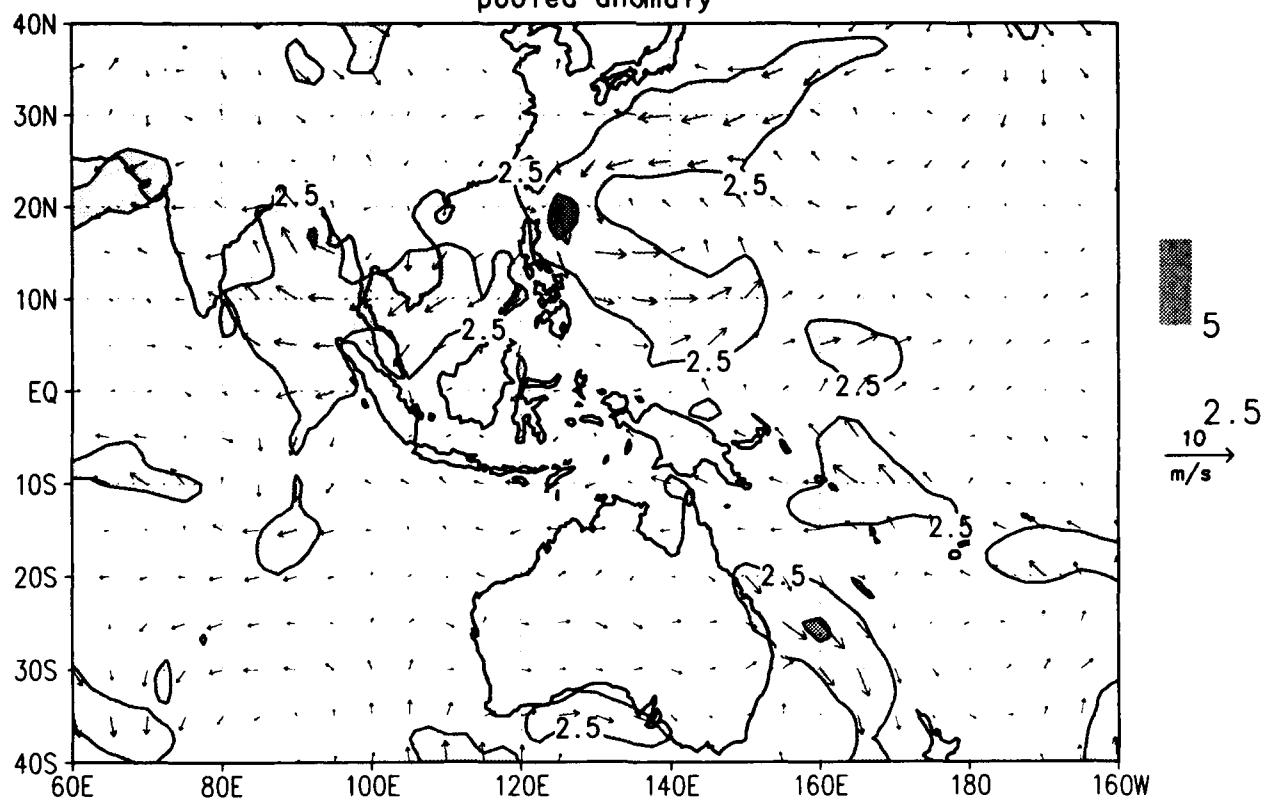


Sfc wind climo for NOV 1992
/d2/toga_coare/c.gs

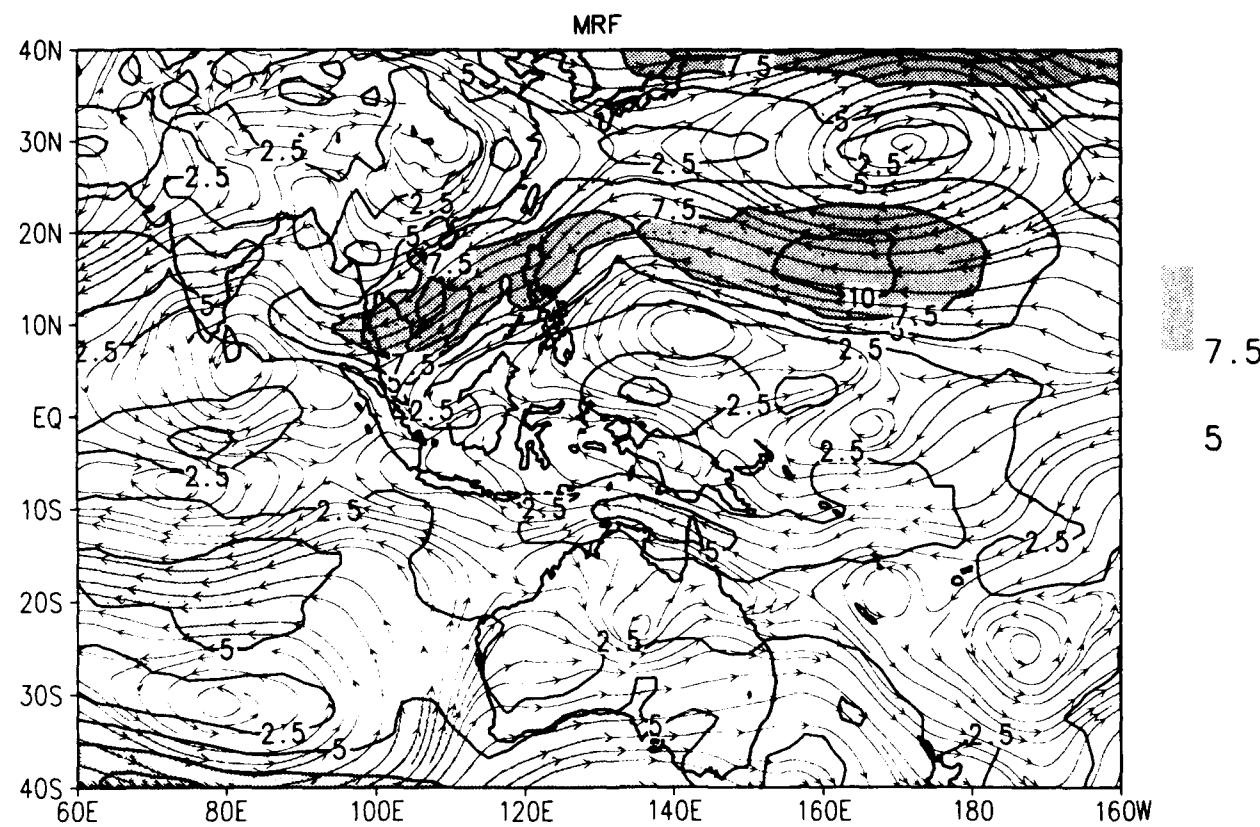
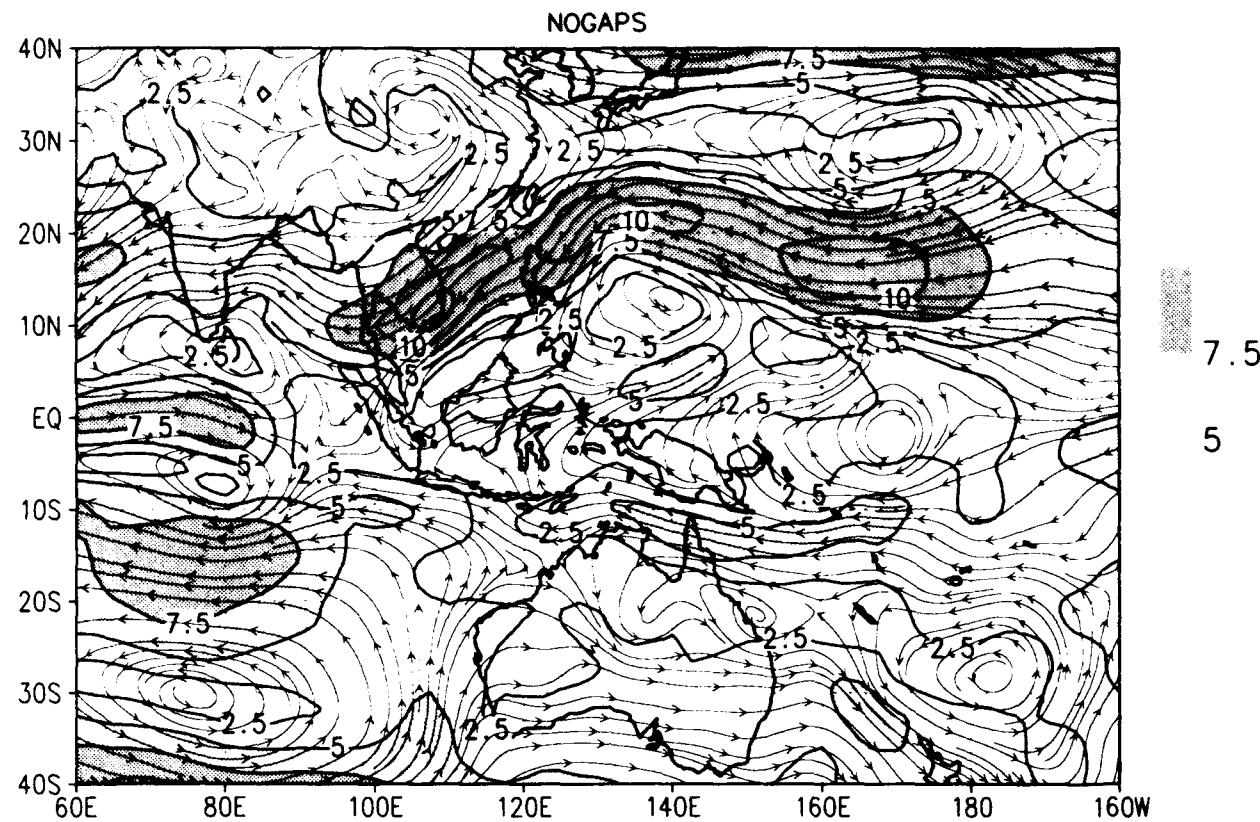
ECMWF climatology



pooled anomaly

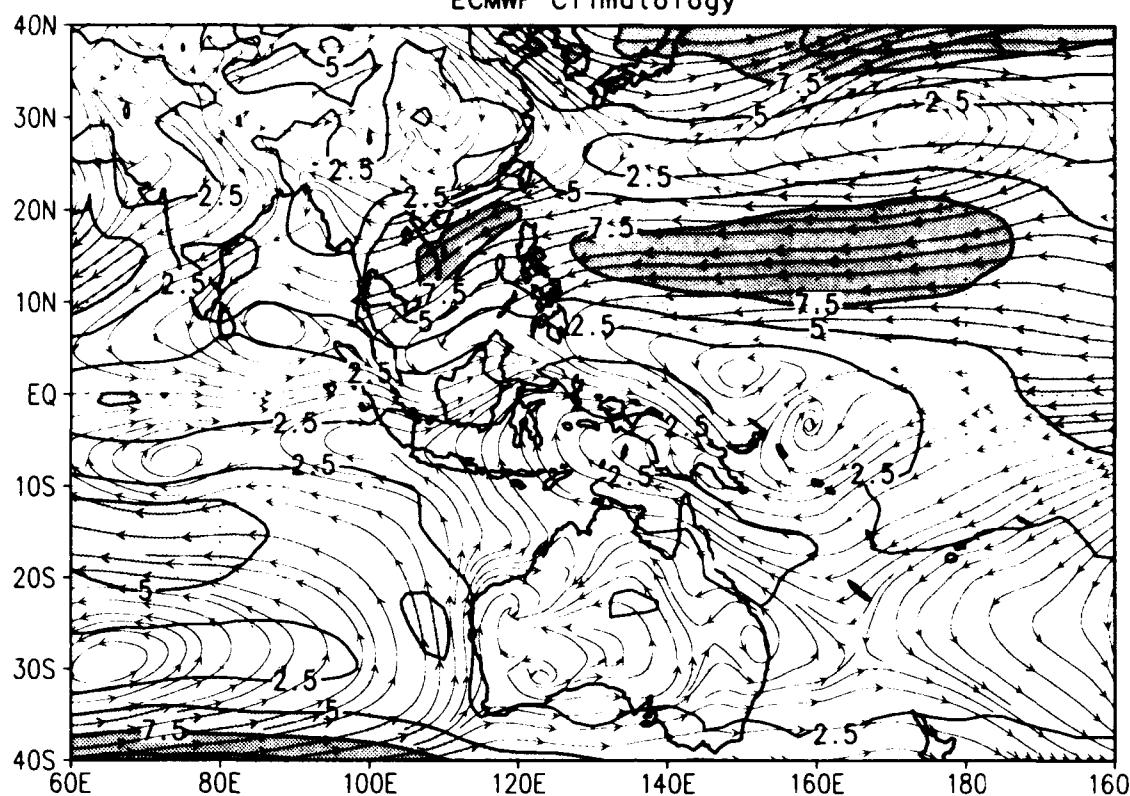


850 mb wind climo for NOV 1992
/d2/toga_coare/c.gs

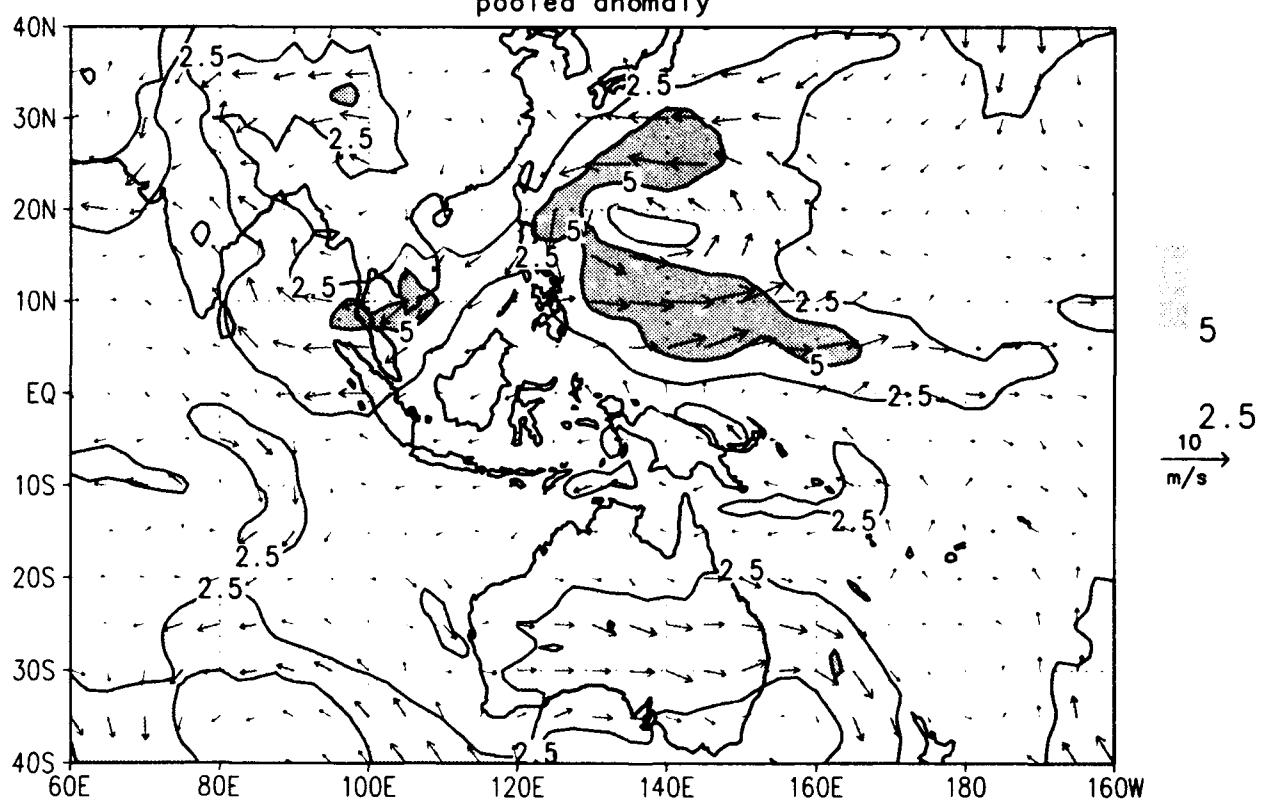


850 mb wind climo for NOV 1992
/d2/toga_coare/c.gs

ECMWF Climatology

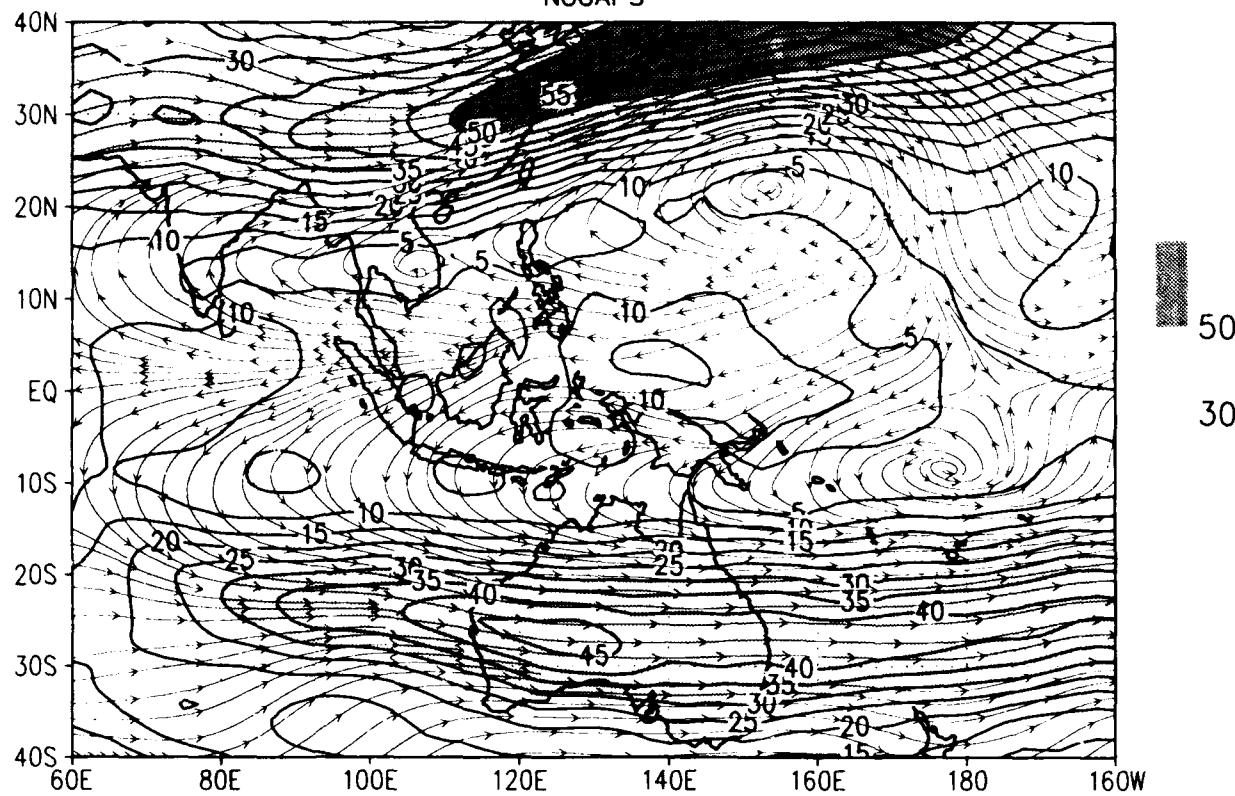


pooled anomaly

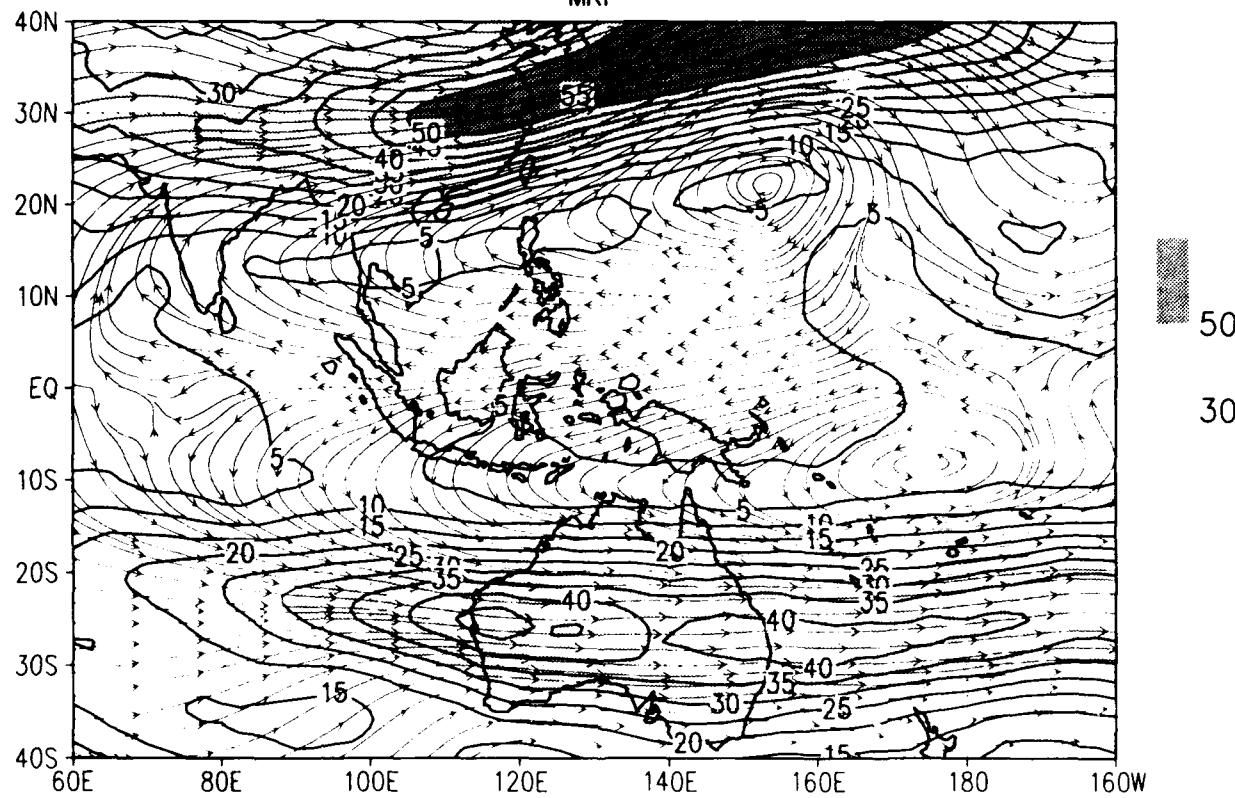


200 mb wind climo for NOV 1992
/d2/toga_coare/c.gs

NOGAPS

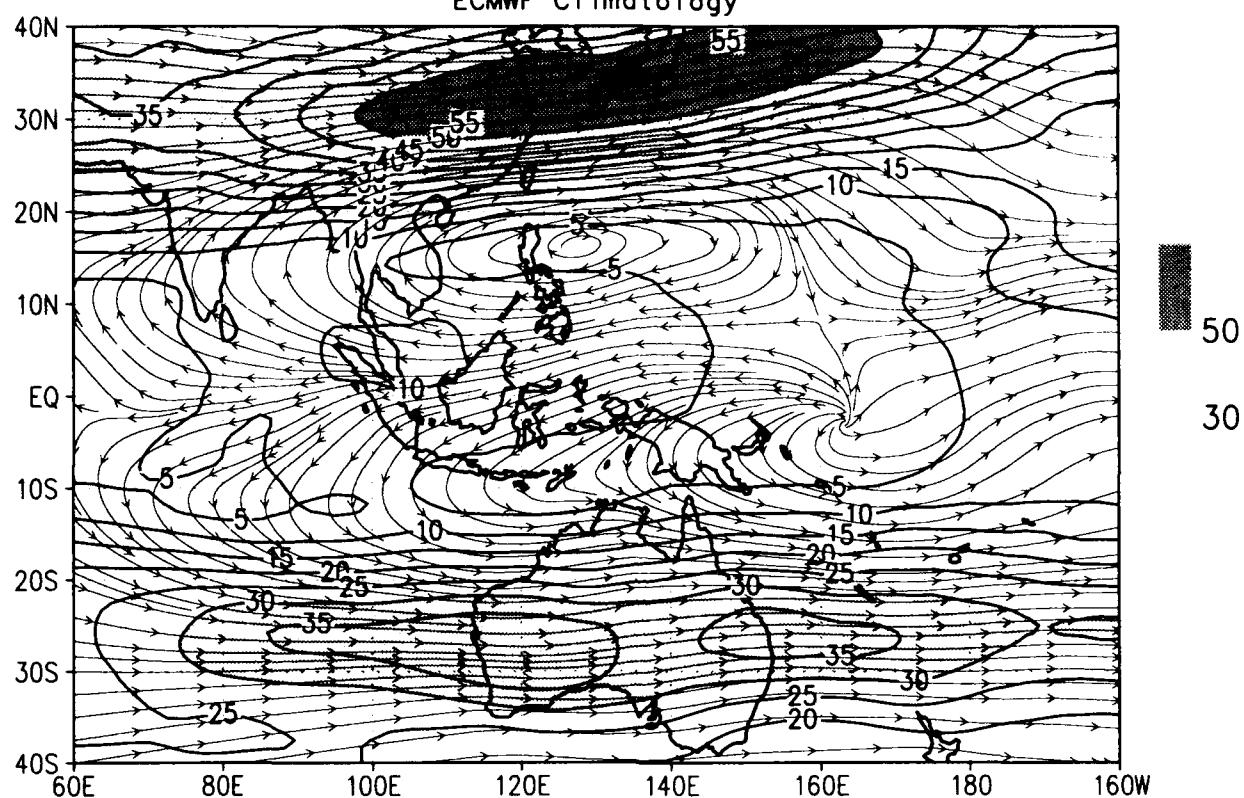


MRF

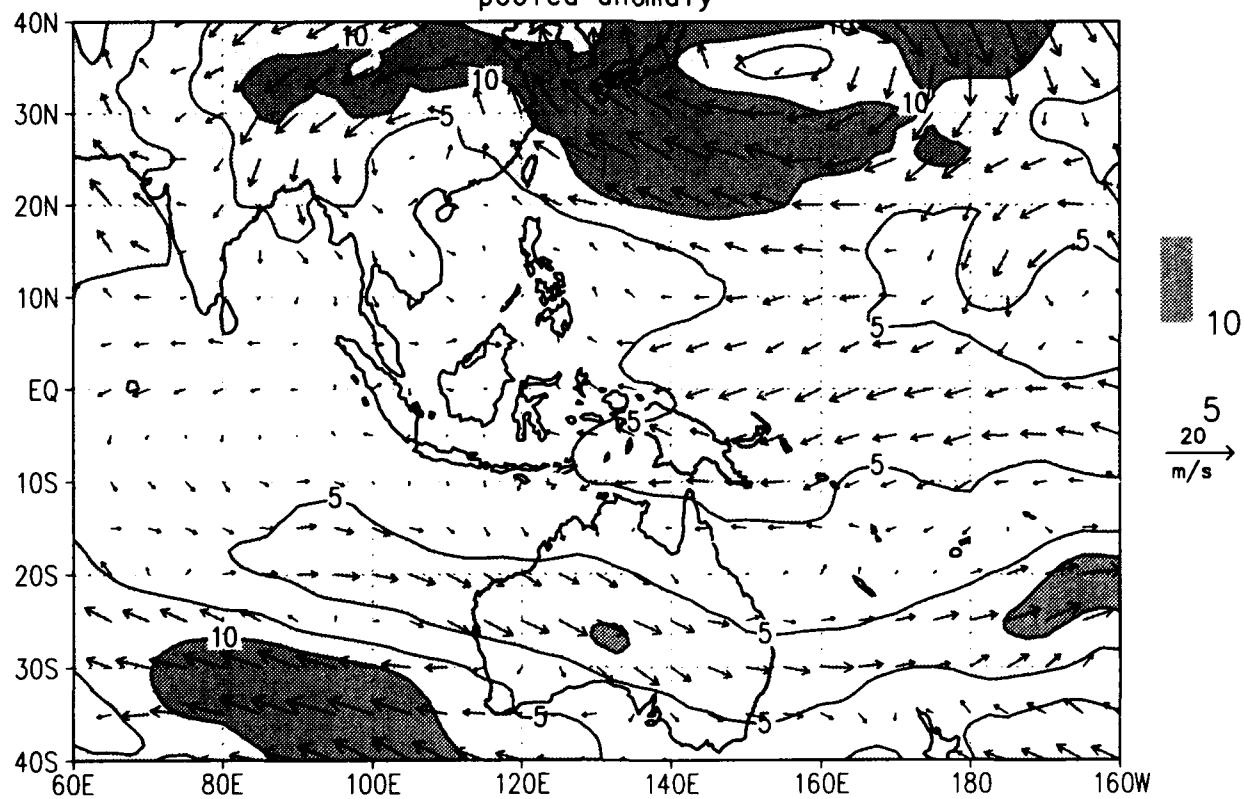


200 mb wind climo for NOV 1992
/d2/toga_coare/c.gs

ECMWF Climatology



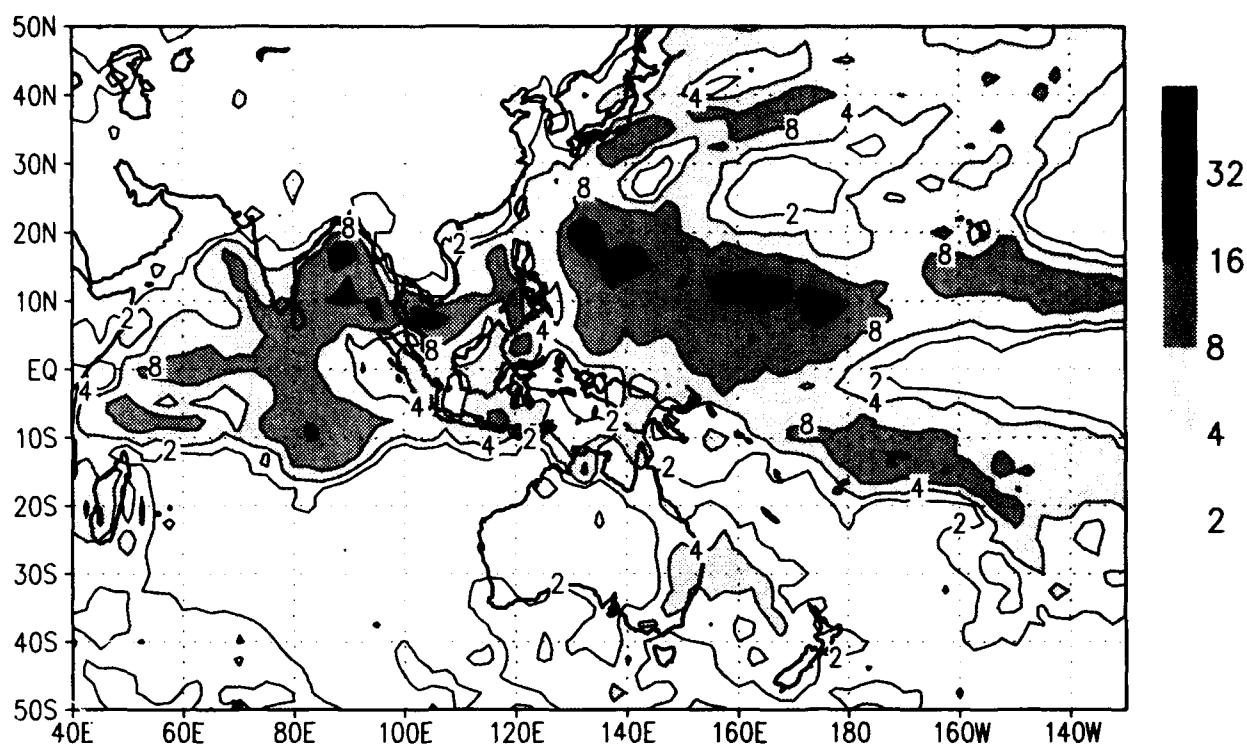
pooled anomaly



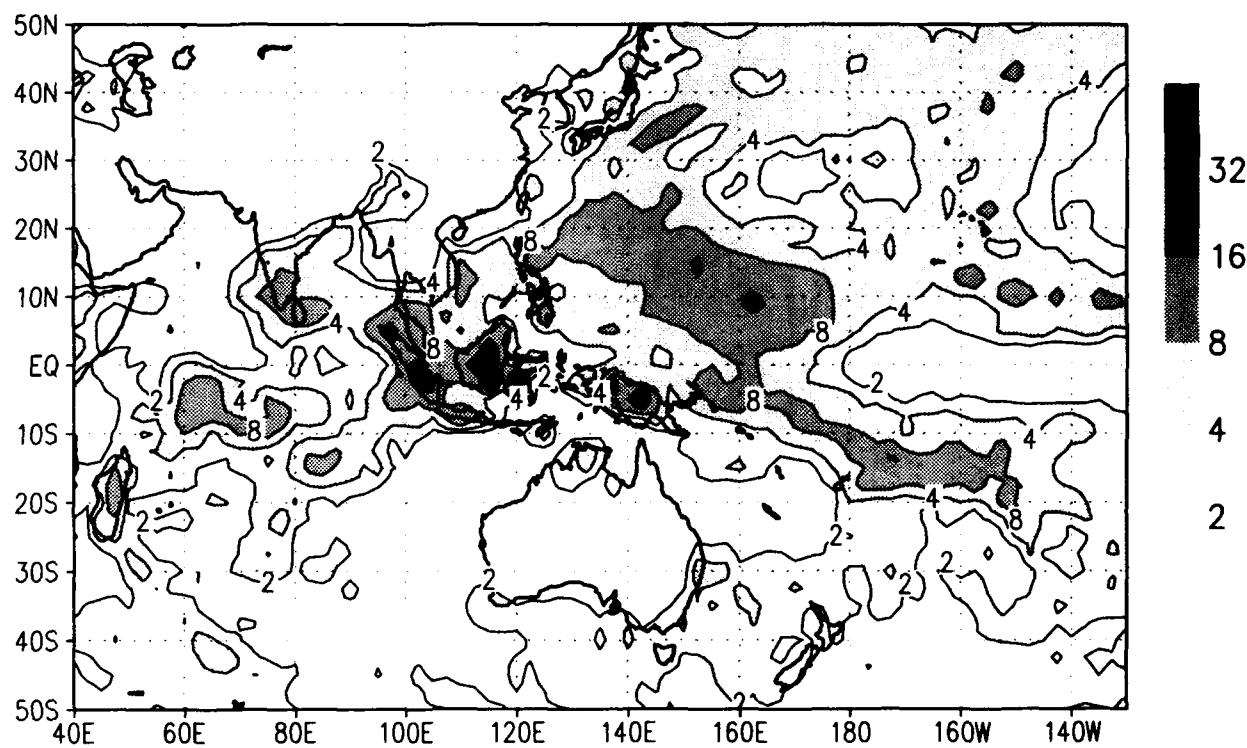
precip climo for NOV 1992

/d2/toga_coare/c.gs

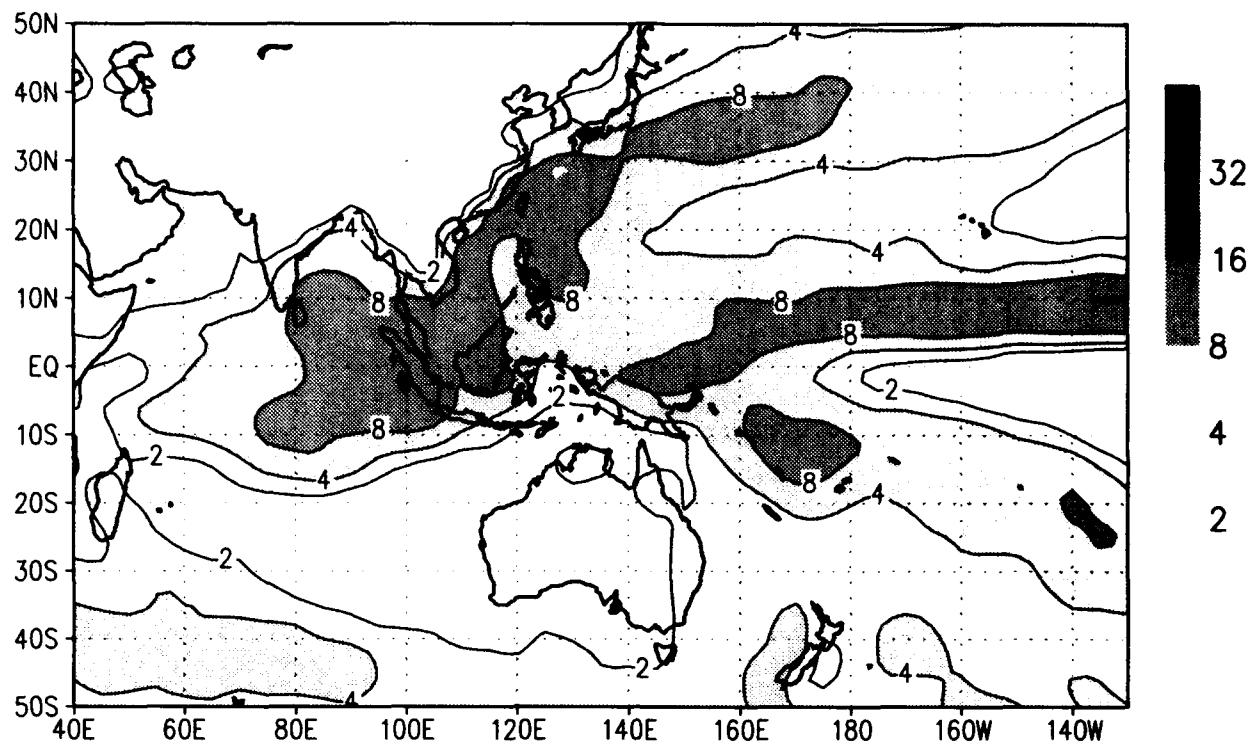
NOGAPS



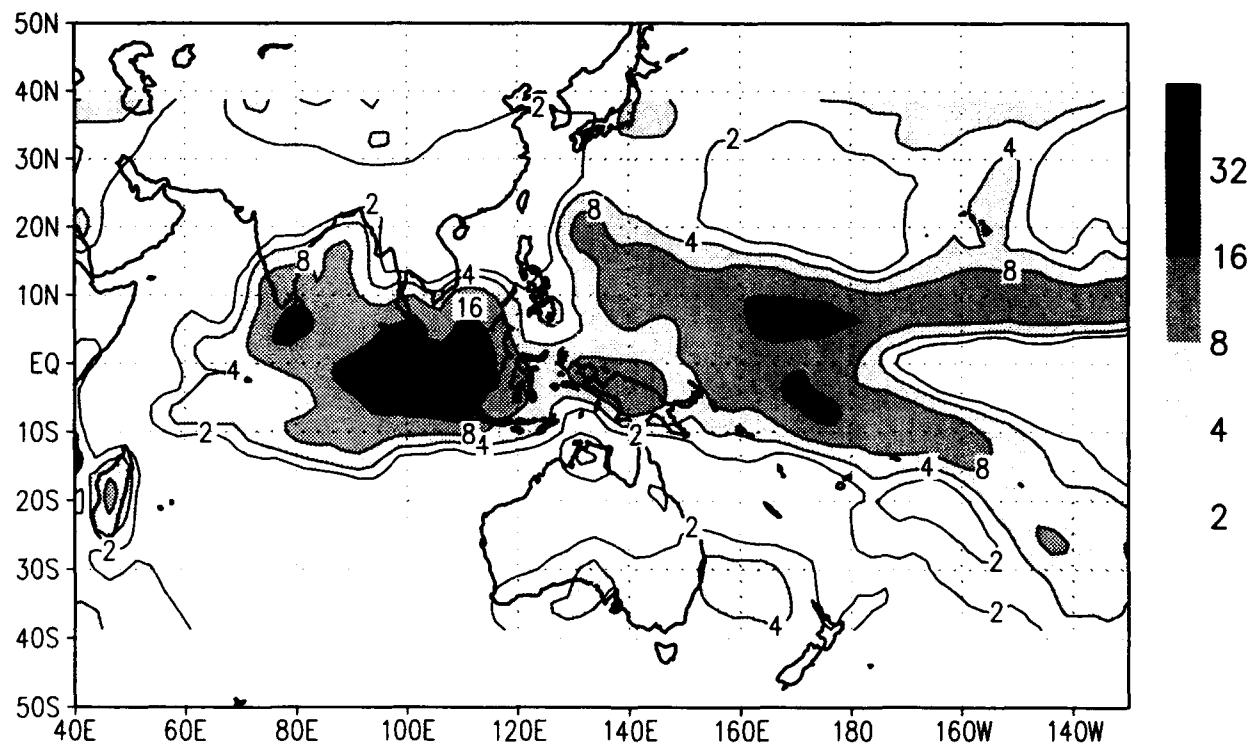
MRF



precip climo for NOV 1992
/d2/toga_coare/c.gs
msu_merged climo



Prelim GPI



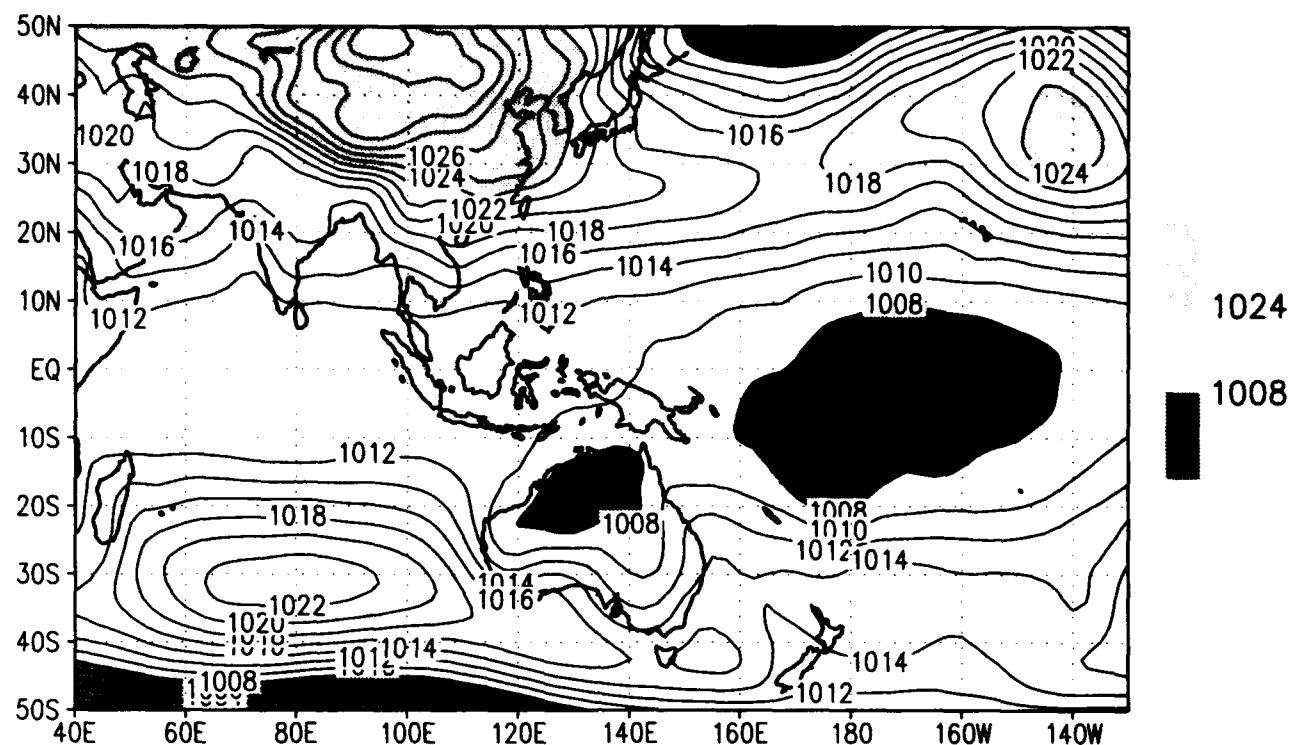
10.2 December 1992

The layout of the plots is the same as in the NDJF seasonal mean section.

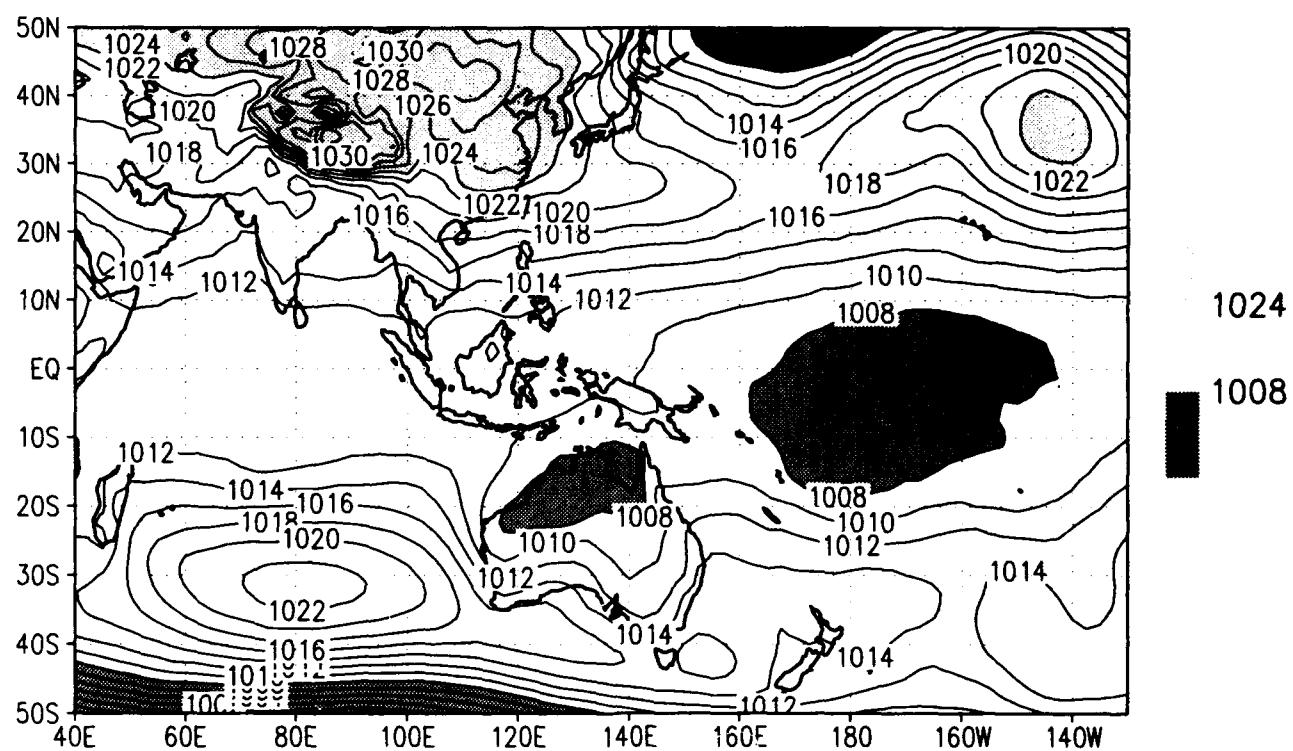
Chart	Description
1	- Sea-level pressure for NOGAPS and MRF
2	- ECMWF climatological Sea-level pressure and the pooled anomaly
3	- Surface wind speed for NOGAPS and MRF
4	- ECMWF climatological surface wind and pooled anomaly
5	- 850 mb wind for NOGAPS and MRF
6	- ECMWF climatological 850 mb wind and pooled anomaly
7	- 200 mb wind for NOGAPS and MRF
8	- ECMWF climatological 200 mb wind and pooled anomaly
9	- 12-h precipitation for NOGAPS and MRF
10	- MSU merged climatological precipitation and GPI

SLP climo for DEC 1992

NOGAPS

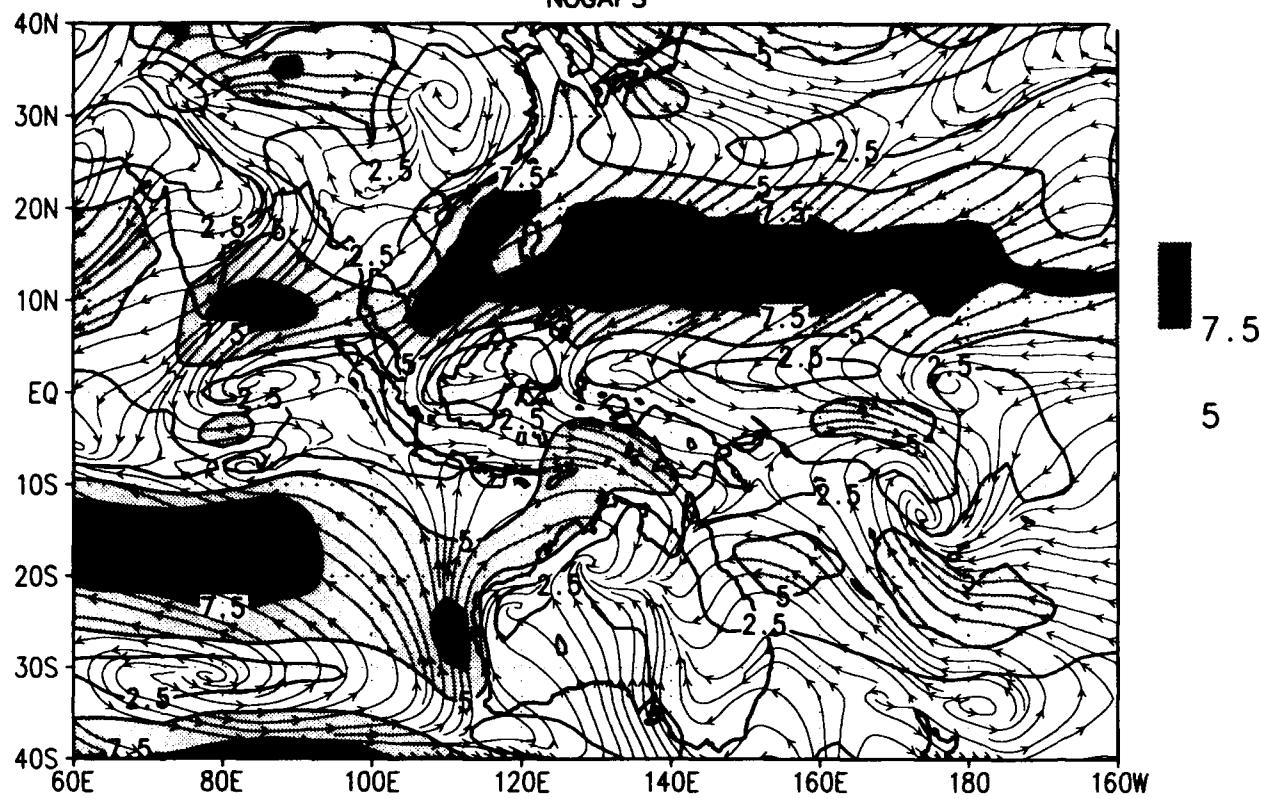


MRF

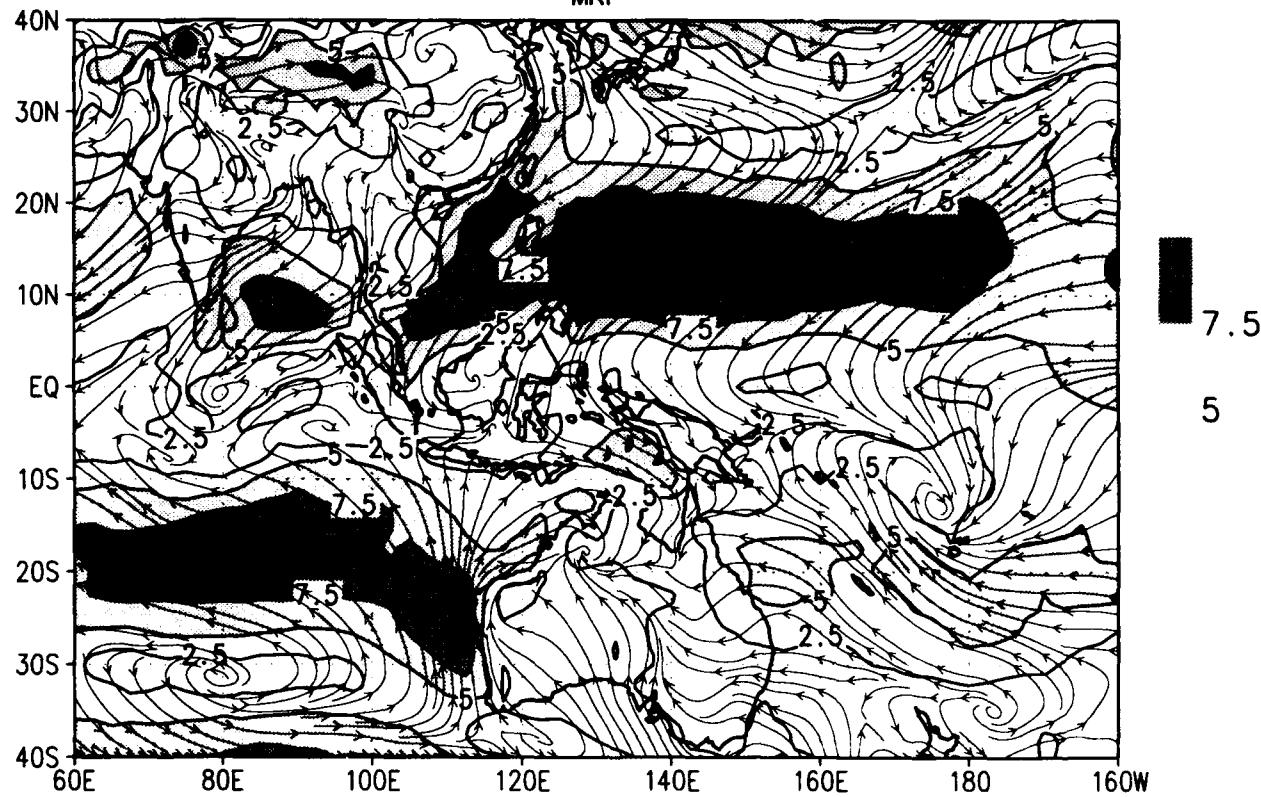


Sfc wind climo for DEC 1992
/d2/toga_coare/c.gs

NOGAPS

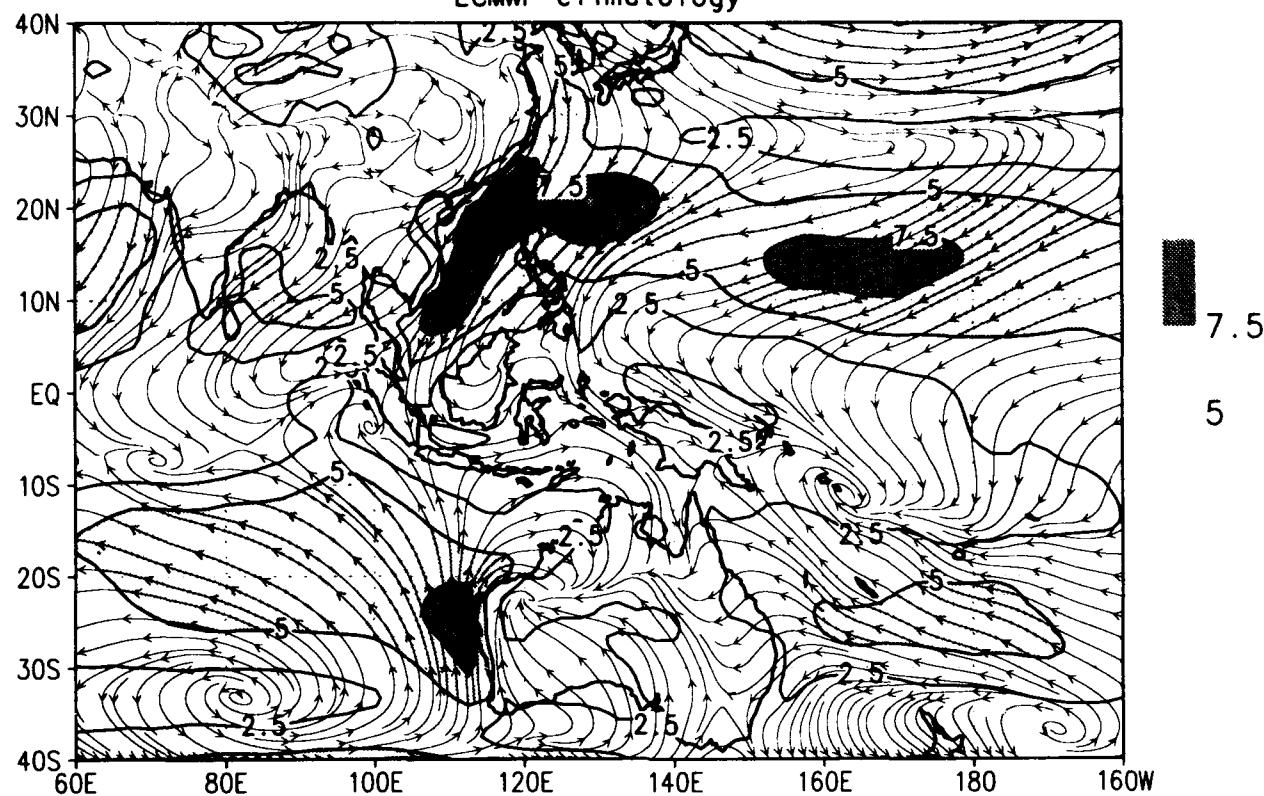


MRF

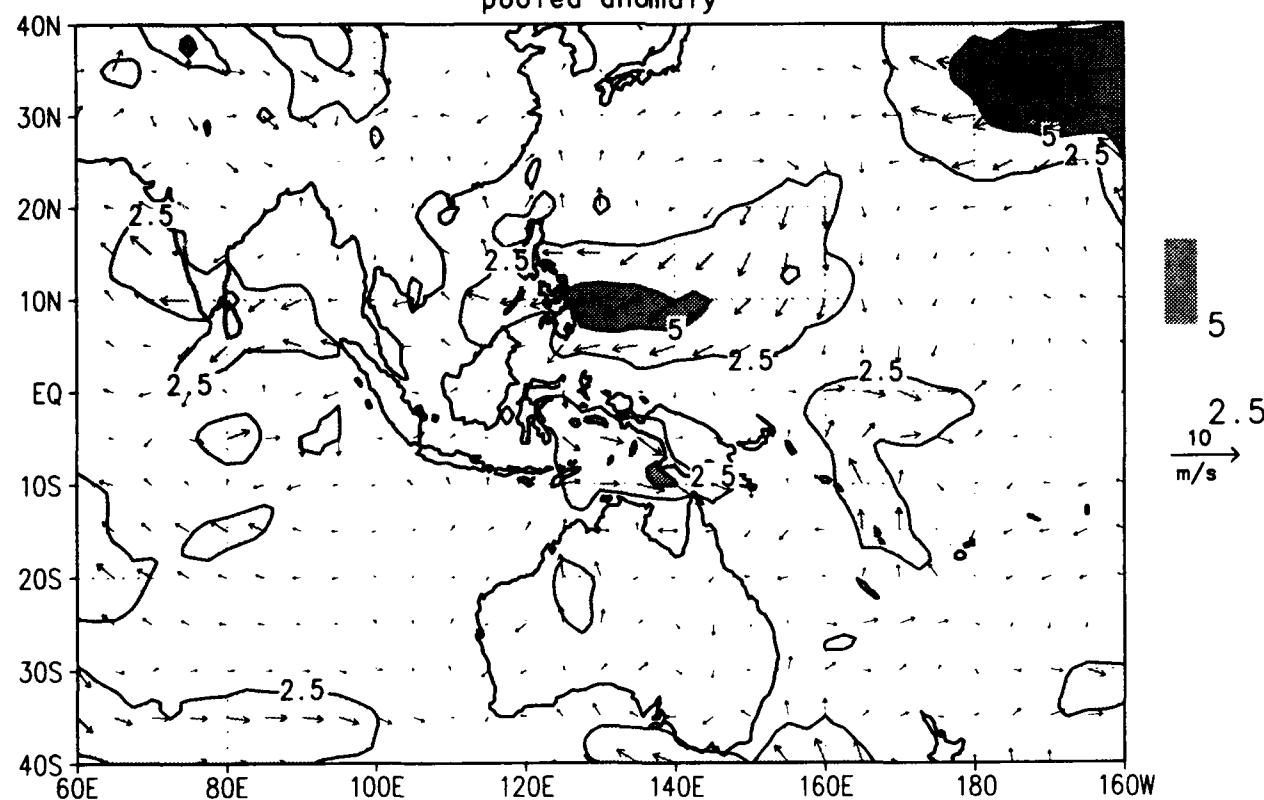


Sfc wind climo for DEC 1992
/d2/toga_coare/c.gs

ECMWF climatology

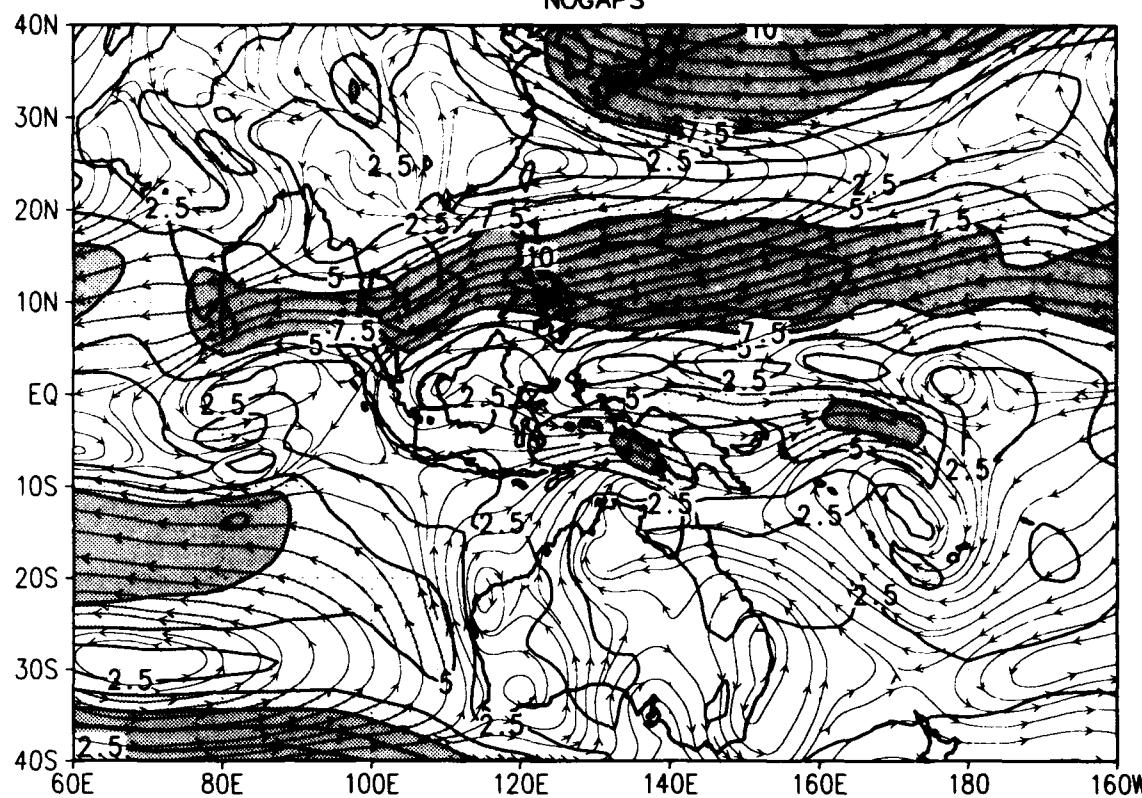


pooled anomaly



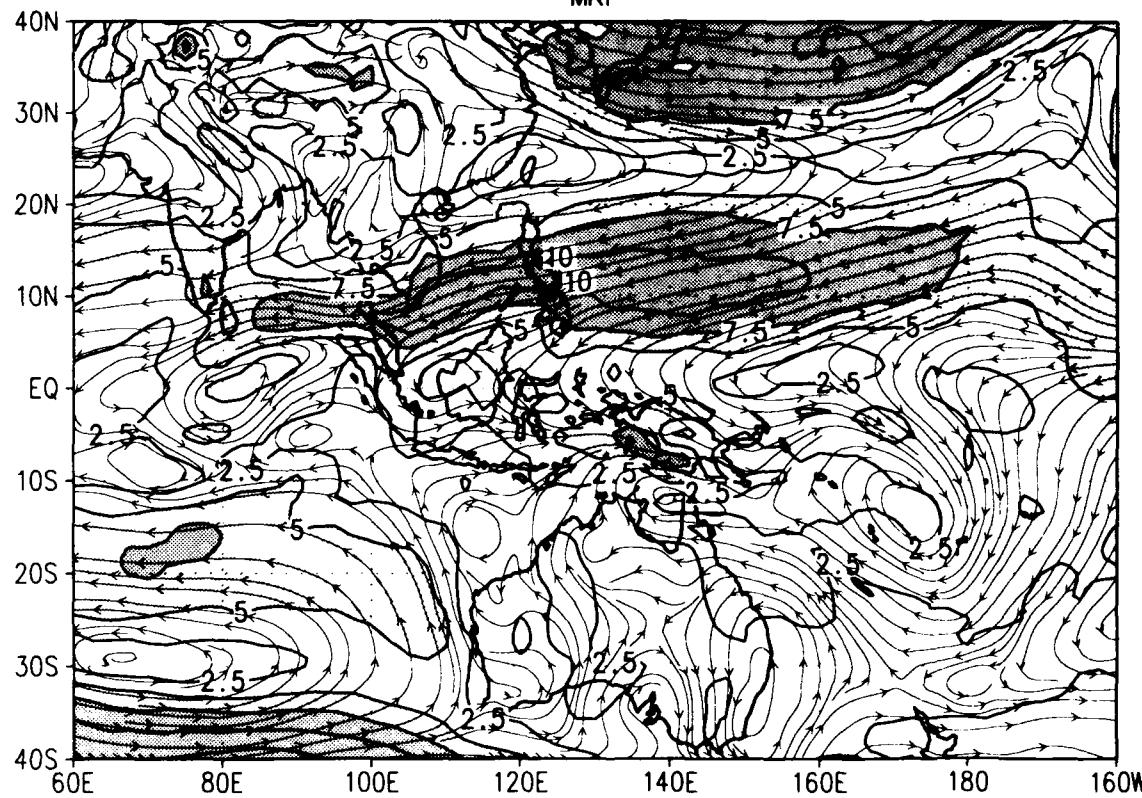
850 mb wind climo for DEC 1992
/d2/toga_coare/c.gs

NOGAPS



7.5
5

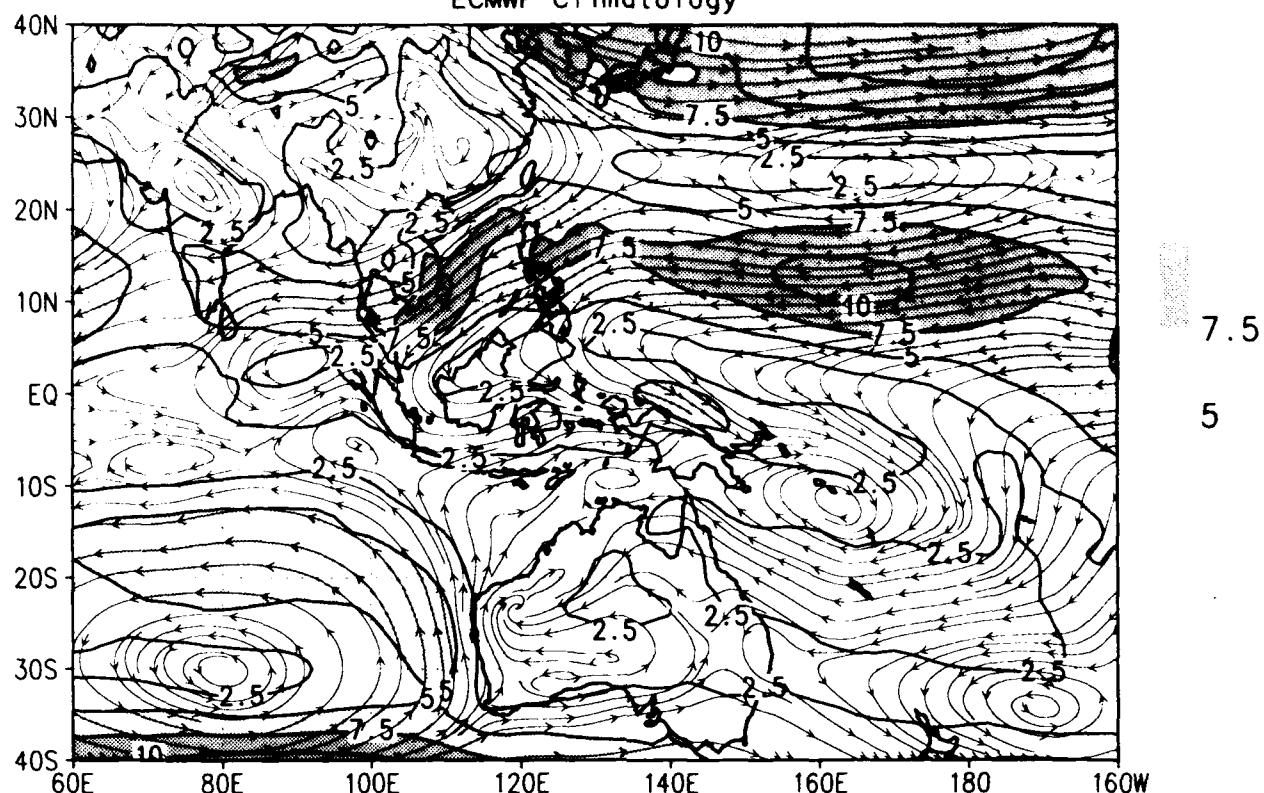
MRF



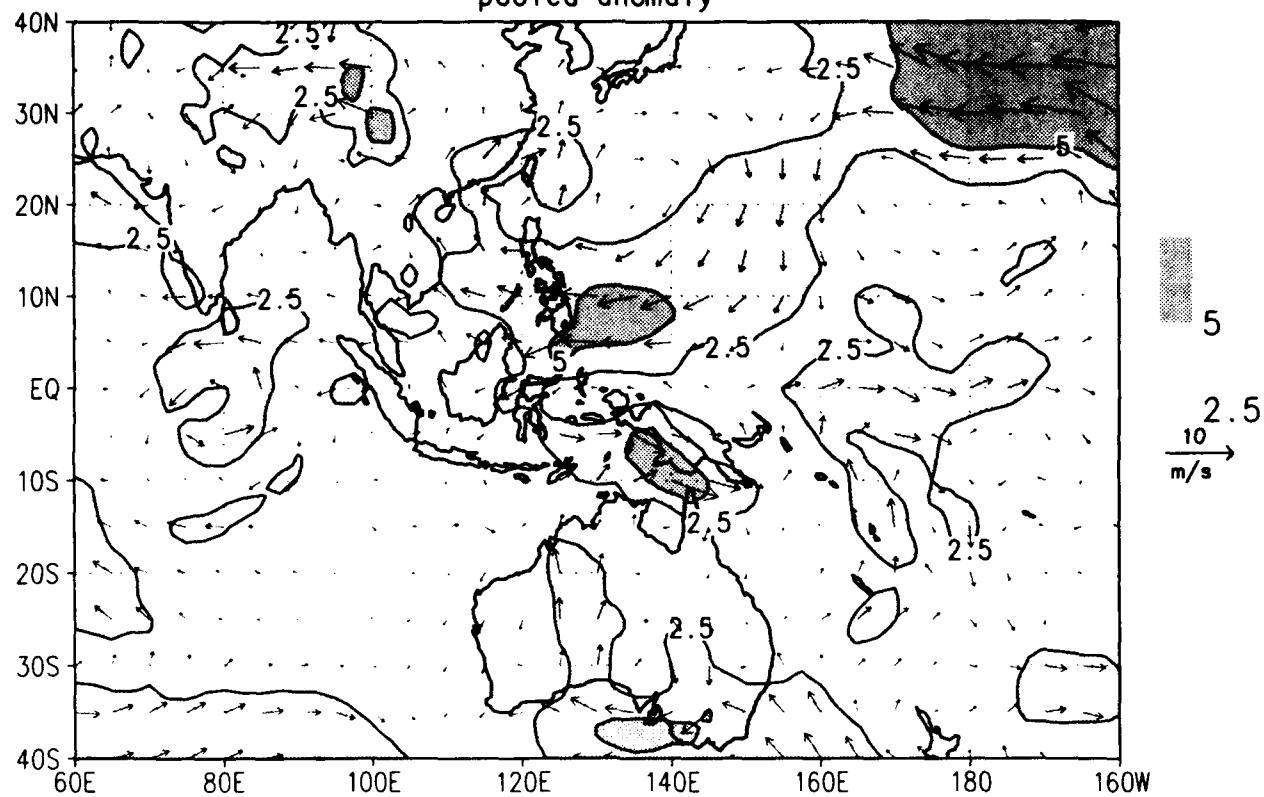
7.5
5

850 mb wind climo for DEC 1992
 /d2/toga_coare/c.gs

ECMWF Climatology

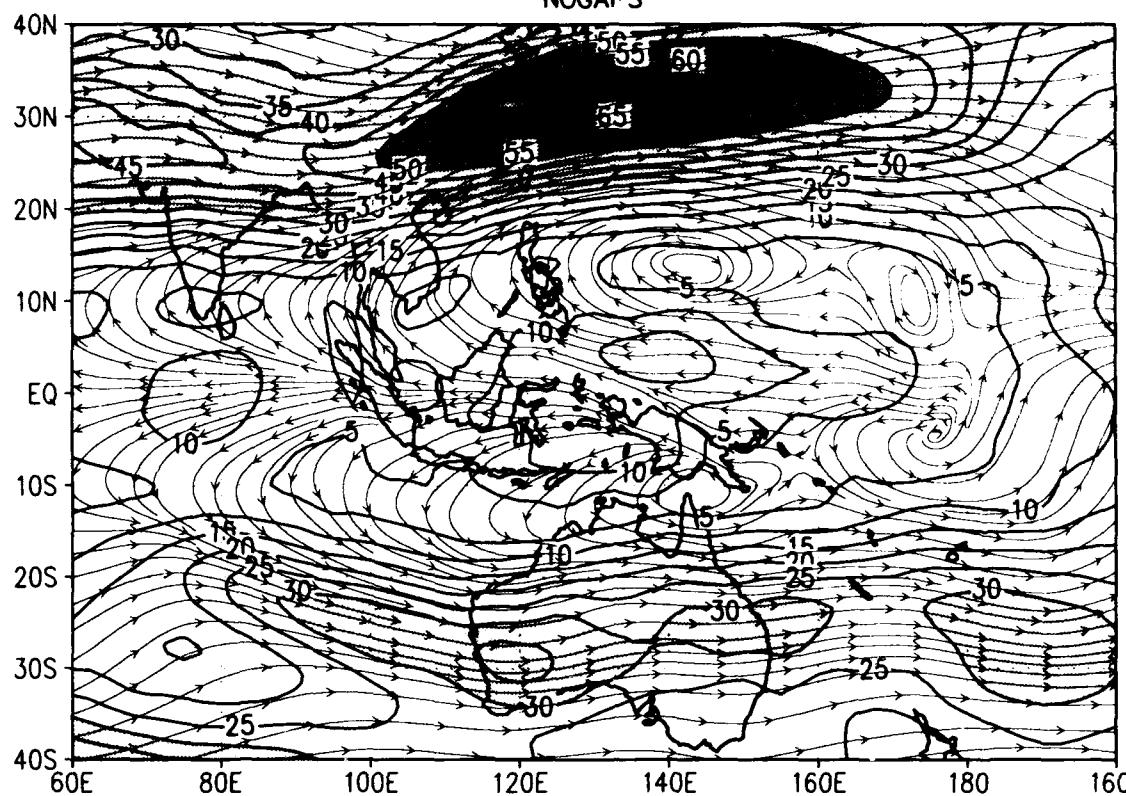


pooled anomaly

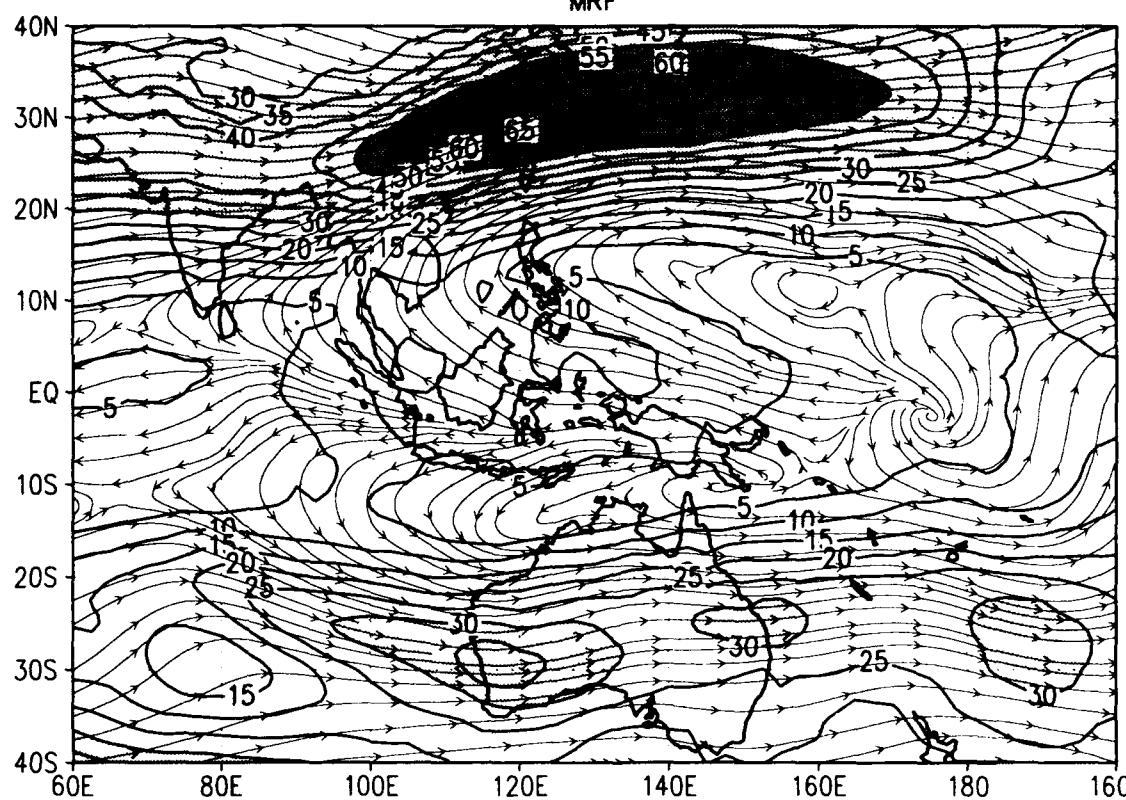


200 mb wind climo for DEC 1992
/d2/toga_coare/c.gs

NOGAPS

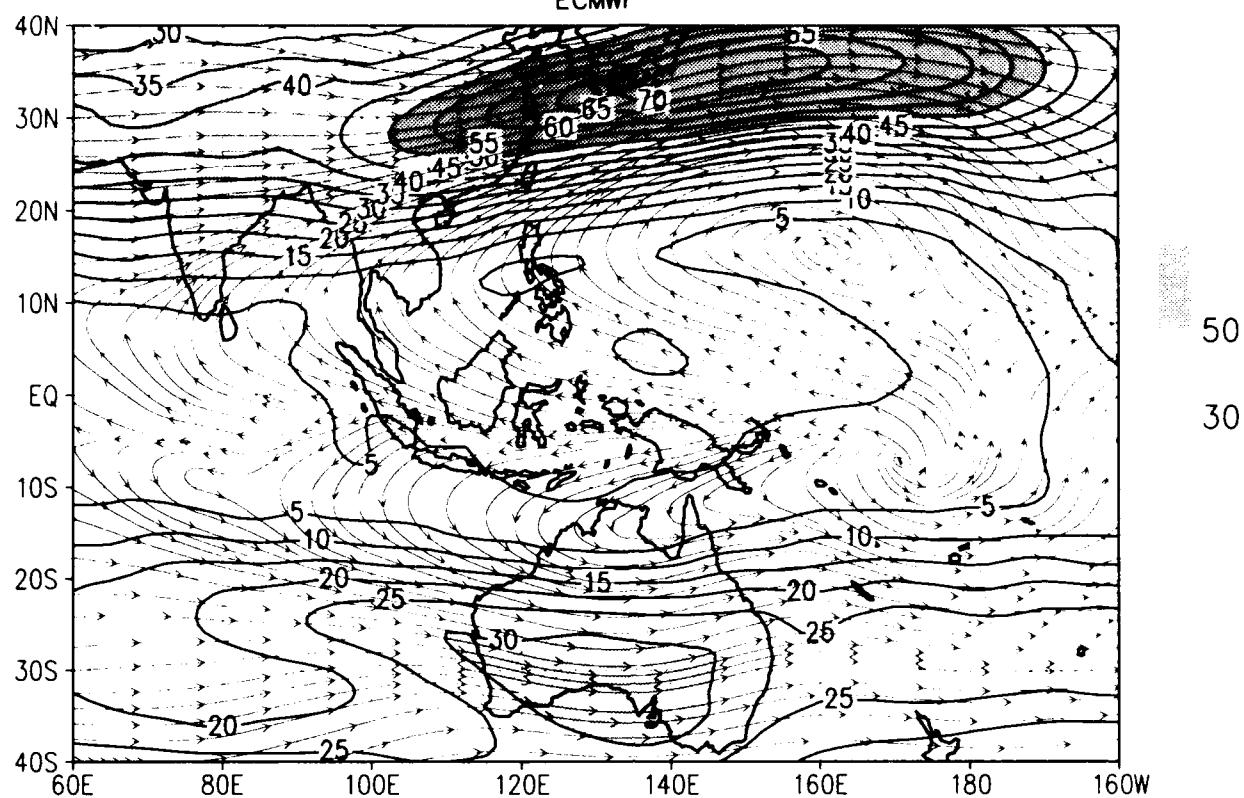


MRF

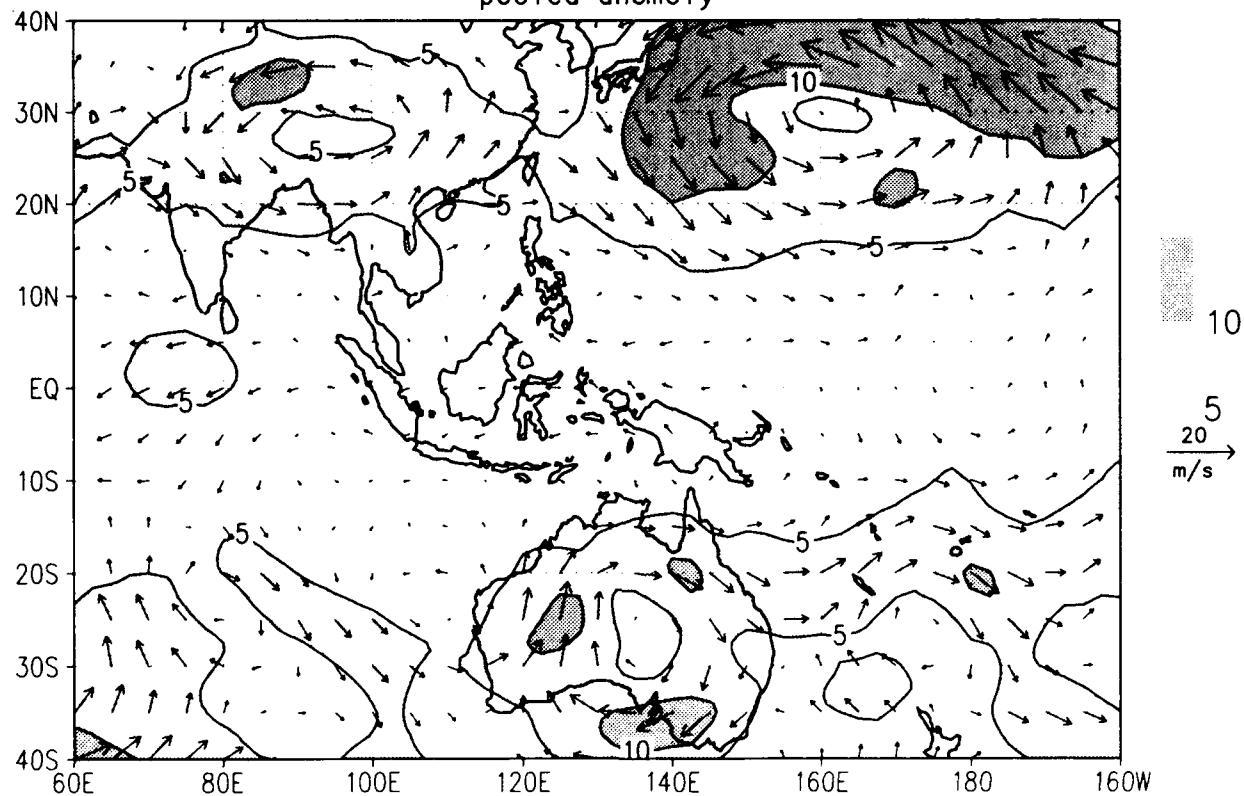


200 mb wind climo for DEC 1992
 /d2/toga_coare/c.gs

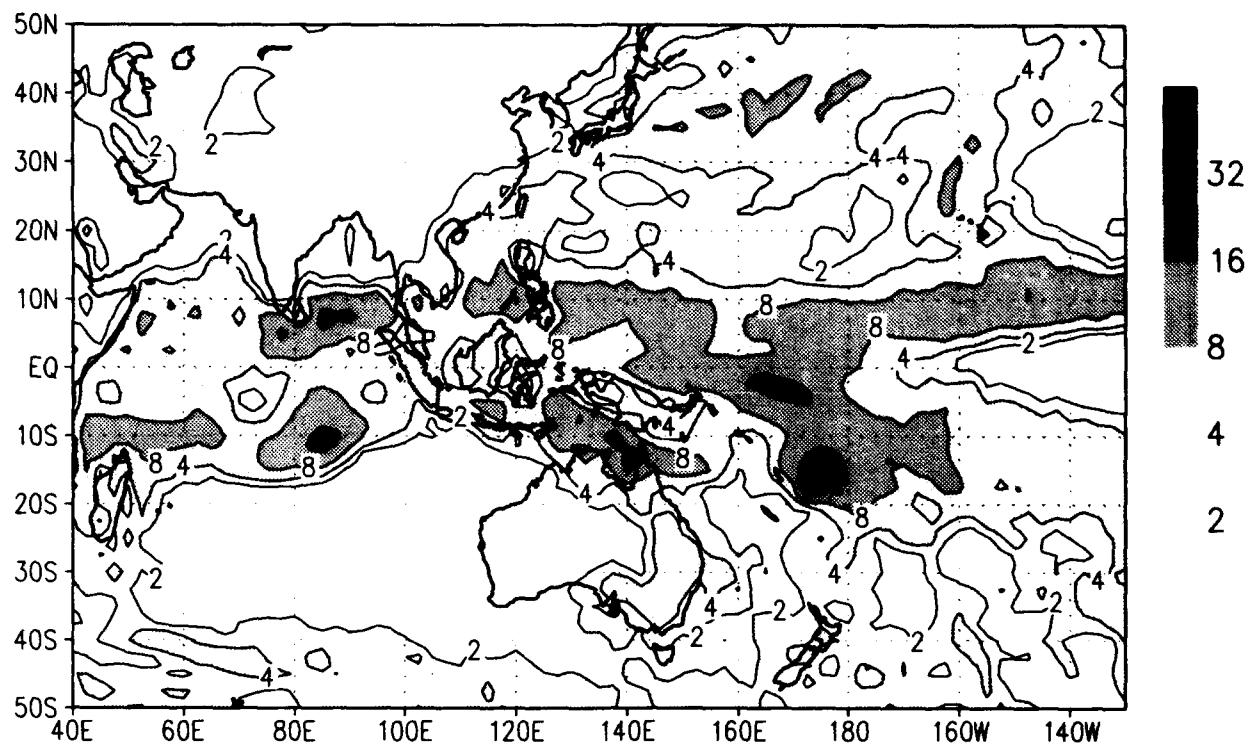
ECMWF



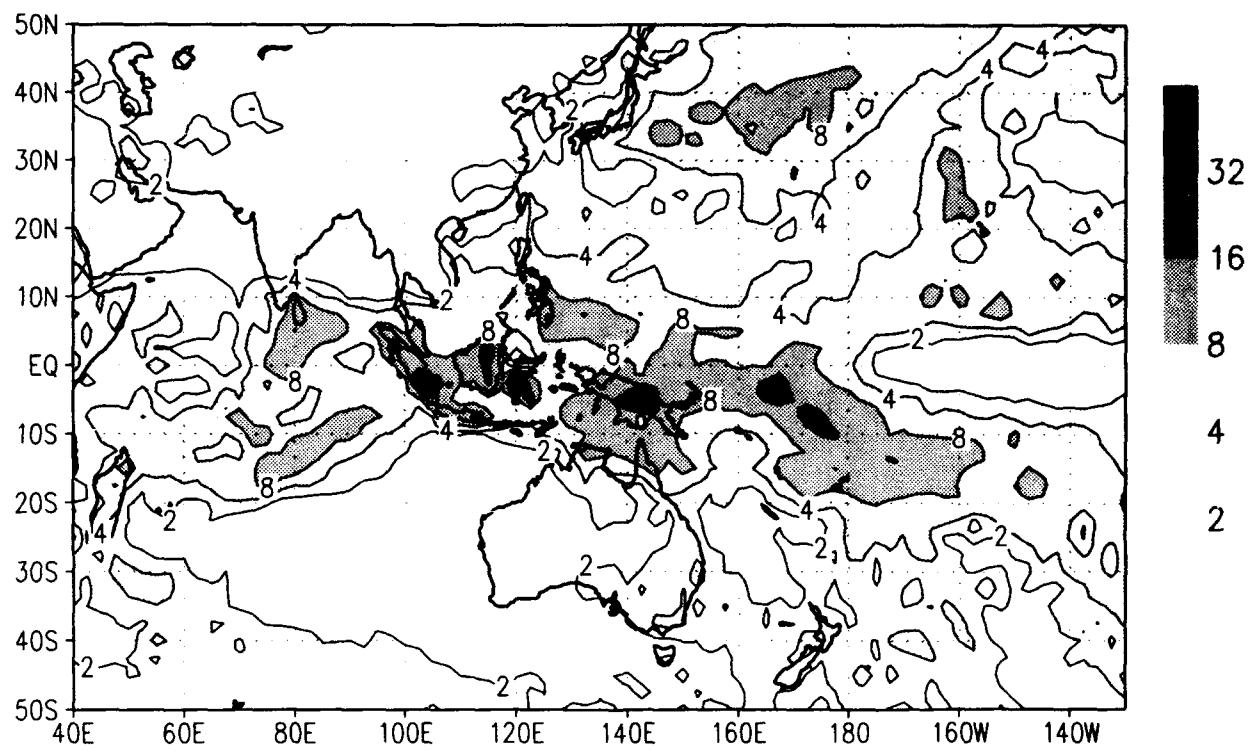
pooled anomaly



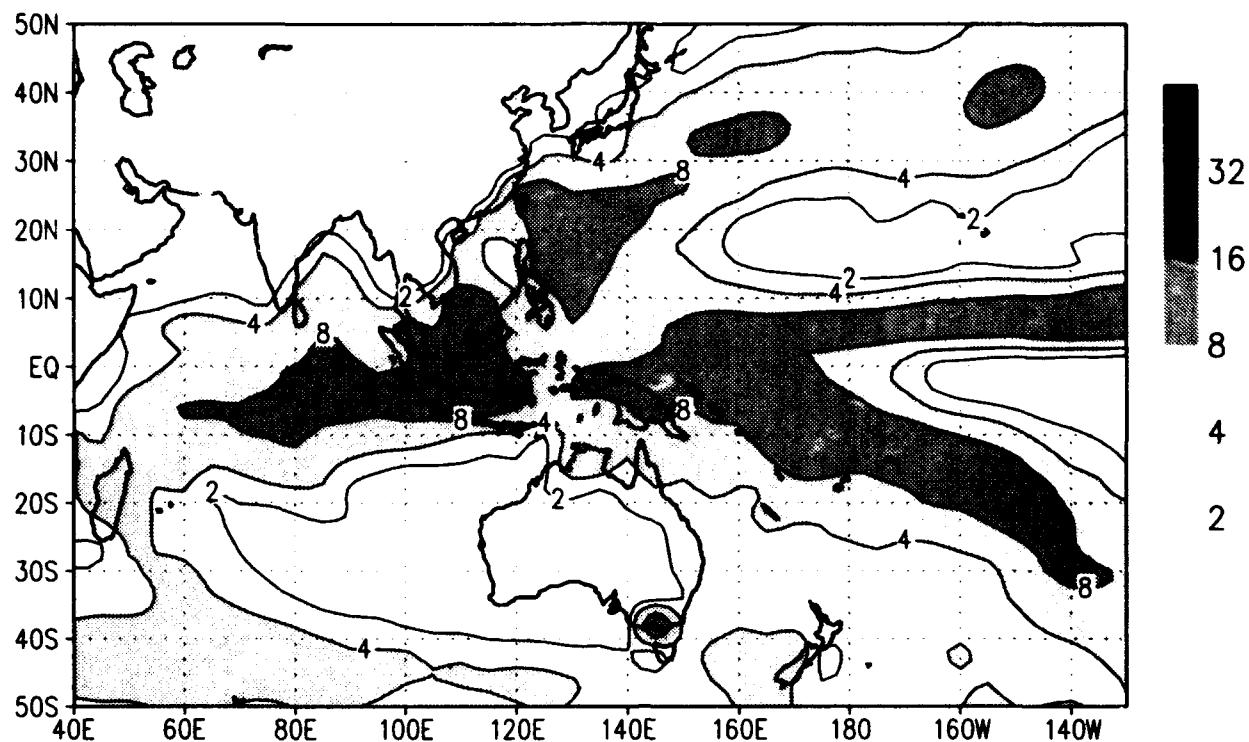
precip climo for DEC 1992
/d2/toga_coare/c.gs
NOGAPS



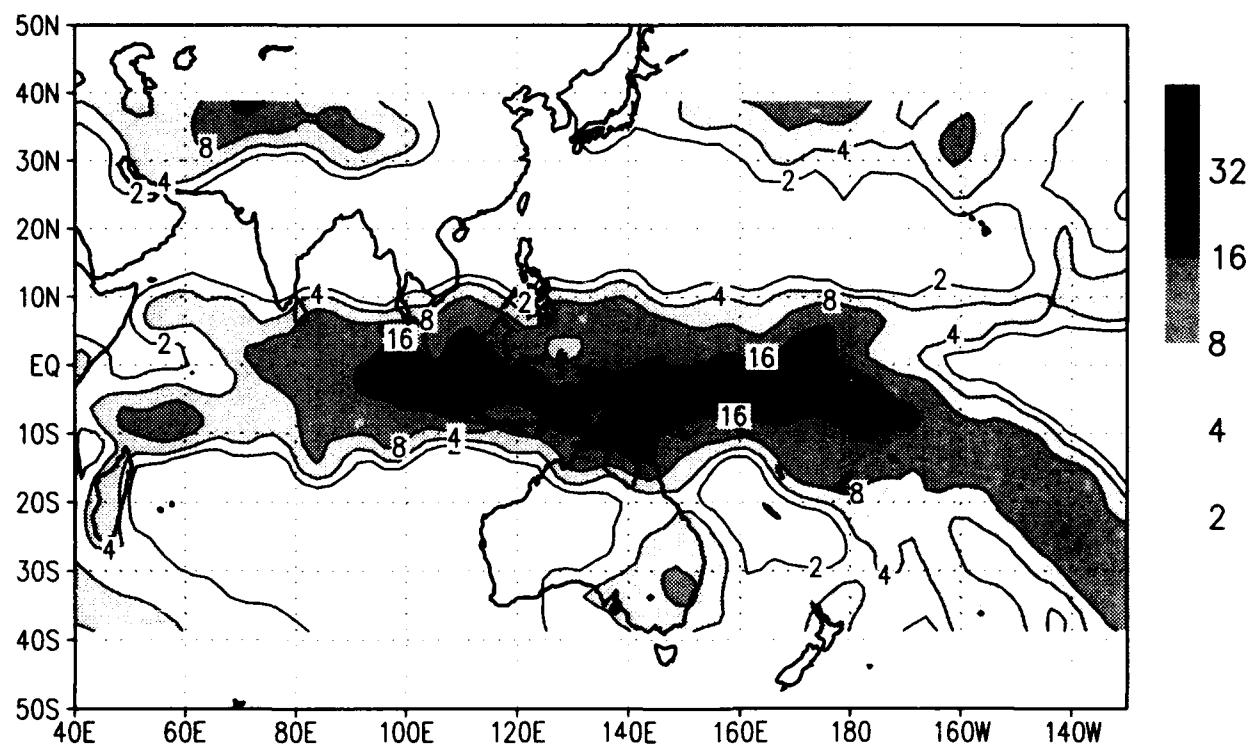
MRF



precip climo for DEC 1992
/d2/toga_coare/c.gs
msu_merged climo



Prelim GPI



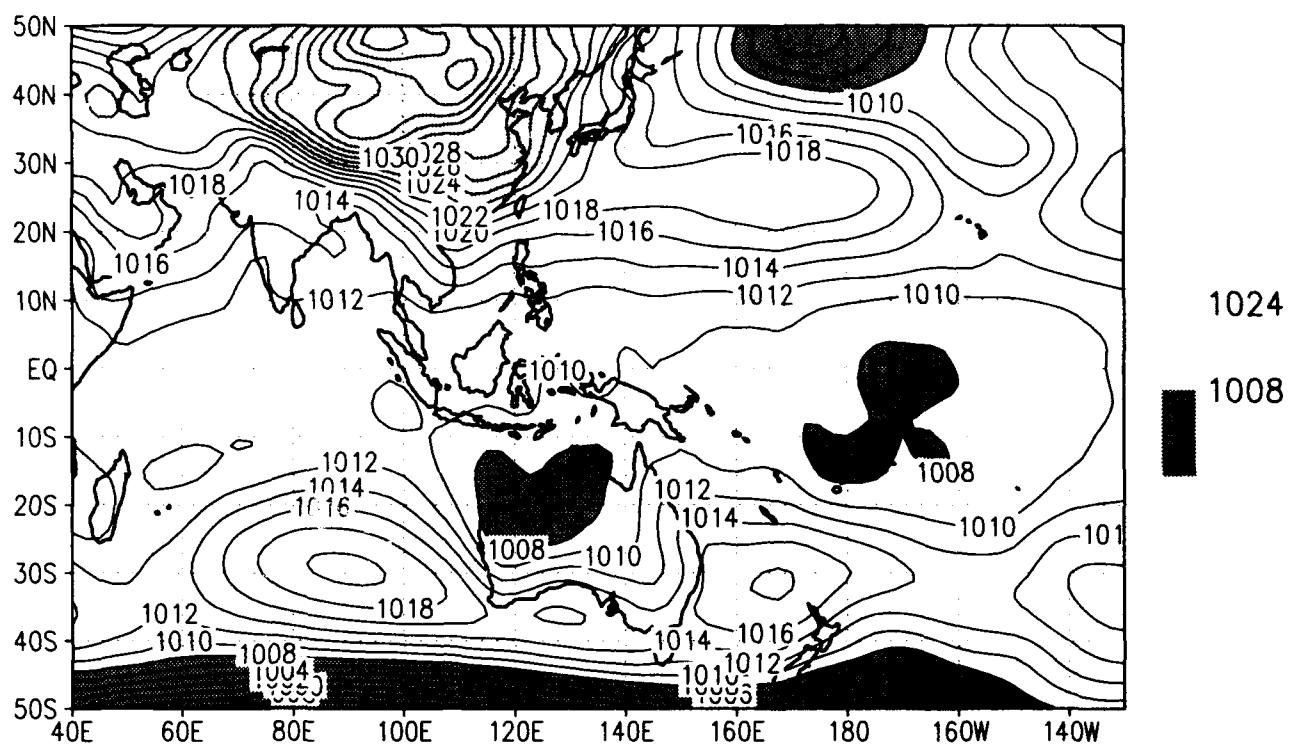
10.3 January 1993

The layout of the plots is the same as in the NDJF seasonal mean section.

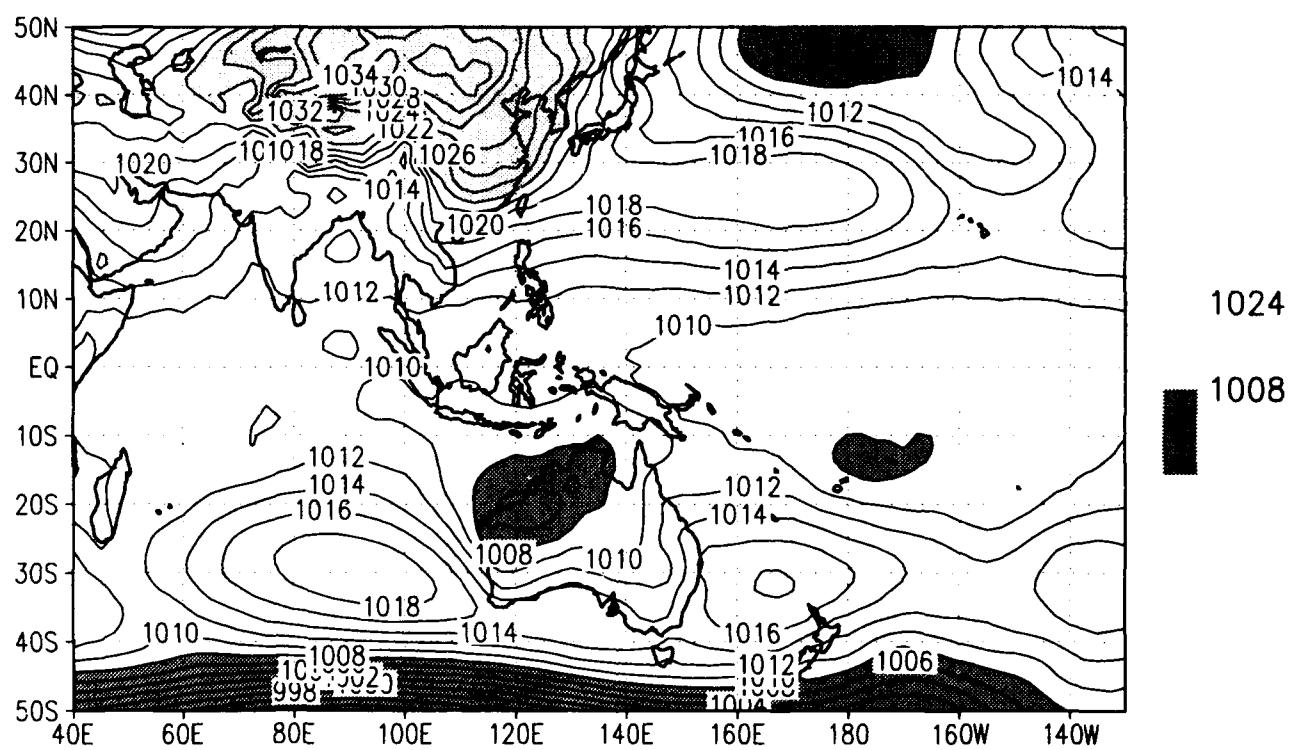
Chart		Description
1	-	Sea-level pressure for NOGAPS and MRF
2	-	ECMWF climatological Sea-level pressure and the pooled anomaly
3	-	Surface wind speed for NOGAPS and MRF
4	-	ECMWF climatological surface wind and pooled anomaly
5	-	850 mb wind for NOGAPS and MRF
6	-	ECMWF climatological 850 mb wind and pooled anomaly
7	-	200 mb wind for NOGAPS and MRF
8	-	ECMWF climatological 200 mb wind and pooled anomaly
9	-	12-h precipitation for NOGAPS and MRF
10	-	MSU merged climatological precipitation and GPI

SLP climo for JAN 1993
 /d2/toga_coare/c.gs

NOGAPS



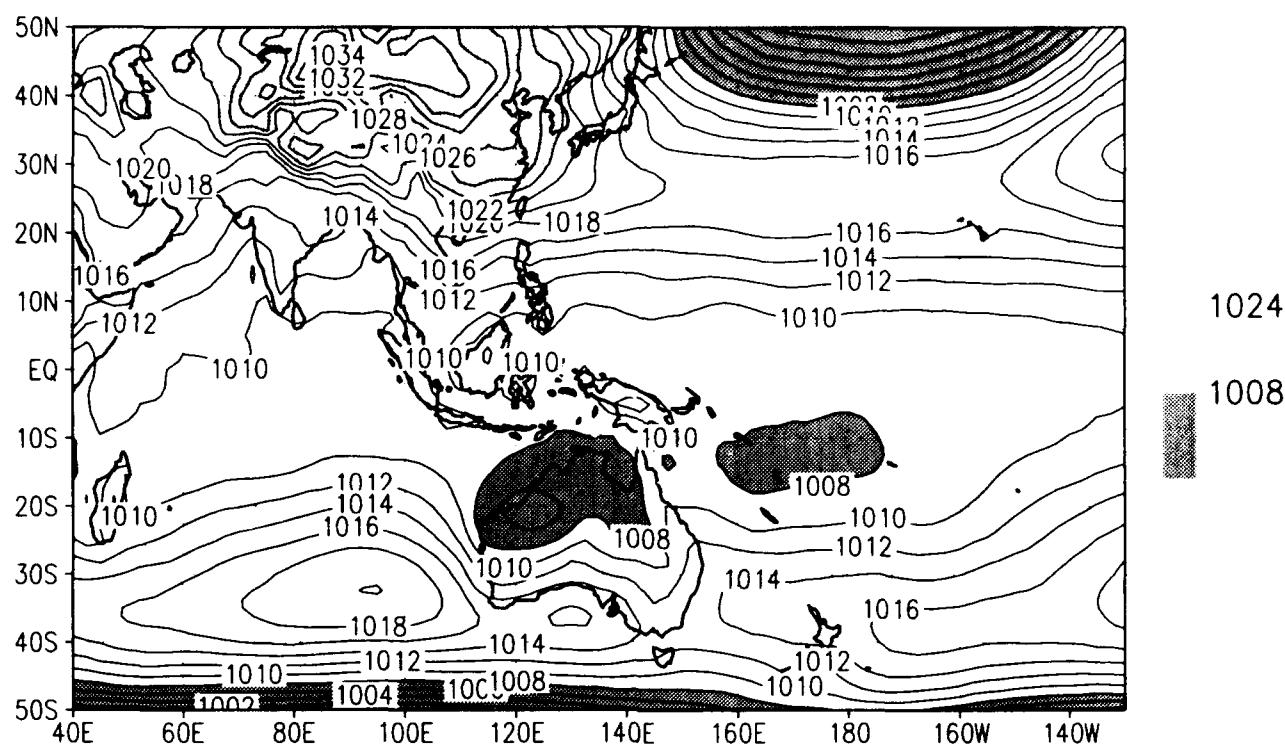
MRF



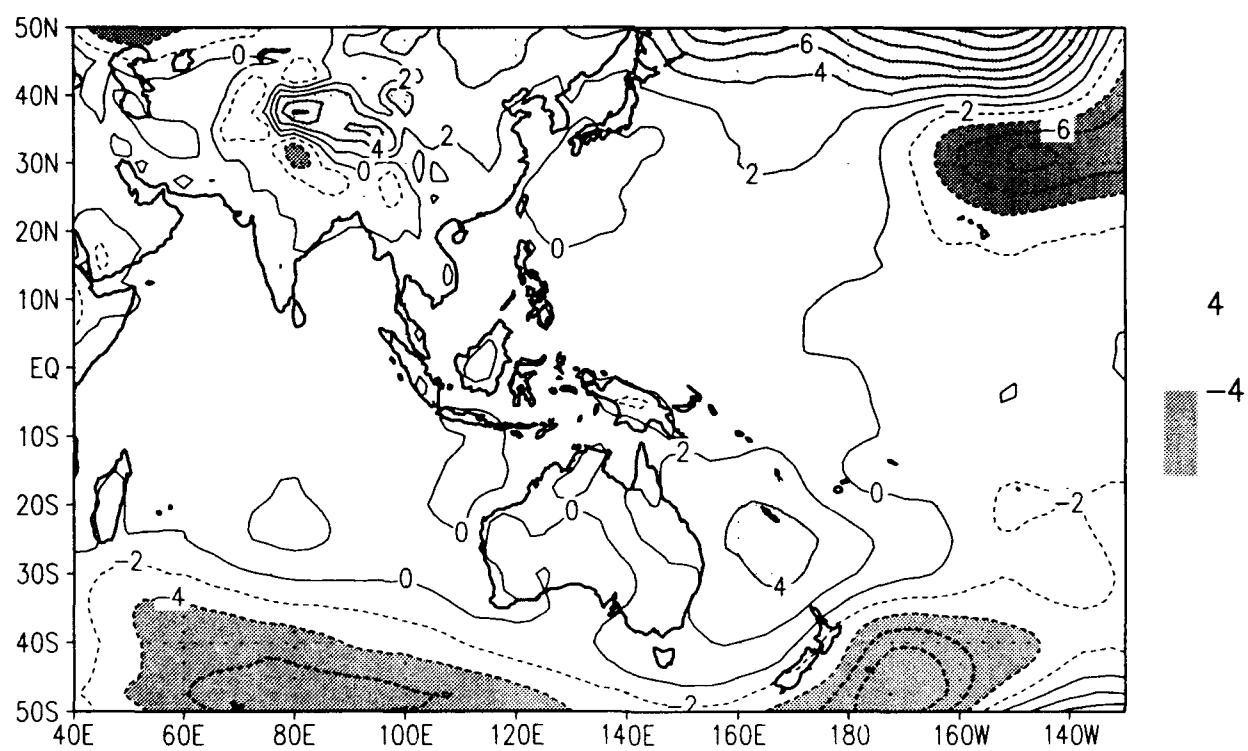
SLP climo for JAN 1993

/d2/toga_coare/c.gs

ECMWF Climatology

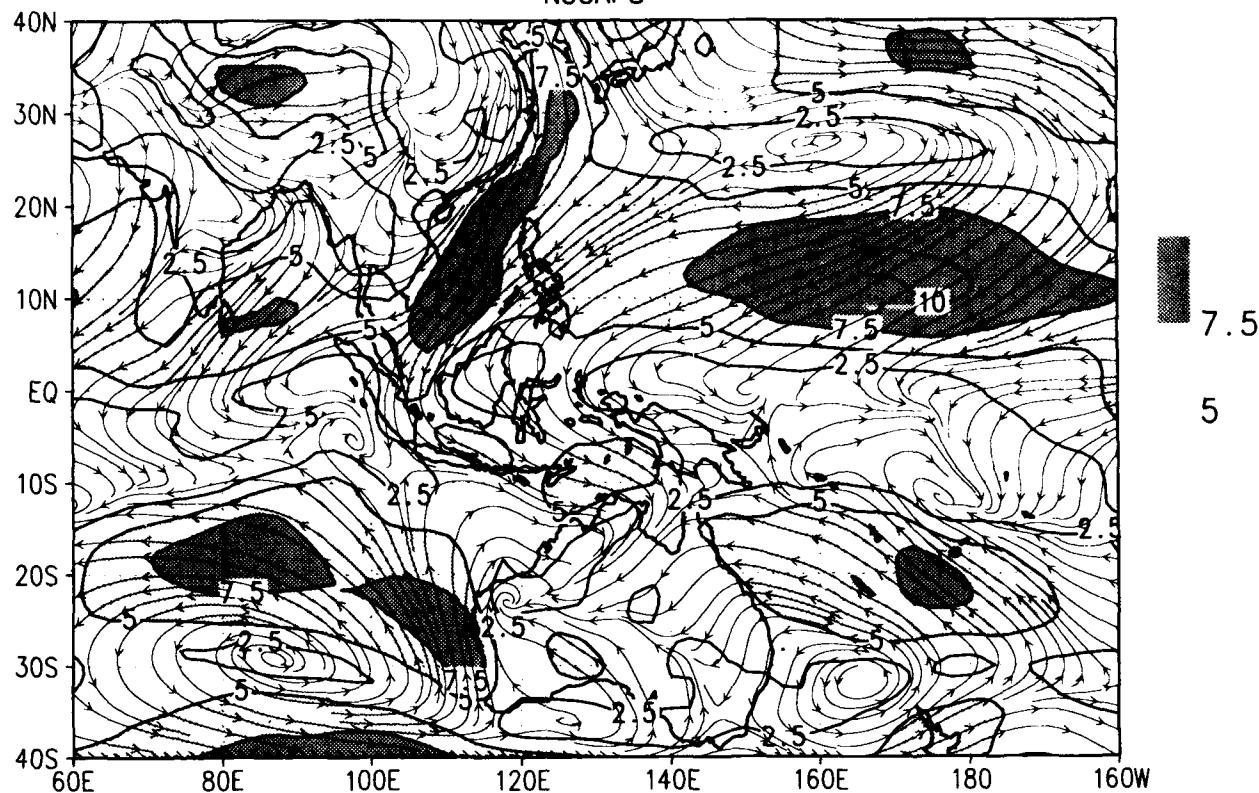


pooled anomaly

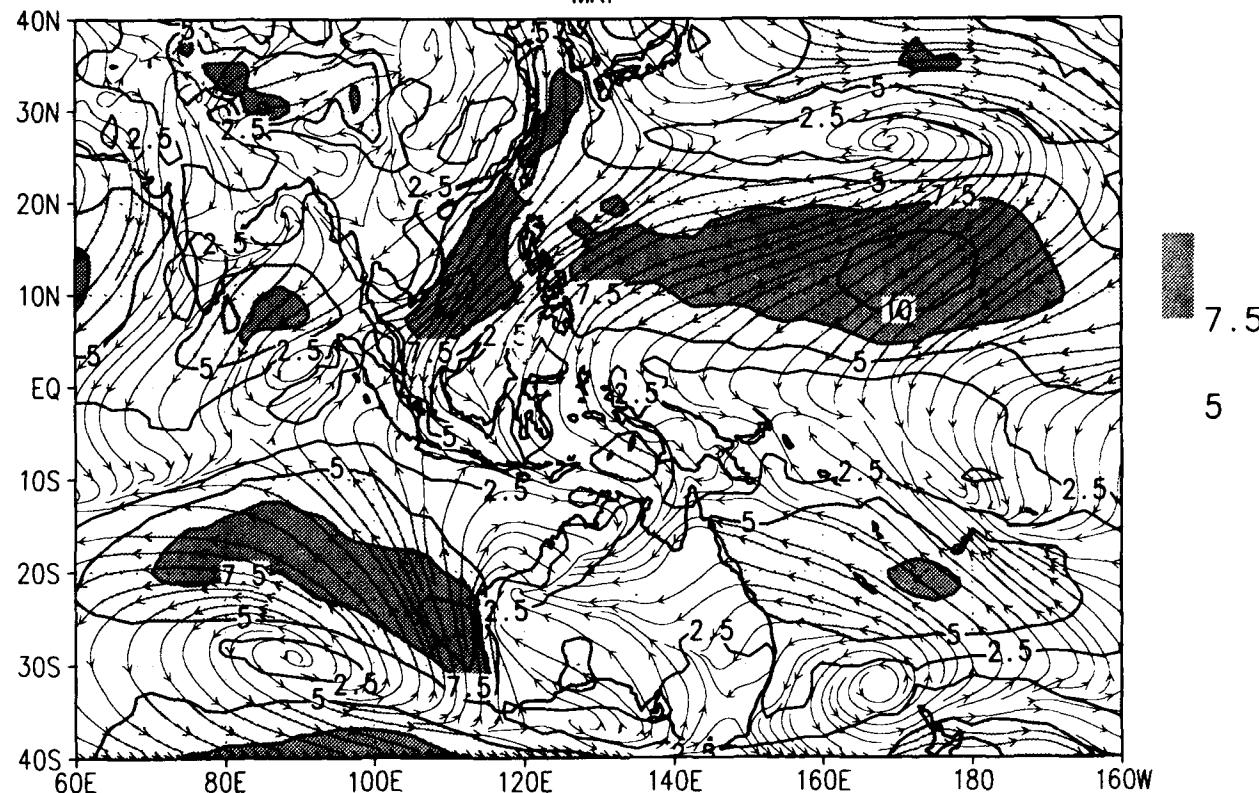


Sfc wind climo for JAN 1993
/d2/toga_coare/c.gs

NOGAPS

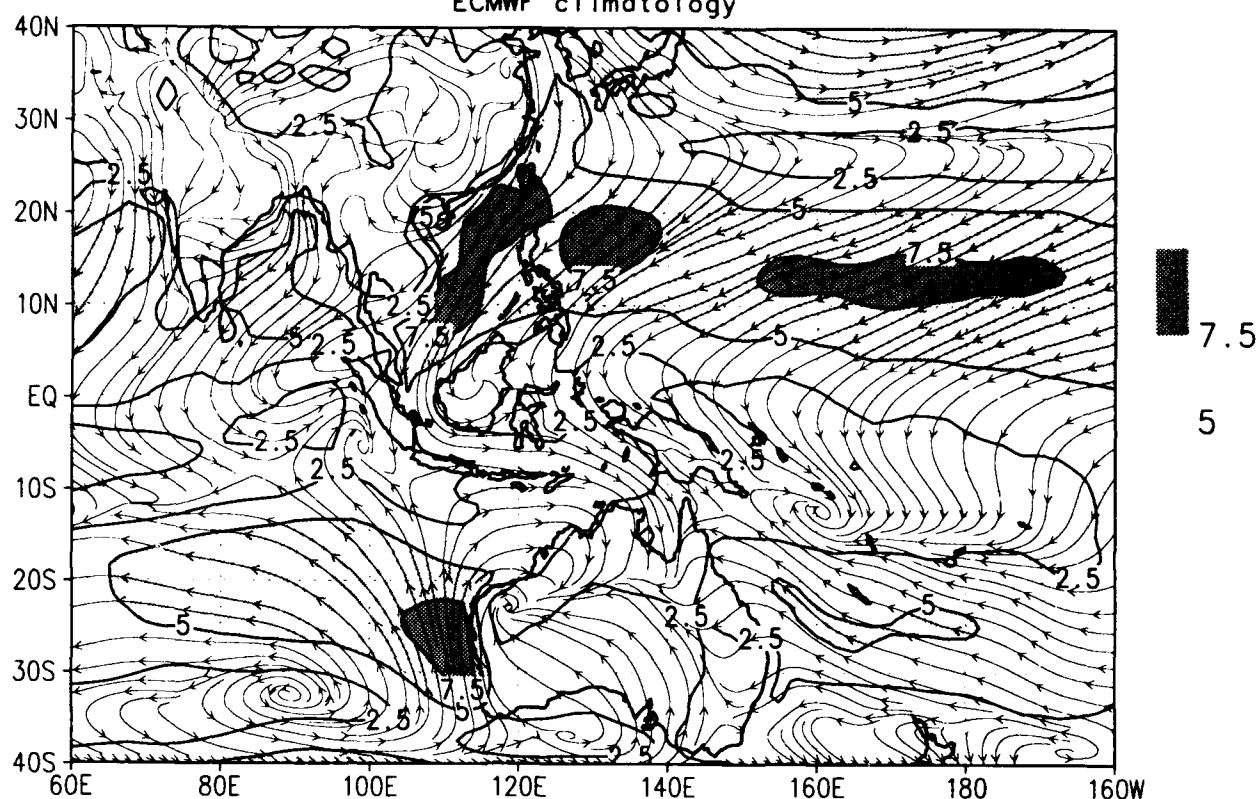


MRF

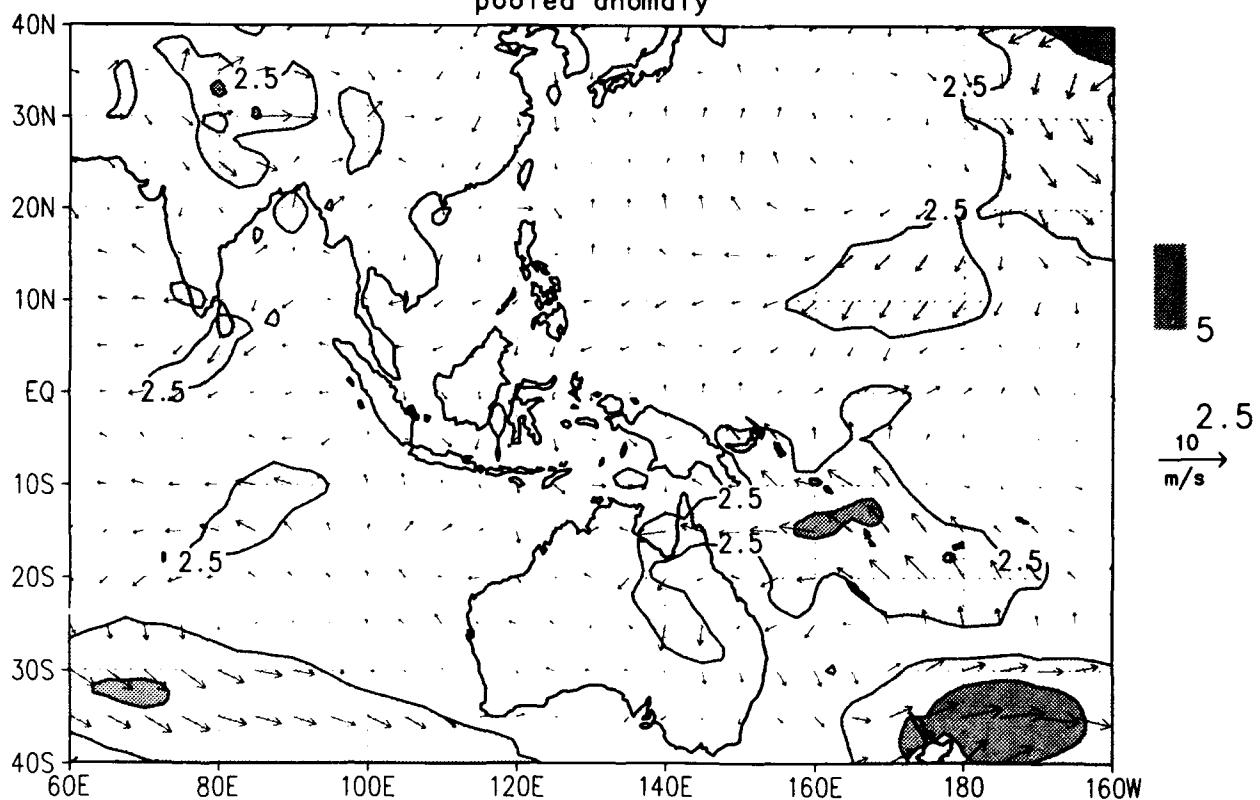


Sfc wind climo for JAN 1993
/d2/toga_coare/c.gs

ECMWF climatology

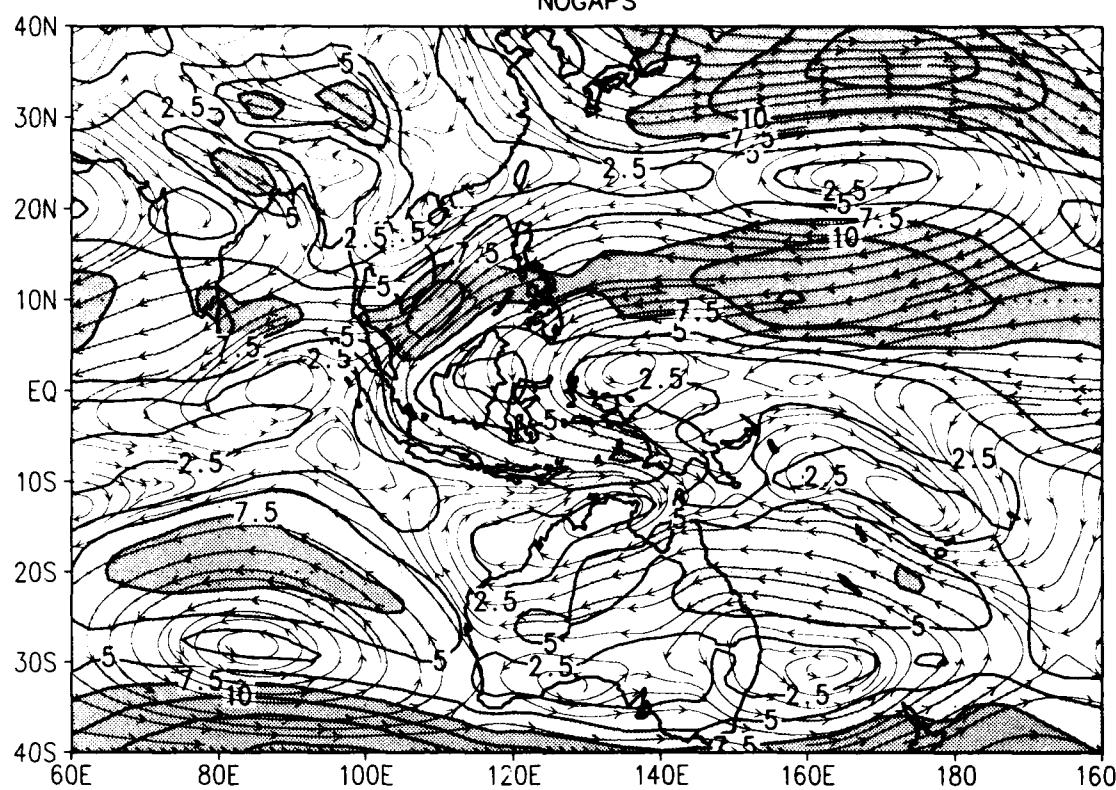


pooled anomaly



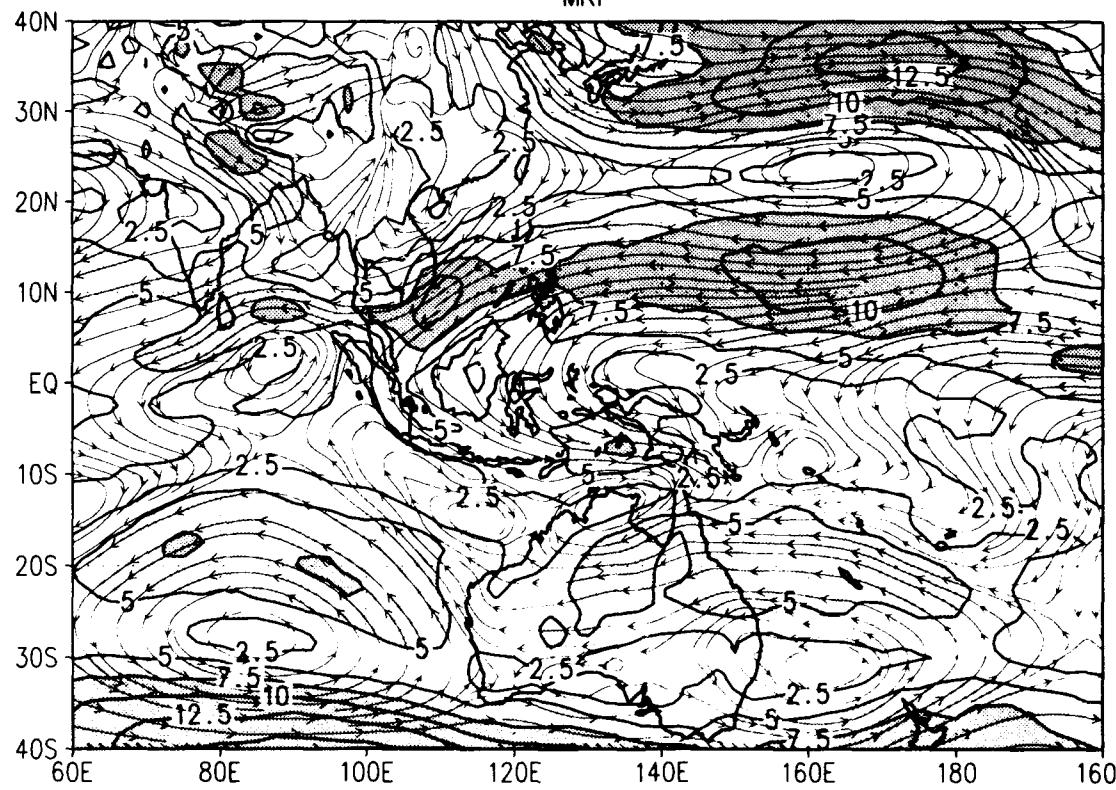
850 mb wind climo for JAN 1993
/d2/toga_coare/c.gs

NOGAPS



7.5
5

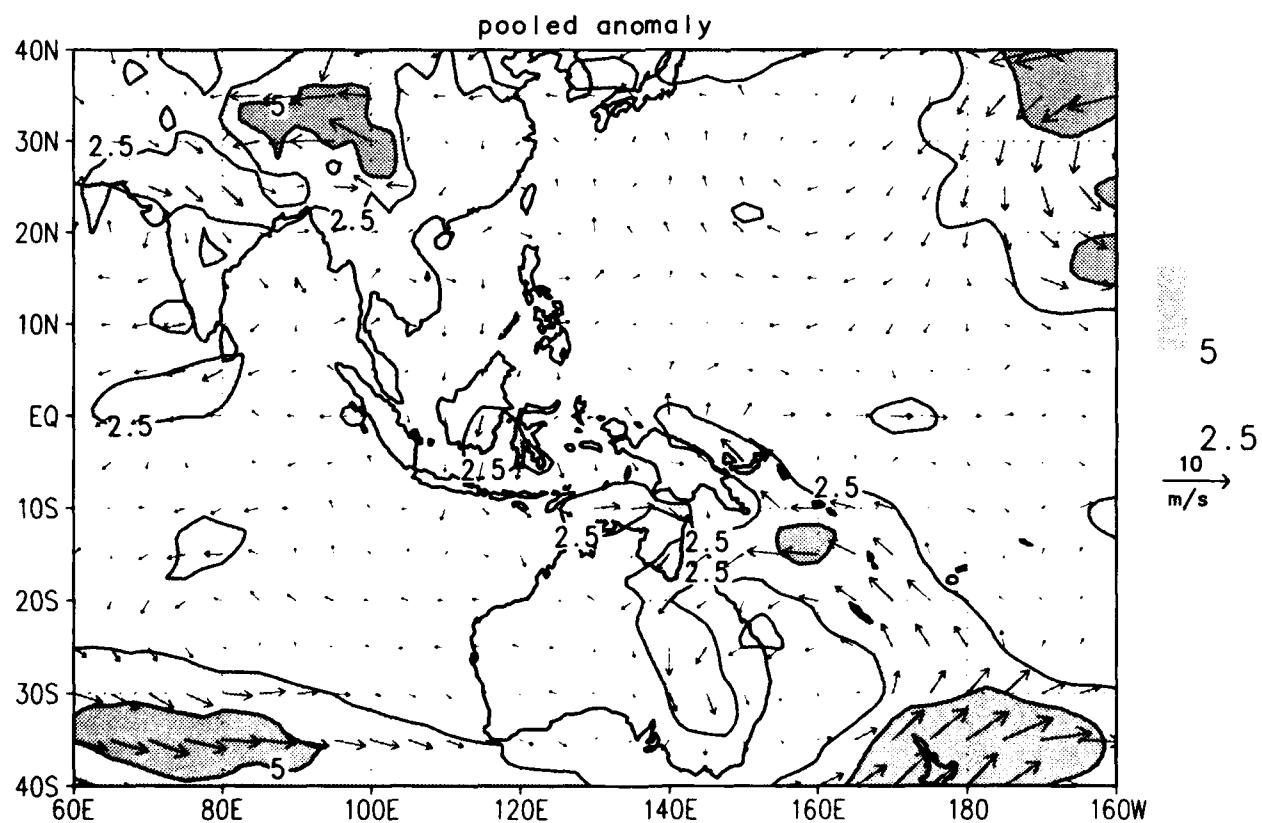
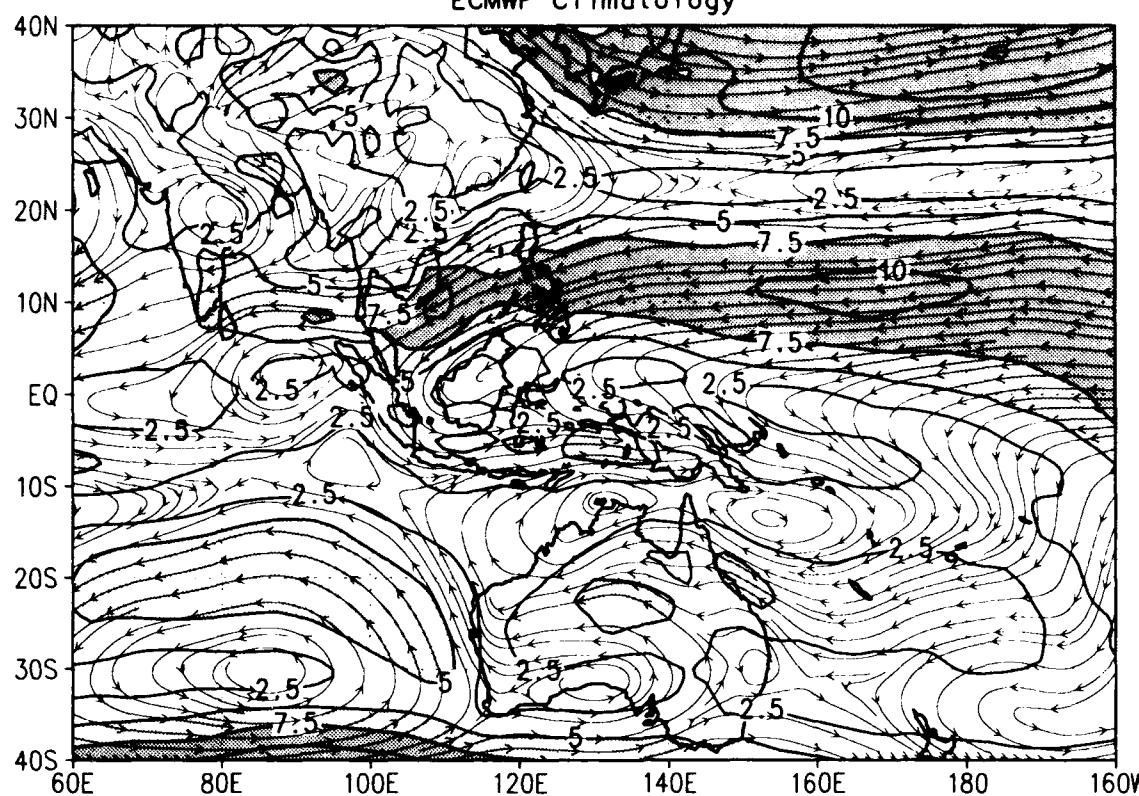
MRF



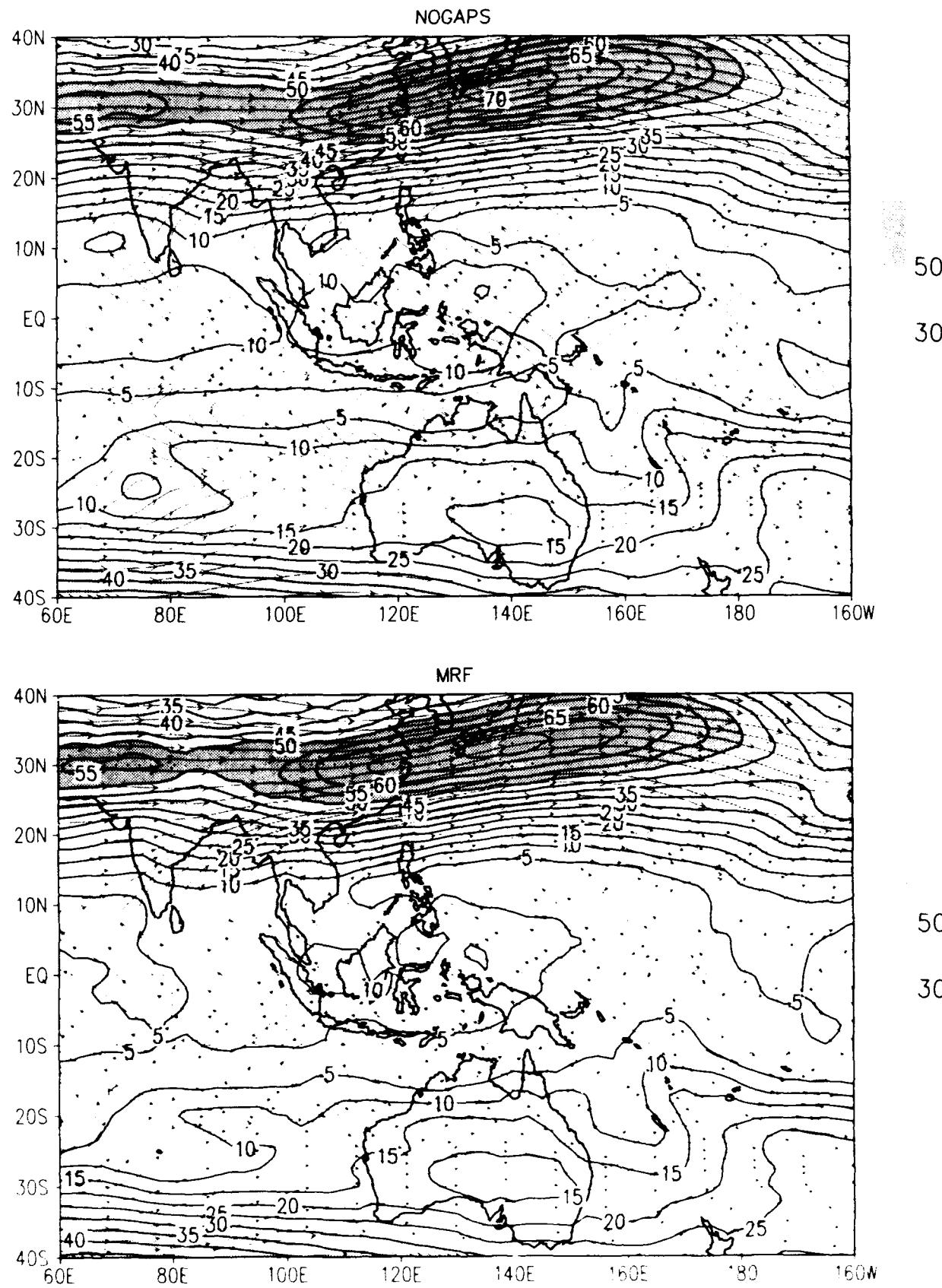
7.5
5

850 mb wind climo for JAN 1993
/d2/toga_coare/c.gs

ECMWF Climatology

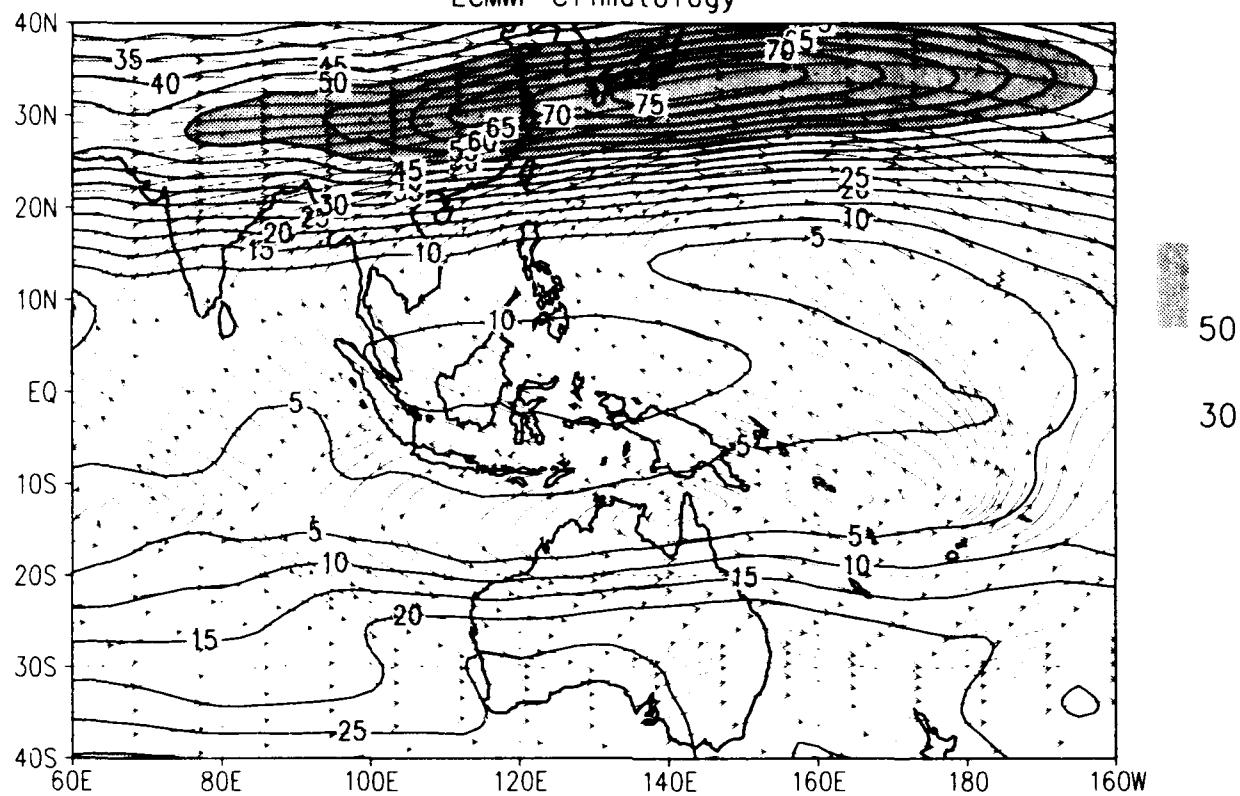


200 mb wind climo for JAN 1993
/d2/toga_coare/c.gs

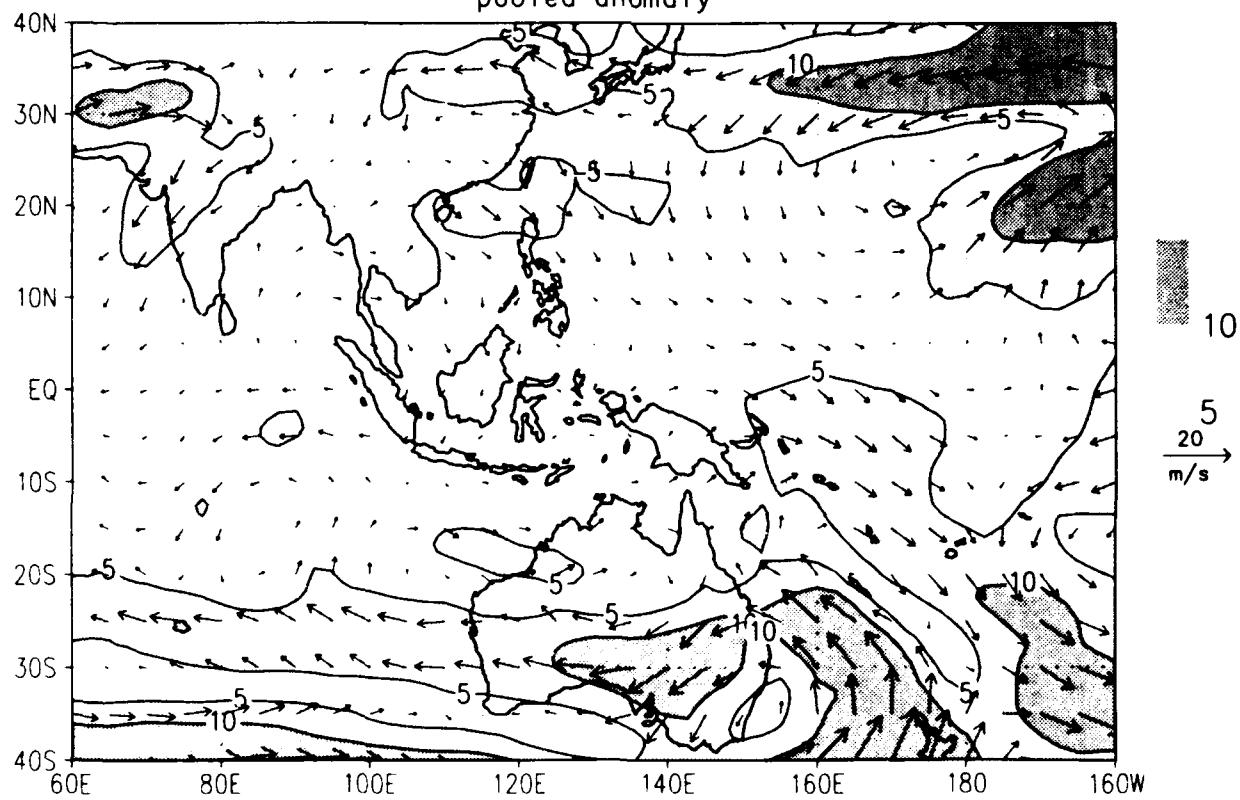


200 mb wind climo for JAN 1993
 /d2/toga_coare/c.gs

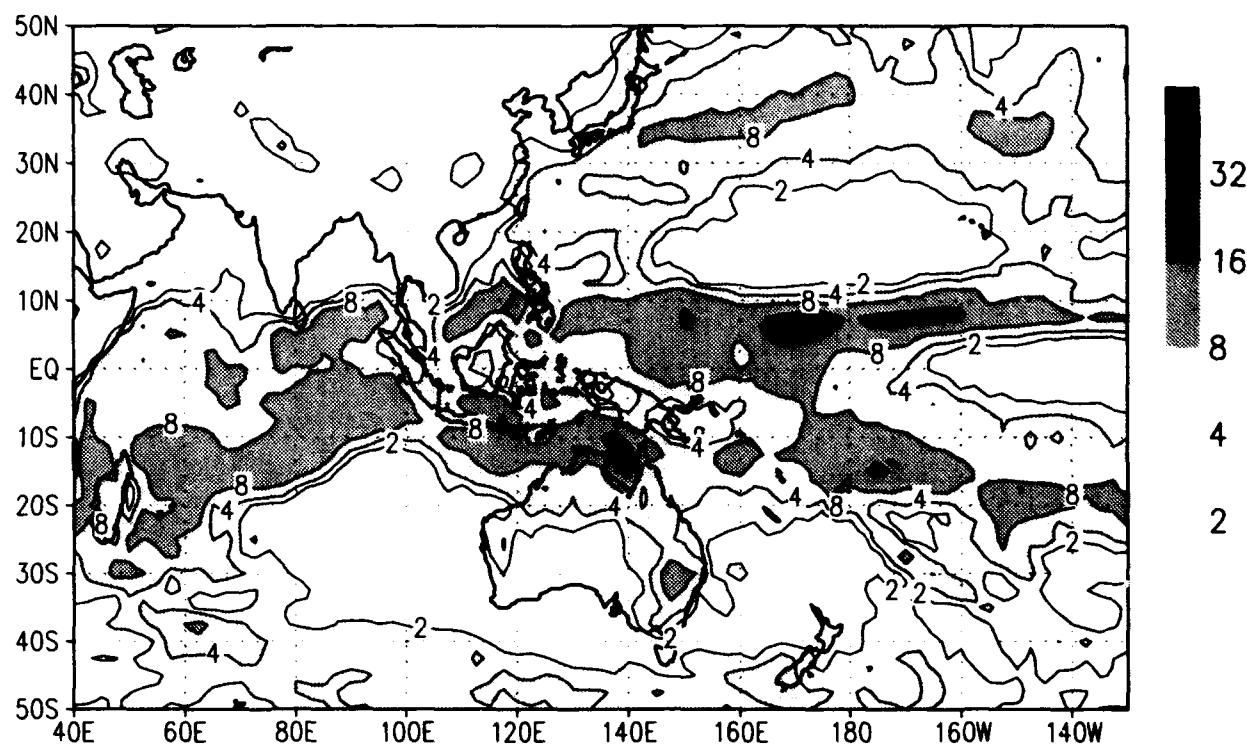
ECMWF Climatology



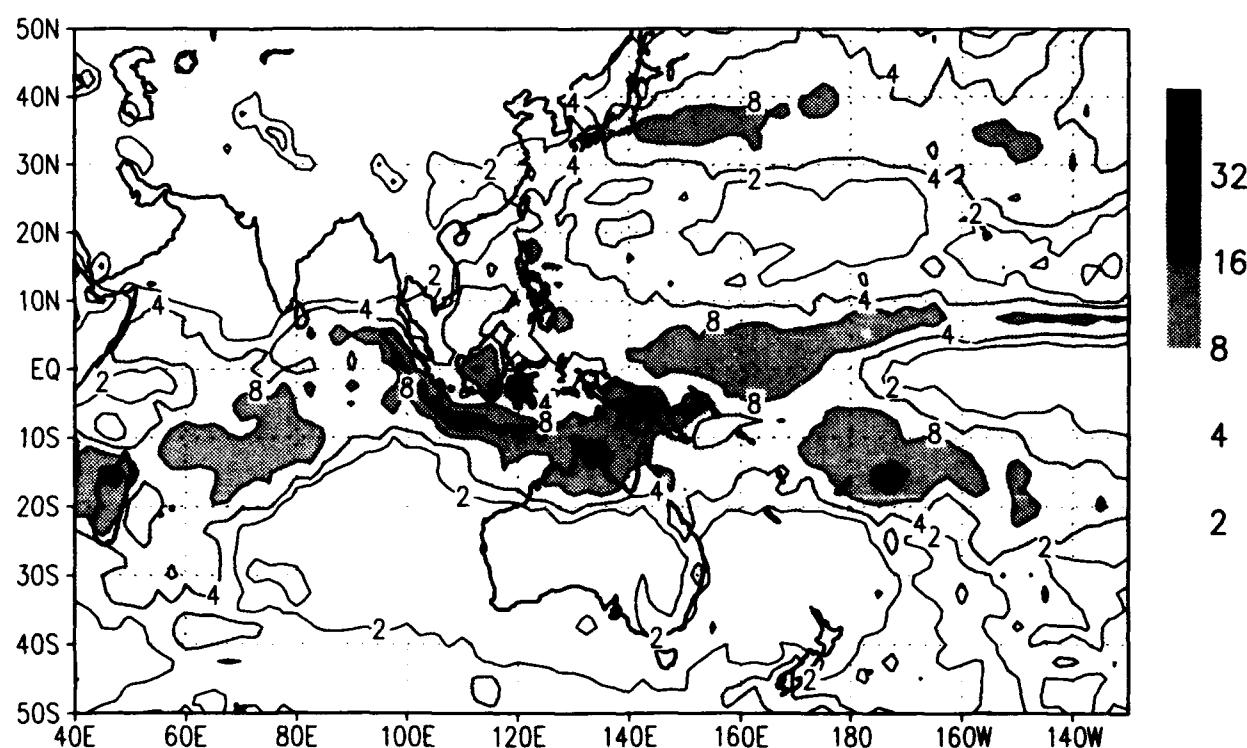
pooled anomaly



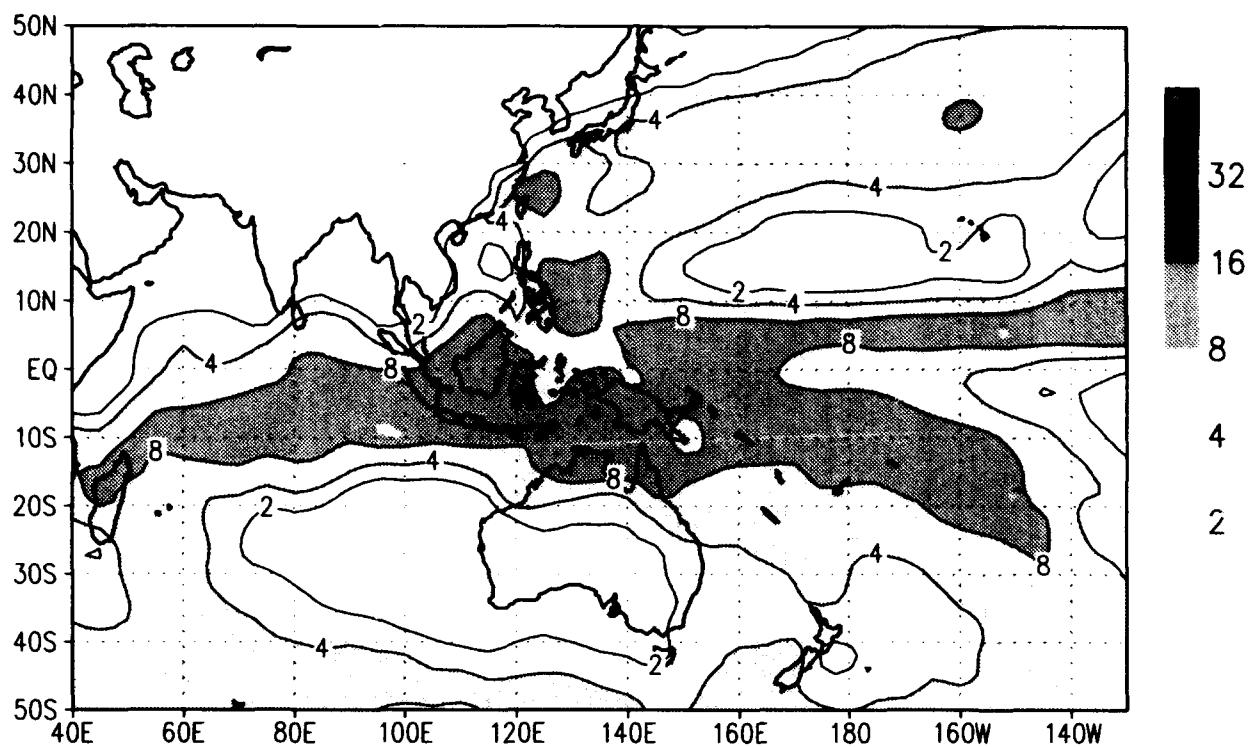
precip climo for JAN 1993
/d2/toga_coare/c.gs
NOGAPS



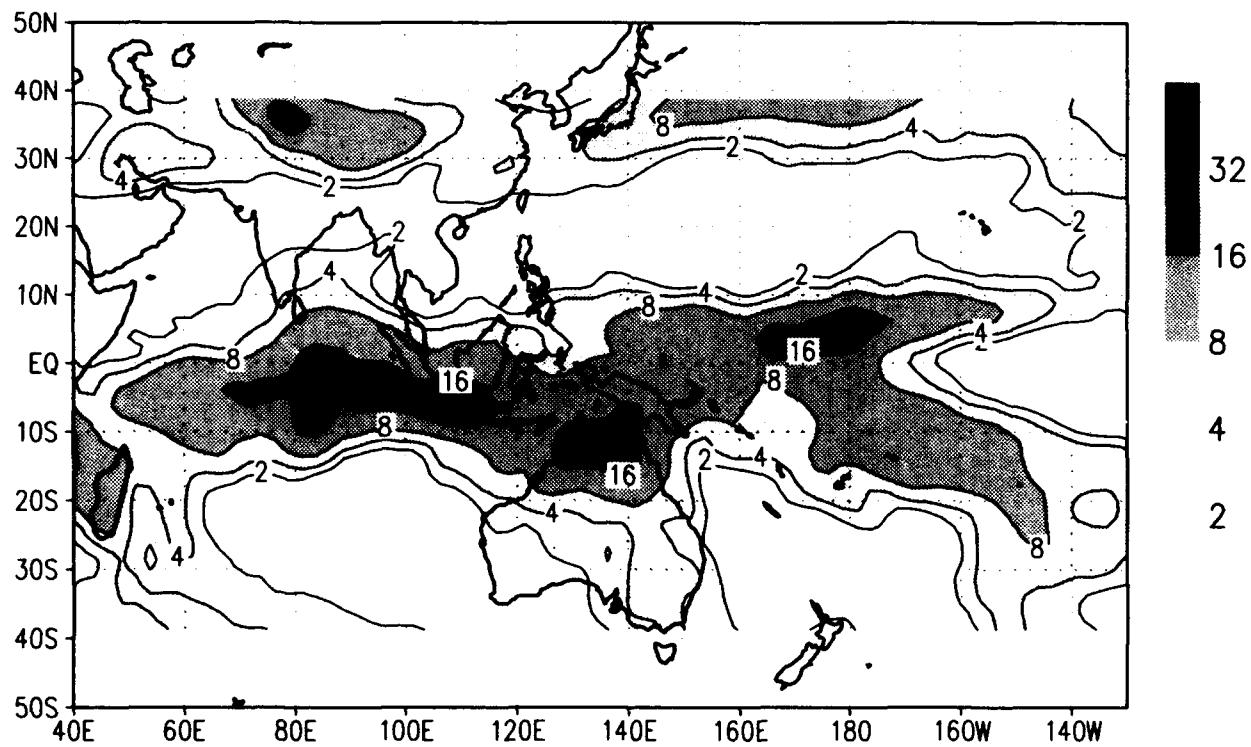
MRF



precip climo for JAN 1993
/d2/toga_coare/c.gs
msu_merged climo



Prelim GPI

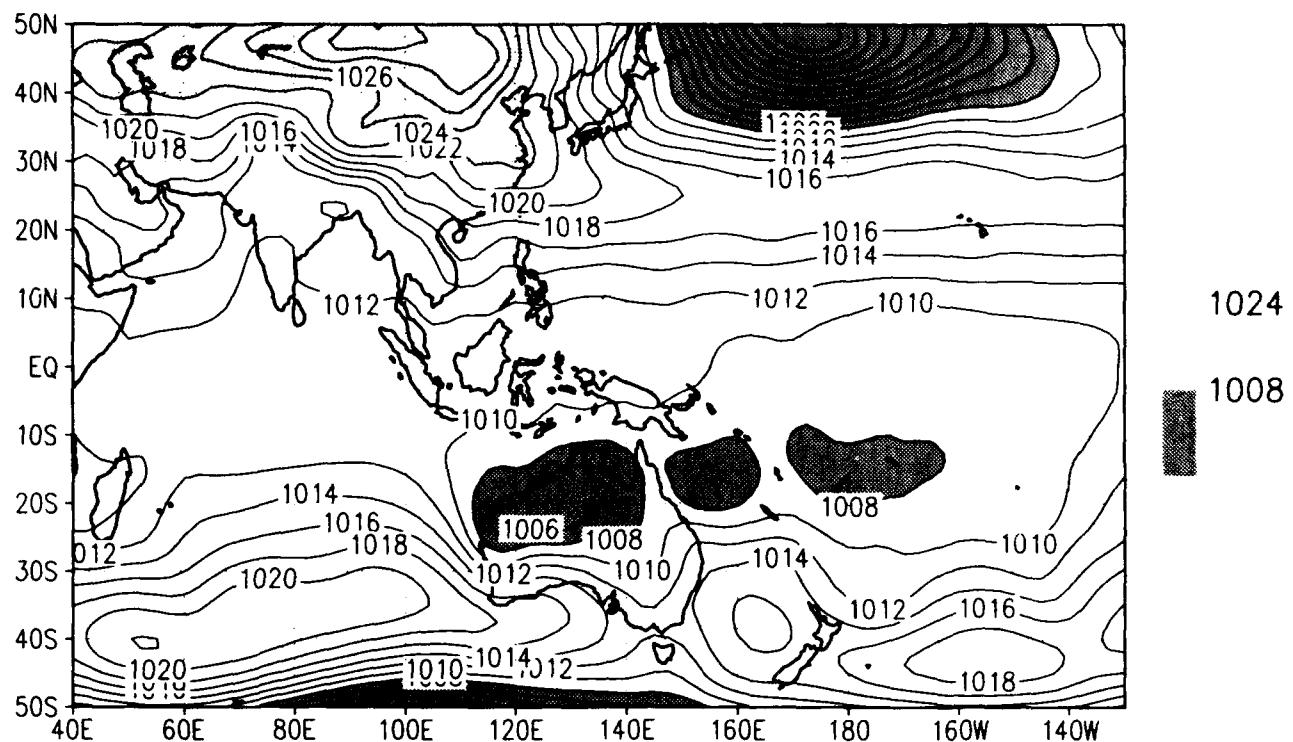


10.4 February 1993

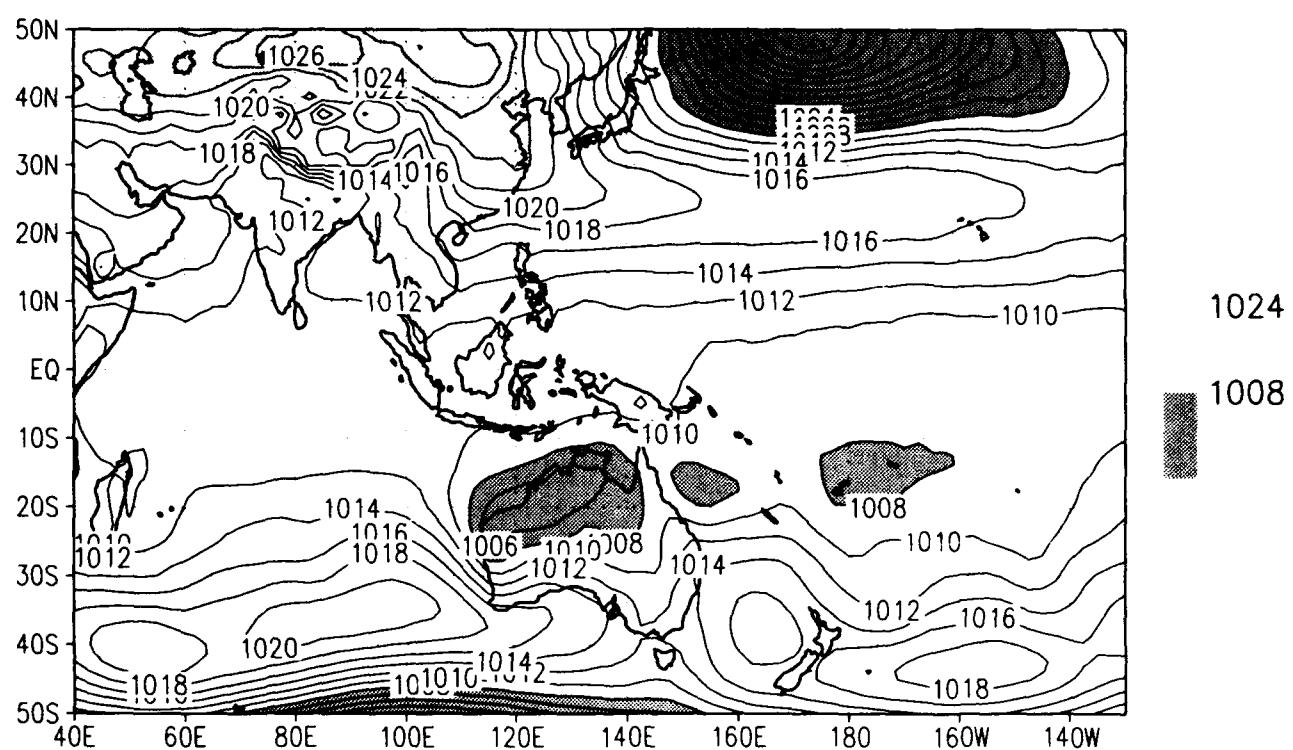
The layout of the plots is the same as in the NDJF seasonal mean section.

Chart		Description
1	-	Sea-level pressure for NOGAPS and MRF
2	-	ECMWF climatological Sea-level pressure and the pooled anomaly
3	-	Surface wind speed for NOGAPS and MRF
4	-	ECMWF climatological surface wind and pooled anomaly
5	-	850 mb wind for NOGAPS and MRF
6	-	ECMWF climatological 850 mb wind and pooled anomaly
7	-	200 mb wind for NOGAPS and MRF
8	-	ECMWF climatological 200 mb wind and pooled anomaly
9	-	12-h precipitation for NOGAPS and MRF
10	-	MSU merged climatological precipitation and GPI

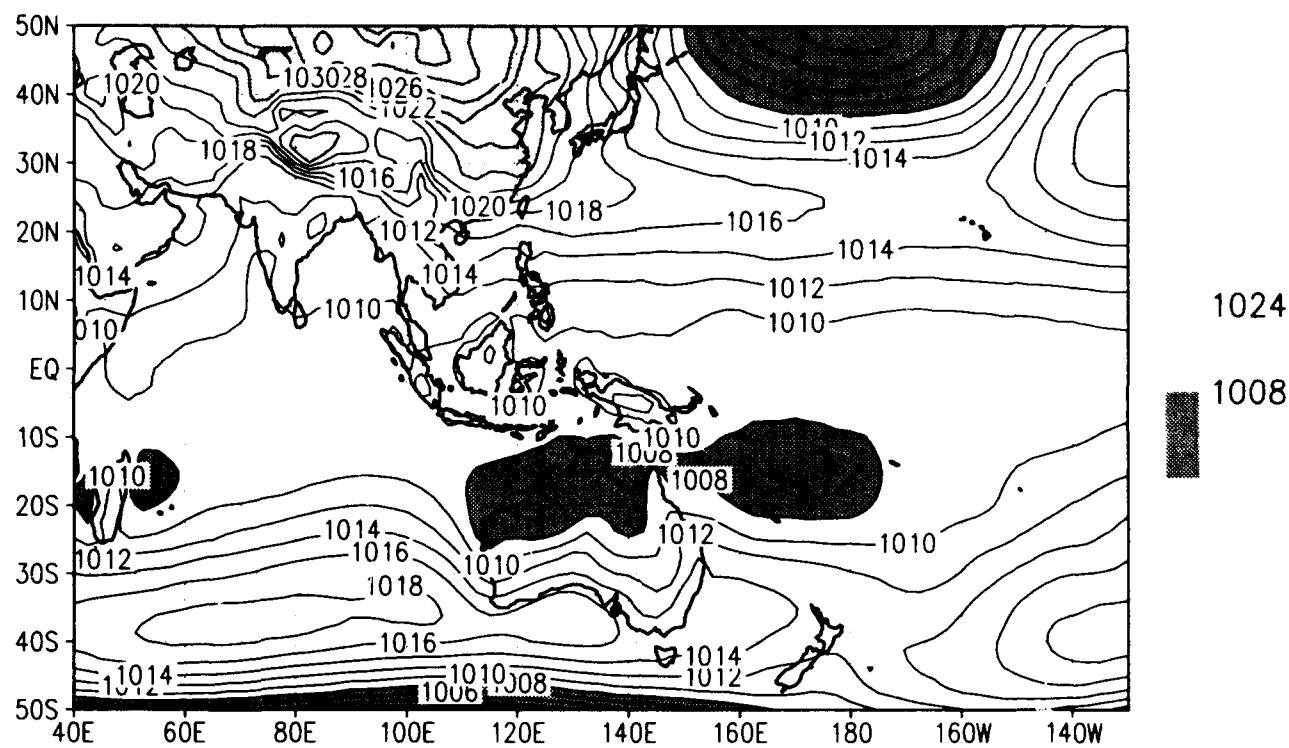
SLP climo for FEB 1993
 /d2/toga_coare/c.gs
 NOGAPS



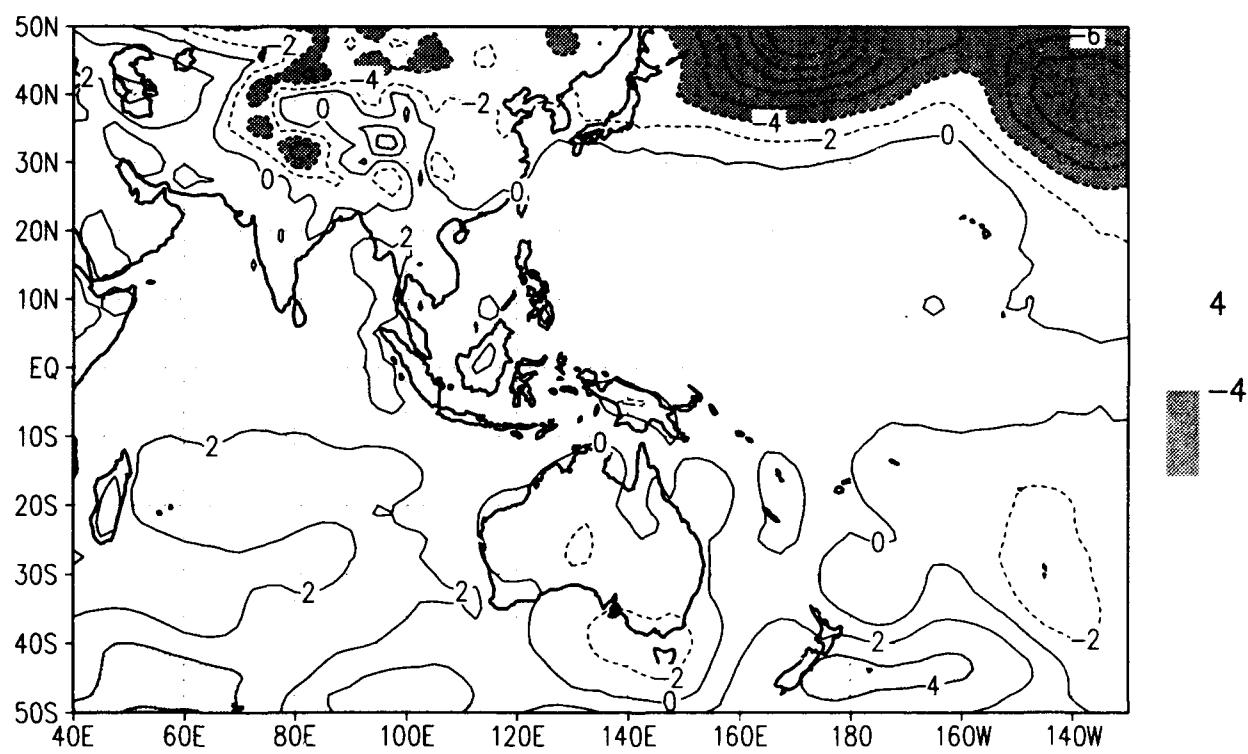
MRF



SLP climo for FEB 1993
/d2/toga_coare/c.gs
ECMWF Climatology

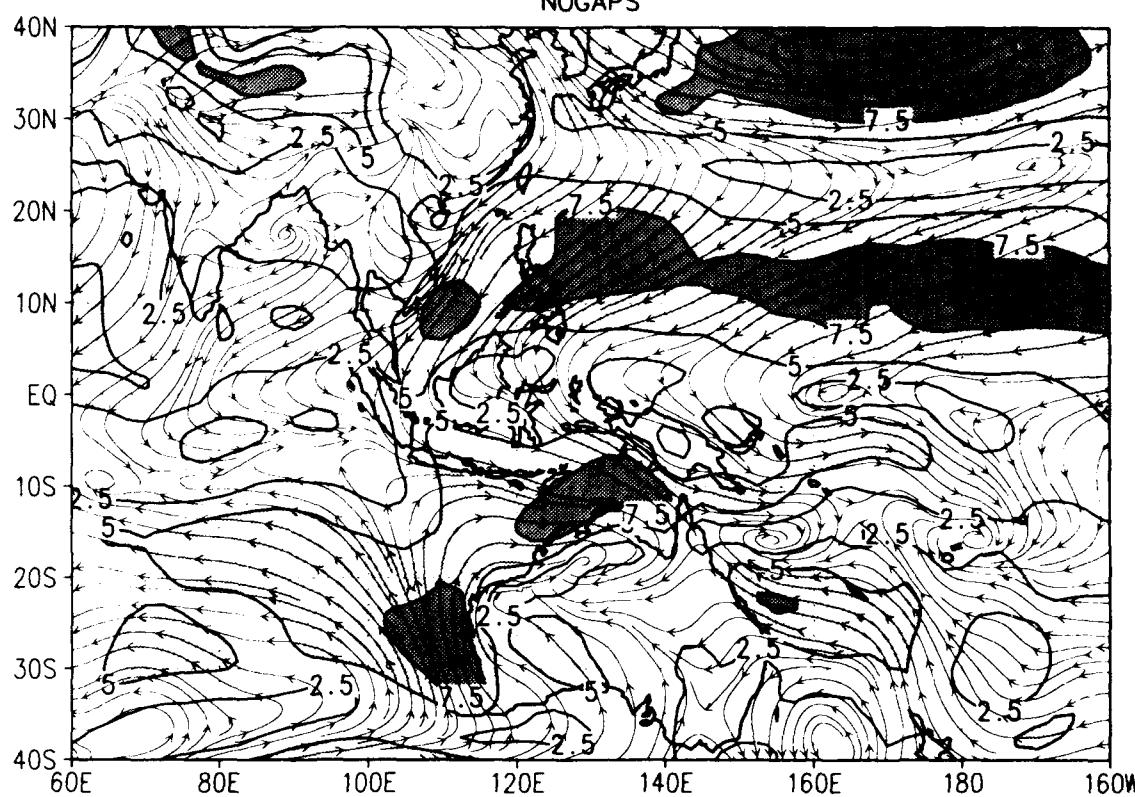


pooled anomaly



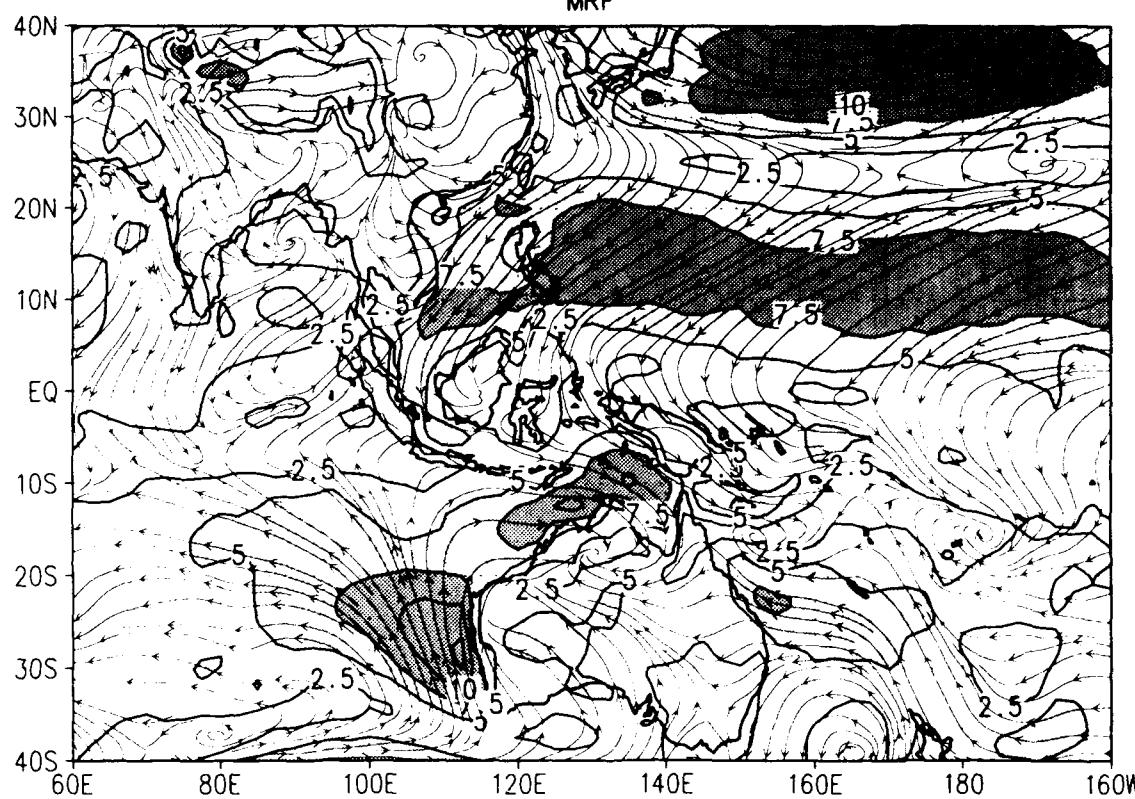
Sfc wind climo for FEB 1993
/d2/toga_coare/c.gs

NOGAPS



7.5
5

MRF

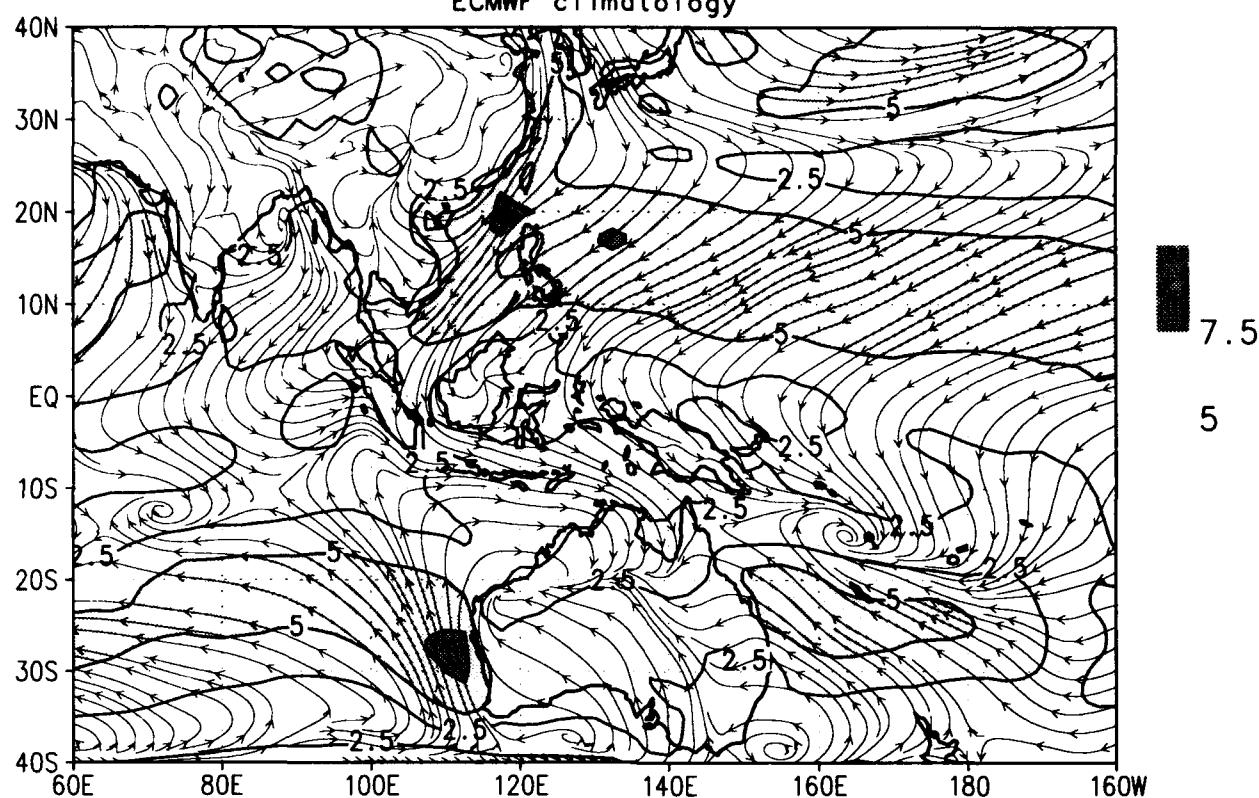


7.5
5

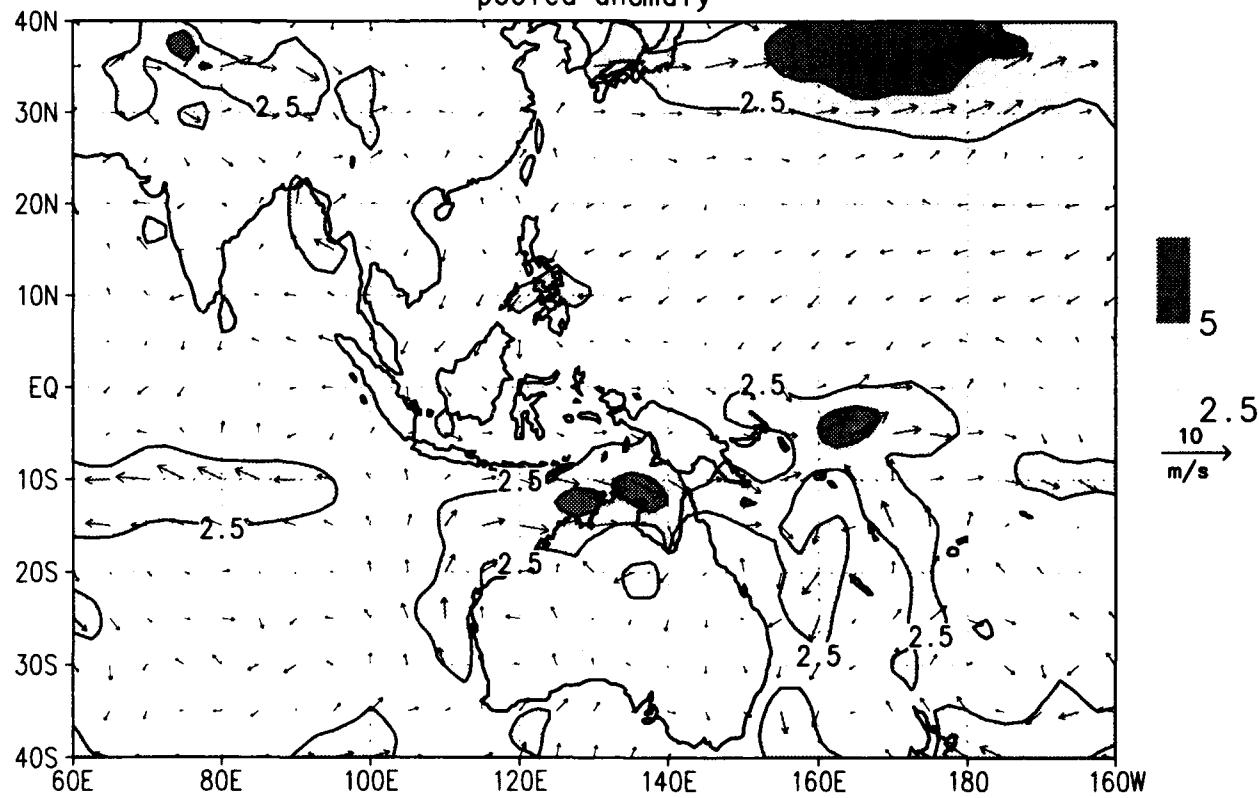
Sfc wind climo for FEB 1993

/d2/toga_coare/c.gs

ECMWF climatology

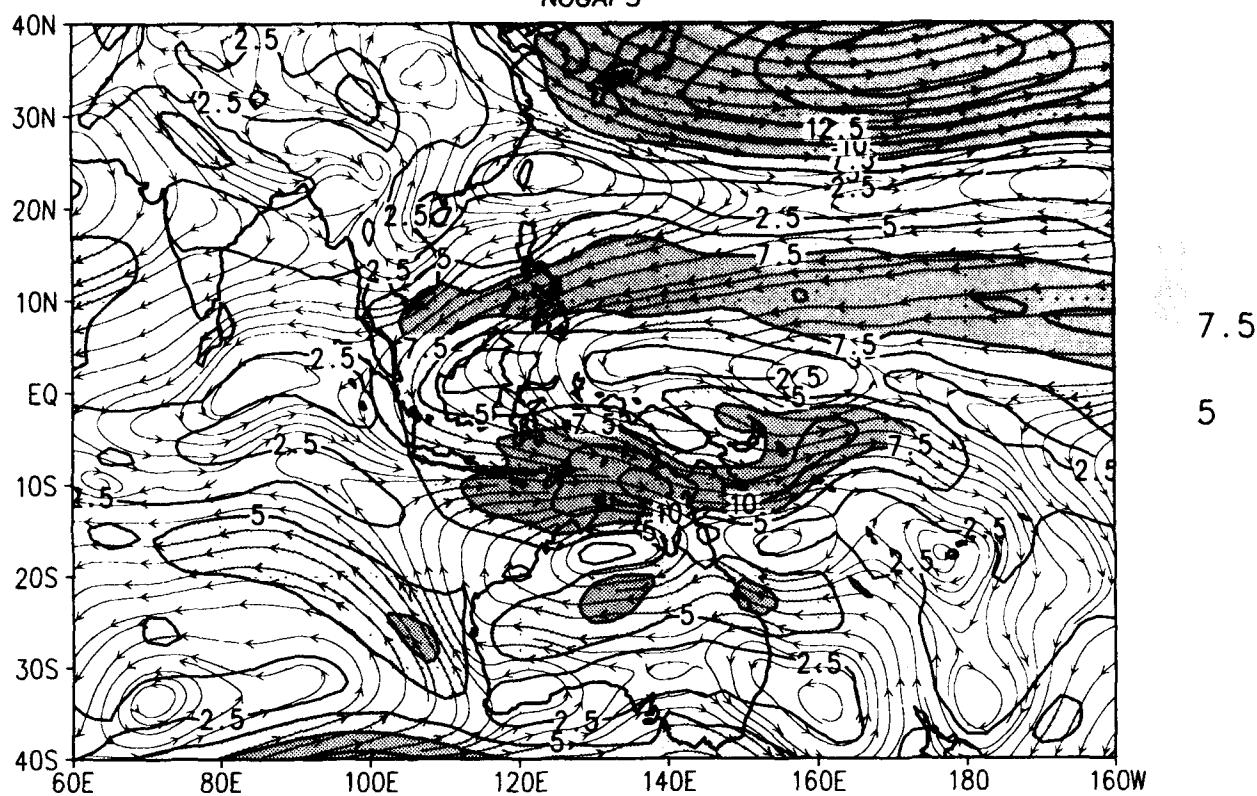


pooled anomaly

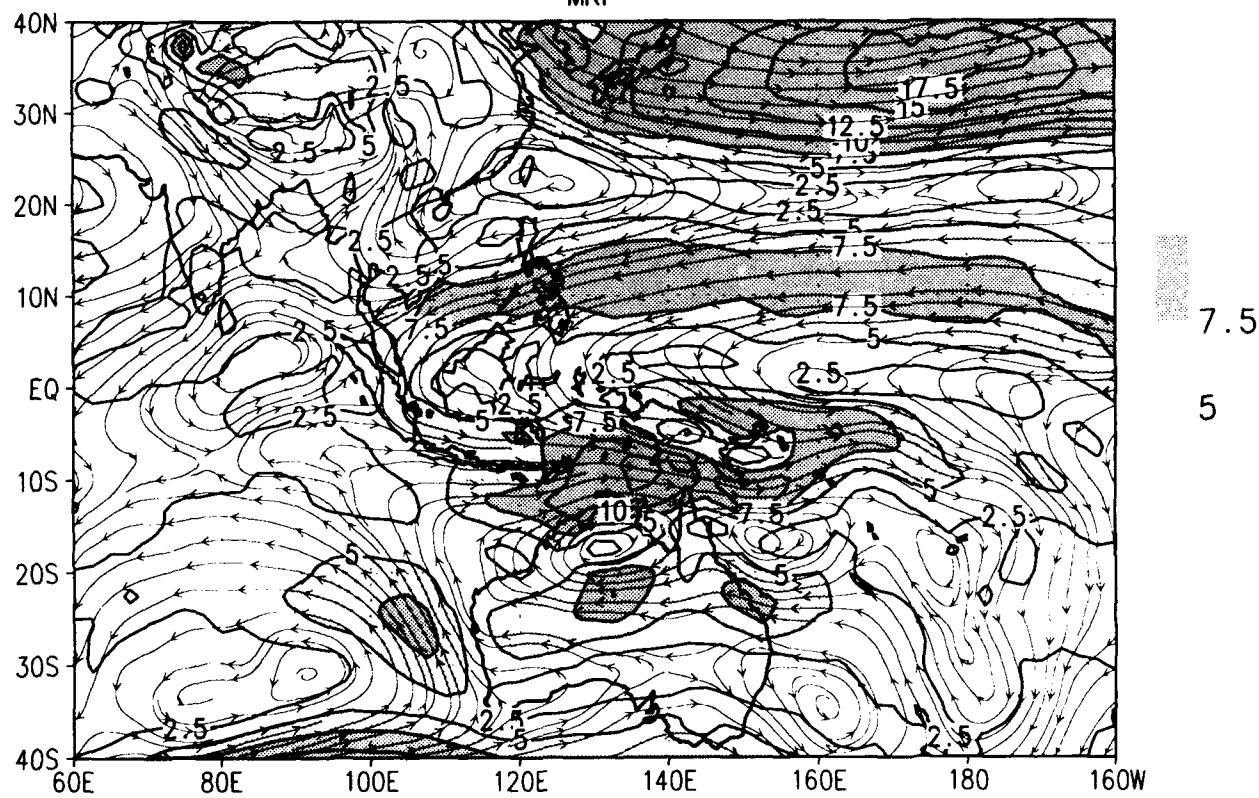


850 mb wind climo for FEB 1993
/d2/toga_coare/c.gs

NOGAPS

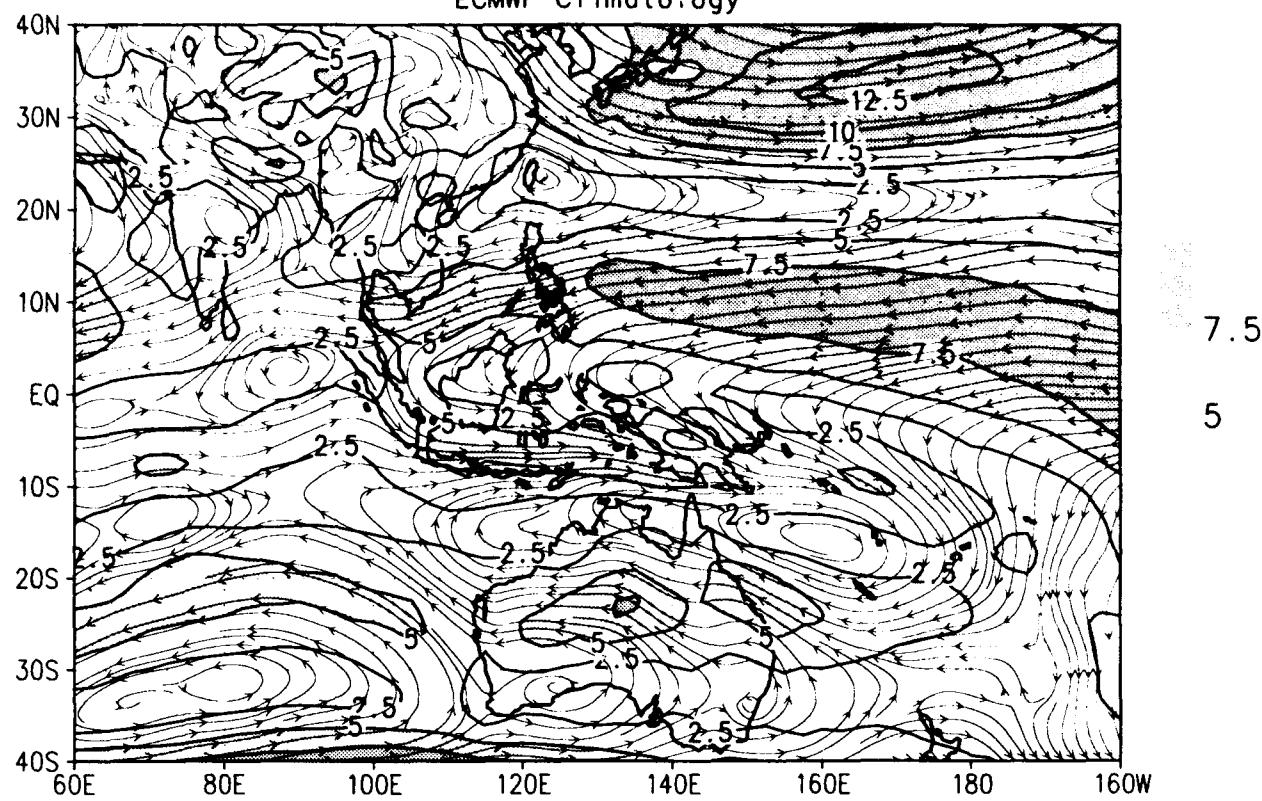


MRF

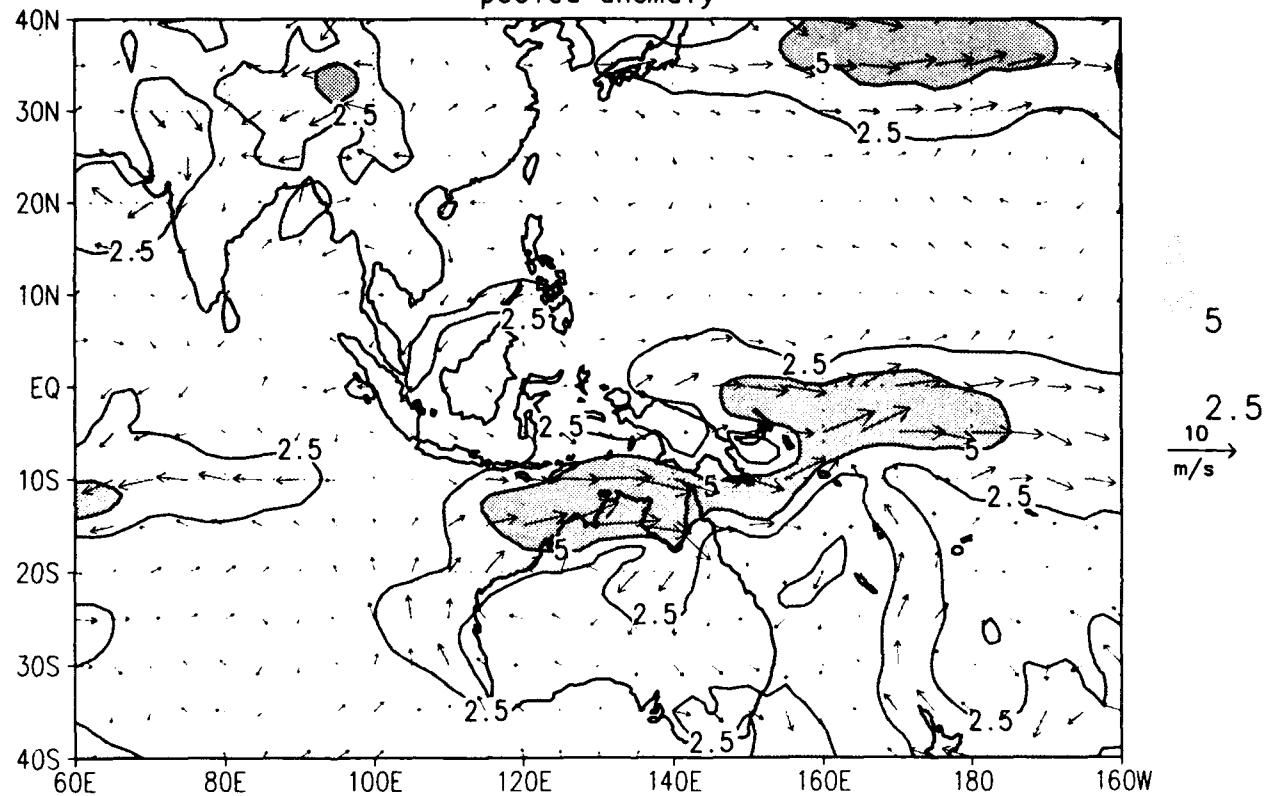


850 mb wind climo for FEB 1993
 /d2/toga_coare/c.gs

ECMWF Climatology

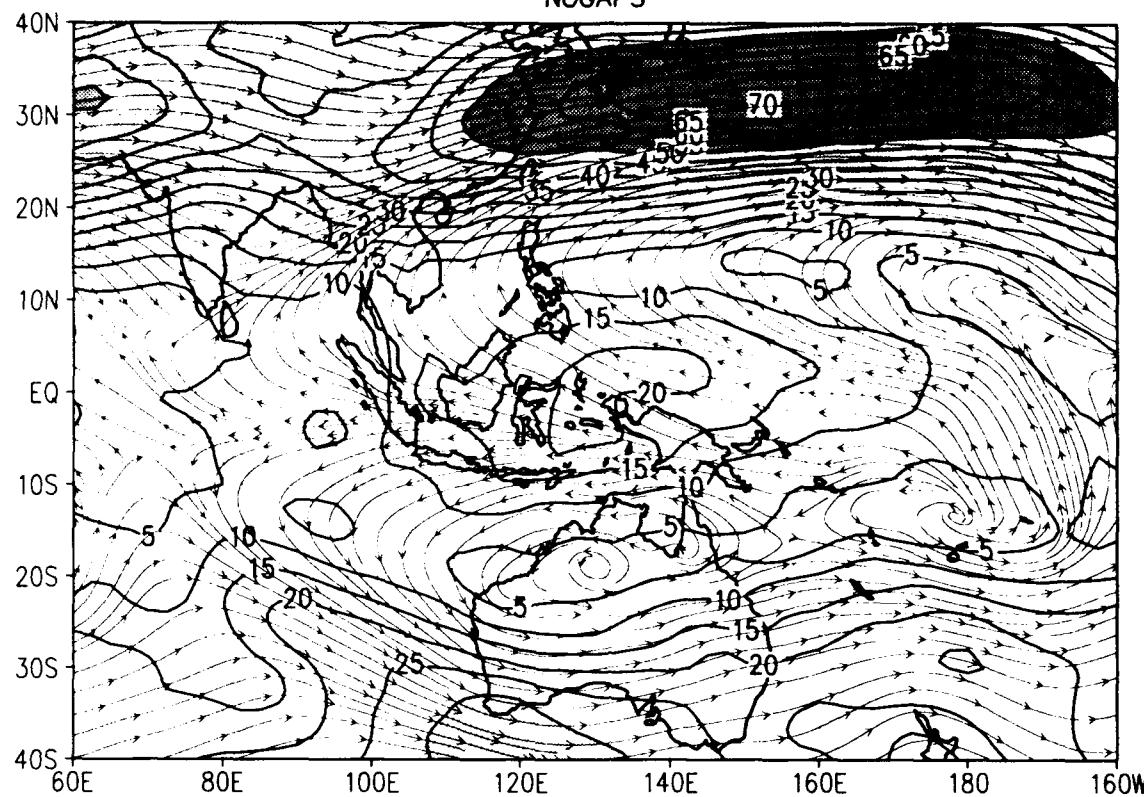


pooled anomaly

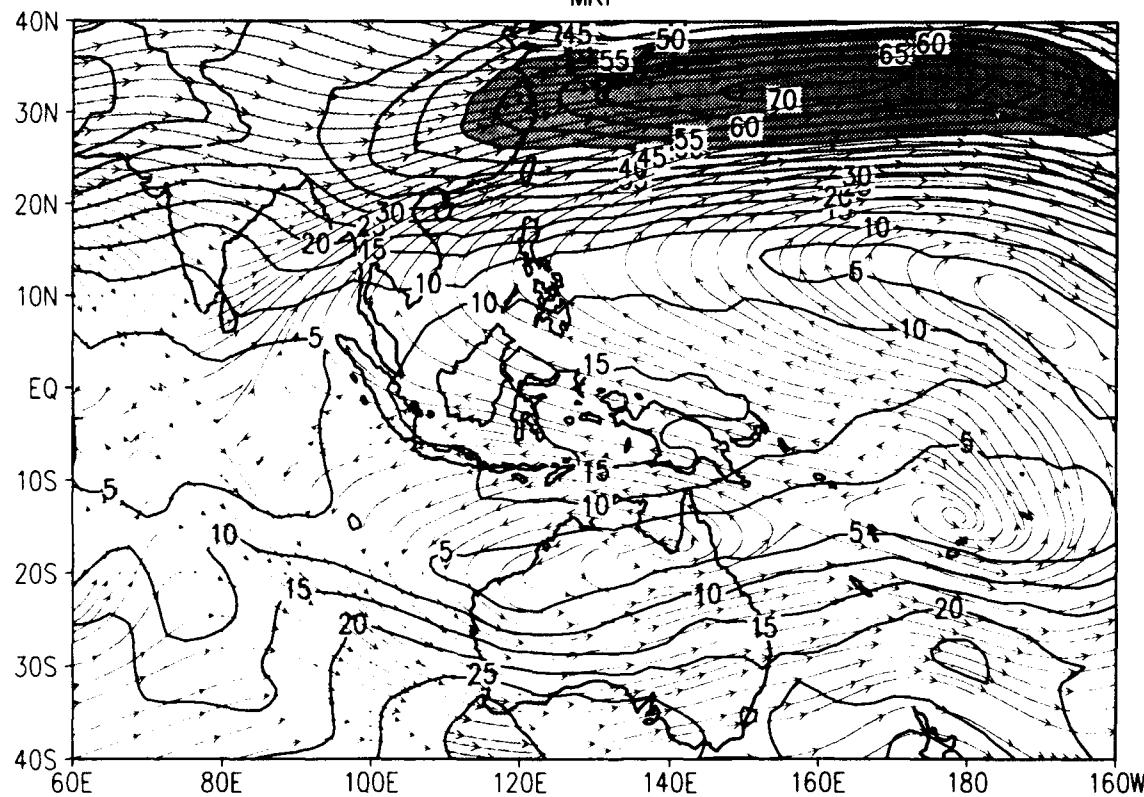


200 mb wind climo for FEB 1993
/d2/toga_coare/c.gs

NOGAPS

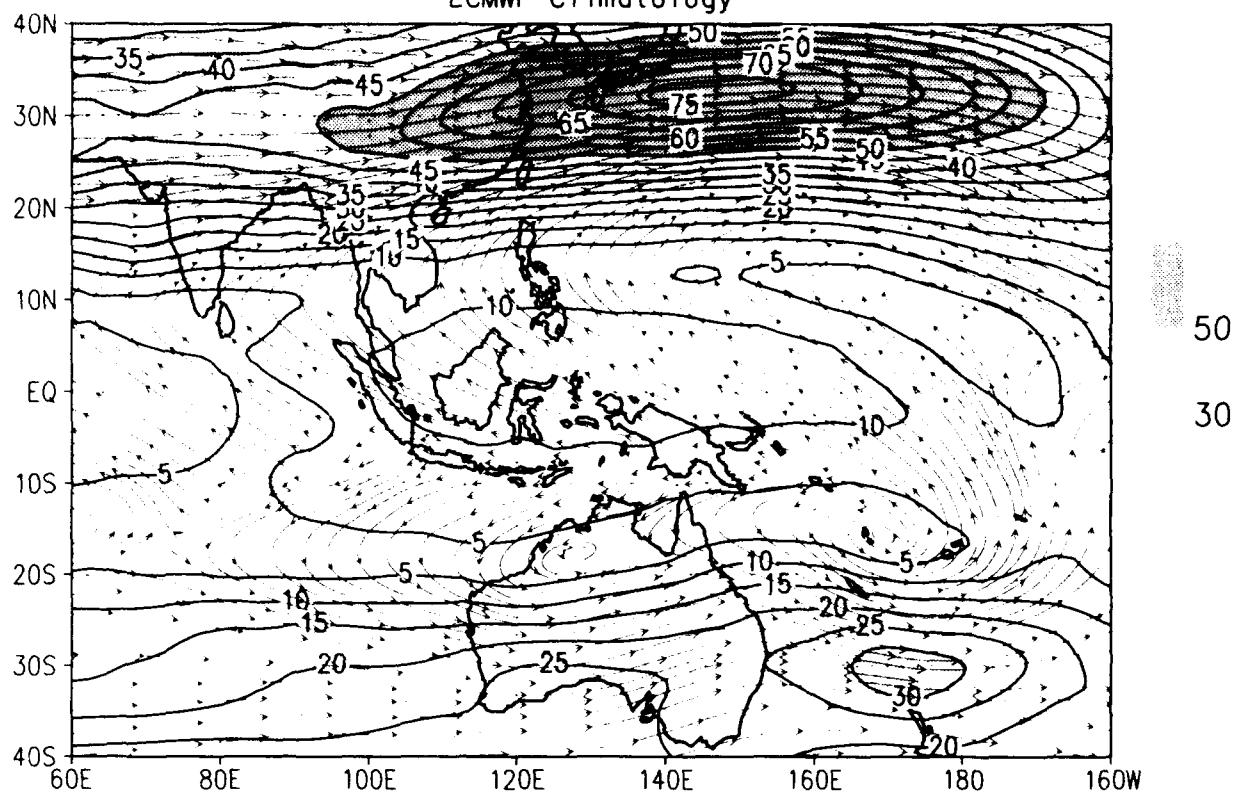


MRF

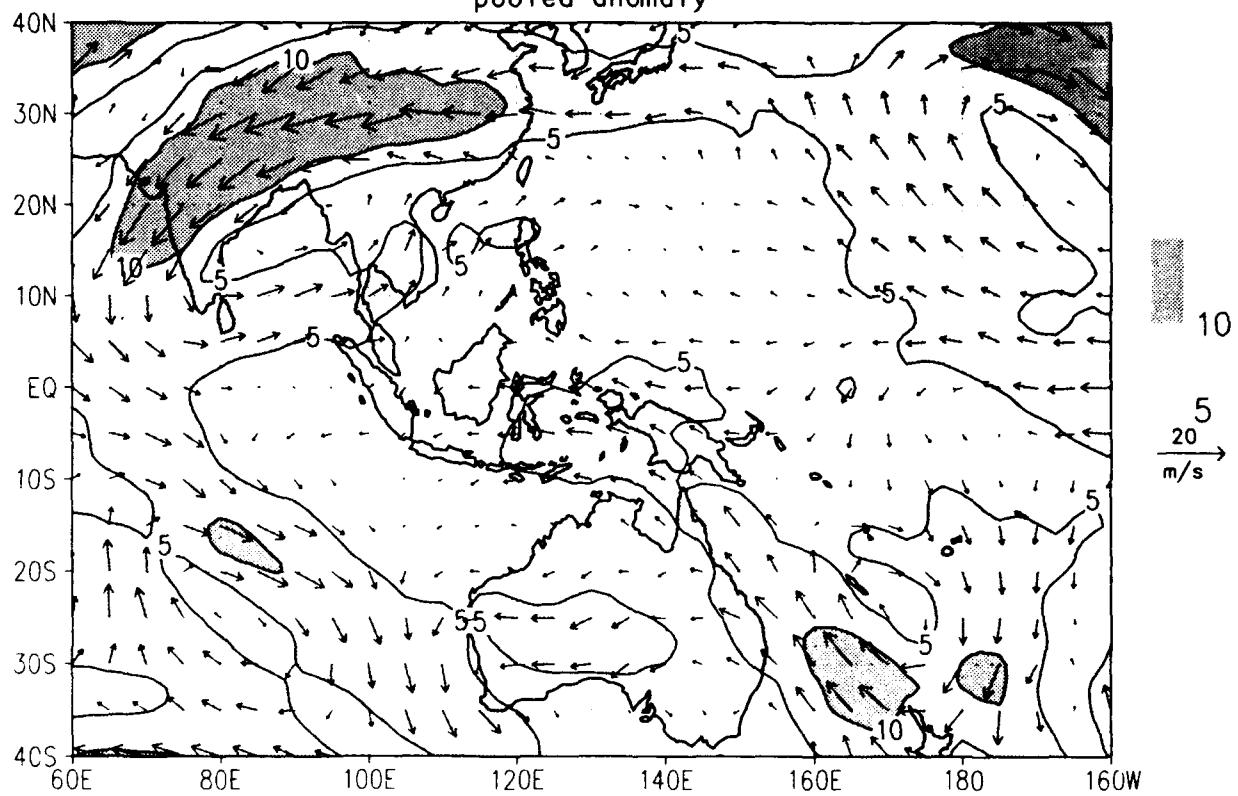


200 mb wind climo for FEB 1993
 /d2/toga_coare/c.gs

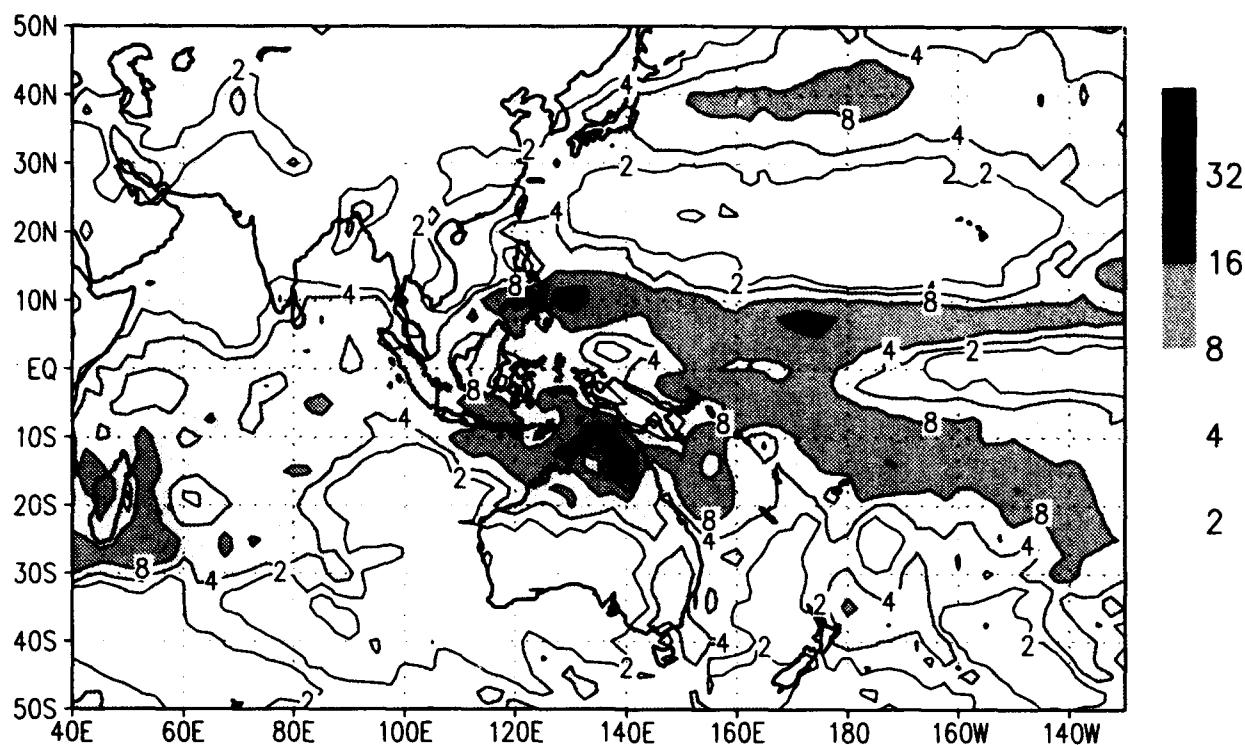
ECMWF Climatology



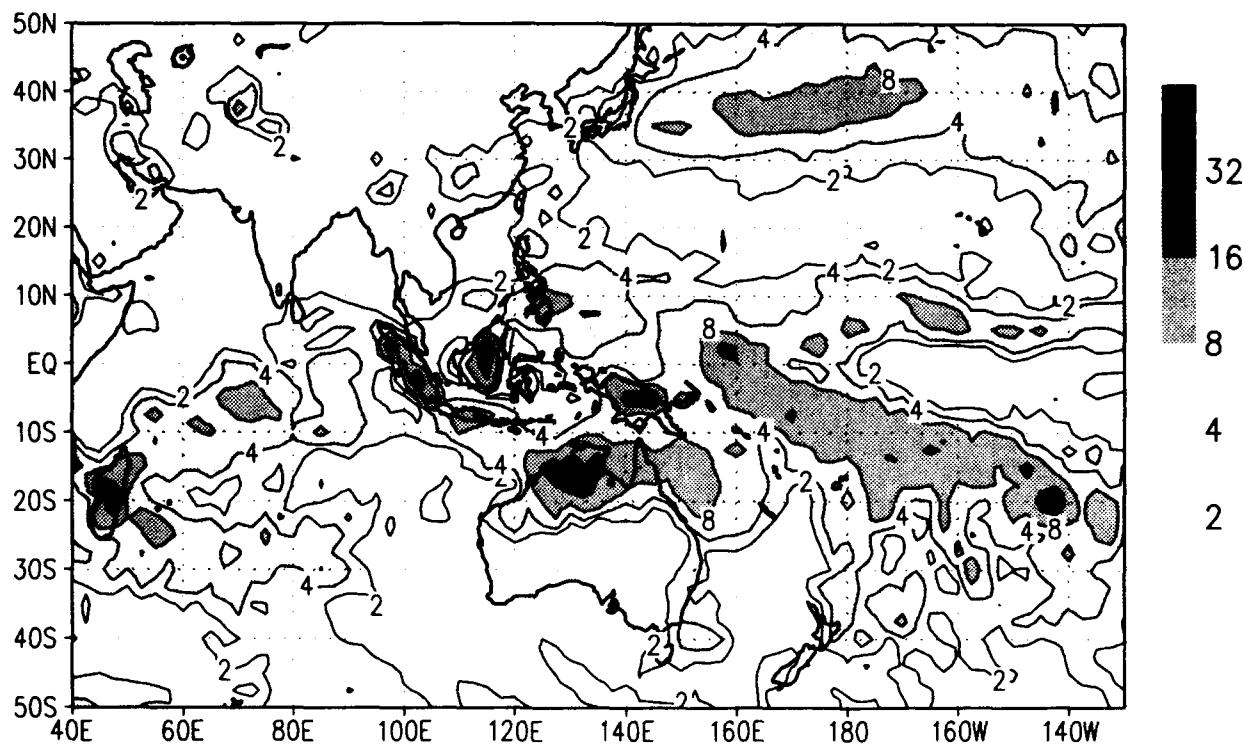
pooled anomaly



precip climo for FEB 1993
/d2/toga_coare/c.gs
NOGAPS



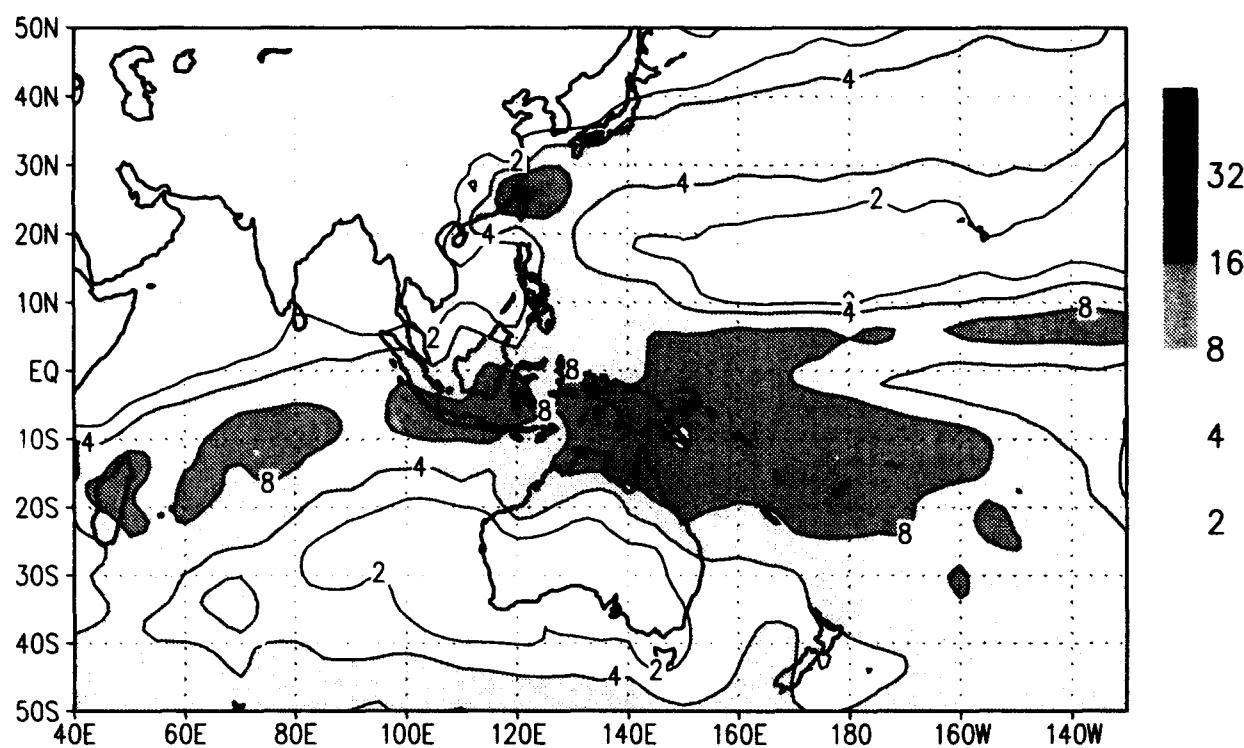
MRF



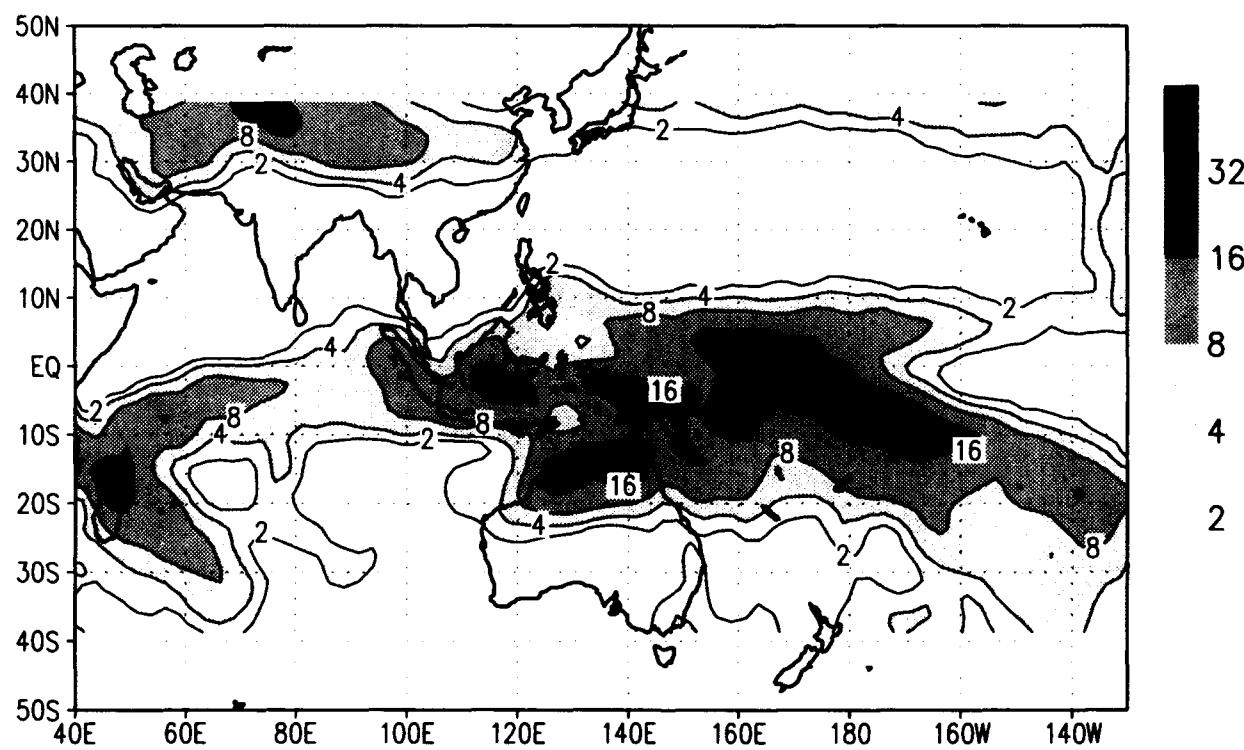
precip climo for FEB 1993

/d2/toga_coare/c.gs

msu_merged climo



Prelim GPI



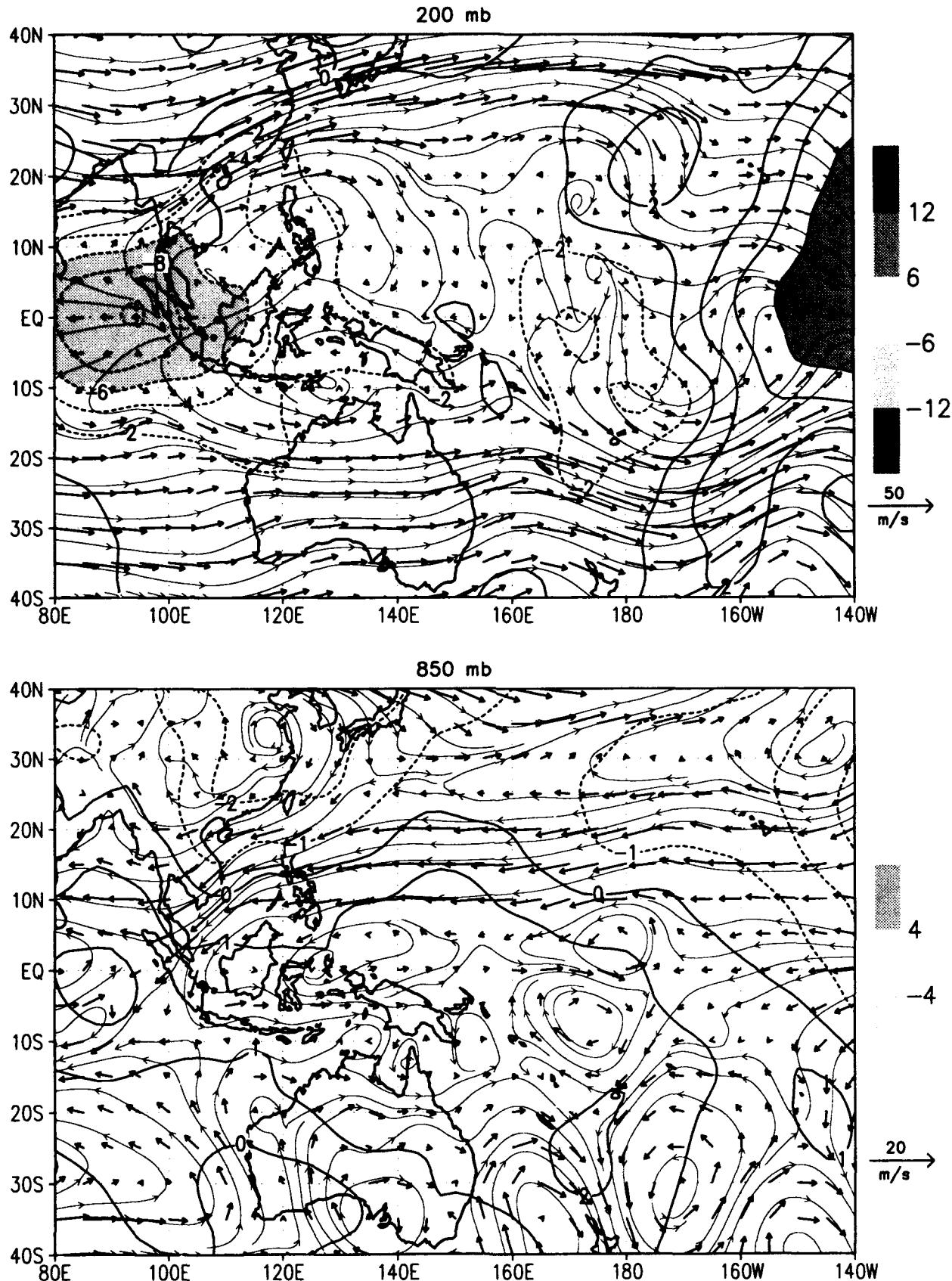
11 NOGAPS and MRF Pentads for Dec 92 - Feb 93

Two charts are given for each five-day period, or pentad, from December 1992 through February 1993: 1) flow and velocity potential at 200 and 850 mb; and 2) the 5-day average of the NOGAPS precipitation and the corresponding GPI estimate. Areas of negative chi indicate divergence (upward motion at 200 mb) and are shaded according to the grey-shade bar.

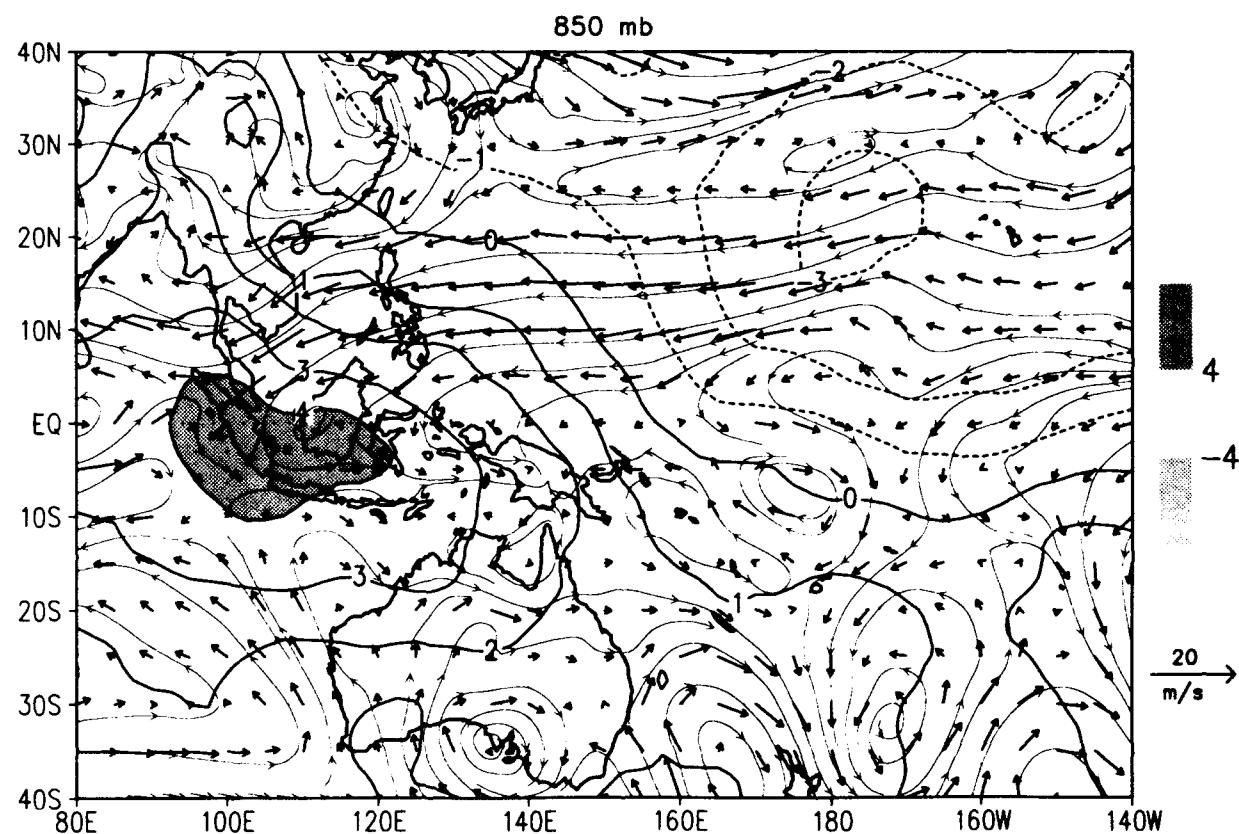
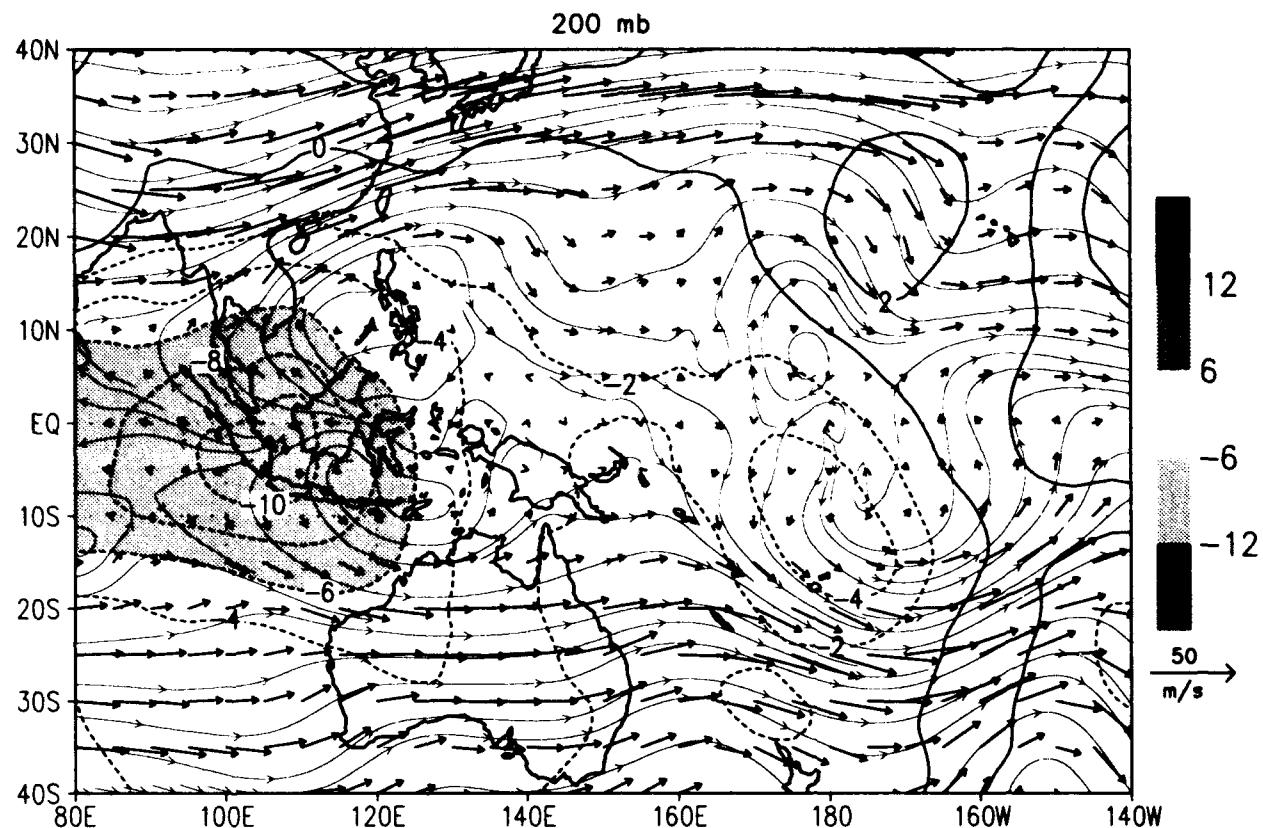
These charts can be used to follow the evolution of the upper level flow as the two ISOs pass through the IFA. In particular, follow the eastward propagation of an area of 200 mb divergence starting 12 January 1993 in the Indian Ocean. By 27 January 1993, this divergence region has intensified and is centered over New Guinea. A similar propagation is found in the GPI rainfall data. The relationship between upper level divergence and the GPI estimates is fairly good, but is less distinct in the model precipitation where we find smaller-scale features.

Chart	Description
1	- 200 and 850 mb flow and velocity potential for NOGAPS; 5-day average centered around 12 UTC 2 Dec 1992
2	- 200 and 850 mb flow and velocity potential for MRF; 5-day average centered around 12 UTC 2 Dec 1992
3	- 12-h NOGAPS precipitation; 5-day average centered around 12 UTC 2 Dec 1992 and corresponding pentad from GPI
4	- 12-h MRF precipitation; 5-day average centered around 12 UTC 2 Dec 1992 and corresponding pentad from GPI
5-8	- same as 1-4 except for 12 UTC 7 Dec 1992
9-12	- same as 1-4 except for 12 UTC 17 Dec 1992
13-16	- same as 1-4 except for 12 UTC 22 Dec 1992
17-20	- same as 1-4 except for 12 UTC 27 Dec 1992
21-24	- same as 1-4 except for 12 UTC 2 Jan 1993
25-28	- same as 1-4 except for 12 UTC 7 Jan 1993
29-32	- same as 1-4 except for 12 UTC 12 Jan 1993
33-36	- same as 1-4 except for 12 UTC 17 Jan 1993
37-40	- same as 1-4 except for 12 UTC 22 Jan 1993
41-44	- same as 1-4 except for 12 UTC 27 Jan 1993
45-48	- same as 1-4 except for 12 UTC 2 Feb 1993
49-52	- same as 1-4 except for 12 UTC 7 Feb 1993
53-56	- same as 1-4 except for 12 UTC 12 Feb 1993
57-60	- same as 1-4 except for 12 UTC 17 Feb 1993
61-64	- same as 1-4 except for 12 UTC 22 Feb 1993
65-68	- same as 1-4 except for 12 UTC 27 Feb 1993

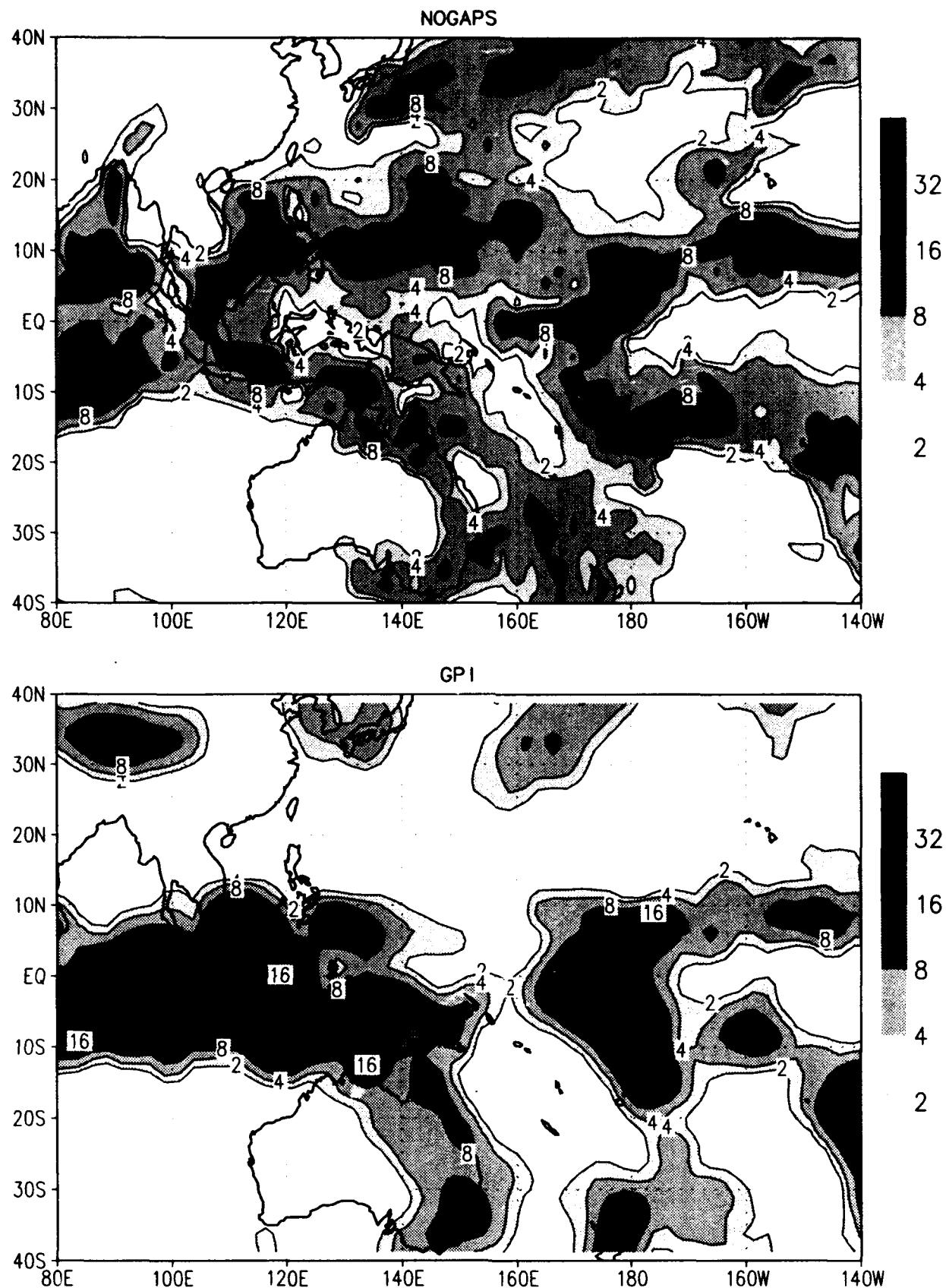
NOGAPS 5-day ave flow and chi ~ 02 DEC 1992
wind (m/s) chi ($1e6\text{ m}^2/\text{s}$) /d2/toga_coare/d5.gs



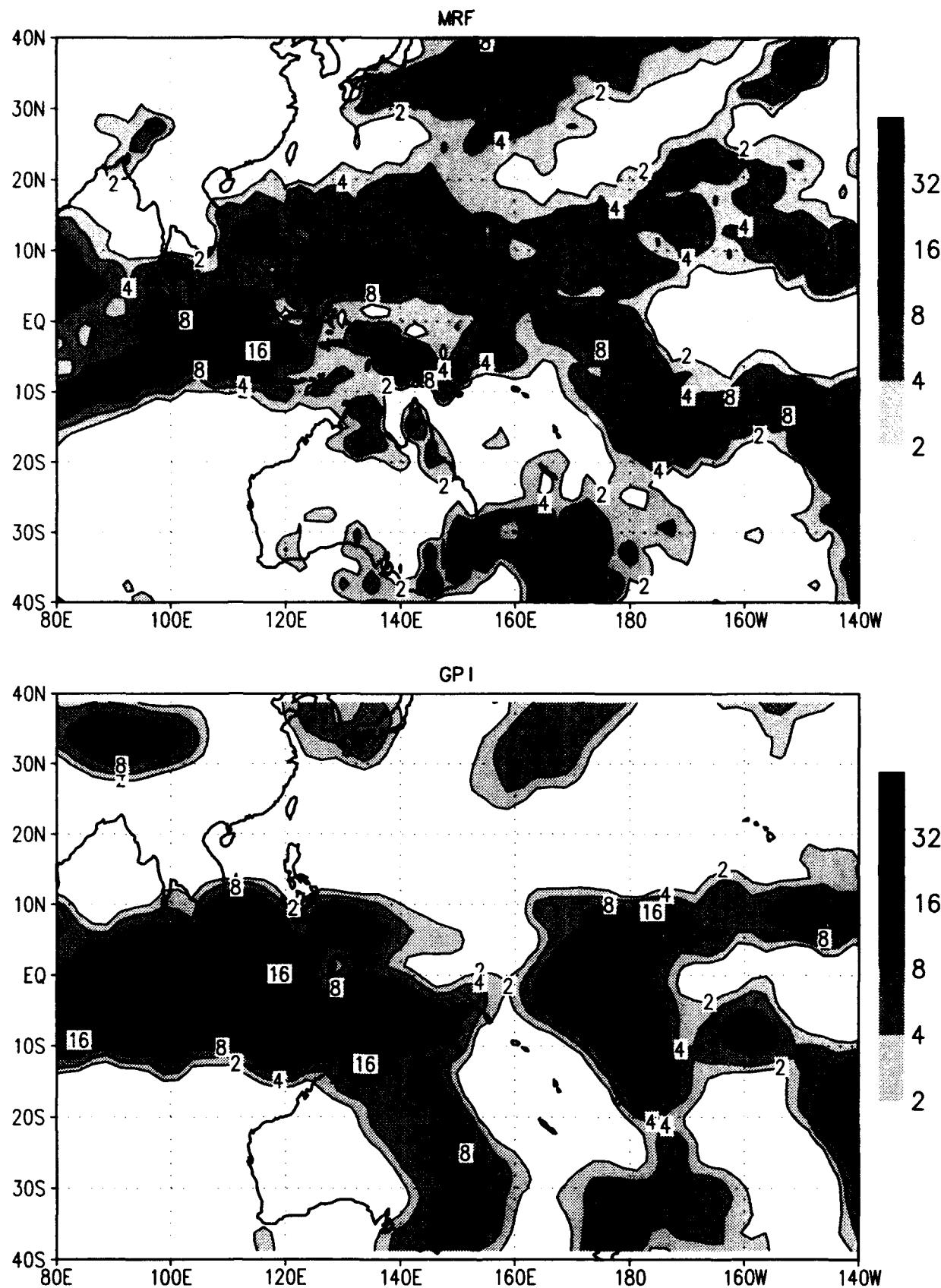
MRF 5-day ave flow and chi ~ 02 DEC 1992
wind (m/s) chi ($10^6 \text{ m}^2/\text{s}$) /d2/toga_coare/d5.gs



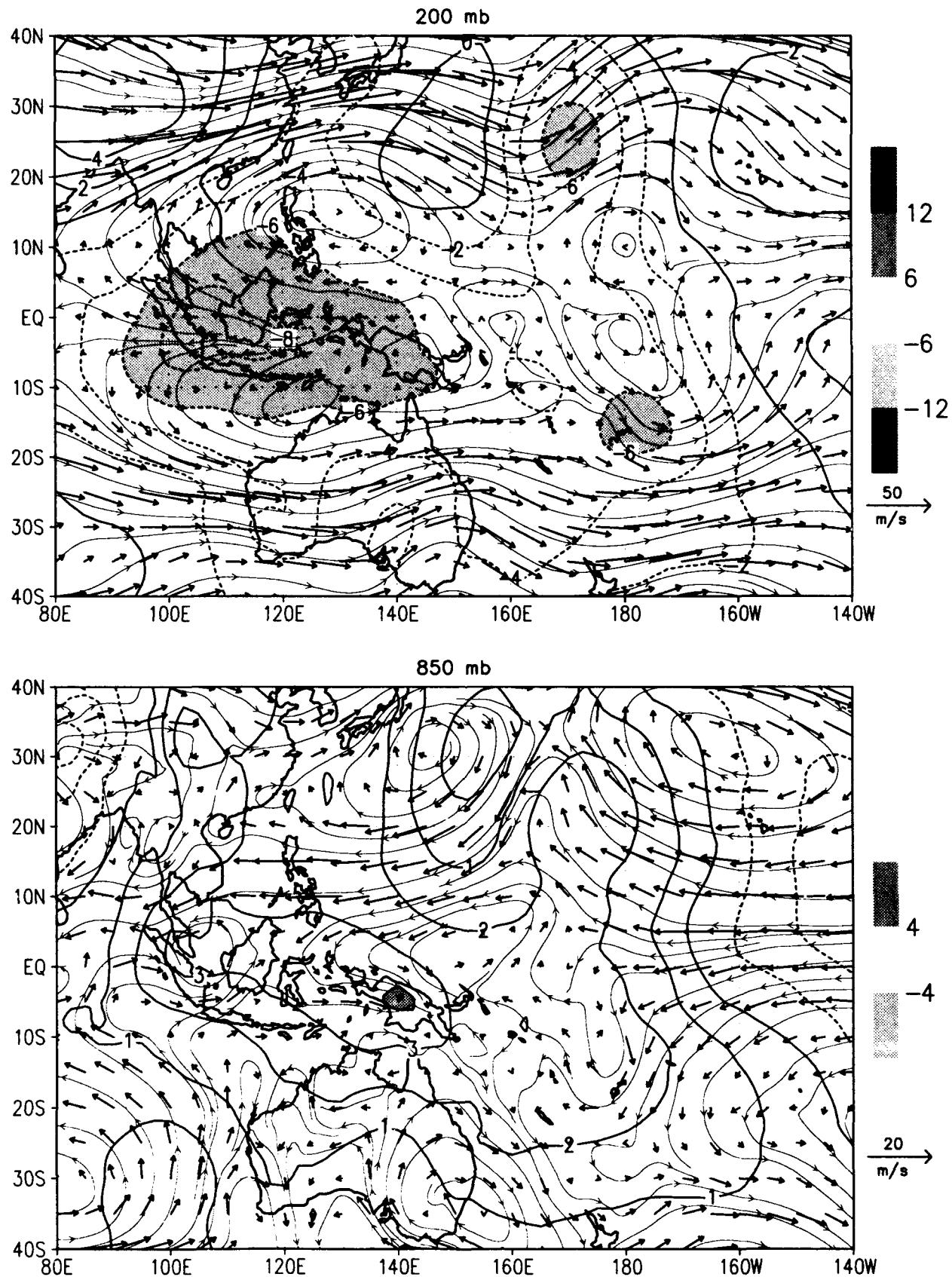
NOGAPS and GPI 5-day ave Precip ~ 02 DEC 1992
(mm/day) /d2/toga_coare/d5.gs



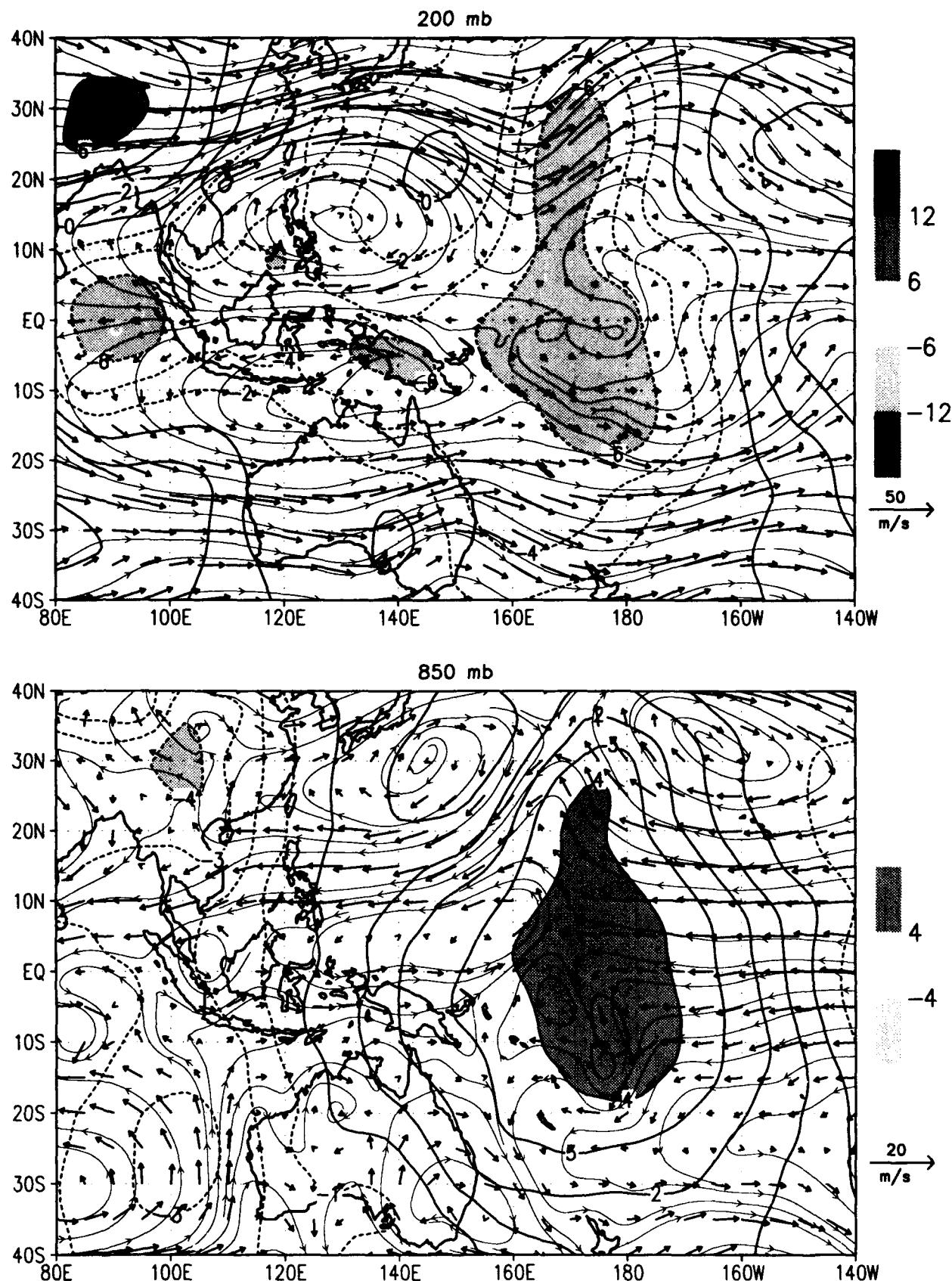
MRF and GPI 5-day ave Precip ~ 02 DEC 1992
(mm/day) /d2/toga_coare/d5.gs



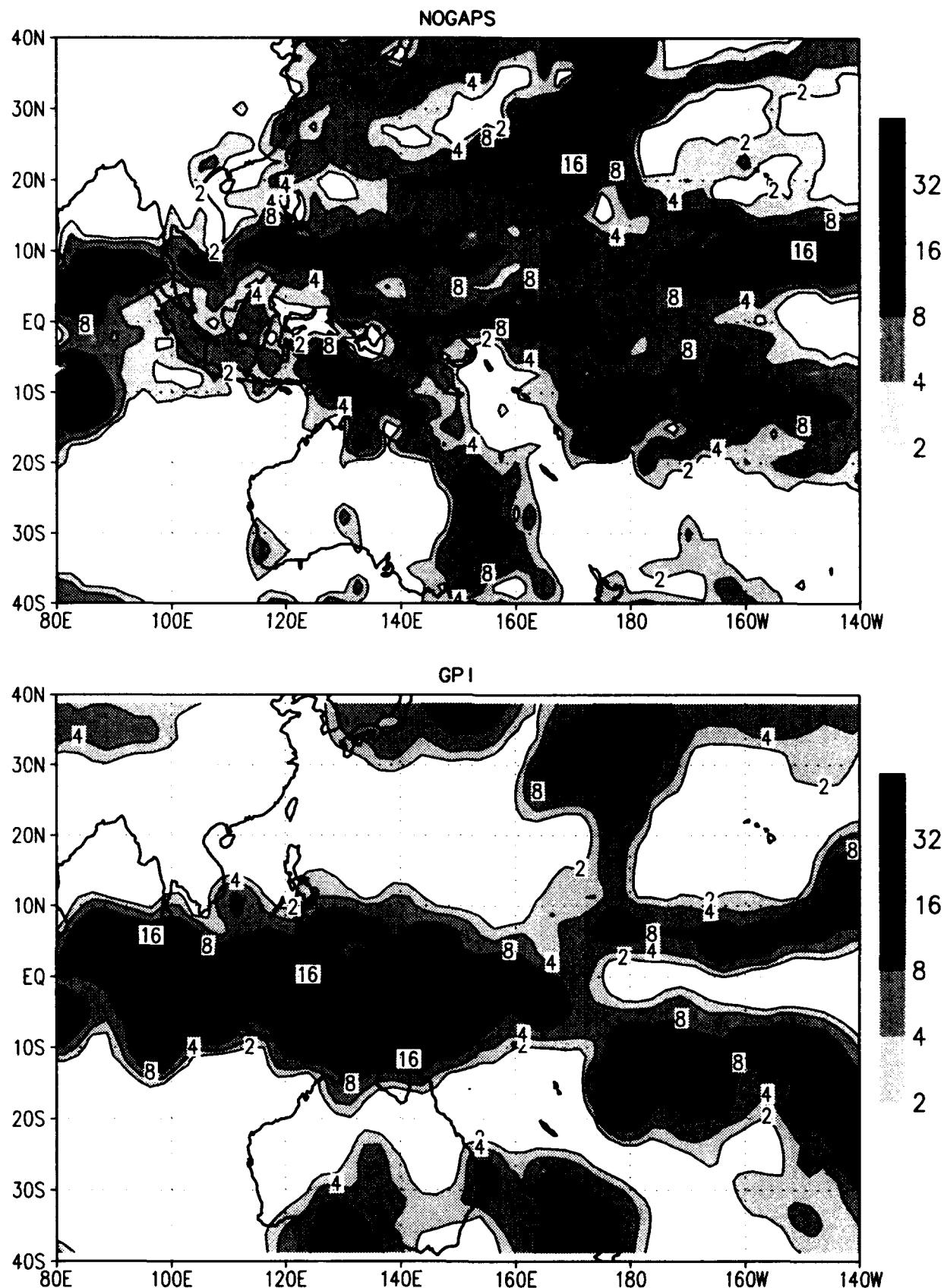
MRF 5-day ave flow and chi ~ 07 DEC 1992
 wind (m/s) chi ($10^6 \text{ m}^2/\text{s}$) /d2/toga_coare/d5.gs



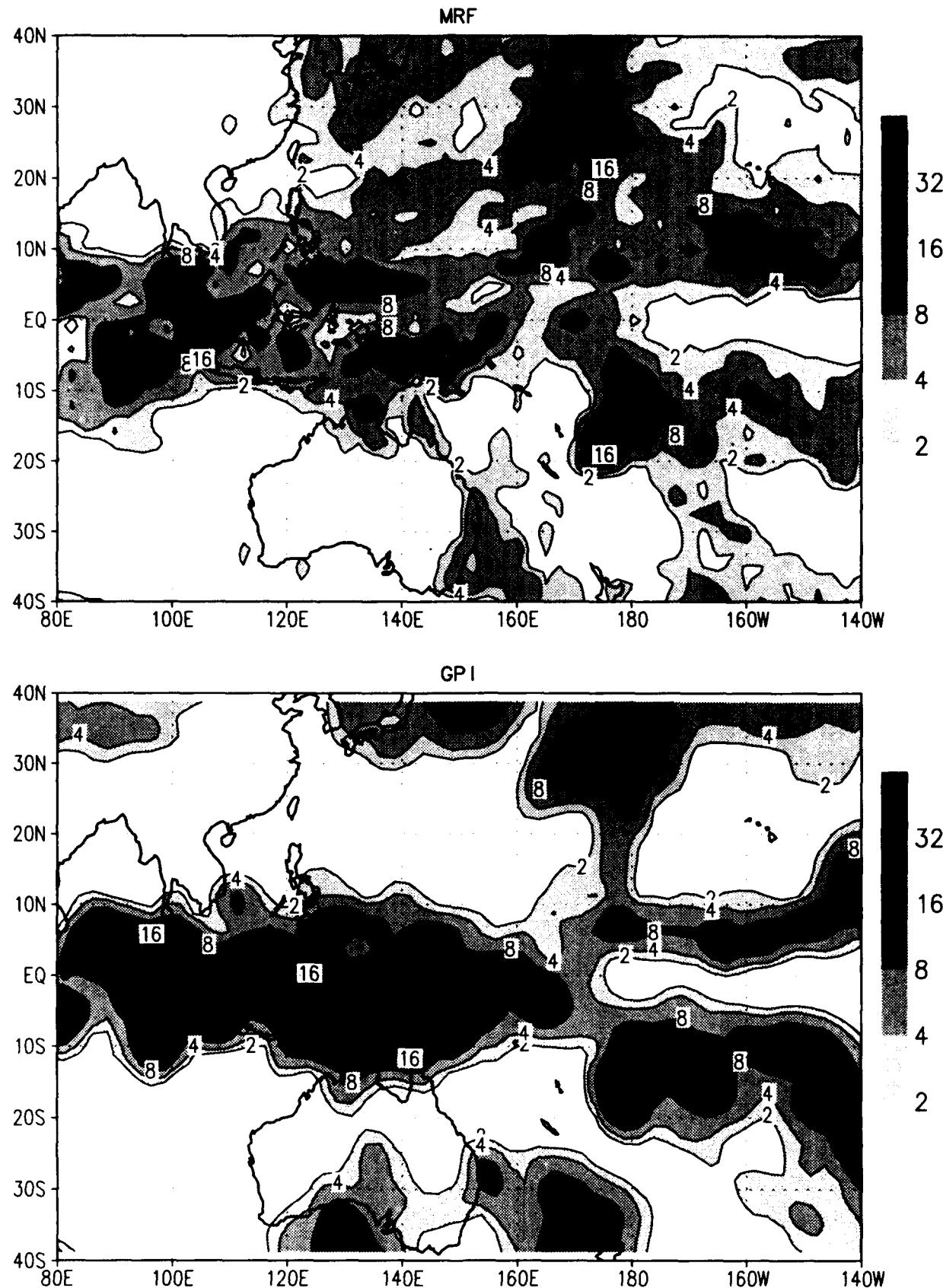
NOGAPS 5-day ave flow and chi ~ 07 DEC 1992
wind (m/s) chi ($1e6\text{ m}^2/\text{s}$) /d2/toga_coare/d5.gs



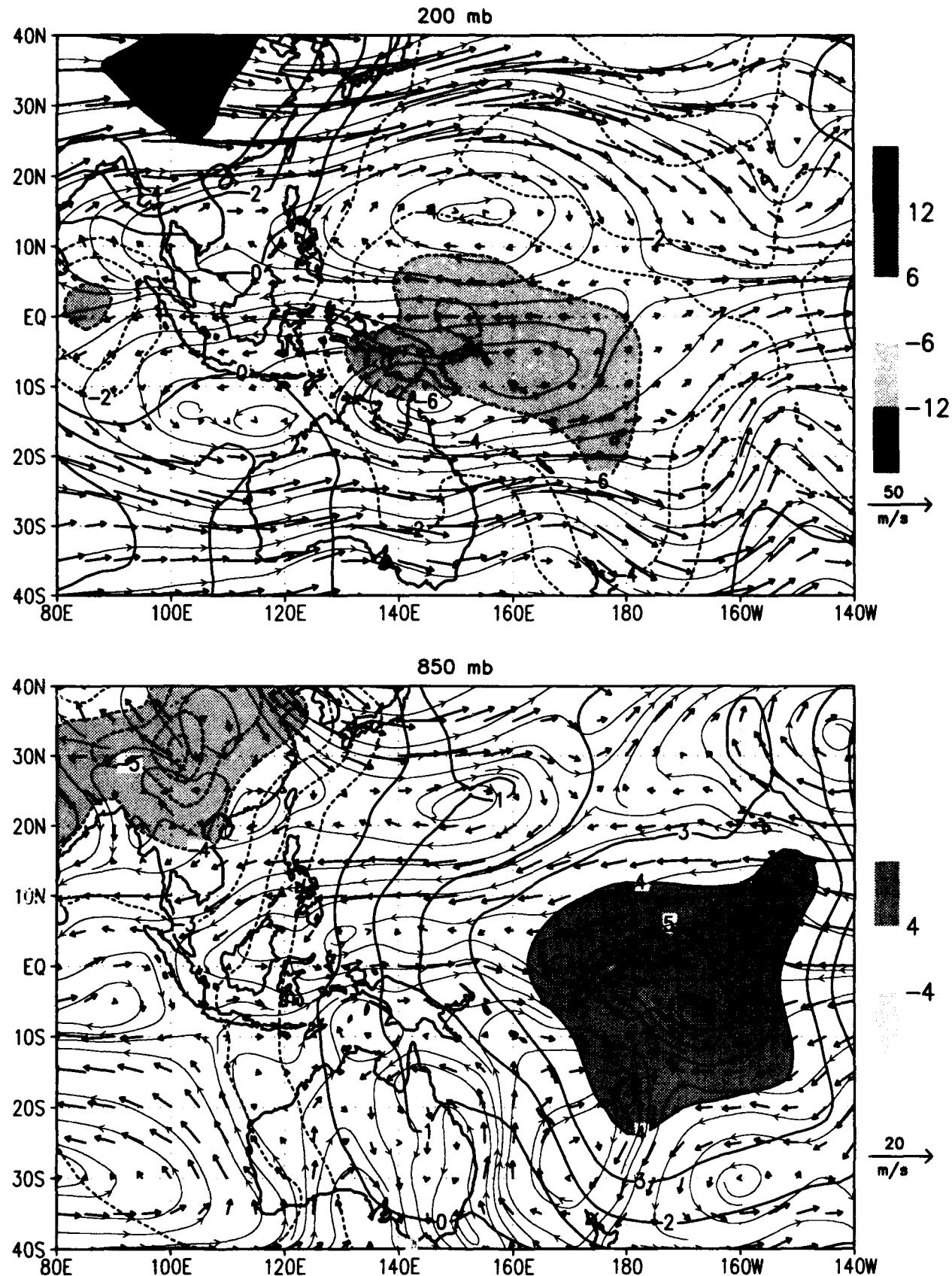
NOGAPS and GPI 5-day ave Precip ~ 07 DEC 1992
(mm/day) /d2/toga_coare/d5.gs



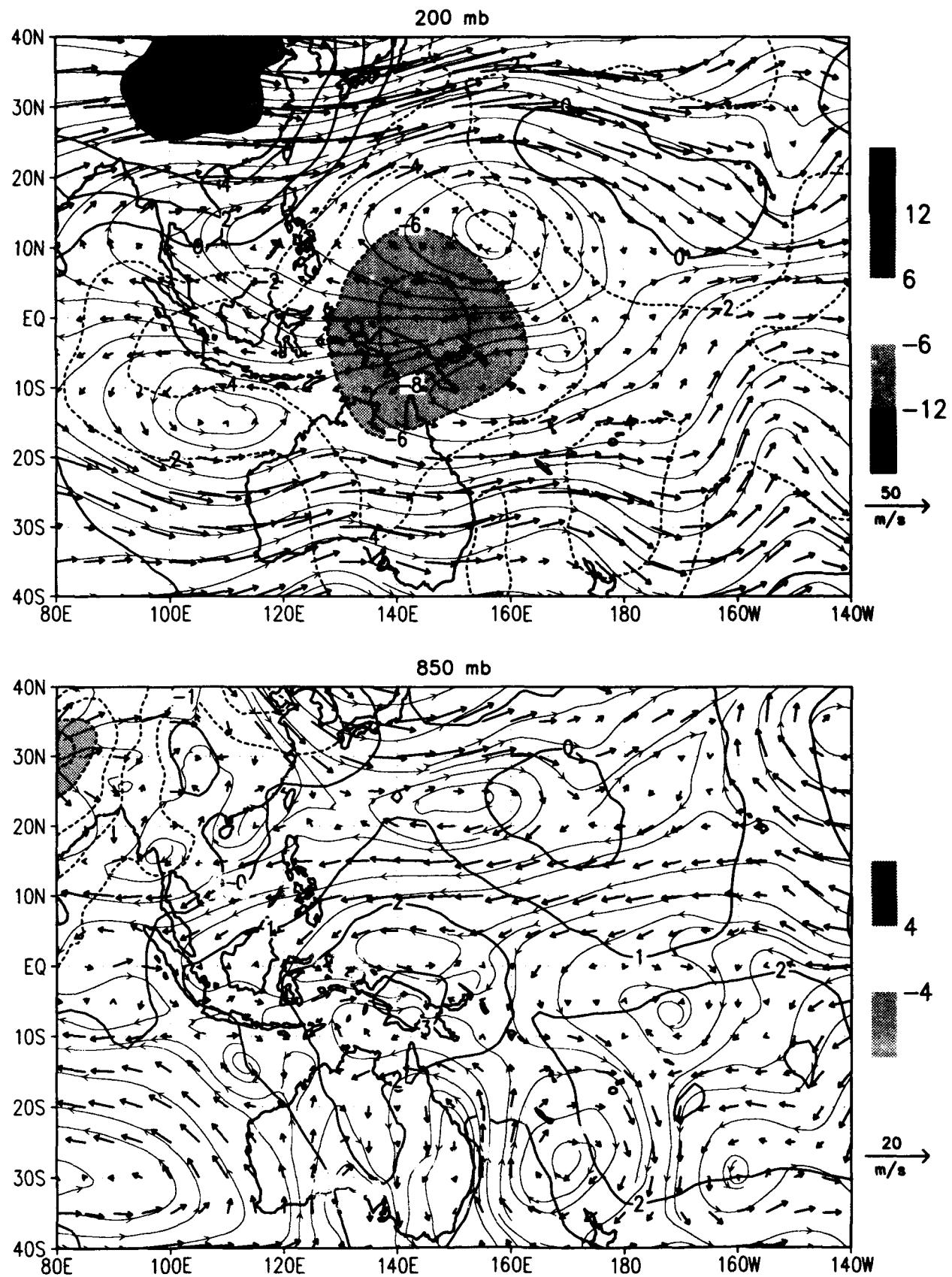
MRF and GPI 5-day ave Precip ~ 07 DEC 1992
(mm/day) /d2/toga_coare/d5.gs



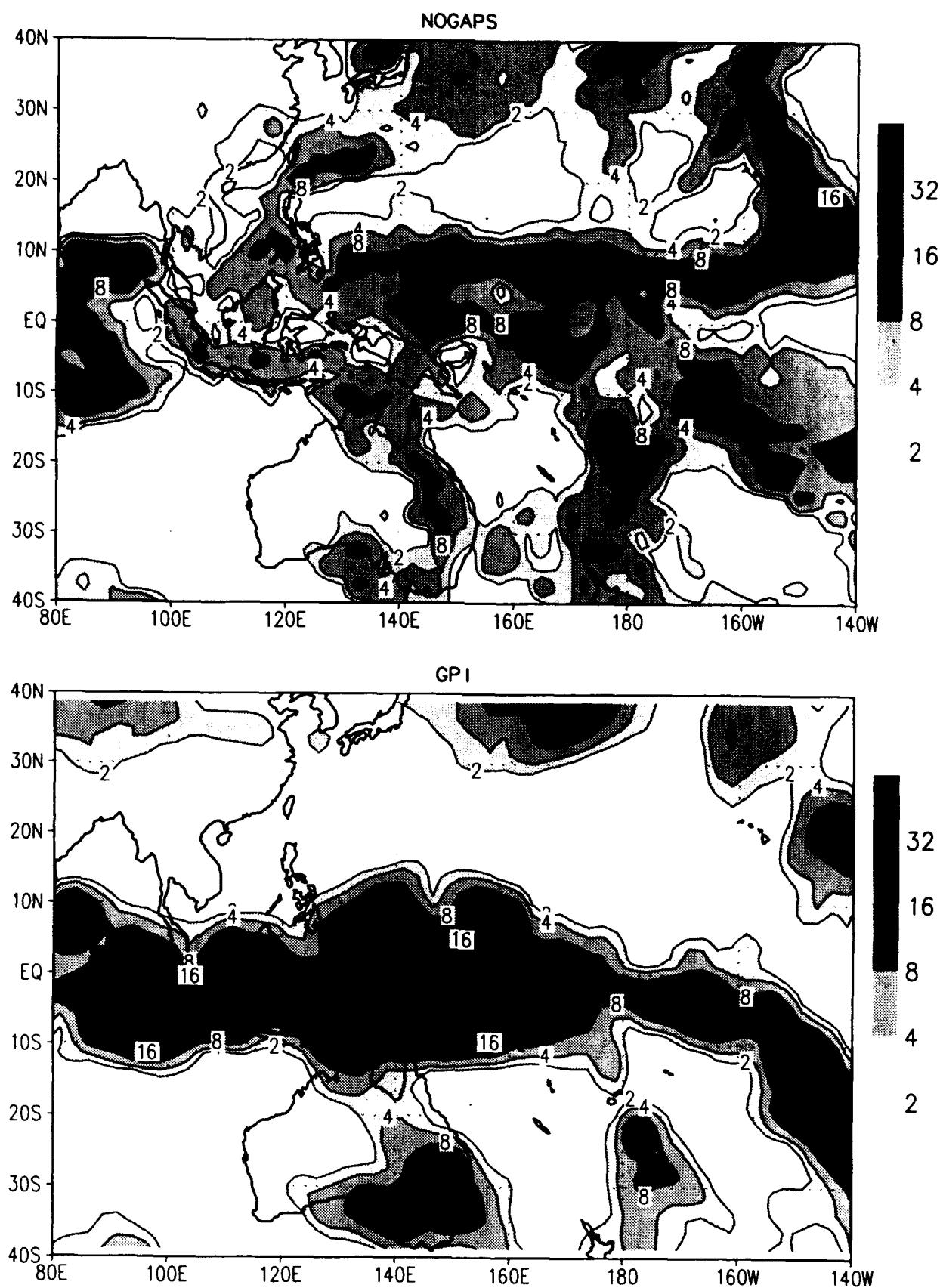
NOGAPS 5-day ave flow and chi ~ 12 DEC 1992
 wind (m/s) chi ($10^6 \text{ m}^2/\text{s}$) /d2/toga_coare/d5.gs



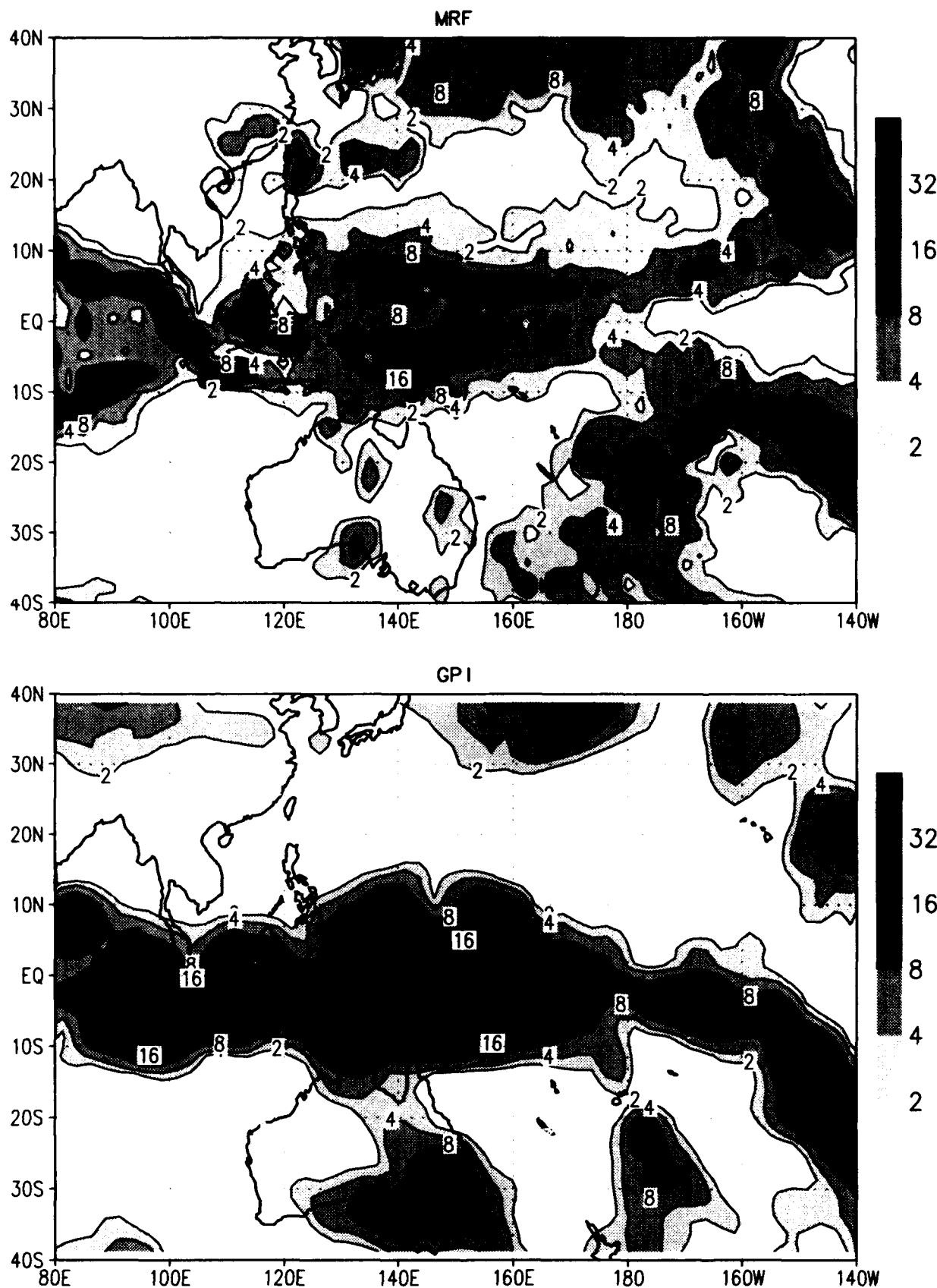
MRF 5-day ave flow and chi ~ 12 DEC 1992
wind (m/s) chi ($10^6 \text{ m}^2/\text{s}$) /d2/toga_coare/d5.gs



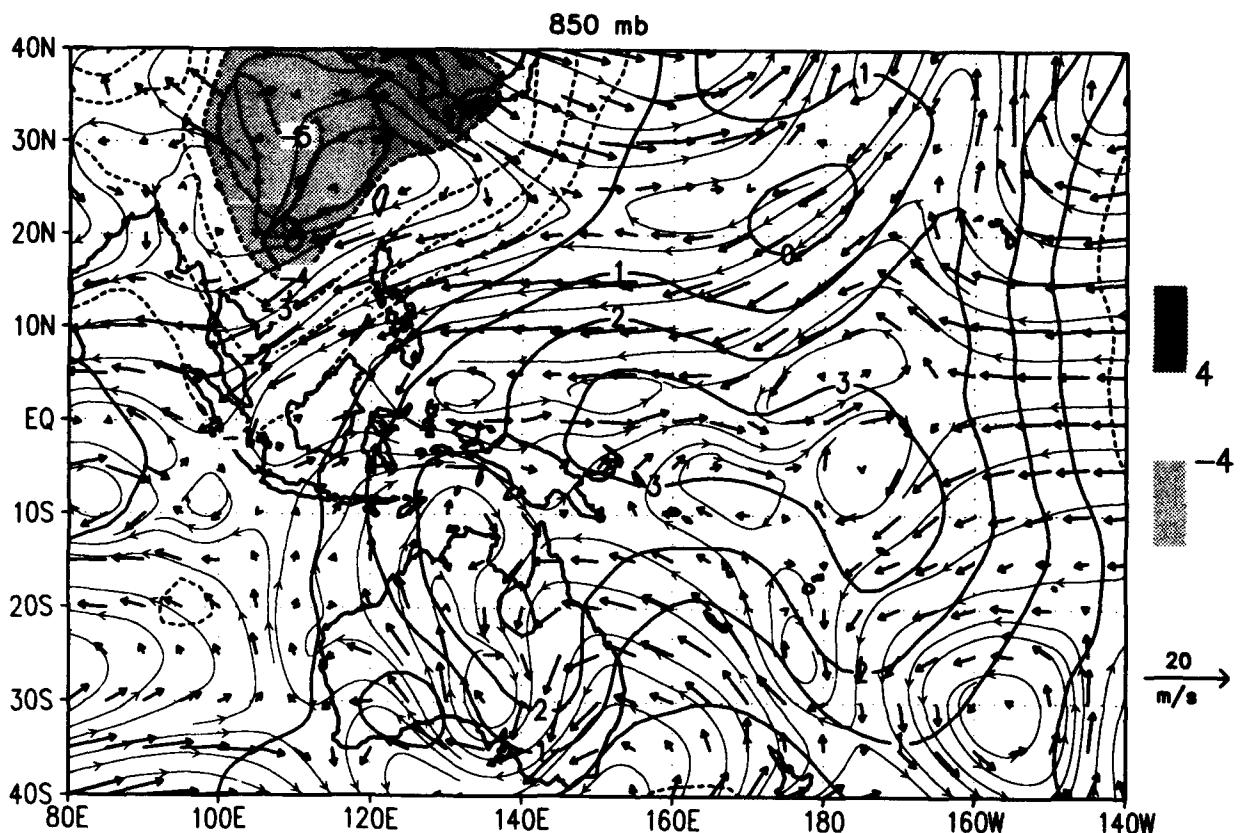
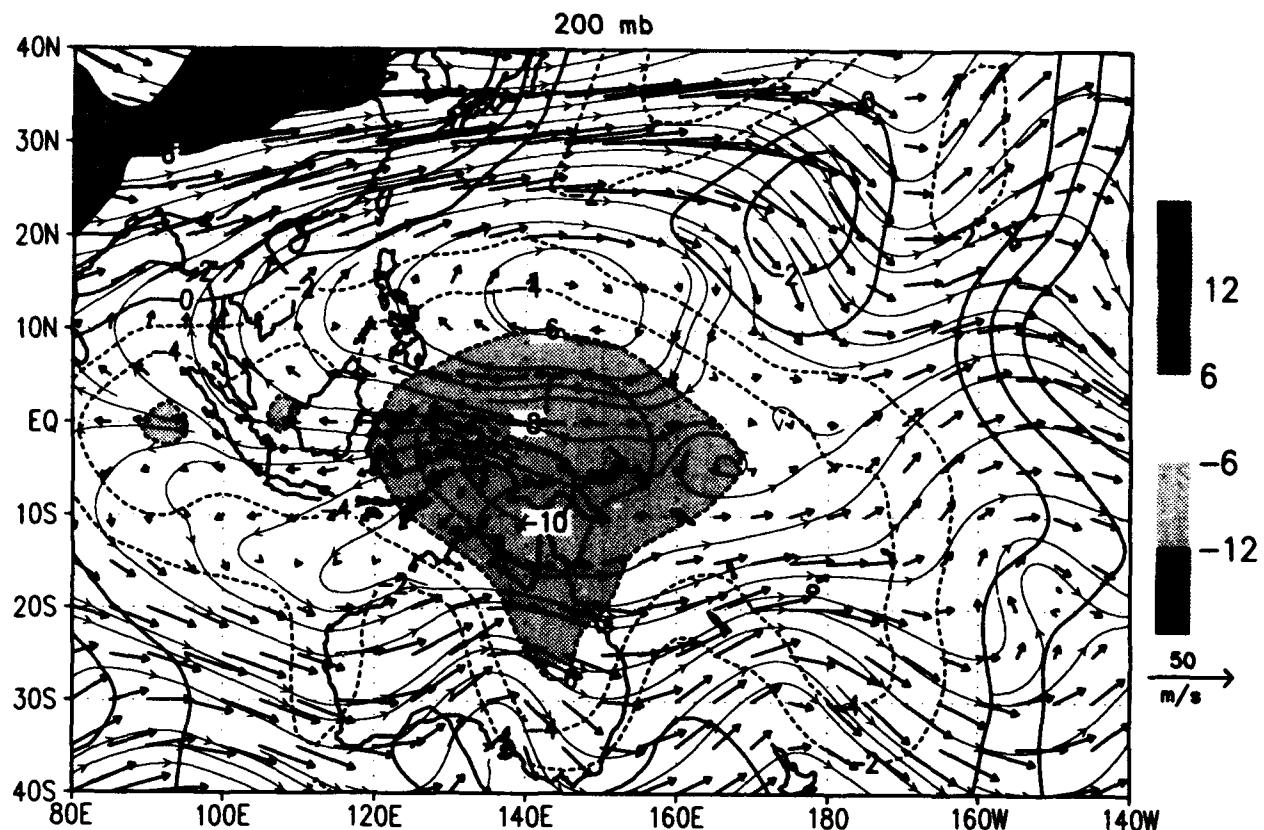
NOGAPS and GPI 5-day ave Precip ~ 12 DEC 1992
(mm/day) /d2/toga_coare/d5.gs



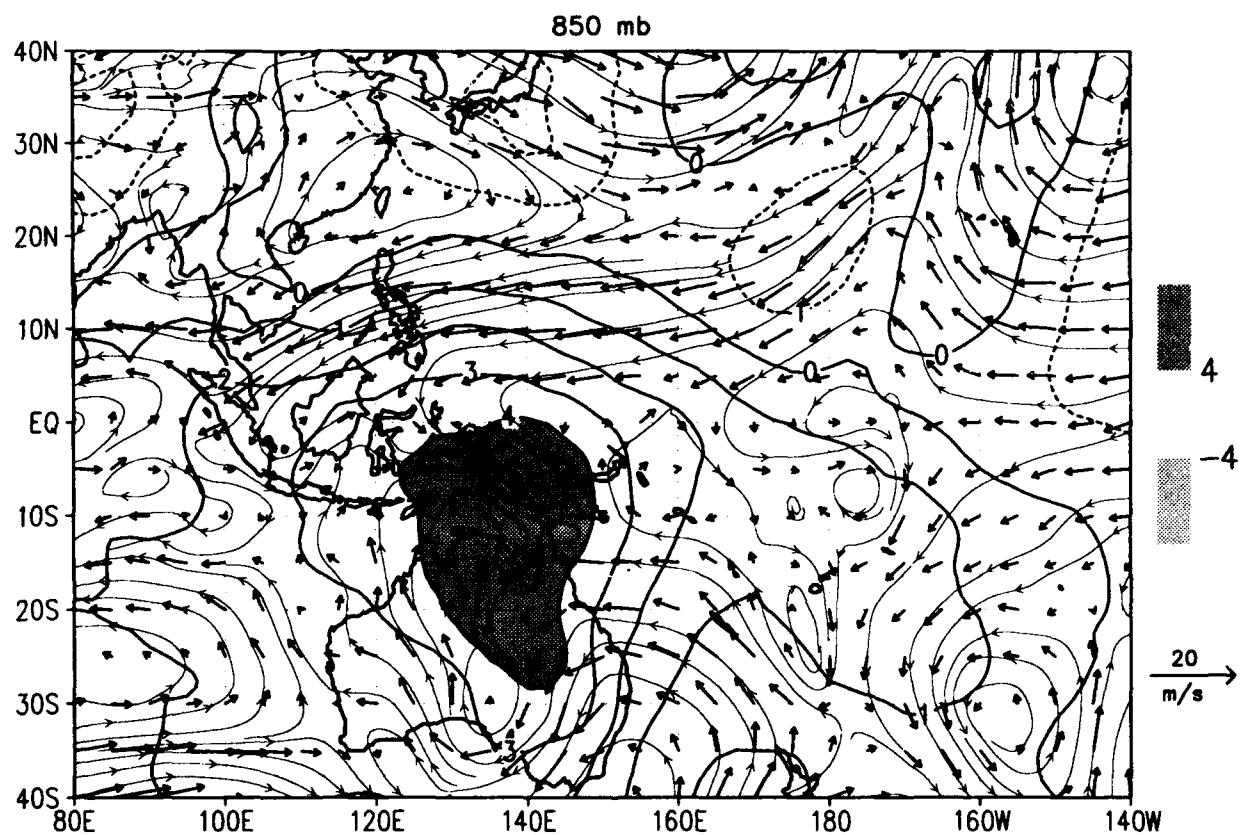
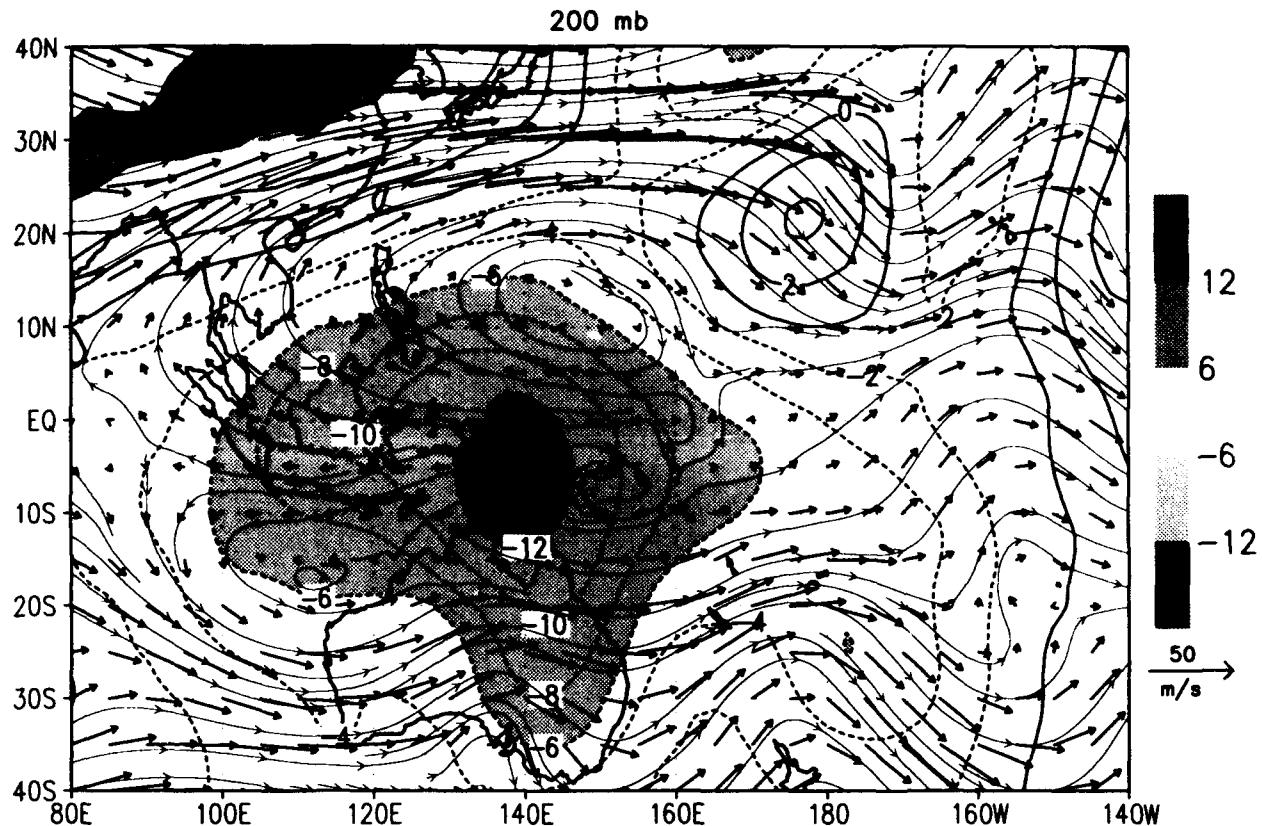
MRF and GPI 5-day ave Precip ~ 12 DEC 1992
(mm/day) /d2/toga_coare/d5.gs



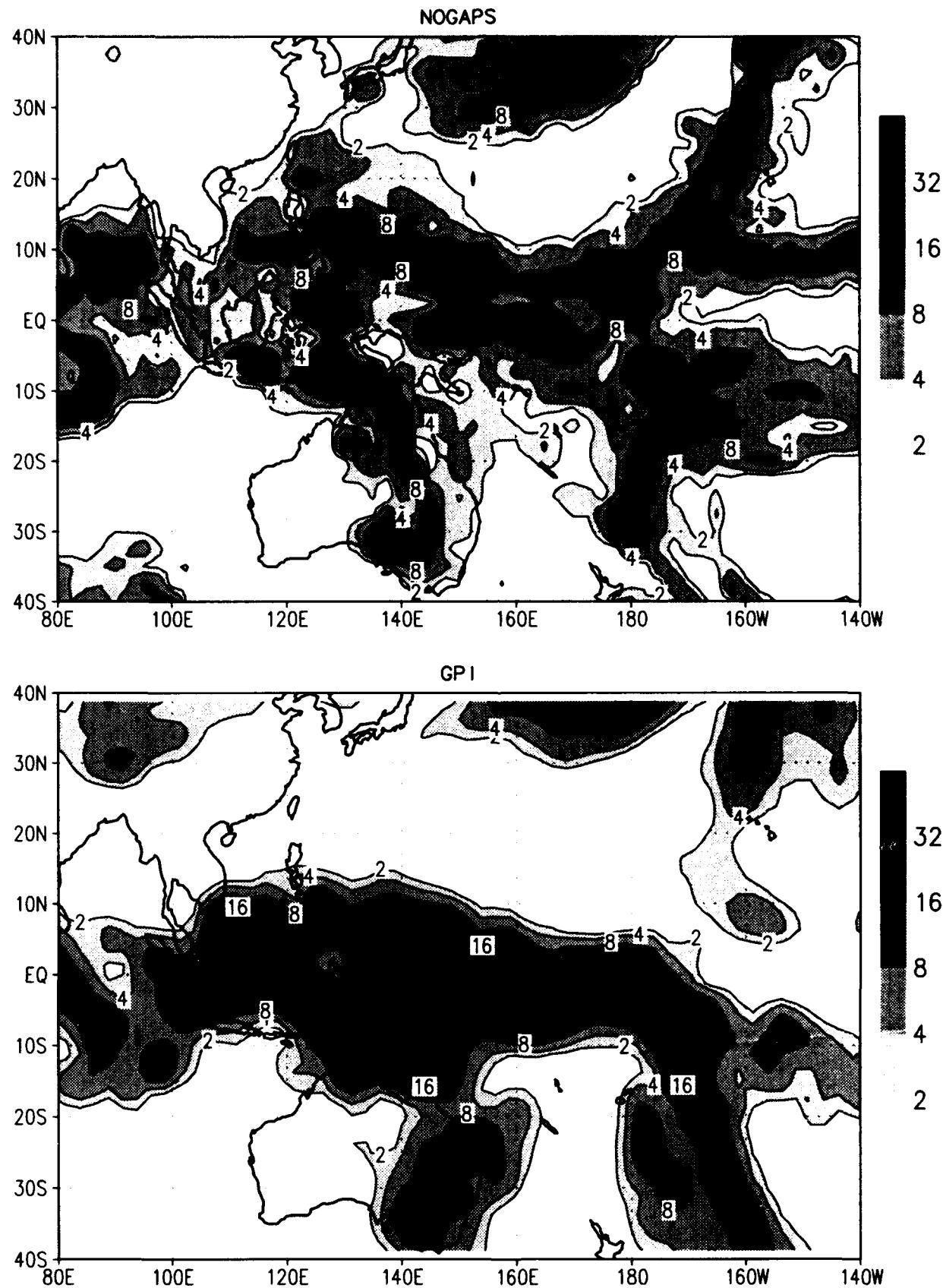
NOGAPS 5-day ave flow and chi ~ 17 DEC 1992
wind (m/s) chi ($10^6 \text{ m}^2/\text{s}$) /d2/toga_coare/d5.gs



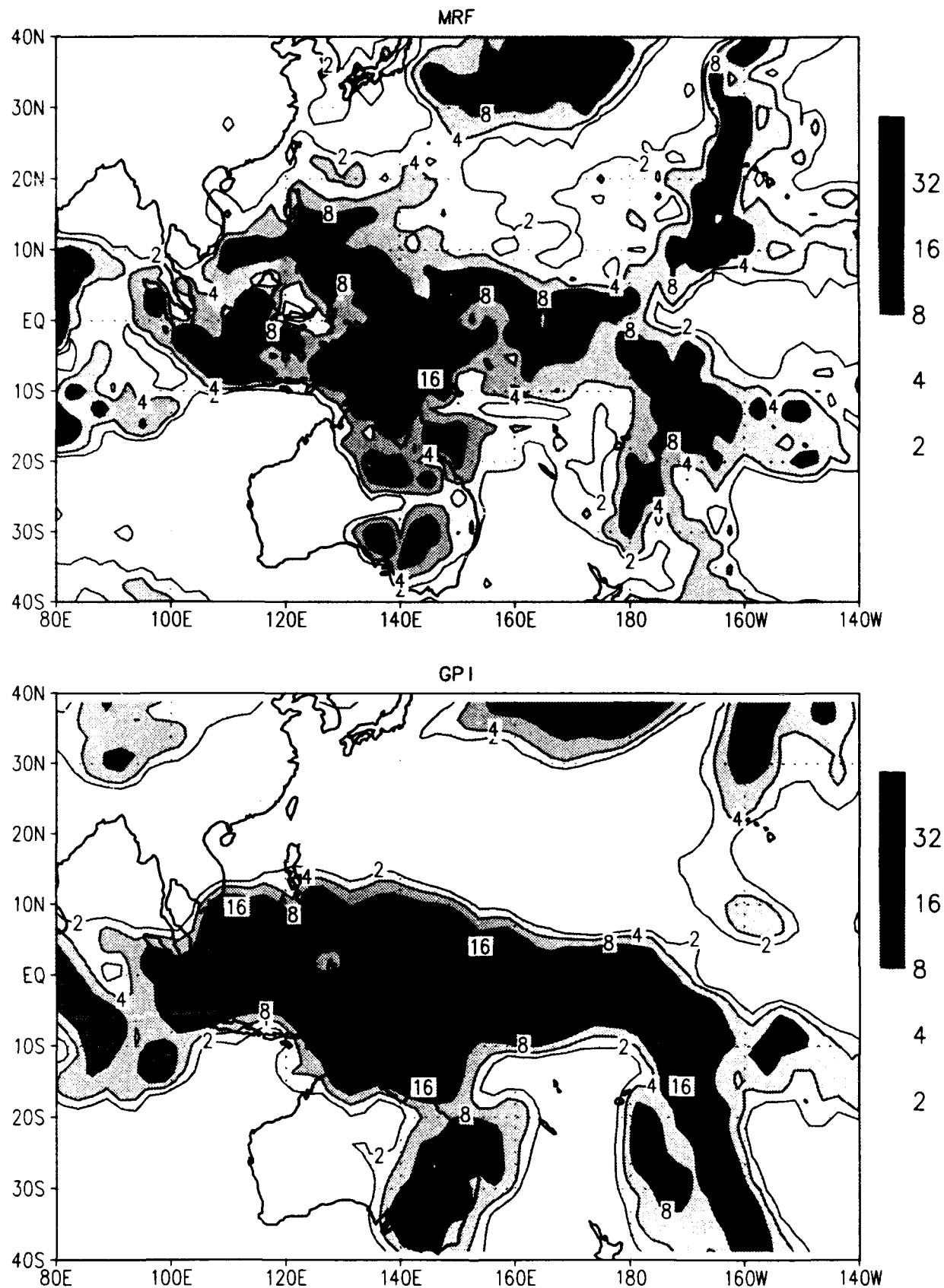
MRF 5-day ave flow and chi ~ 17 DEC 1992
wind (m/s) chi ($10^6 \text{ m}^2/\text{s}$) /d2/toga_coare/d5.gs



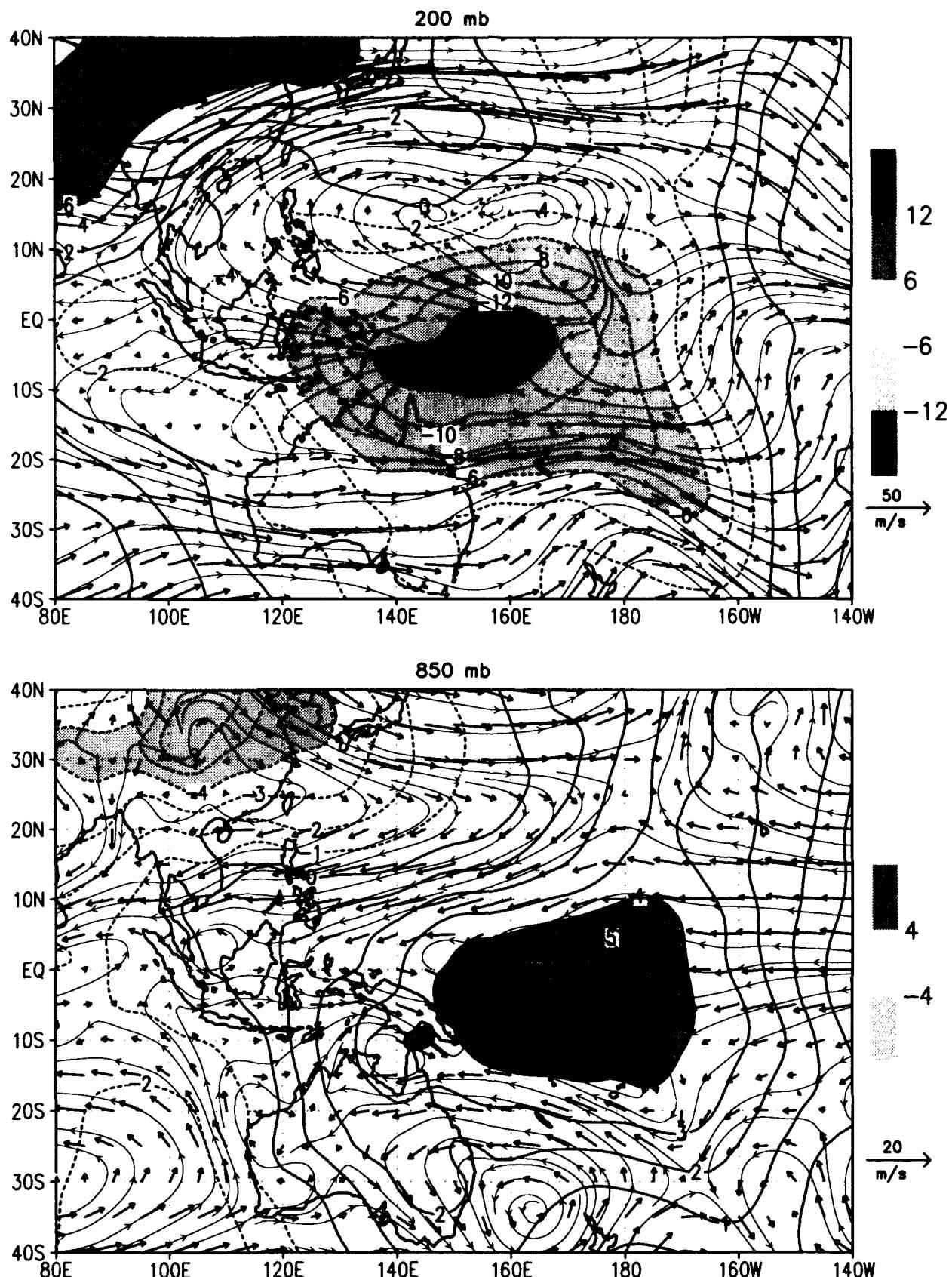
NOGAPS and GPI 5-day ave Precip ~ 17 DEC 1992
(mm/day) /d2/toga_coare/d5.gs



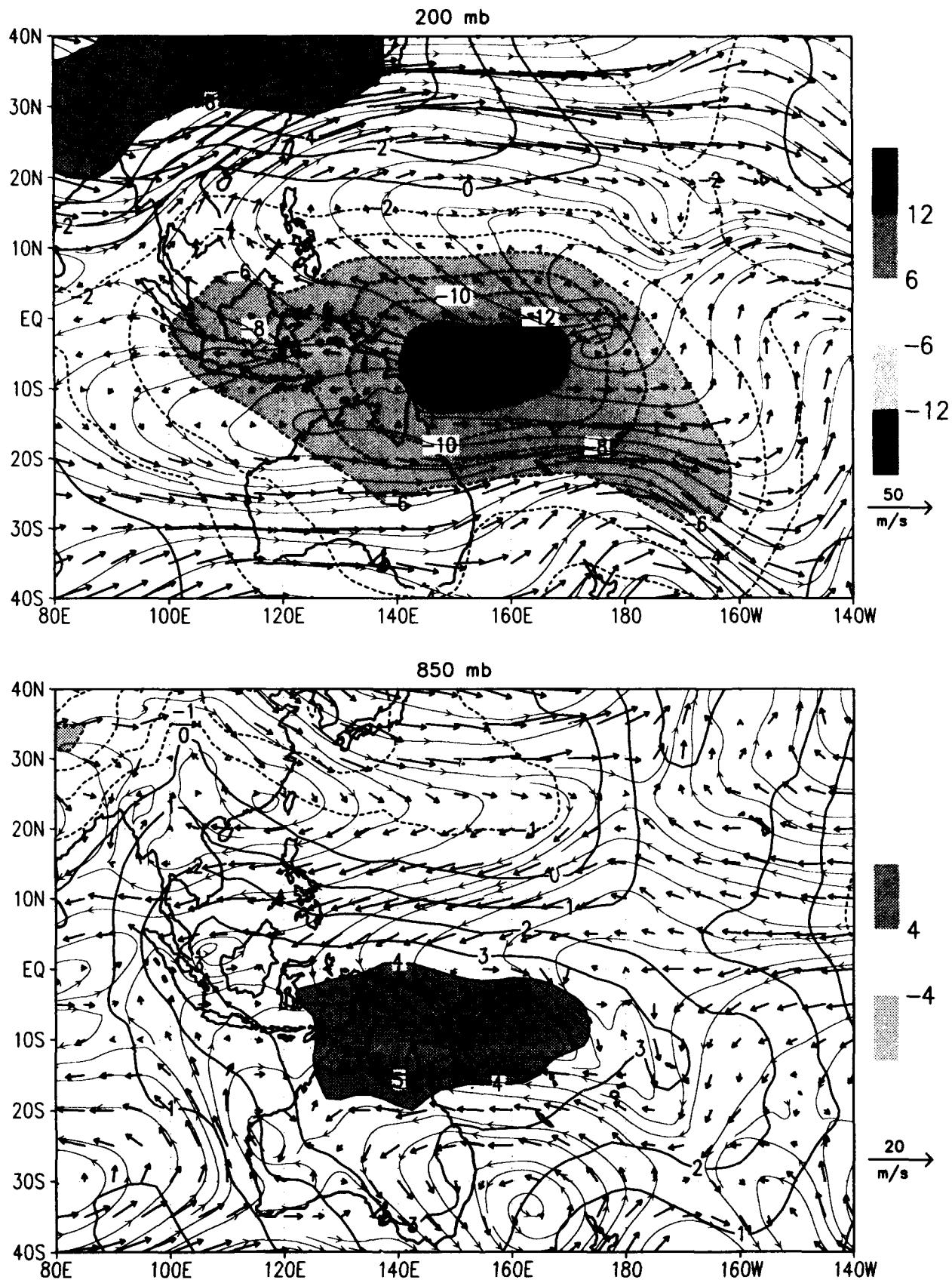
MRF and GPI 5-day ave Precip ~ 17 DEC 1992
(mm/day) /d2/toga_coare/d5.gs



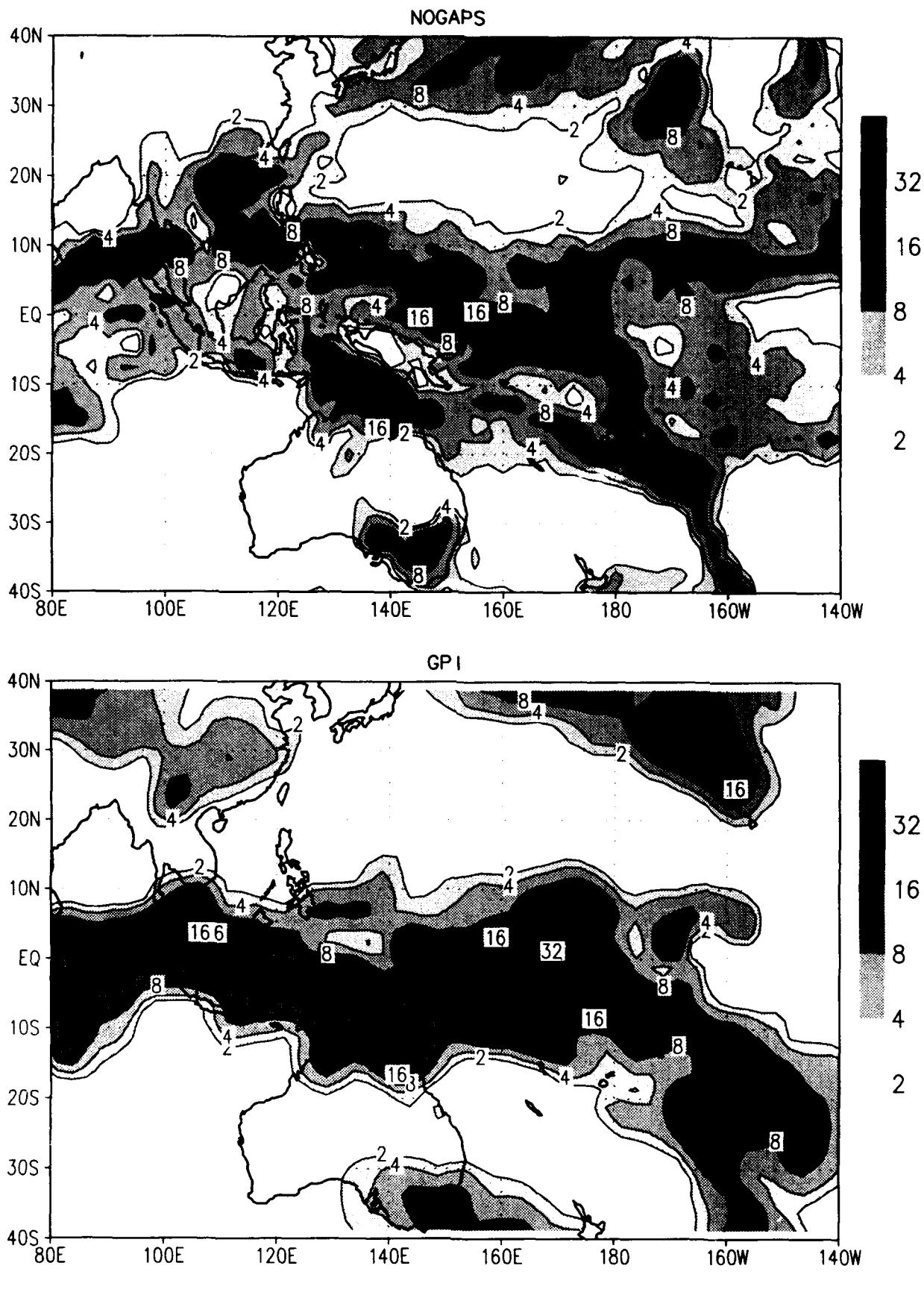
NOGAPS 5-day ave flow and chi ~ 22 DEC 1992
wind (m/s) chi ($10^6 \text{ m}^2/\text{s}$) /d2/toga_coare/d5.gs



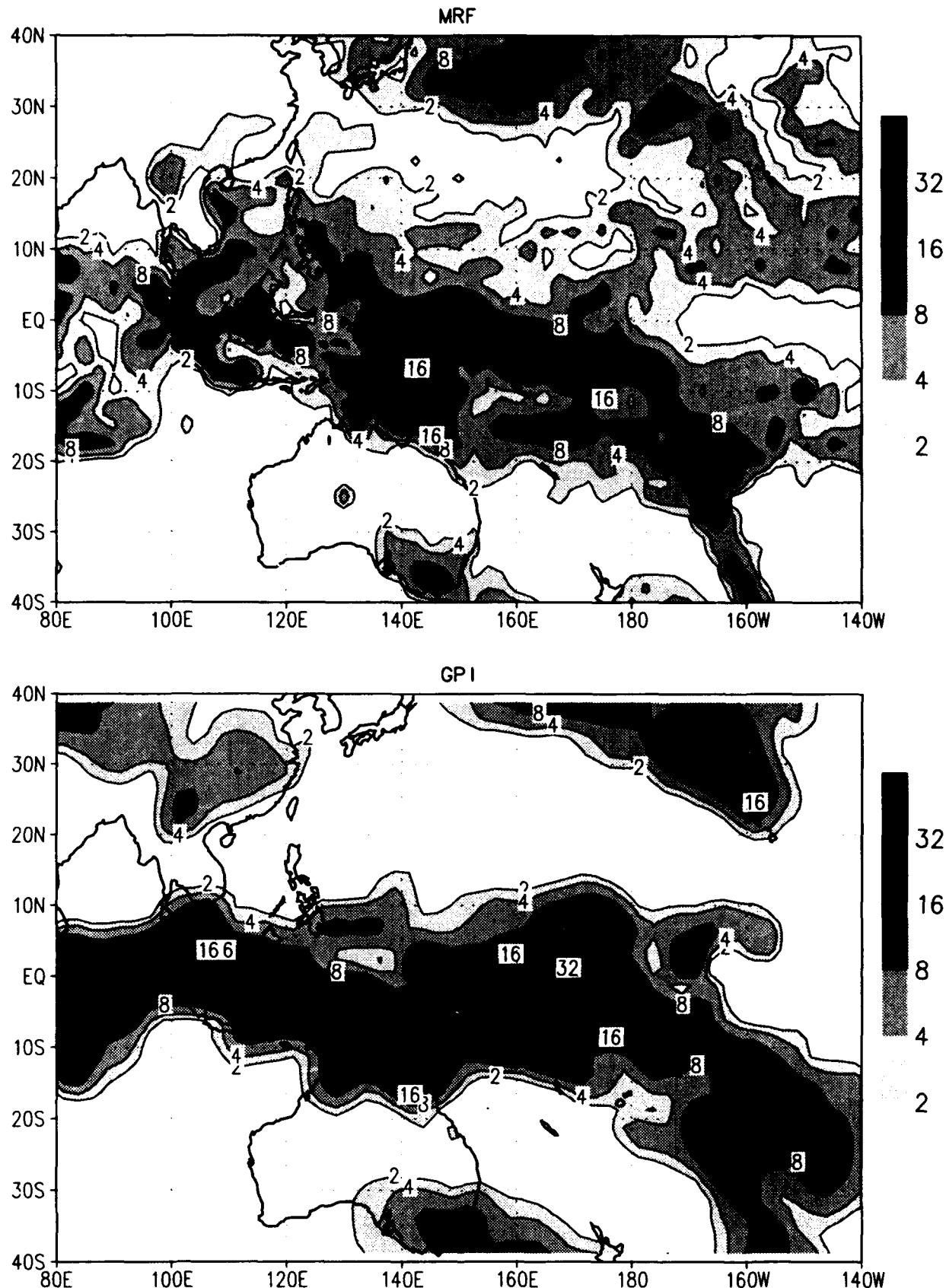
MRF 5-day ave flow and chi ~ 22 DEC 1992
 wind (m/s) chi ($10^6 \text{ m}^{-2}/\text{s}$) /d2/toga_coare/d5.gs



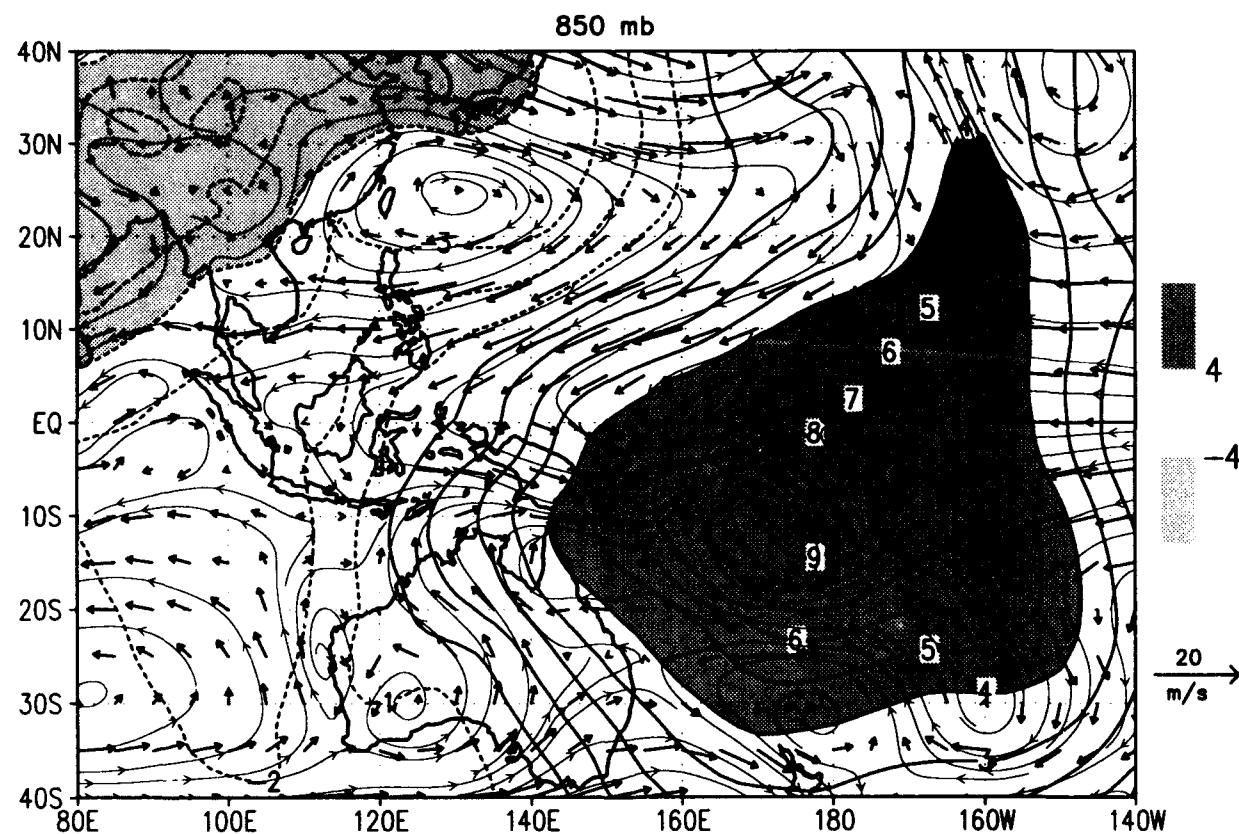
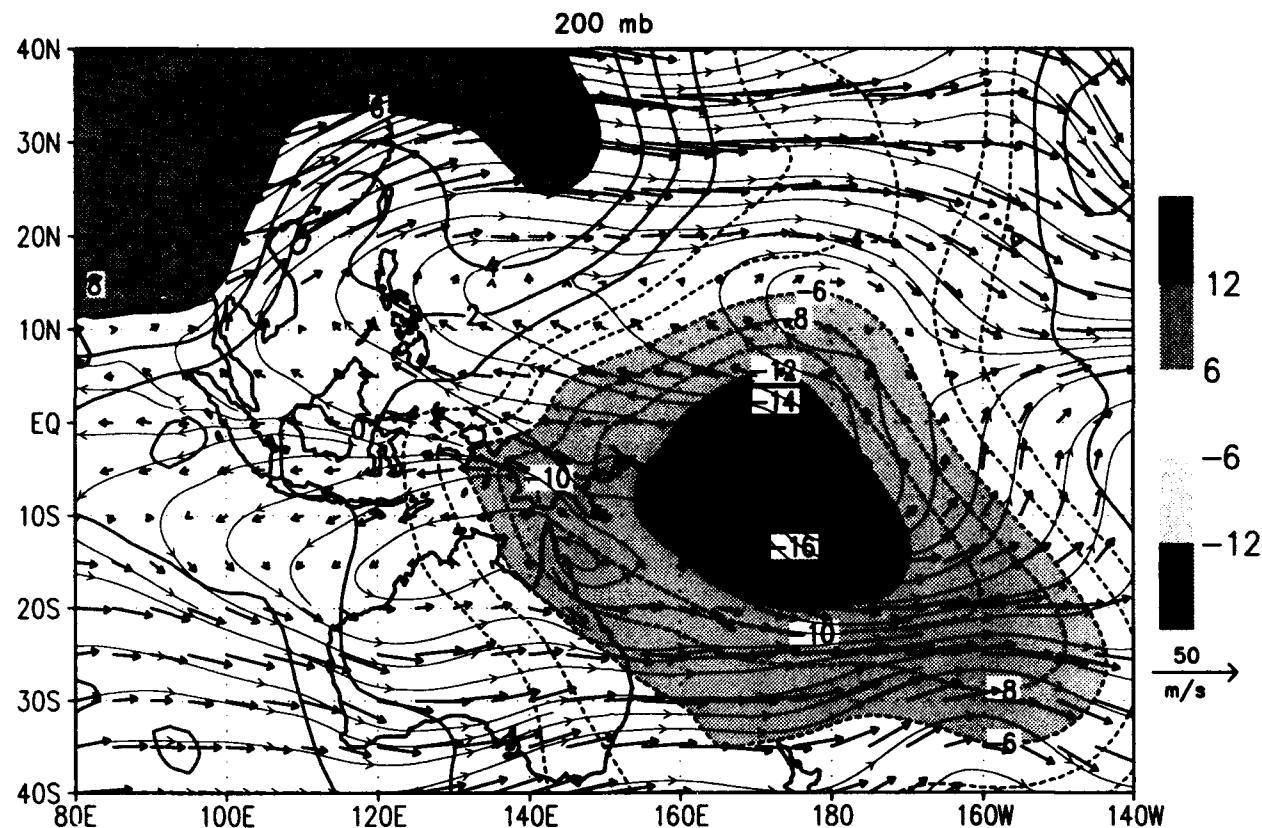
NOGAPS and GPI 5-day ave Precip ~ 22 DEC 1992
(mm/day) /d2/toga_coare/d5.gs



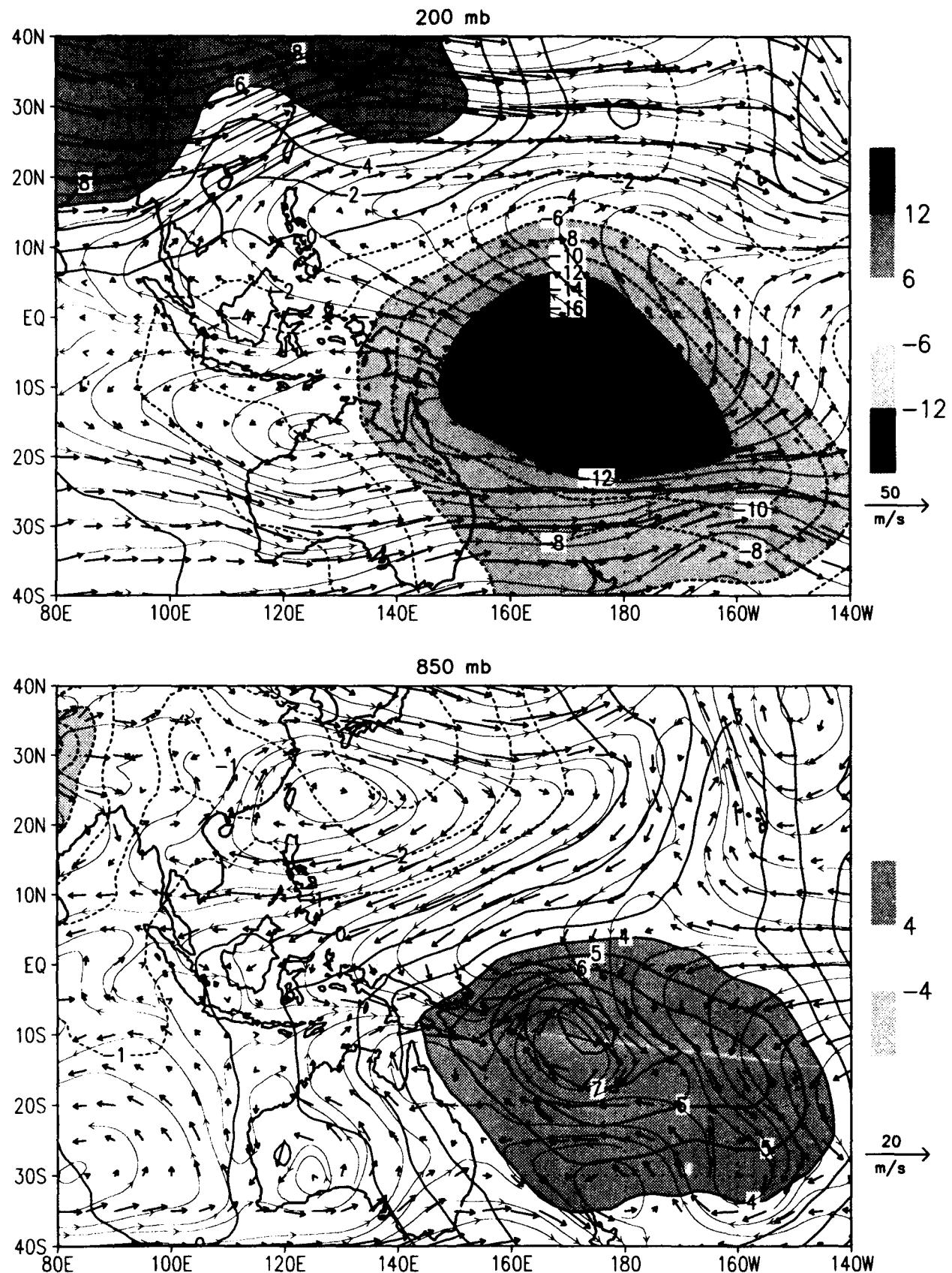
MRF and GPI 5-day ave Precip ~ 22 DEC 1992
(mm/day) /d2/toga_coare/d5.gs



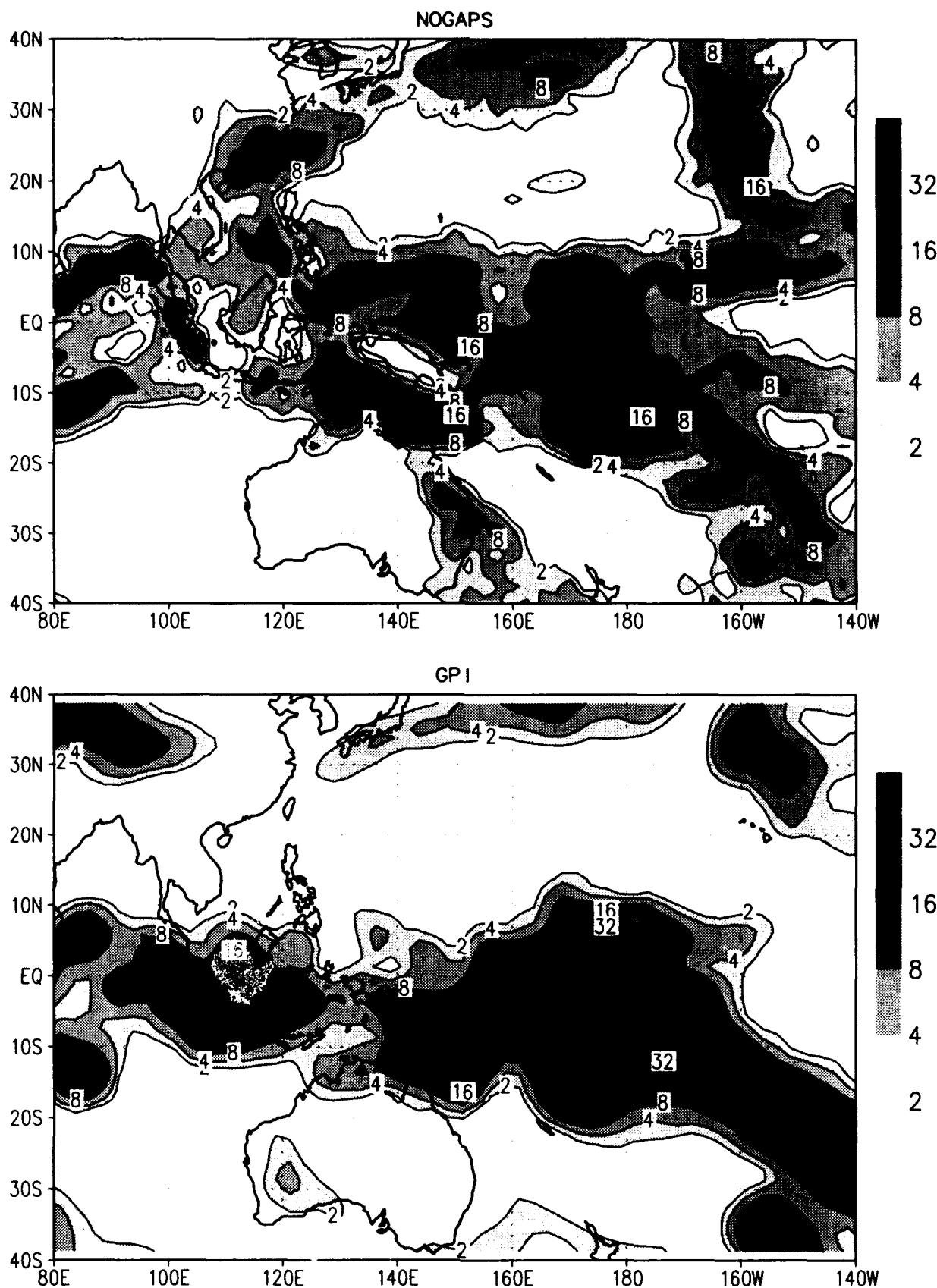
NOGAPS 5-day ave flow and chi ~ 27 DEC 1992
 wind (m/s) chi ($10^6 \text{ m}^2/\text{s}$) /d2/toga_coare/d5.gs



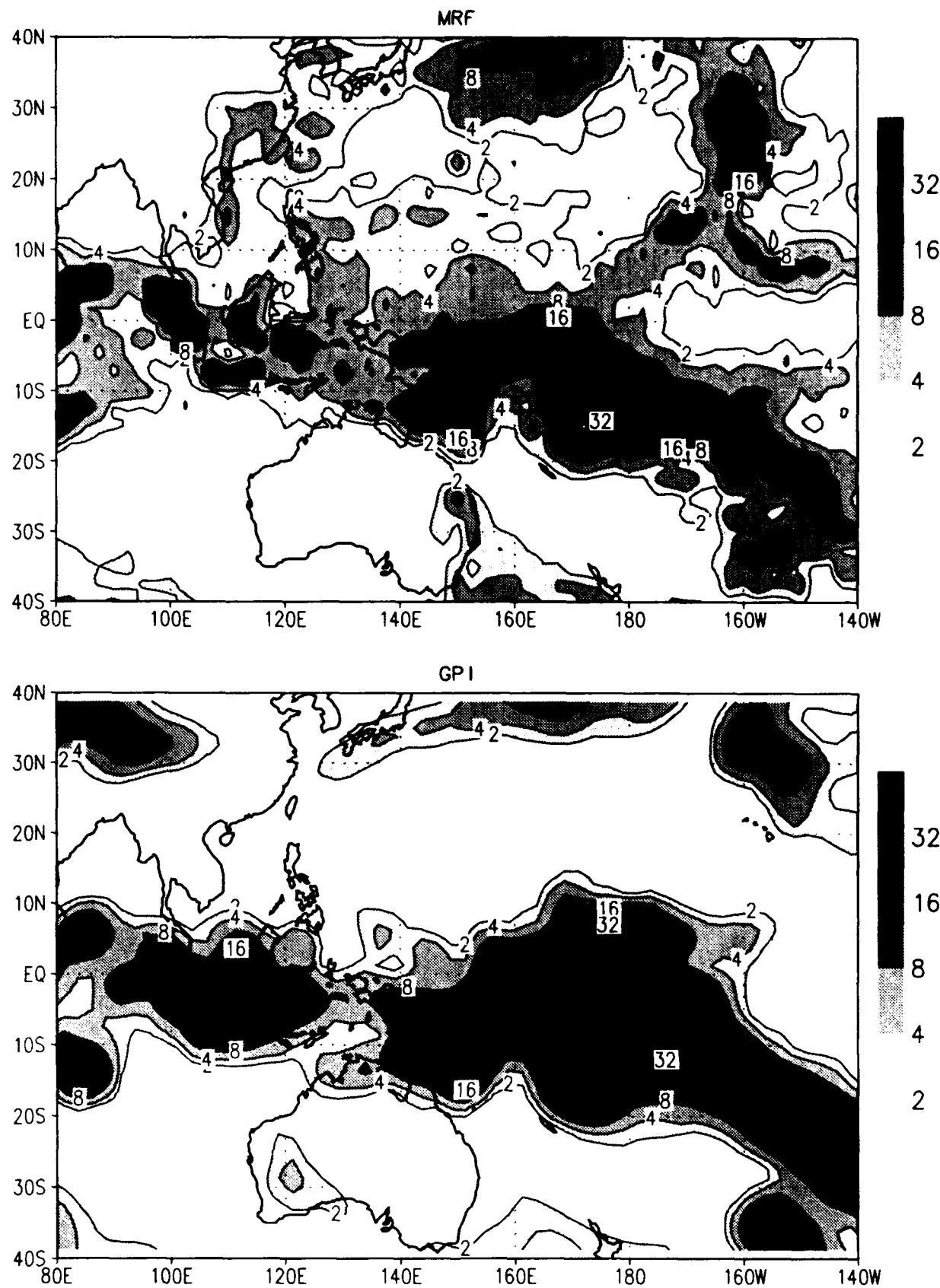
MRF 5-day ave flow and chi ~ 27 DEC 1992
 wind (m/s) chi ($1e6 \text{ m}^2/\text{s}$) /d2/toga_coare/d5.gs



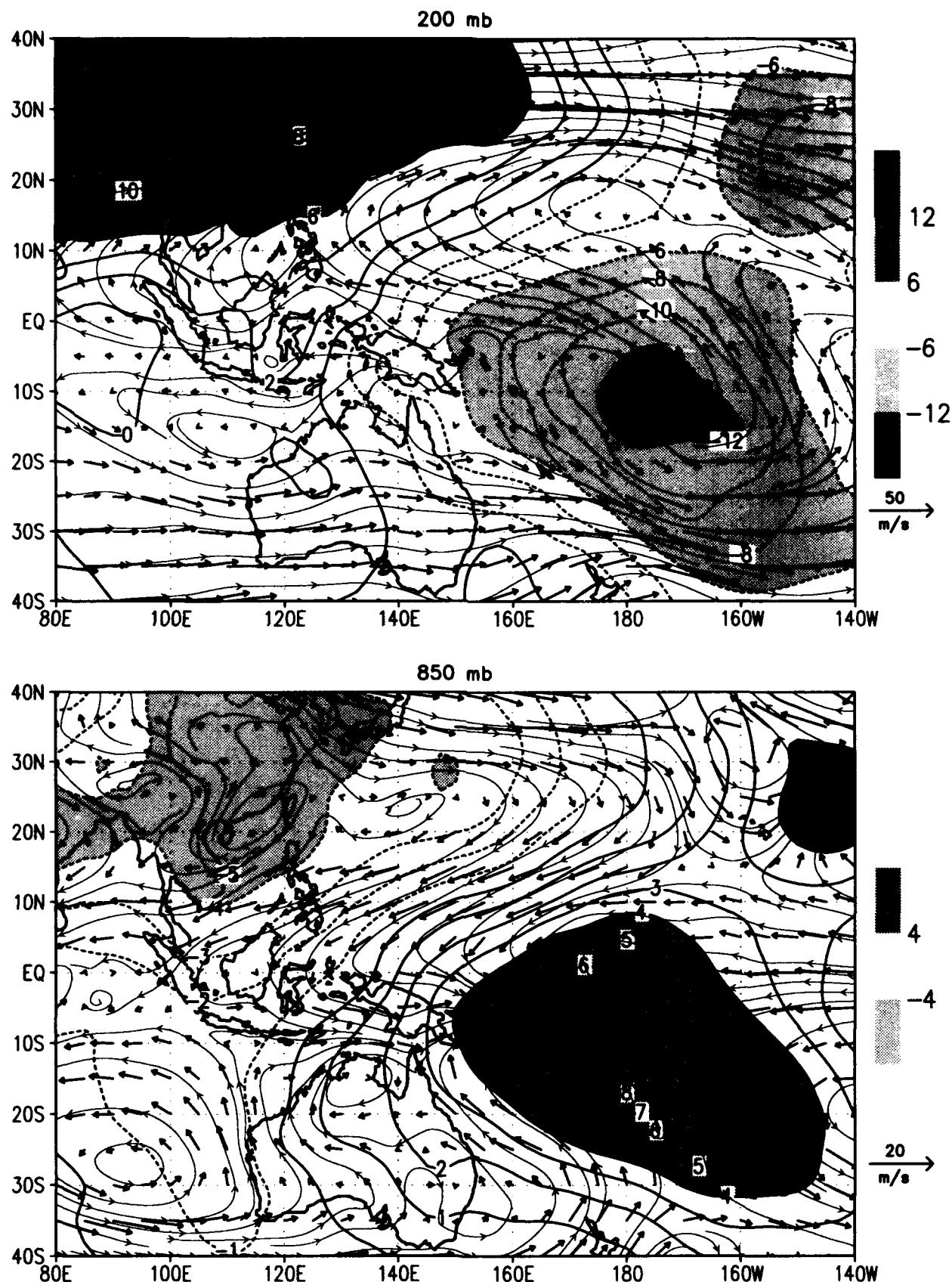
NOGAPS and GPI 5-day ave Precip ~ 27 DEC 1992
(mm/day) /d2/toga_coare/d5.gs



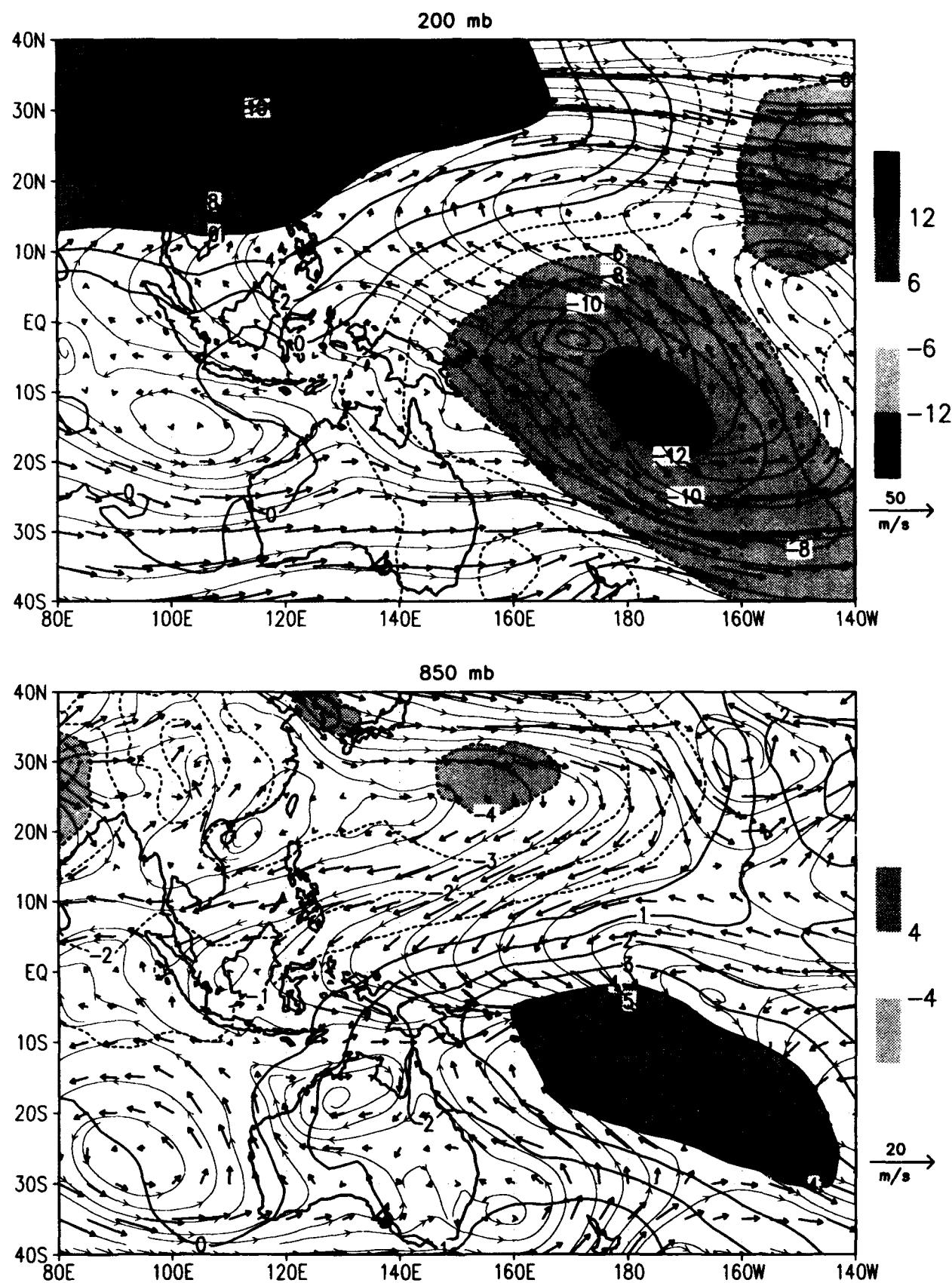
MRF and GPI 5-day ave Precip ~ 27 DEC 1992
(mm/day) /d2/toga_coare/d5.gs



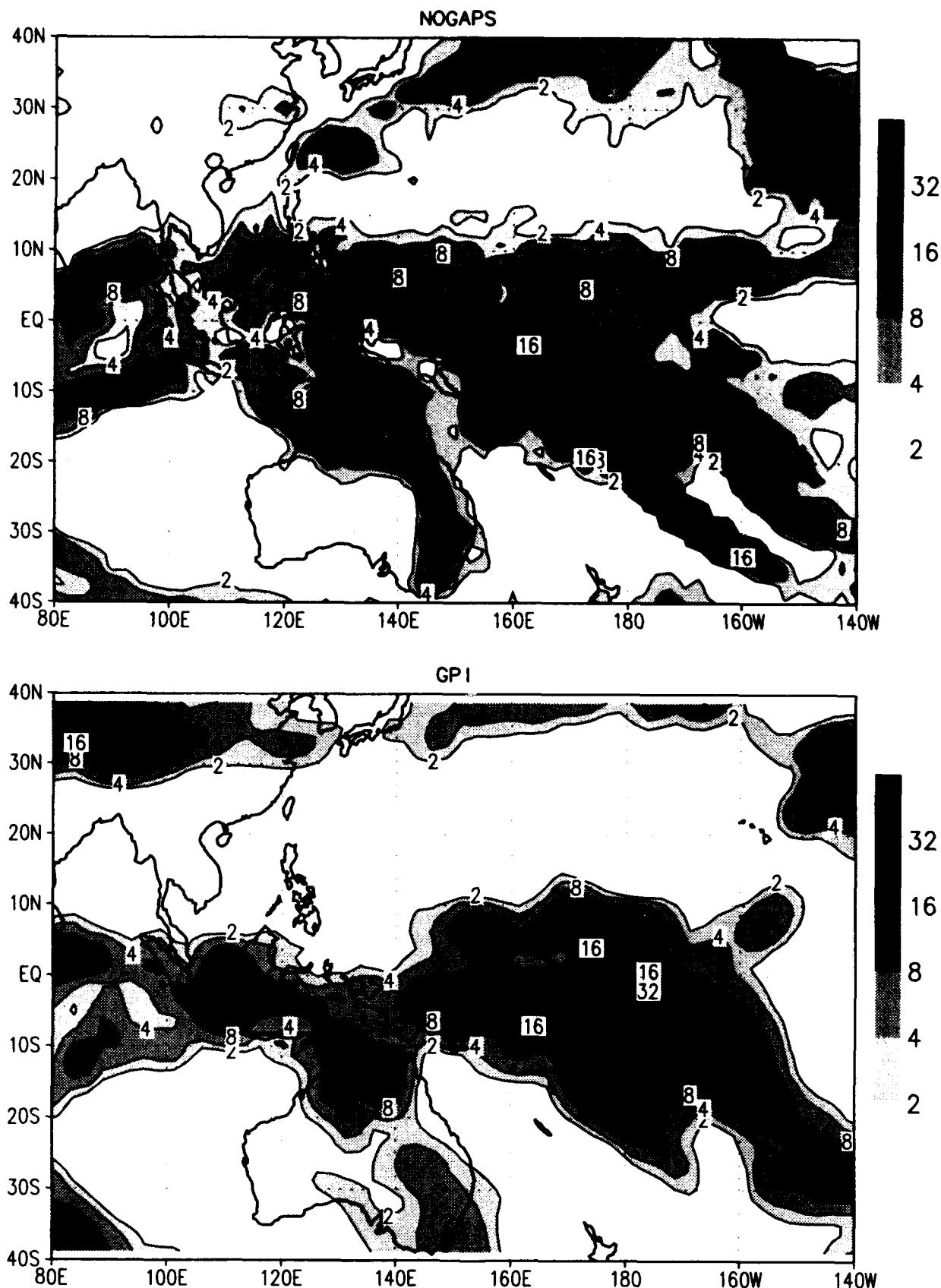
NOGAPS 5-day ave flow and chi ~ 02 JAN 1993
wind (m/s) chi ($10^6 \text{ m}^2/\text{s}$) /d2/toga_coare/d5.gs



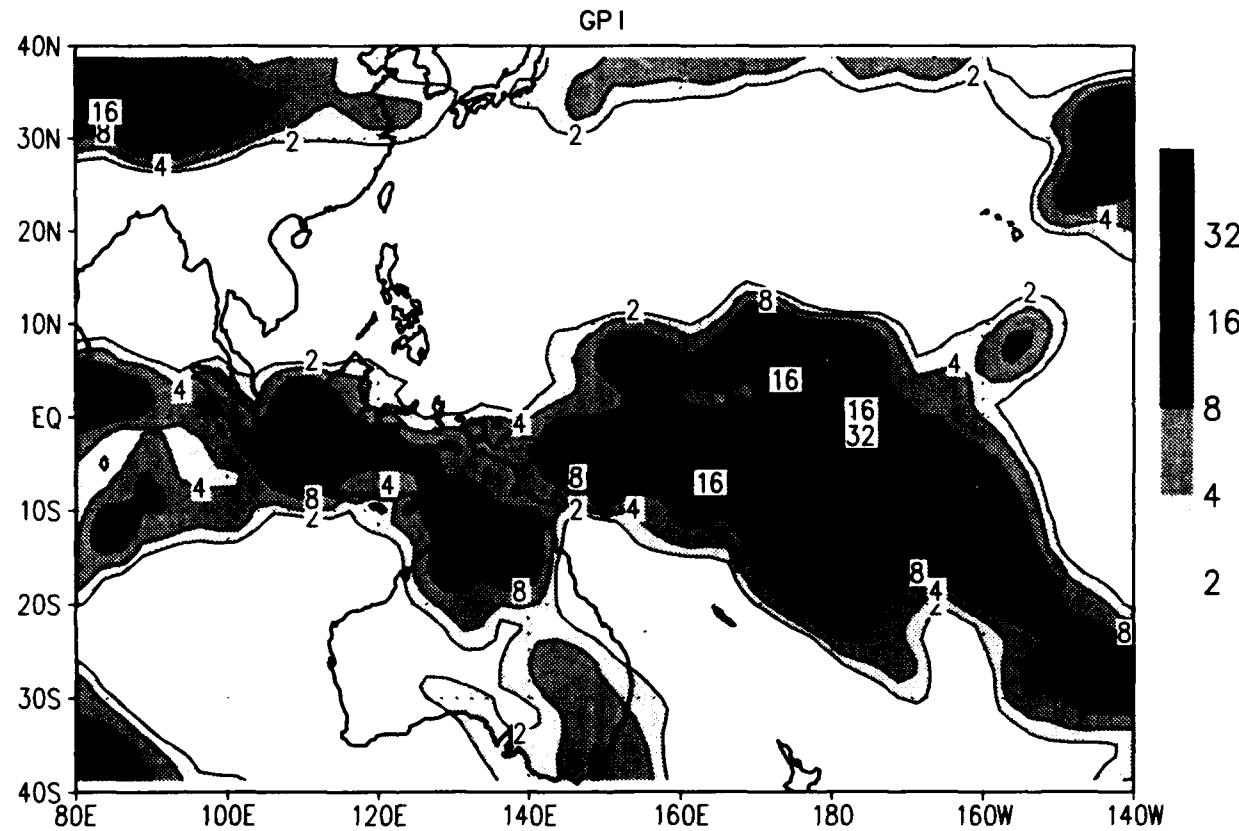
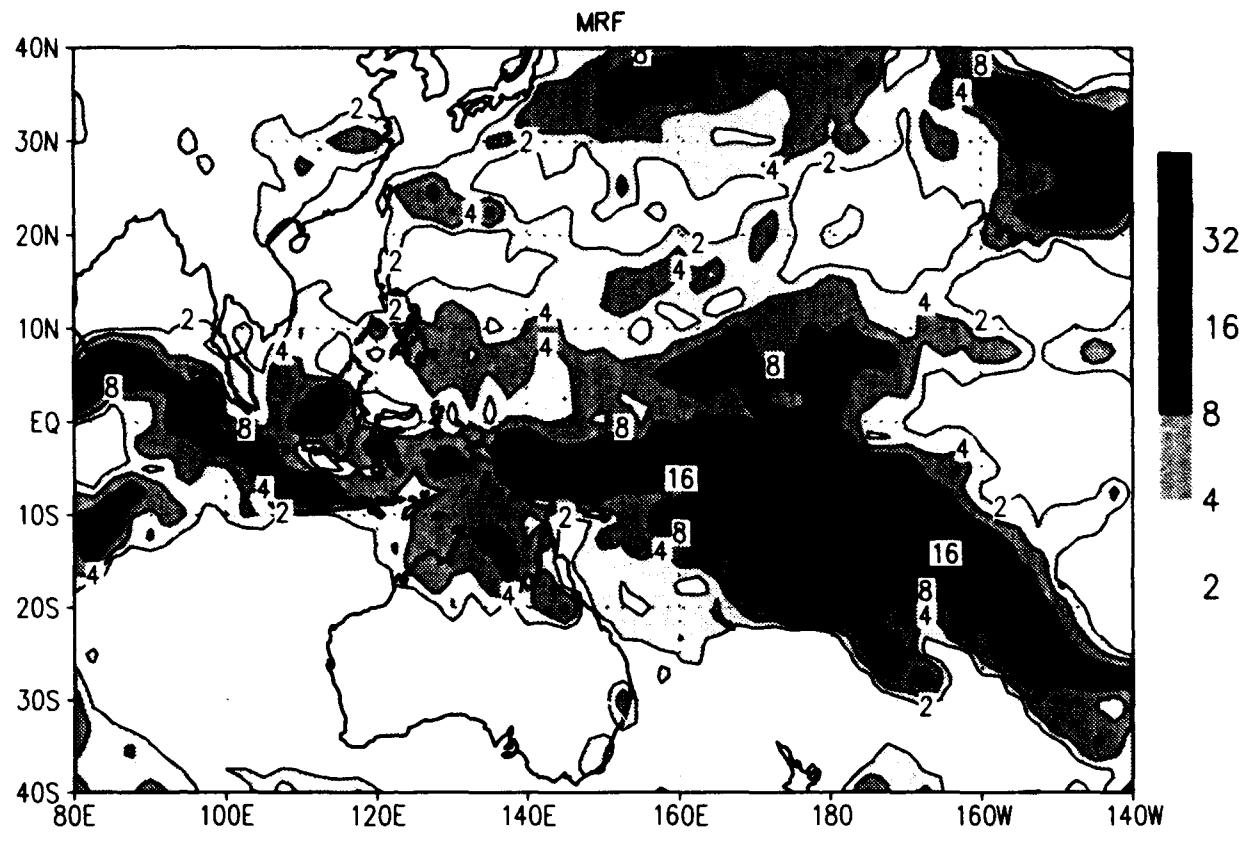
MRF 5-day ave flow and chi ~ 02 JAN 1993
wind (m/s) chi ($10^6 \text{ m}^{-2}/\text{s}$) /d2/toga_coare/d5.gs



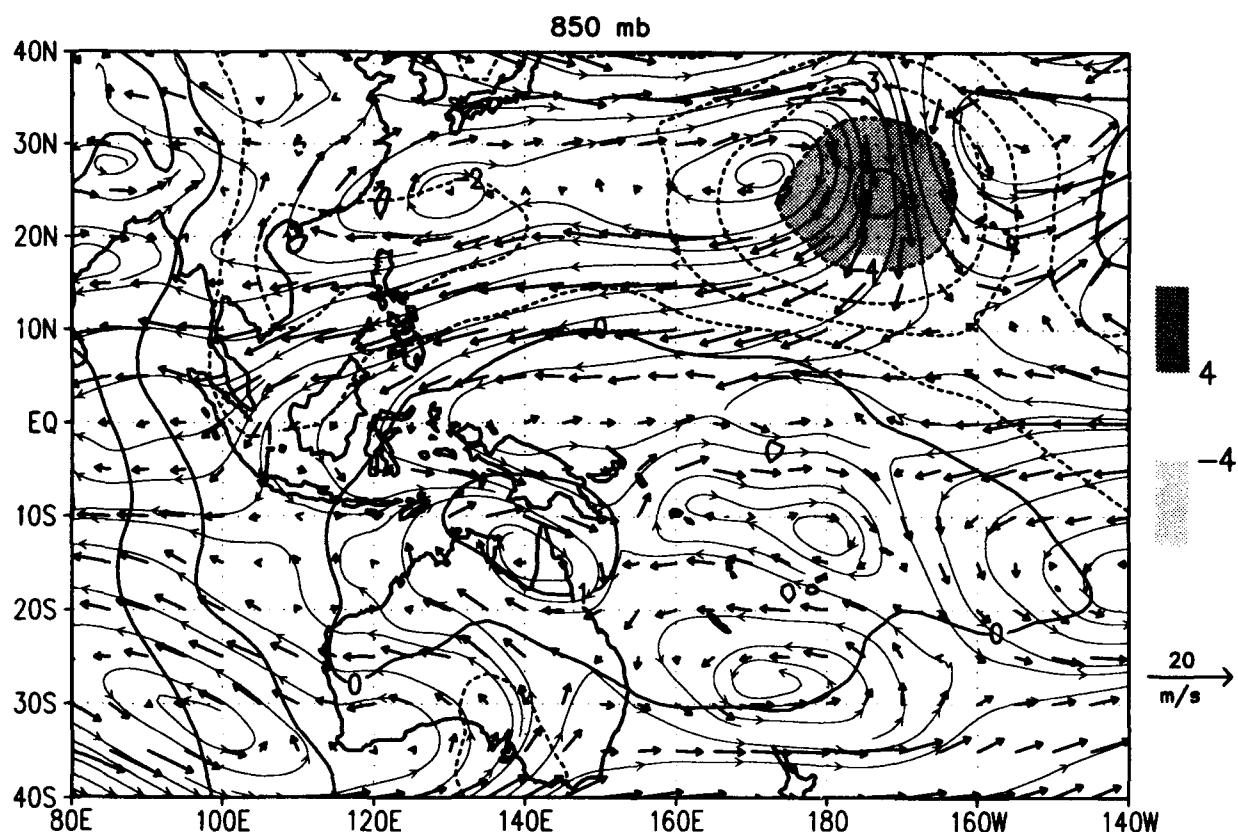
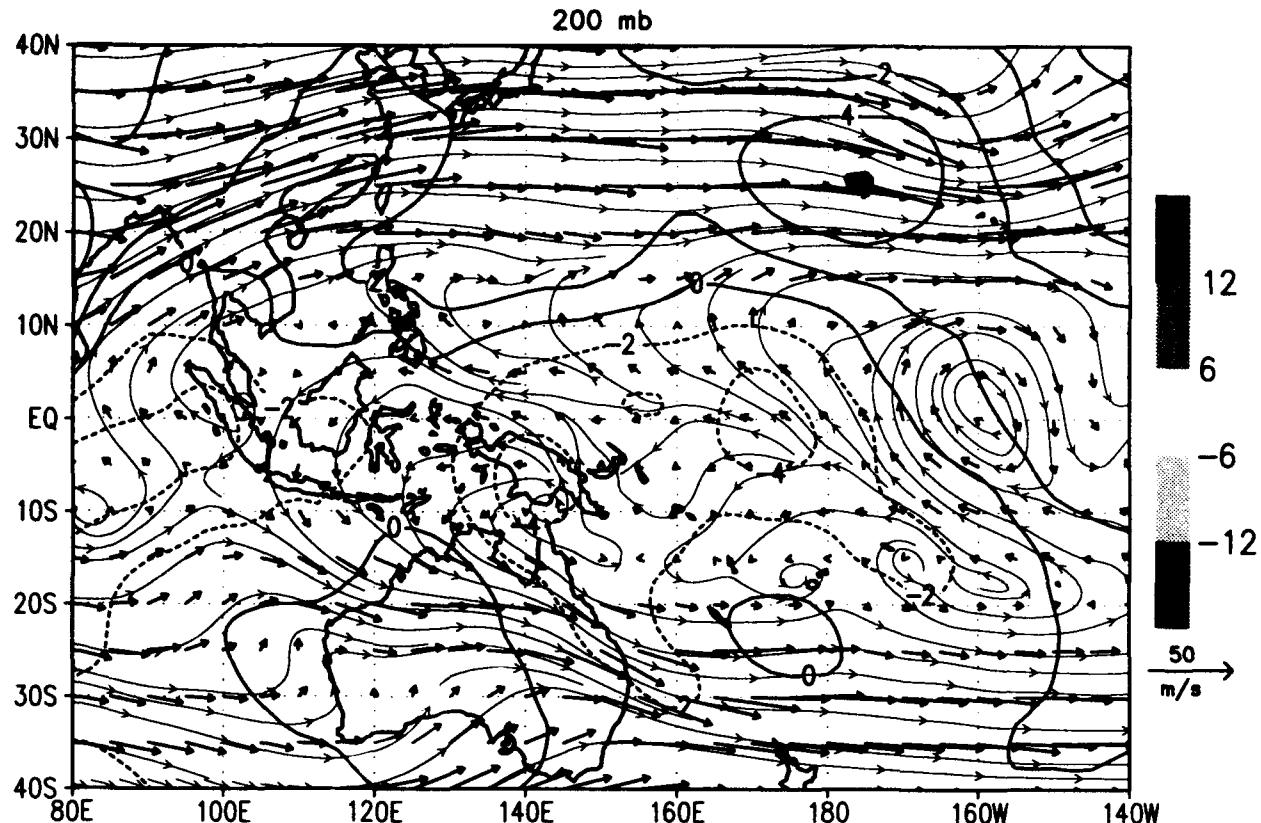
NOGAPS and GPI 5-day ave Precip ~ 02 JAN 1993
(mm/day) /d2/toga_coare/d5.gs



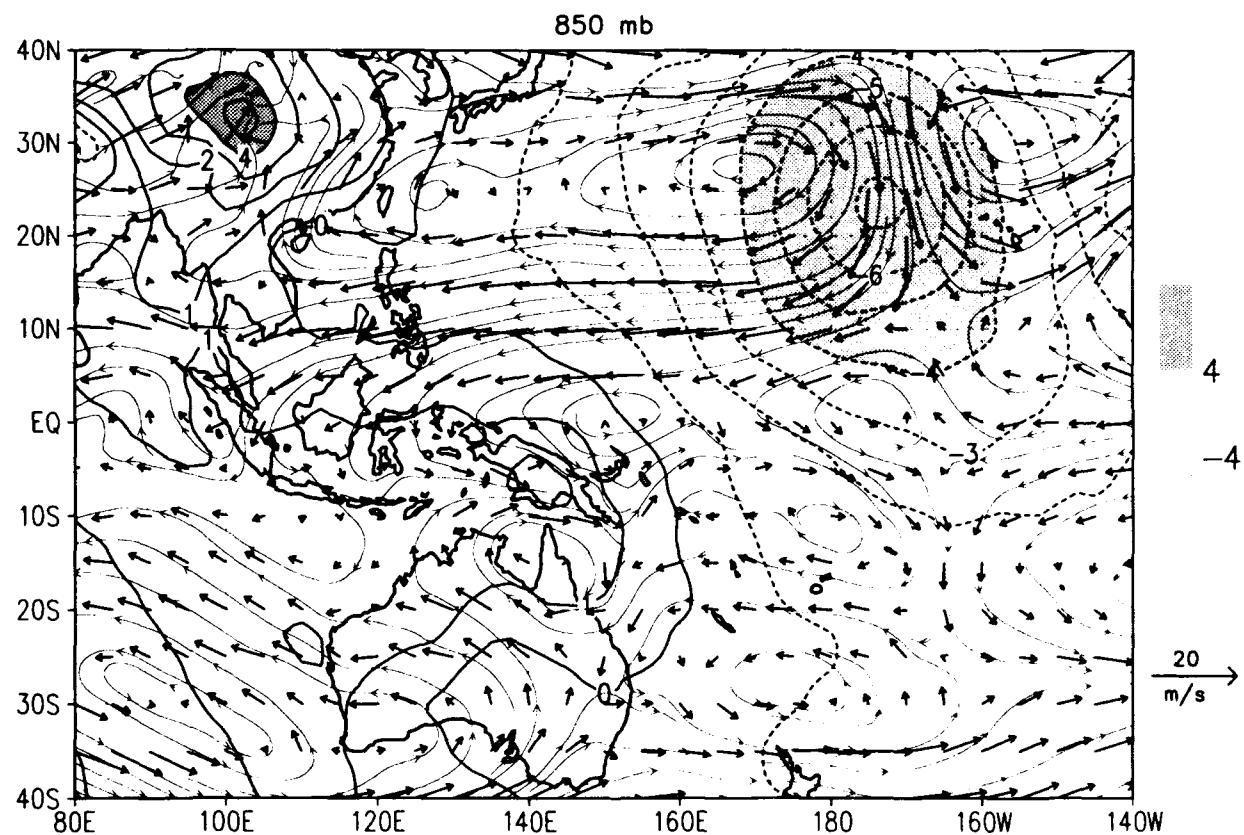
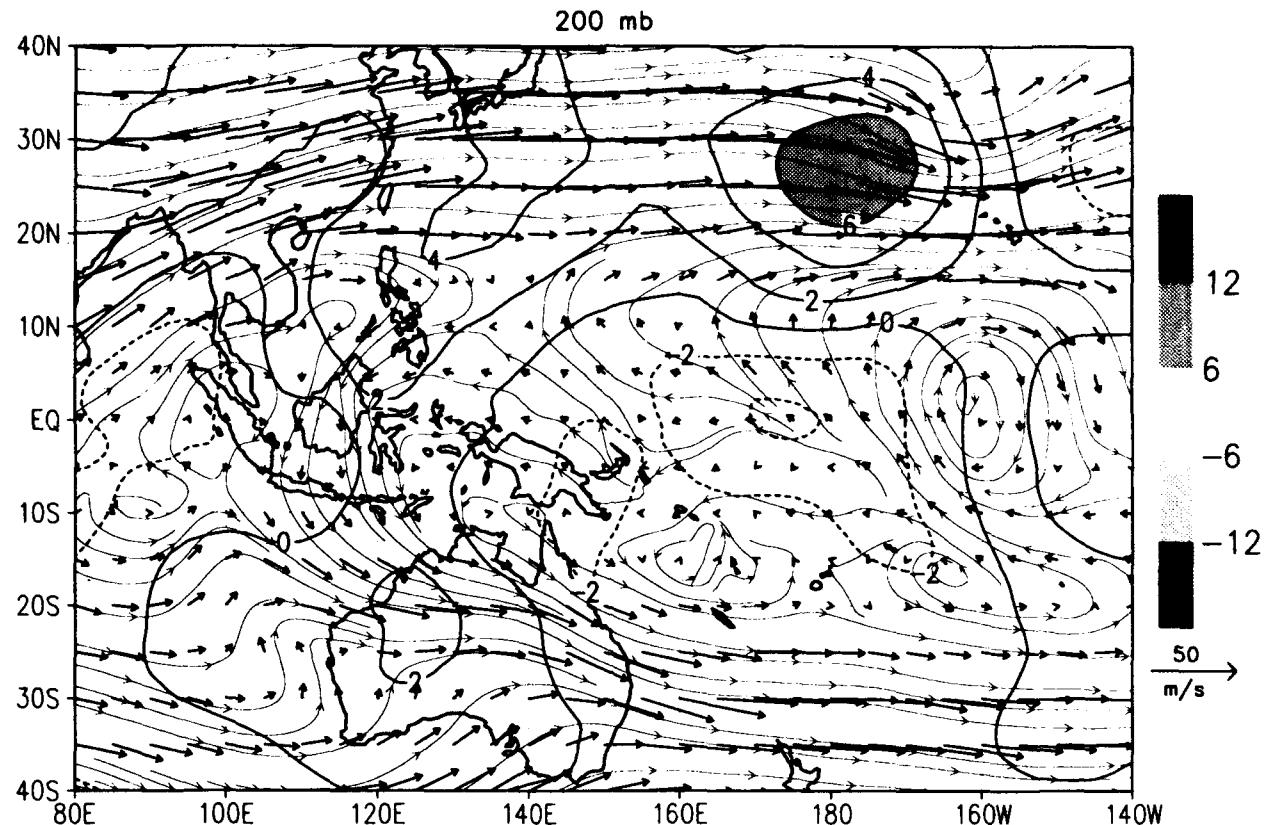
MRF and GPI 5-day ave Precip ~ 02 JAN 1993
(mm/day) /d2/toga_coare/d5.gs



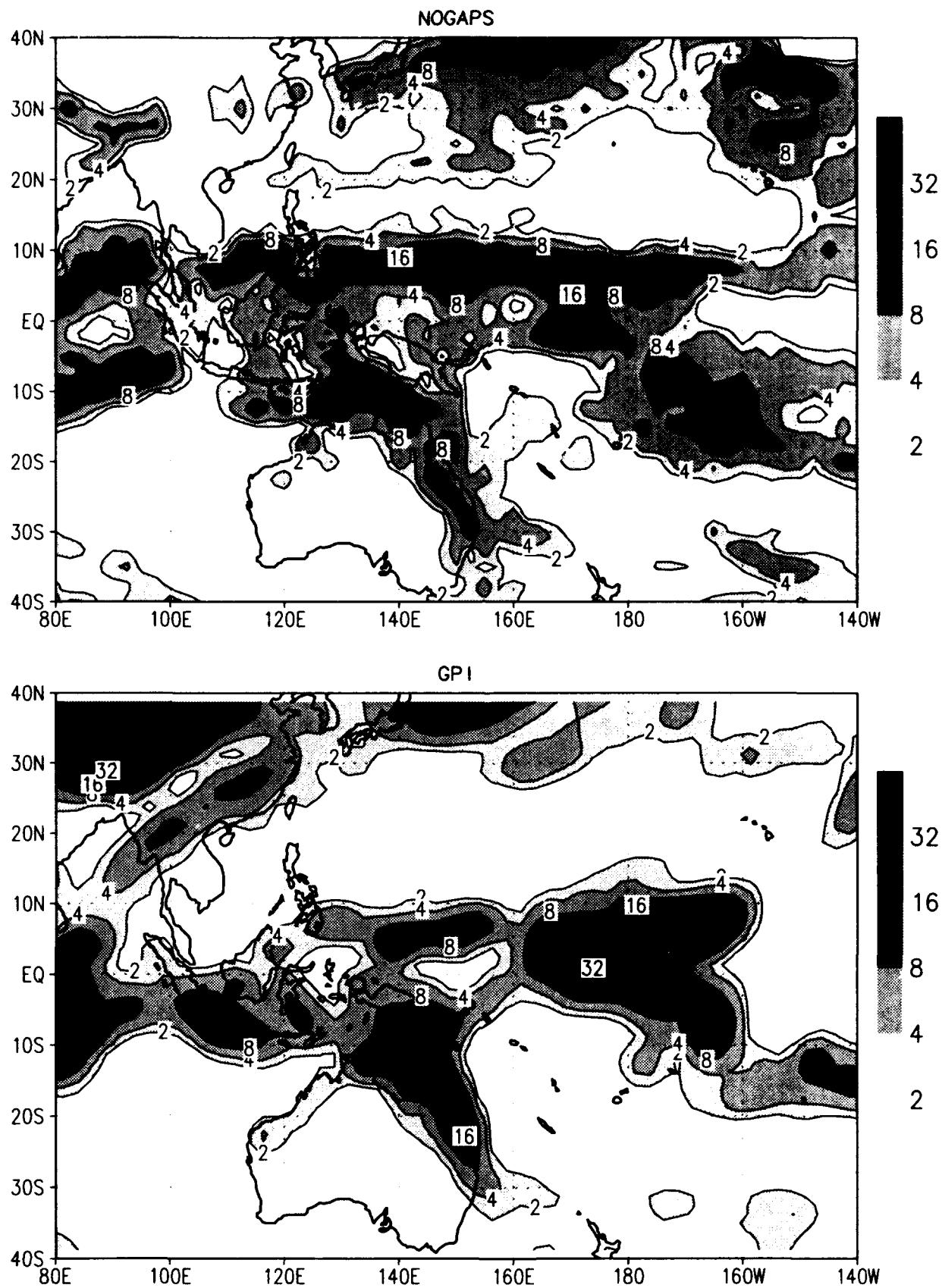
NOGAPS 5-day ave flow and chi ~ 07 JAN 1993
wind (m/s) chi ($10^6 \text{ m}^2/\text{s}$) /d2/toga_coare/d5.gs



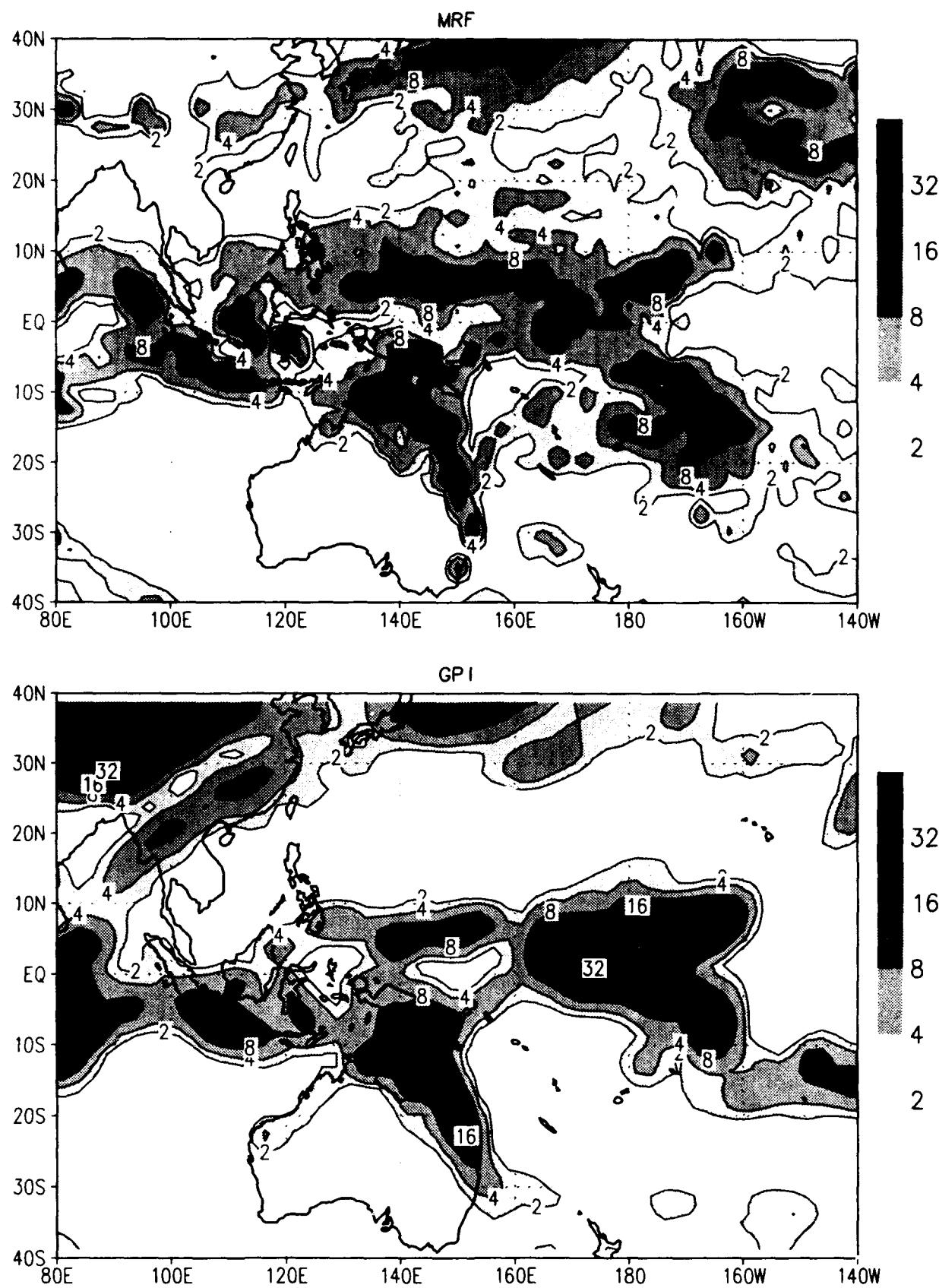
MRF 5-day ave flow and chi ~ 07 JAN 1993
wind (m/s) chi ($1e6 \text{ m}^2/\text{s}$) /d2/toga_coare/d5.gs



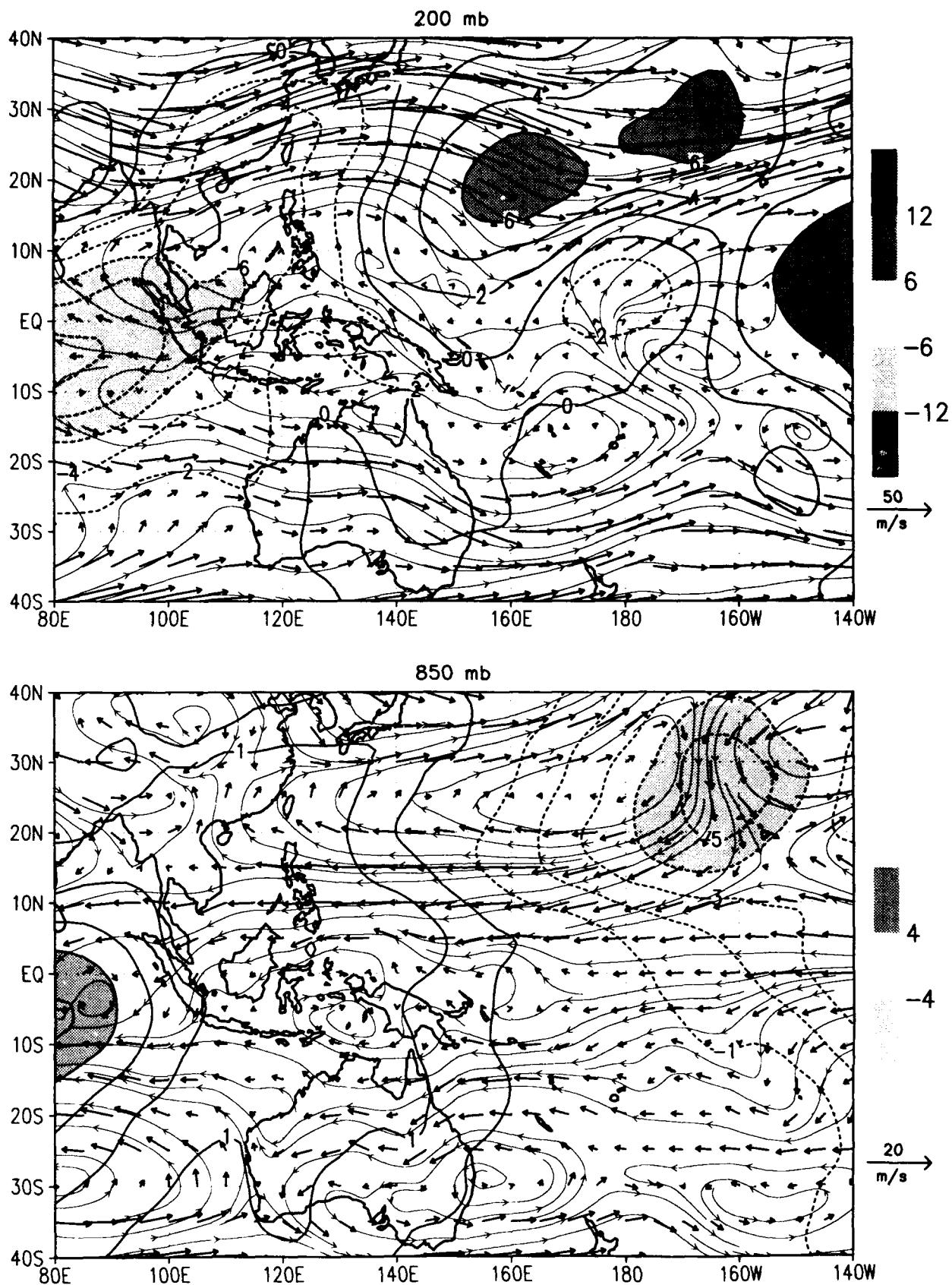
NOGAPS and GPI 5-day ave Precip ~ 07 JAN 1993
(mm/day) /d2/toga_coare/d5.gs



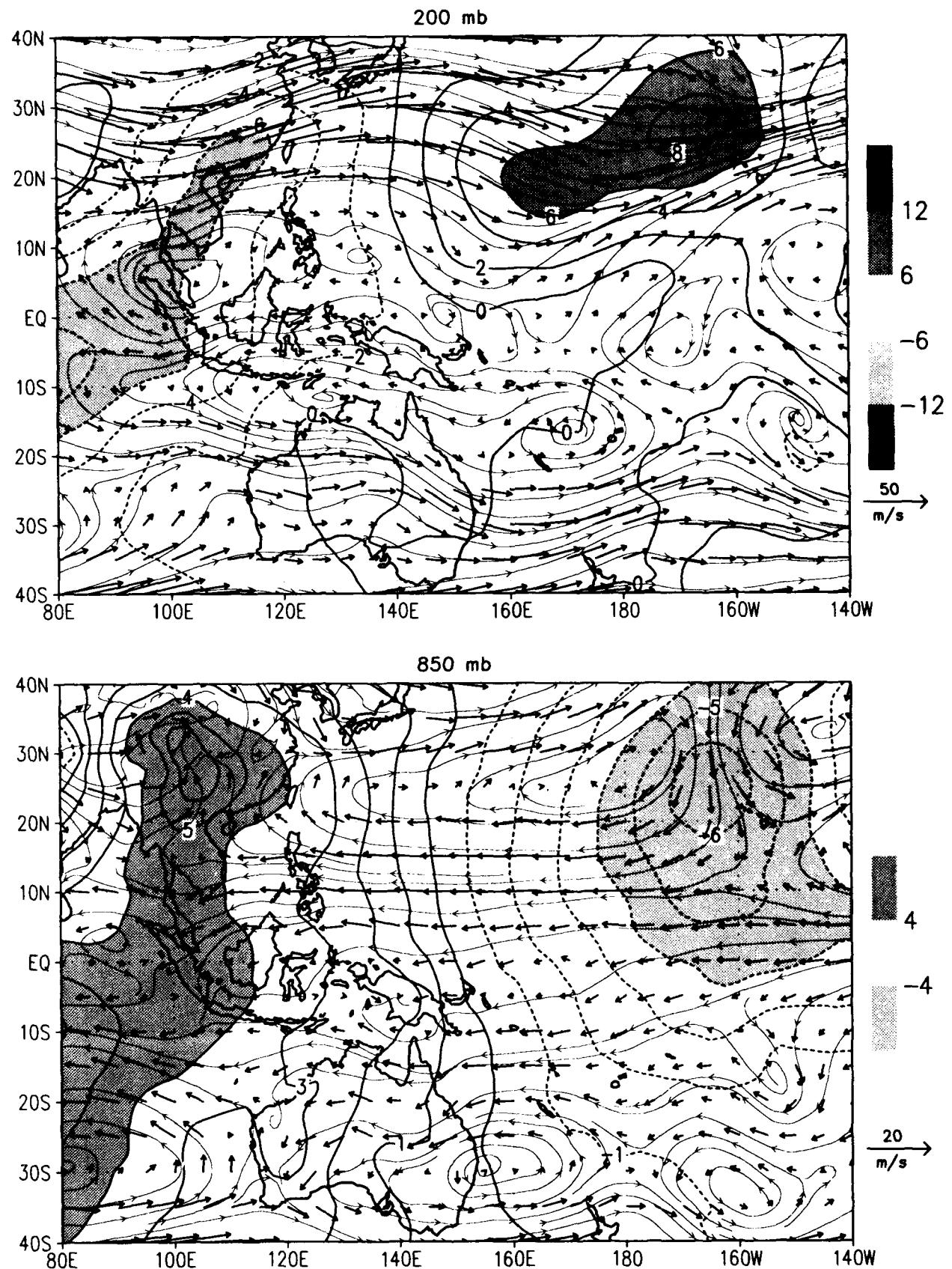
MRF and GPI 5-day ave Precip ~ 07 JAN 1993
(mm/day) /d2/toga_coare/d5.gs



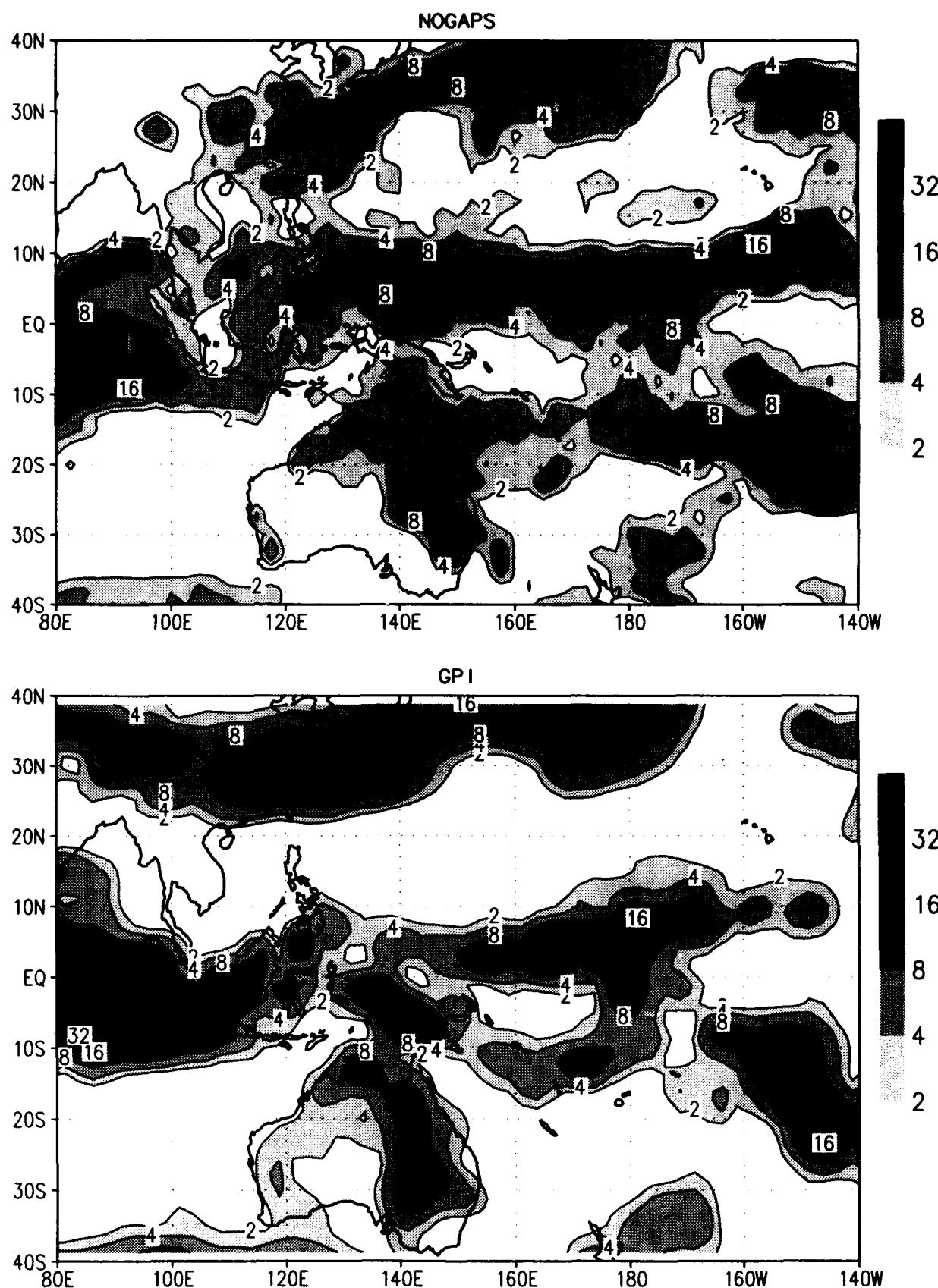
NOGAPS 5-day ave flow and chi ~ 12 JAN 1993
wind (m/s) chi (1e6 m²/s) /d2/toga_coare/d5.gs



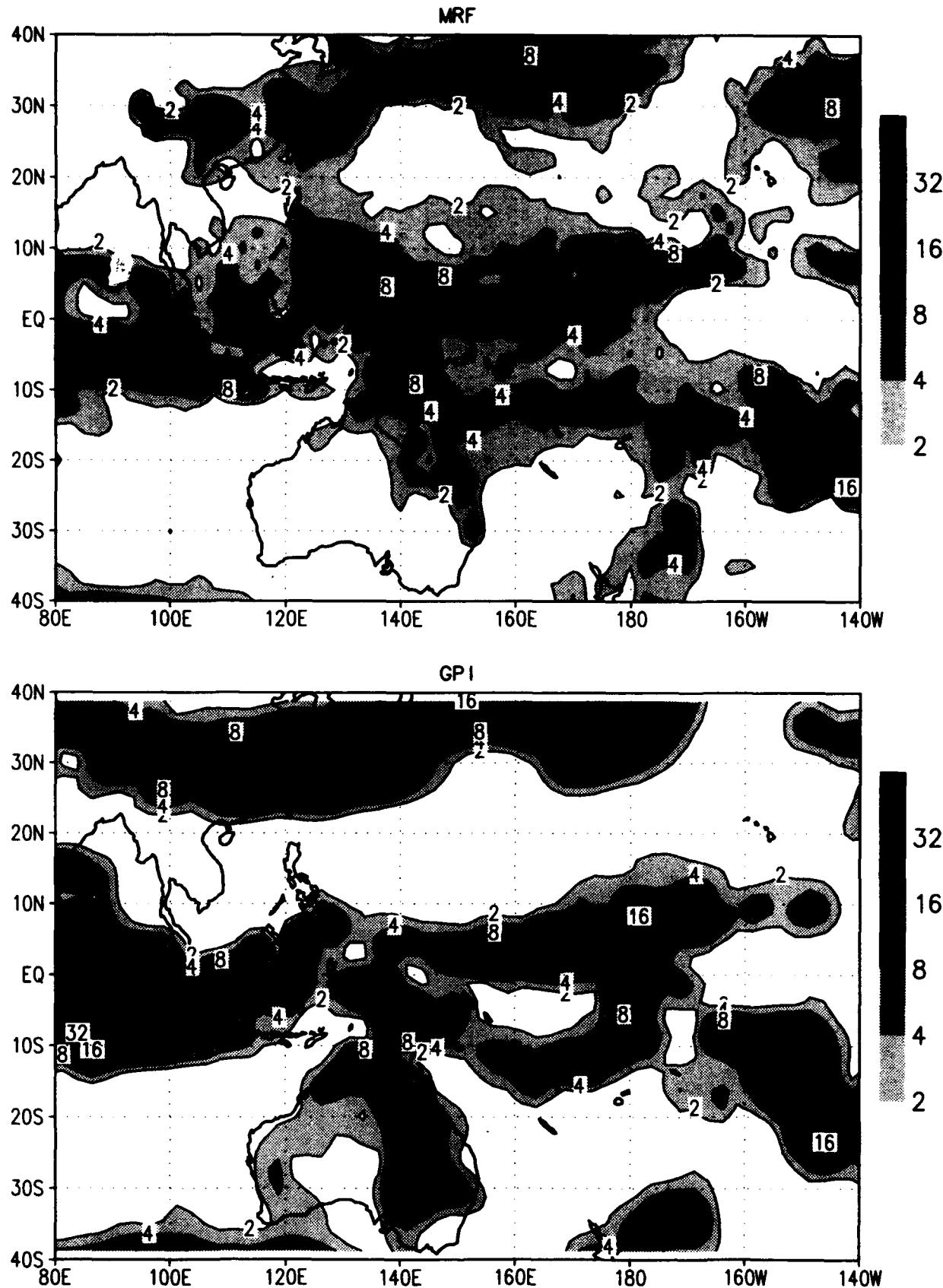
MRF 5-day ave flow and chi ~ 12 JAN 1993
 wind (m/s) chi ($1e6 \text{ m}^2/\text{s}$) /d2/toga_coare/d5.gs



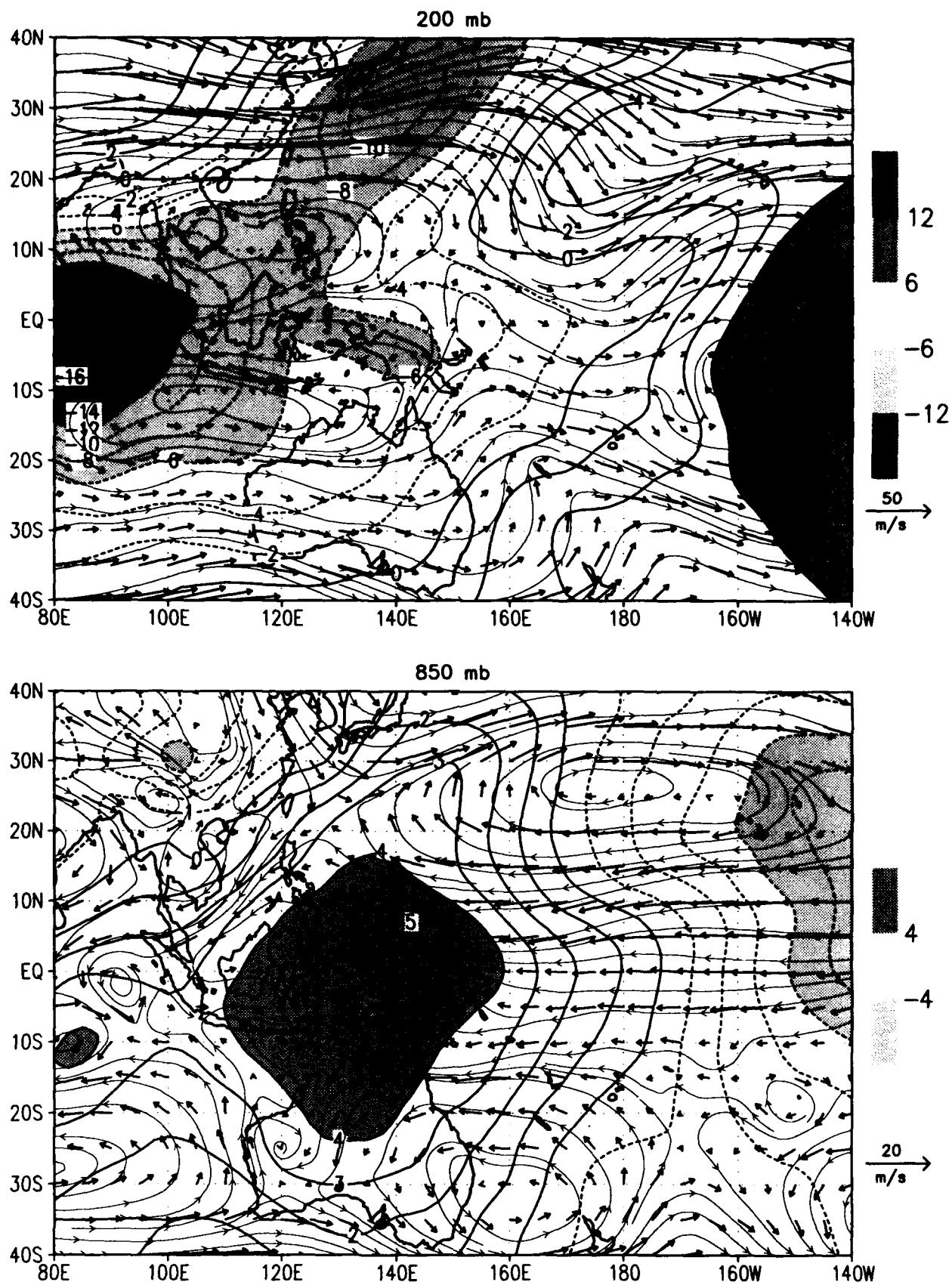
NOGAPS and GPI 5-day ave Precip ~ 12 JAN 1993
(mm/day) /d2/toga_coare/d5.gs



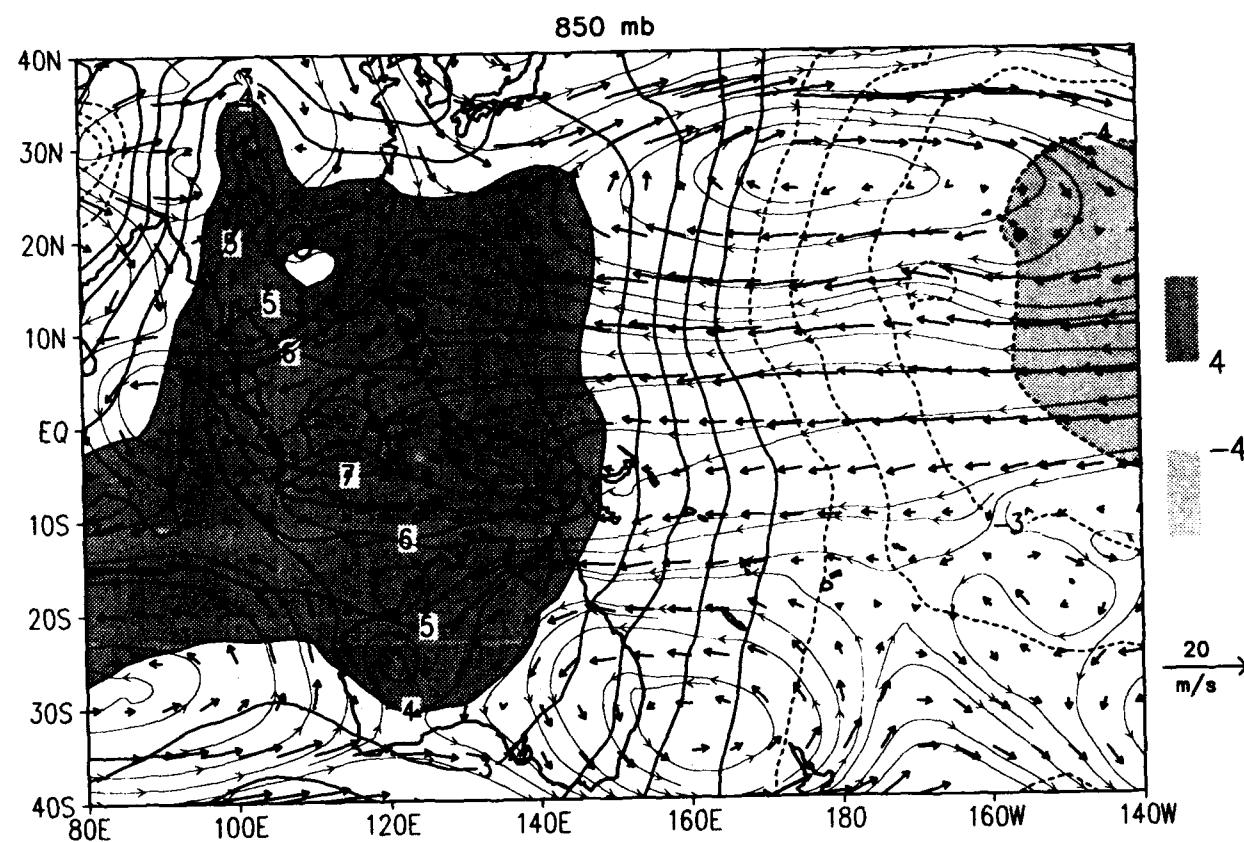
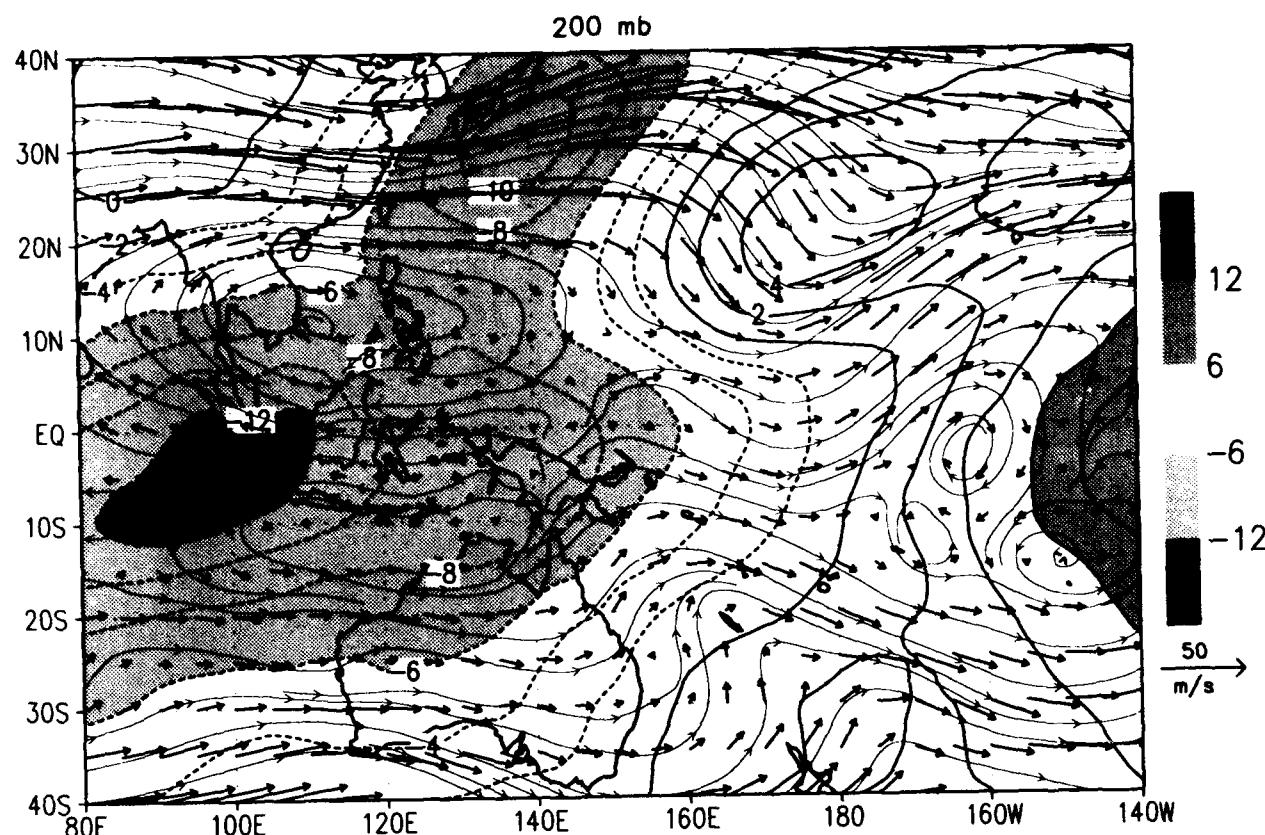
MRF and GPI 5-day ave Precip ~ 12 JAN 1993
(mm/day) /d2/toga_coare/d5.gs



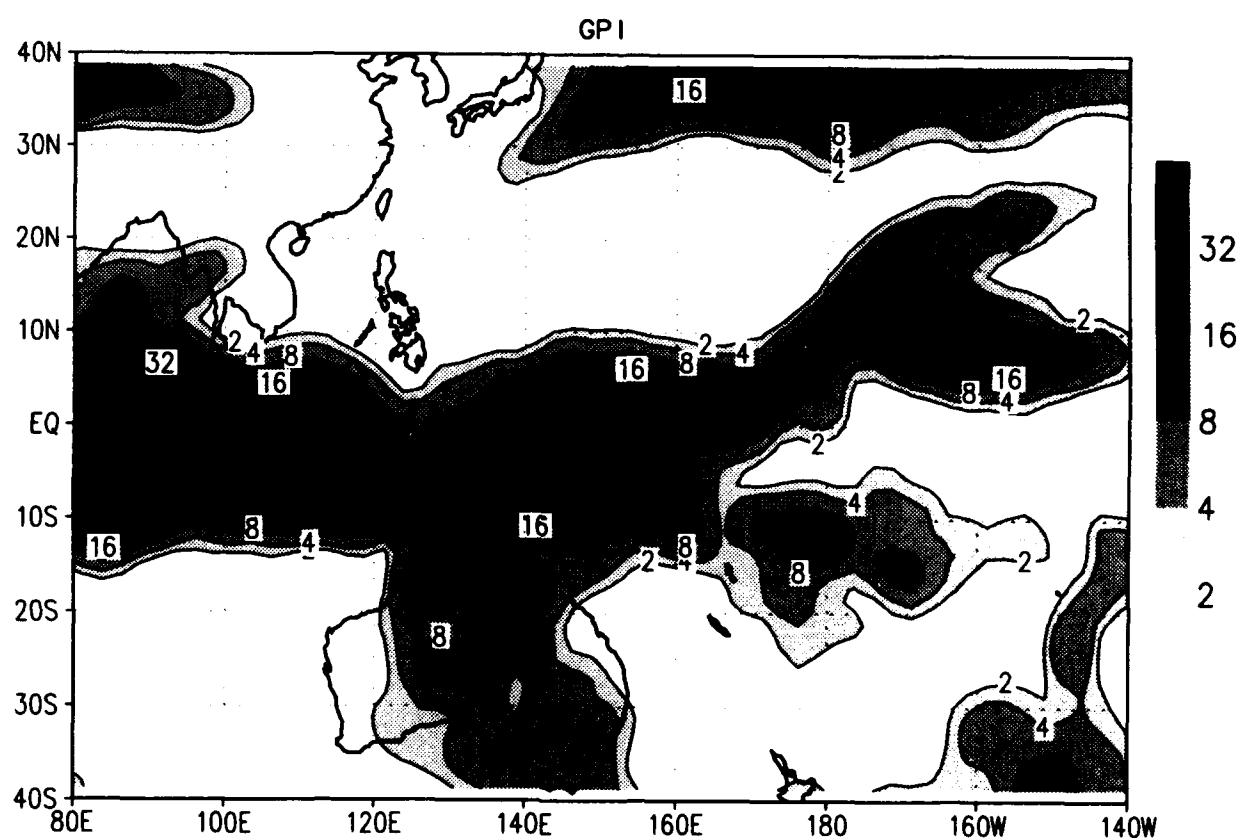
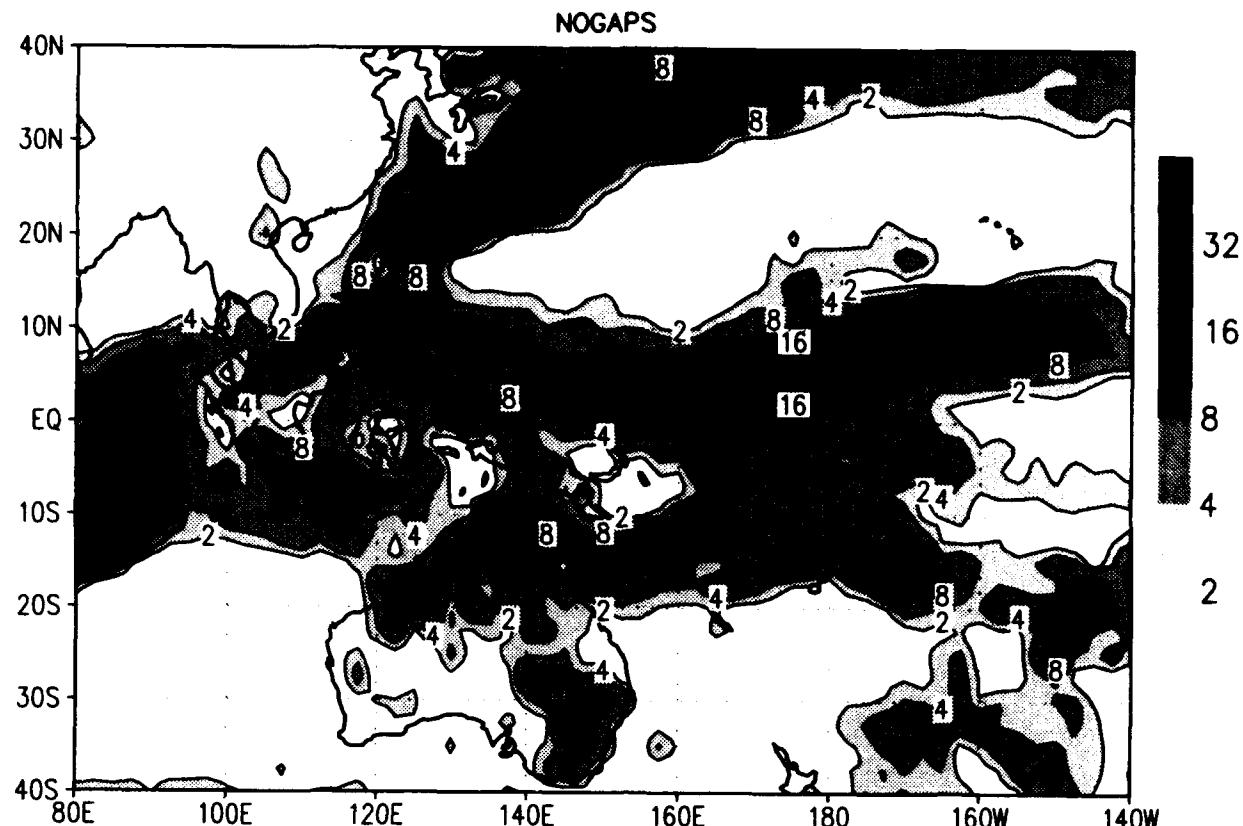
NOGAPS 5-day ave flow and chi ~ 17 JAN 1993
wind (m/s) chi ($10^6 \text{ m}^2/\text{s}$) /d2/toga_coare/d5.gs



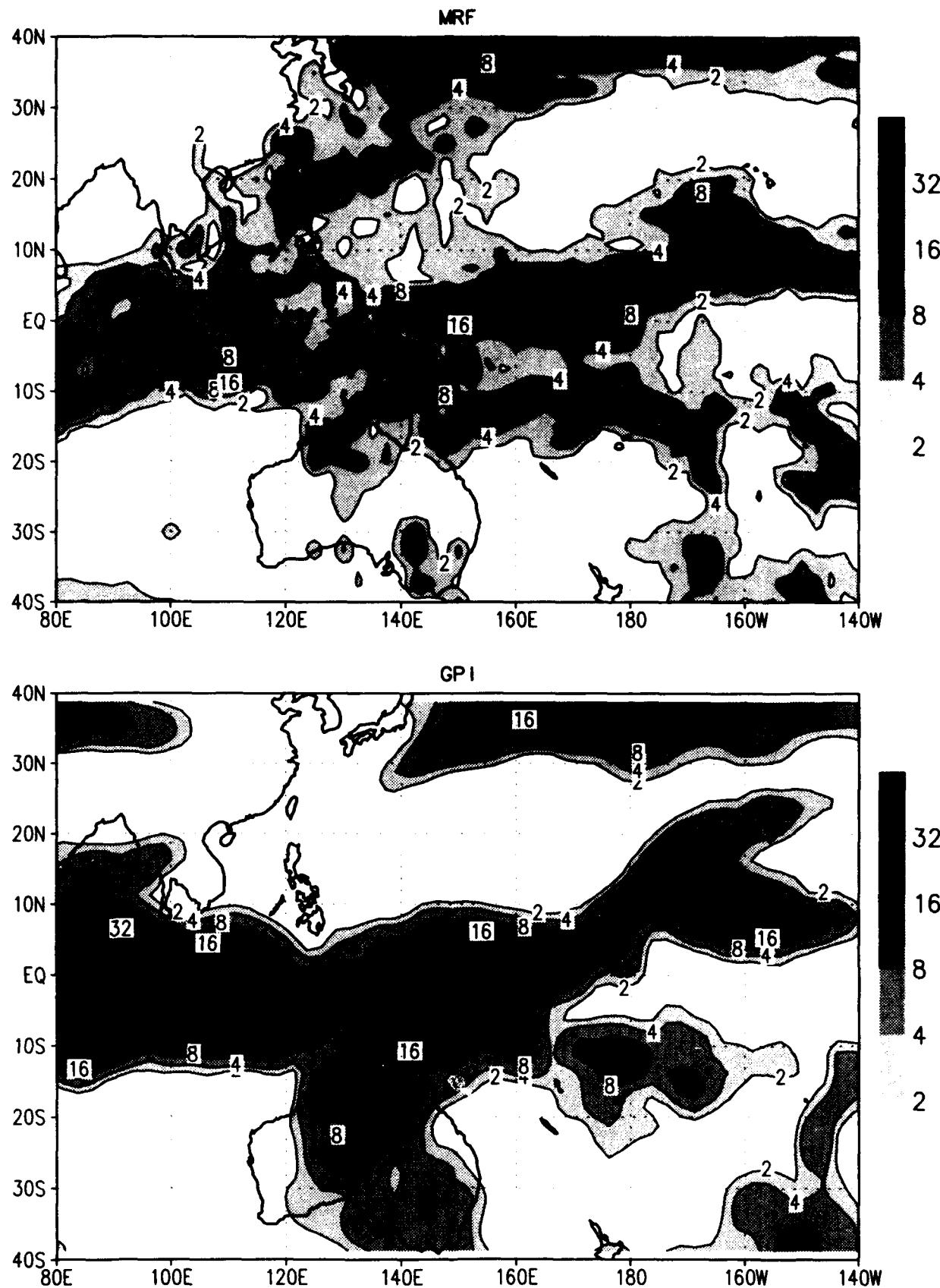
MRF 5-day ave flow and chi ~ 17 JAN 1993
wind (m/s) chi ($10^6 \text{ m}^{-2}/\text{s}$) /d2/toga_coare/d5.gs



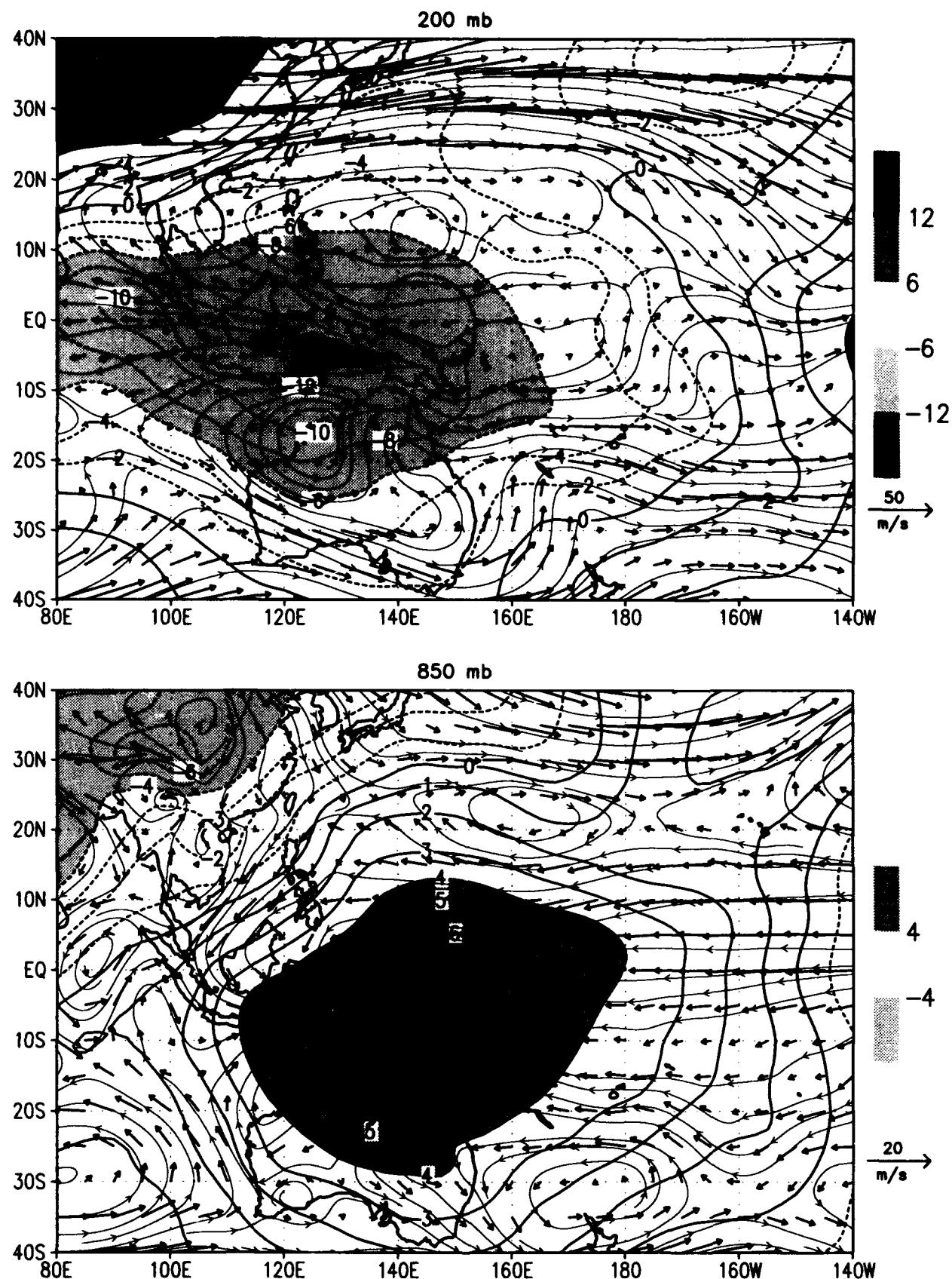
NOGAPS and GPI 5-day ave Precip ~ 17 JAN 1993
(mm/day) /d2/toga_coare/d5.gs



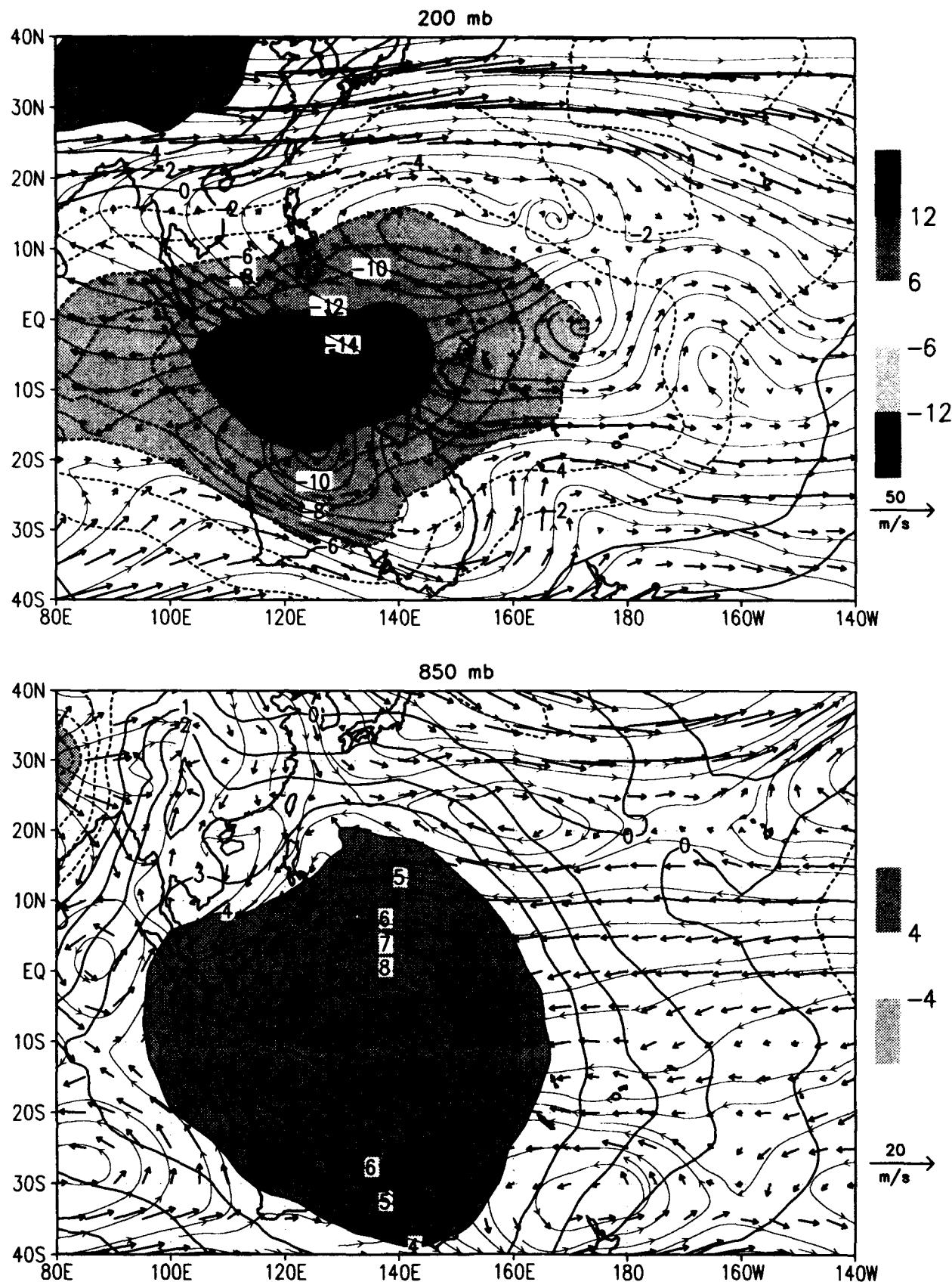
MRF and GPI 5-day ave Precip ~ 17 JAN 1993
(mm/day) /d2/toga_coare/d5.gs



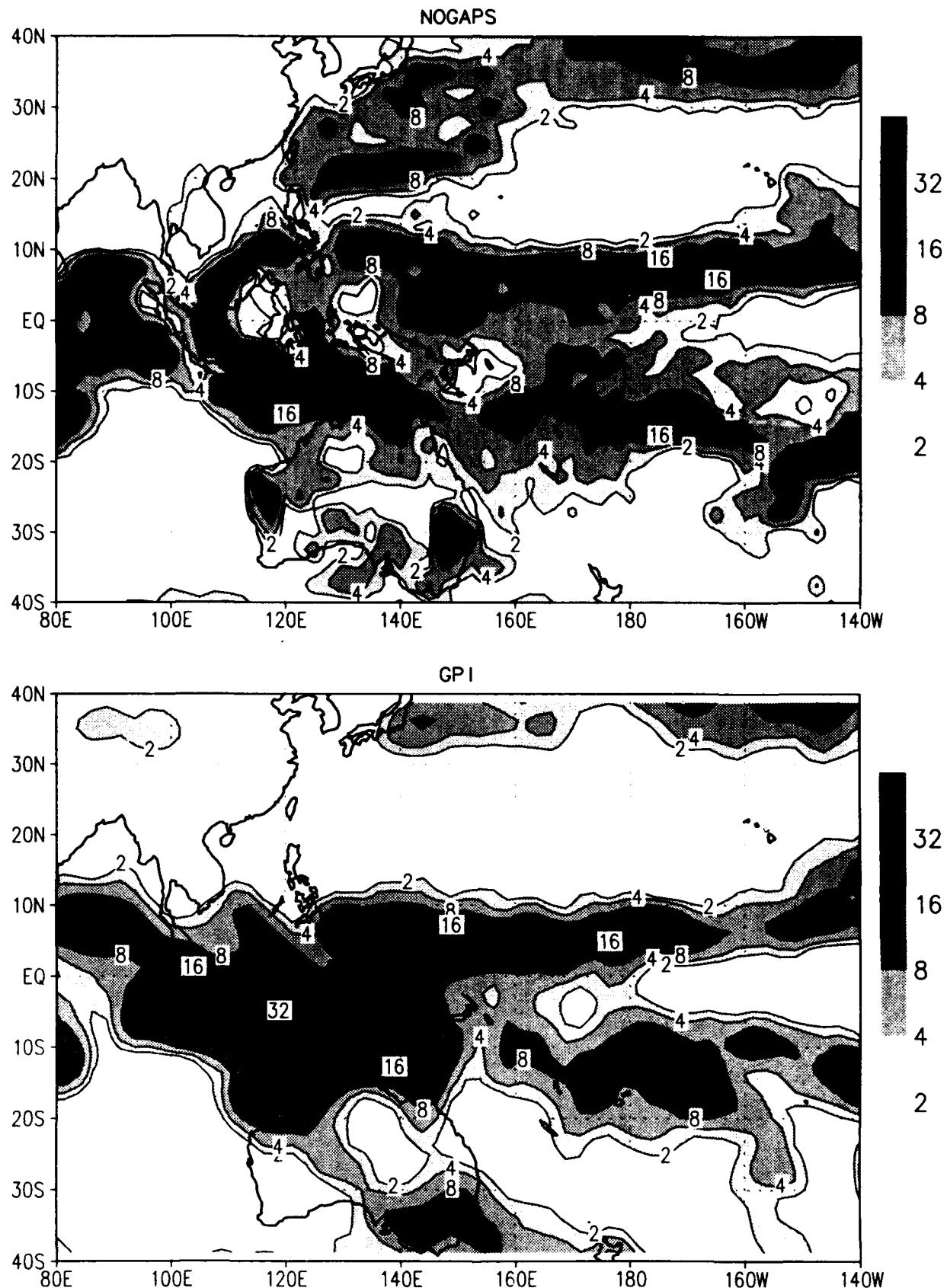
NOGAPS 5-day ave flow and chi ~ 22 JAN 1993
wind (m/s) chi ($10^6 \text{ m}^2/\text{s}$) /d2/toga_coare/d5.gs



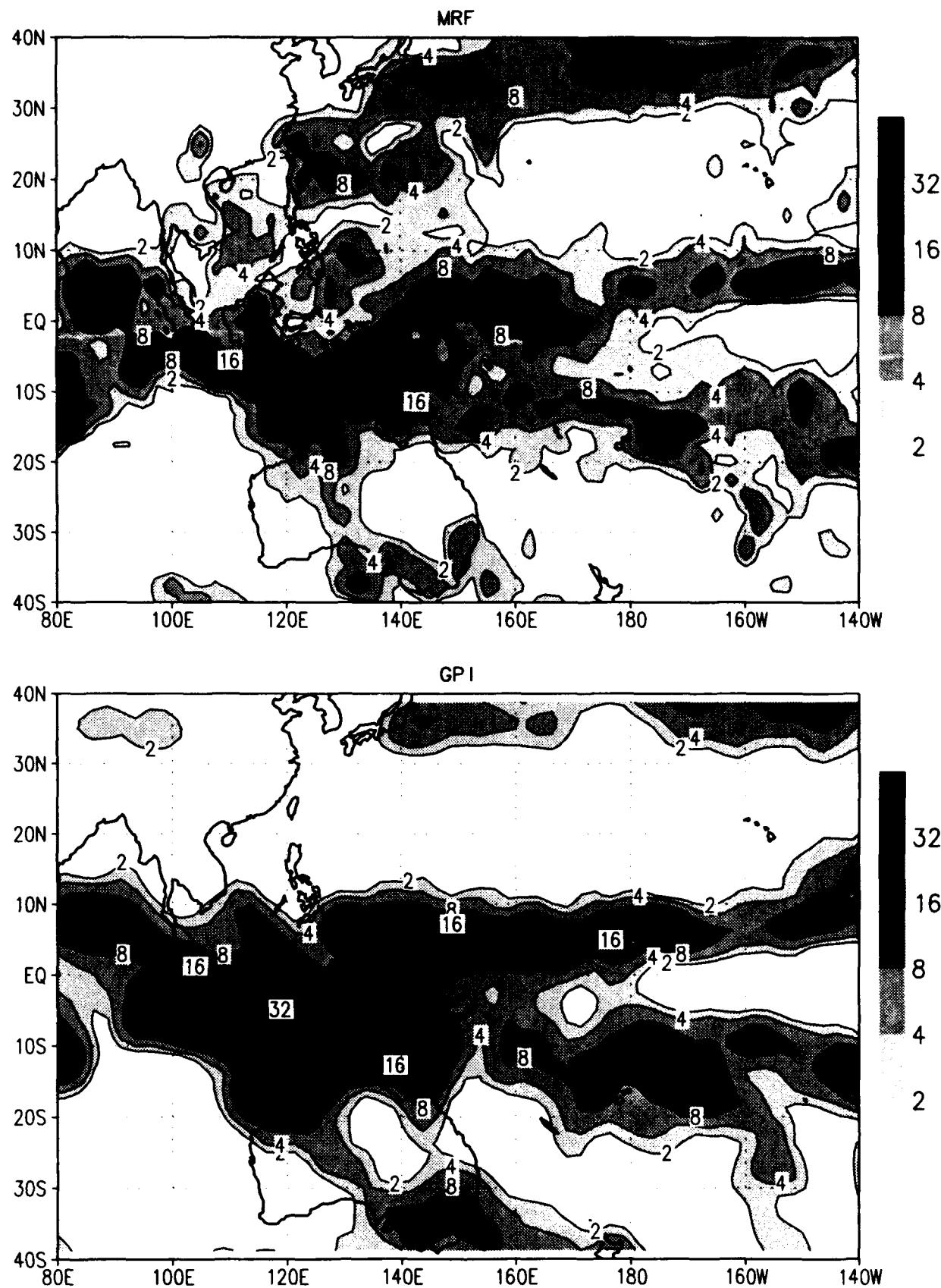
MRF 5-day ave flow and chi ~ 22 JAN 1993
wind (m/s) chi ($10^6 \text{ m}^2/\text{s}$) /d2/toga_coare/d5.gs



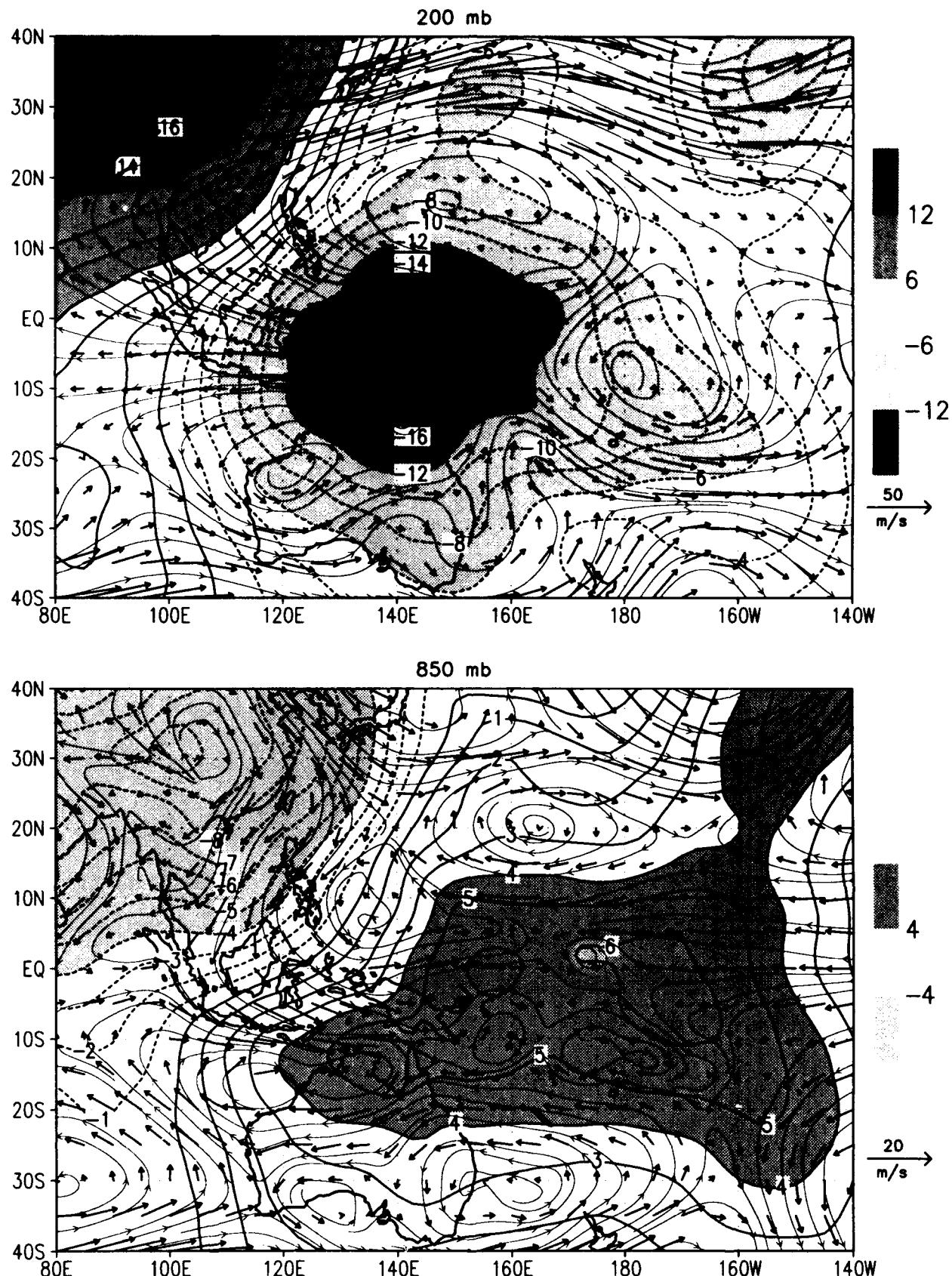
NOGAPS and GPI 5-day ave Precip ~ 22 JAN 1993
(mm/day) /d2/toga_coare/d5.gs



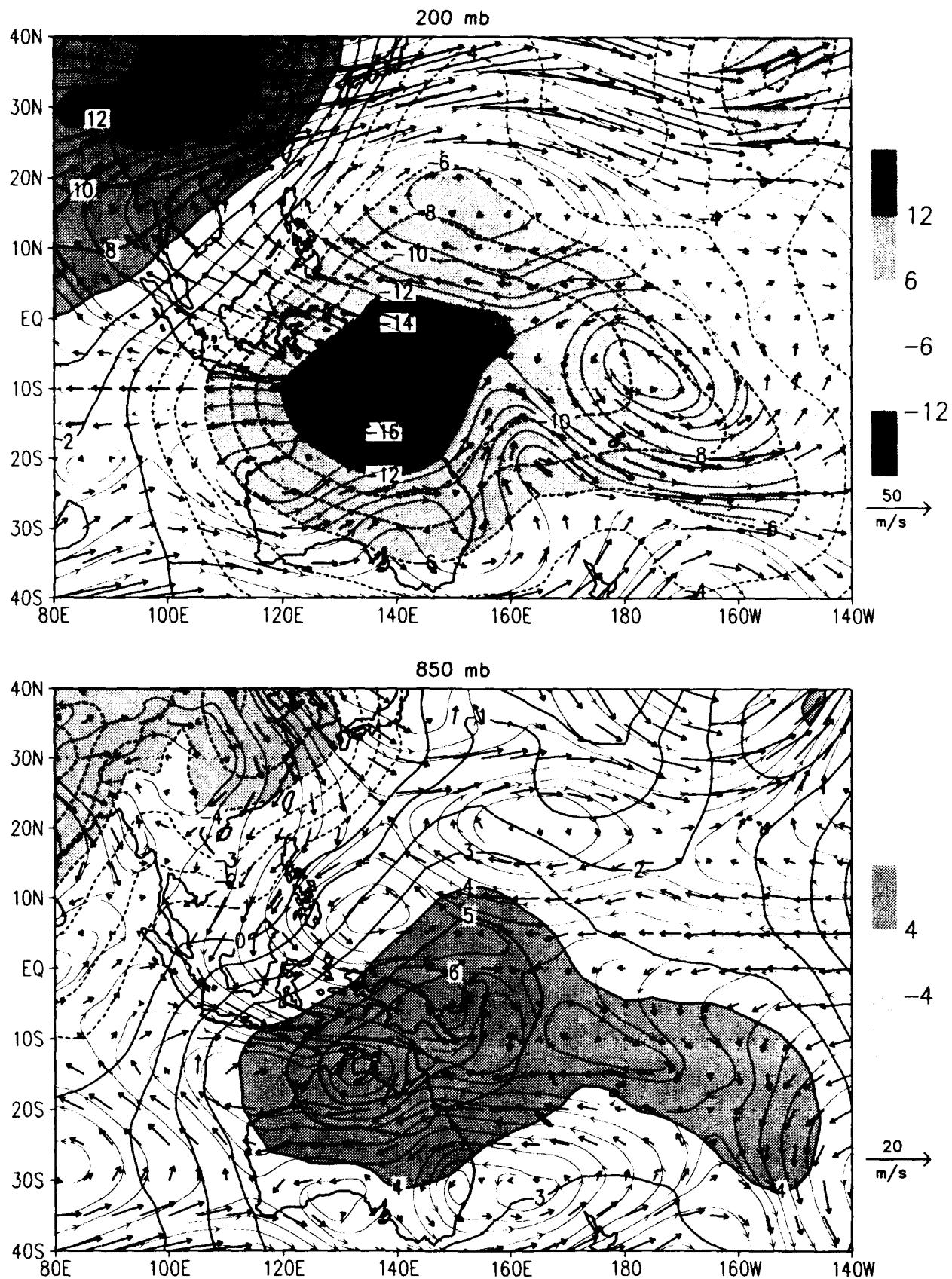
MRF and GPI 5-day ave Precip ~ 22 JAN 1993
(mm/day) /d2/toga_coare/d5.gs



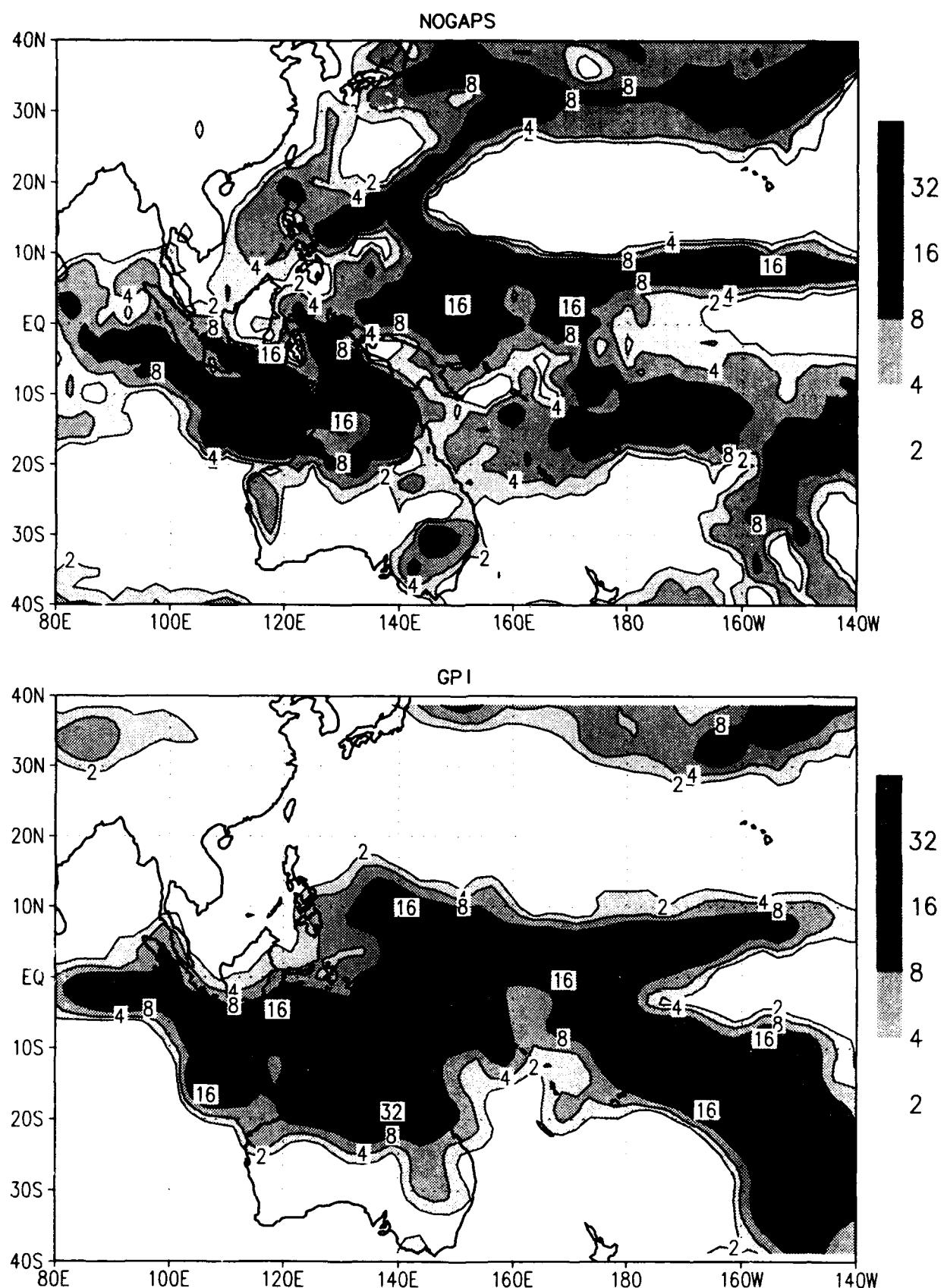
NOGAPS 5-day ave flow and chi ~ 27 JAN 1993
wind (m/s) chi ($1e6 \text{ m}^2/\text{s}$) /d2/toga_coare/d5.gs



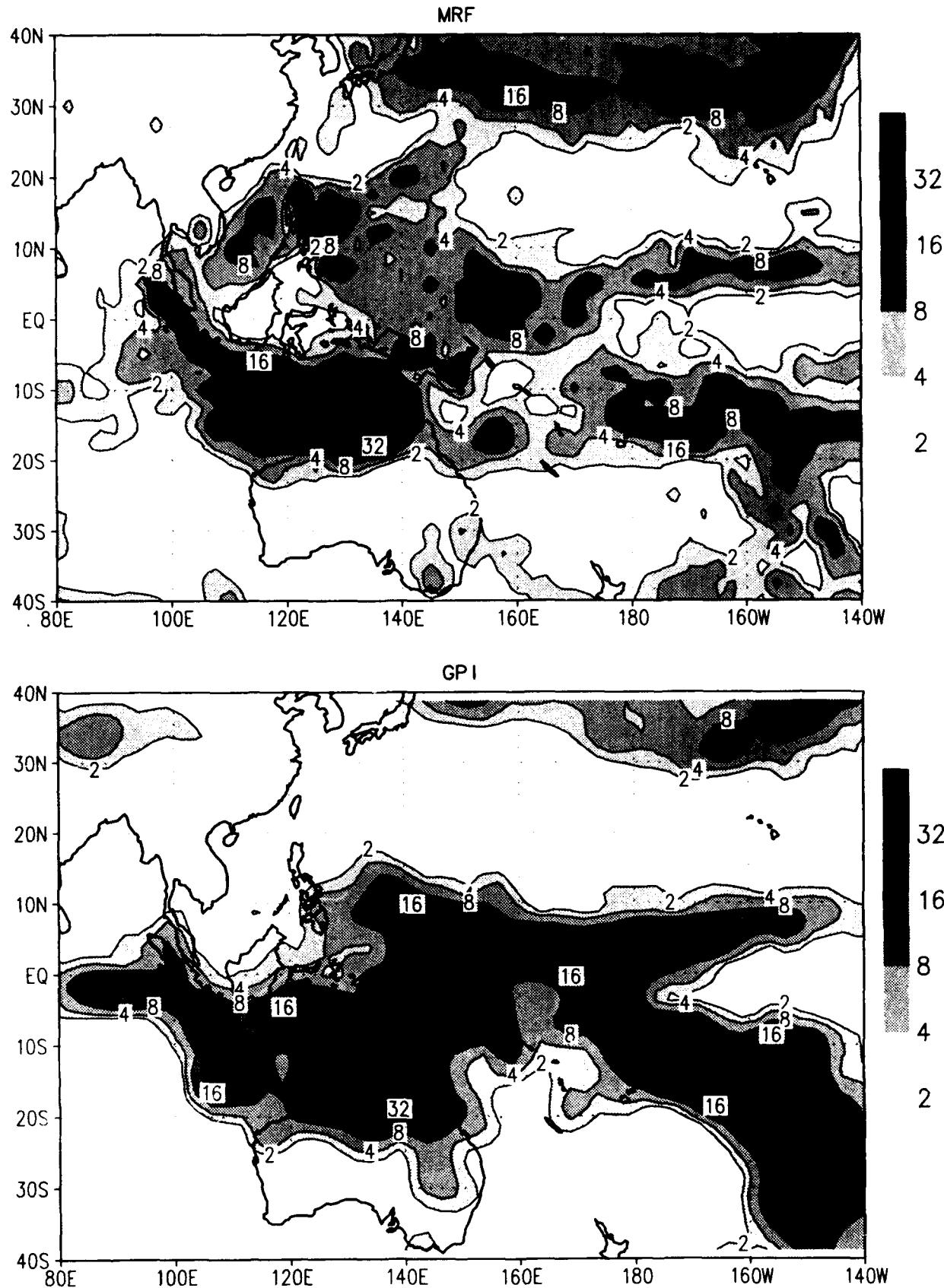
MRF 5-day ave flow and chi ~ 27 JAN 1993
 wind (m/s) chi ($1e6\text{ m}^2/\text{s}$) /d2/toga_coare/d5.gs



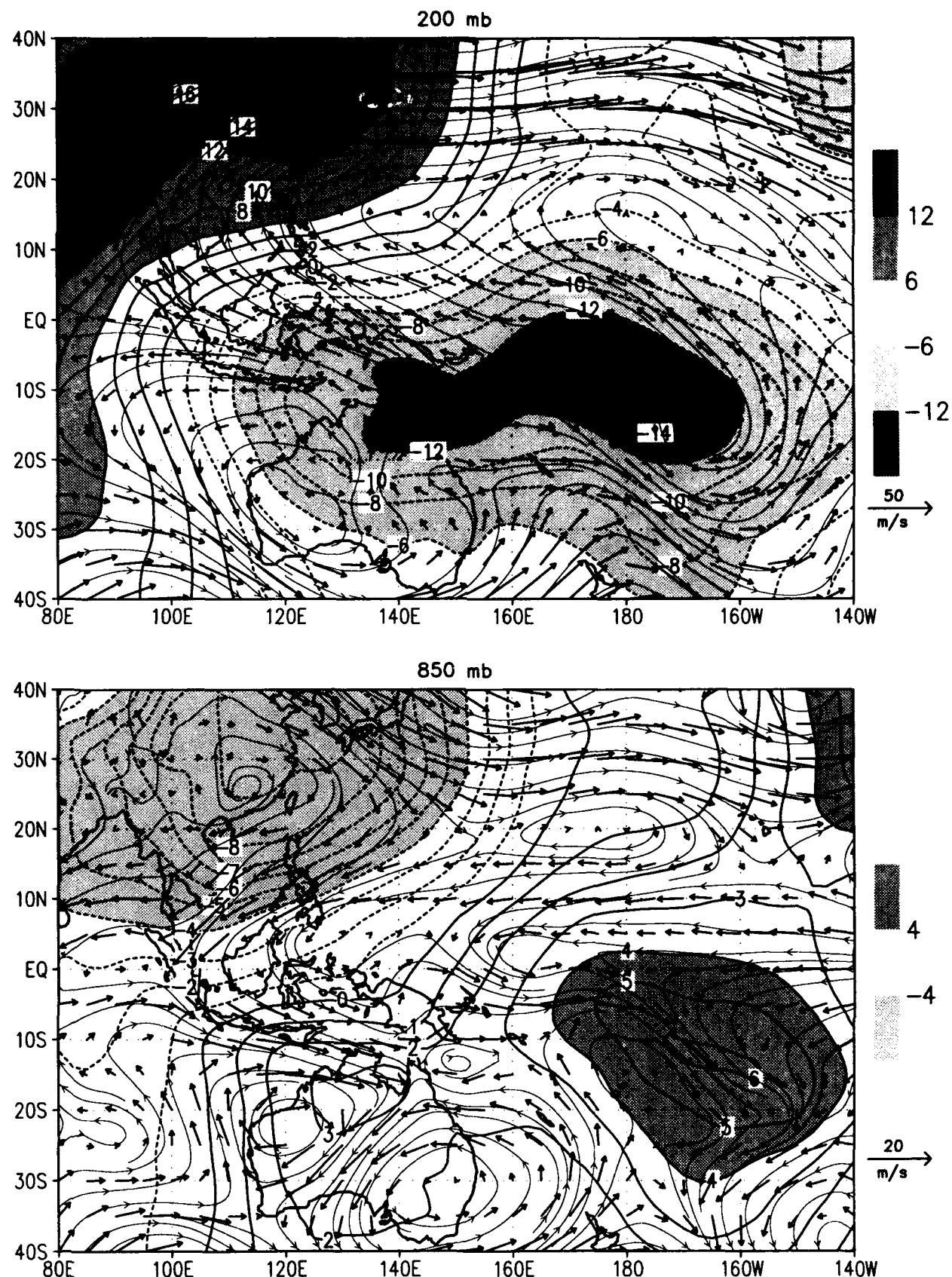
NOGAPS and GPI 5-day ave Precip ~ 27 JAN 1993
(mm/day) /d2/toga_coare/d5.gs



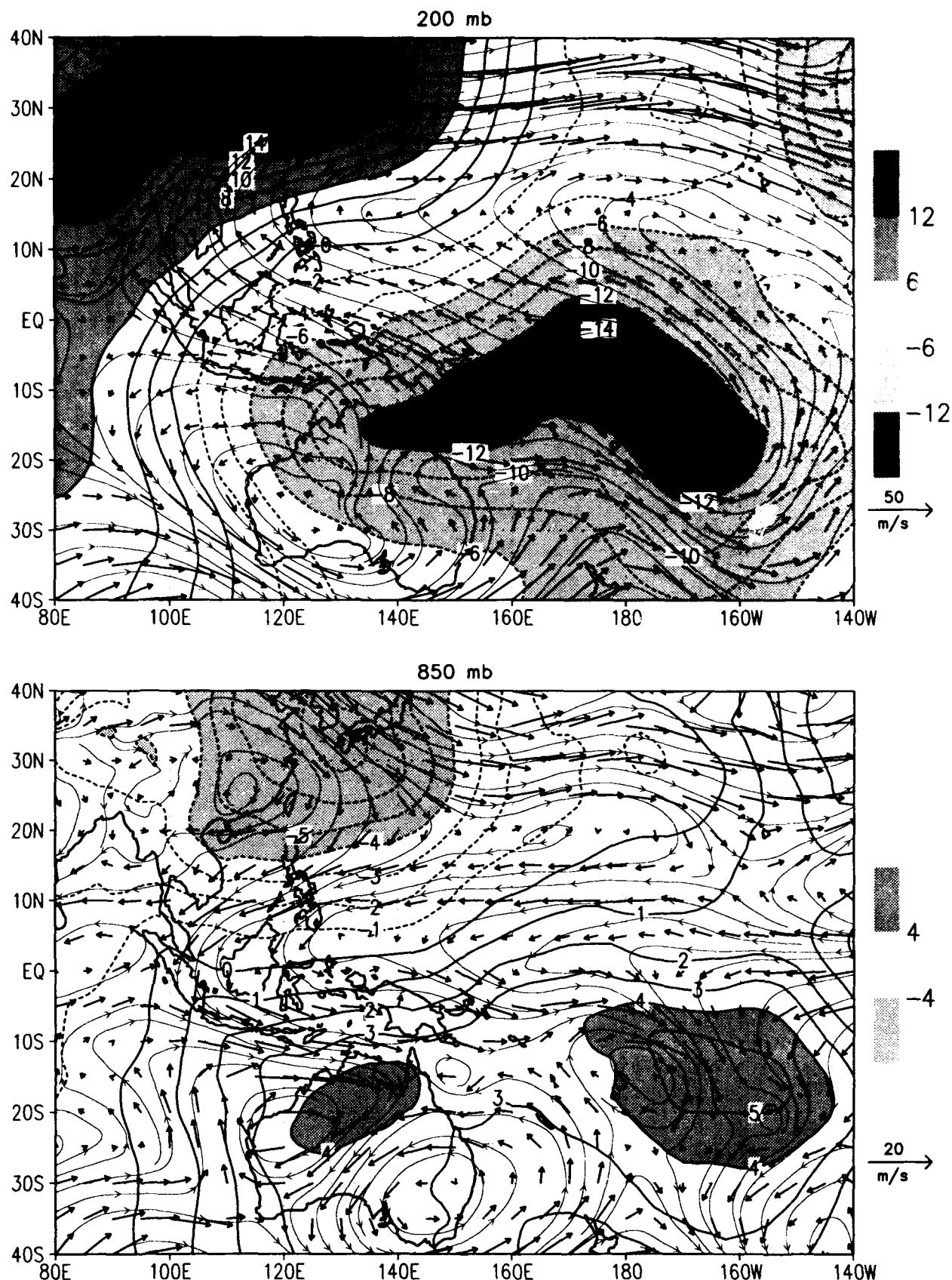
MRF and GPI 5-day ave Precip ~ 27 JAN 1993
 (mm/day) /d2/toga_coare/d5.gs



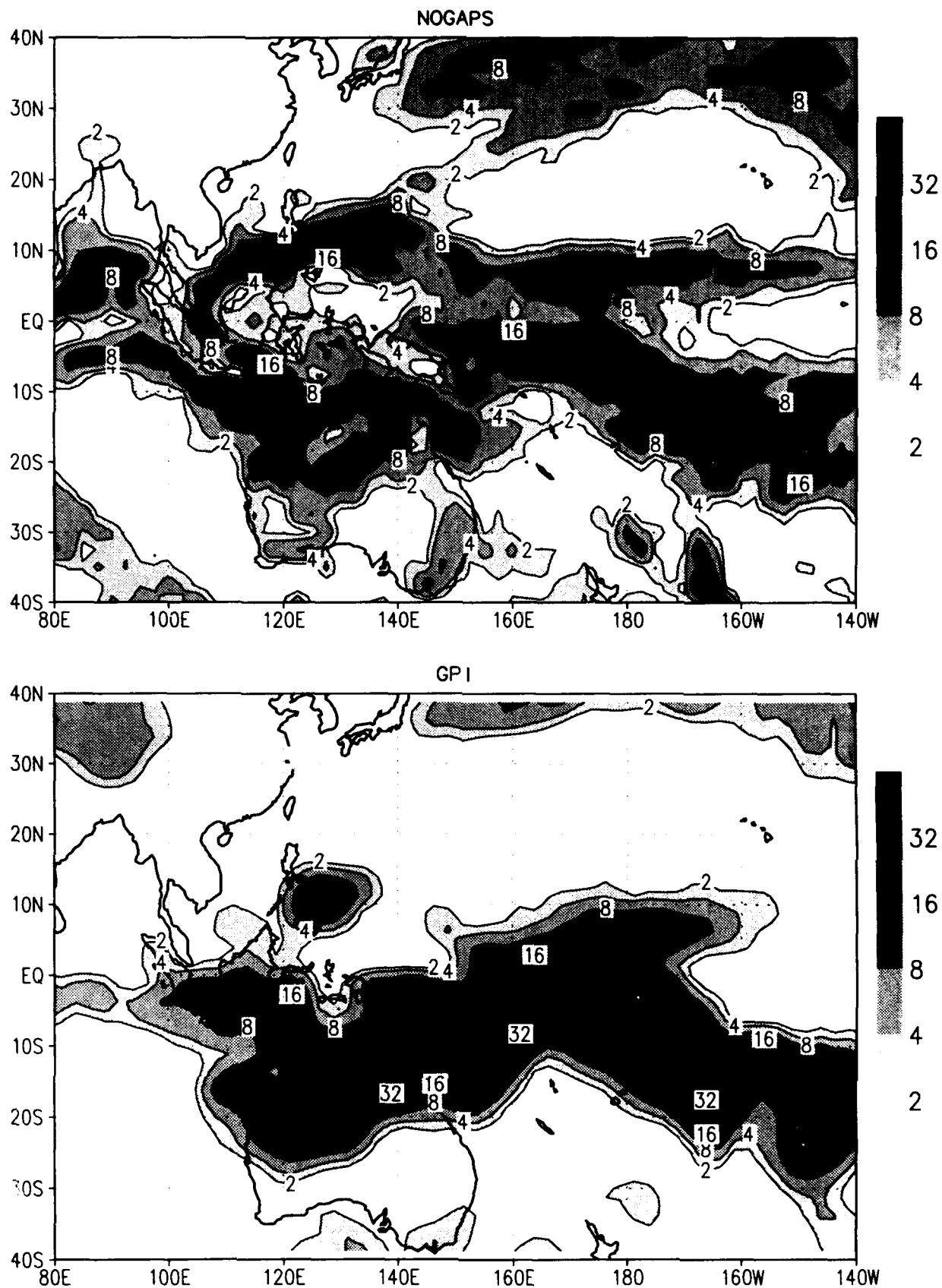
NOGAPS 5-day ave flow and chi ~ 02 FEB 1993
 wind (m/s) chi ($1e6\text{ m}^2/\text{s}$) /d2/toga_coare/d5.gs



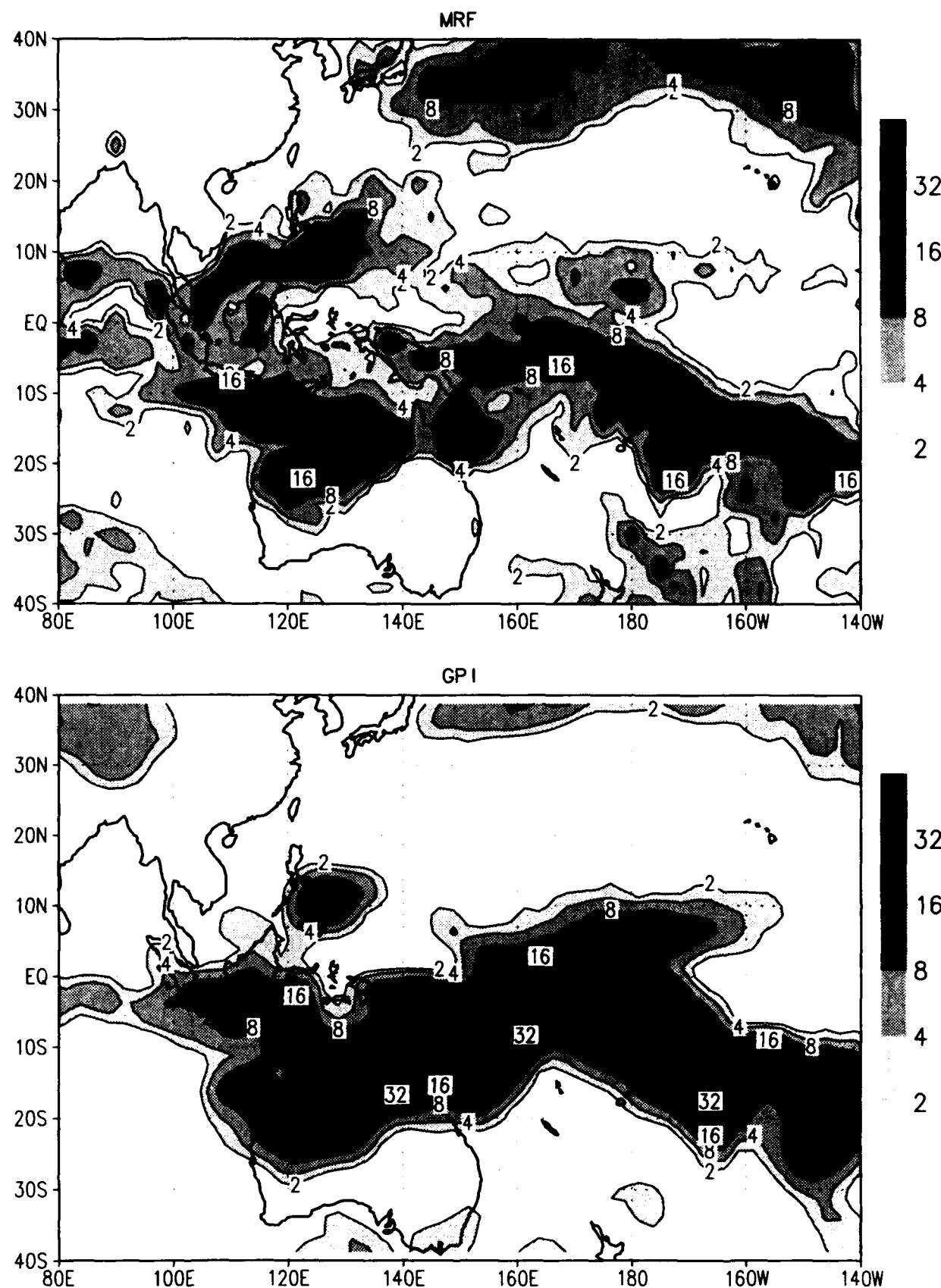
MRF 5-day ave flow and chi ~ 02 FEB 1993
wind (m/s) chi ($1e6 \text{ m}^2/\text{s}$) /d2/toga_coare/d5.gs



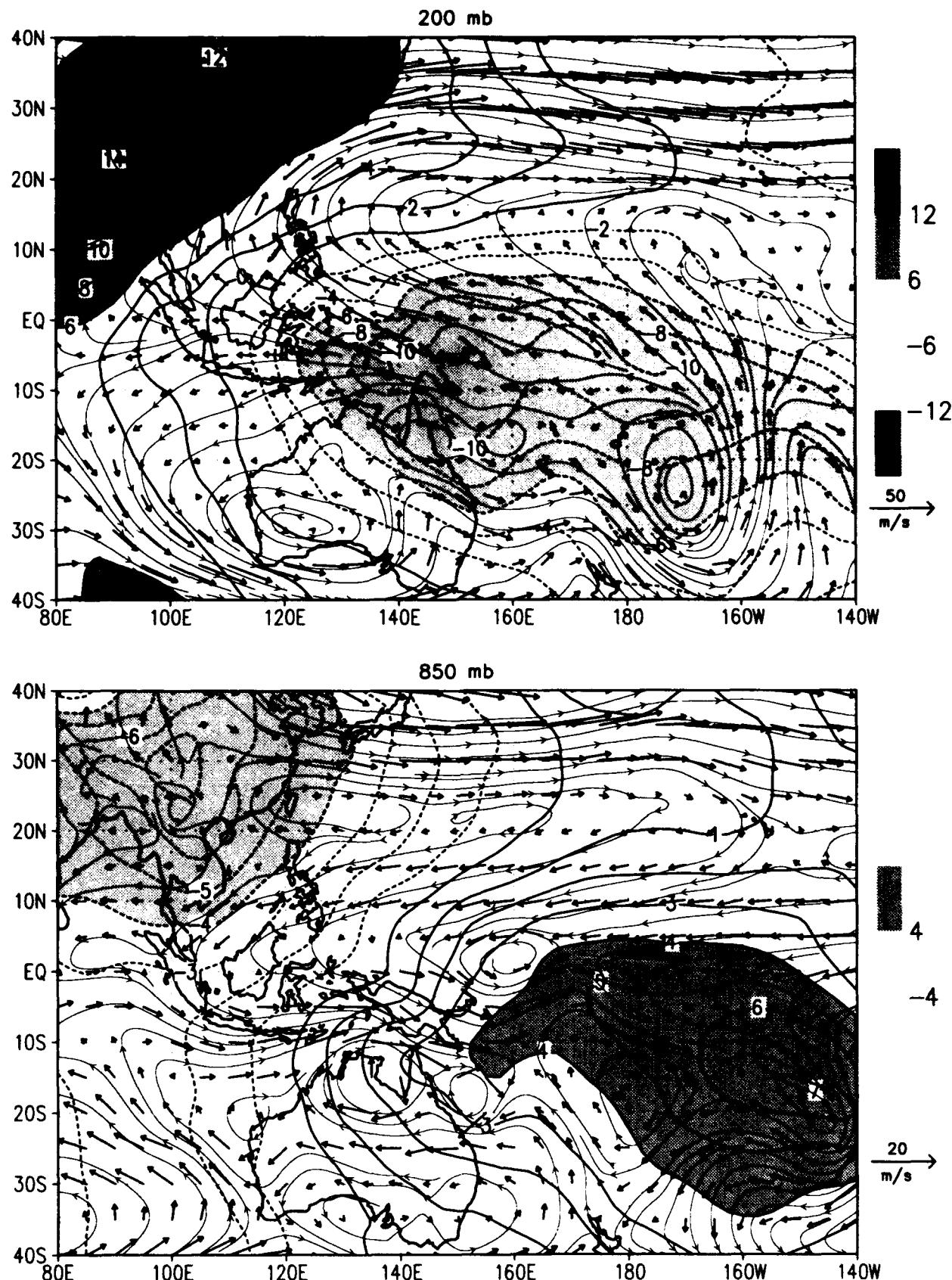
NOGAPS and GPI 5-day ave Precip ~ 02 FEB 1993
(mm/day) /d2/toga_coare/d5.gs



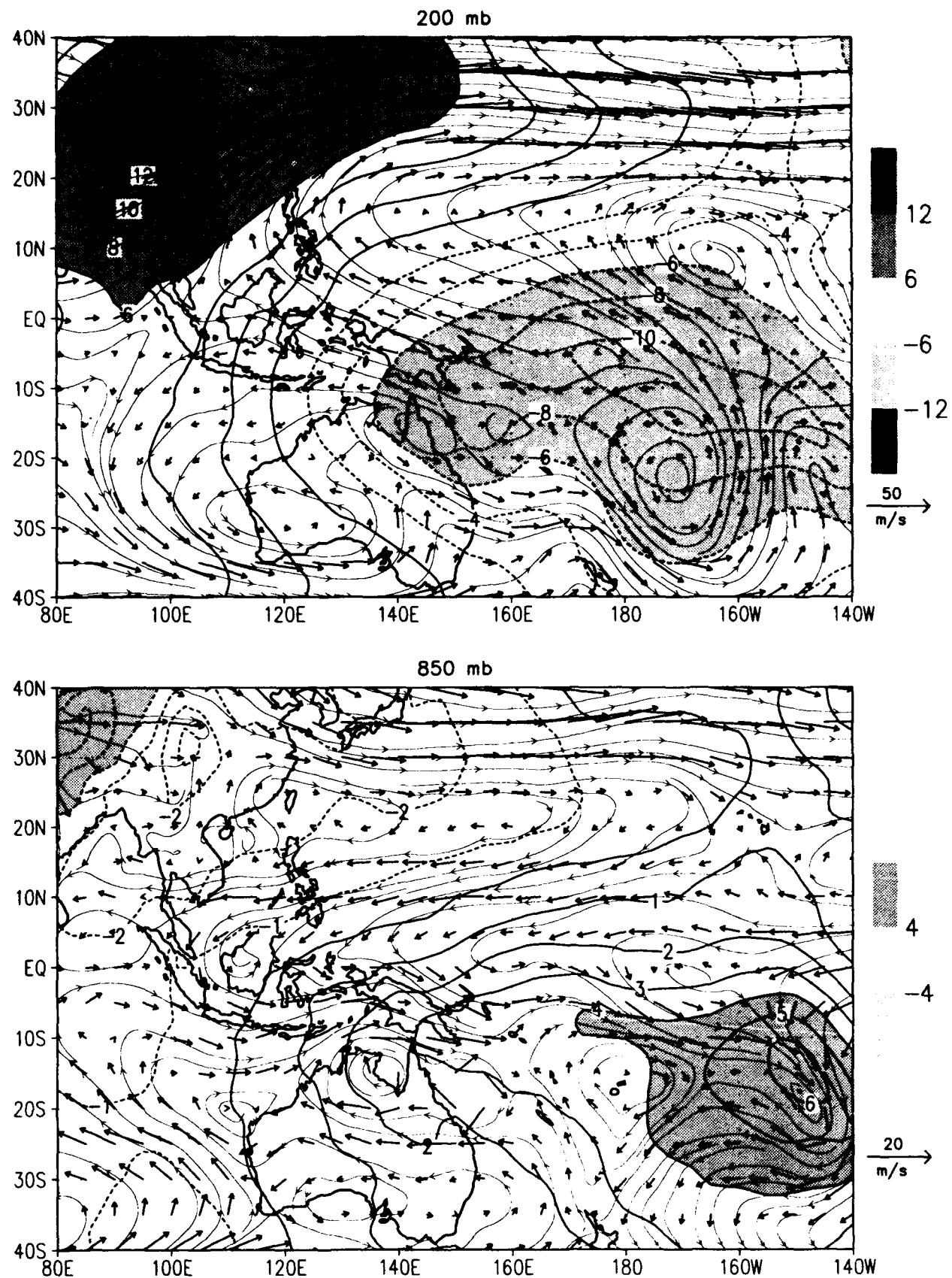
MRF and GPI 5-day ave Precip ~ 02 FEB 1993
(mm/day) /d2/toga_coare/d5.gs



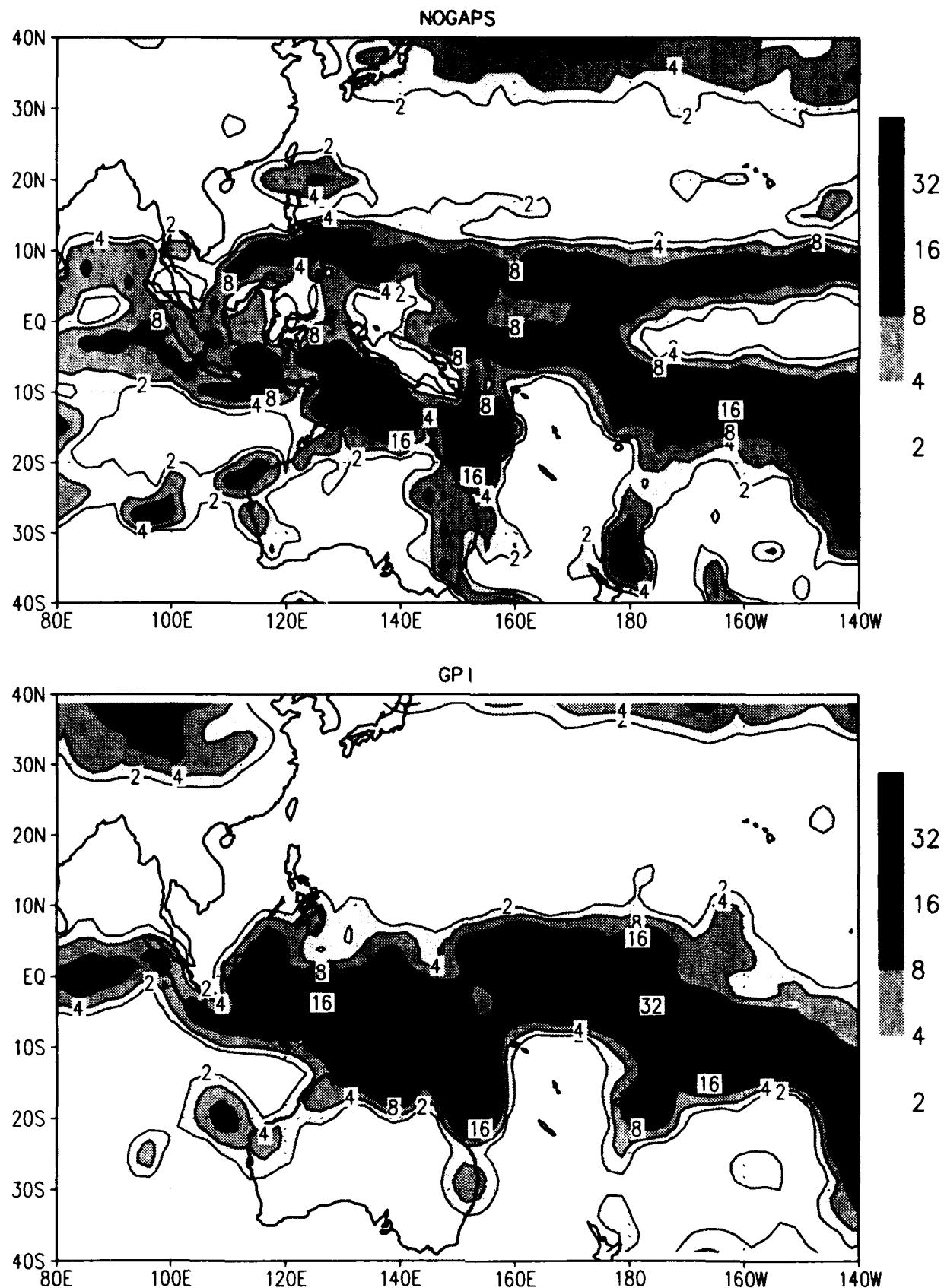
NOGAPS 5-day ave flow and chi ~ 07 FEB 1993
wind (m/s) chi ($10^6 \text{ m}^2/\text{s}$) /d2/toga_coare/d5.gs



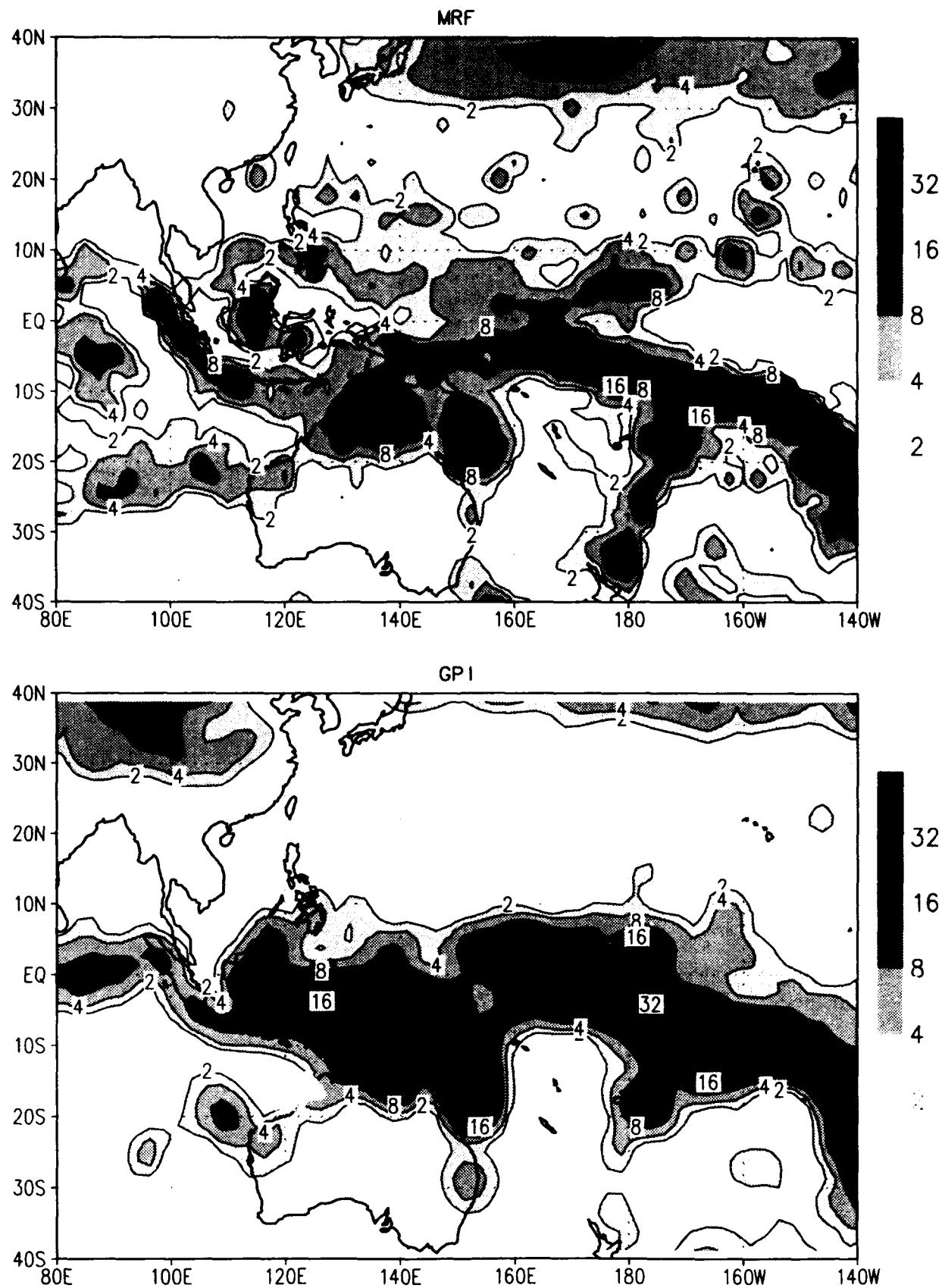
MRF 5-day ave flow and chi ~ 07 FEB 1993
wind (m/s) chi ($10^6 \text{ m}^2/\text{s}$) /d2/toga_coare/d5.gs



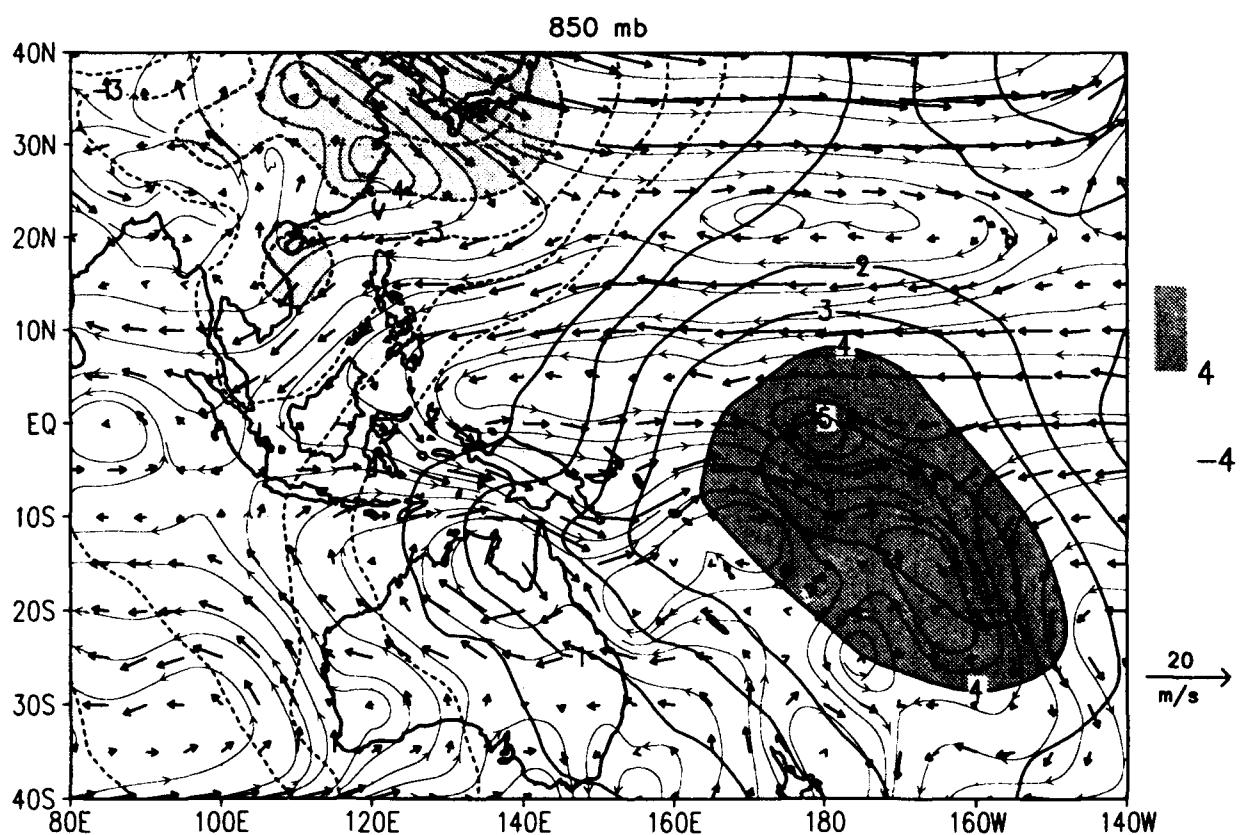
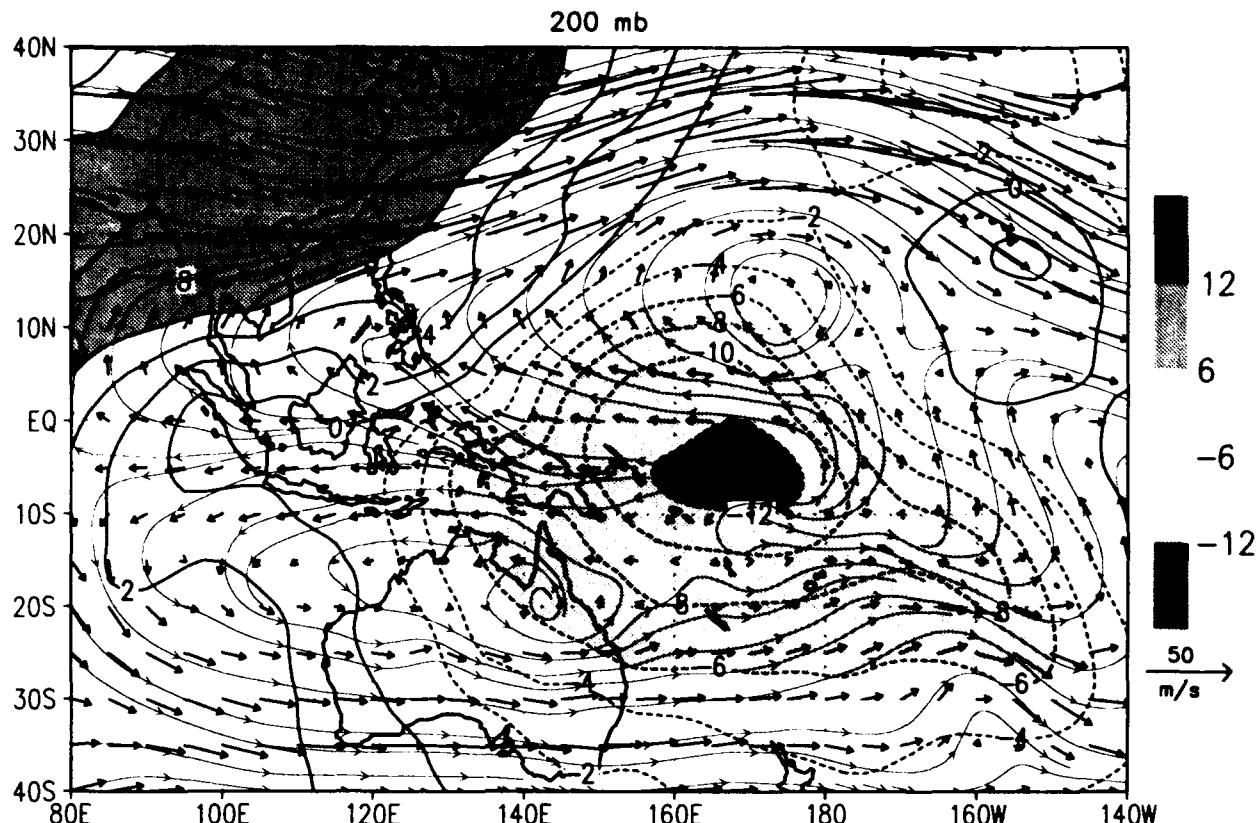
NOGAPS and GPI 5-day ave Precip ~ 07 FEB 1993
(mm/day) /d2/toga_coare/d5.gs



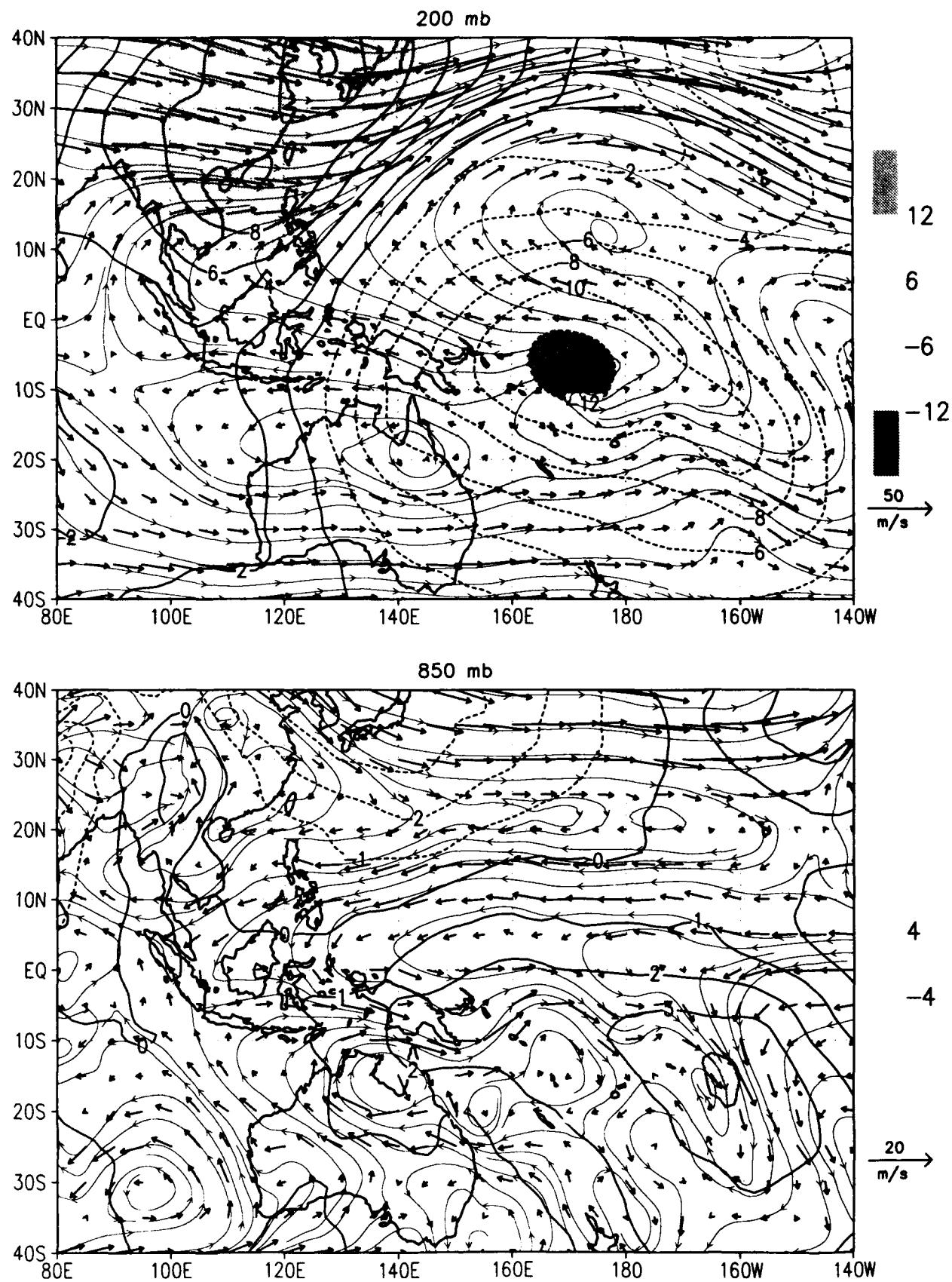
MRF and GPI 5-day ave Precip ~ 07 FEB 1993
(mm/day) /d2/toga_coare/d5.gs



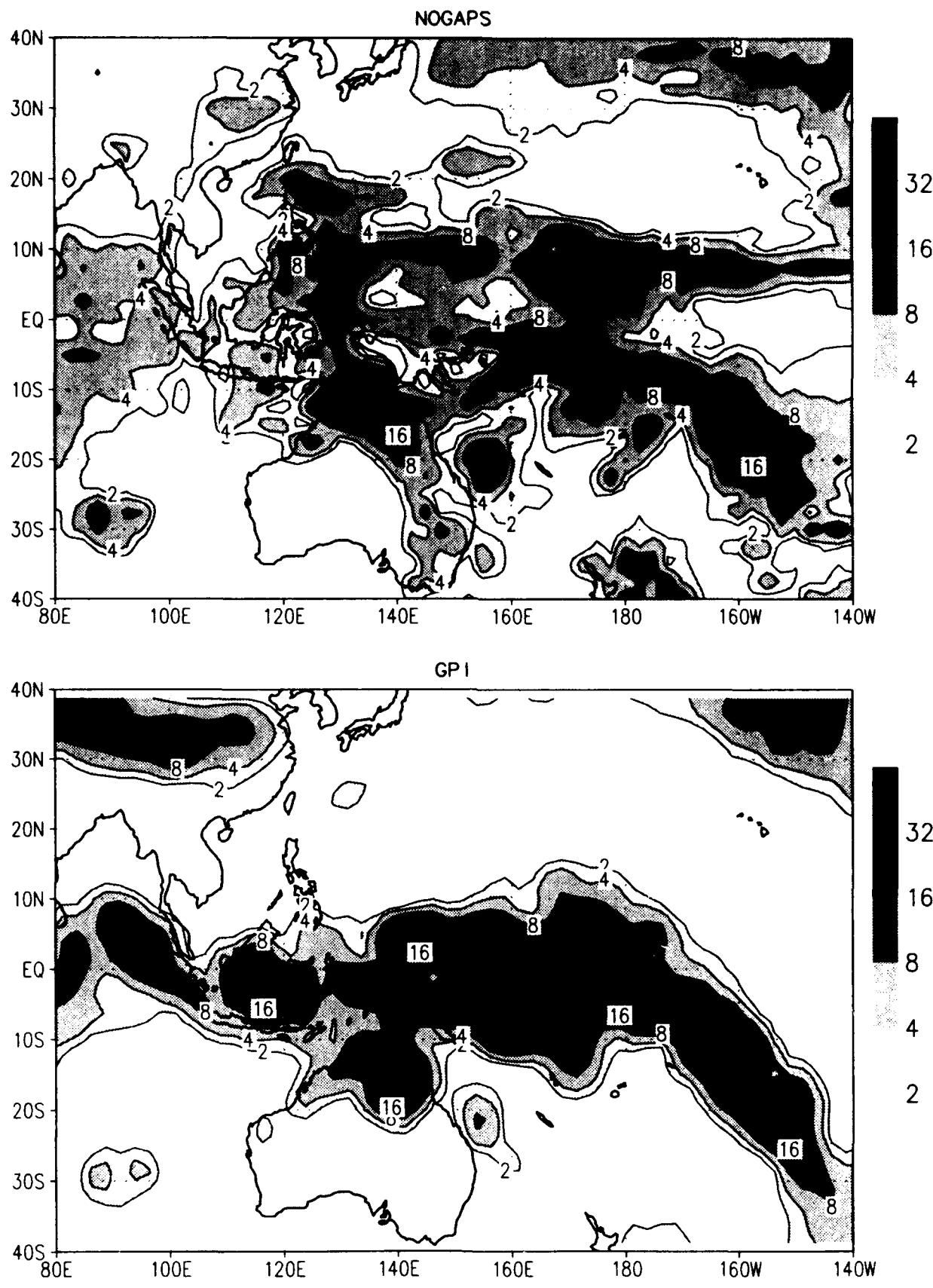
NOGAPS 5-day ave flow and chi ~ 12 FEB 1993
wind (m/s) chi ($10^6 \text{ m}^2/\text{s}$) /d2/toga_coare/d5.gs



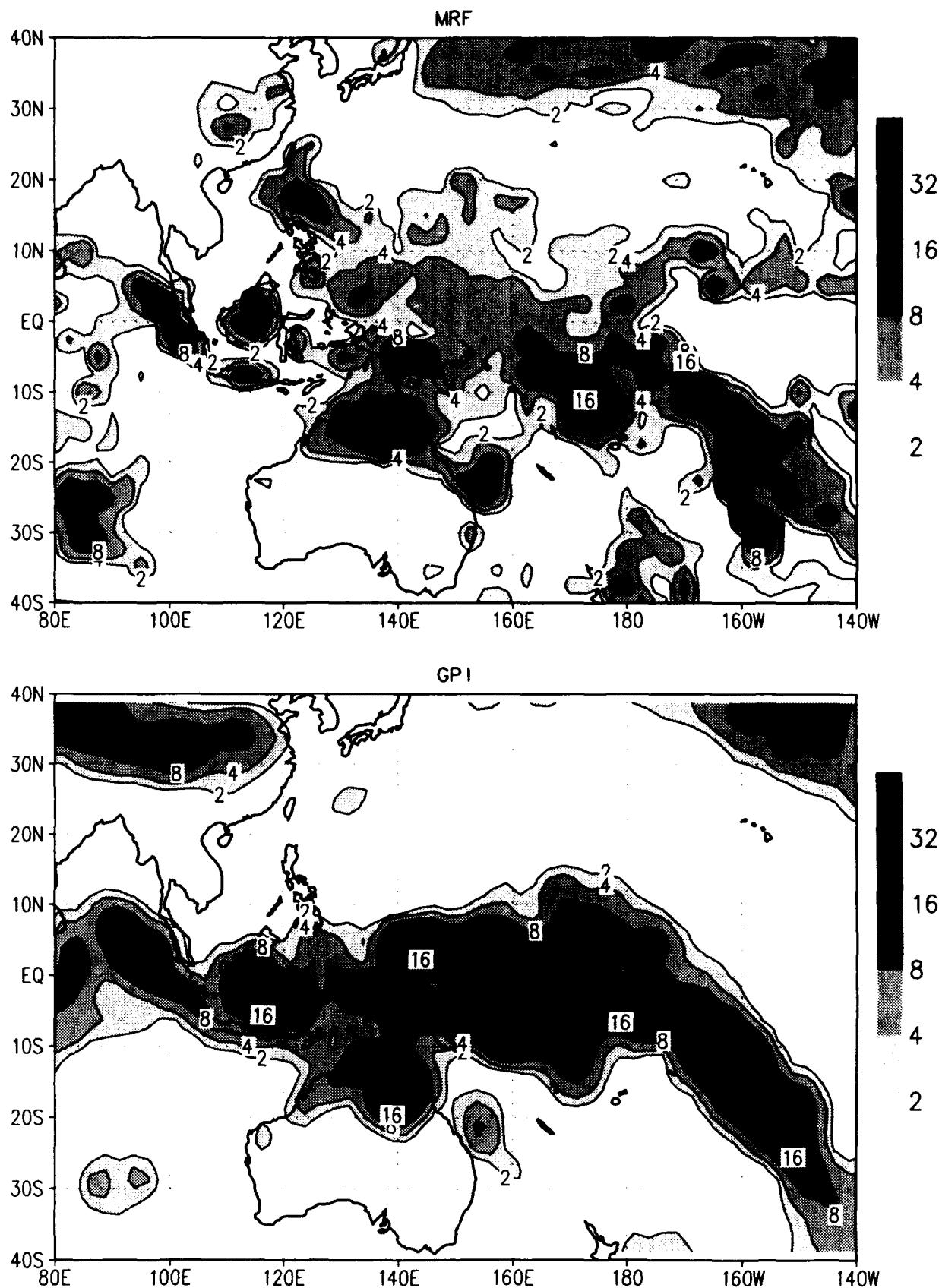
MRF 5-day ave flow and chi ~ 12 FEB 1993
wind (m/s) chi ($10^6 \text{ m}^2/\text{s}$) /d2/toga_coare/d5.gs



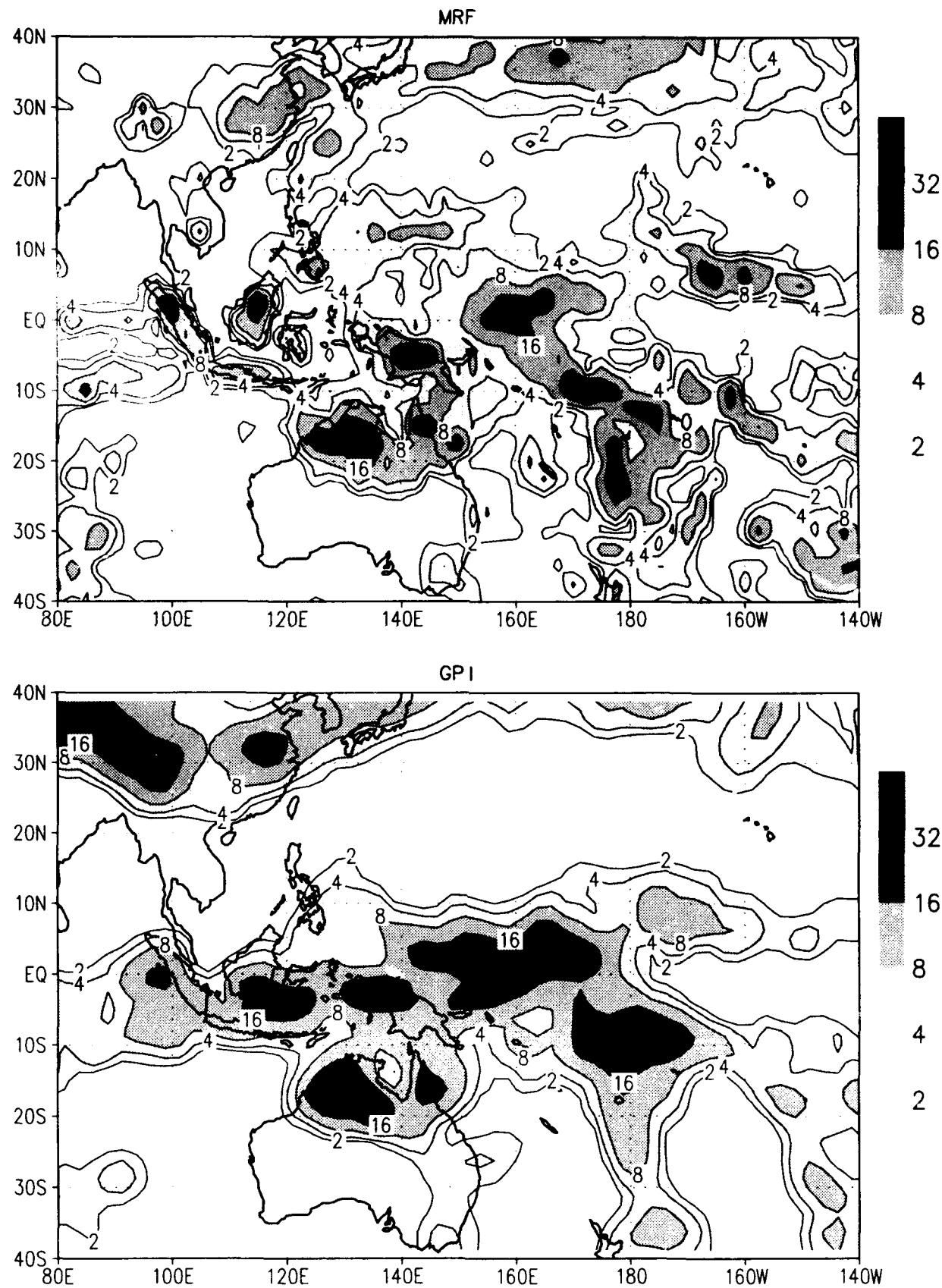
NOGAPS and GPI 5-day ave Precip ~ 12 FEB 1993
(mm/day) /d2/toga_coare/d5.gs



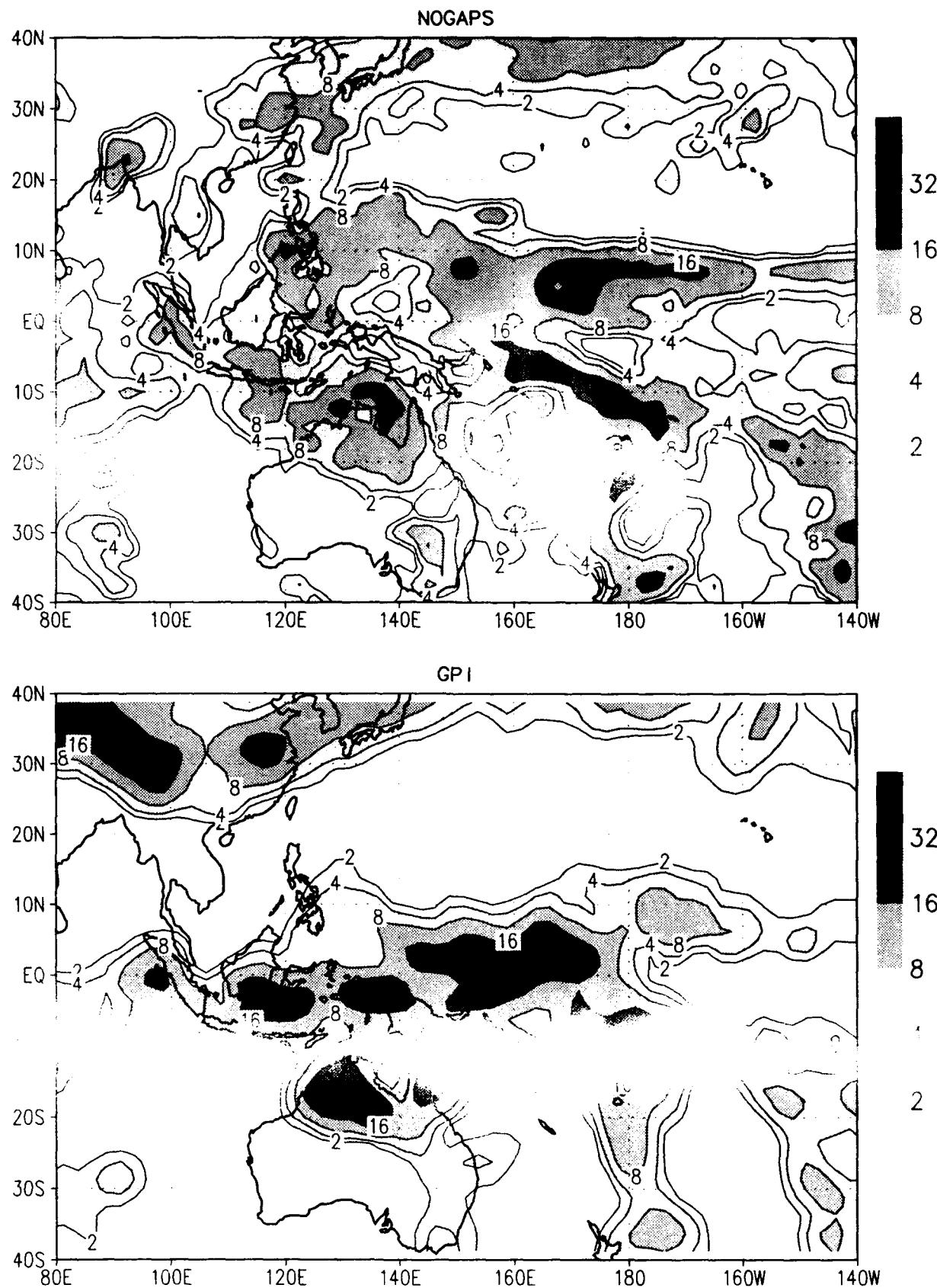
MRF and GPI 5-day ave Precip ~ 12 FEB 1993
(mm/day) /d2/toga_coare/d5.gs



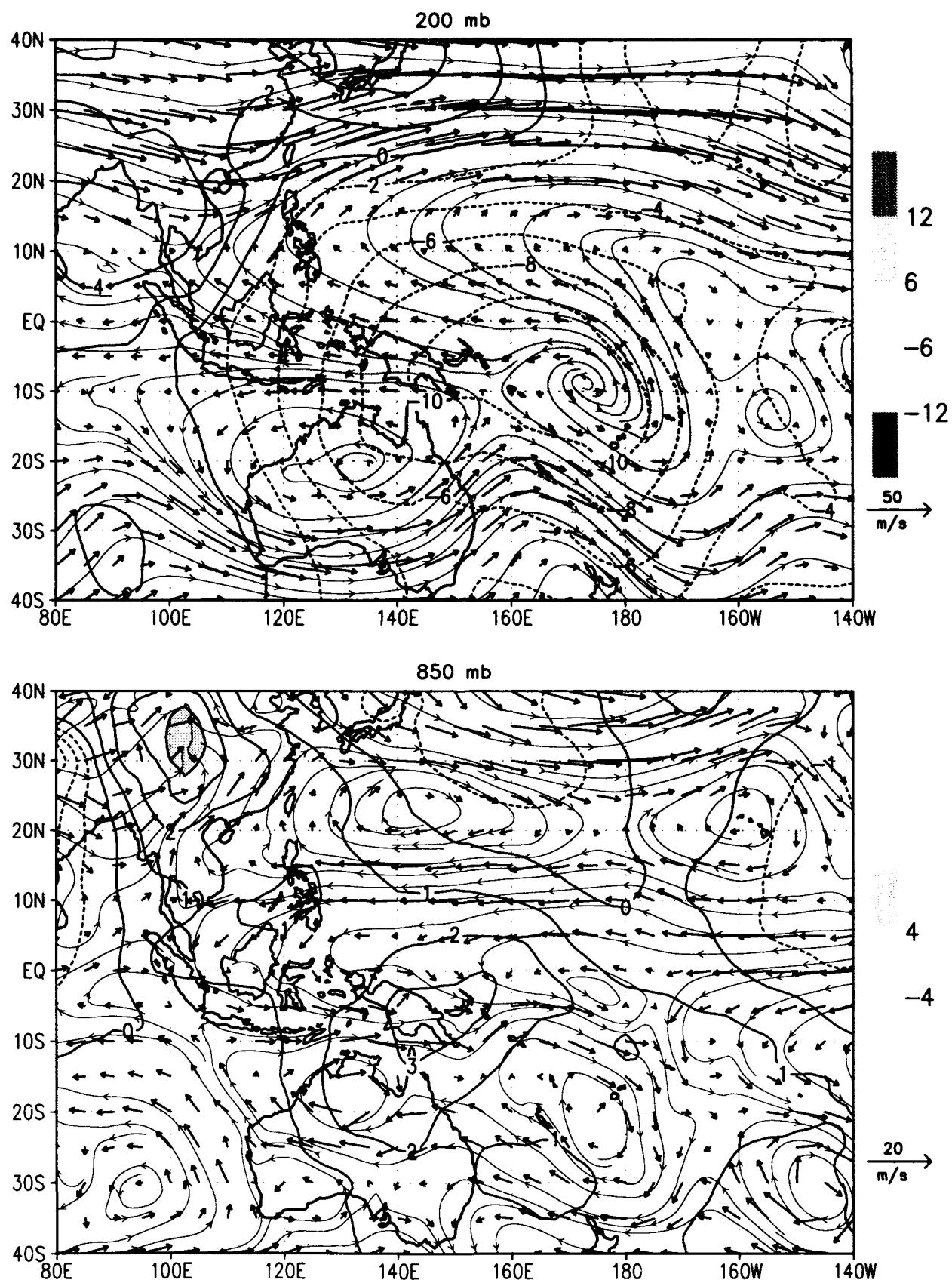
MRF and GPI 5-day ave Precip ~ 17 FEB 1993
(mm/day) /d2/toga_coare/d5.gs



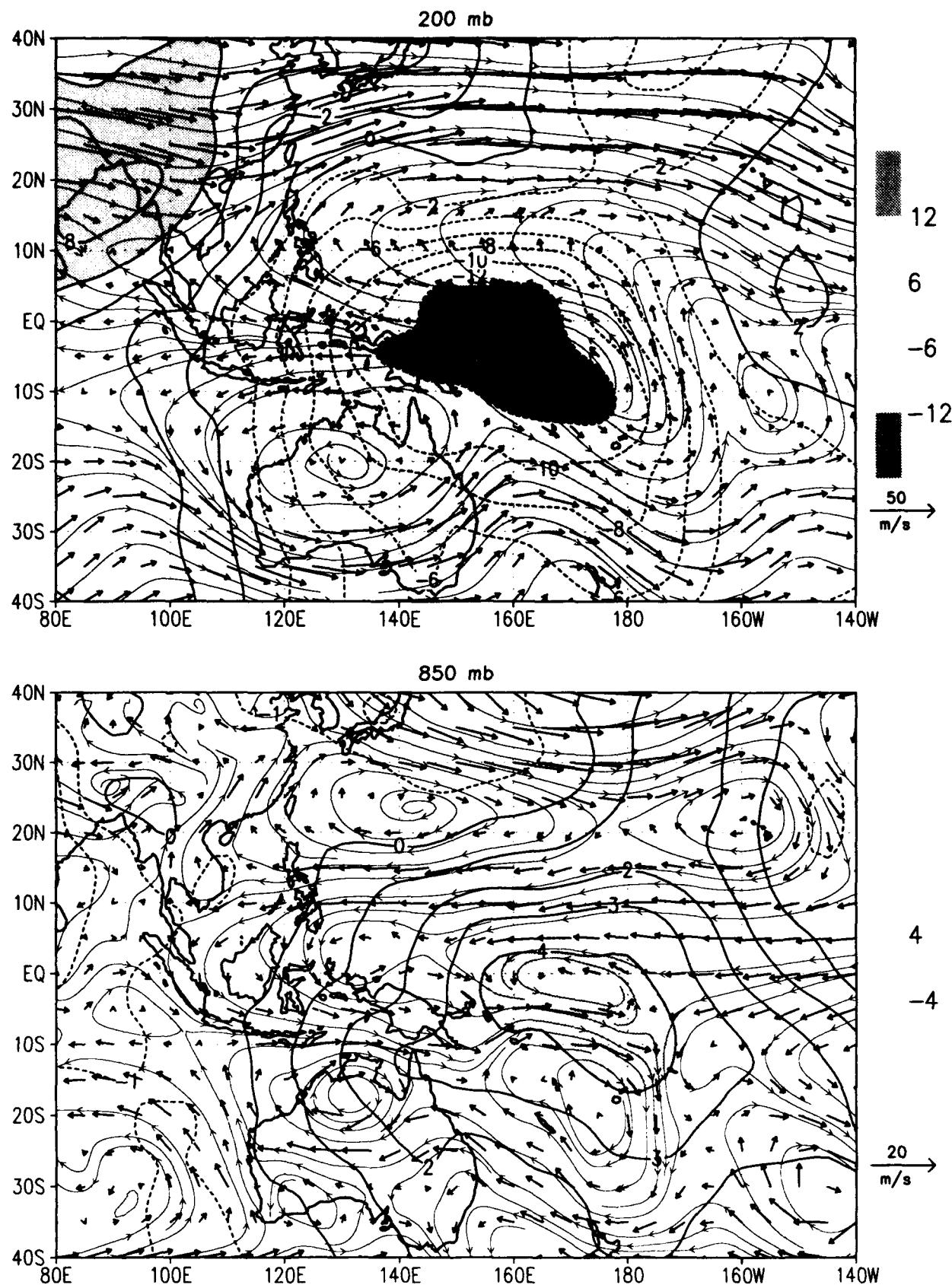
NOGAPS and GPI 5-day ave Precip ~ 17 FEB 1993
 (mm/day) /d2/toga_coare/d5.gs



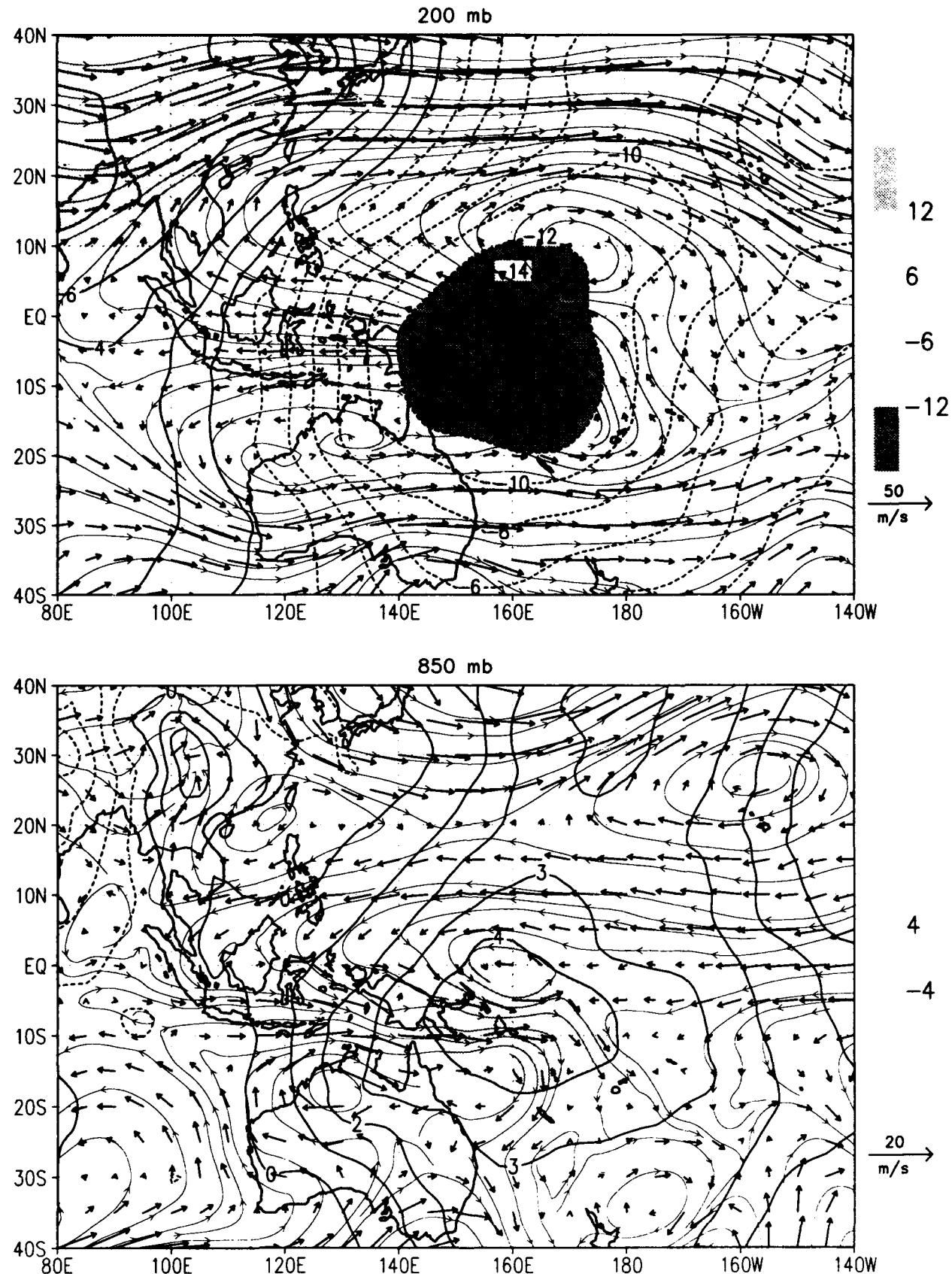
MRF 5-day ave flow and chi ~ 17 FEB 1993
wind (m/s) chi ($10^6 \text{ m}^2/\text{s}$) /d2/toga_coare/d5.gs



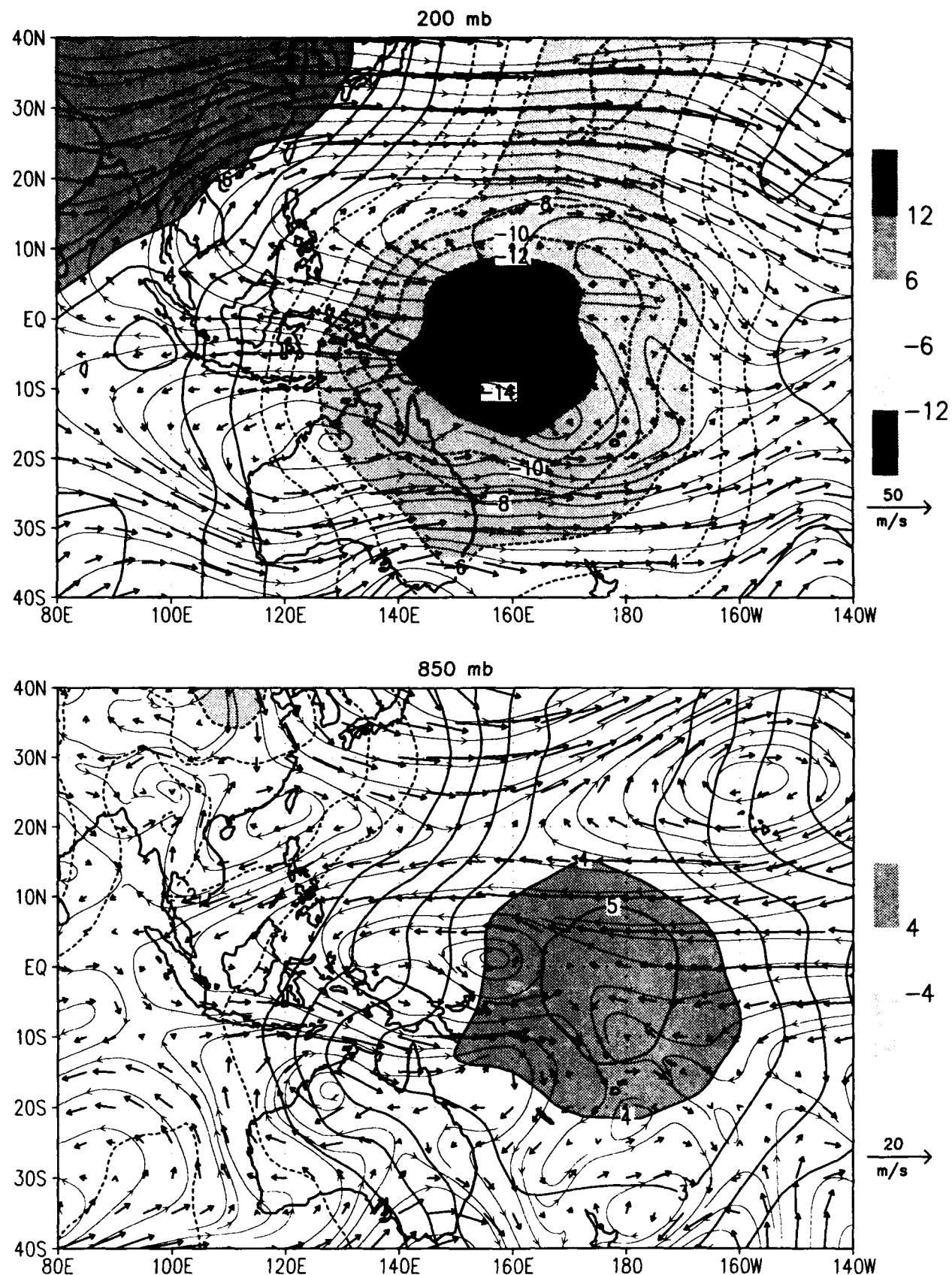
NOGAPS 5-day ave flow and chi ~ 17 FEB 1993
wind (m/s) chi ($10^6 \text{ m}^2/\text{s}$) /d2/toga_coare/d5.gs



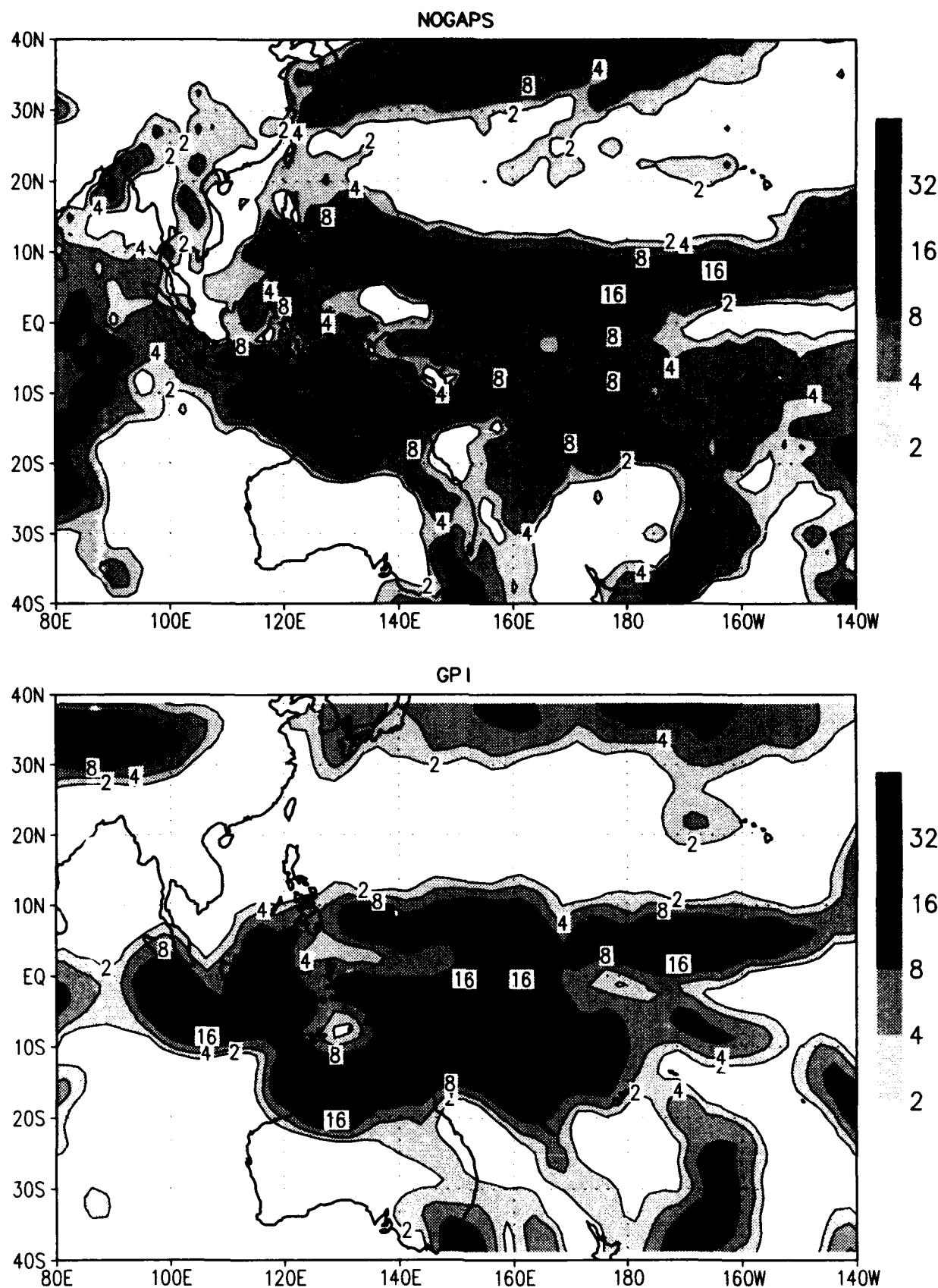
MRF 5-day ave flow and chi ~ 22 FEB 1993
wind (m/s) chi ($10^6 \text{ m}^2/\text{s}$) /d2/toga_coare/d5.gs



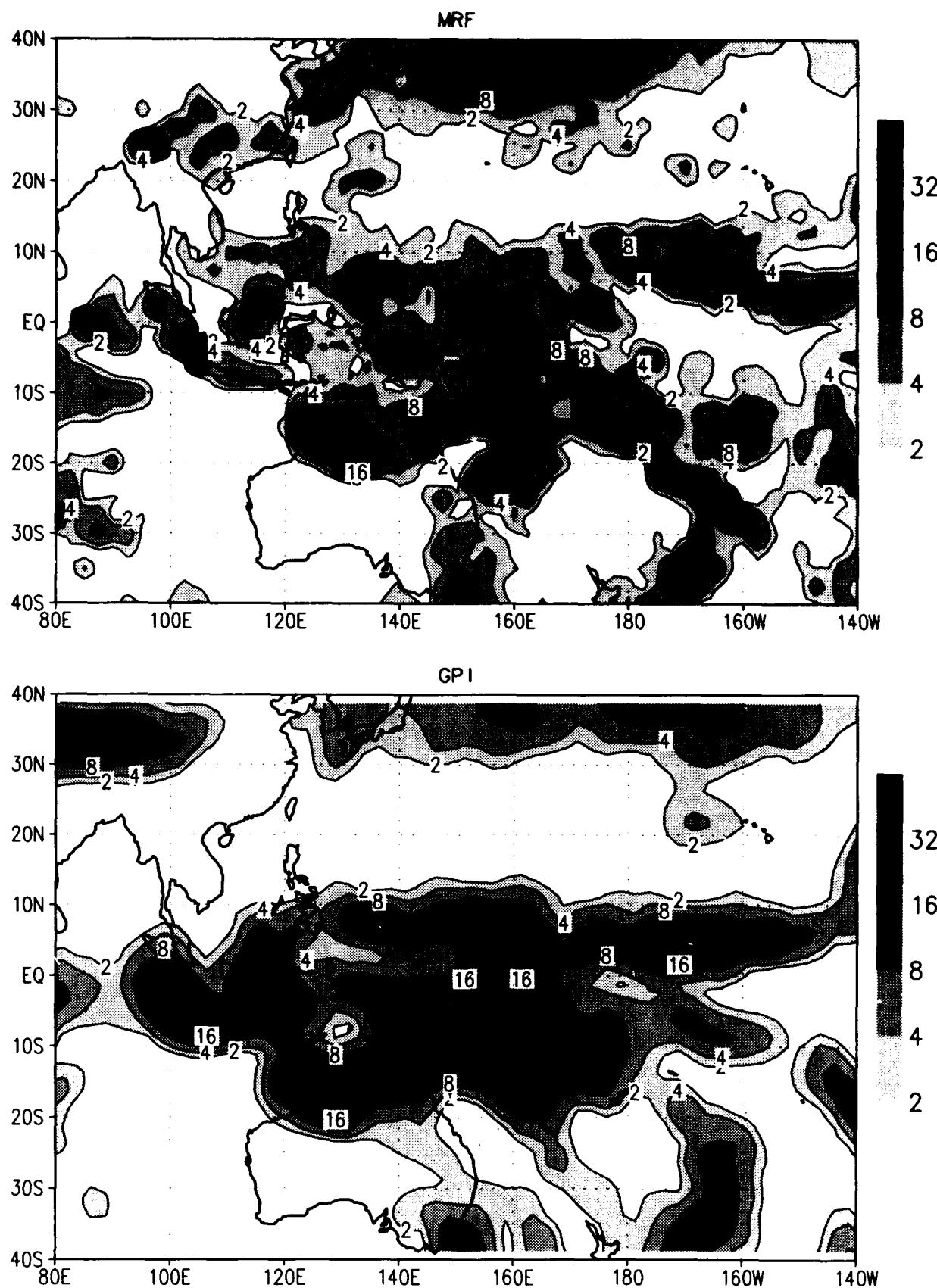
NOGAPS 5-day ave flow and chi ~ 22 FEB 1993
 wind (m/s) chi ($10^6 \text{ m}^2/\text{s}$) /d2/toga_coare/d5.gs



NOGAPS and GPI 5-day ave Precip ~ 22 FEB 1993
(mm/day) /d2/toga_coare/d5.gs



MRF and GPI 5-day ave Precip ~ 22 FEB 1993
(mm/day) /d2/toga_coare/d5.gs



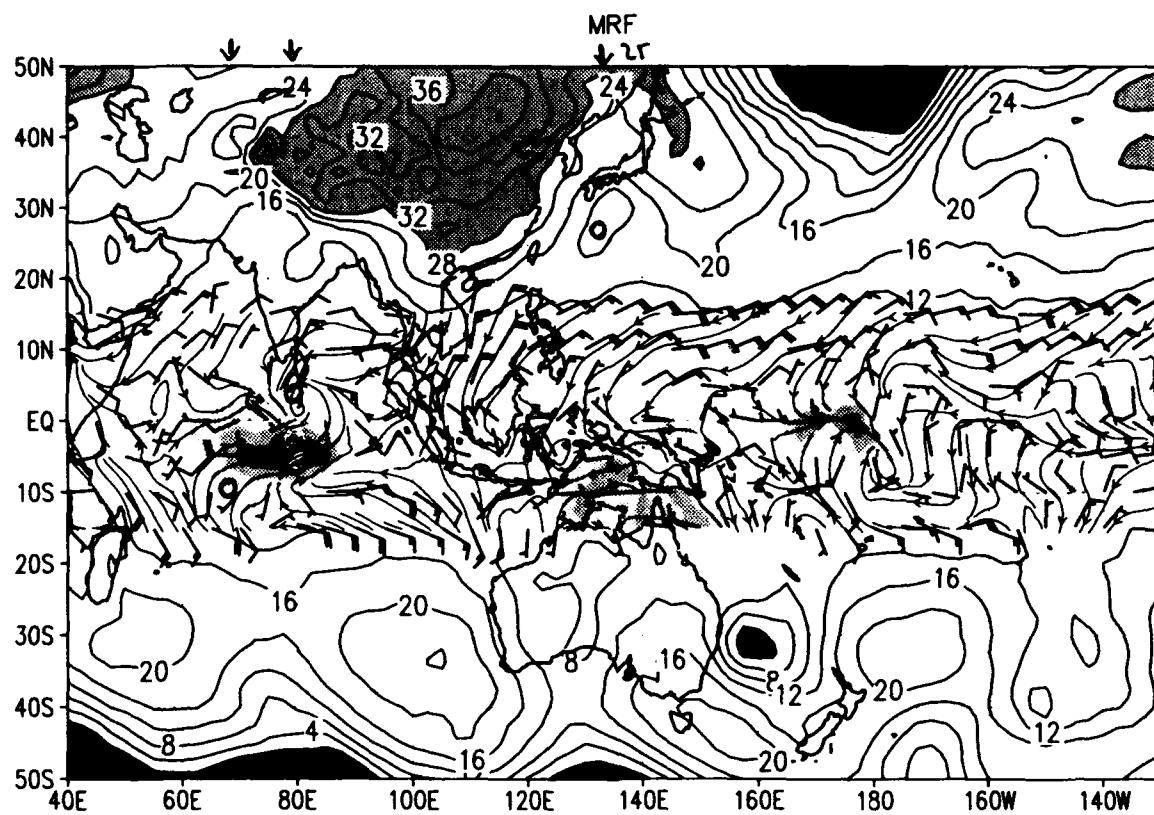
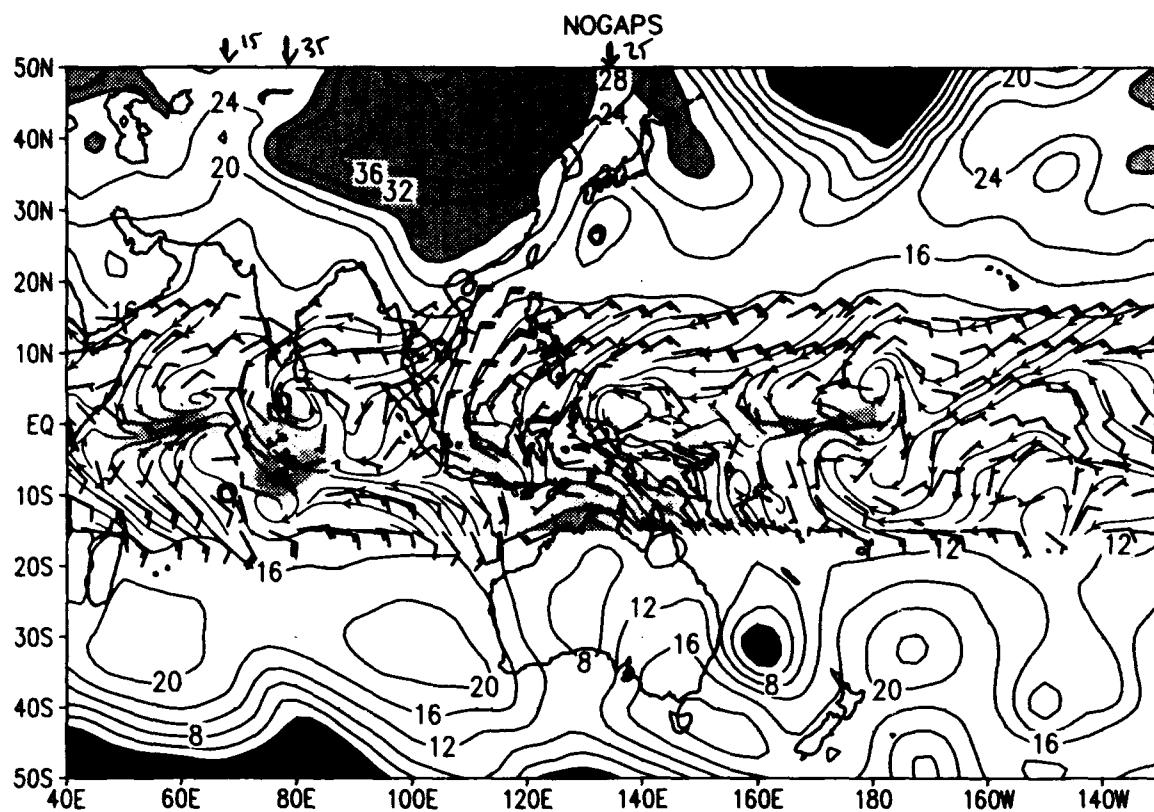
12 00 UTC Synoptic Charts for 1 Dec 92 - 31 Dec 92

The following sections contains 00 UTC surface synoptic charts for the period December 1992 - February 1993. We choose this period because the ISO and Australian monsoon were active and we display a larger area than in the monthly climatology to give an even broader scale view of the synoptic conditions. In the deep tropics (15S-15N) we show surface wind barbs (kts) and streamlines with positive u component shaded in the intervals 5-10 kts (light), 10-20 kts (medium) and over 20 kts (dark). Outside the deep tropics we show sea-level pressure with a contour interval of 2 mb and areas < 1004 mb and > 1028 shaded. Tropical cyclone positions at 00 UTC are drawn using a circle for tropical depressions (<35 kts), an open hurricane symbol for tropical storms (< 65 kts) and a closed hurricane symbol for typhoons (> 65 kts).

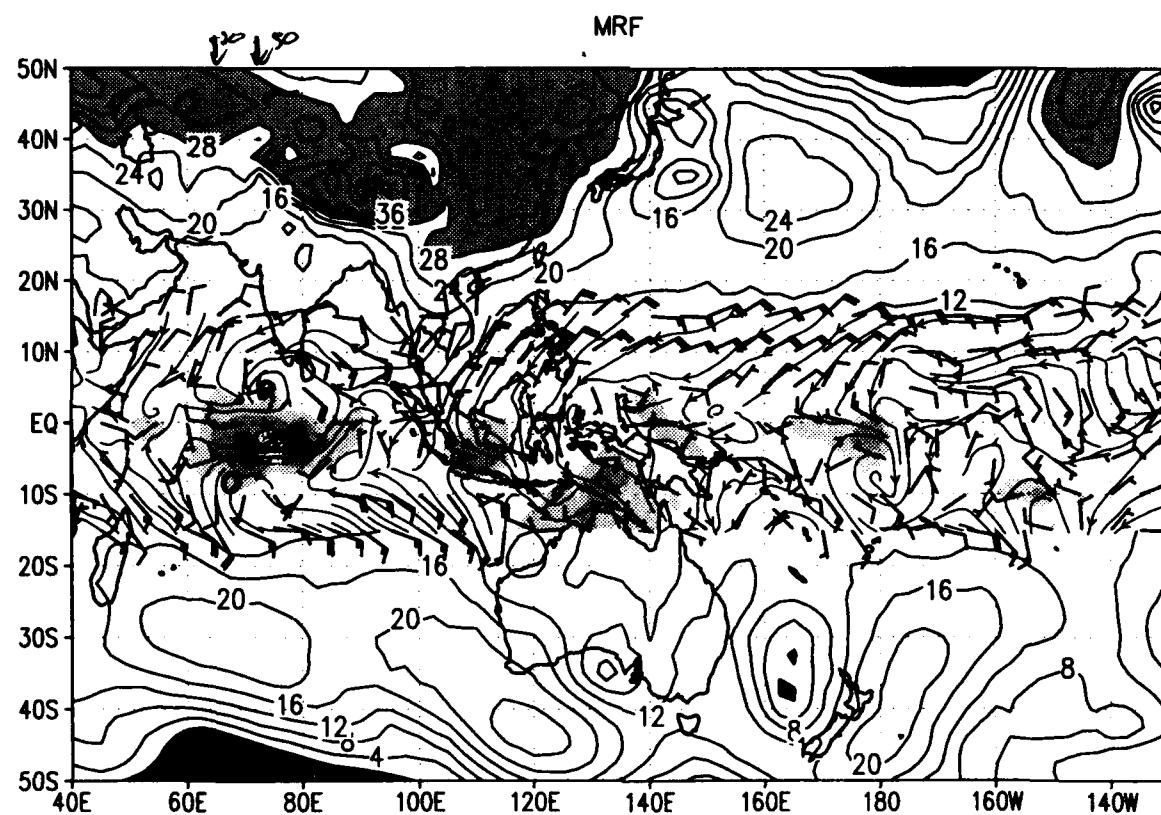
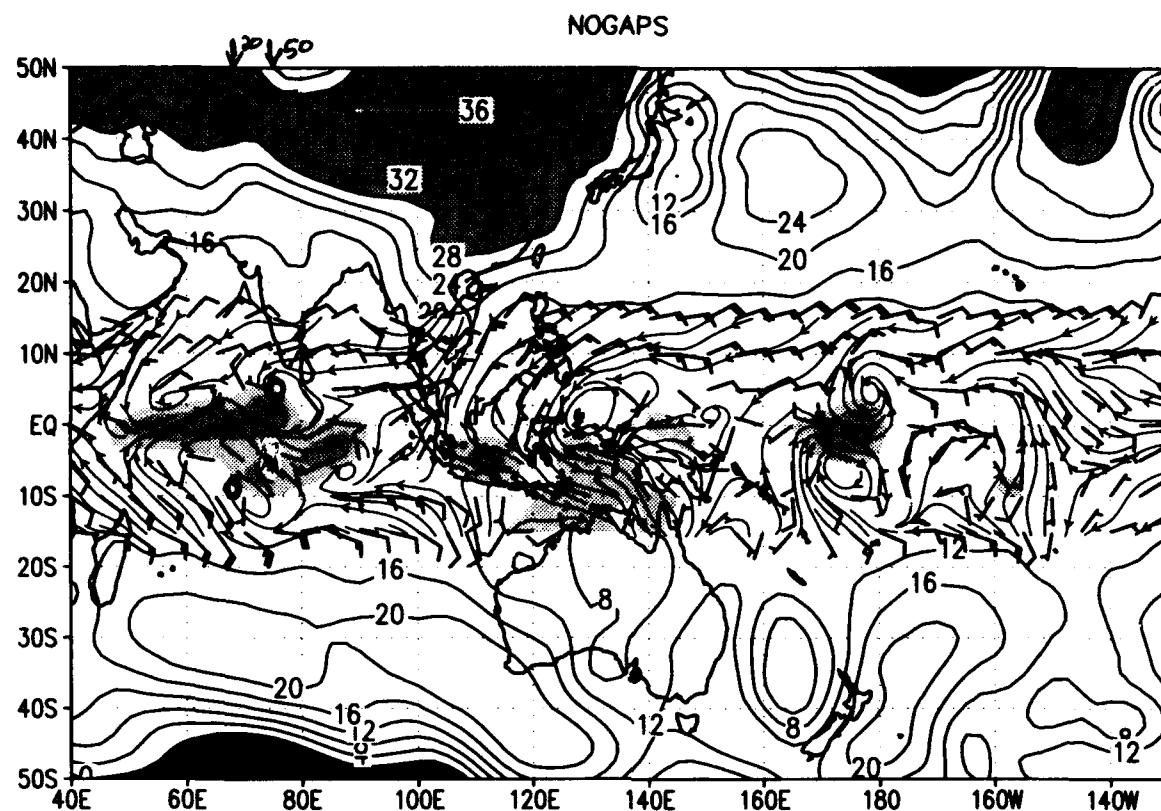
The large differences in SLP between NOGAPS and MRF over mountainous terrain is an artifact of the method of estimating sea-level pressure from 1000 mb geopotential heights and temperature for the MRF. The correspondence was very good outside these regions. However, there were notable differences between the MRF and NOGAPS analyses with regards to the strength of the westerly winds in the tropics and the strength of tropical cyclones, with NOGAPS depicting stronger and more organized WWBs and deeper cyclones. The arrow above the northern border of the map indicates the longitude of the observed TC and the max wind speed in kts is given to the right of the arrow.

Chart	Description
1-31 -	Synoptic charts for NOGAPS and MRF

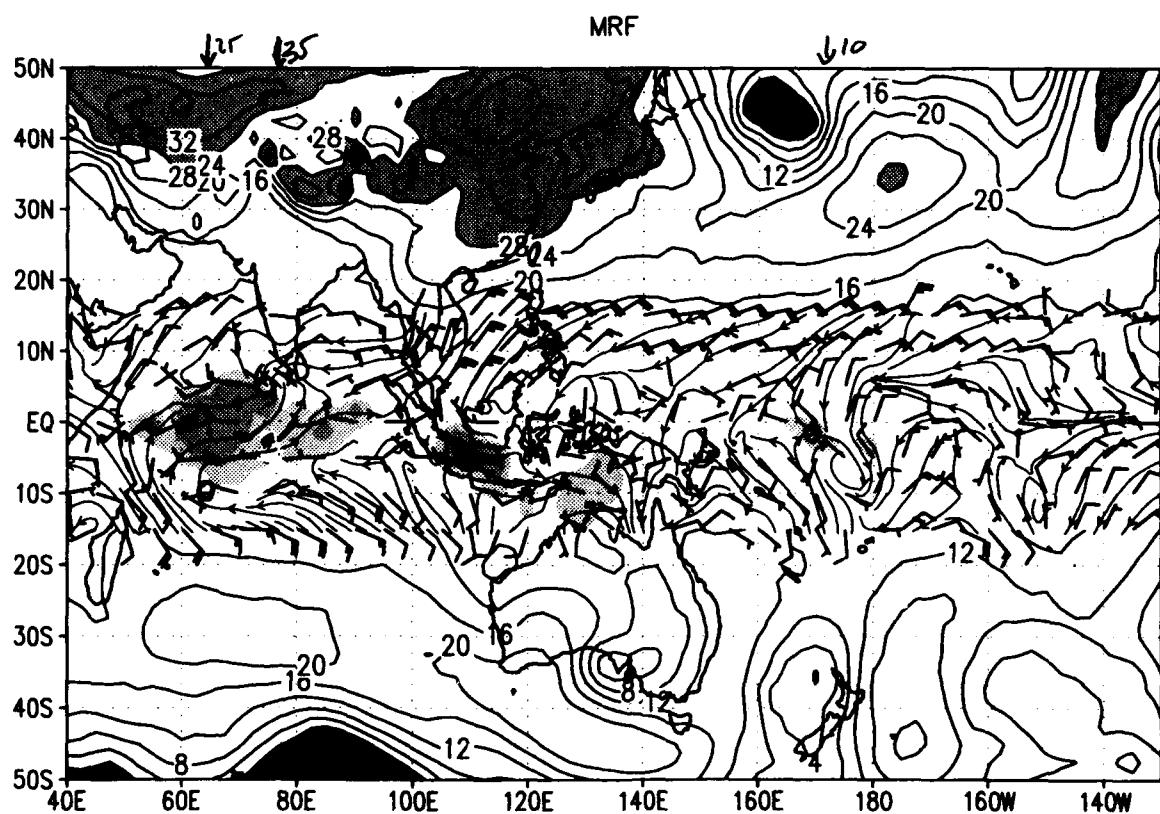
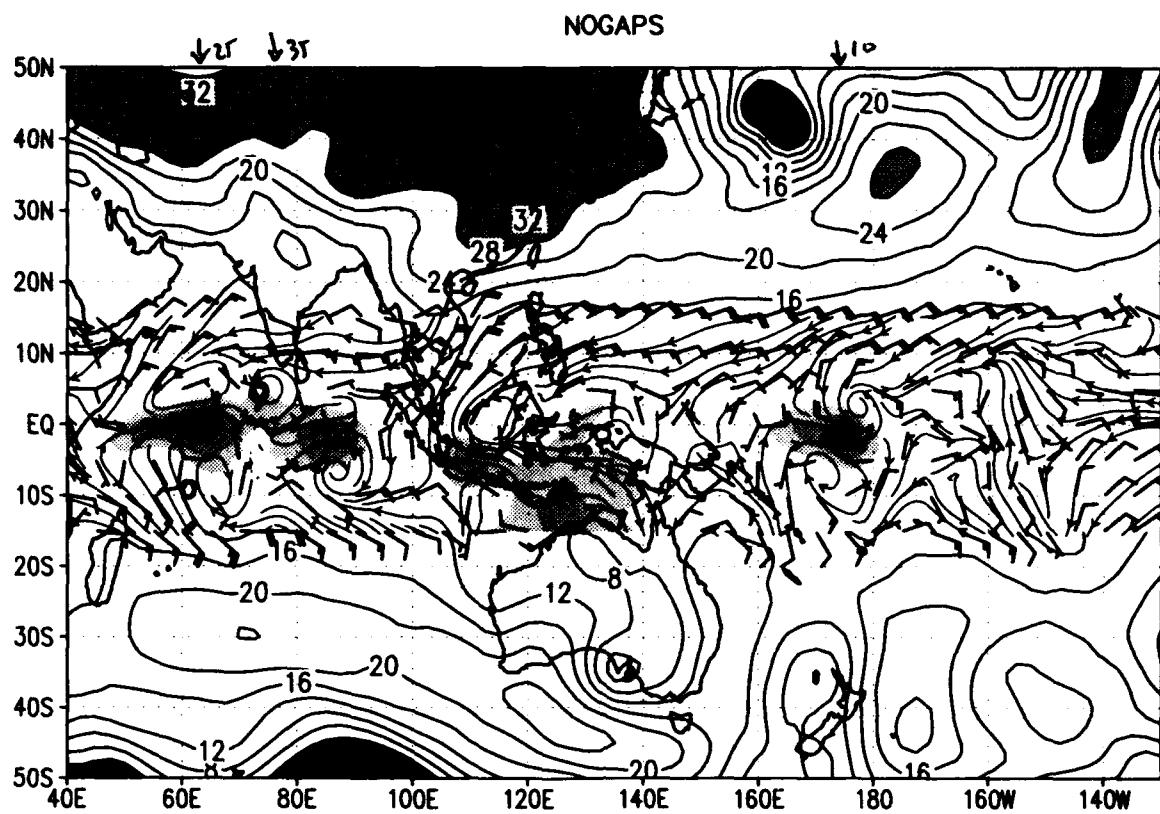
SLP and sfc winds ($u>0$ shaded) for 00Z 01 DEC 1992
slp (mb) wind barbs (kts) /d2/toga_coare/d2.gs



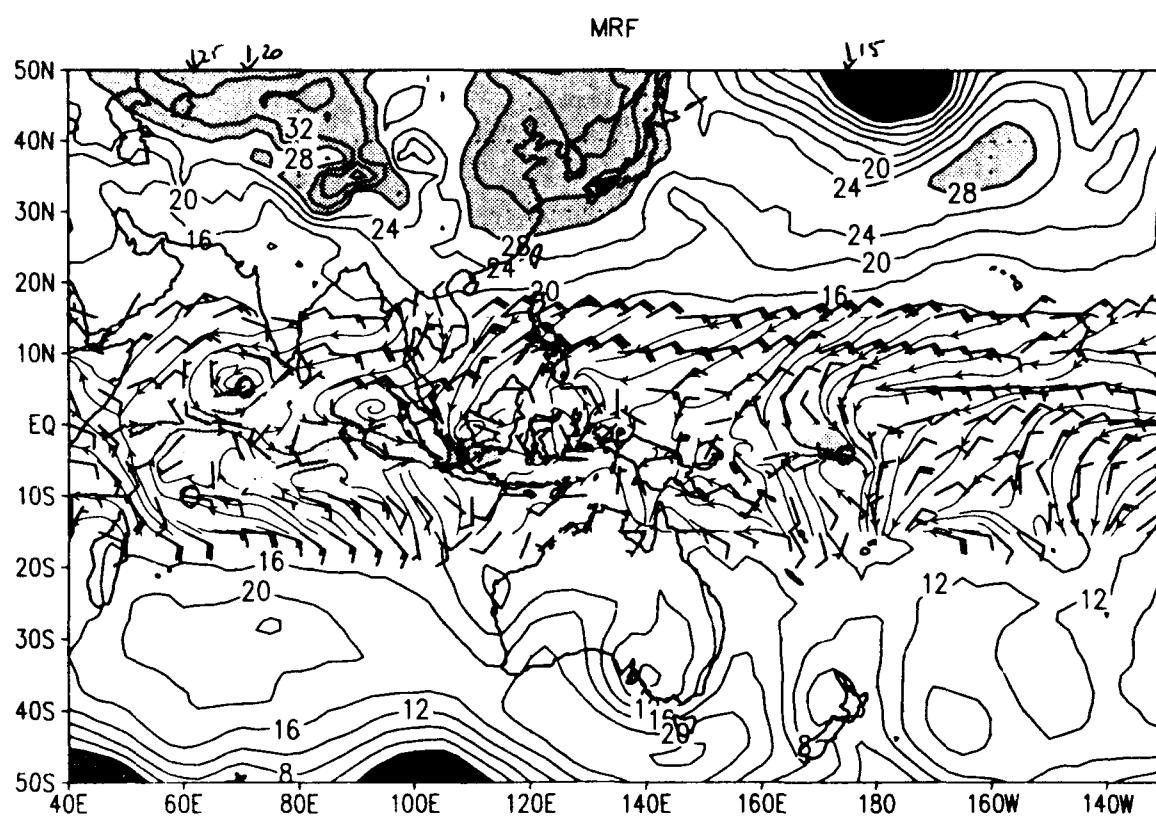
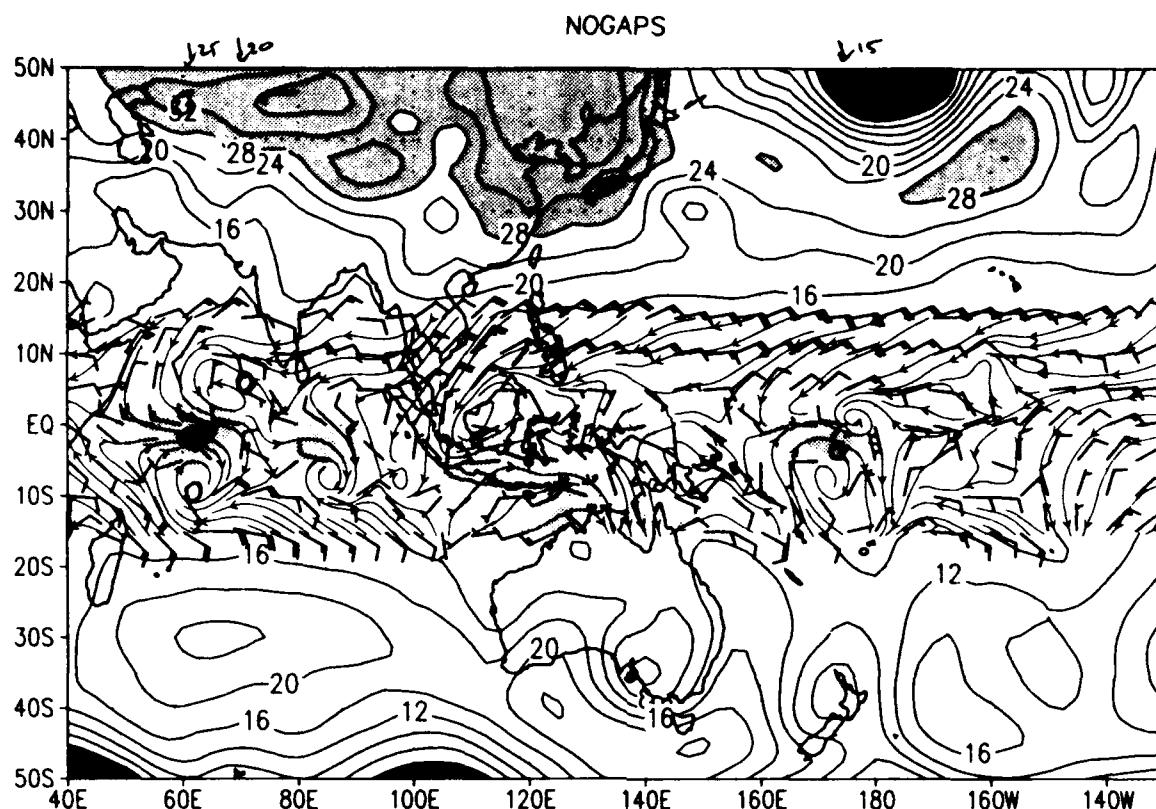
SLP and sfc winds ($u>0$ shaded) for 00Z 02 DEC 1992
slp (mb) wind barbs (kts) /d2/toga_coare/d2.gs



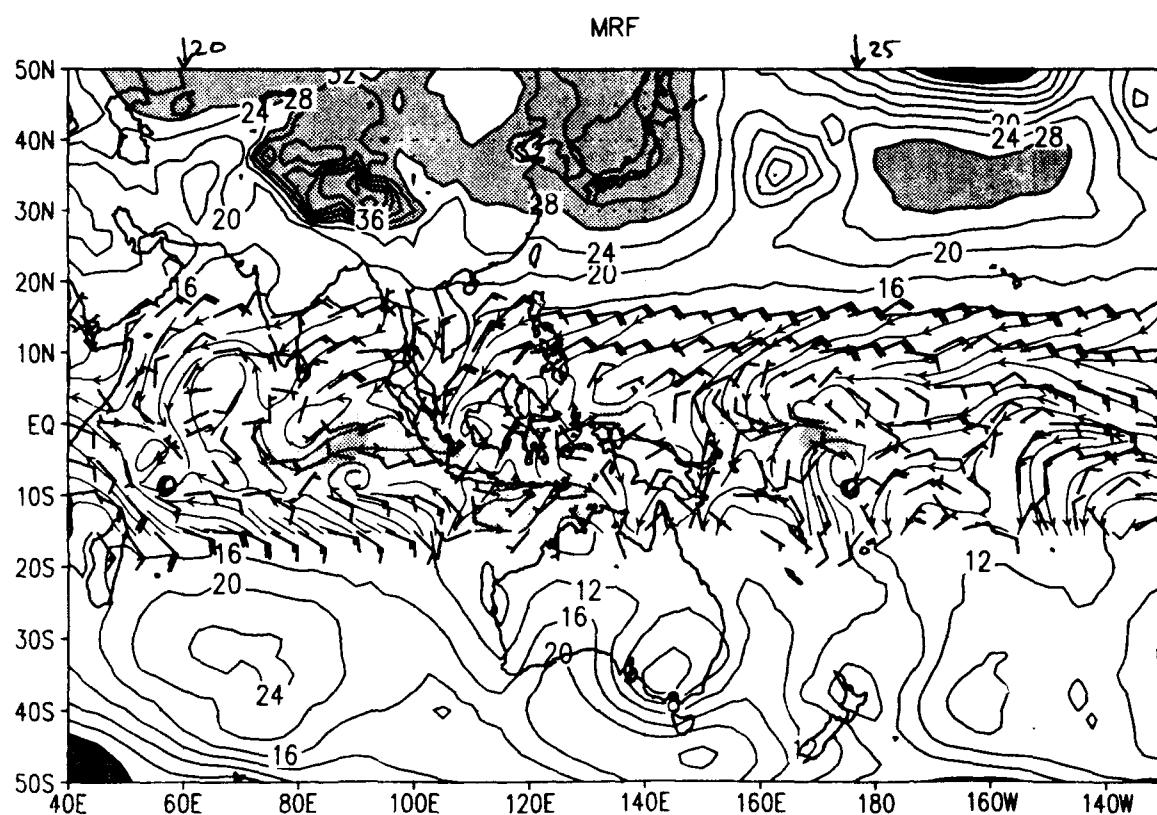
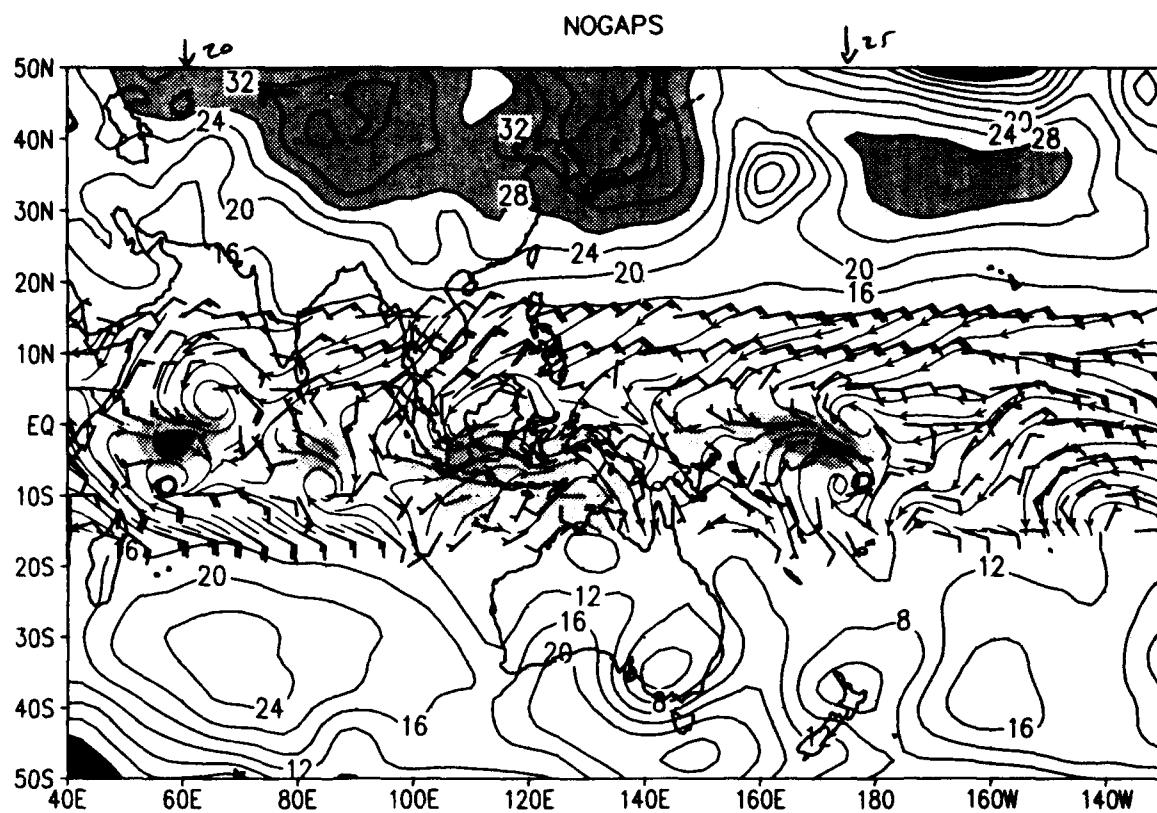
SLP and sfc winds ($u>0$ shaded) for 00Z 03 DEC 1992
slp (mb) wind barbs (kts) /d2/toga_cocre/d2.gs



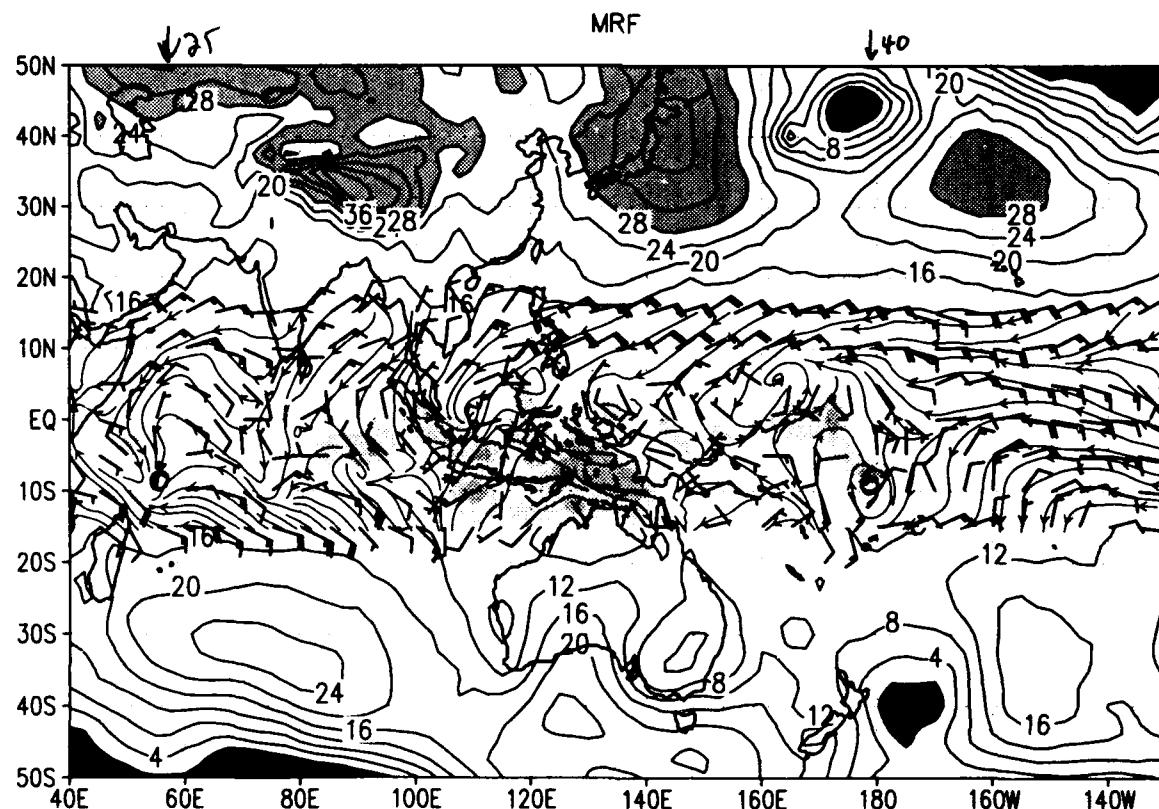
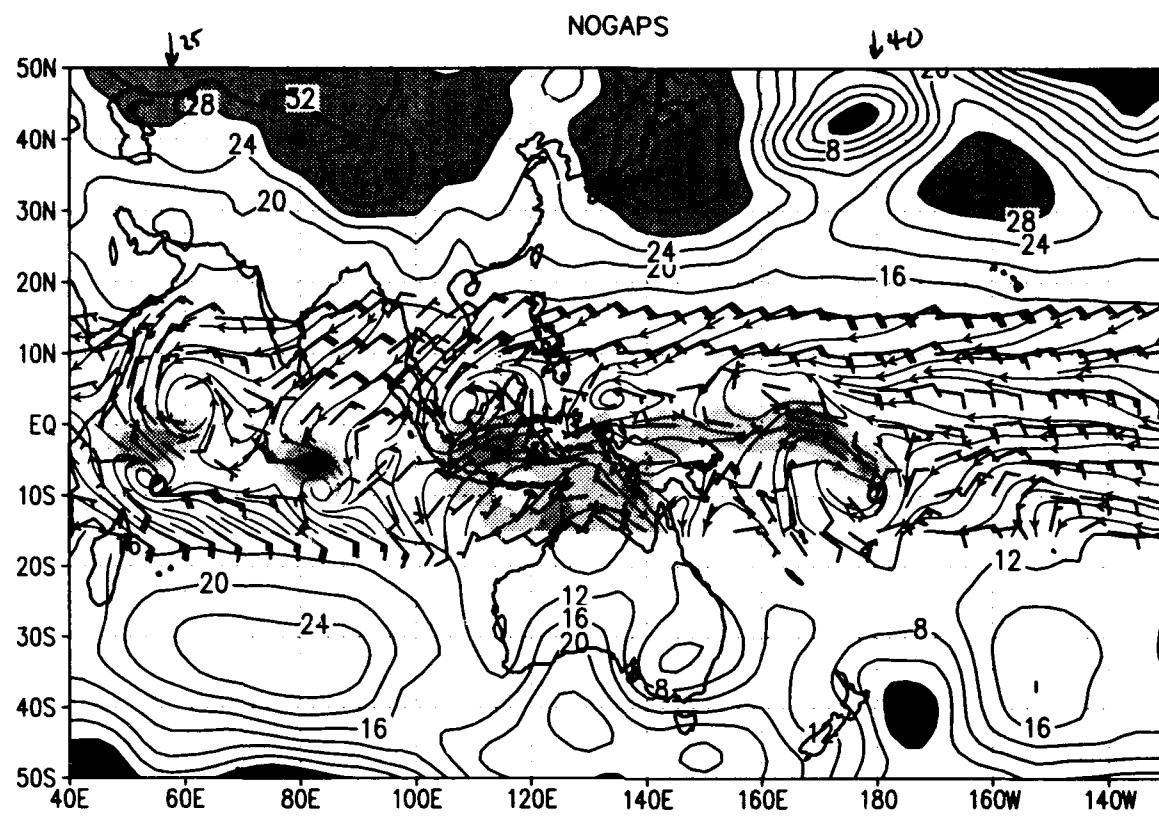
SLP and sfc winds ($u>0$ shaded) for 00Z 04 DEC 1992
slp (mb) wind barbs (kts) /d2/toga_coare/d2.gs



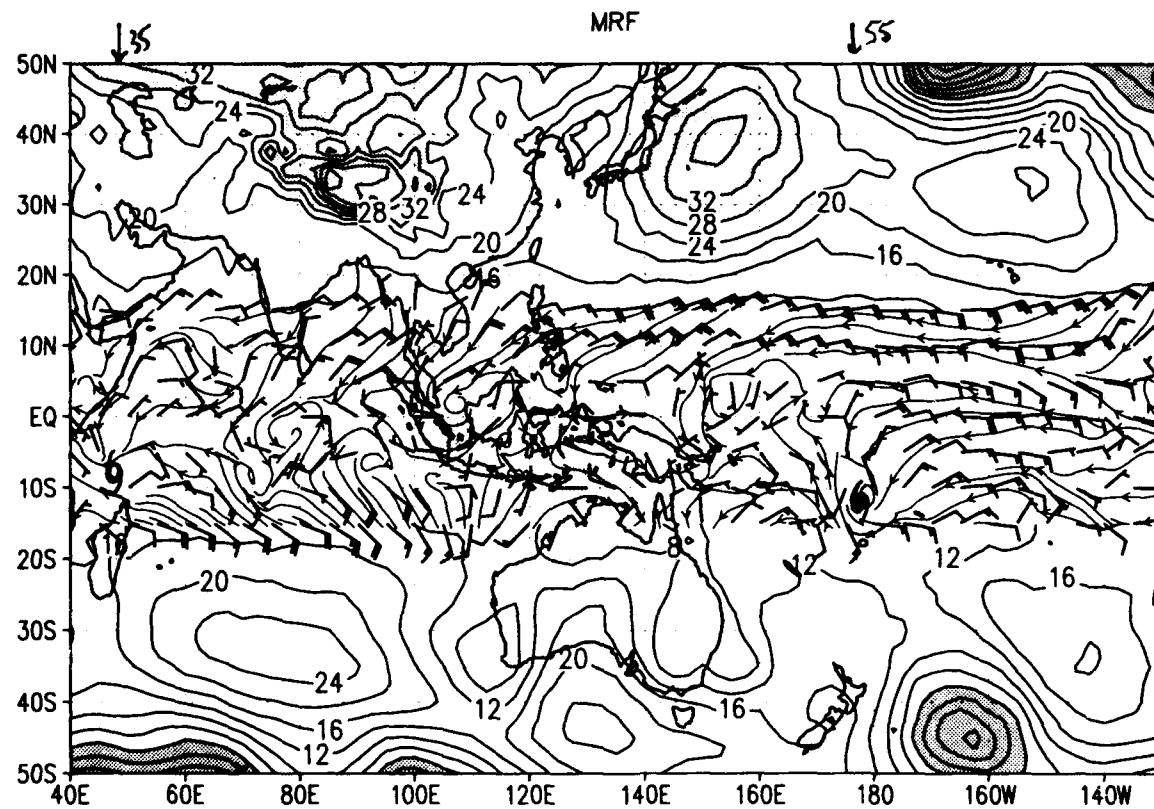
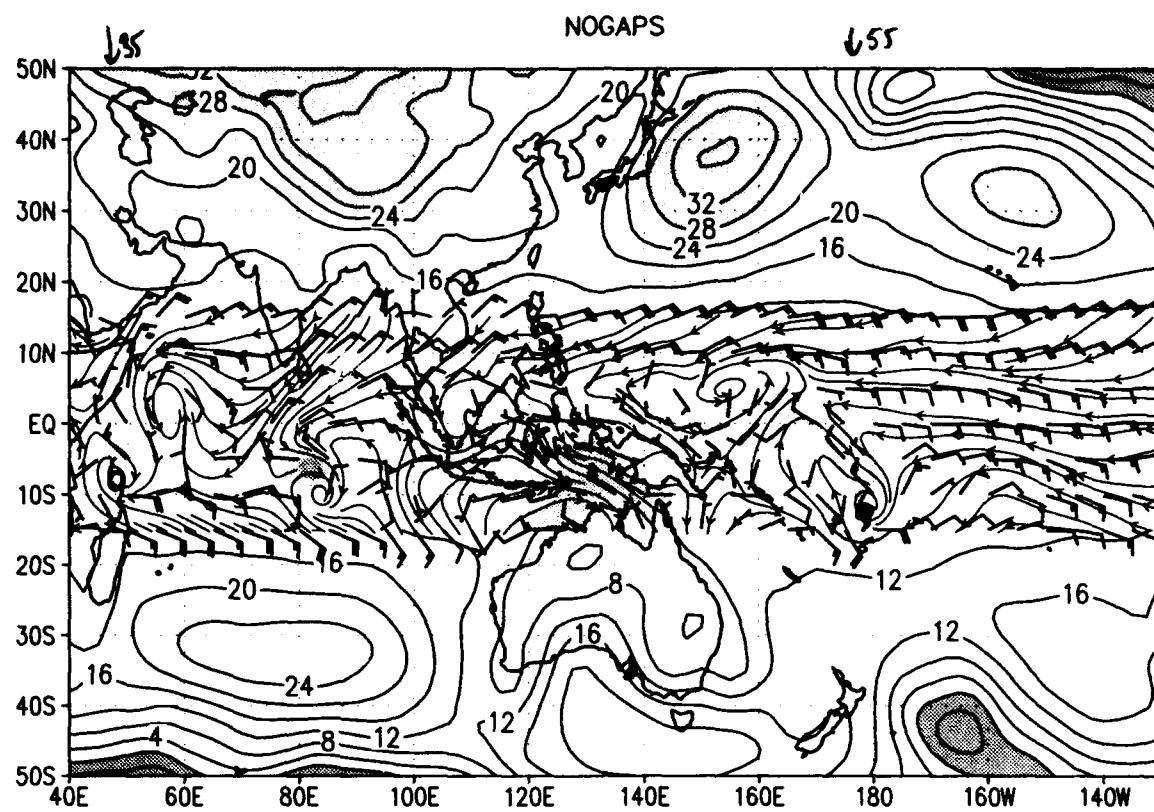
SLP and sfc winds ($u>0$ shaded) for 00Z 05 DEC 1992
slp (mb) wind barbs (kts) /d2/toga_coare/d2.gs



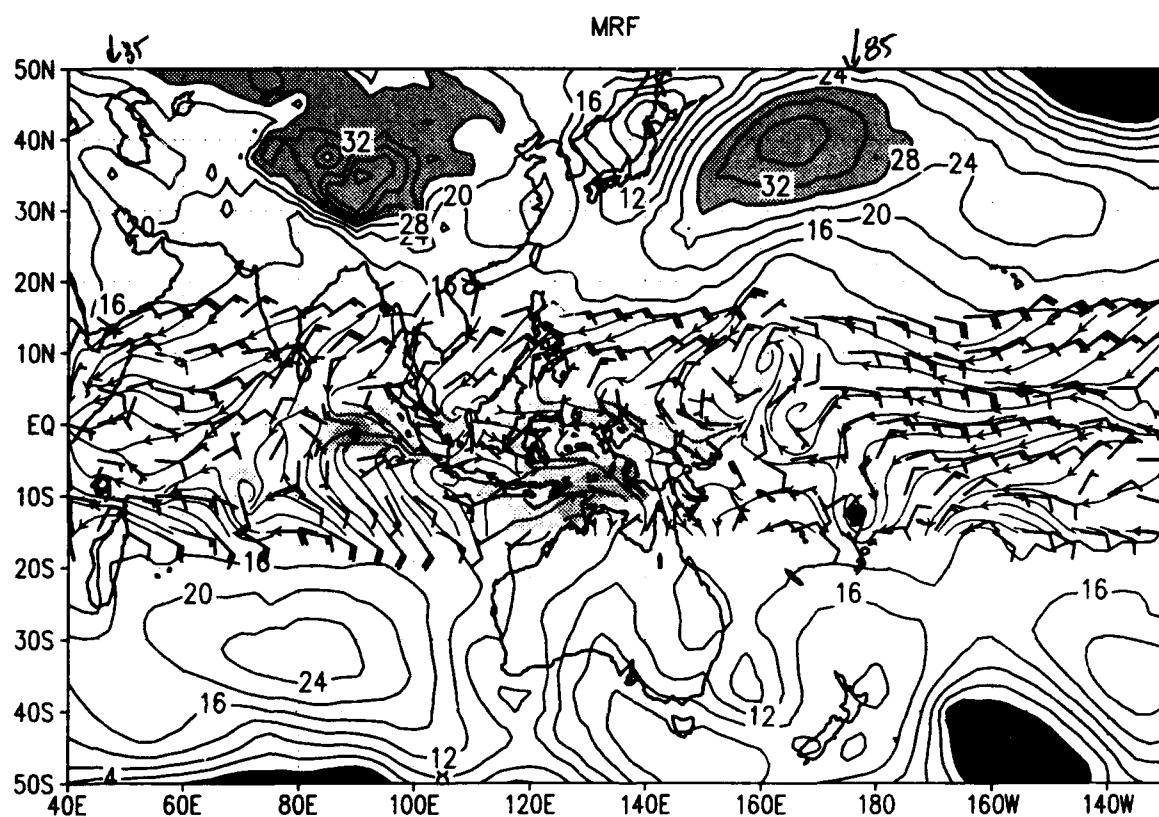
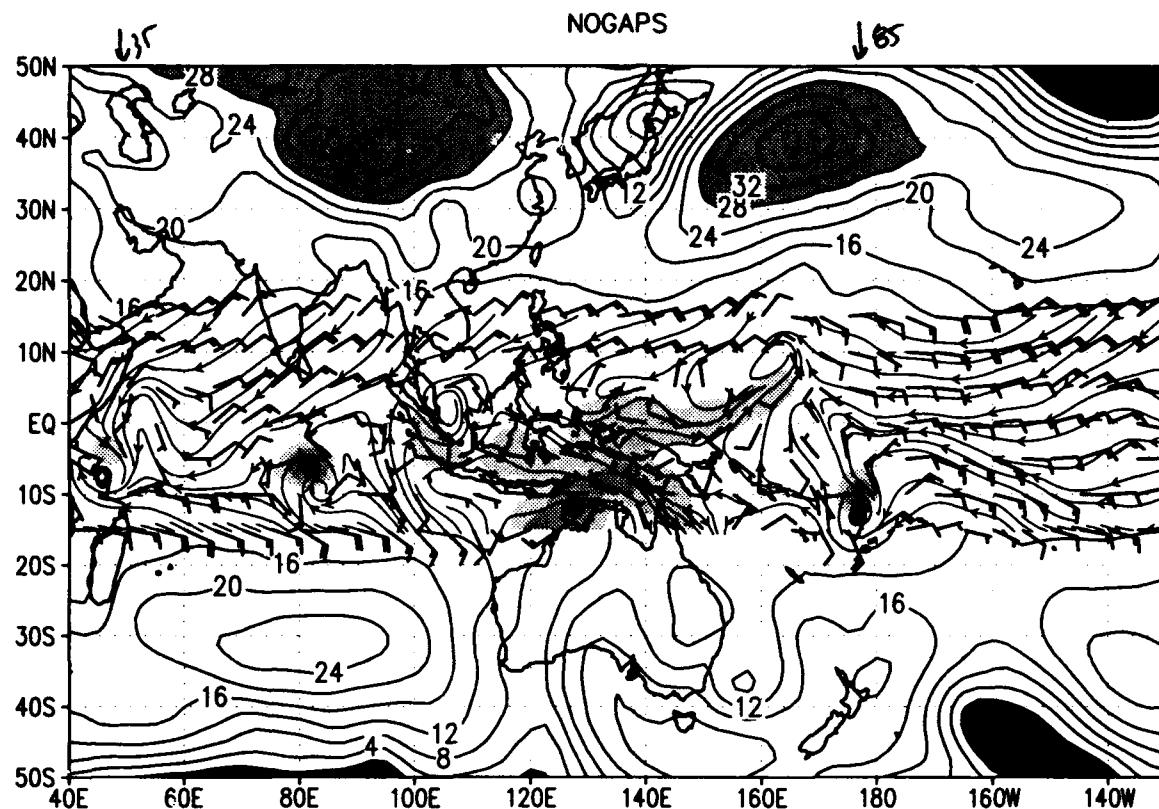
SLP and sfc winds ($u>0$ shaded) for 00Z 06 DEC 1992
slp (mb) wind barbs (kts) /d2/toga_coare/d2.gs



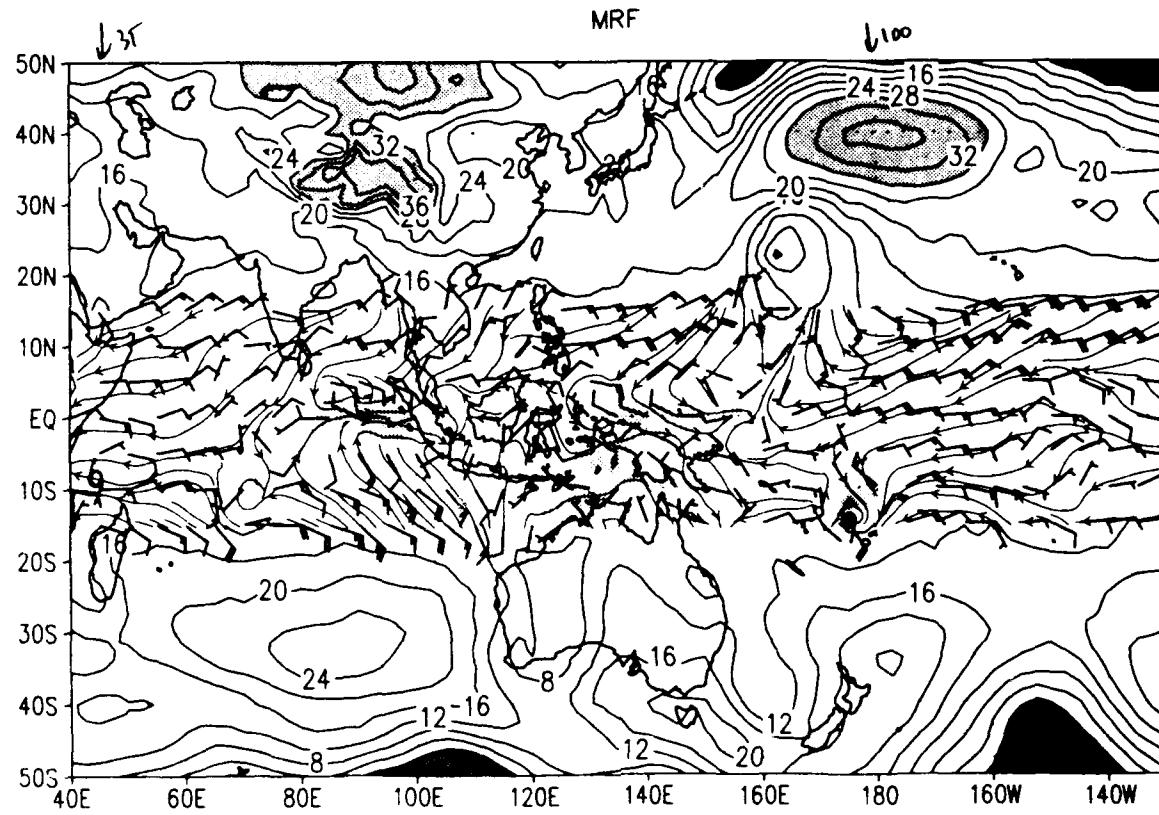
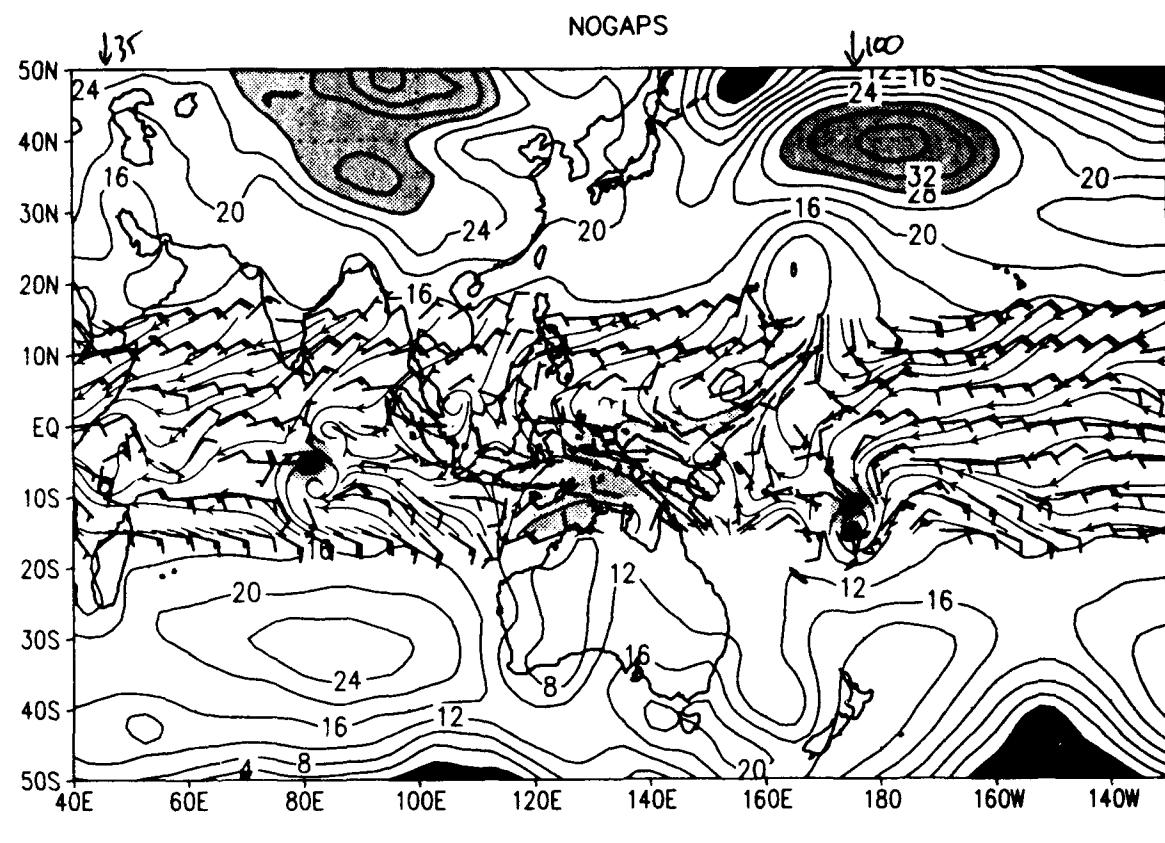
SLP and sfc winds ($u>0$ shaded) for 00Z 07 DEC 1992
slp (mb) wind barbs (kts) /d2/toga_coare/apps/d2.gs



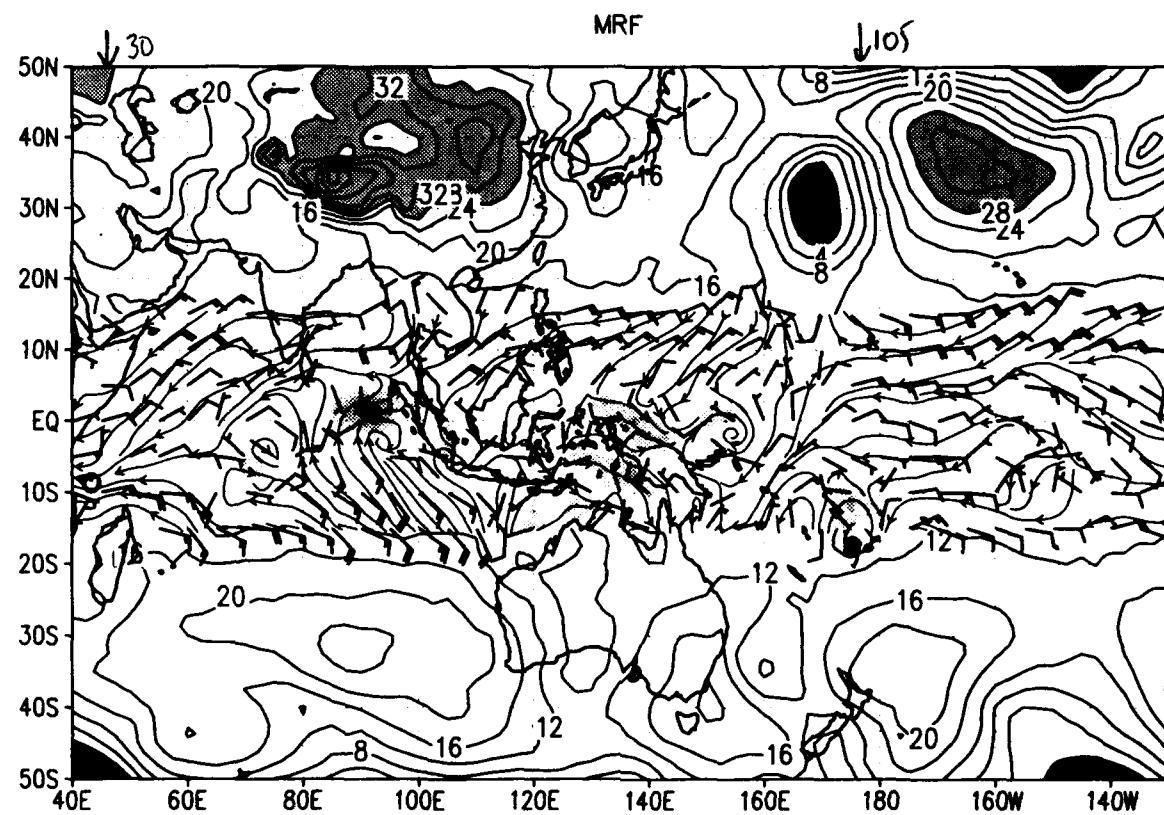
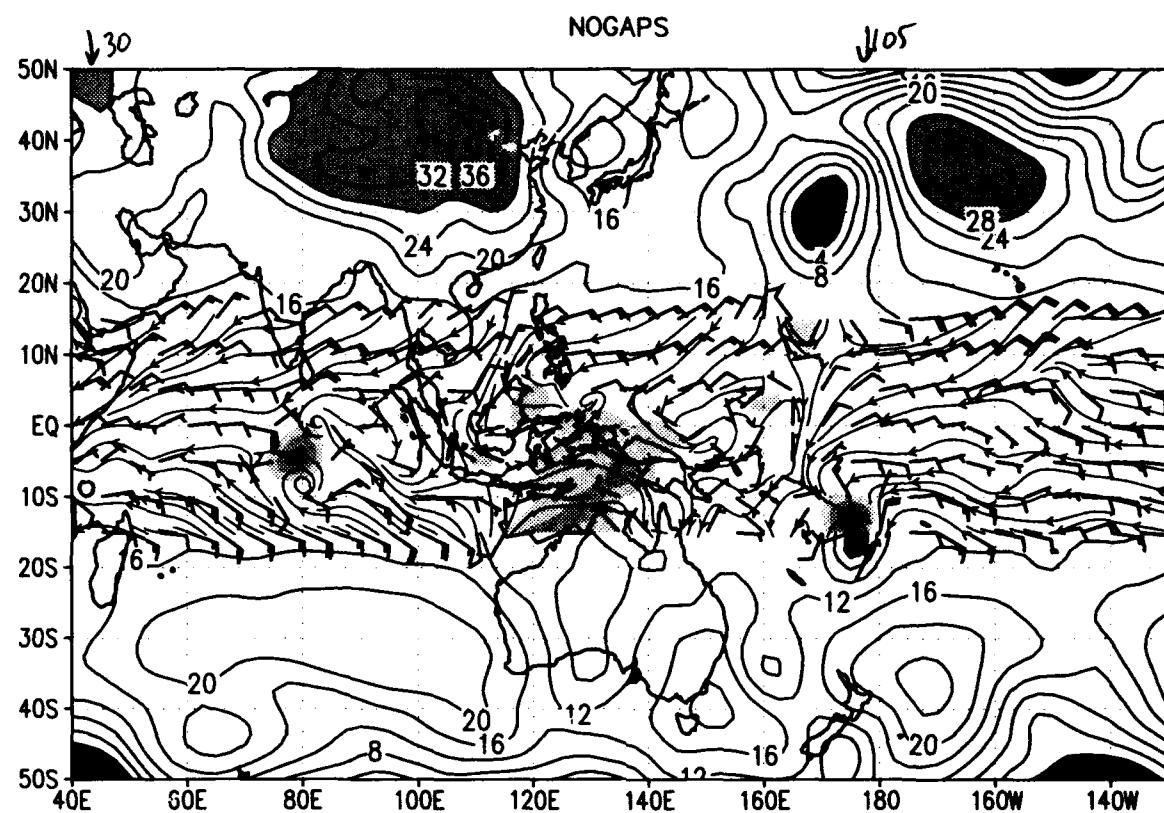
SLP and sfc winds ($u>0$ shaded) for 00Z 08 DEC 1992
slp (mb) wind barbs (kts) /d2/toga_coare/d2.gs



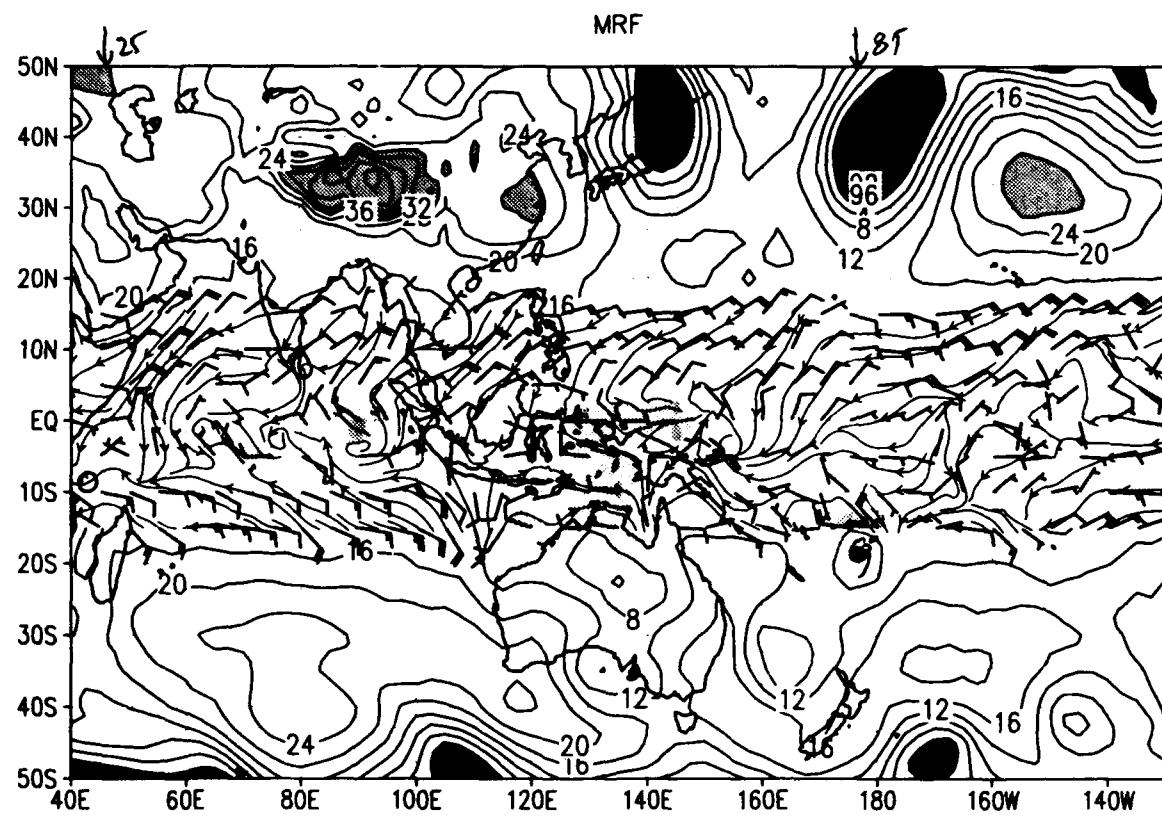
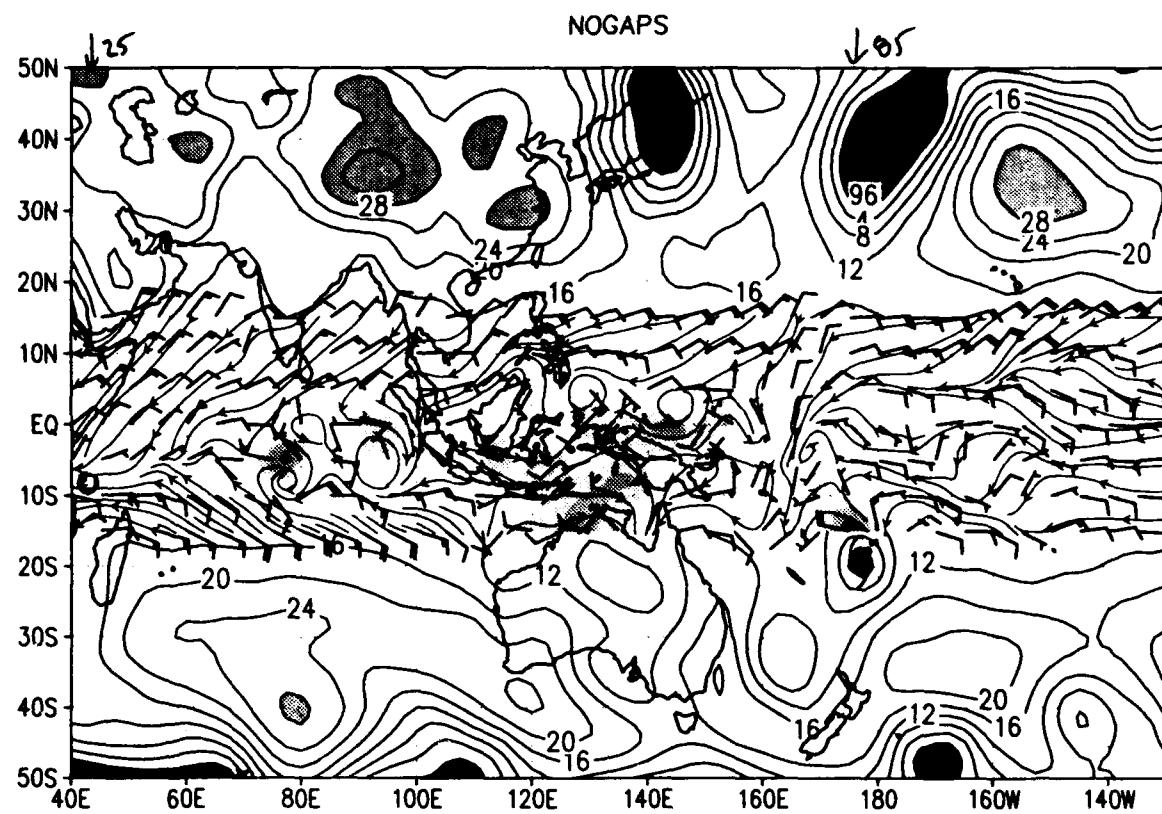
SLP and sfc winds ($u>0$ shaded) for 00Z 09 DEC 1992
slp (mb) wind barbs (kts) /d2/toga_coare/d2.gs



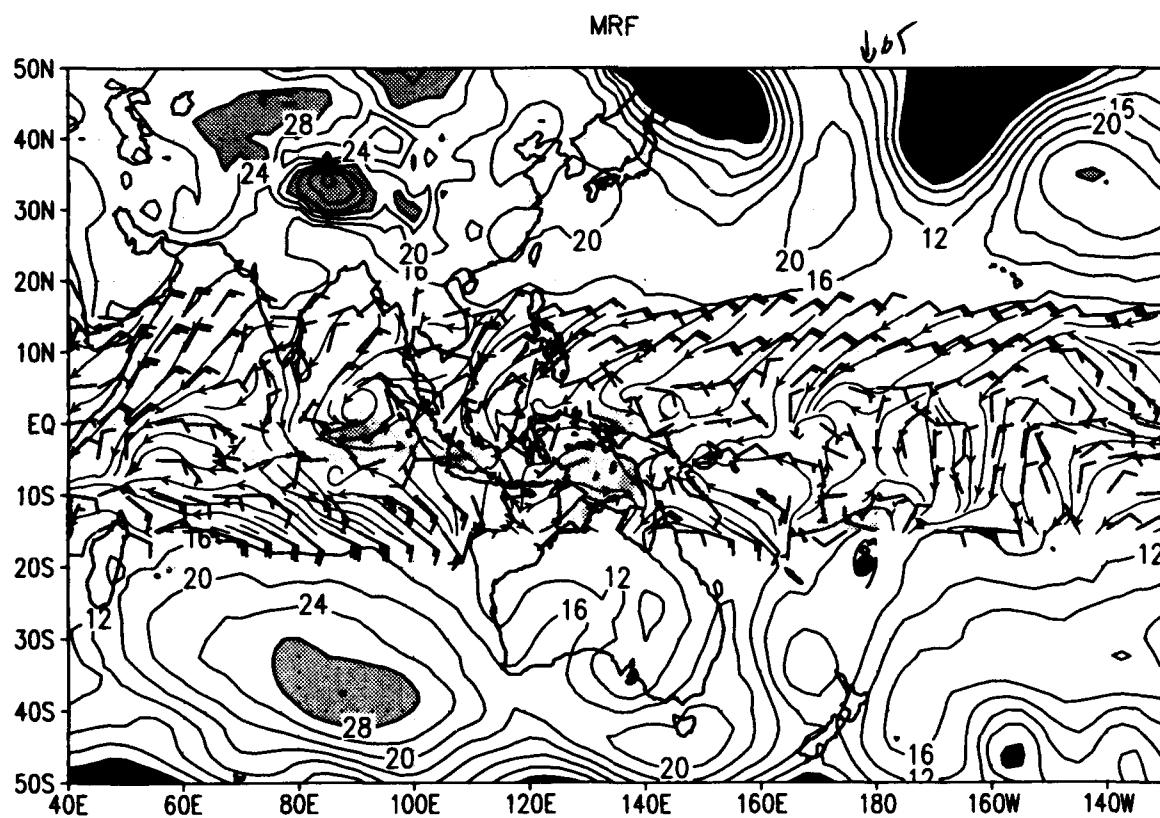
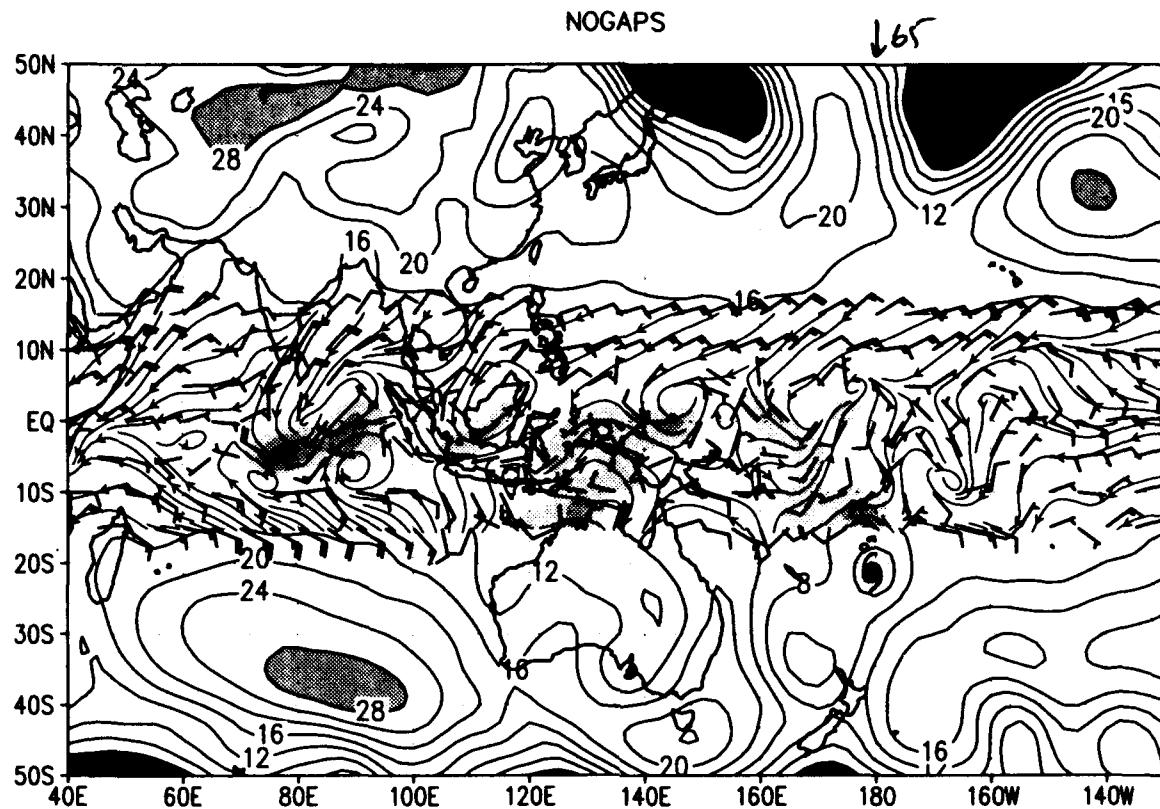
SLP and sfc winds ($u>0$ shaded) for 00Z 10 DEC 1992
 slp (mb) wind barbs (kts) /d2/toga_coare/d2.gs



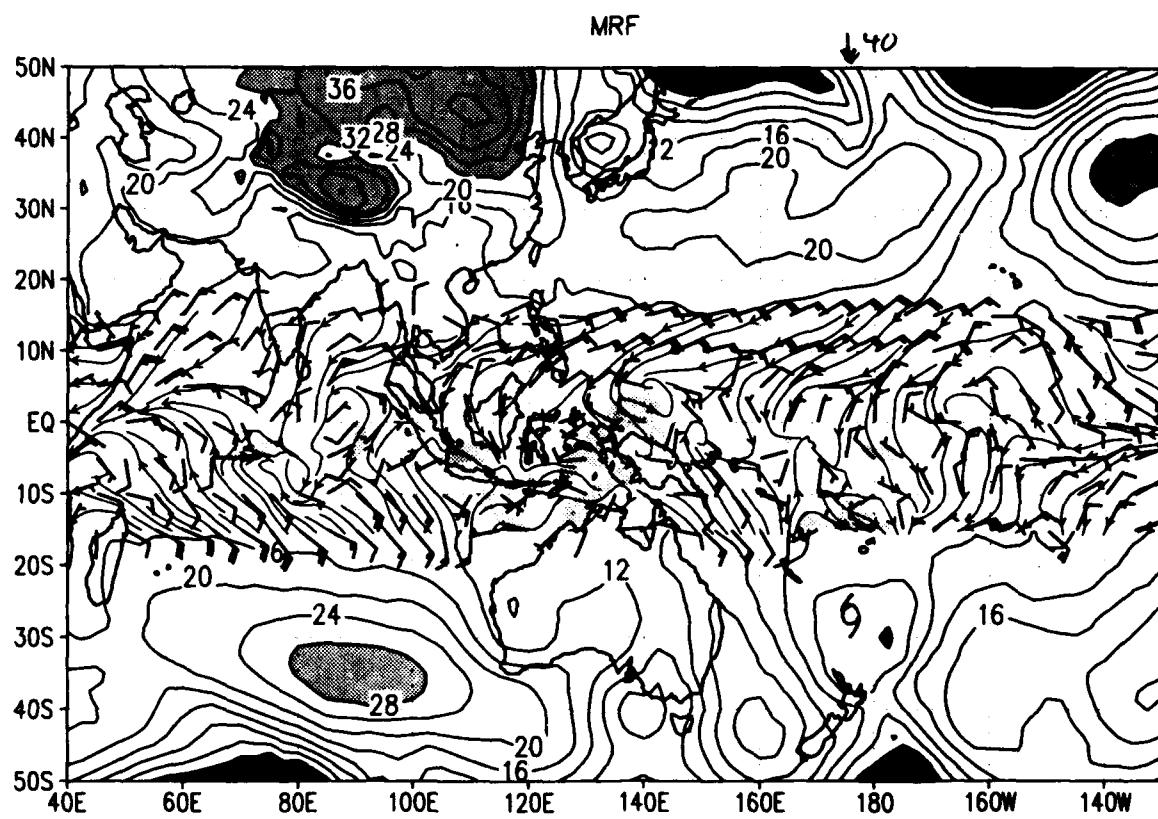
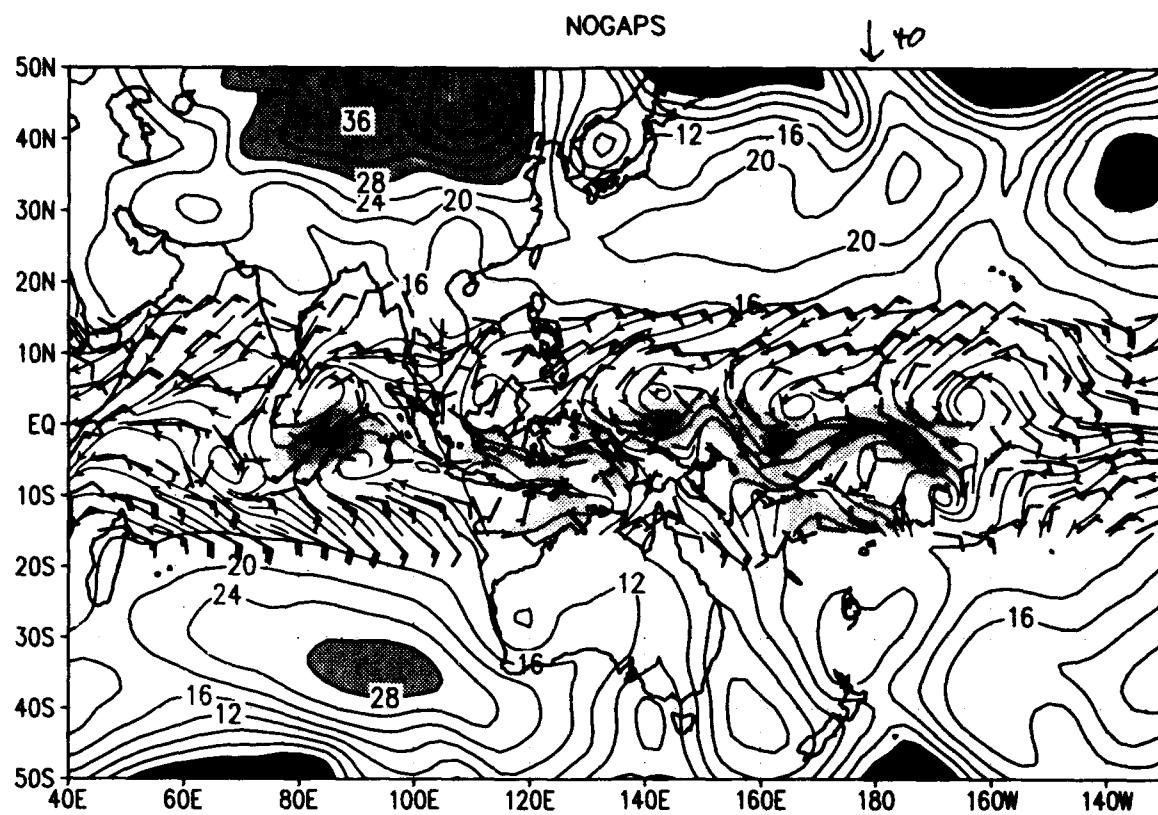
SLP and sfc winds ($u > 0$ shaded) for 00Z 11 DEC 1992
slp (mb) wind barbs (kts) /d2/toga_coare/d2.gs



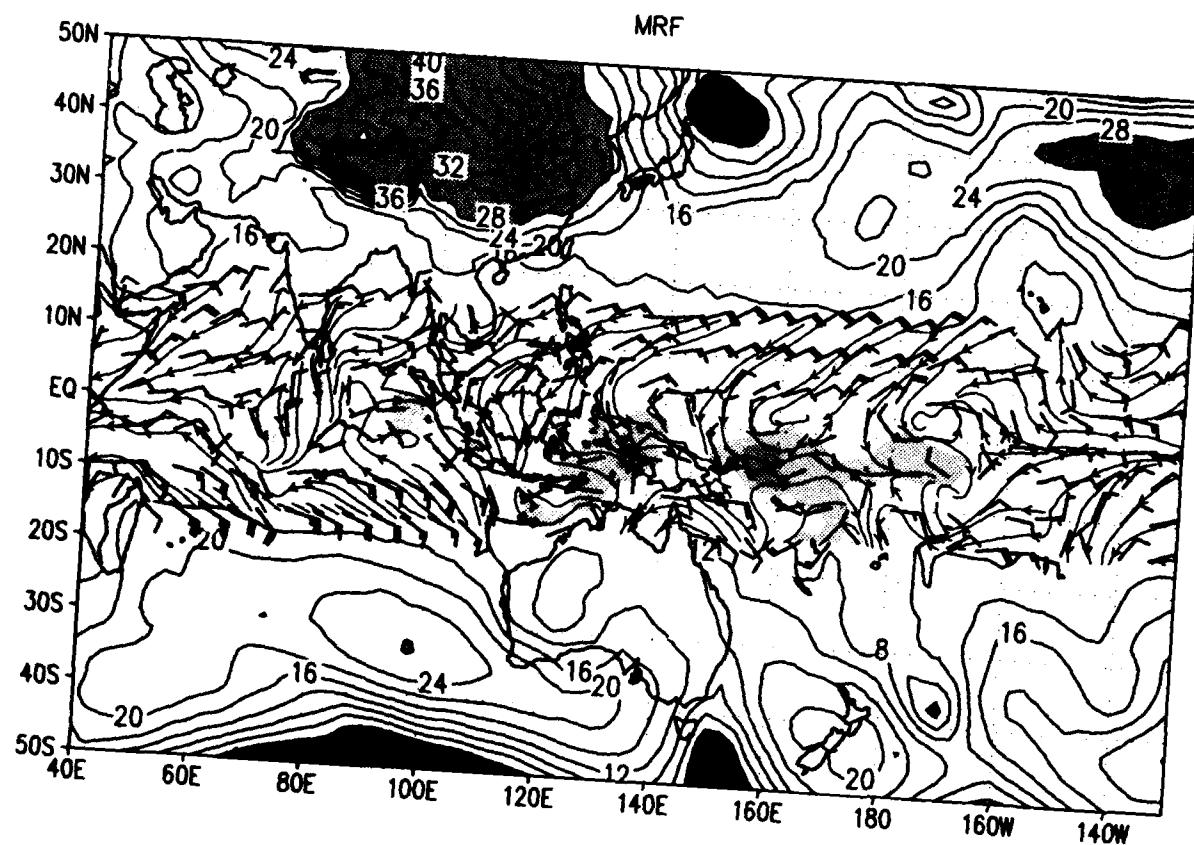
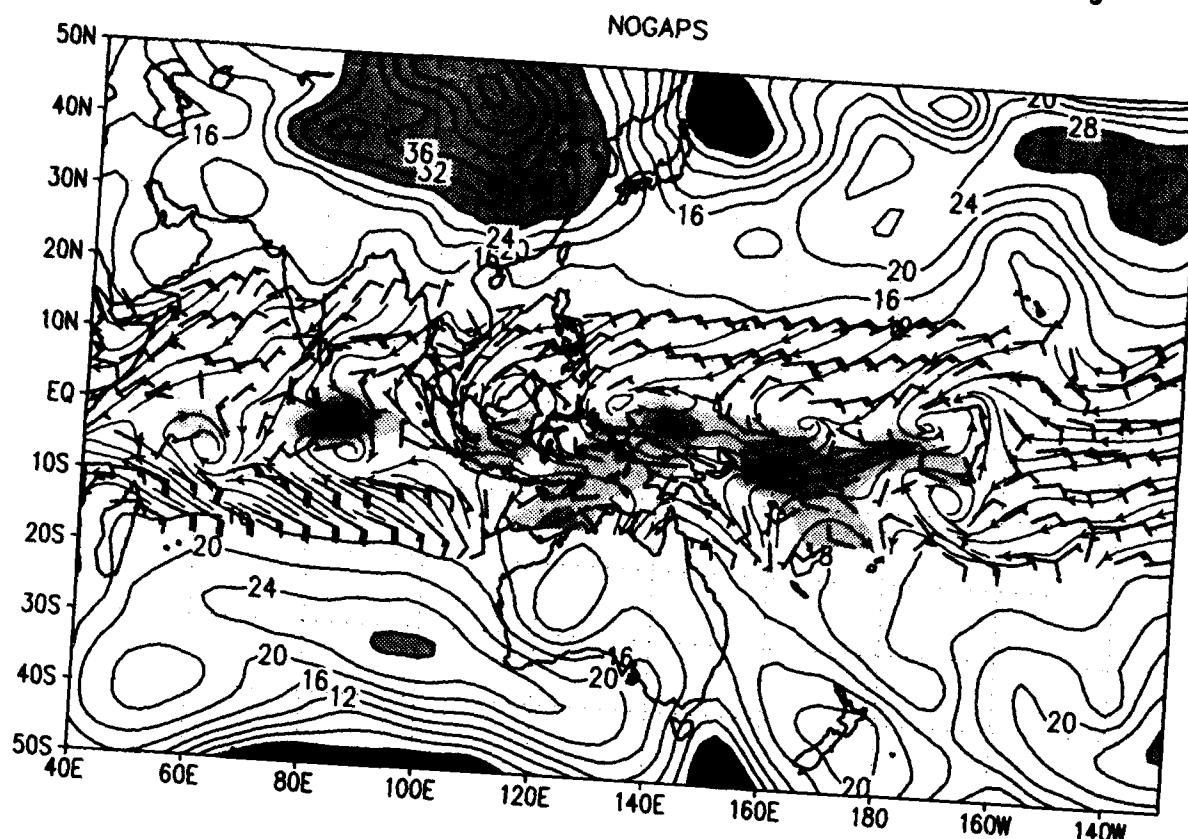
SLP and sfc winds ($u>0$ shaded) for 00Z 12 DEC 1992
slp (mb) wind barbs (kts) /d2/toga_coare/d2.gs



SLP and sfc winds ($u > 0$ shaded) for 00Z 13 DEC 1992
slp (mb) wind barbs (kts) /d2/toga_coare/d2.gs

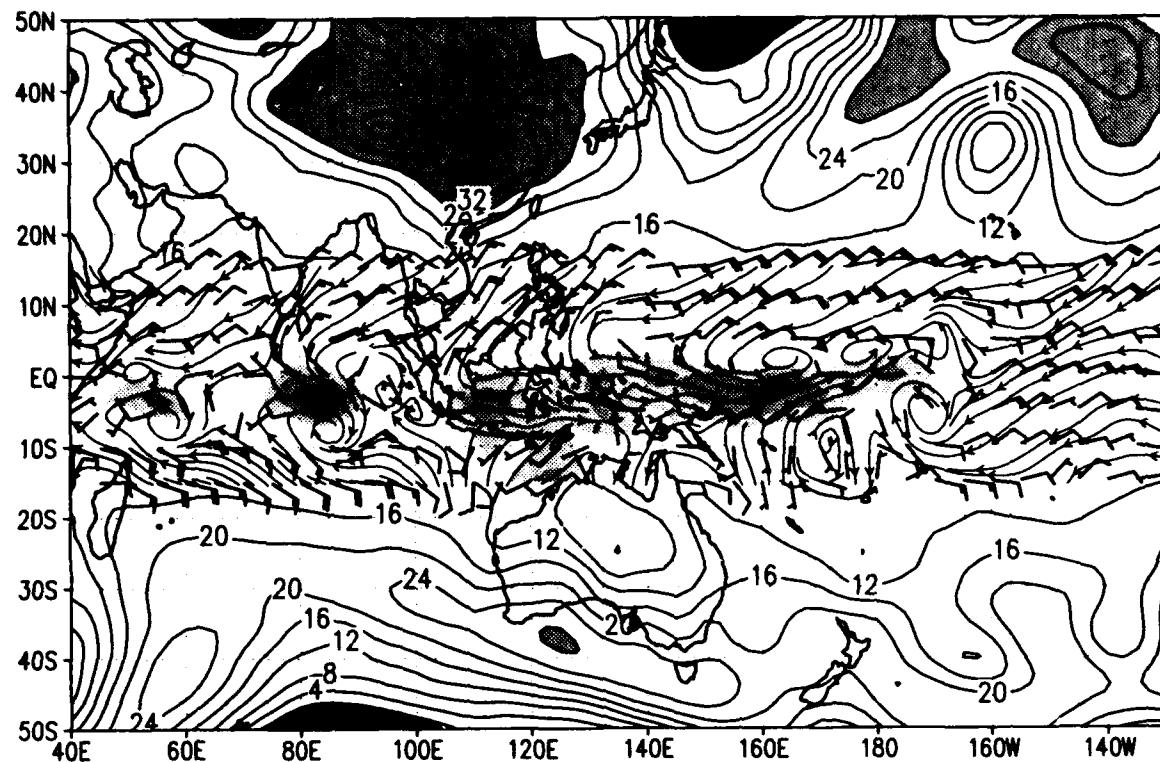


SLP and sfc winds ($u > 0$ shaded)
slp (mb) wind barbs (kts) /d2/toga_coare/d2.gs
for 00Z 14 DEC 1992

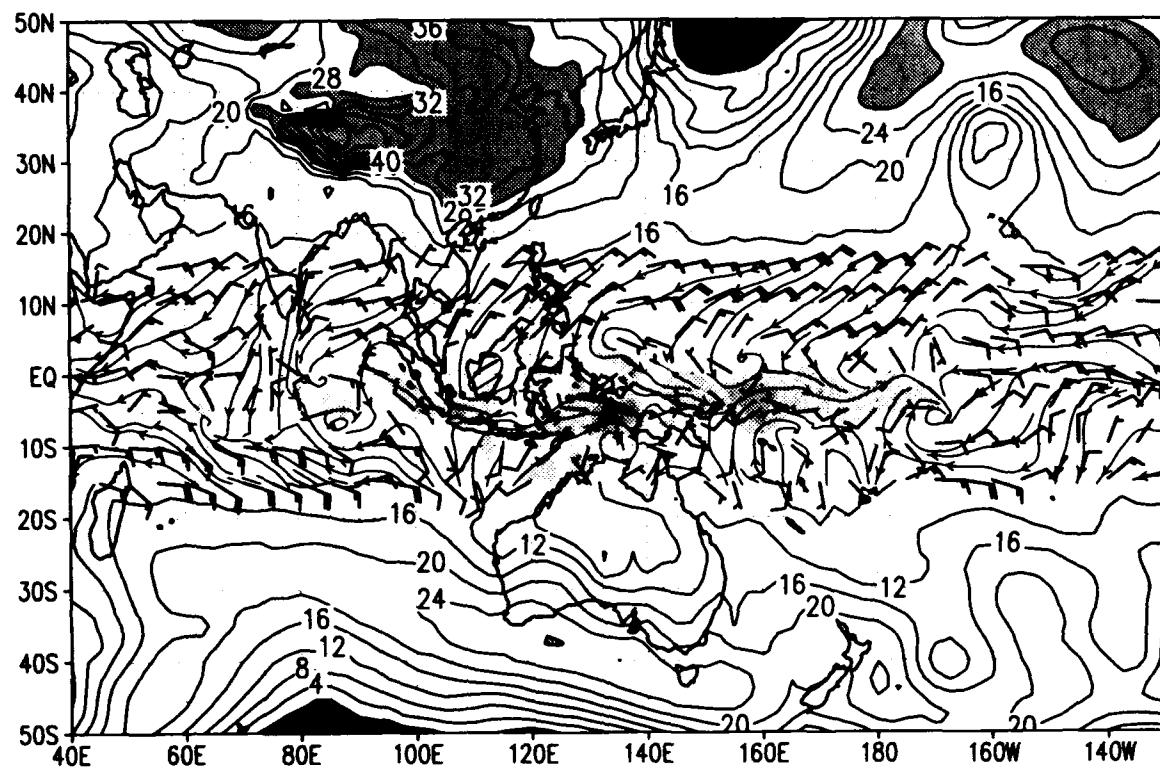


SLP and sfc winds ($u>0$ shaded) for 00Z 15 DEC 1992
slp (mb) wind barbs (kts) /d2/toga_coare/d2.gs

NOGAPS

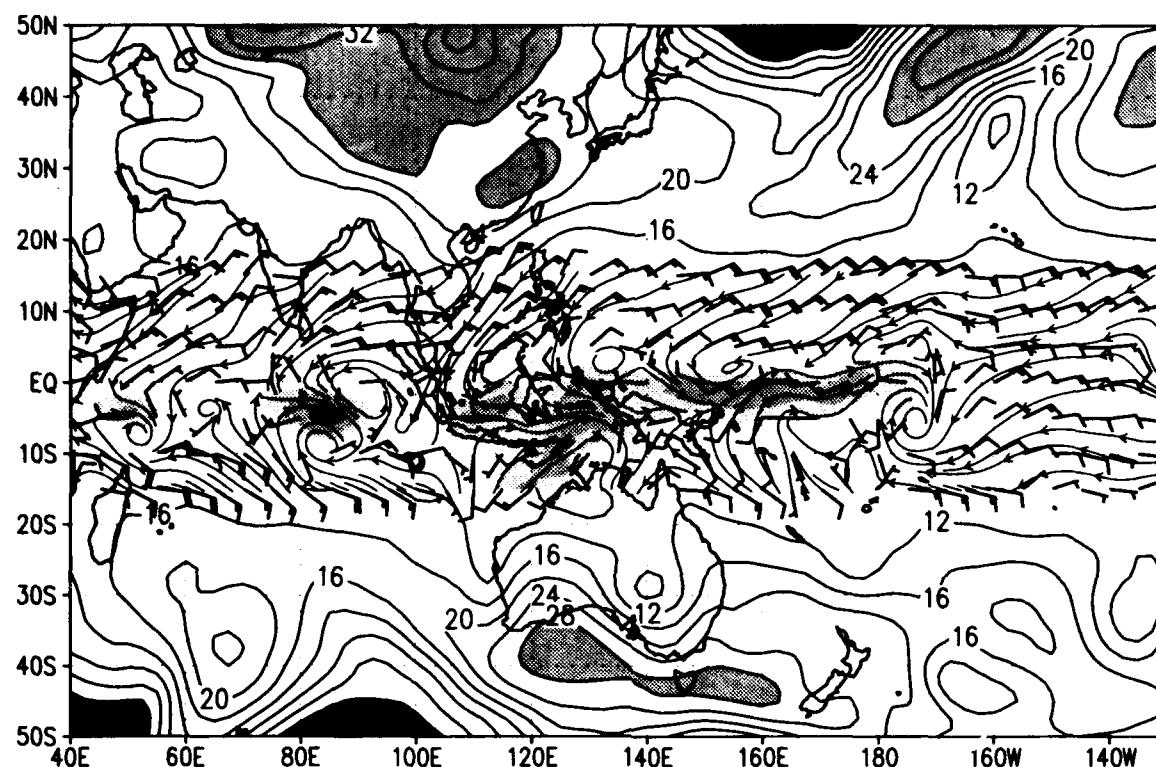


MRF

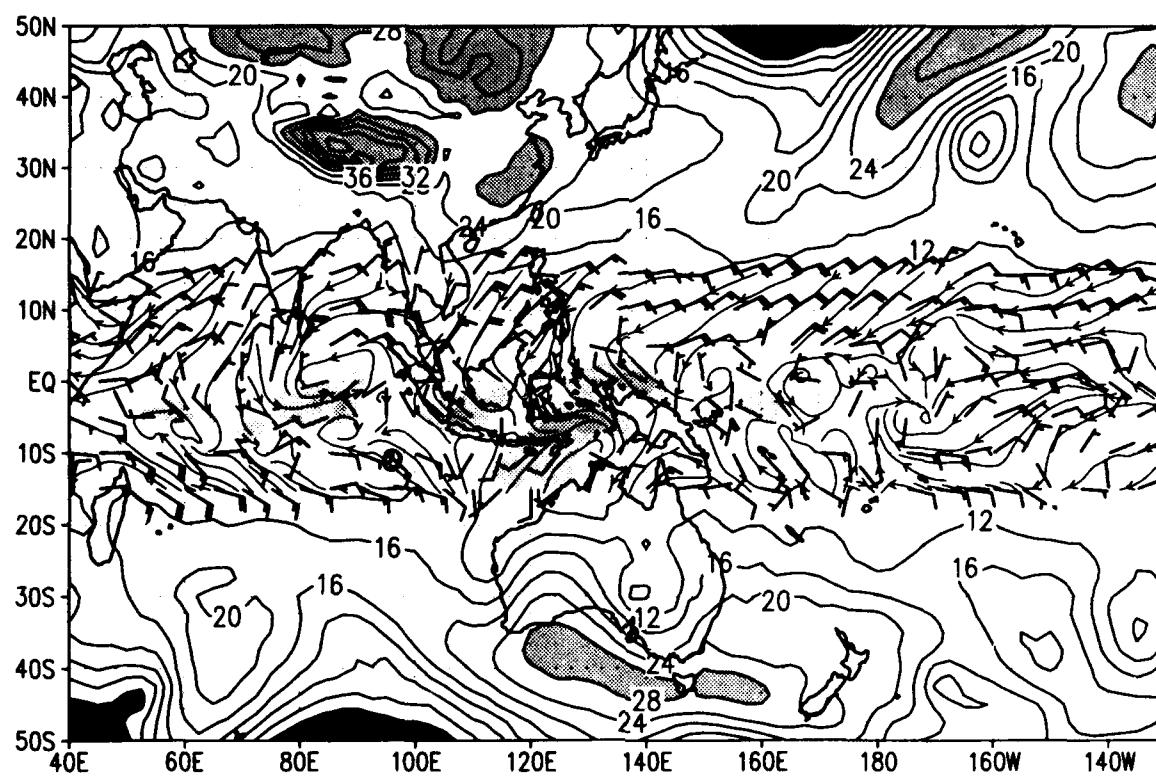


SLP and sfc winds ($u>0$ shaded) for 00Z 16 DEC 1992
slp (mb) wind barbs (kts) /d2/toga_coare/d2.gs

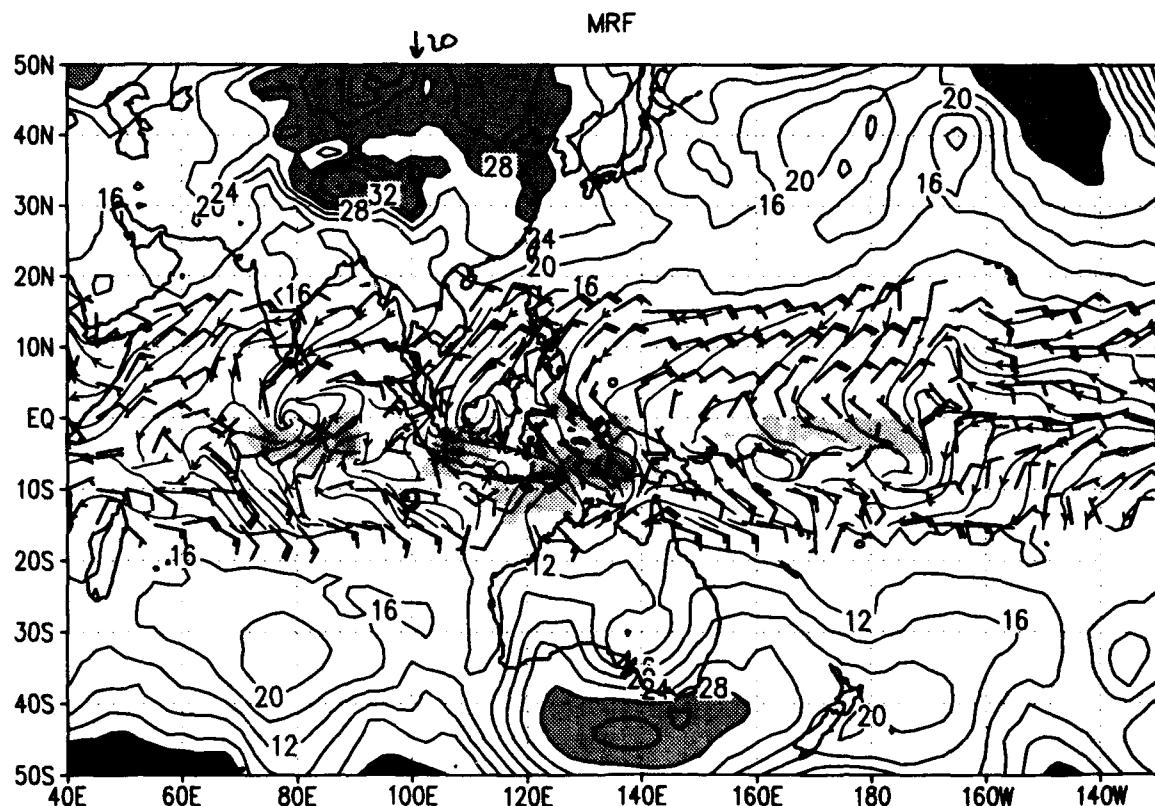
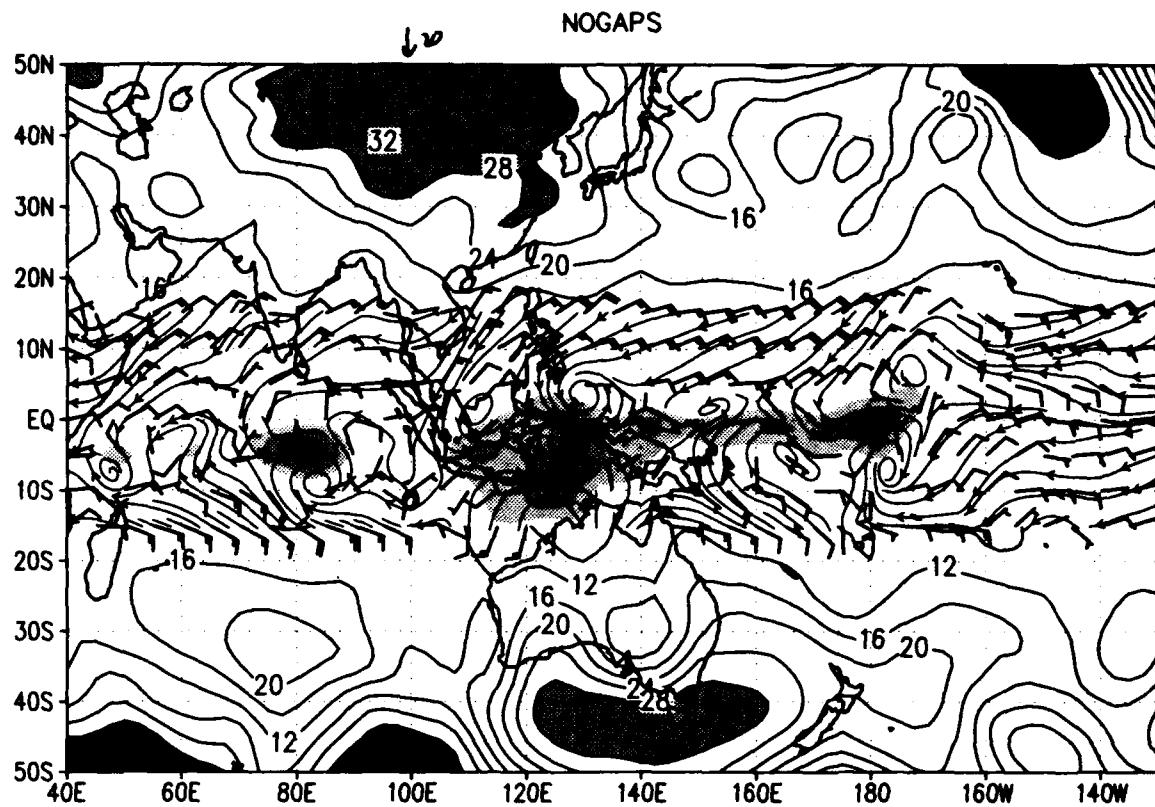
NOGAPS



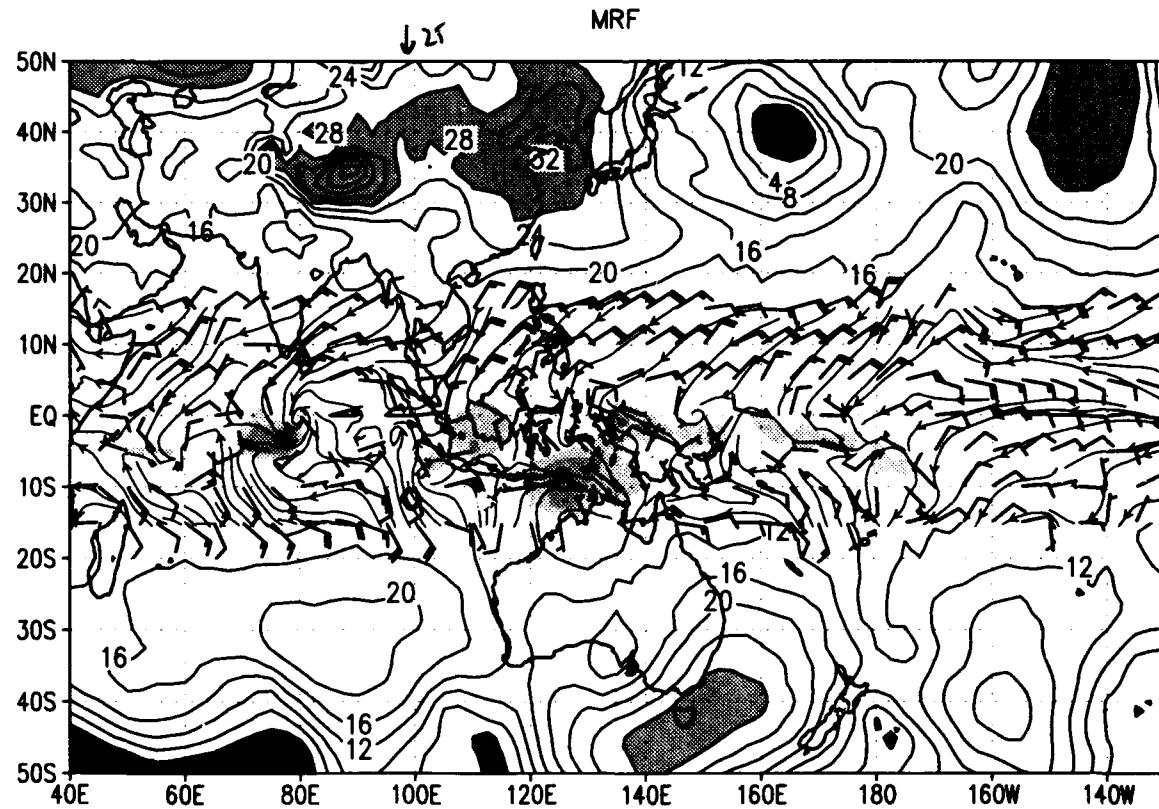
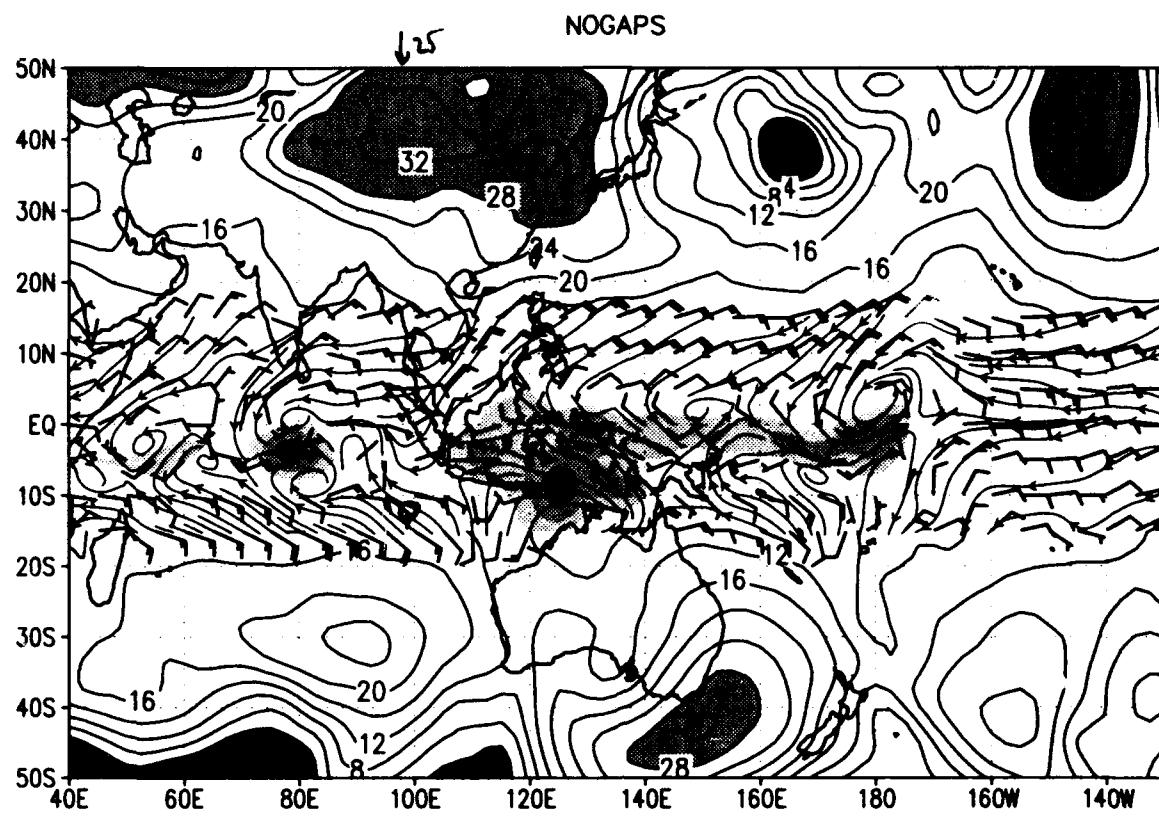
MRF



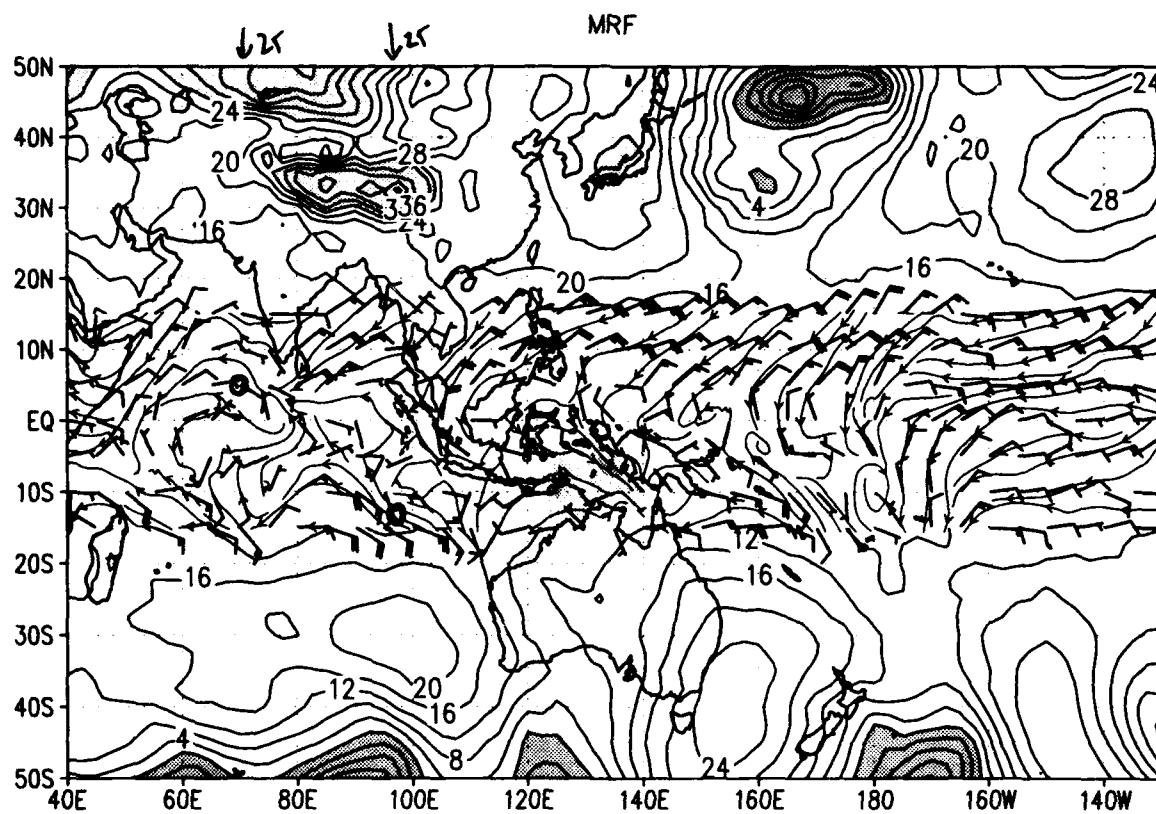
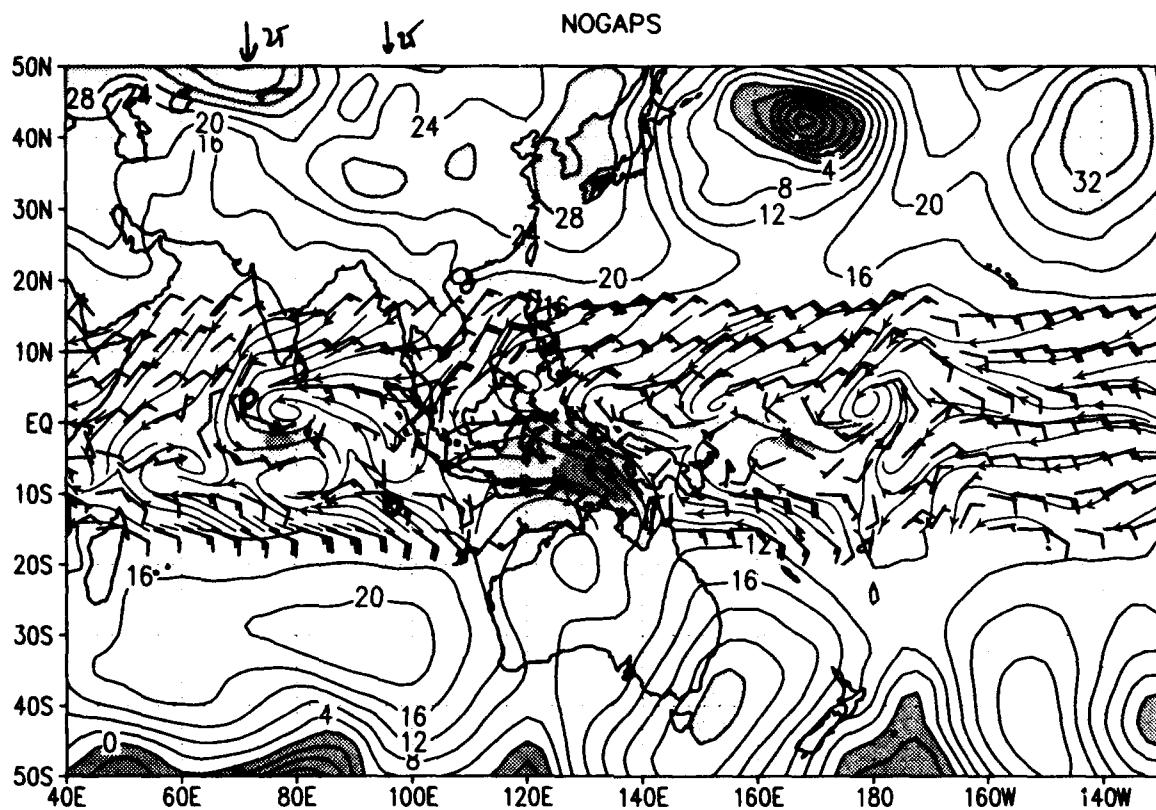
SLP and sfc winds ($u>0$ shaded) for 00Z 17 DEC 1992
slp (mb) wind barbs (kts) /d2/toga_coare/d2.gs



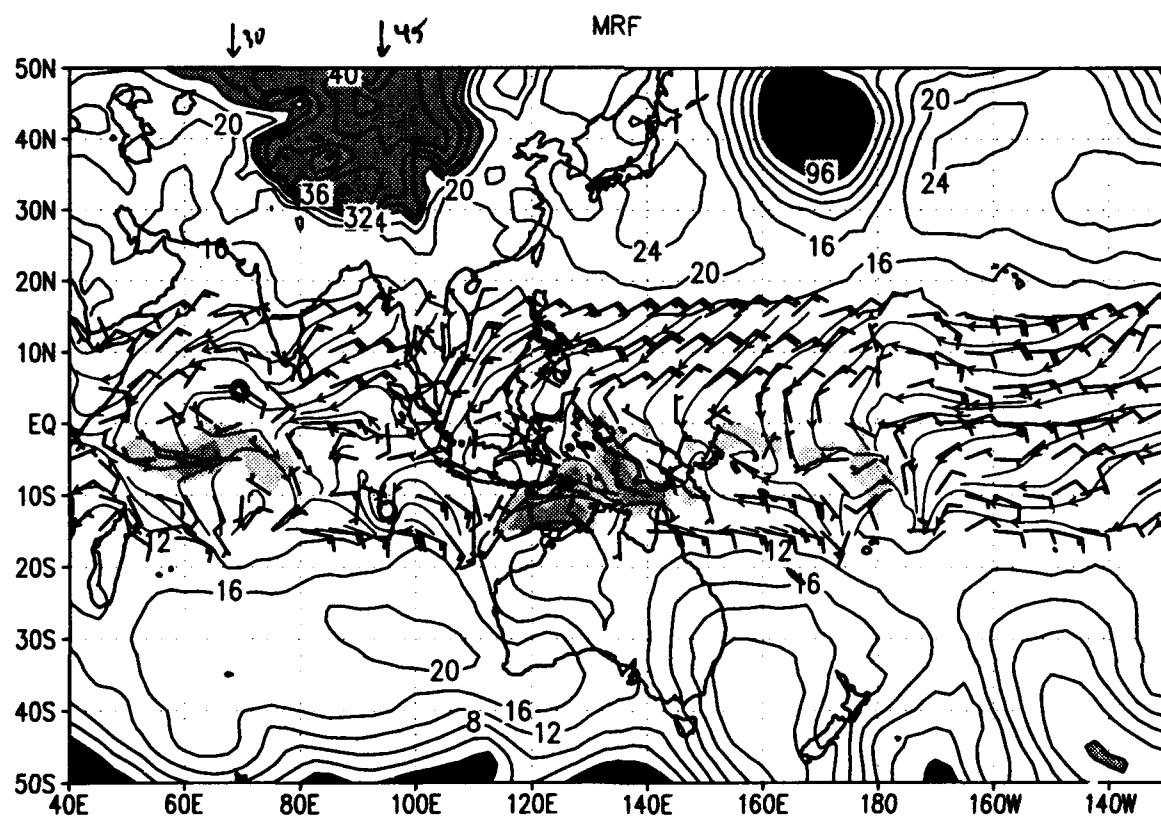
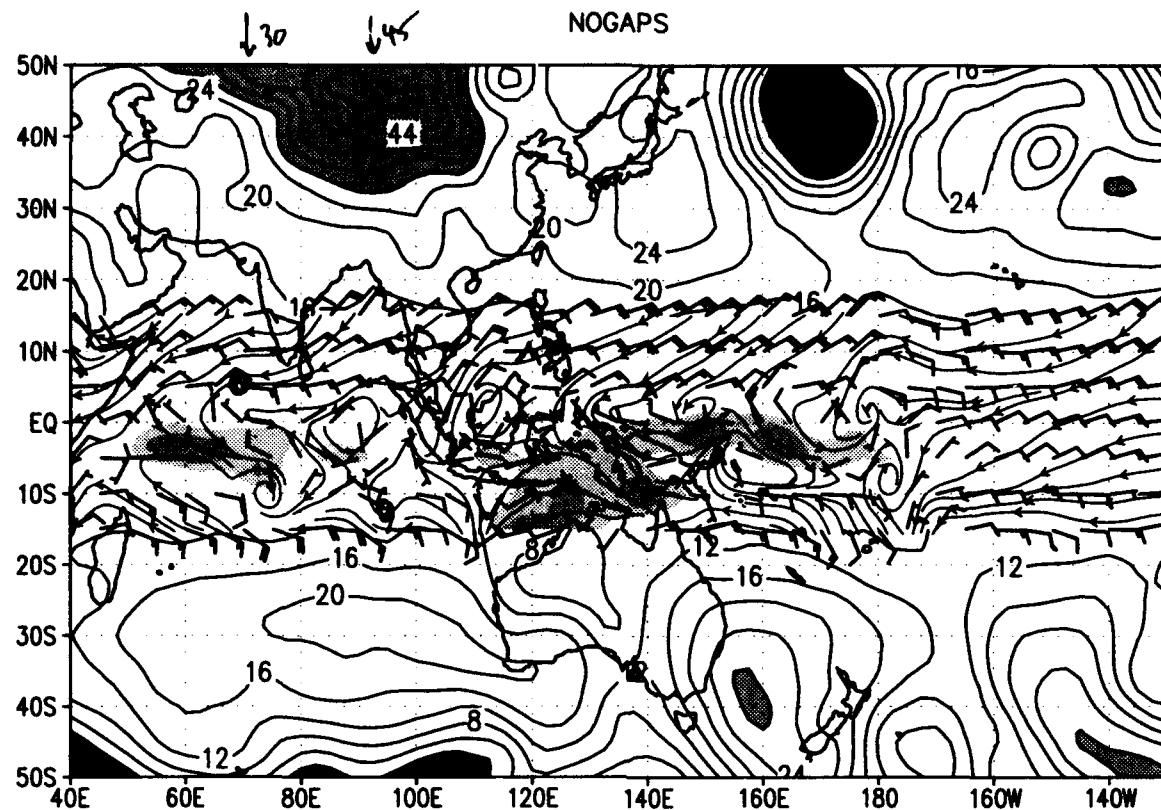
SLP and sfc winds ($u>0$ shaded) for 00Z 18 DEC 1992
slp (mb) wind barbs (kts) /d2/toga_coare/d2.gs



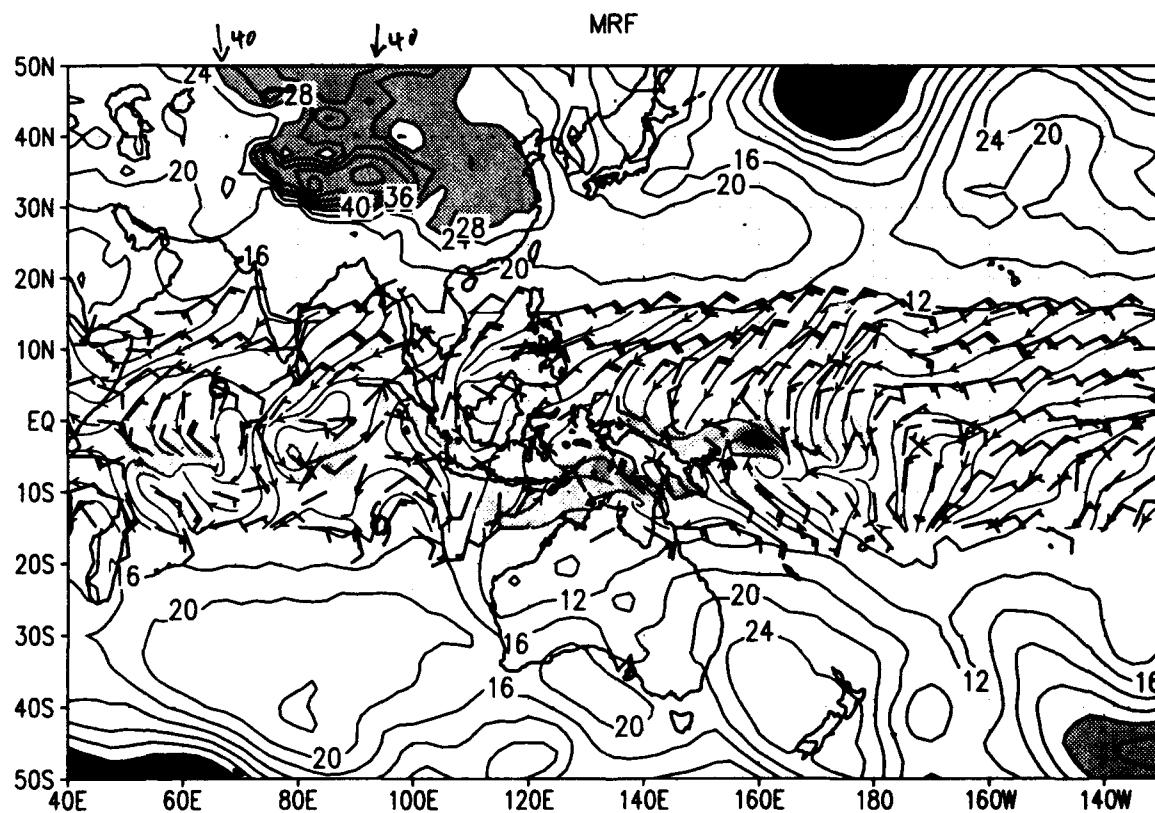
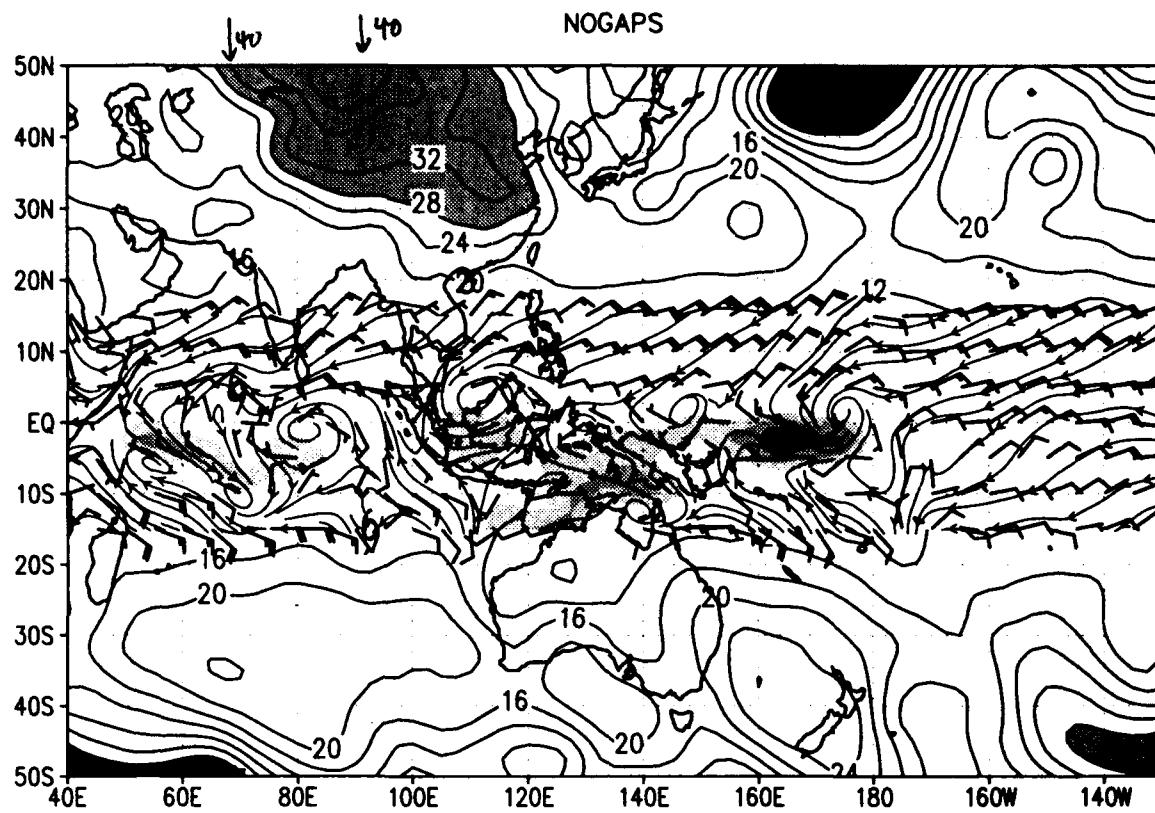
SLP and sfc winds ($u > 0$ shaded) for 00Z 19 DEC 1992
slp (mb) wind barbs (kts) /d2/toga_coare/apps/d2.gs



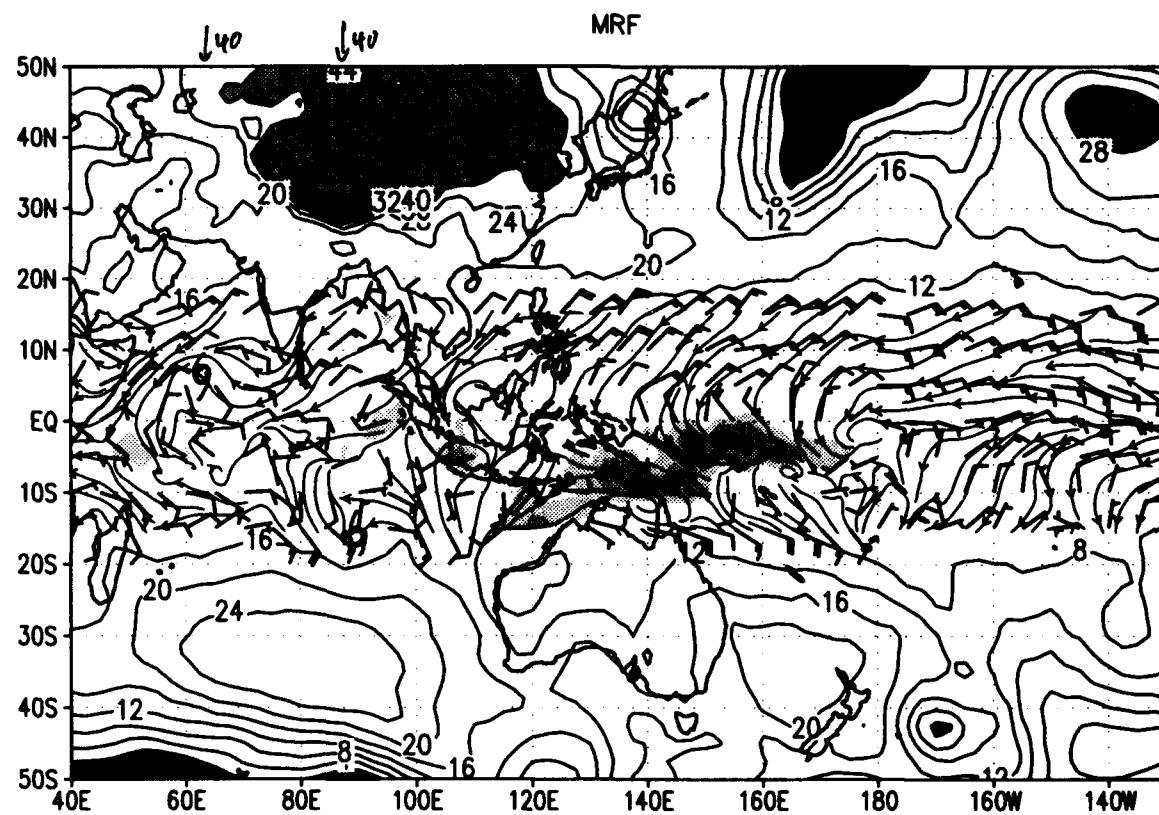
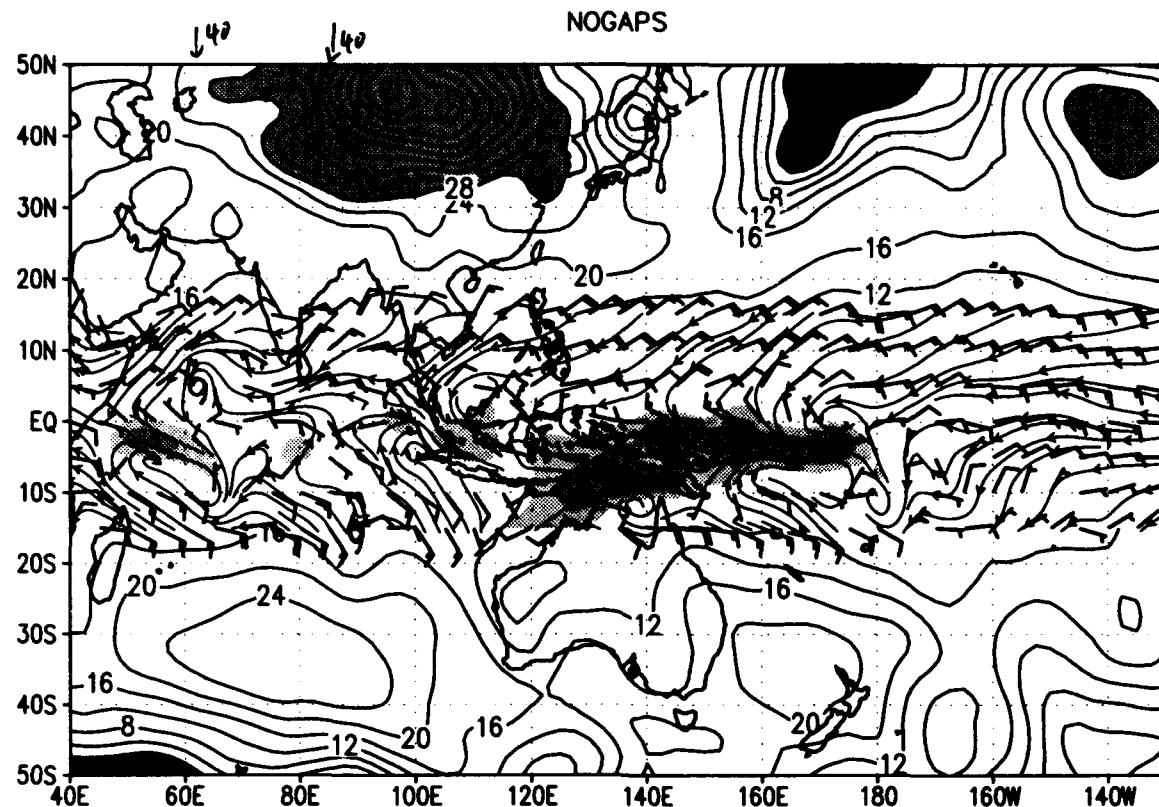
SLP and sfc winds ($u>0$ shaded) for 00Z 20 DEC 1992
slp (mb) wind barbs (kts) /d2/toga_coare/d2.gs



SLP and sfc winds ($u > 0$ shaded) for 00Z 21 DEC 1992
slp (mb) wind barbs (kts) /d2/toga_coare/d2.gs

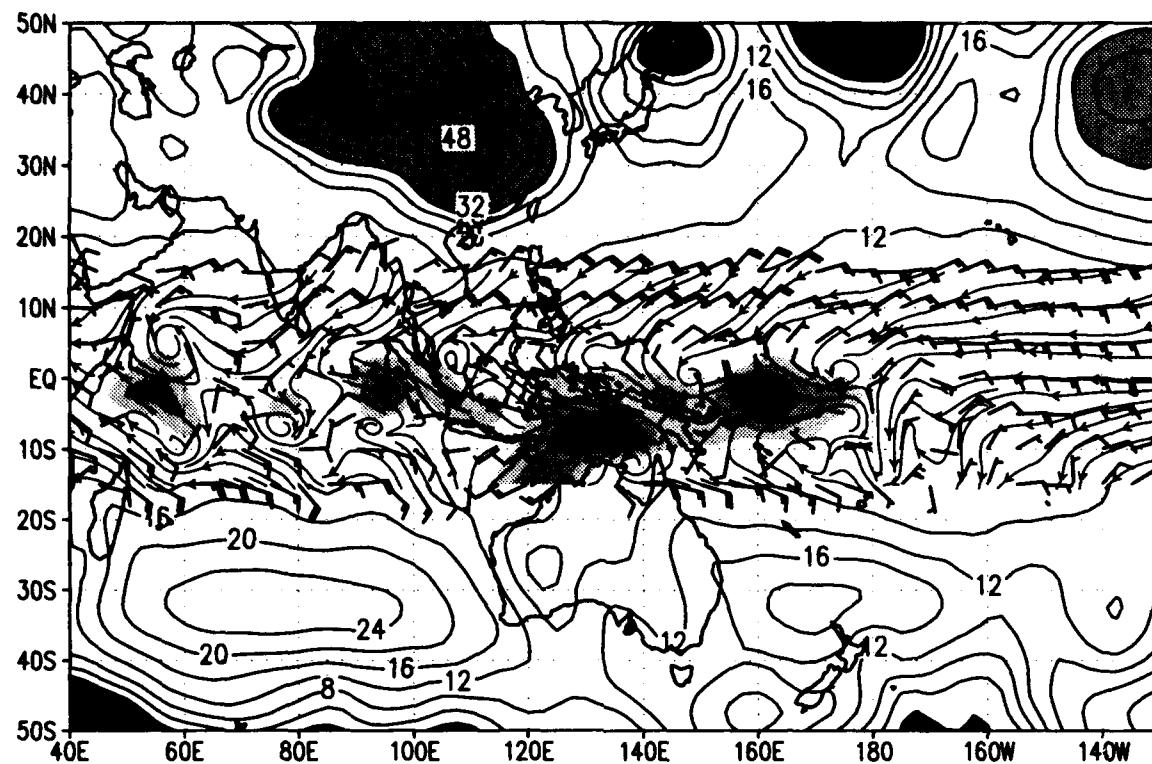


SLP and sfc winds ($u>0$ shaded) for 00Z 22 DEC 1992
slp (mb) wind barbs (kts) /d2/toga_coare/d2.gs

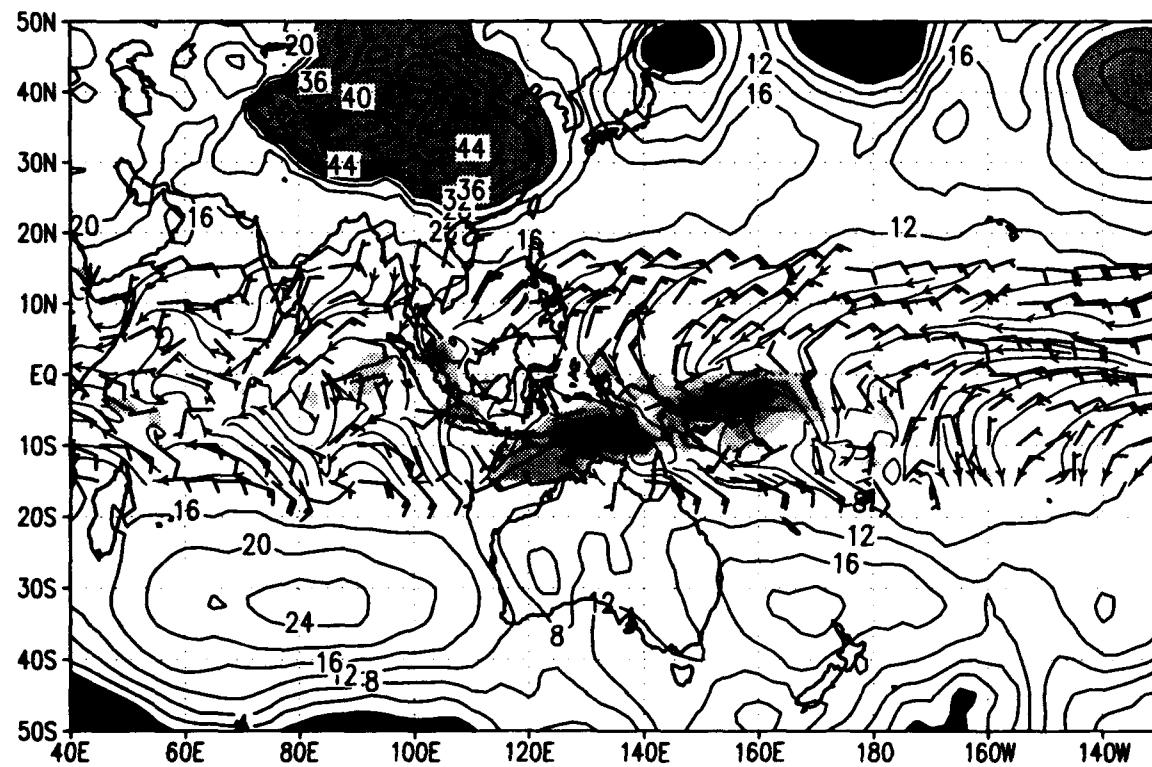


SLP and sfc winds ($u>0$ shaded) for 00Z 23 DEC 1992
slp (mb) wind barbs (kts) /d2/toga_coare/d2.gs

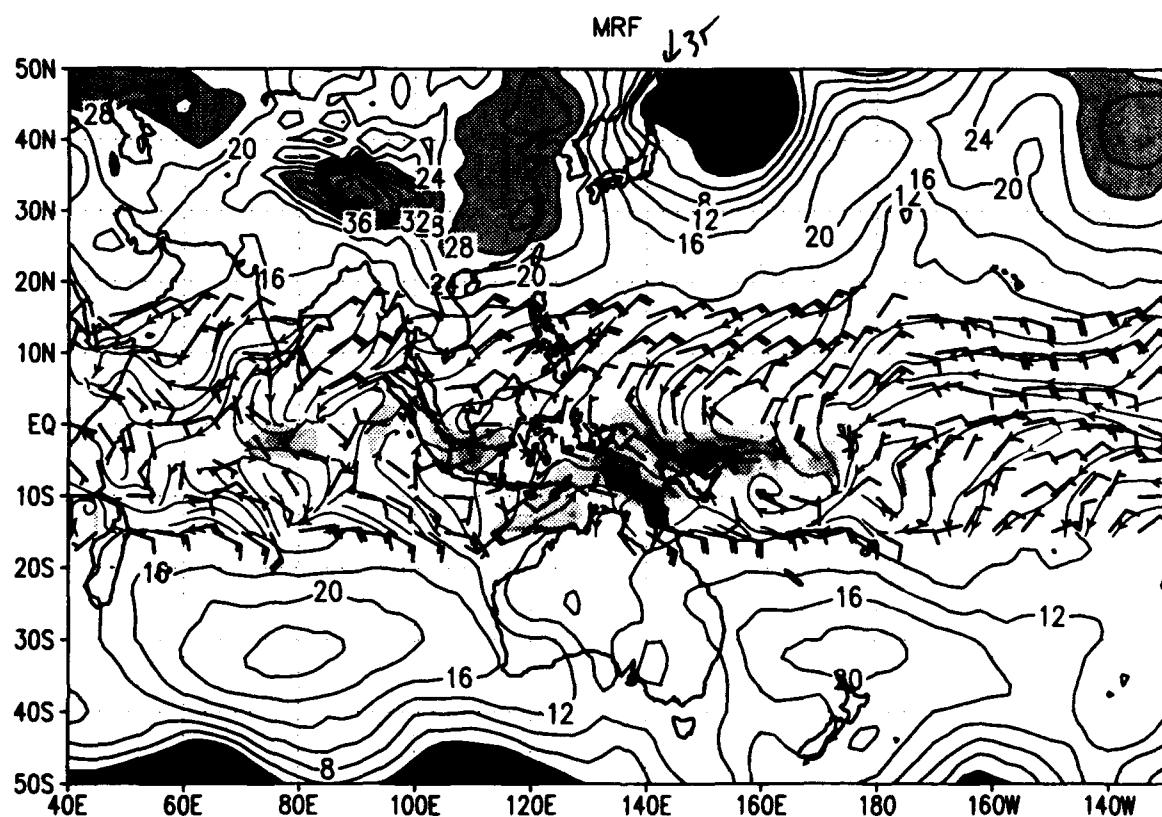
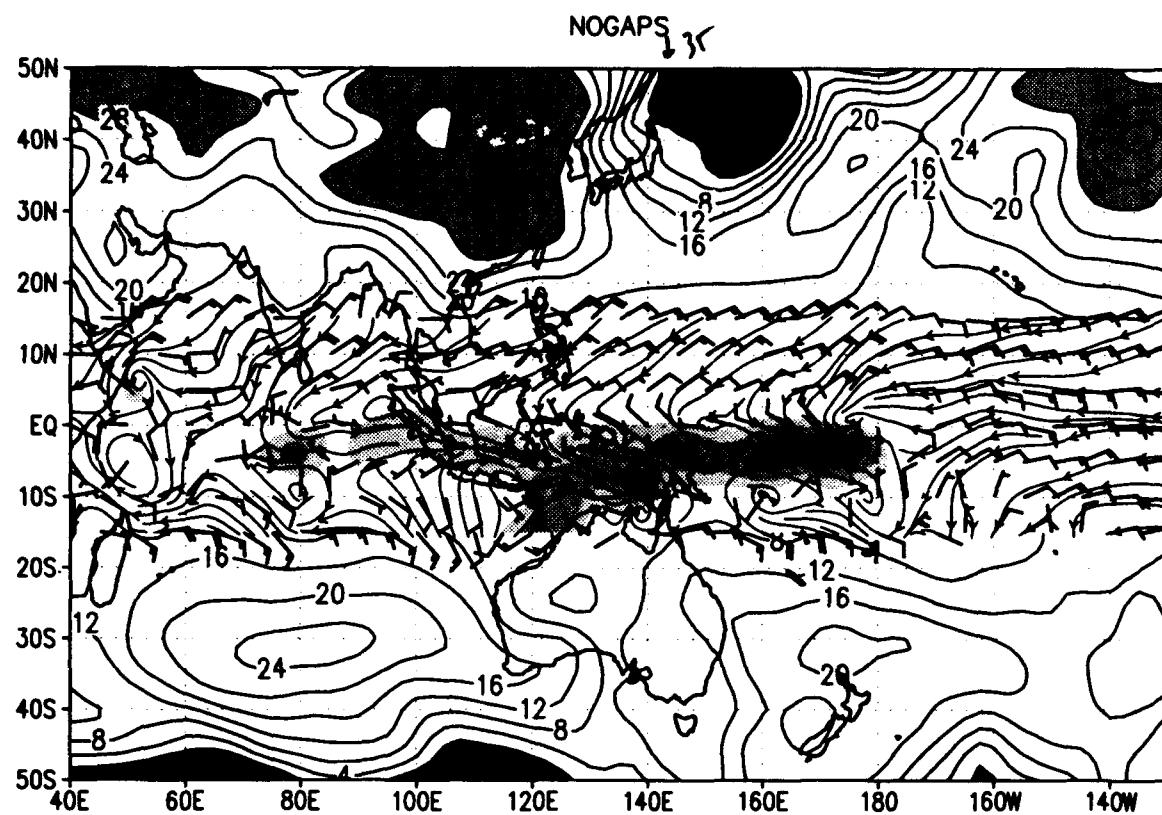
NOGAPS



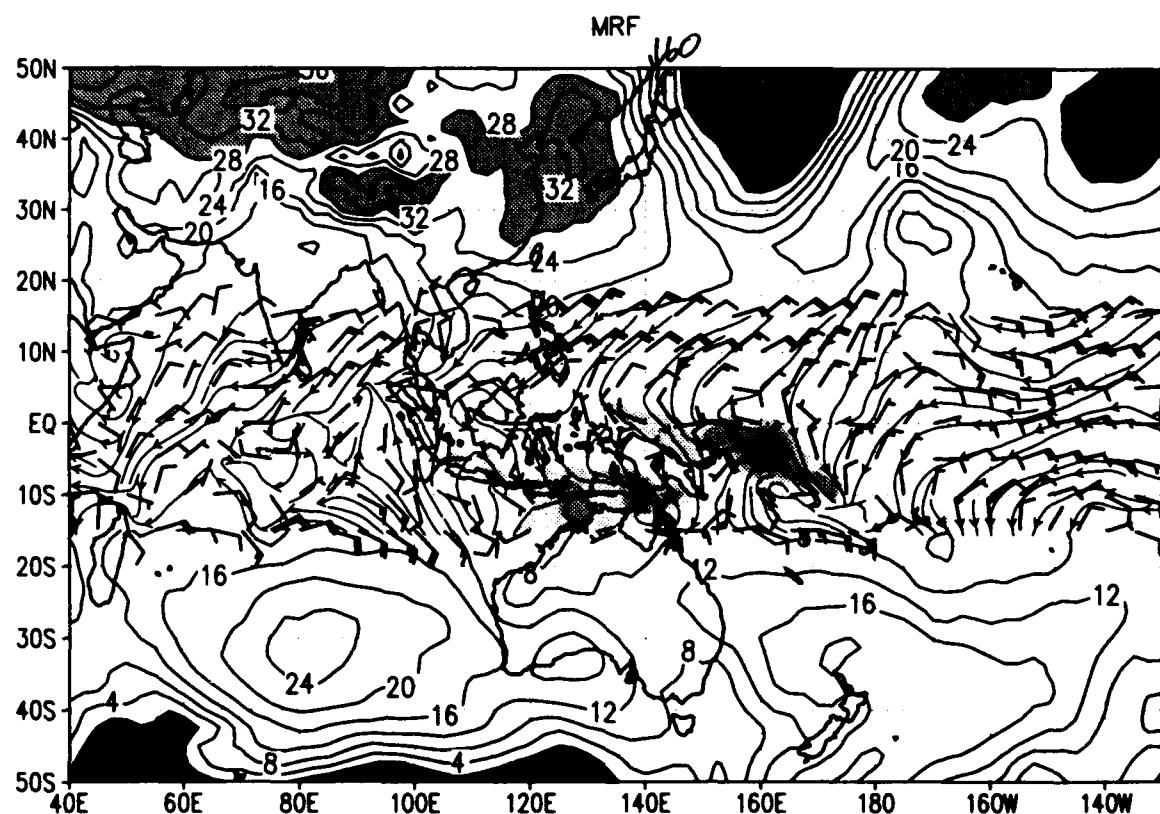
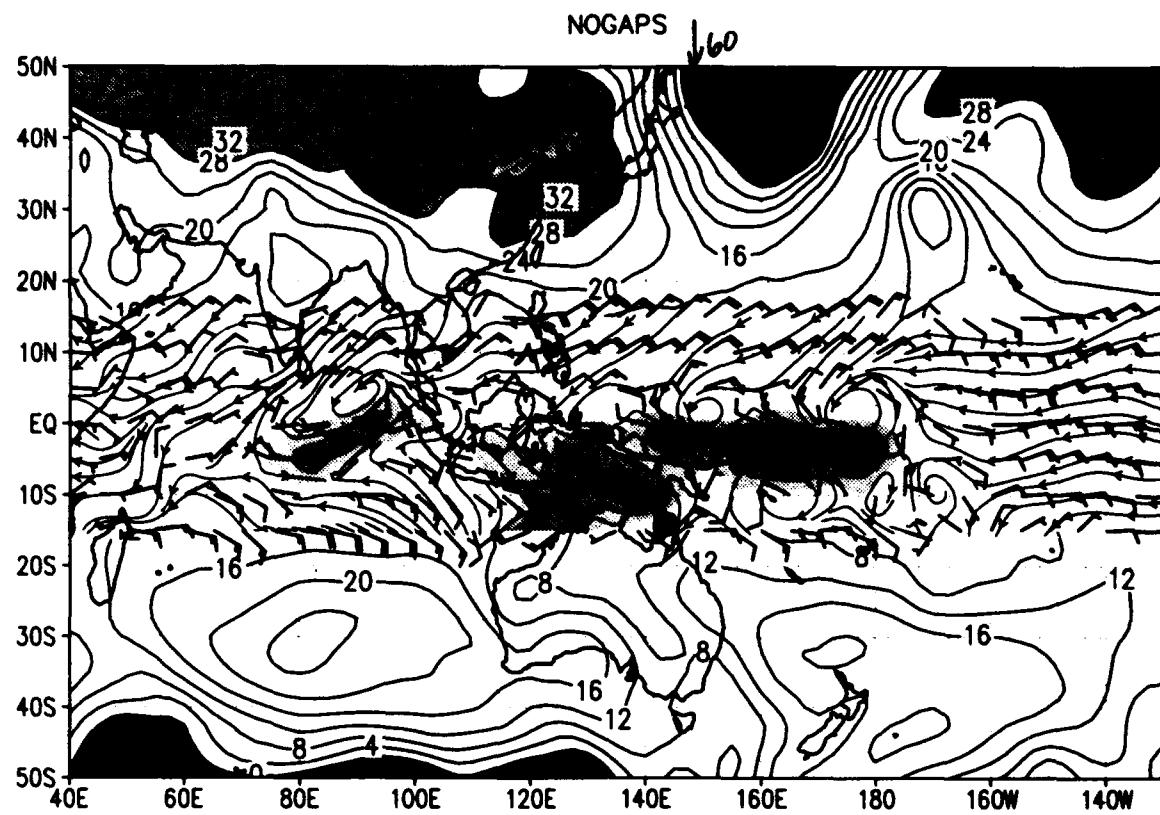
MRF



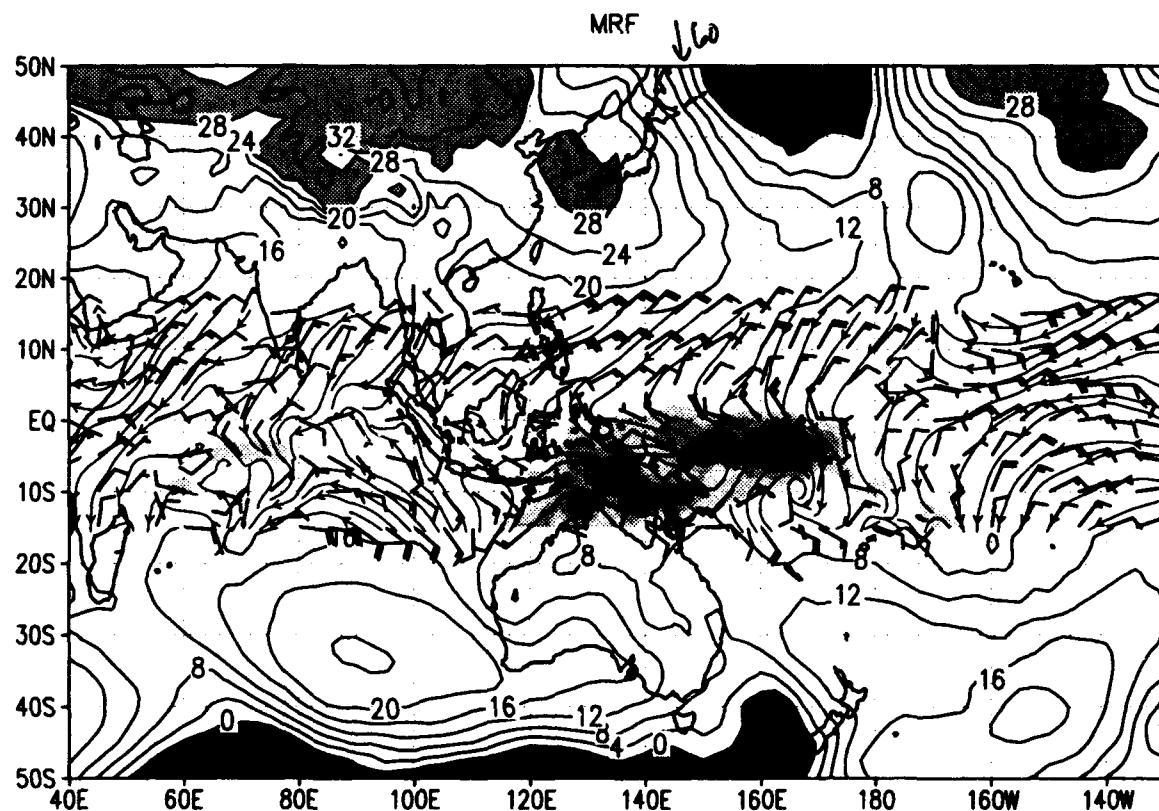
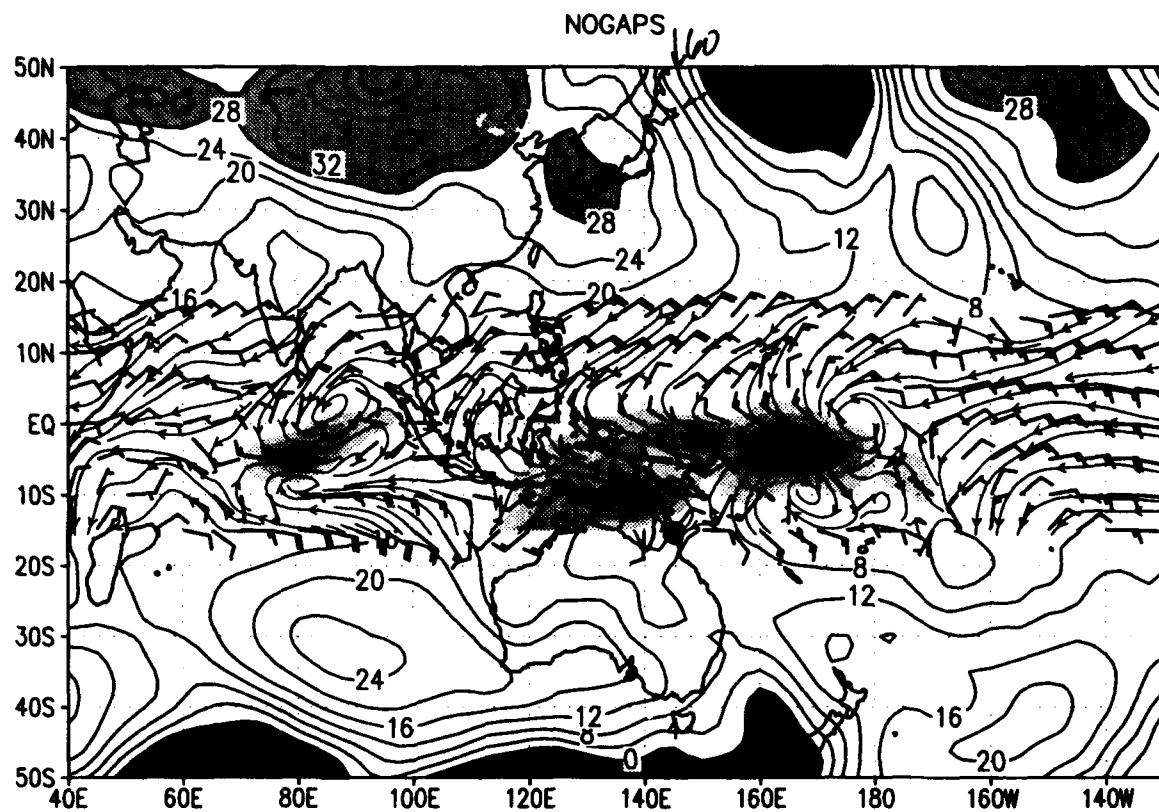
SLP and sfc winds ($u>0$ shaded) for 00Z 24 DEC 1992
slp (mb) wind barbs (kts) /d2/toga_coare/d2.gs



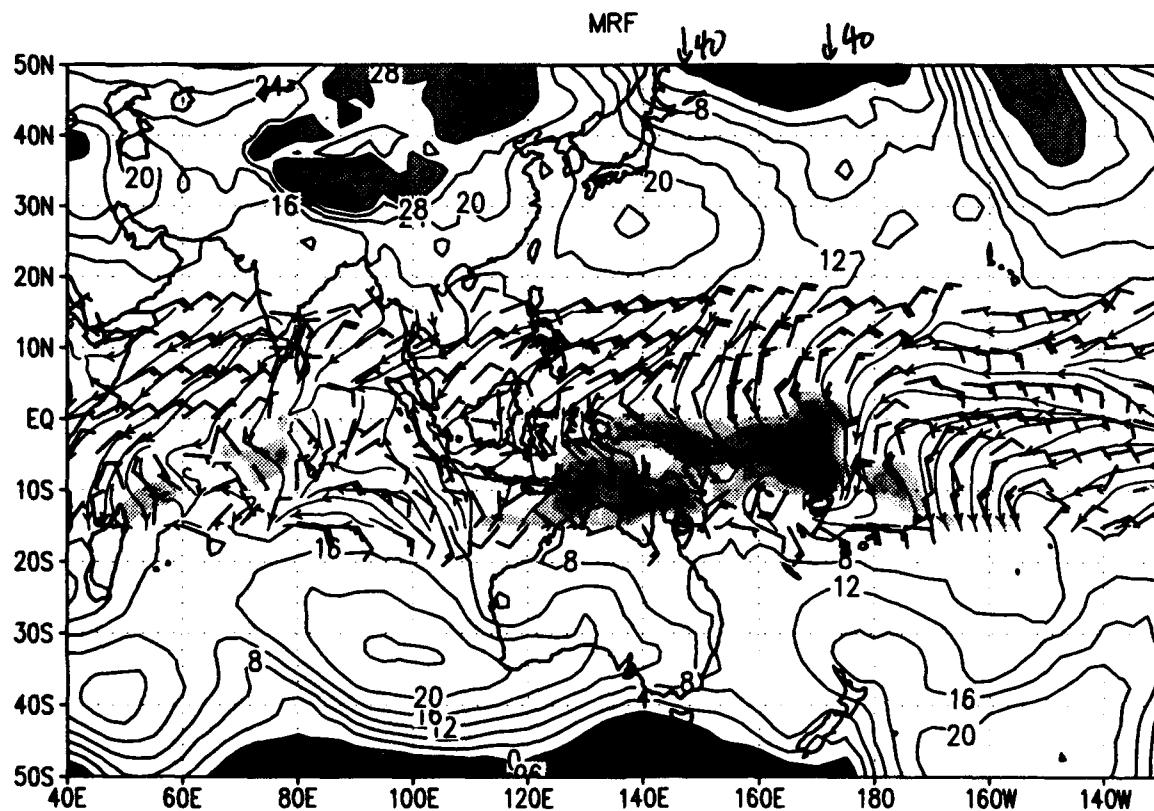
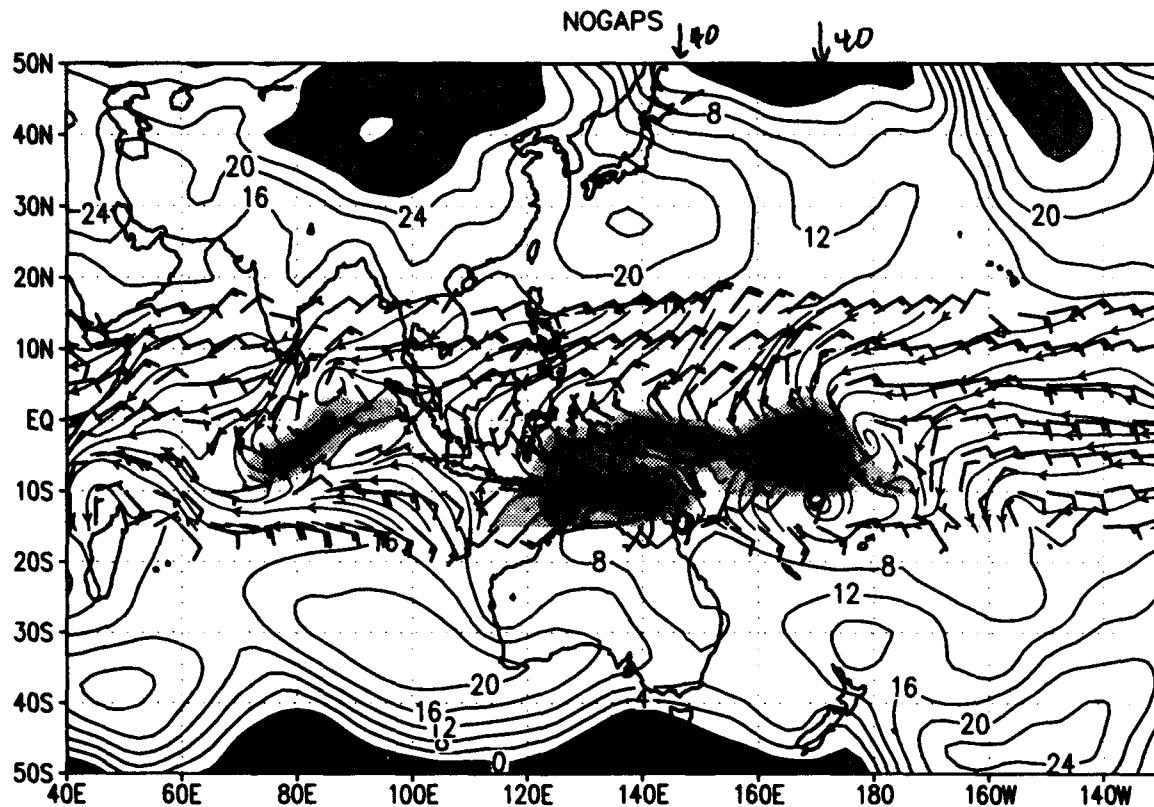
SLP and sfc winds ($u>0$ shaded) for 00Z 25 DEC 1992
slp (mb) wind barbs (kts) /d2/toga_coare/d2.gs



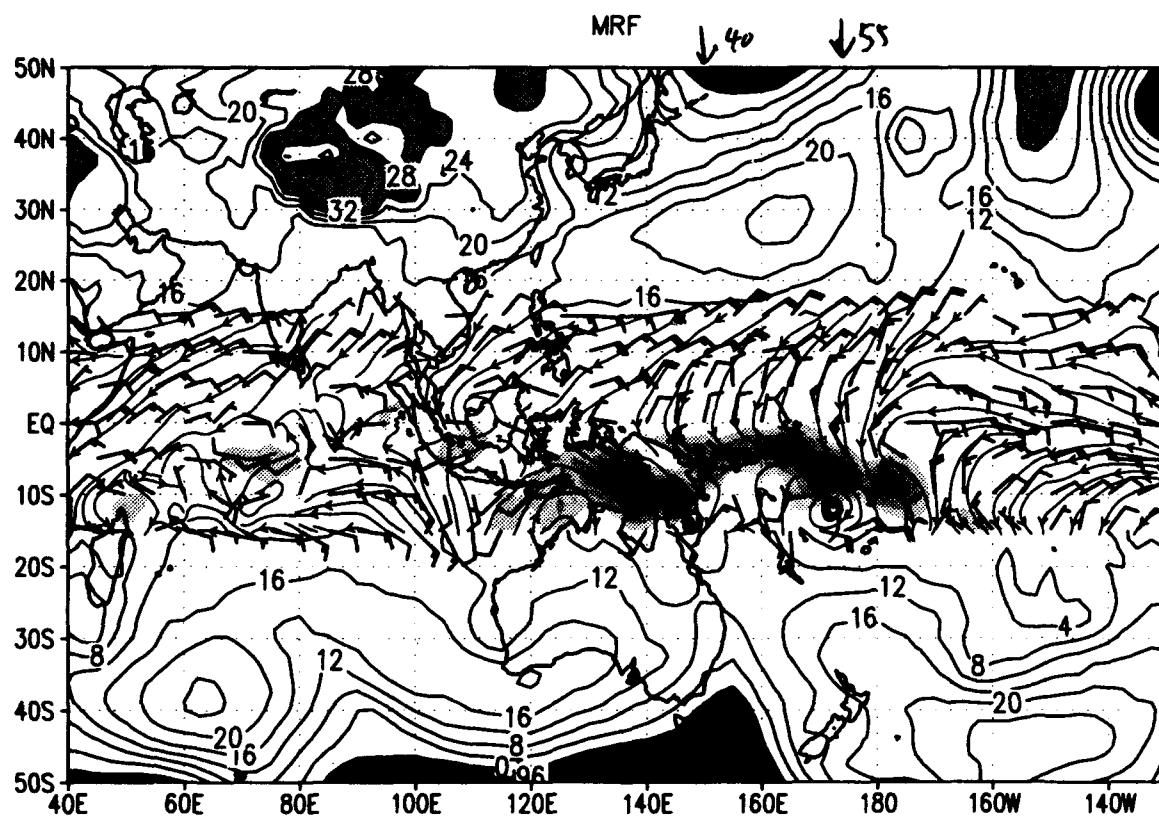
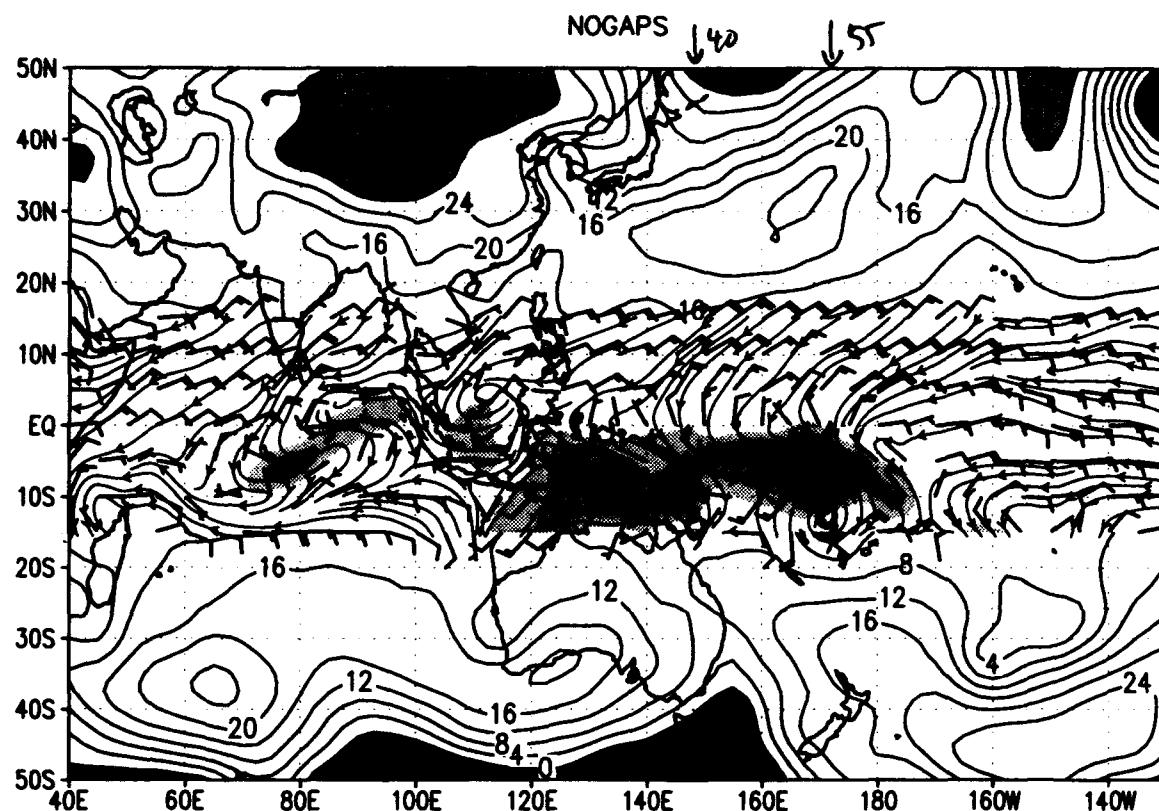
SLP and sfc winds ($u>0$ shaded) for 00Z 26 DEC 1992
slp (mb) wind barbs (kts) /d2/toga_coare/d2.gs



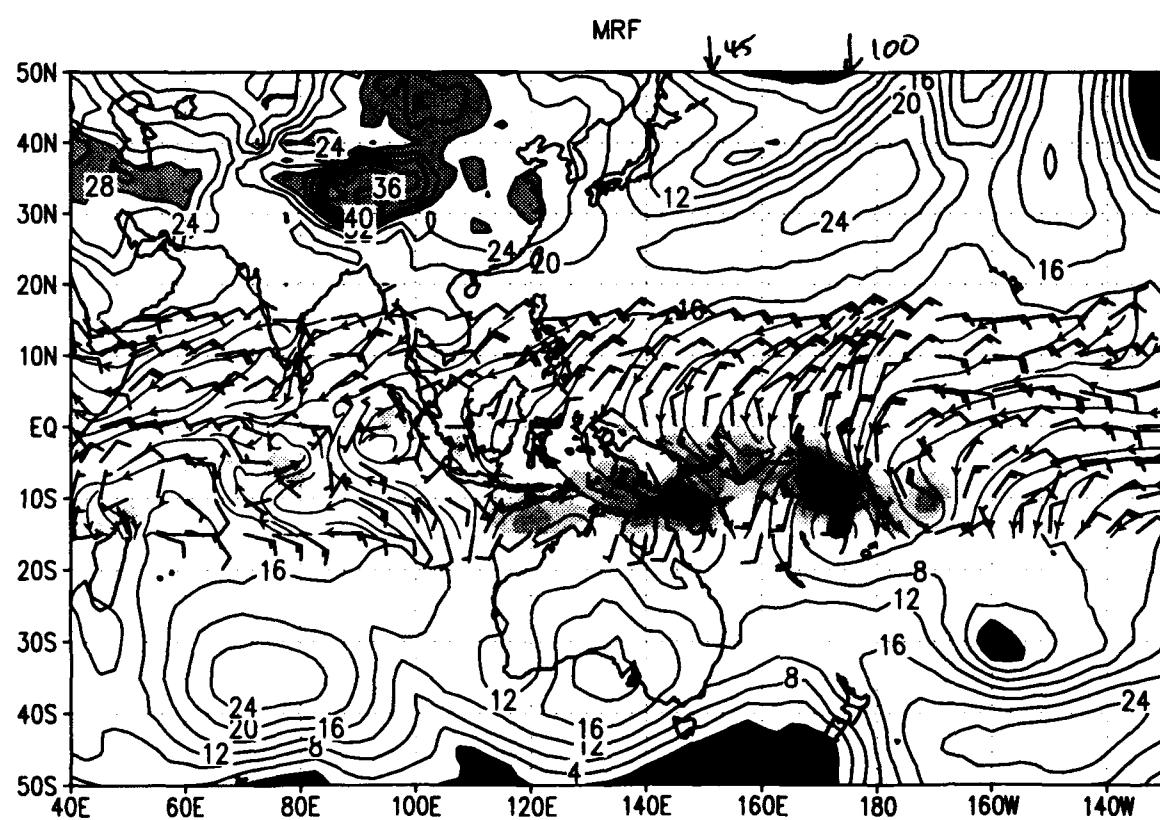
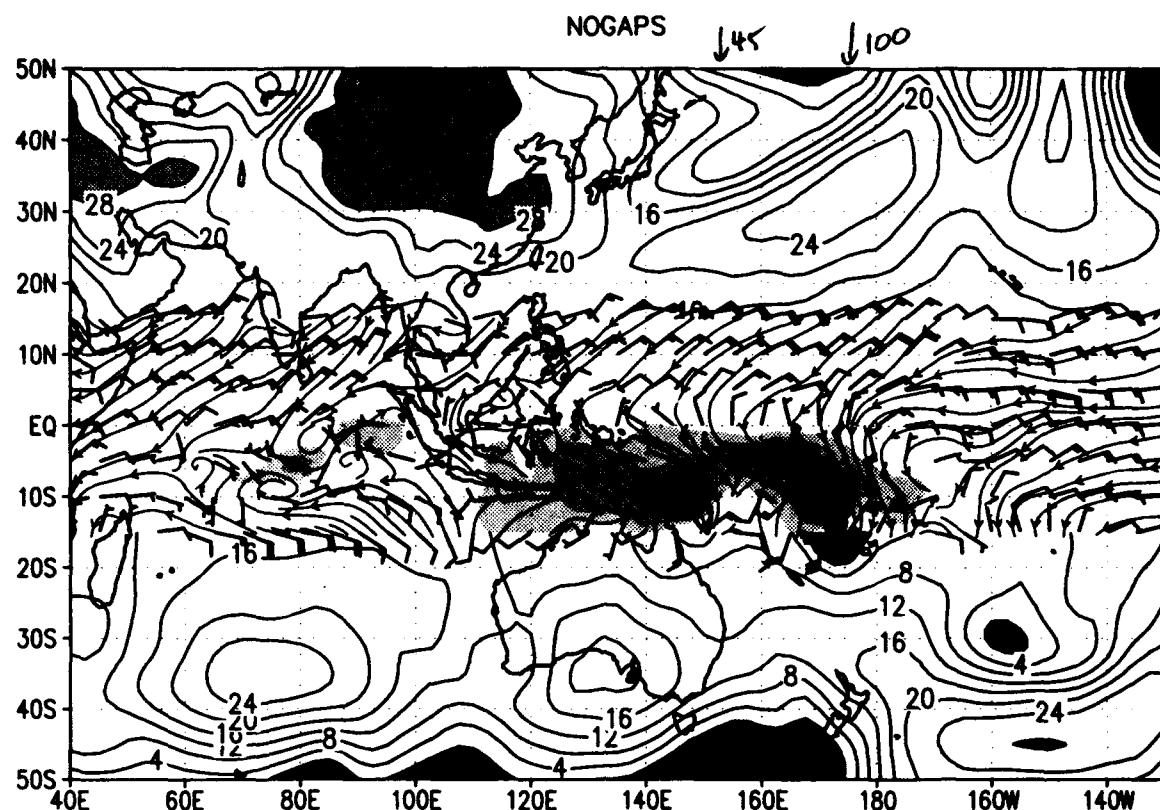
SLP and sfc winds ($u>0$ shaded) for 00Z 27 DEC 1992
slp (mb) wind barbs (kts) /d2/toga_coare/d2.gs



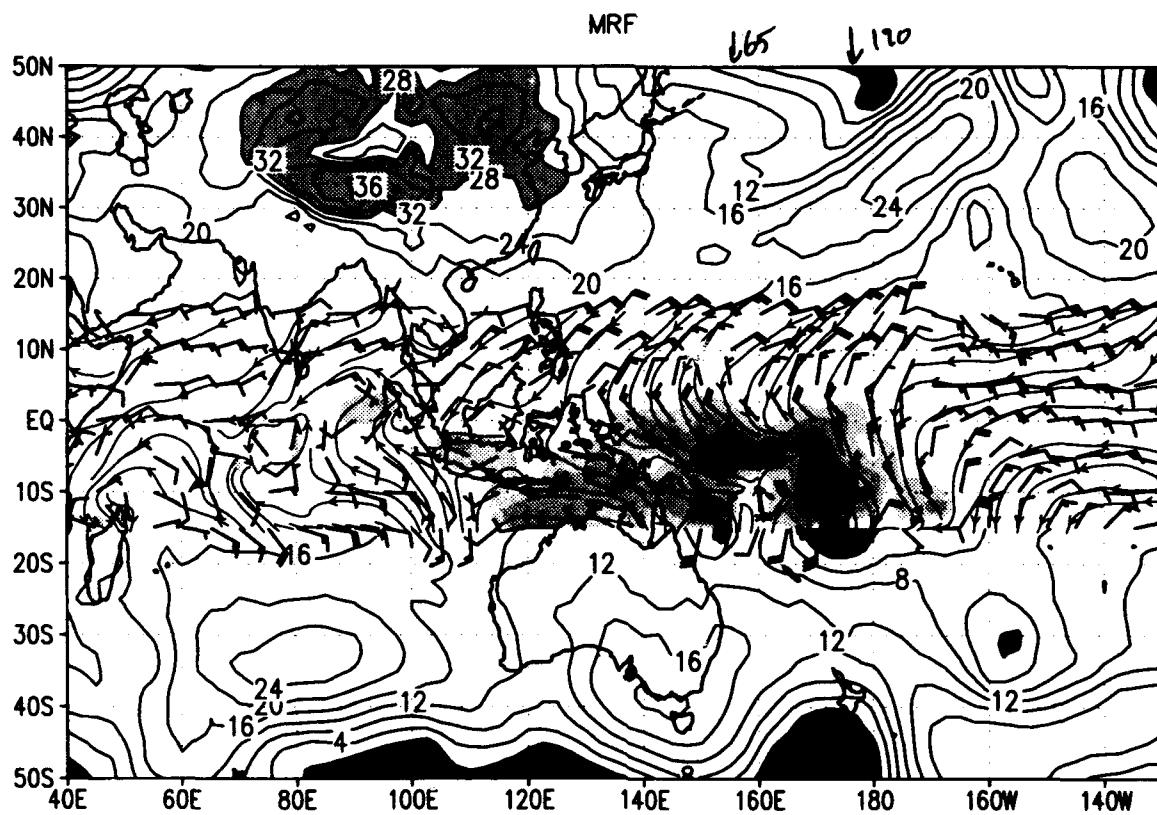
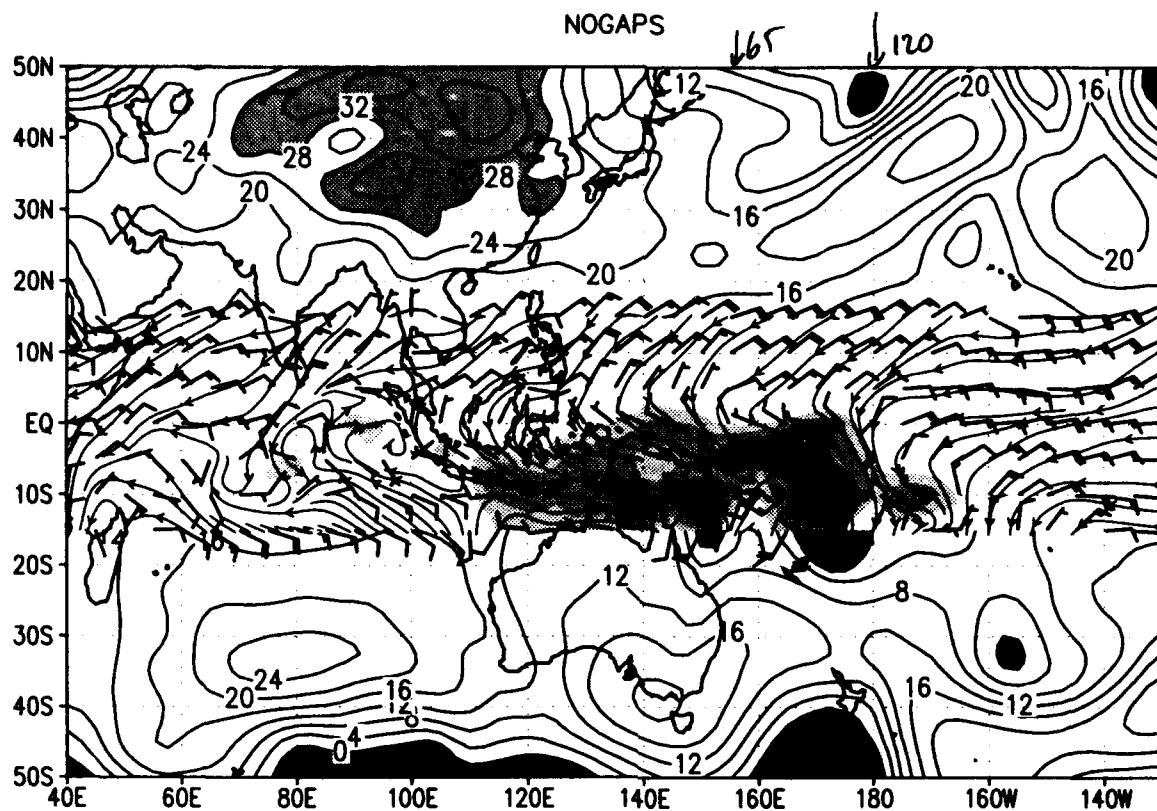
SLP and sfc winds ($u>0$ shaded) for 00Z 28 DEC 1992
 slp (mb) wind barbs (kts) /d2/toga_coare/d2.gs



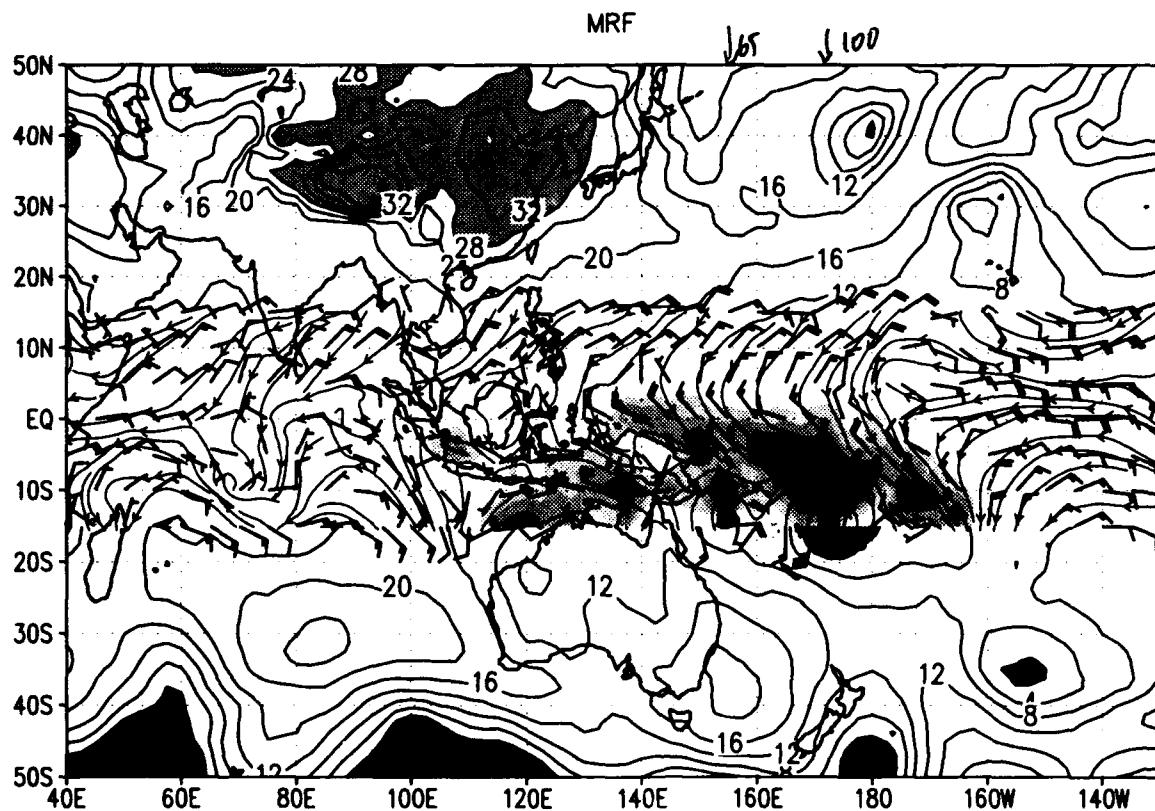
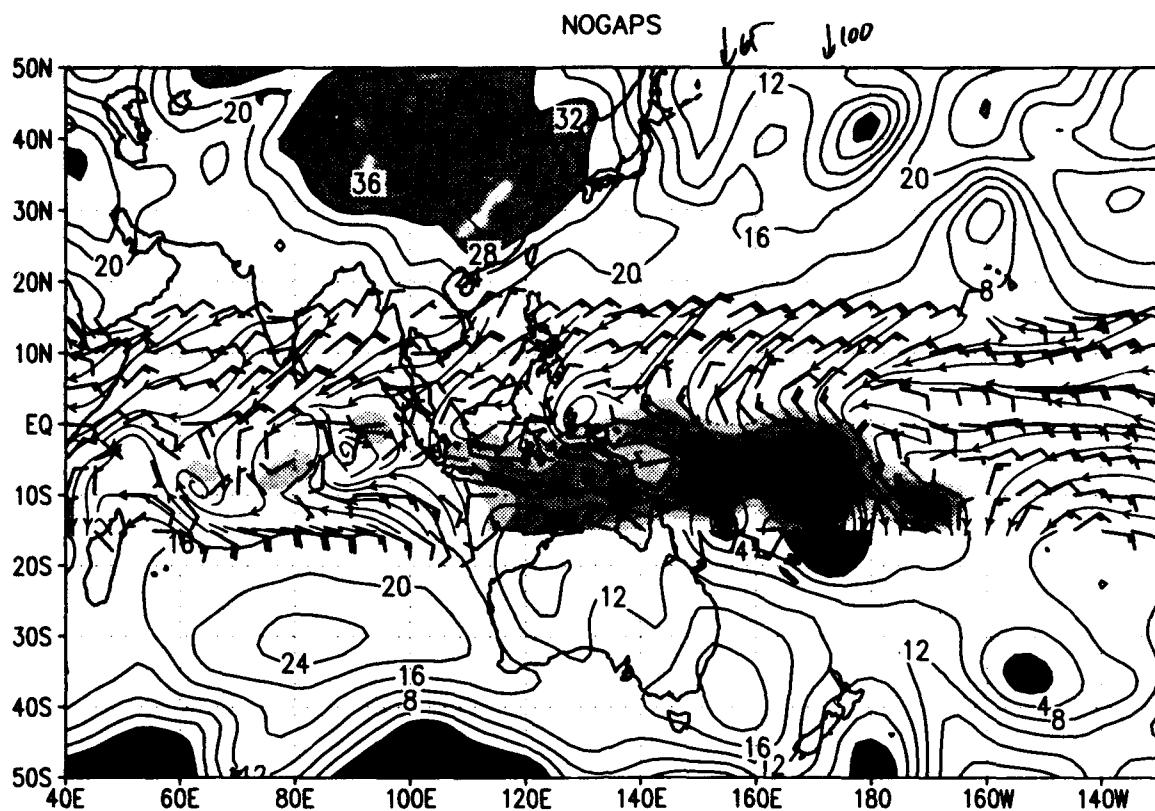
SLP and sfc winds ($u > 0$ shaded) for 00Z 29 DEC 1992
slp (mb) wind barbs (kts) /d2/toga_coare/d2.gs



SLP and sfc winds ($u>0$ shaded) for 00Z 30 DEC 1992
slp (mb) wind barbs (kts) /d2/toga_coare/d2.gs



SLP and sfc winds ($u>0$ shaded) for 00Z 31 DEC 1992
slp (mb) wind barbs (kts) /d2/toga_coare/d2.gs



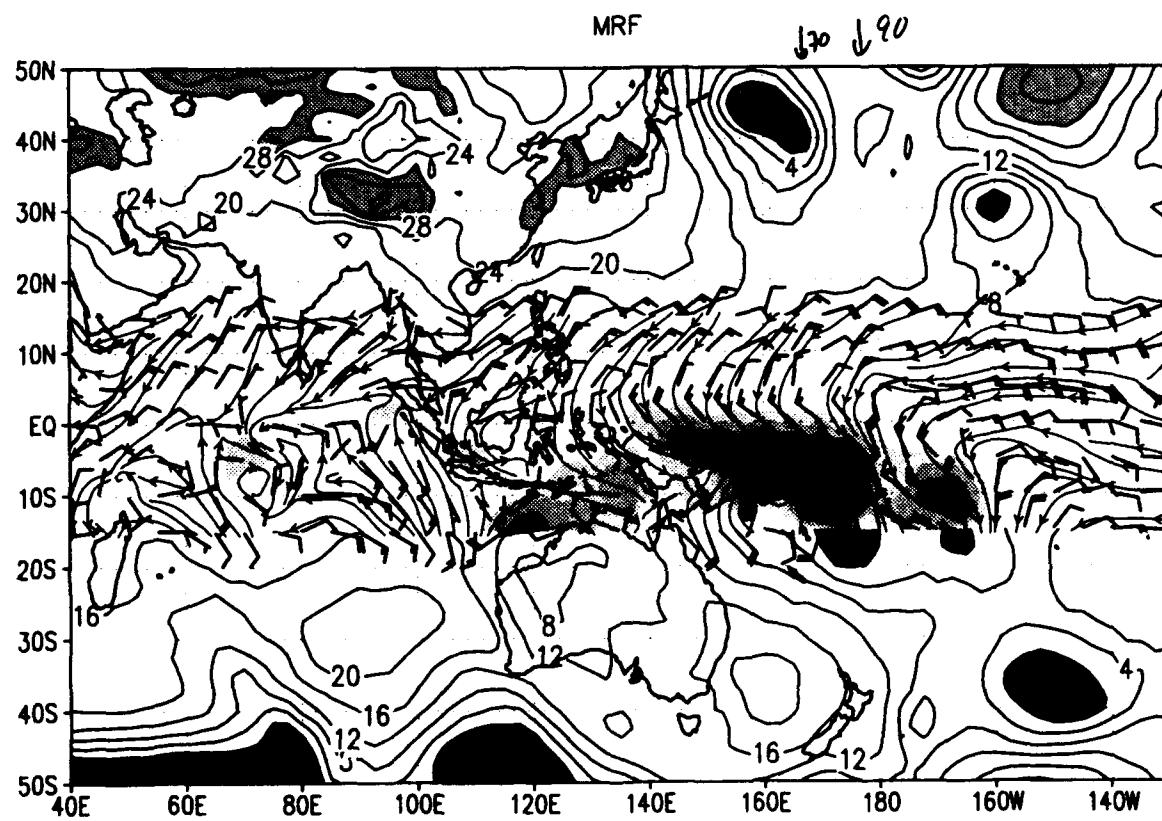
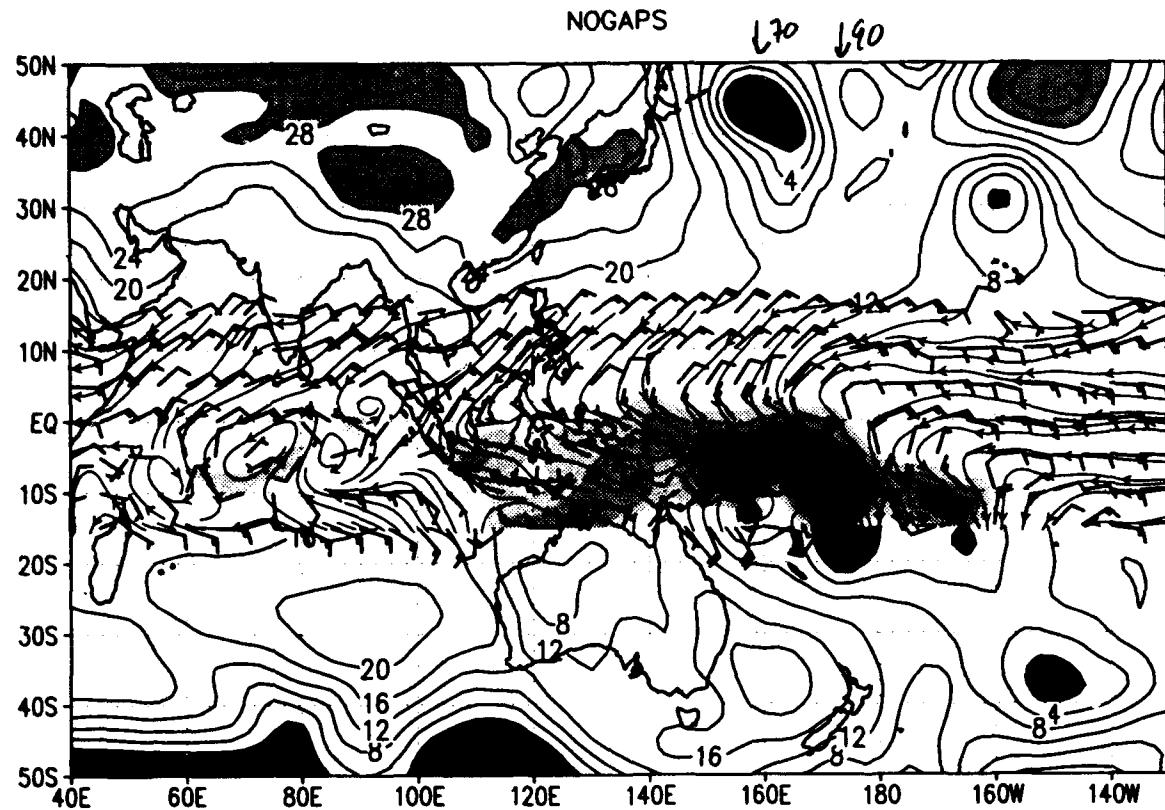
13 00 UTC Synoptic Charts for 1 - 31 January 1993

In the deep tropics (15S-15N) we show surface wind barbs (kts) and streamlines with positive u component shaded in the intervals 5-10 kts (light), 10-20 kts (medium) and over 20 kts (dark). Outside the deep tropics we show sea-level pressure with a contour interval of 2 mb and areas < 1004 mb and > 1028 shaded.

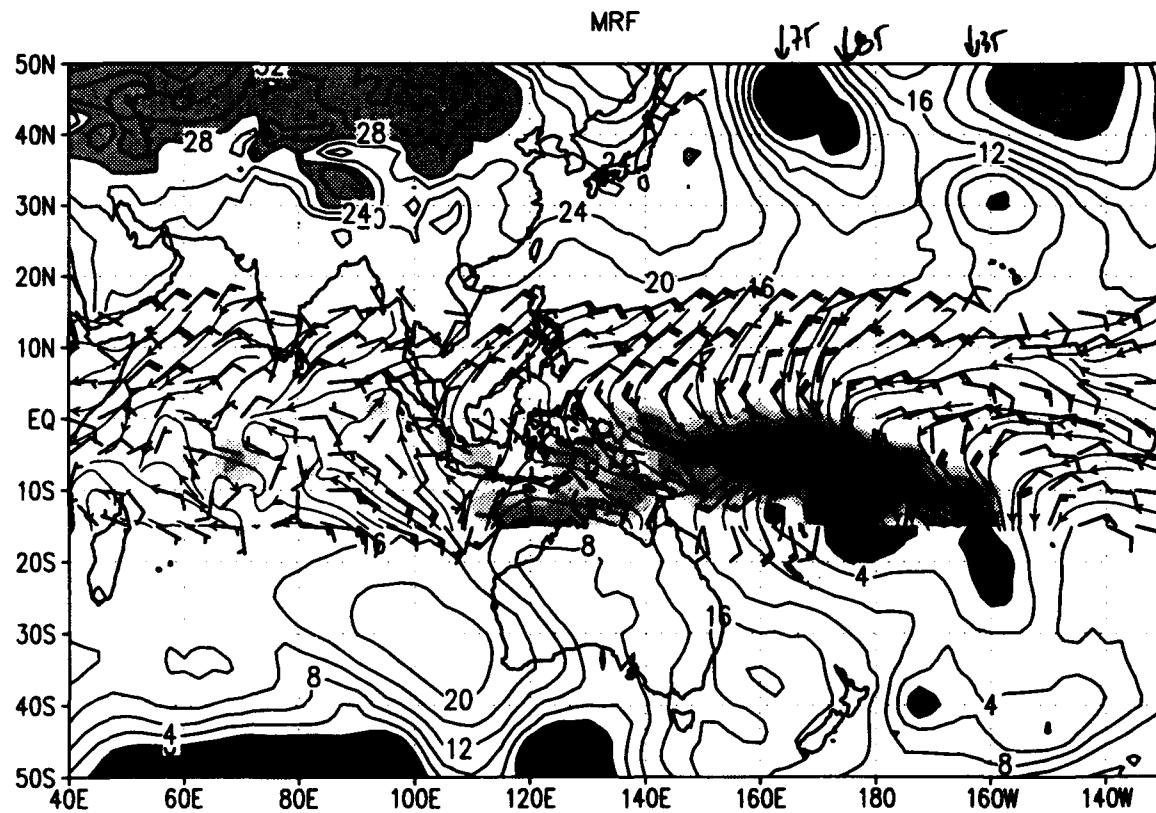
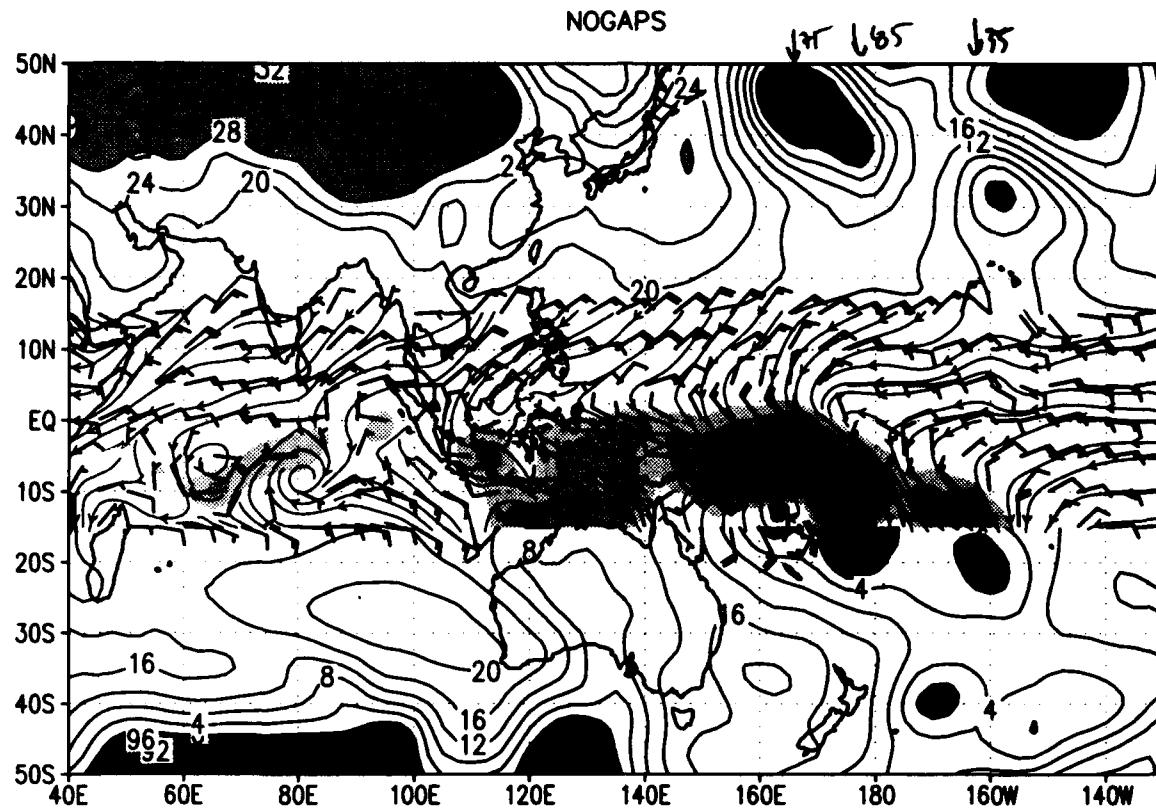
The large differences in SLP between NOGAPS and MRF over mountainous terrain is an artifact of the method of estimating sea-level pressure from 1000 mb geopotential heights and temperature for the MRF. The correspondence was very good outside these regions. However, there were notably differences between the MRF and NOGAPS analyses with regards to the strength of the westerly winds in the tropics and the strength of tropical cyclones. Tropical cyclone positions at 00 UTC are drawn using a circle for tropical depressions (<35 kts), an open hurricane symbol for tropical storms (< 65 kts) and a closed hurricane symbol for typhoons (> 65 kts). The arrow above the northern border of the map indicates the longitude of the observed TC and the max wind speed in kts is given to the right of the arrow.

Chart	Description
1-31 -	Synoptic charts for NOGAPS and MRF

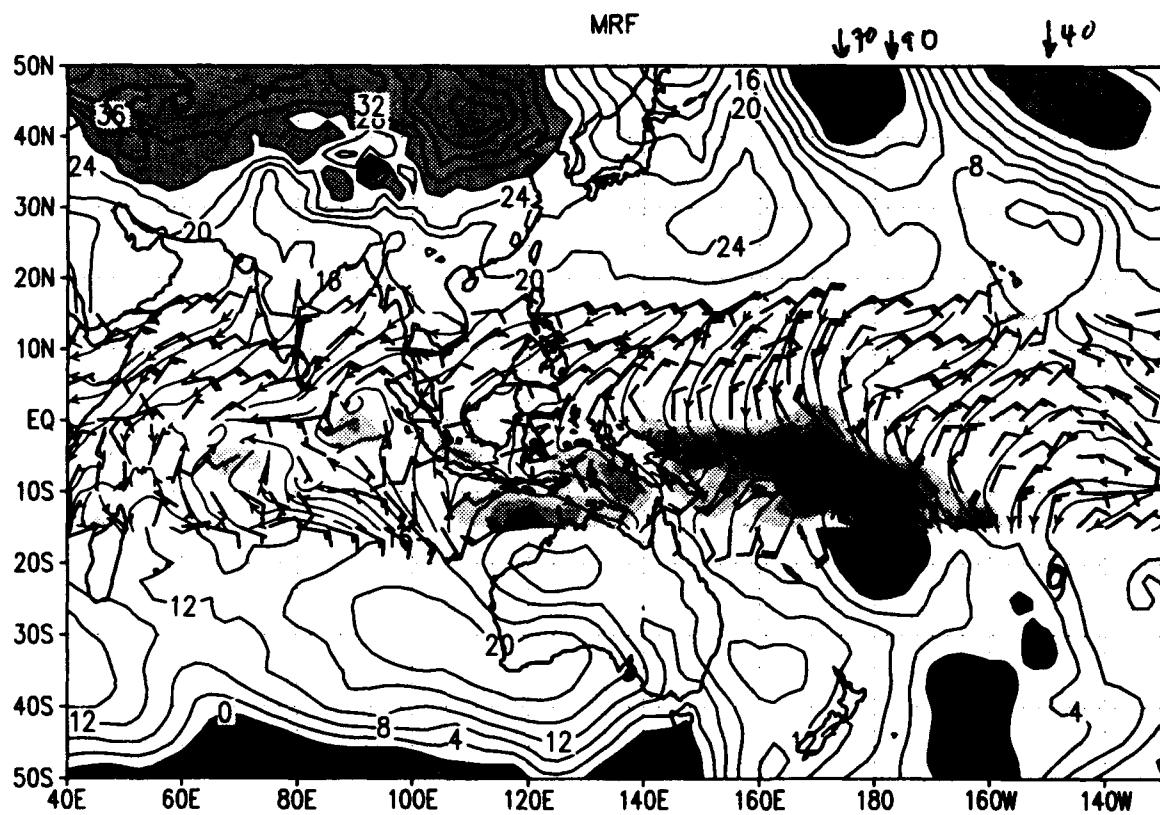
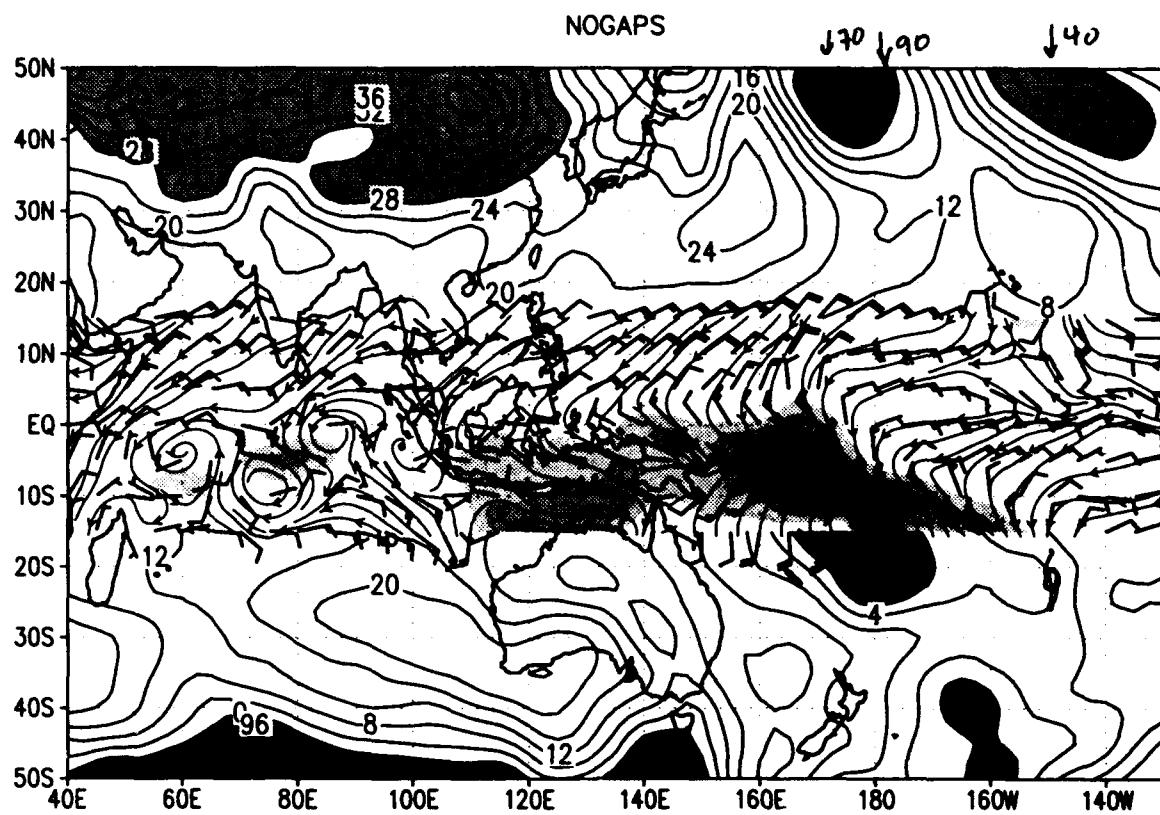
SLP and sfc winds ($u>0$ shaded) for 00Z 01 JAN 1993
slp (mb) wind barbs (kts) /d2/toga_coare/d2.gs



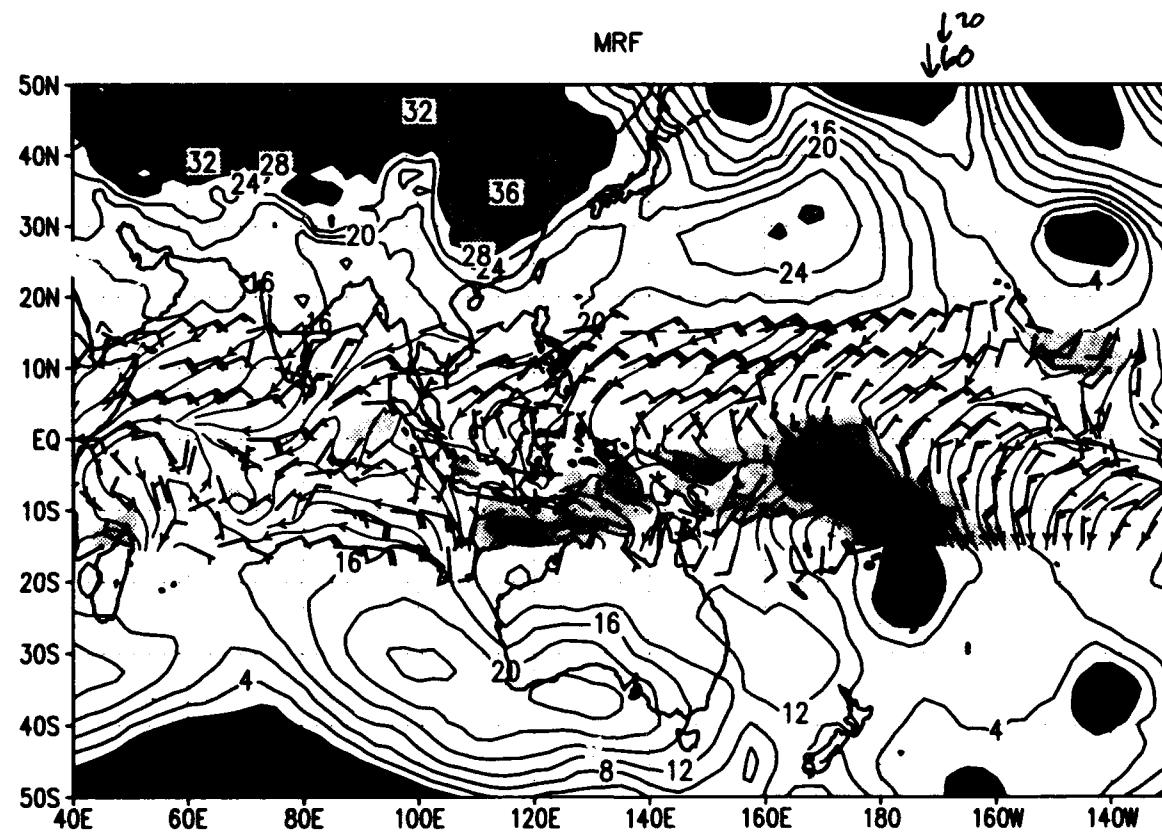
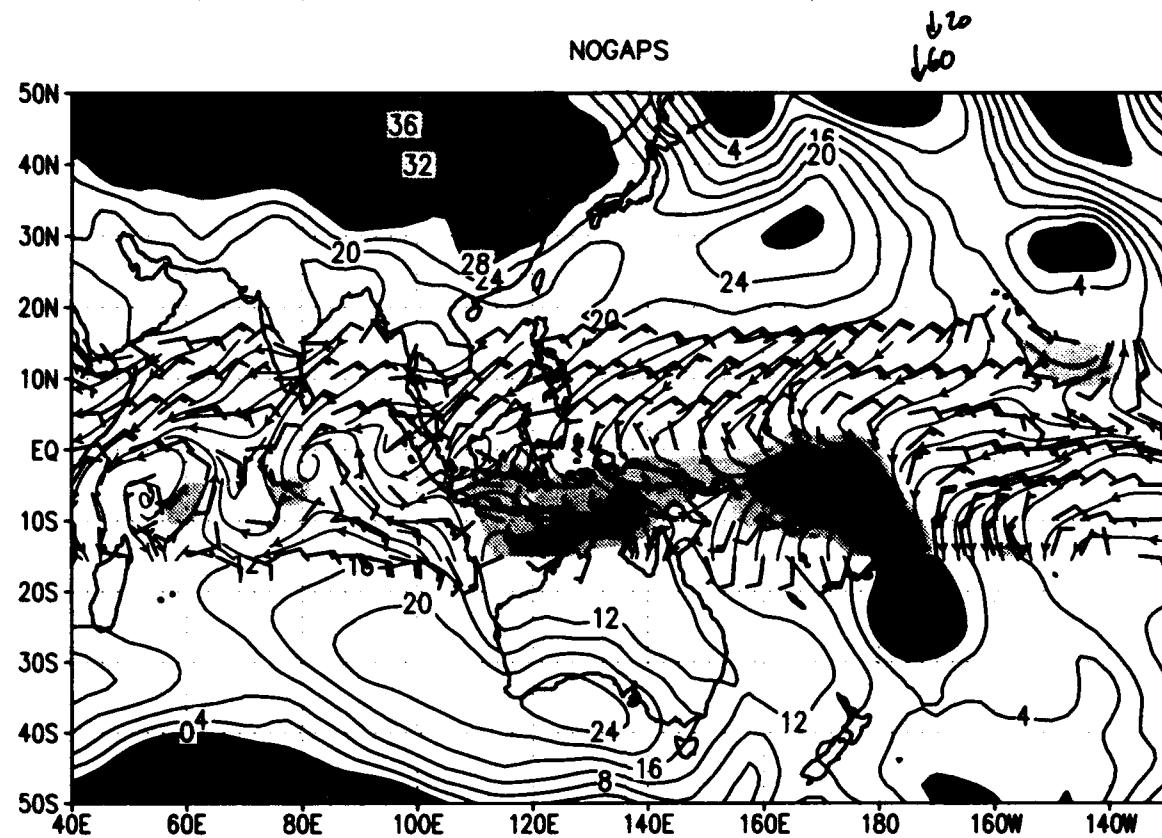
SLP and sfc winds ($u>0$ shaded) for 00Z 02 JAN 1993
slp (mb) wind barbs (kts) /d2/toga_coare/d2.gs



SLP and sfc winds ($u>0$ shaded) for 00Z 03 JAN 1993
slp (mb) wind barbs (kts) /d2/toga_coare/d2.gs

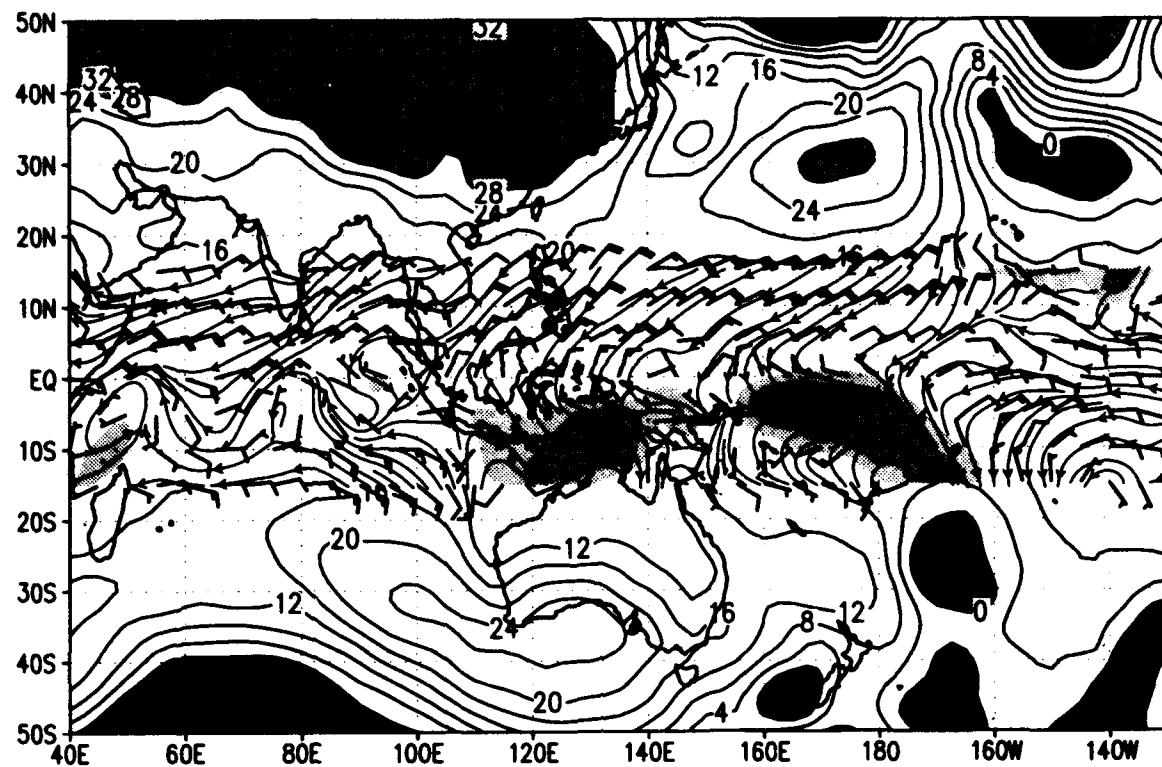


SLP and sfc winds ($u>0$ shaded) for 00Z 04 JAN 1993
 slp (mb) wind barbs (kts) /d2/toga_coare/d2.gs

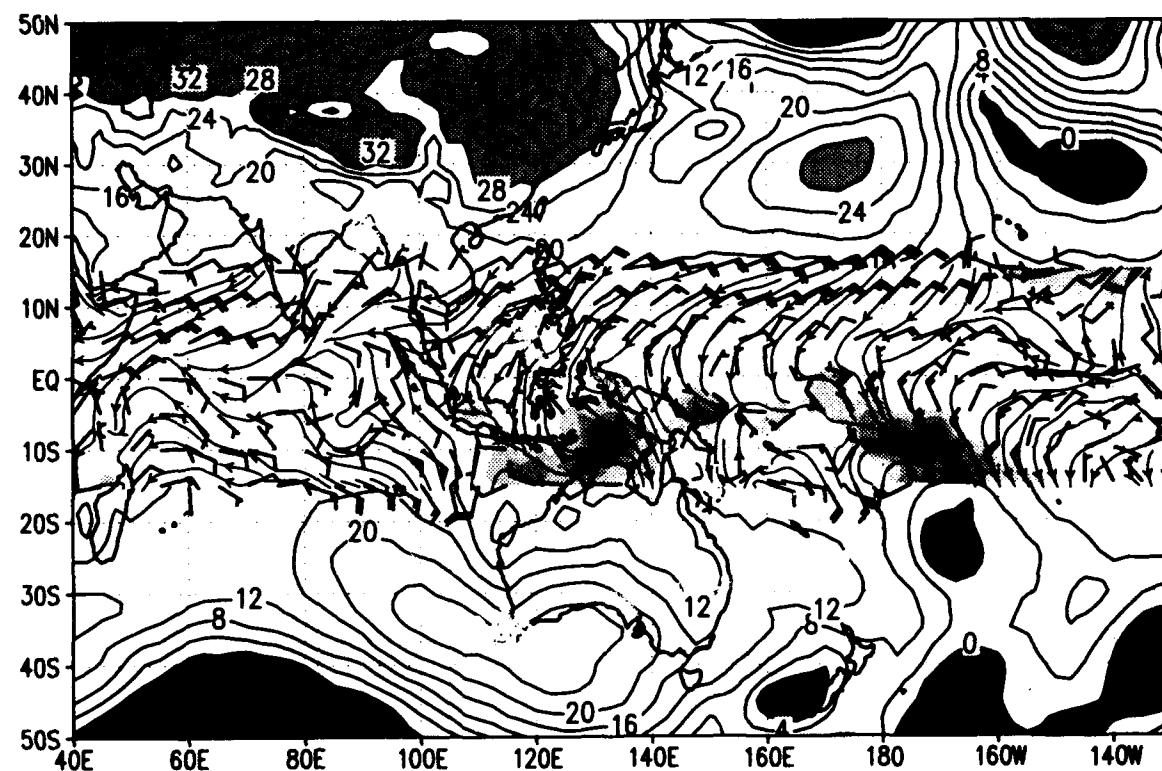


SLP and sfc winds ($u > 0$ shaded) for 00Z 05 JAN 1993
slp (mb) wind barbs (kts) /d2/toga_coare/d2.gs

NOGAPS

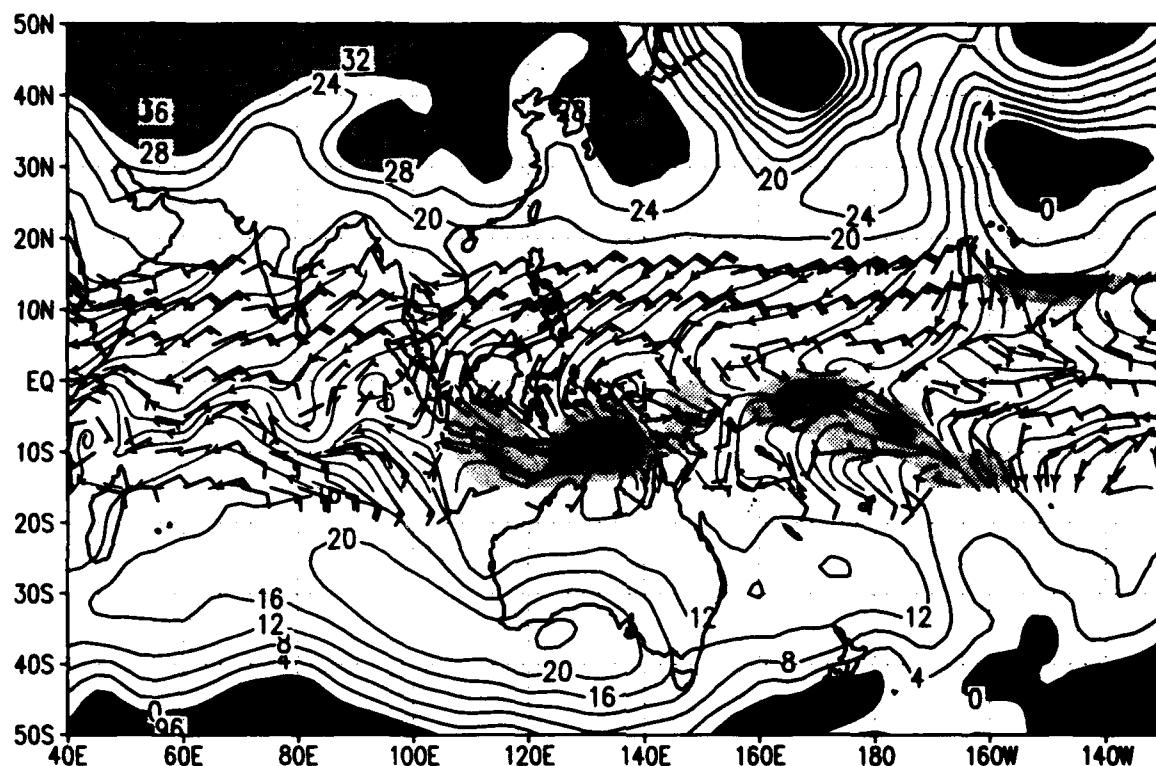


MRF

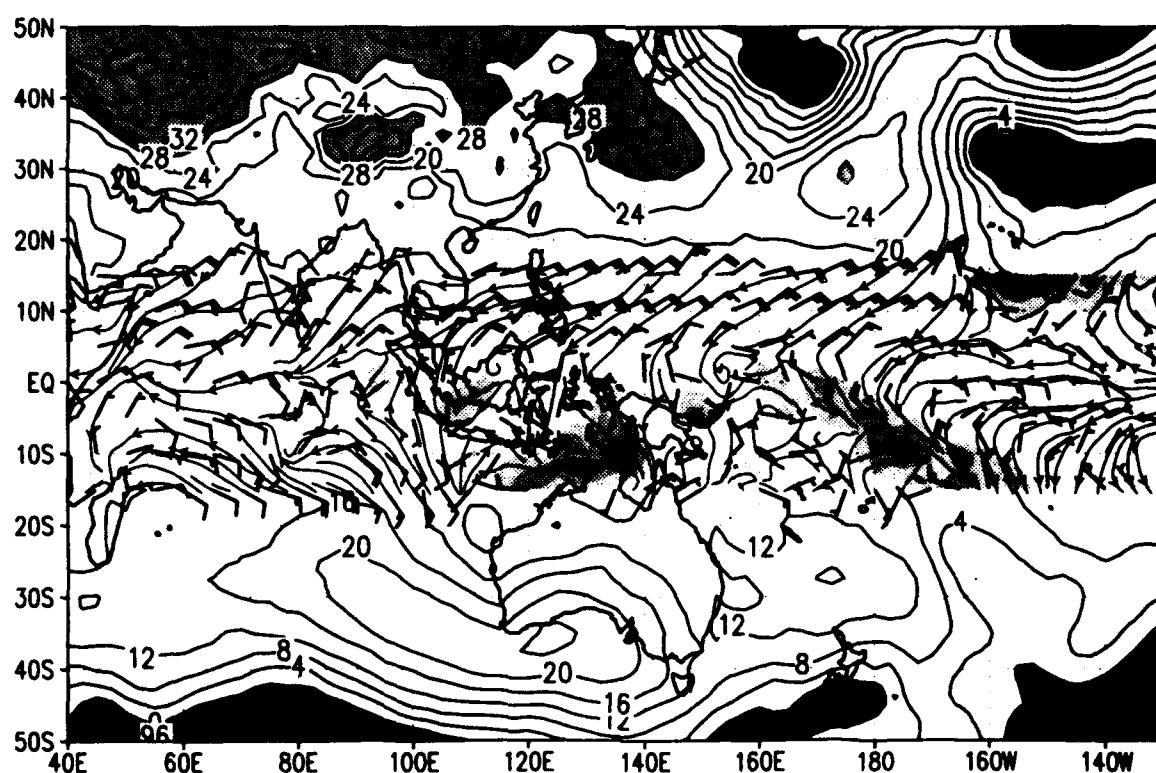


SLP and sfc winds ($u>0$ shaded) for 00Z 06 JAN 1993
slp (mb) wind barbs (kts) /d2/toga_coare/d2.gs

NOGAPS

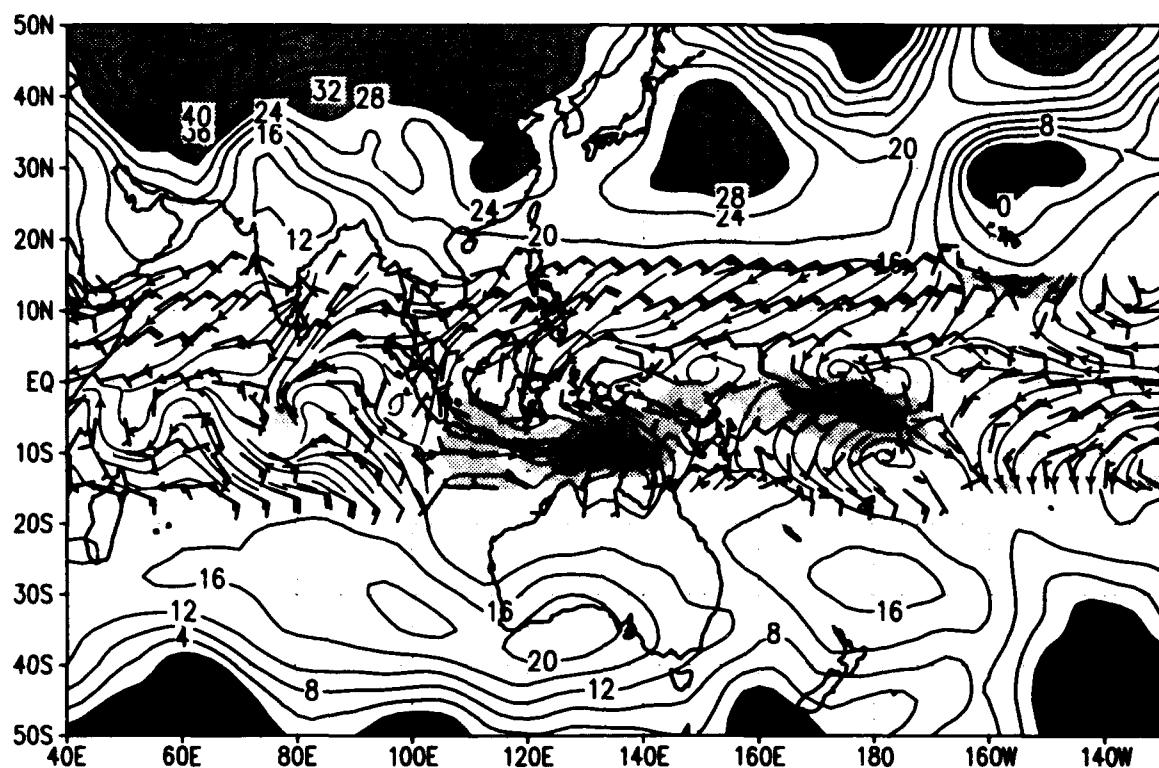


MRF

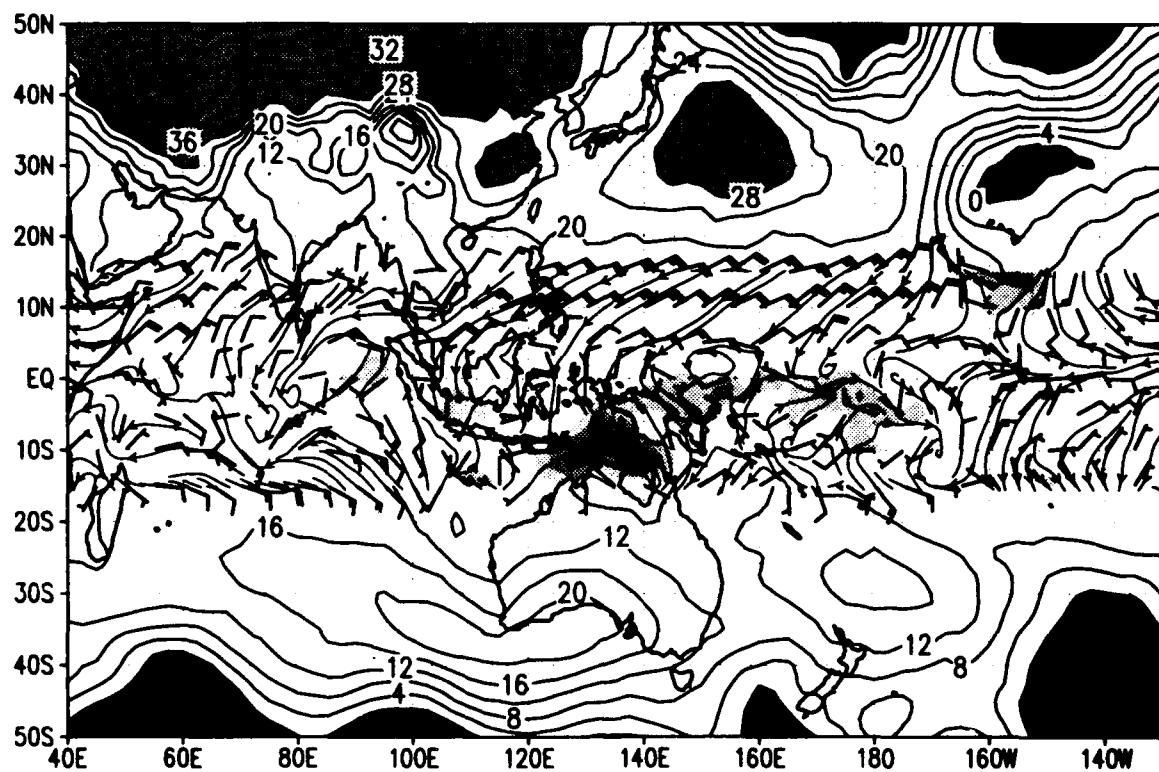


SLP and sfc winds ($u > 0$ shaded) for 00Z 07 JAN 1993
slp (mb) wind barbs (kts) /d2/toga_coare/d2.gs

NOGAPS

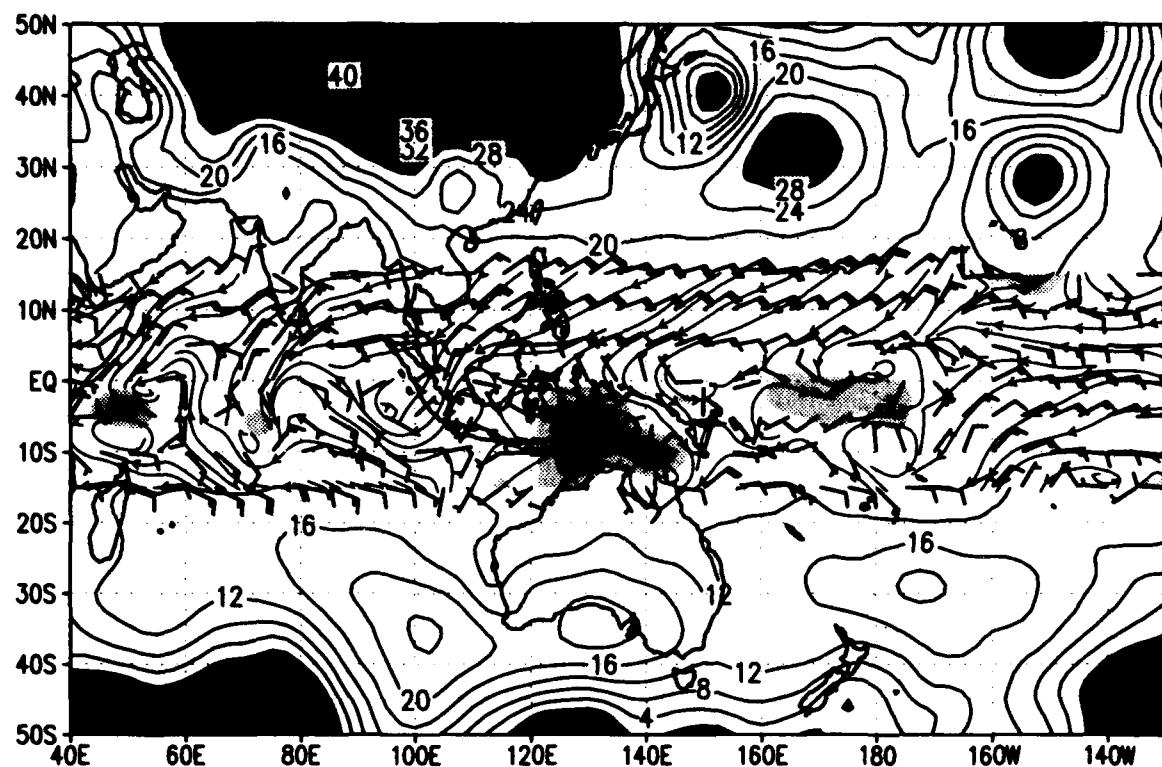


MRF

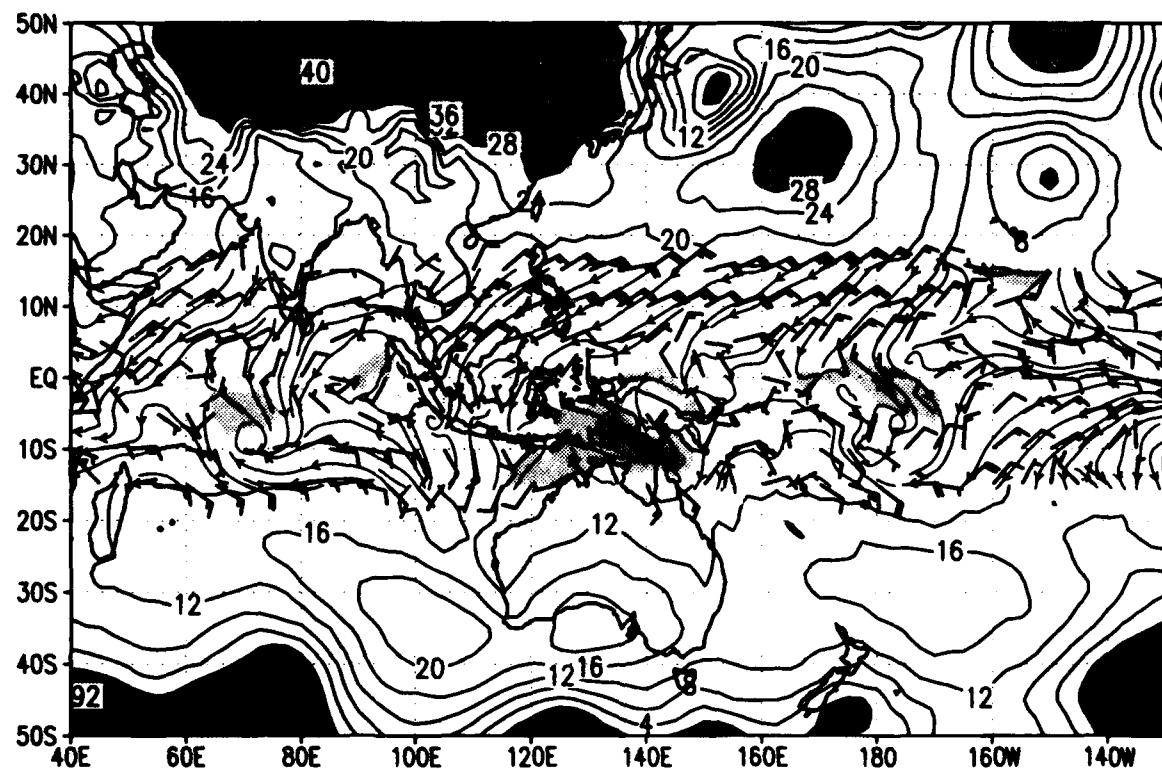


SLP and sfc winds ($u>0$ shaded) for 00Z 08 JAN 1993
slp (mb) wind barbs (kts) /d2/toga_coare/d2.gs

NOGAPS

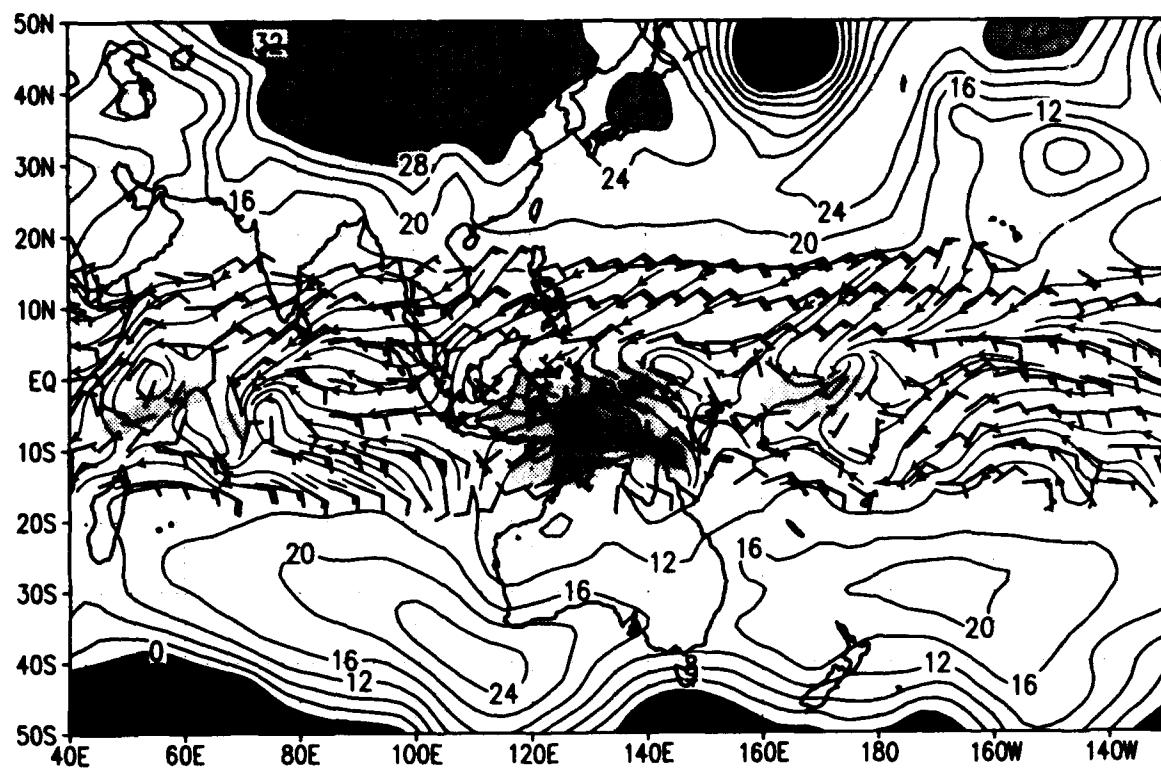


MRF

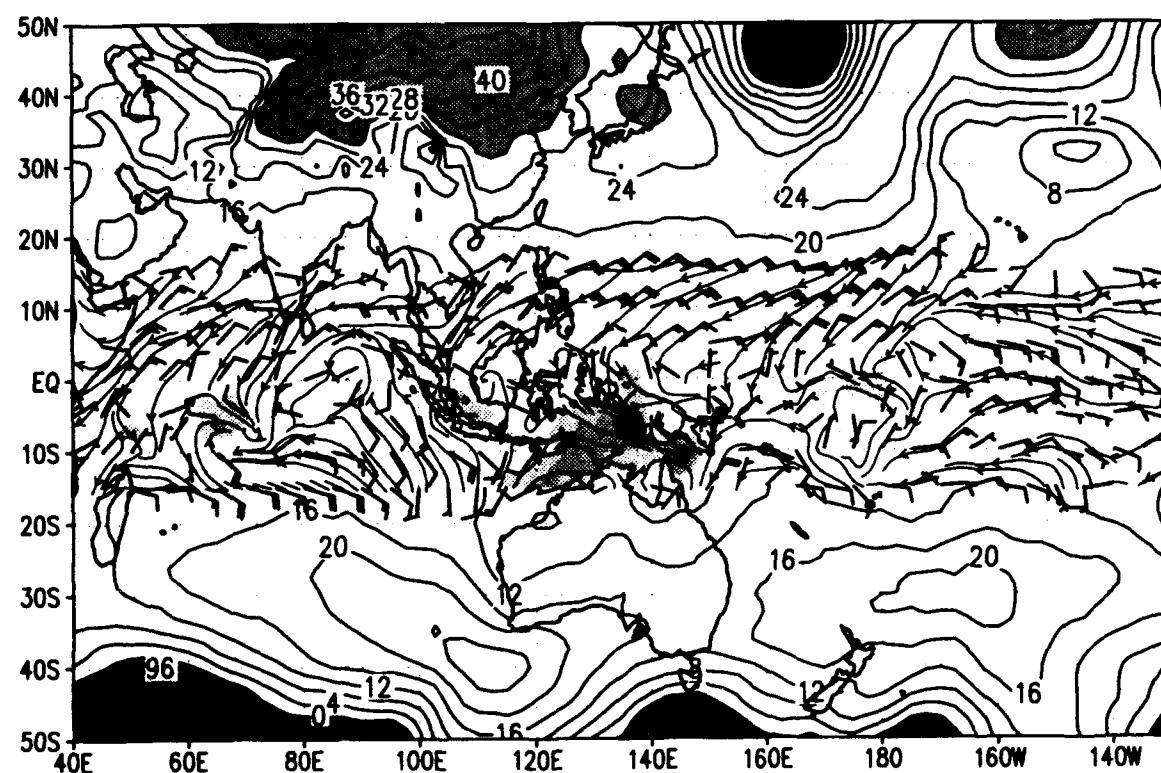


SLP and sfc winds ($u>0$ shaded) for 00Z 09 JAN 1993
slp (mb) wind barbs (kts) /d2/toga_coare/d2.gs

NOGAPS

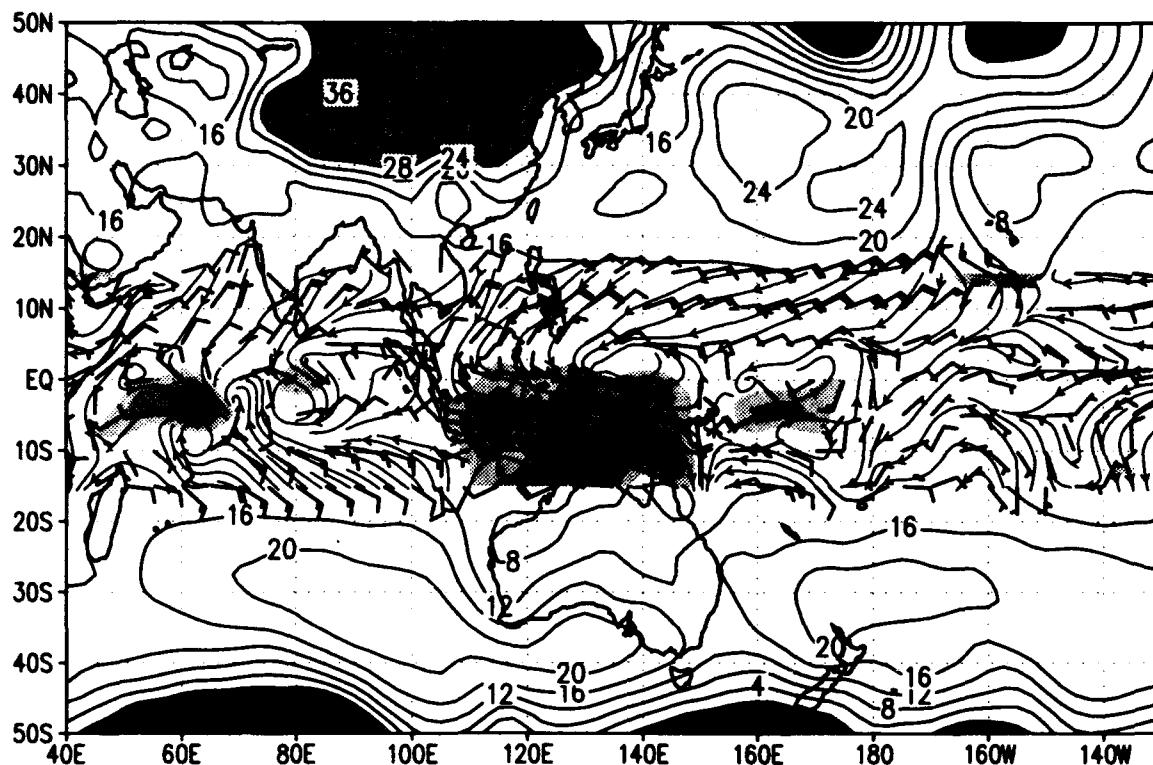


MRF

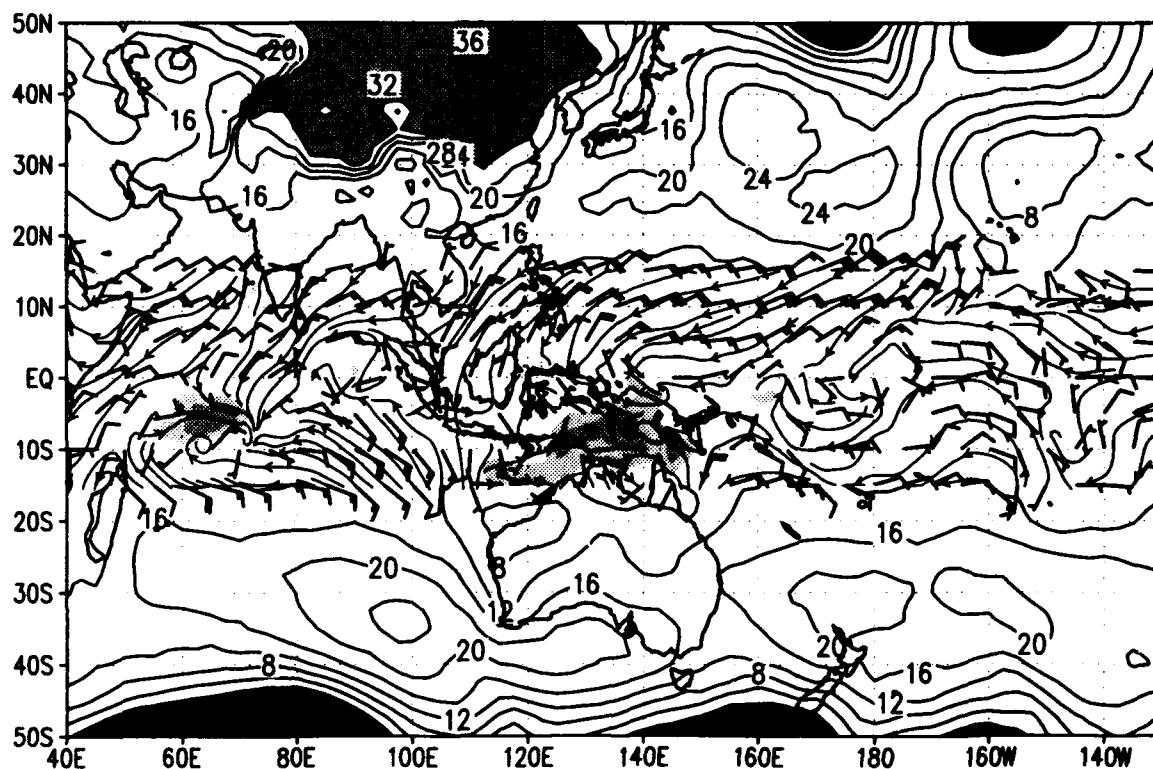


SLP and sfc winds ($u>0$ shaded) for 00Z 10 JAN 1993
slp (mb) wind barbs (kts) /d2/toga_coare/d2.gs

NOGAPS

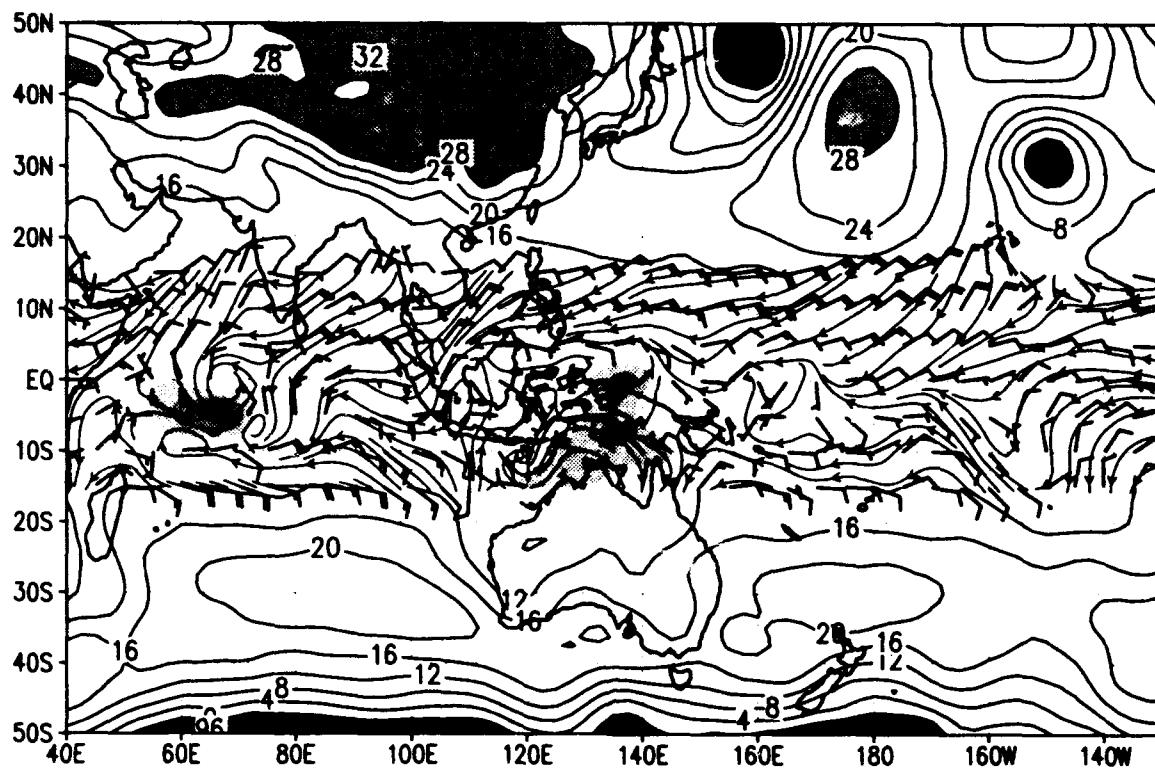


MRF

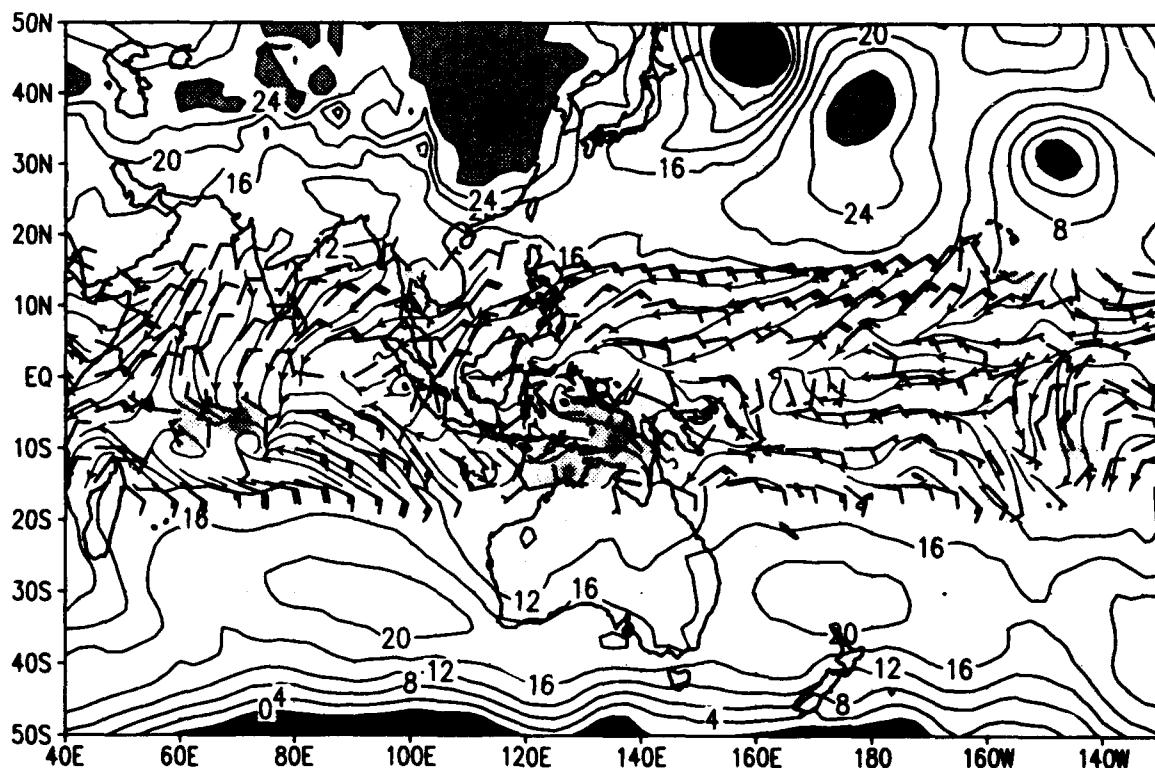


SLP and sfc winds ($u>0$ shaded) for 00Z 11 JAN 1993
slp (mb) wind barbs (kts) /d2/toga_coare/d2.gs

NOGAPS

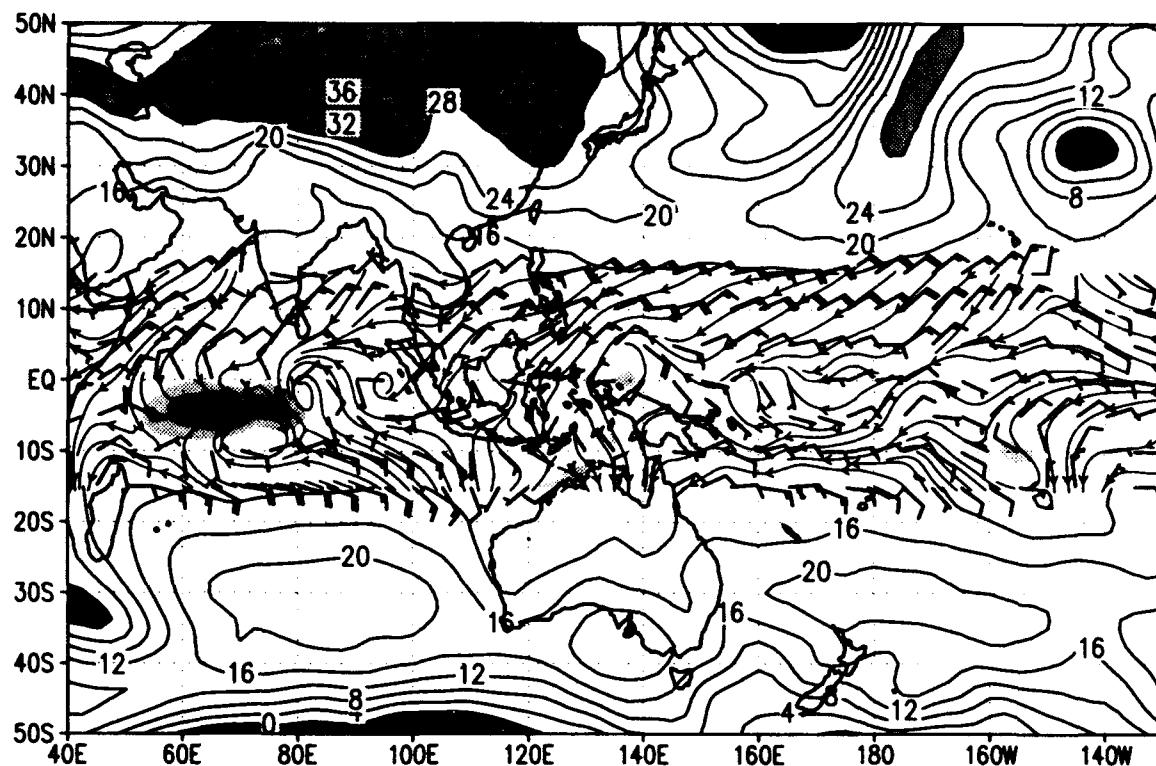


MRF

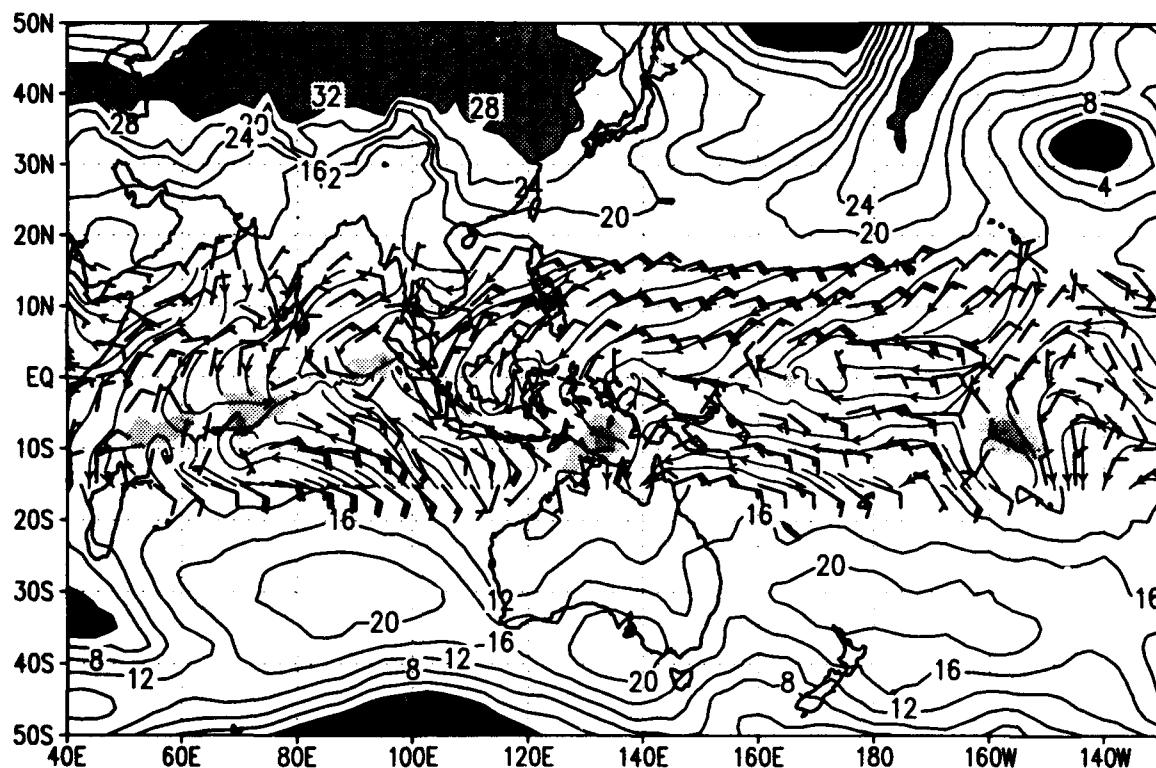


SLP and sfc winds ($u>0$ shaded) for 00Z 12 JAN 1993
slp (mb) wind barbs (kts) /d2/toga_coare/d2.gs

NOGAPS

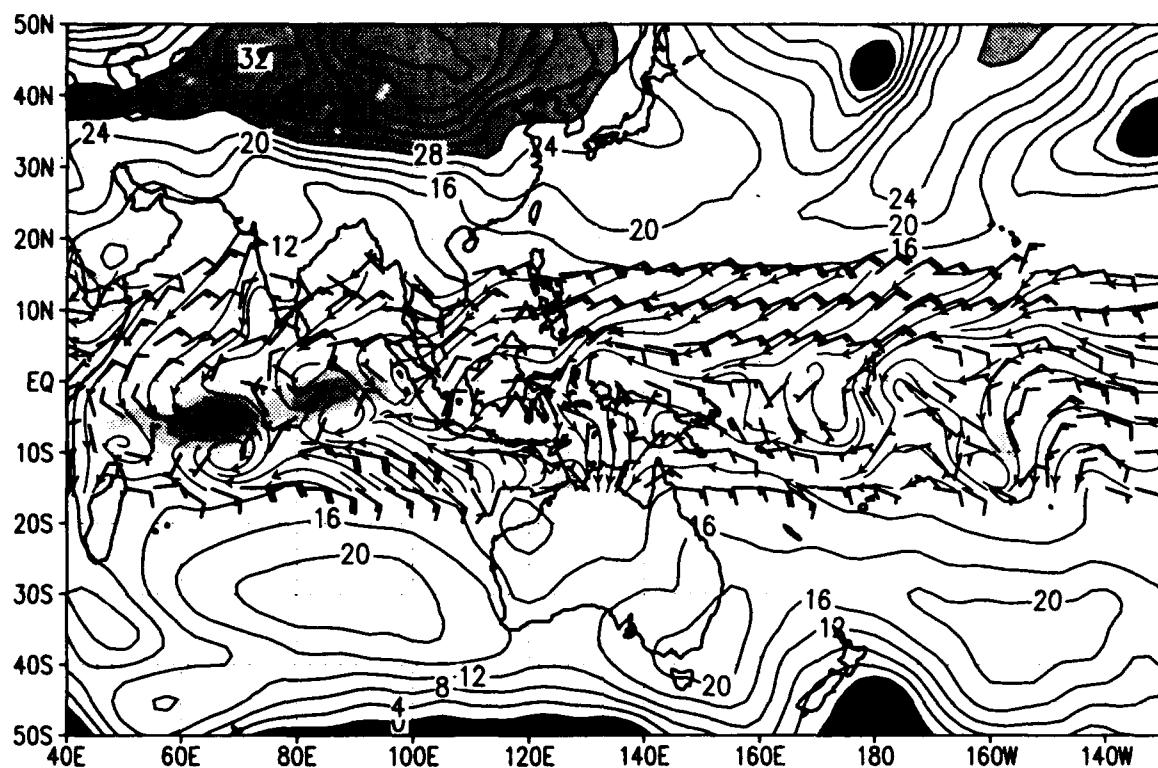


MRF

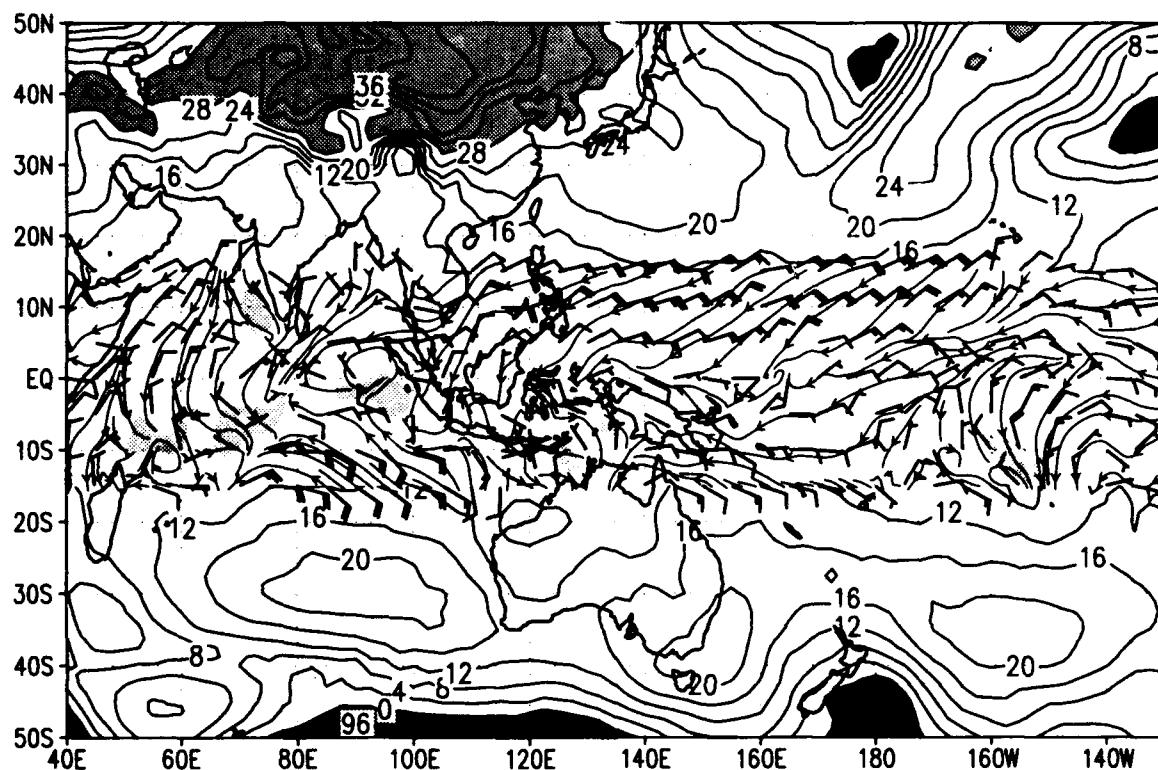


SLP and sfc winds ($u>0$ shaded) for 00Z 13 JAN 1993
slp (mb) wind barbs (kts) /d2/toga_coare/d2.gs

NOGAPS

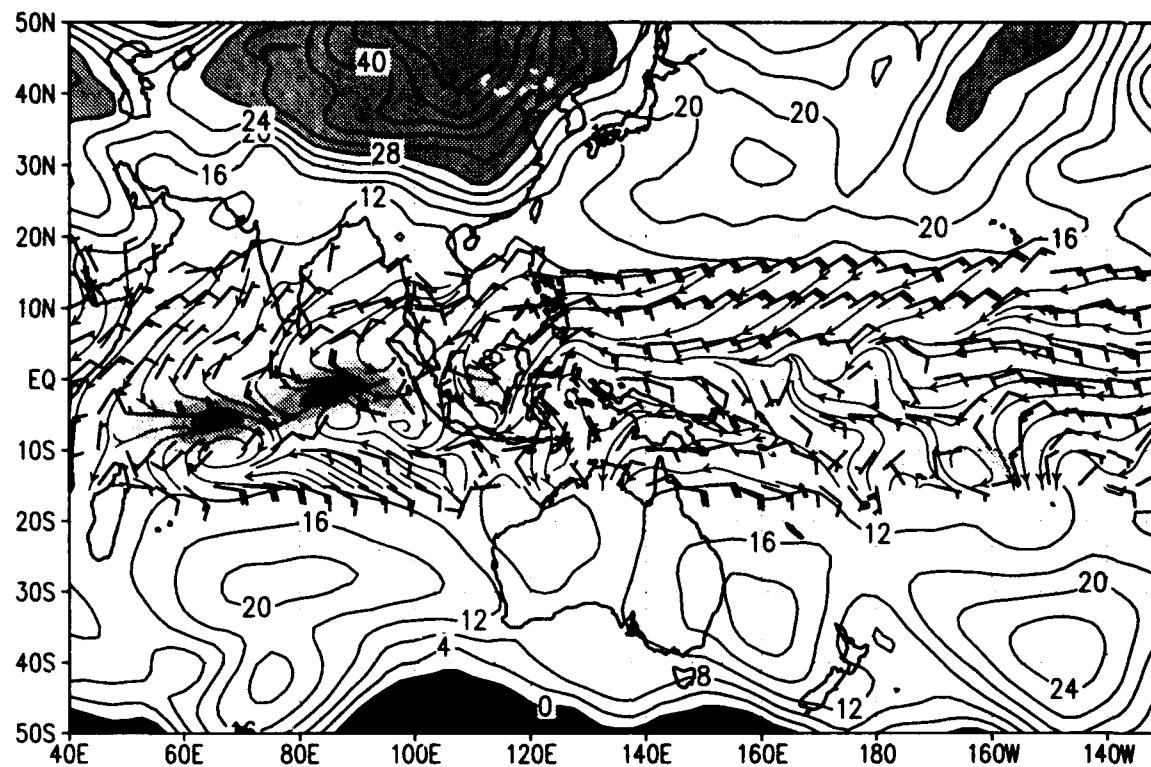


MRF

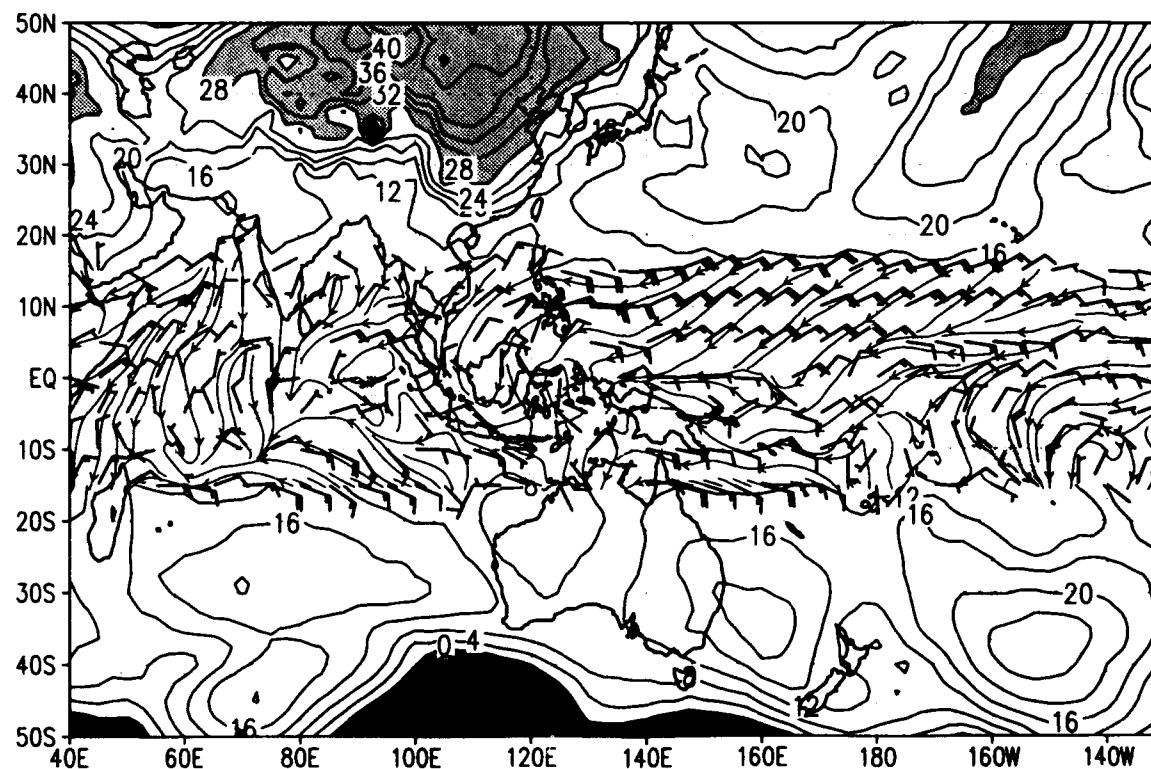


SLP and sfc winds ($u>0$ shaded) for 00Z 14 JAN 1993
slp (mb) wind barbs (kts) /d2/toga_coare/d2.gs

NOGAPS

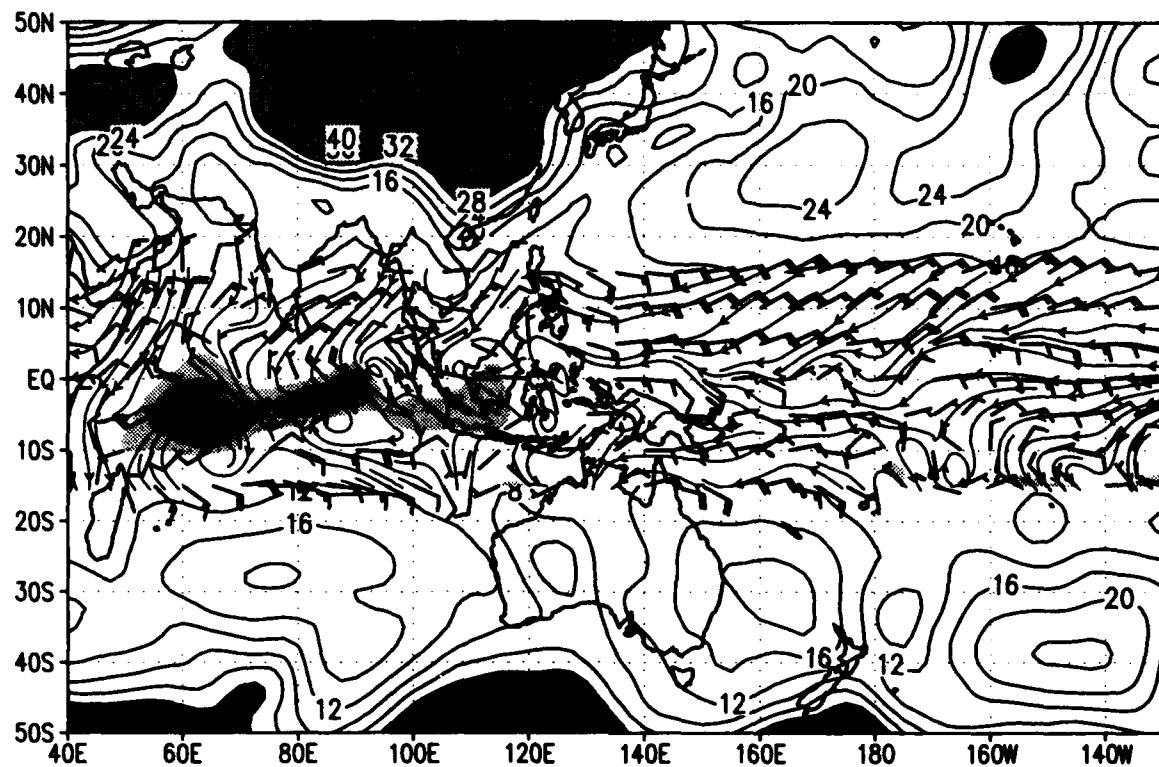


MRF

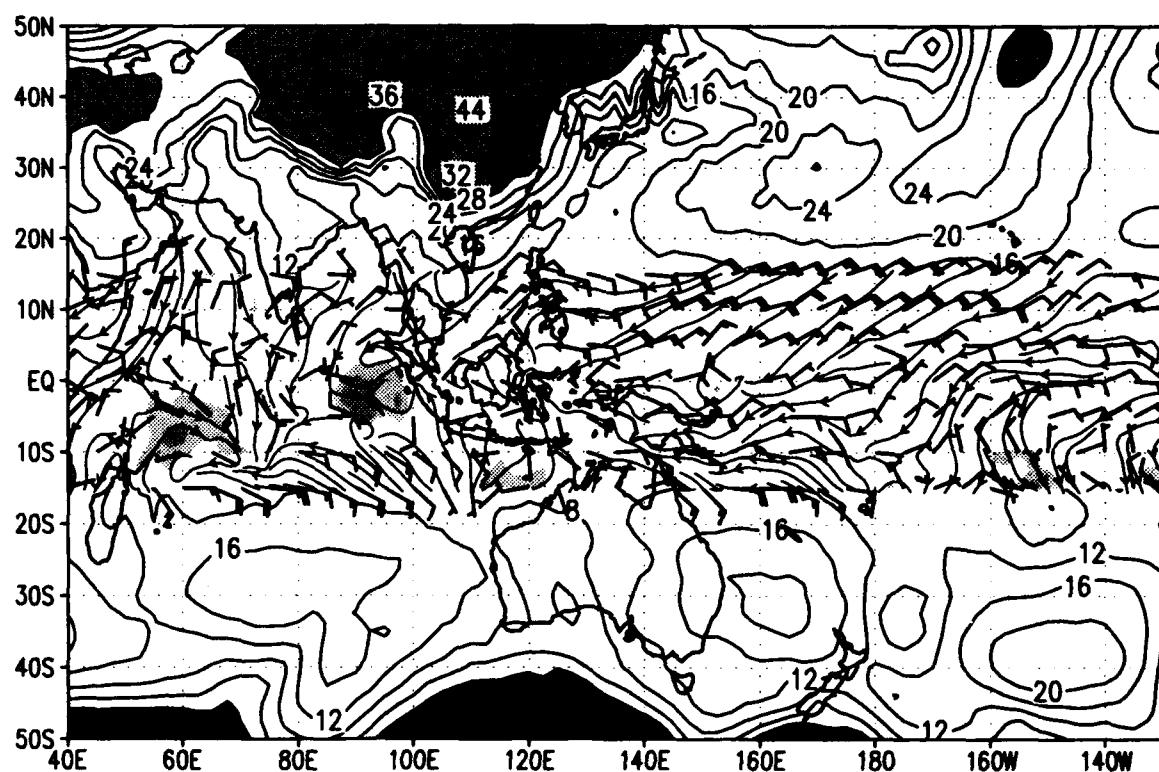


SLP and sfc winds ($u>0$ shaded) for 00Z 15 JAN 1993
slp (mb) wind barbs (kts) /d2/toga_coare/d2.gs

NOGAPS

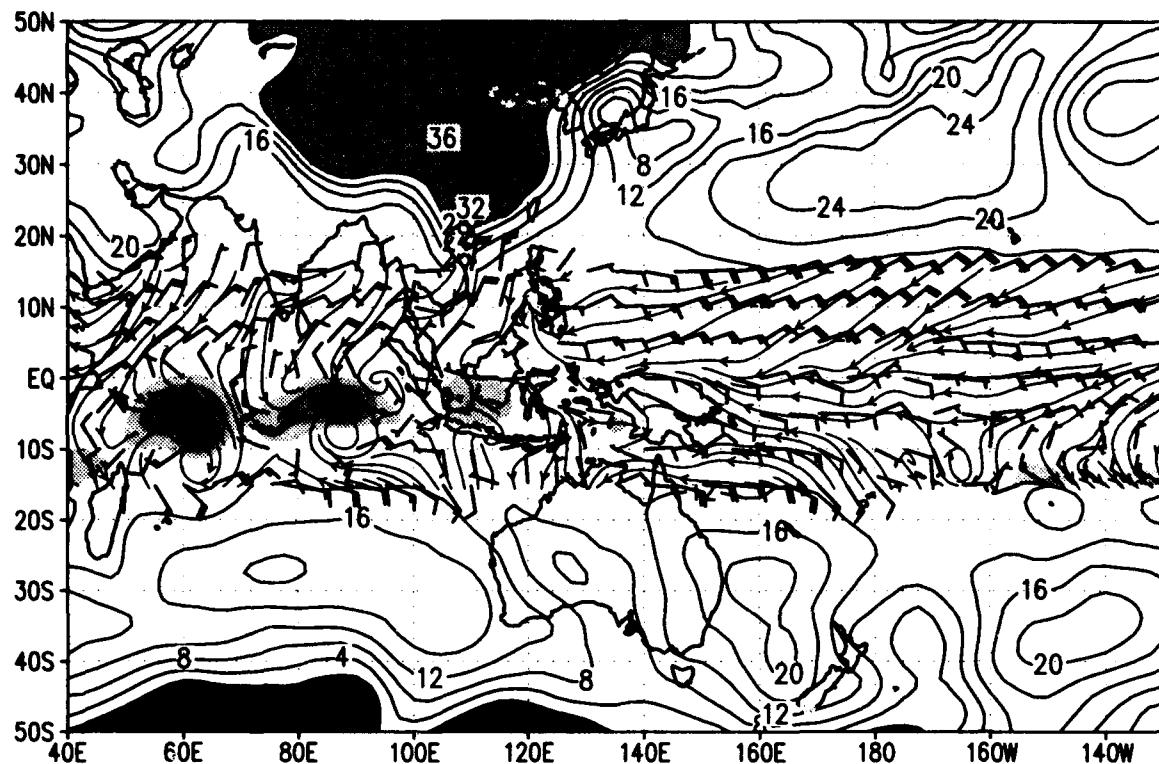


MRF

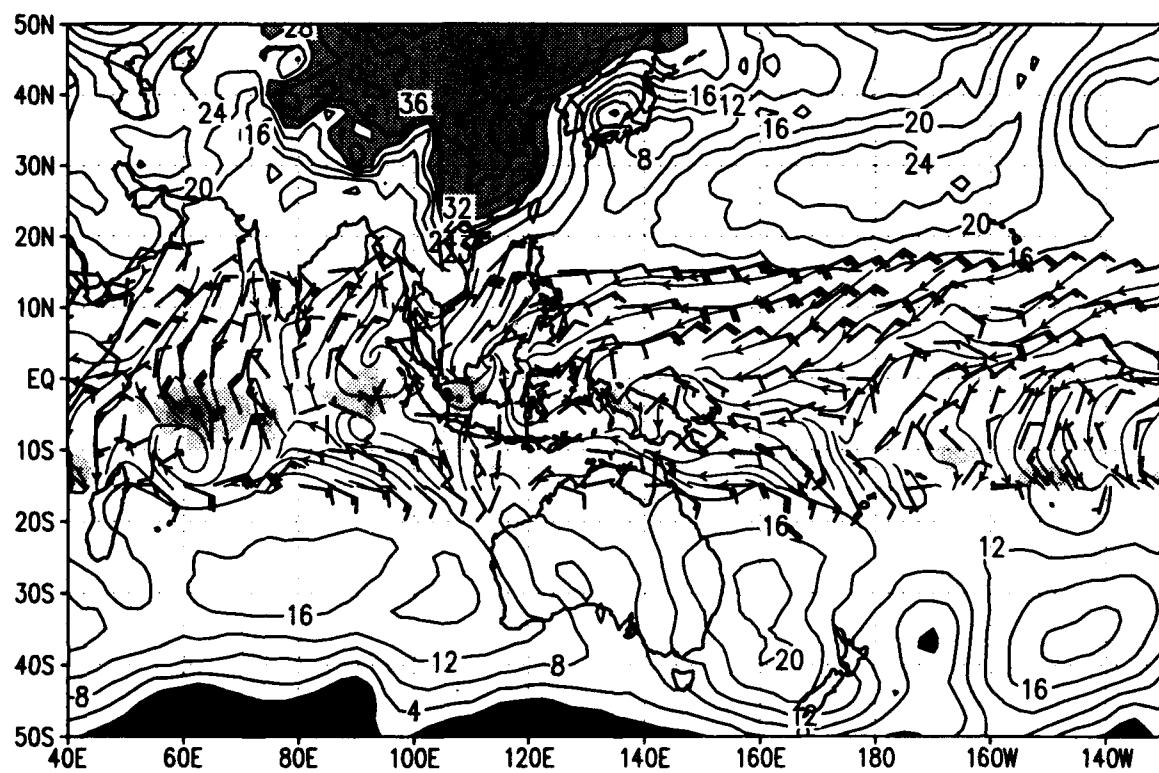


SLP and sfc winds ($u>0$ shaded) for 00Z 16 JAN 1993
slp (mb) wind barbs (kts) /d2/toga_coare/d2.gs

NOGAPS

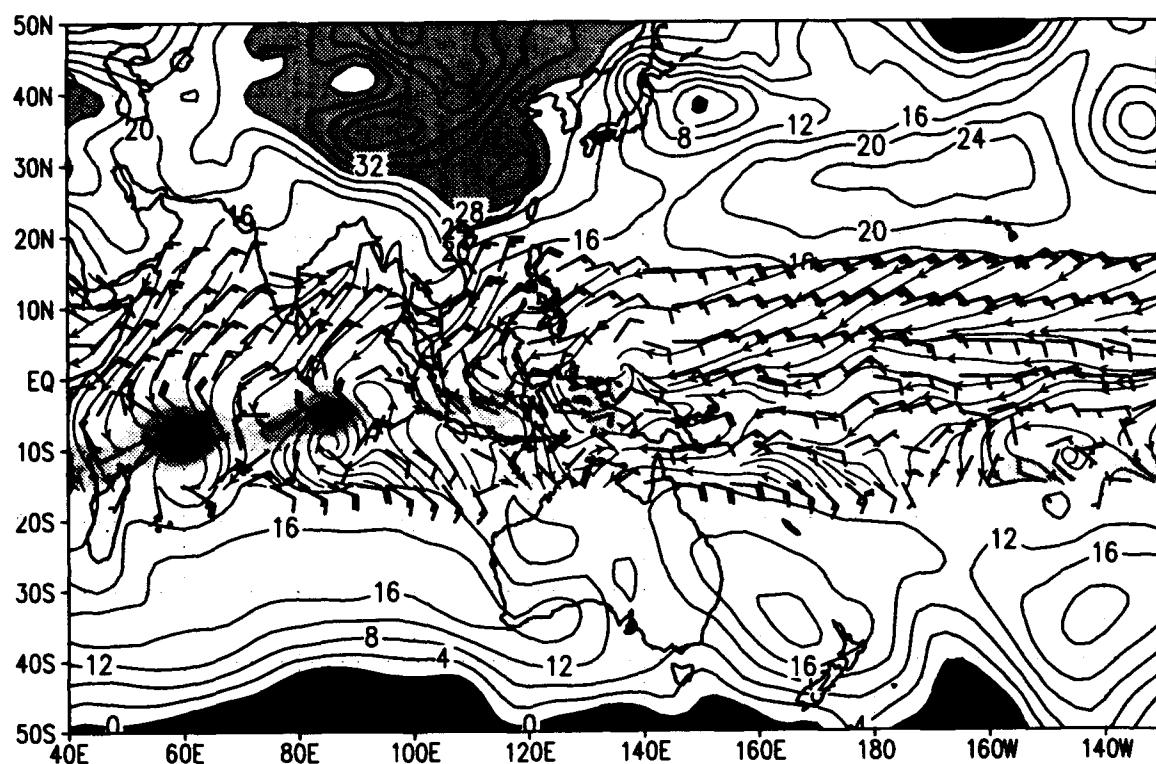


MRF

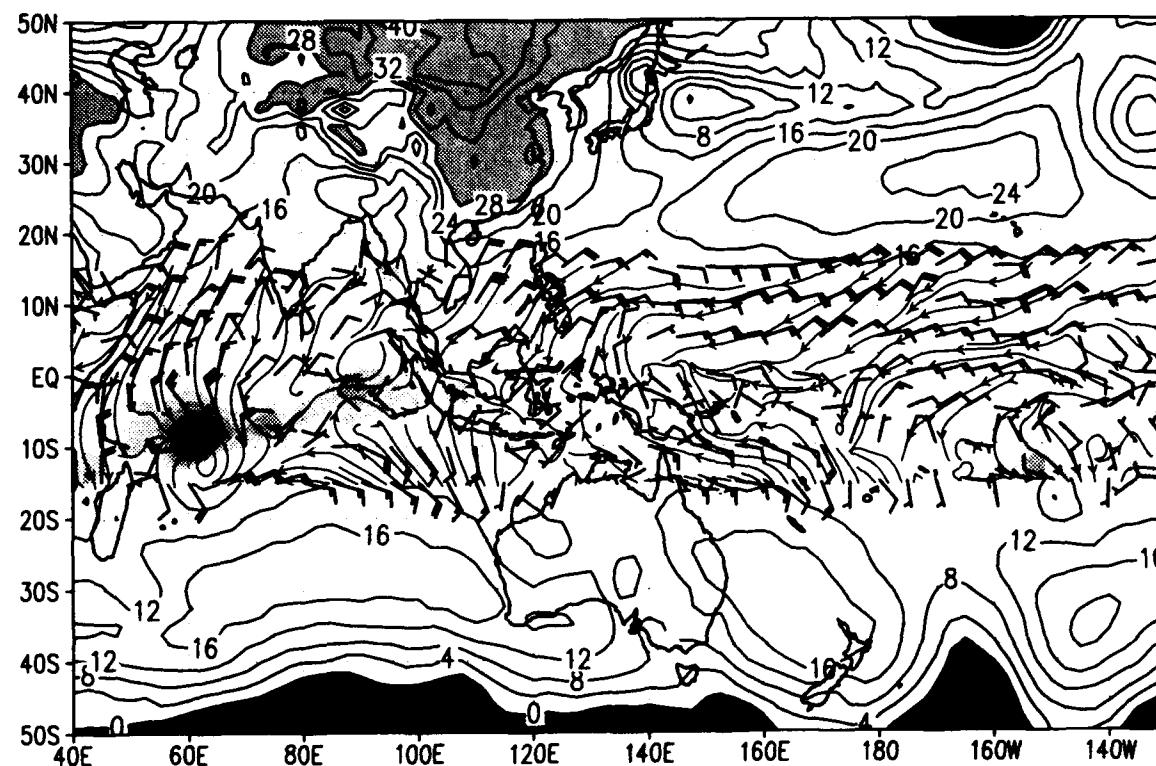


SLP and sfc winds ($u>0$ shaded) for 00Z 17 JAN 1993
slp (mb) wind barbs (kts) /d2/toga_coare/d2.gs

NOGAPS

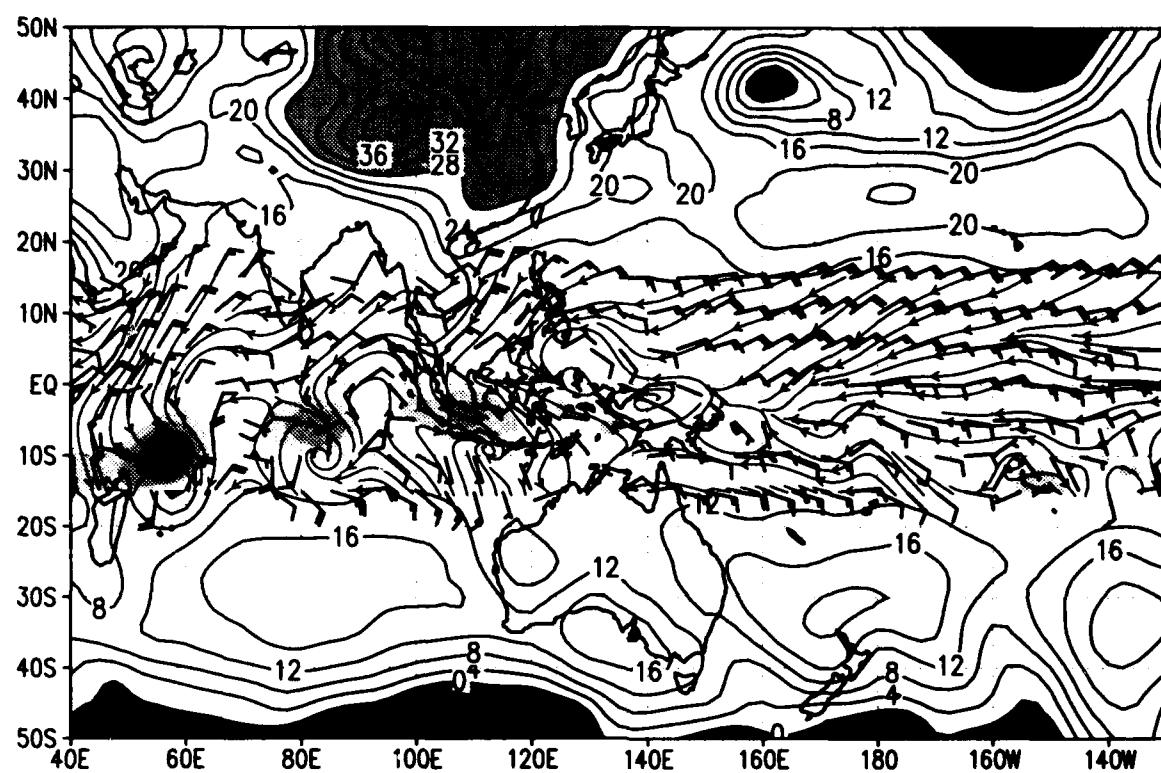


MRF

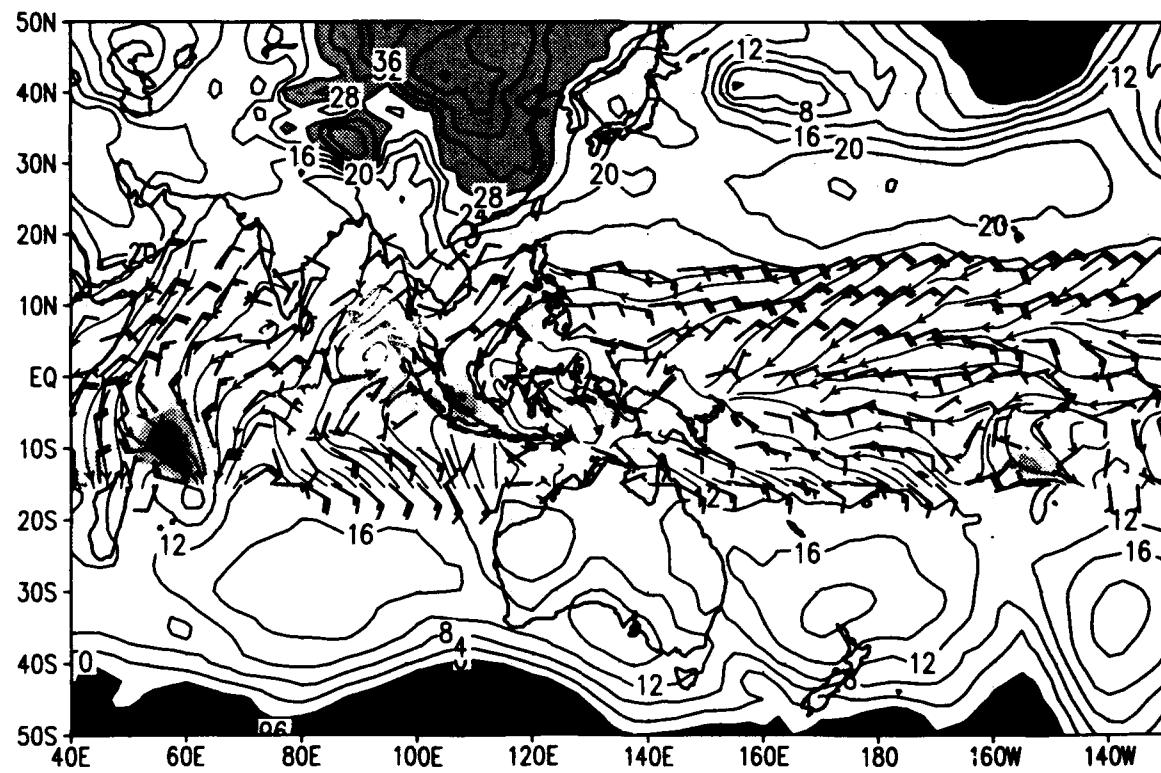


SLP and sfc winds ($u>0$ shaded) for 00Z 18 JAN 1993
slp (mb) wind barbs (kts) /d2/toga_coare/d2.gs

NOGAPS

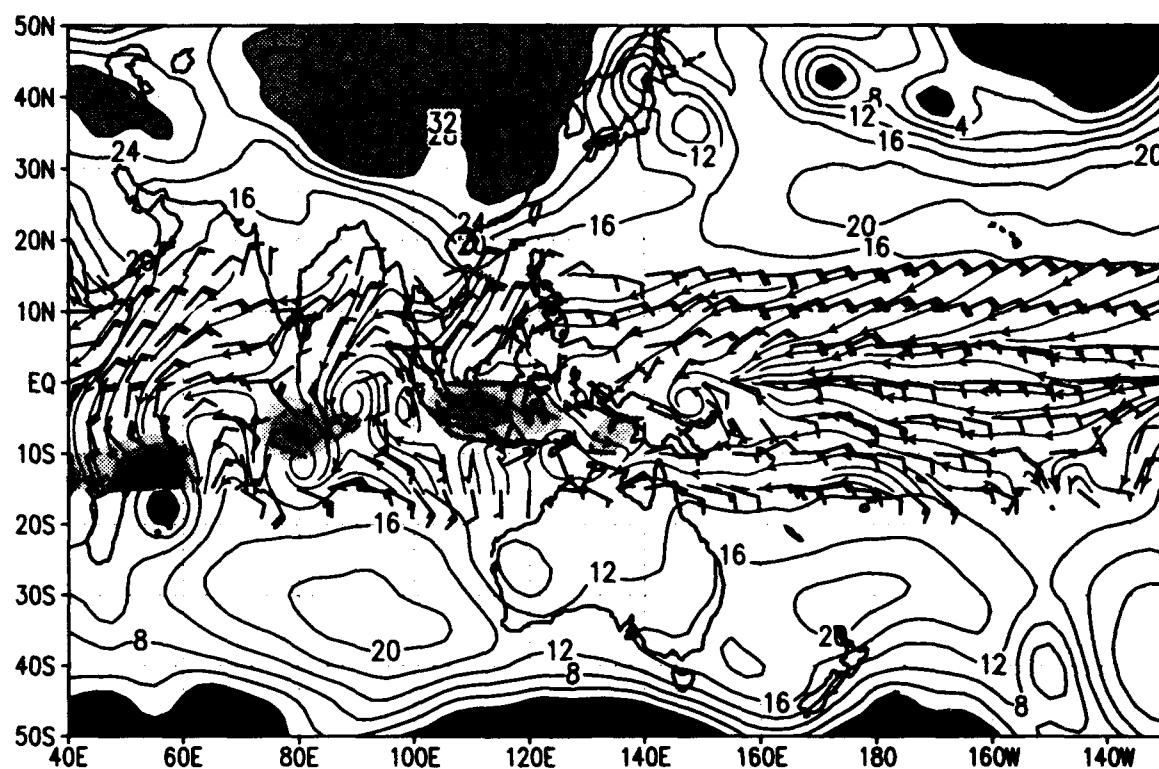


MRF

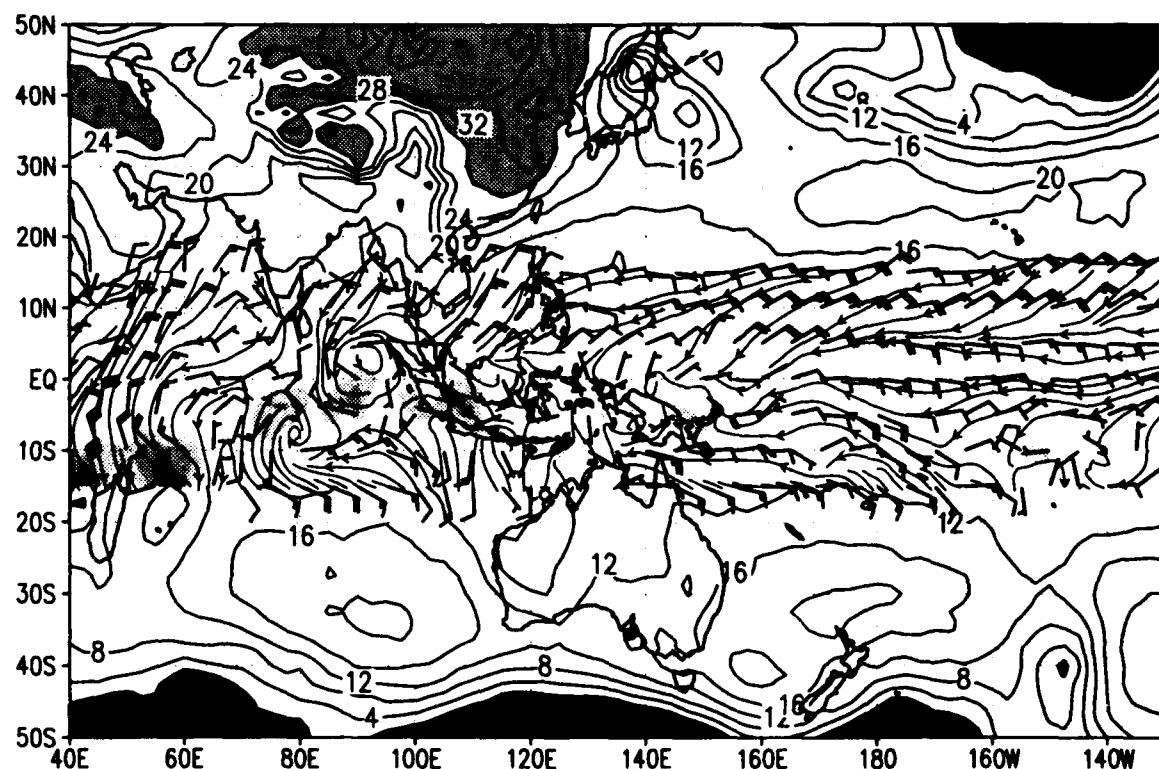


SLP and sfc winds ($u>0$ shaded) for 00Z 19 JAN 1993
slp (mb) wind barbs (kts) /d2/toga_coare/d2.gs

NOGAPS

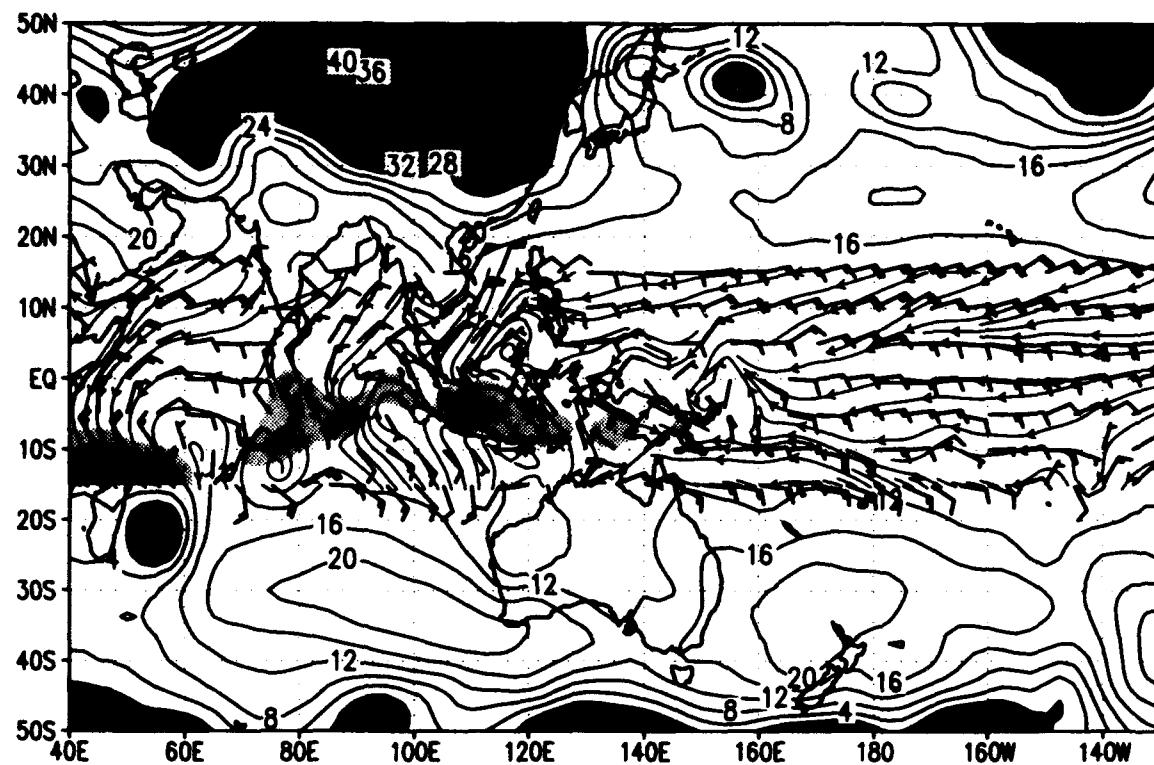


MRF

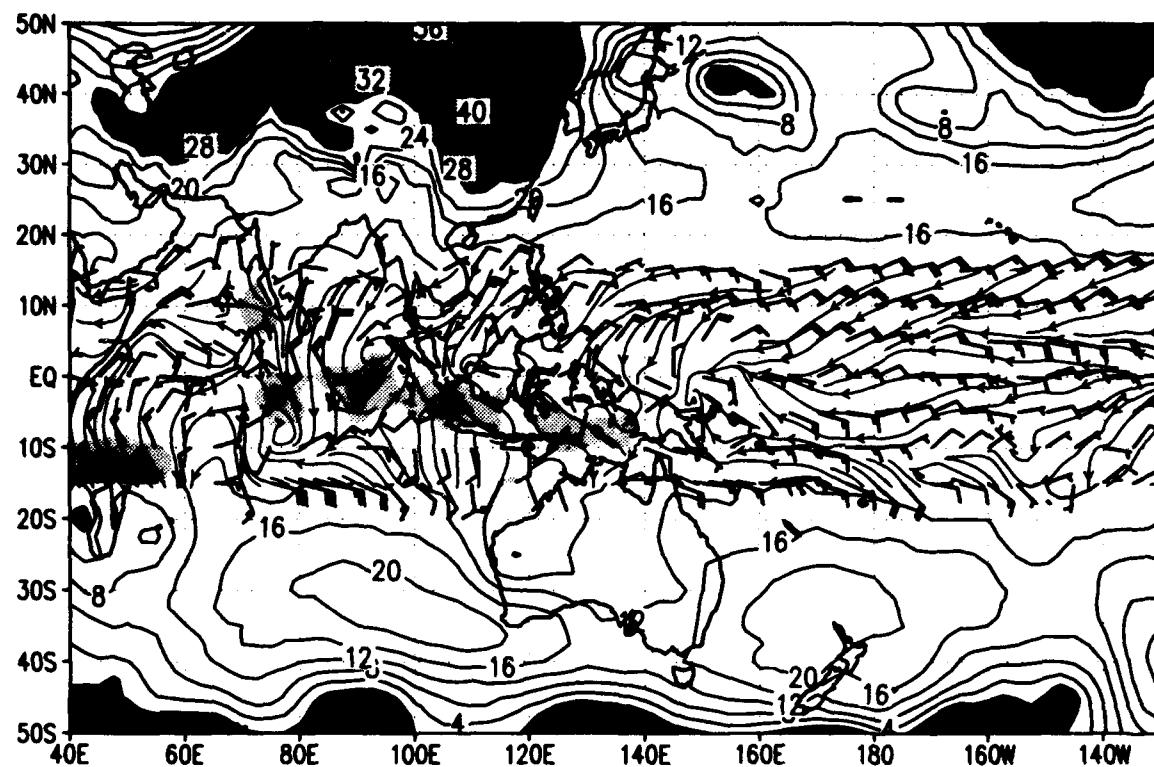


SLP and sfc winds ($u>0$ shaded) for 00Z 20 JAN 1993
slp (mb) wind barbs (kts) /d2/toga_coare/d2.gs

NOGAPS

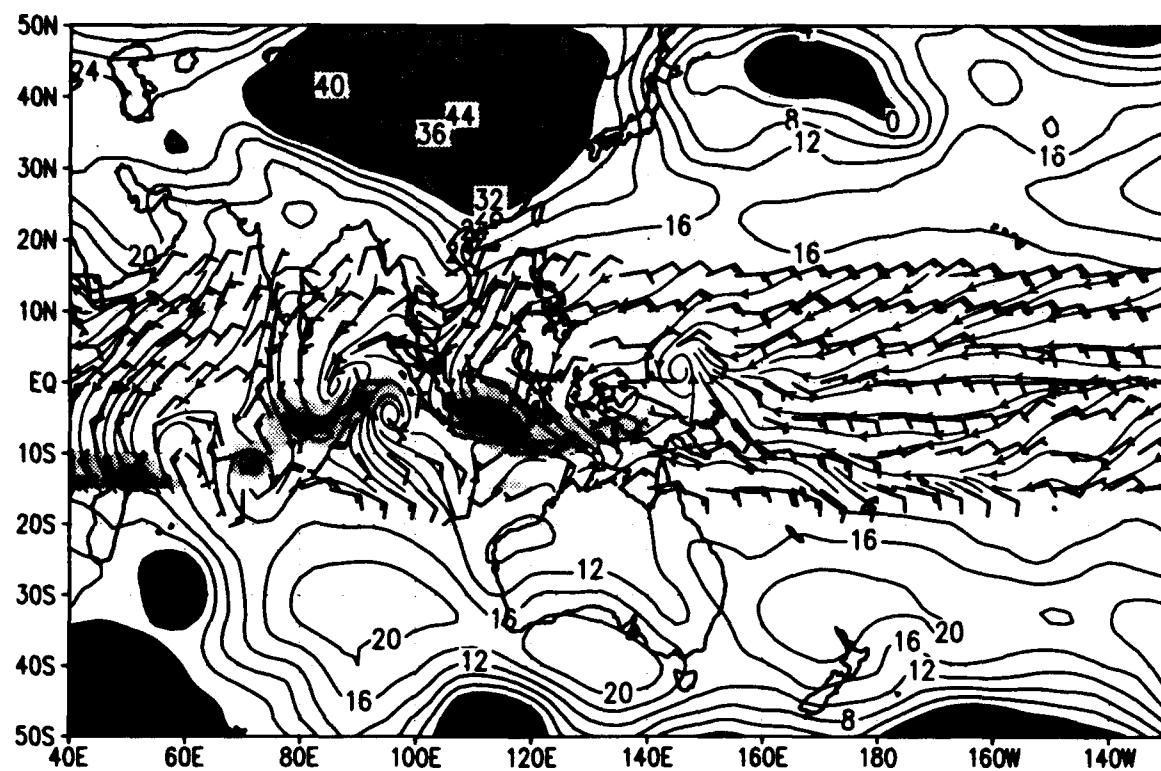


MRF

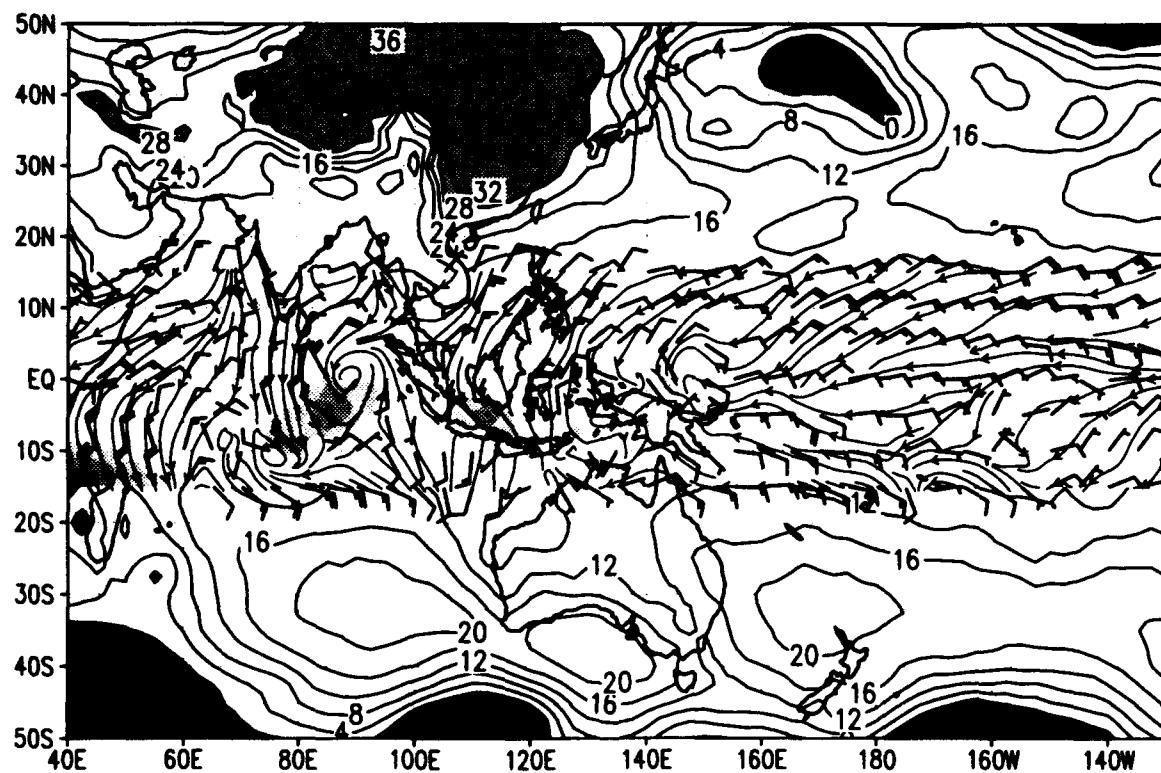


SLP and sfc winds ($u > 0$ shaded) for 00Z 21 JAN 1993
slp (mb) wind barbs (kts) /d2/toga_coare/d2.qs

NOGAPS

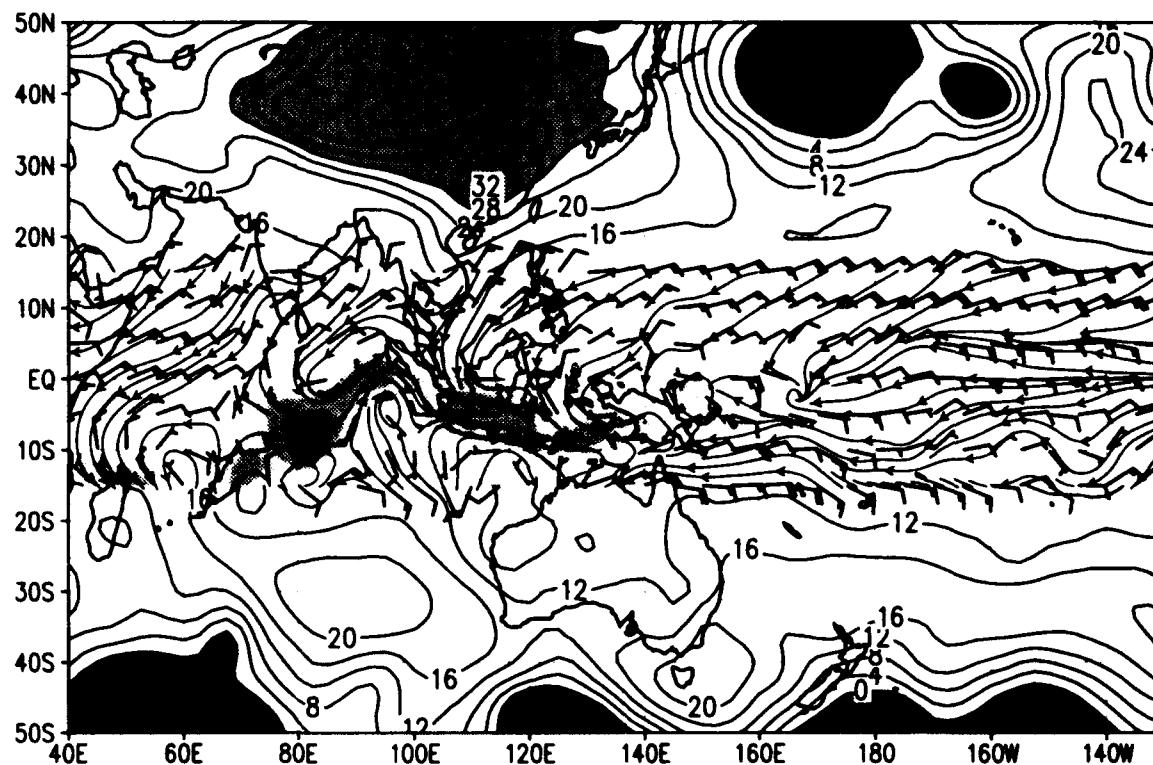


MRF

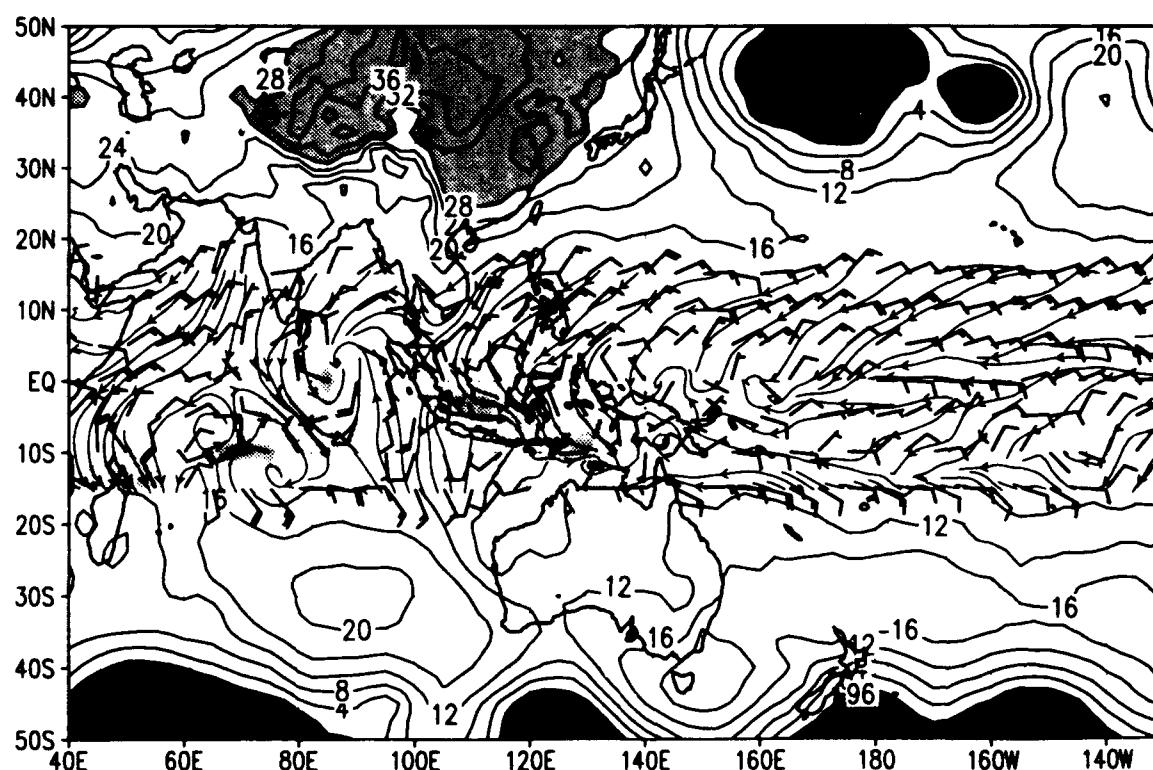


SLP and sfc winds ($u > 0$ shaded) for 00Z 22 JAN 1993
slp (mb) wind barbs (kts) /d2/toga_coare/d2.gs

NOGAPS

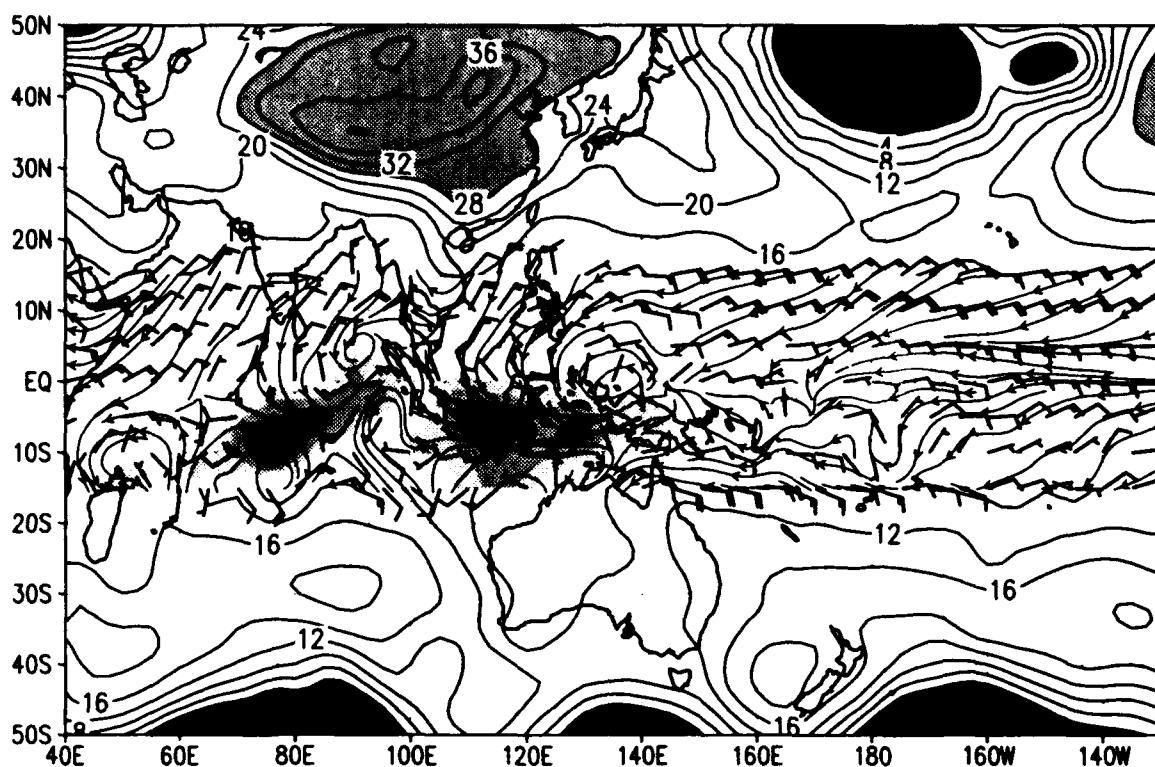


MRF

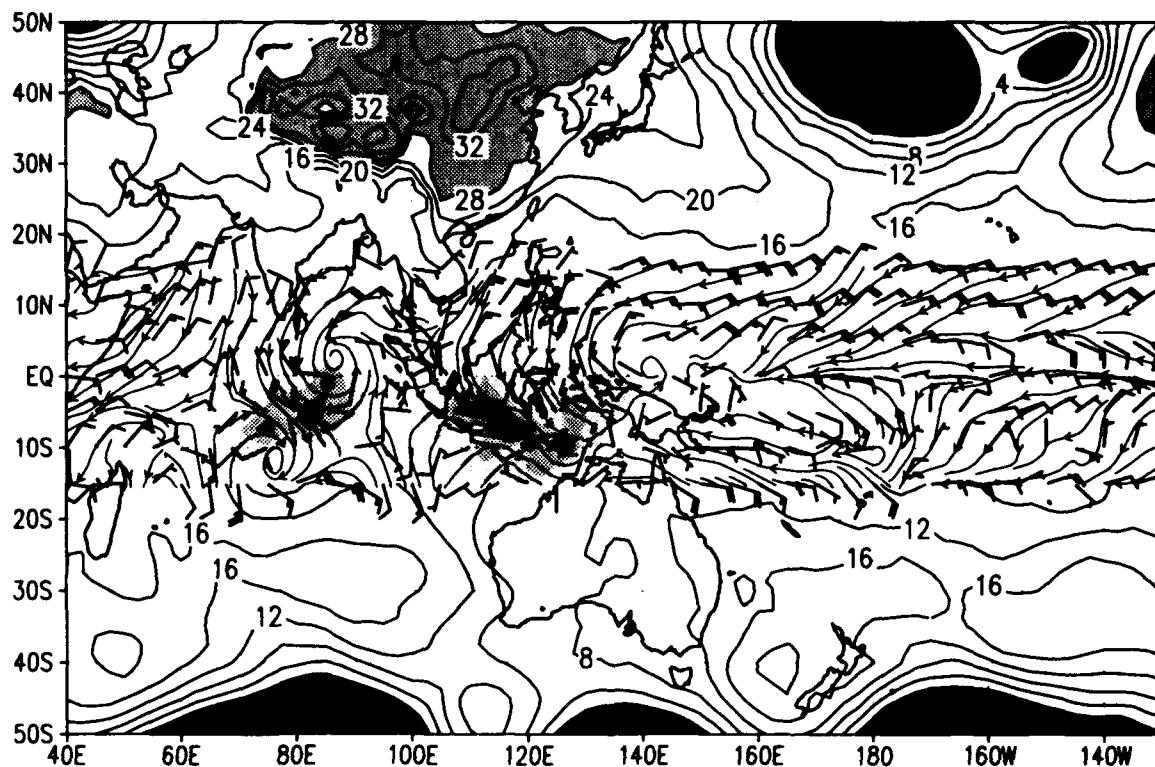


SLP and sfc winds ($u > 0$ shaded) for 00Z 23 JAN 1993
slp (mb) wind barbs (kts) /d2/toga_coare/d2.gs

NOGAPS

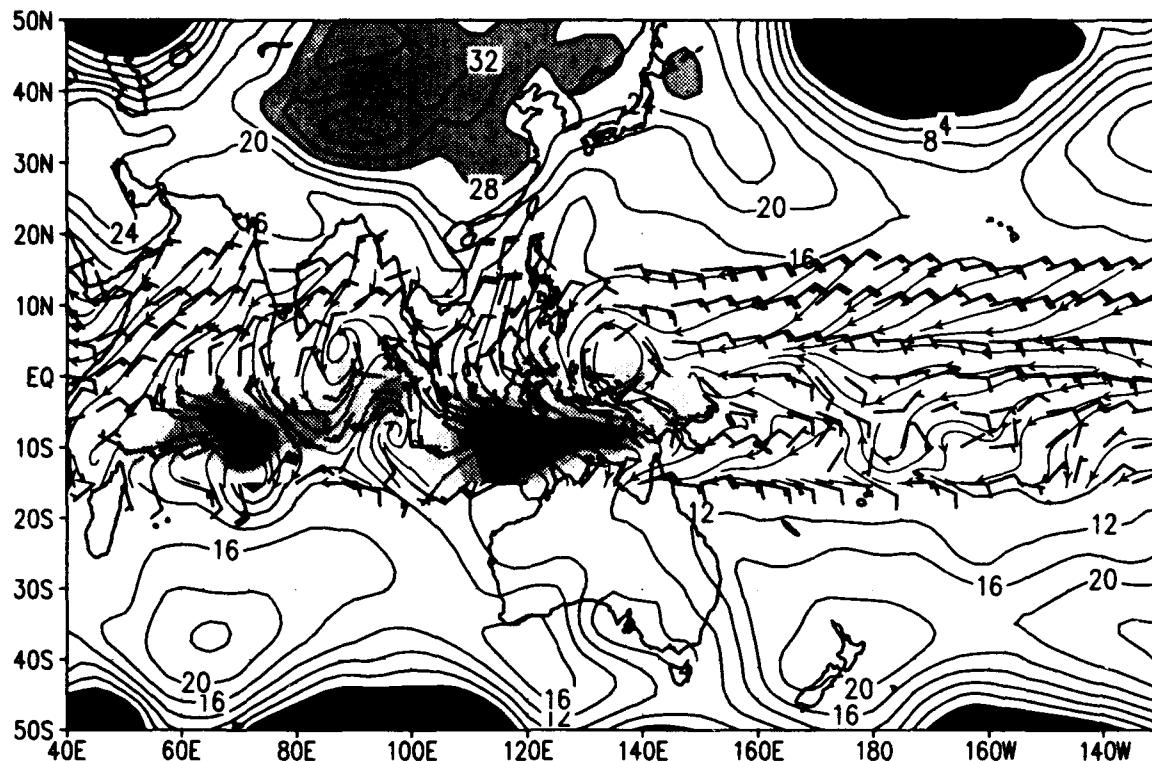


MRF

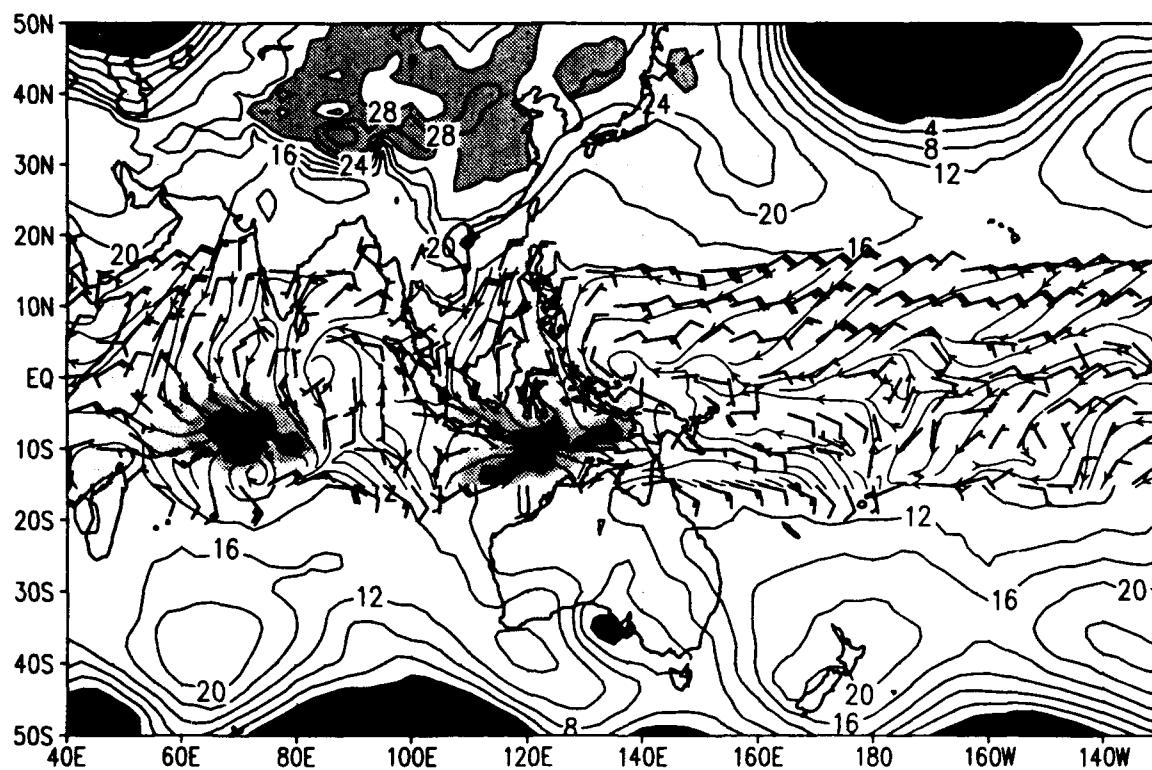


SLP and sfc winds ($u > 0$ shaded) for 00Z 24 JAN 1993
slp (mb) wind barbs (kts) /d2/toga_coare/d2.gs

NOGAPS

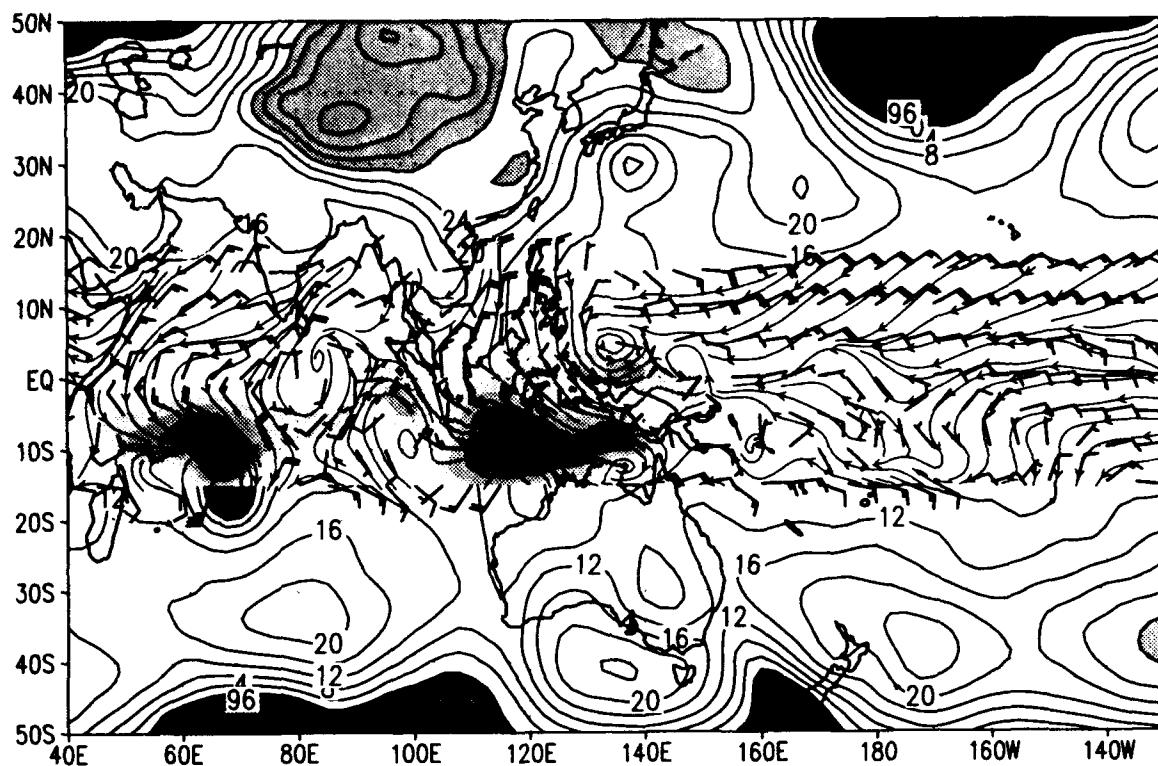


MRF

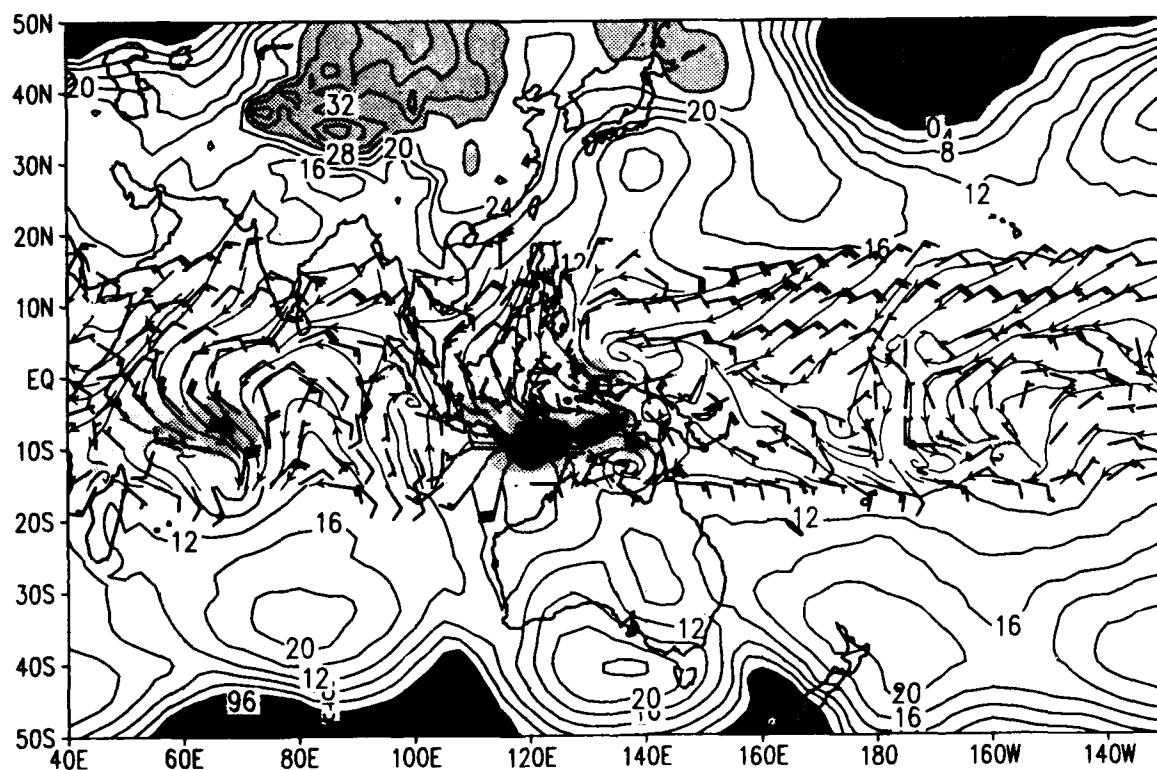


SLP and sfc winds ($u > 0$ shaded) for 00Z 25 JAN 1993
slp (mb) wind barbs (kts) /d2/toga_coare/d2.gs

NOGAPS

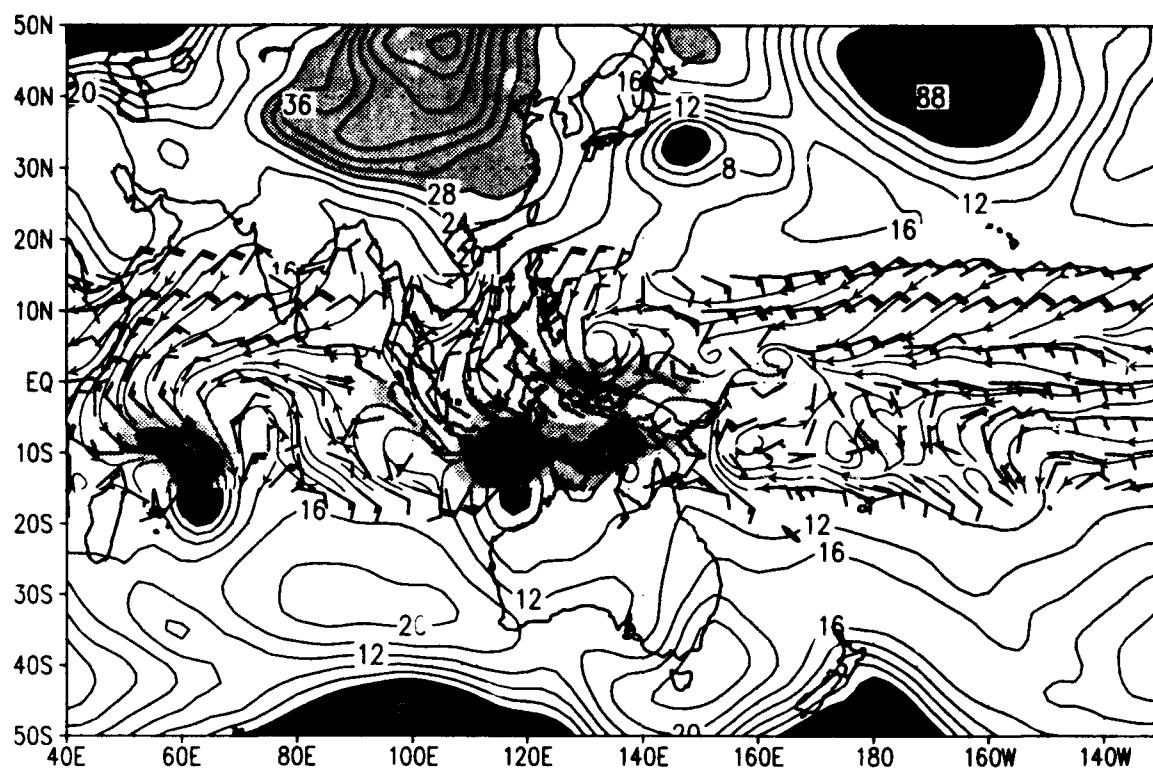


MRF

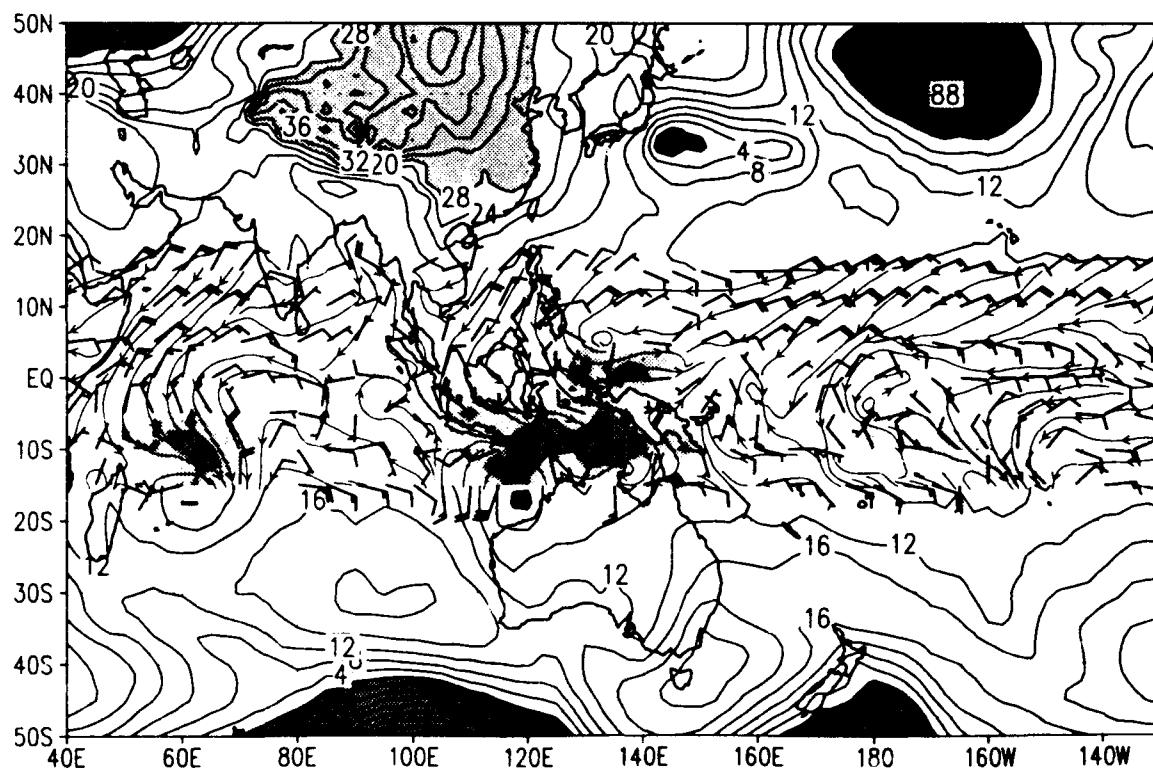


SLP and sfc winds ($u>0$ shaded) for 00Z 26 JAN 1993
slp (mb) wind barbs (kts) /d2/toga_coare/d2.gs

NOGAPS

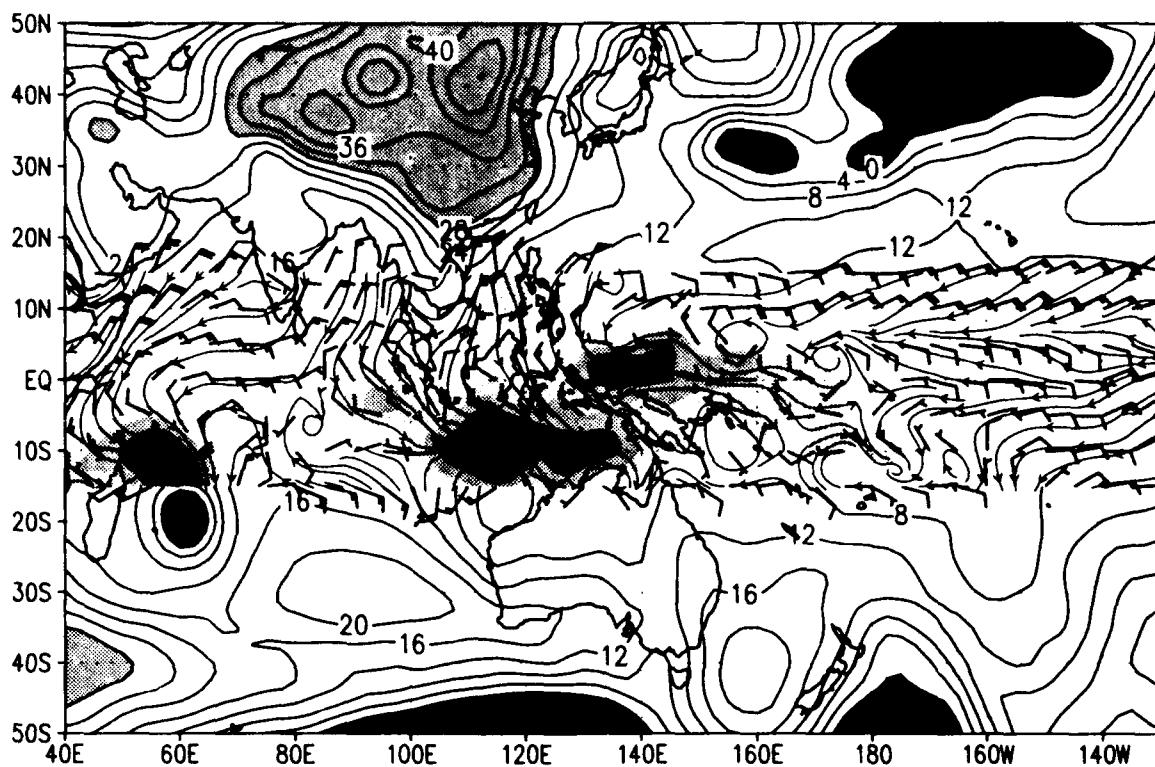


MRF

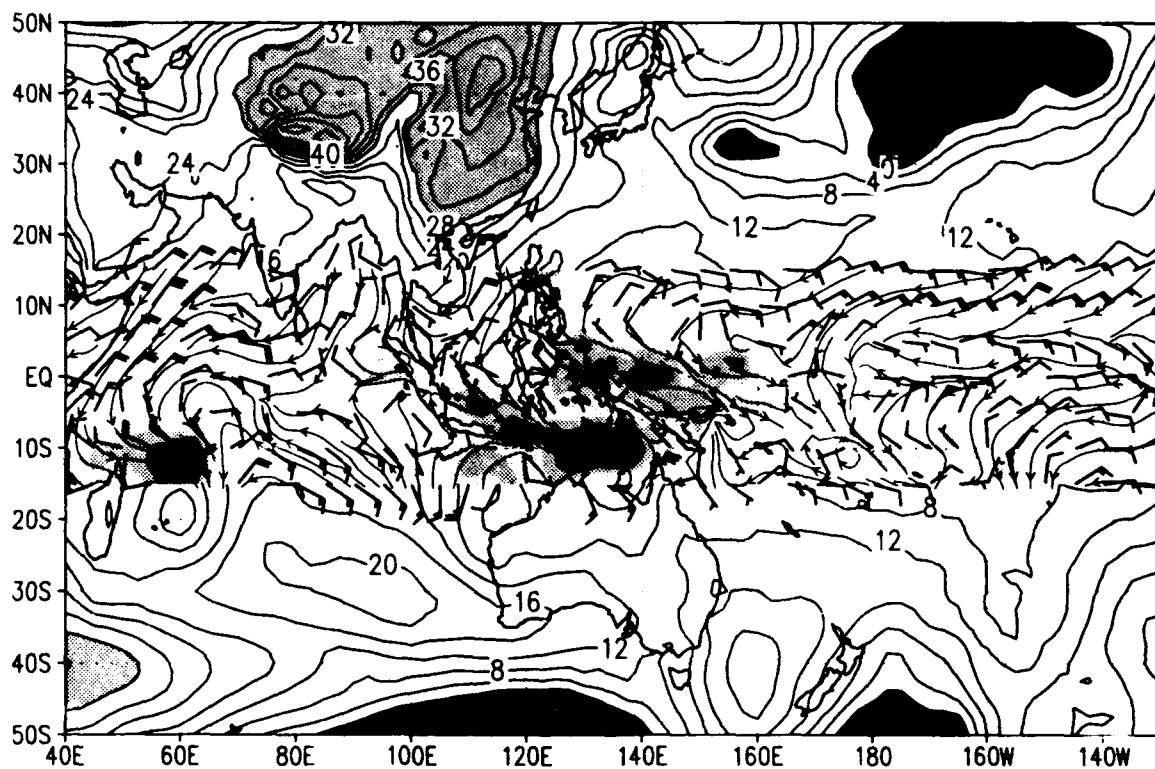


SLP and sfc winds ($u > 0$ shaded) for 00Z 27 JAN 1993
slp (mb) wind barbs (kts) /d2/toga_cocre/d2.gs

NOGAPS

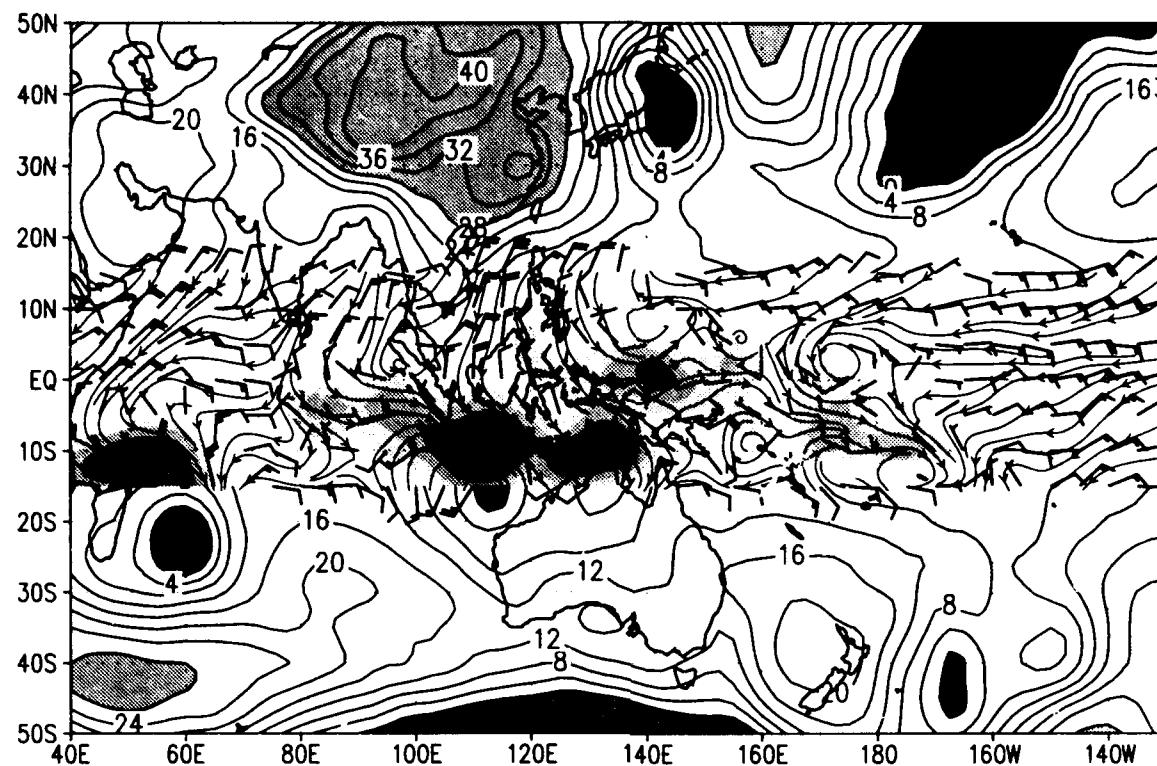


MRF

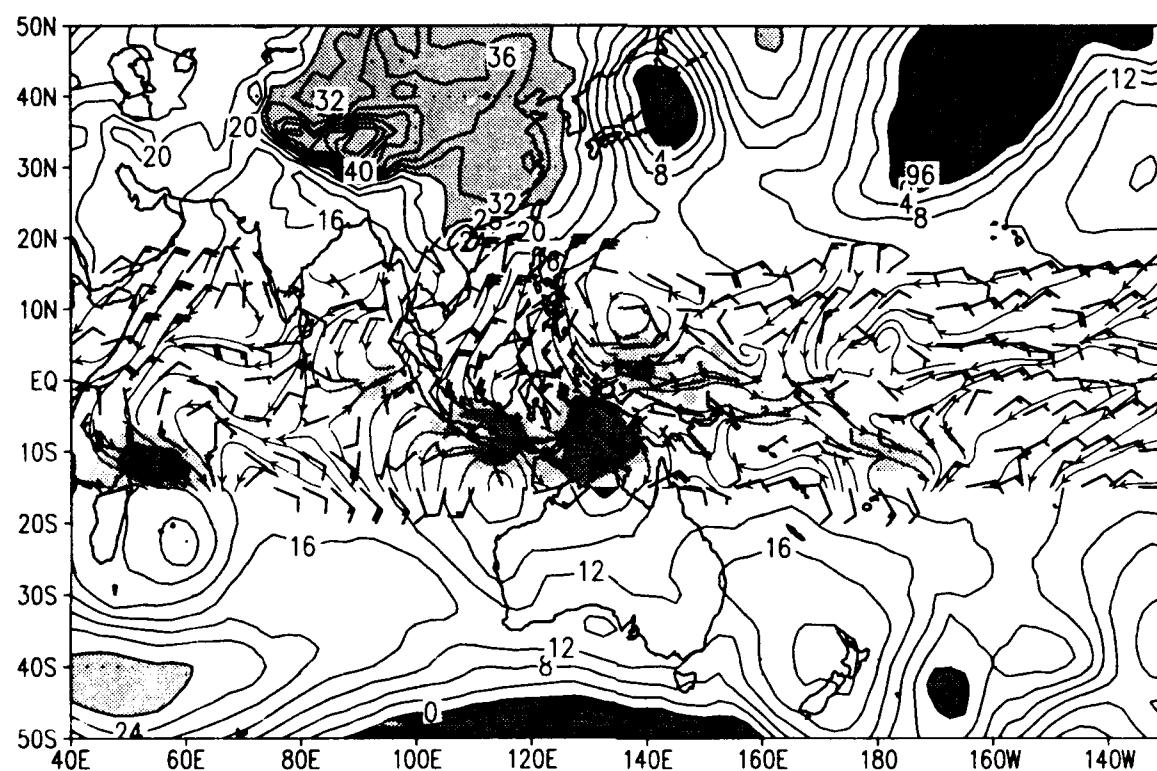


SLP and sfc winds ($u>0$ shaded) for 00Z 28 JAN 1993
slp (mb) wind barbs (kts) /d2/toga_coare/d2.gs

NOGAPS

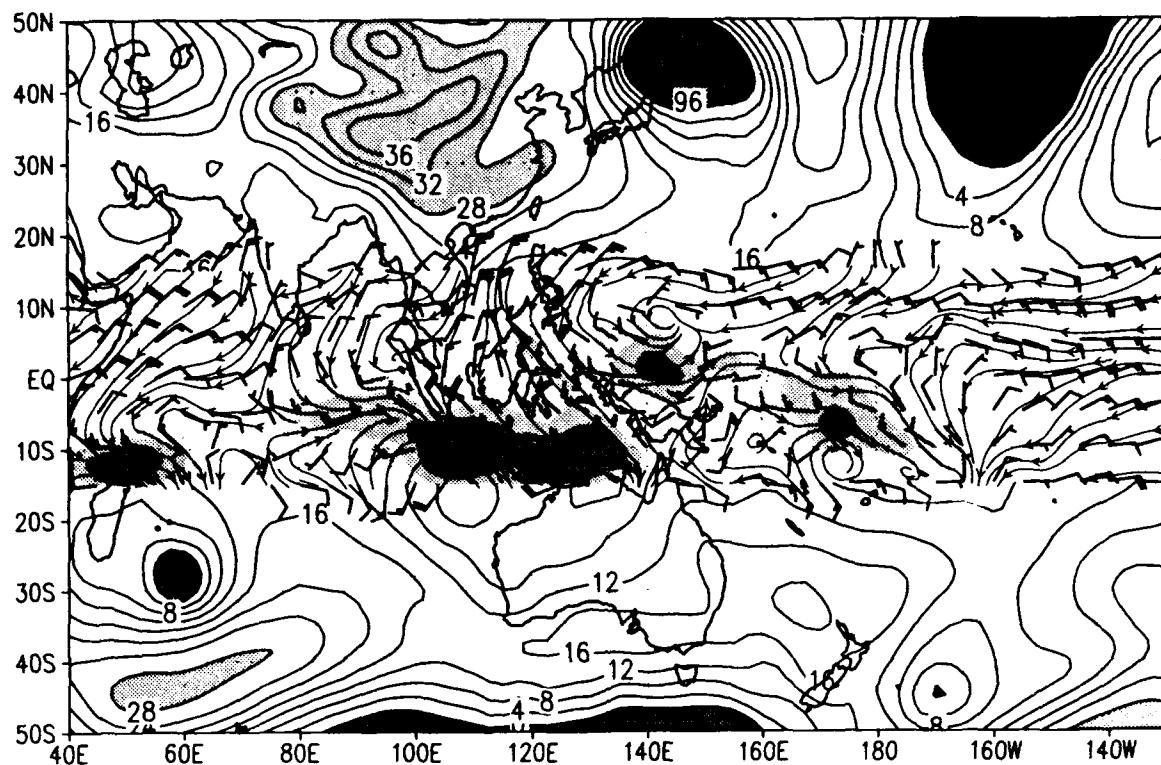


MRF

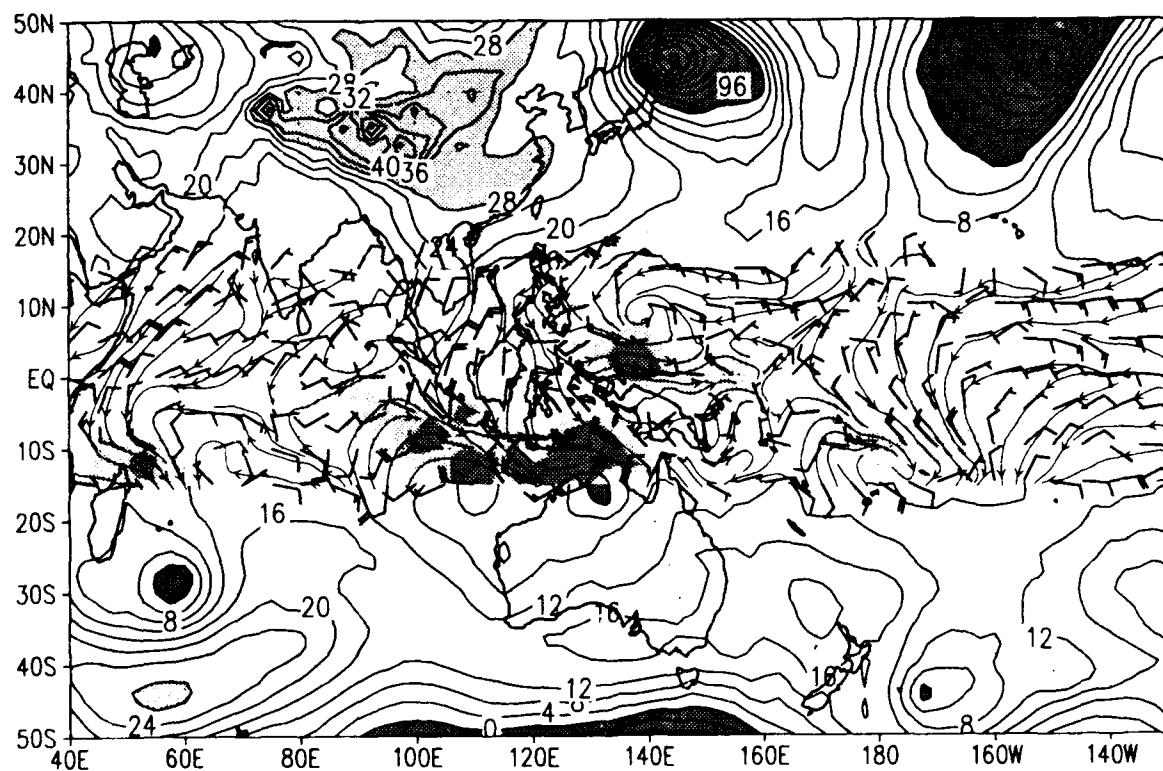


SLP and sfc winds ($u>0$ shaded) for 00Z 29 JAN 1993
slp (mb) wind barbs (kts) /d2/toga_coare/d2.gs

NOGAPS

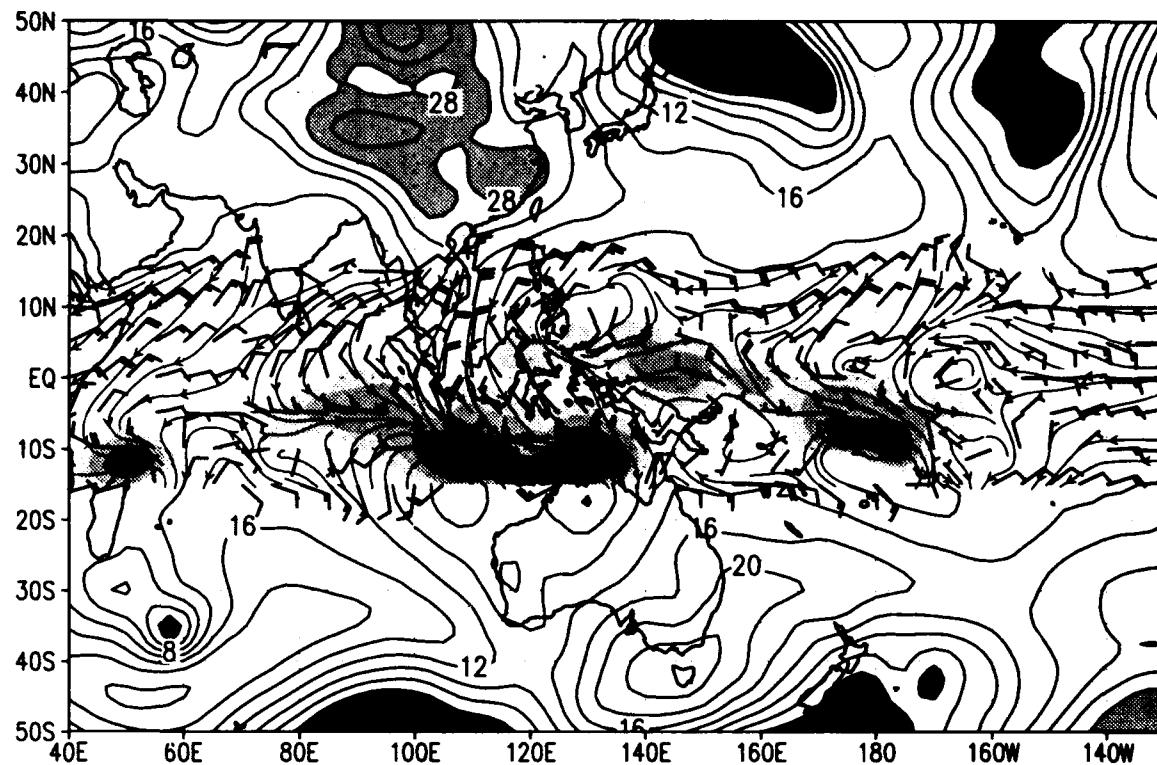


MRF

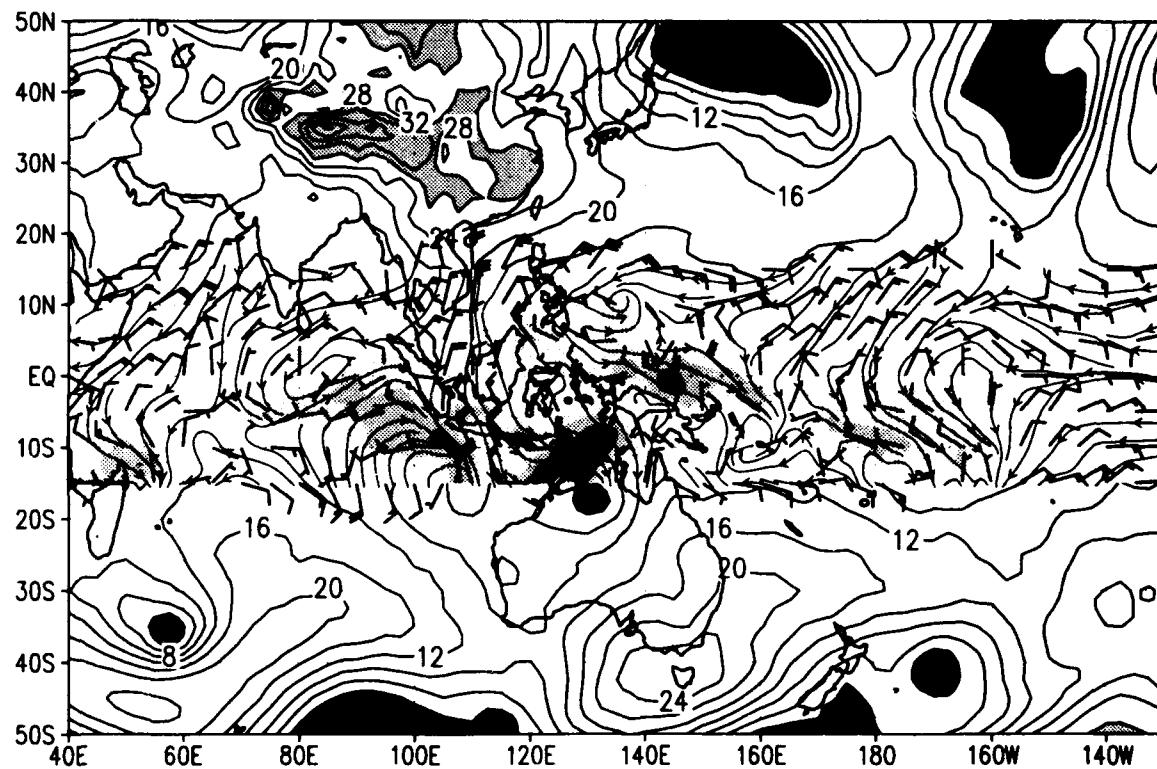


SLP and sfc winds ($u>0$ shaded) for 00Z 30 JAN 1993
slp (mb) wind barbs (kts) /d2/toga_coare/d2.gs

NOGAPS

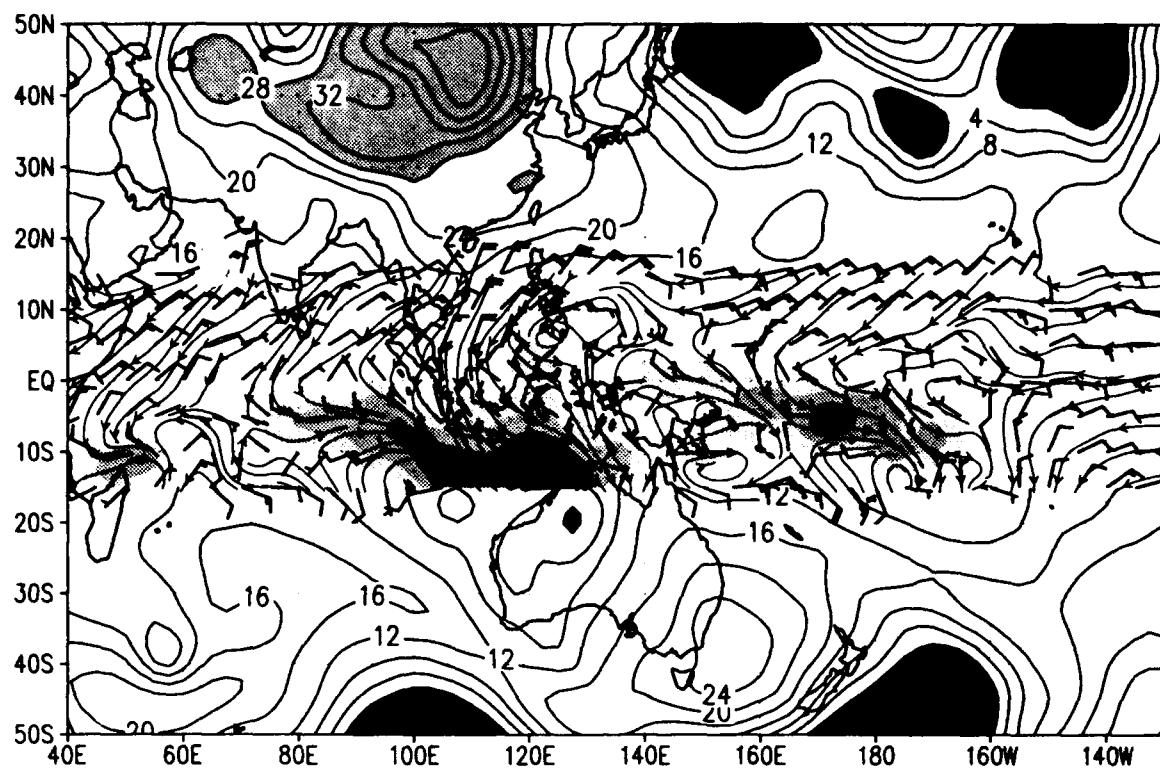


MRF

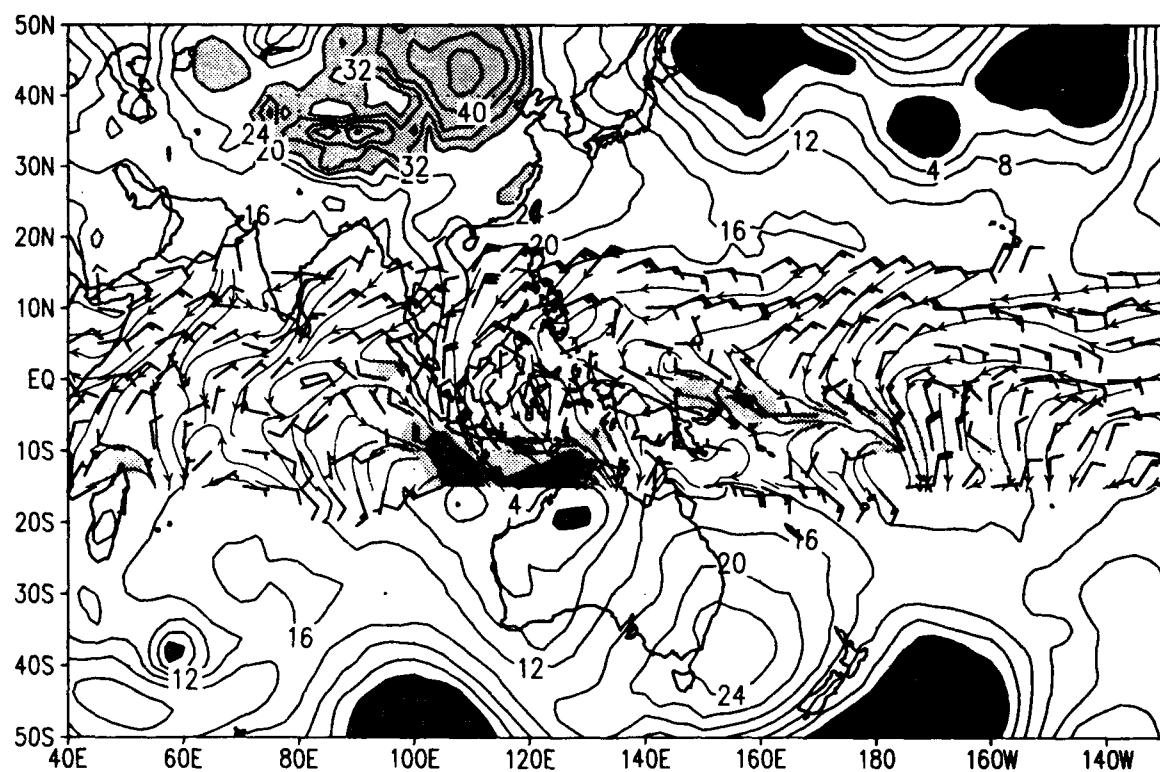


SLP and sfc winds ($u>0$ shaded) for 00Z 31 JAN 1993
slp (mb) wind barbs (kts) /d2/toga_coare/d2.gs

NOGAPS



MRF



14 00 UTC Synoptic Charts for 1 - 28 February 1993

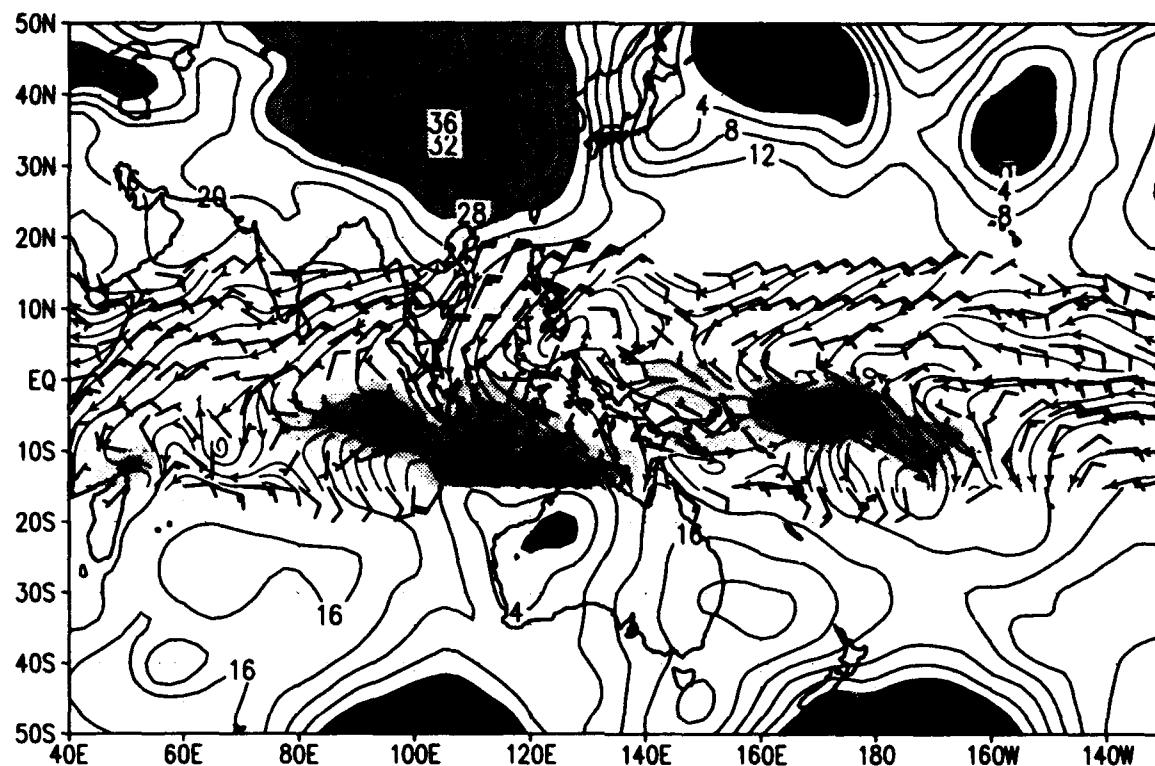
In the deep tropics (15S-15N) we show surface wind barbs (kts) and streamlines with positive u component shaded in the intervals 5-10 kts (light), 10-20 kts (medium) and over 20 kts (dark). Outside the deep tropics we show sea-level pressure with a contour interval of 2 mb and areas < 1004 mb and > 1028 shaded.

The large differences in SLP between NOGAPS and MRF over mountainous terrain is an artifact of the method of estimating sea-level pressure from 1000 mb geopotential heights and temperature for the MRF. The correspondence was very good outside these regions. However, there were notably differences between the MRF and NOGAPS analyses with regards to the strength of the westerly winds in the tropics and the strength of tropical cyclones. Tropical cyclone positions at 00 UTC are drawn using a circle for tropical depressions (<35 kts), an open hurricane symbol for tropical storms (< 65 kts) and a closed hurricane symbol for typhoons (> 65 kts). The arrow above the northern border of the map indicates the longitude of the observed TC and the max wind speed in kts is given to the right of the arrow.

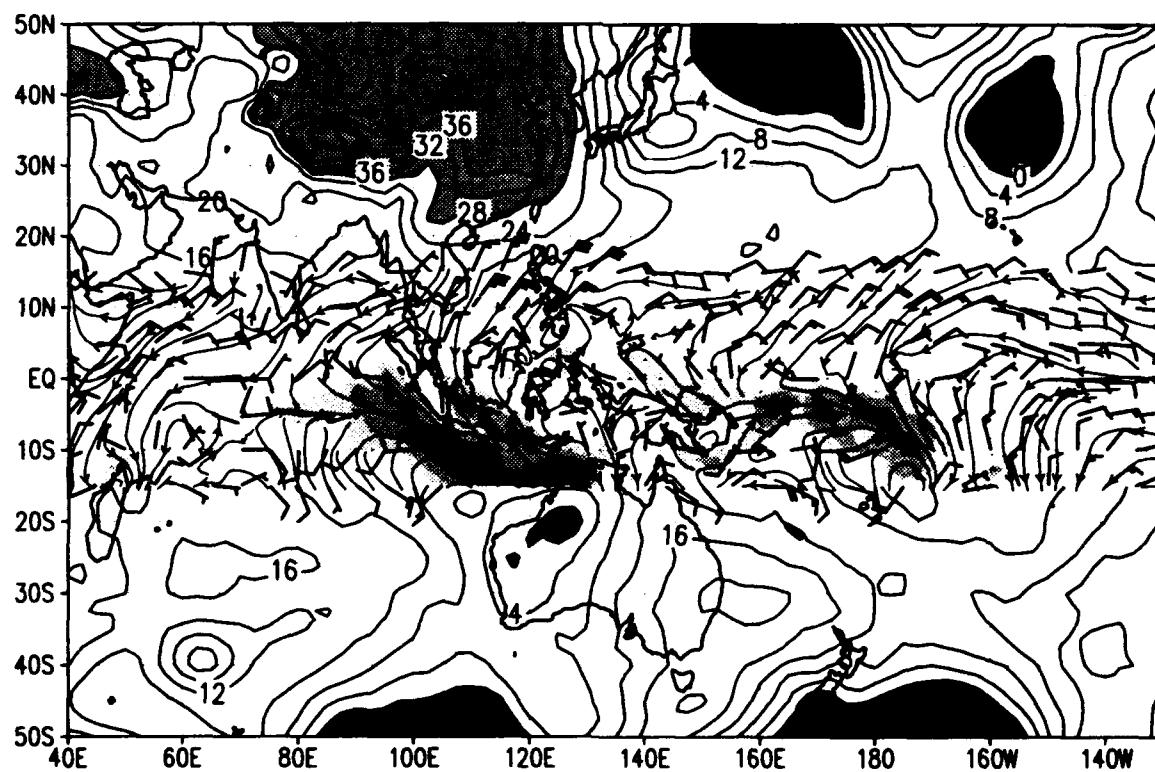
Chart	Description
1-28 -	Synoptic charts for NOGAPS and MRF

SLP and sfc winds ($u > 0$ shaded) for 00Z 01 FEB 1993
slp (mb) wind barbs (kts) /d2/toga_coare/d2.gs

NOGAPS

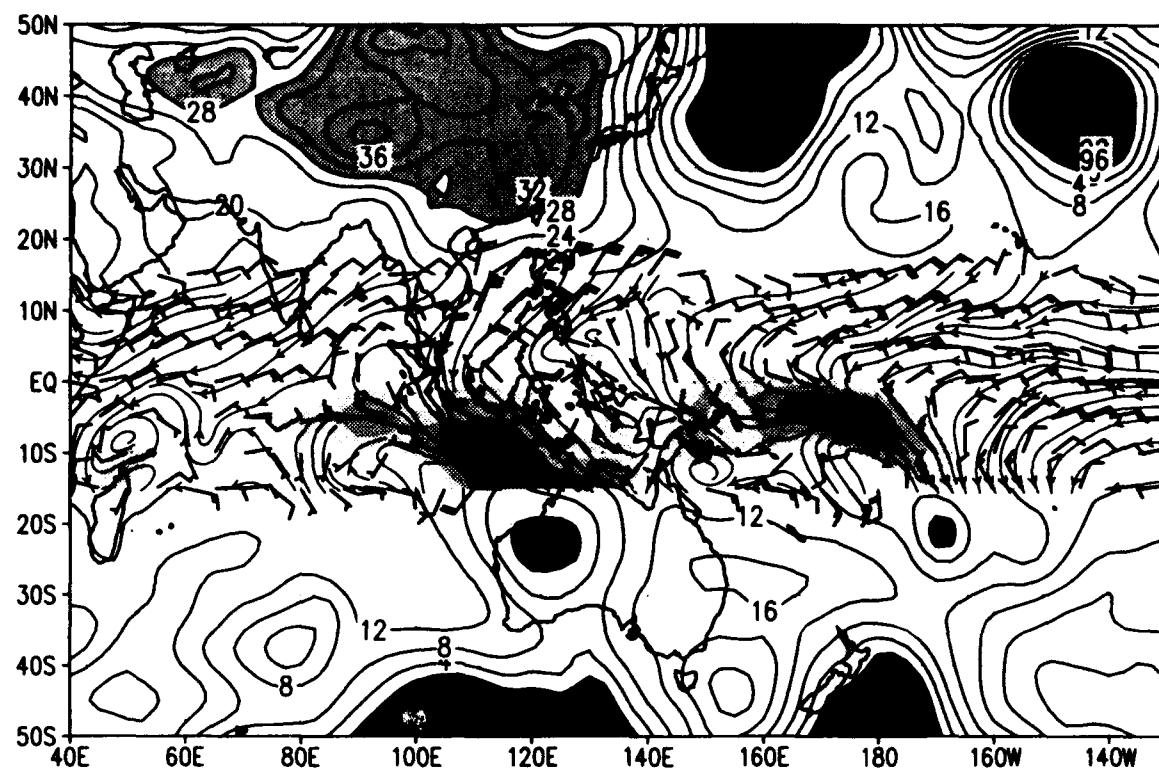


MRF

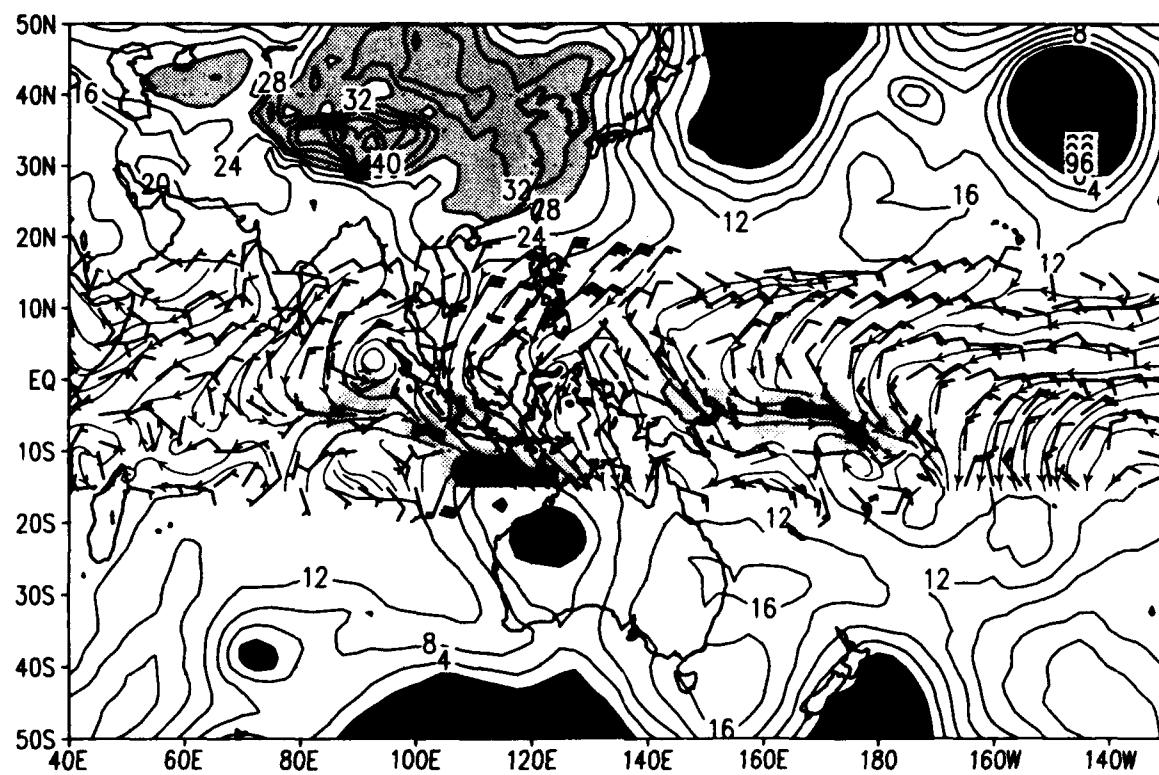


SLP and sfc winds ($u>0$ shaded) for 00Z 02 FEB 1993
slp (mb) wind barbs (kts) /d2/toga_coare/d2.gs

NOGAPS

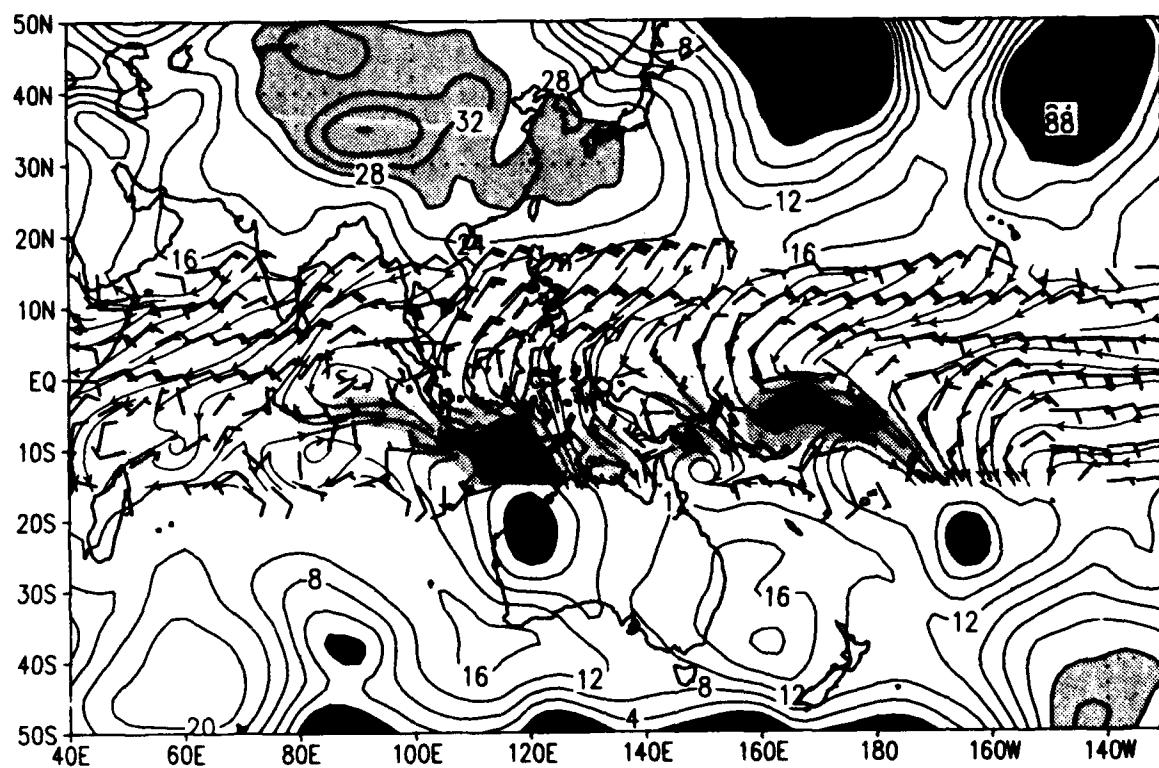


MRF

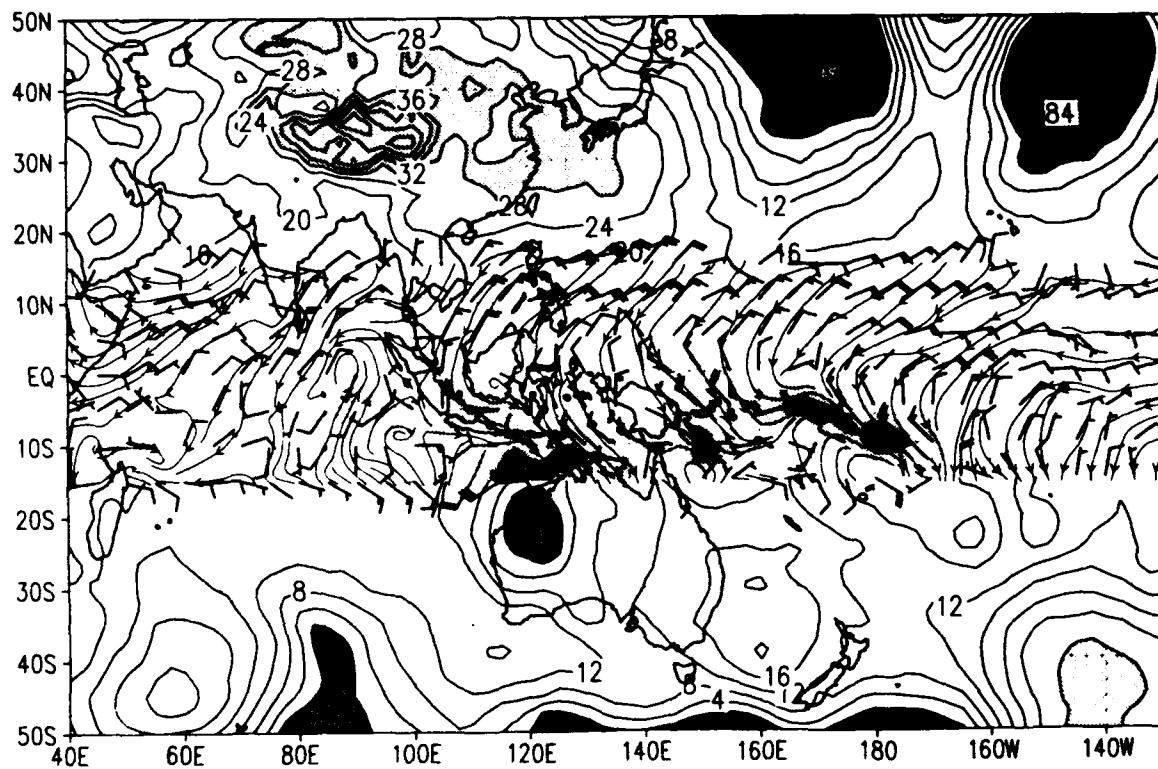


SLP and sfc winds ($u > 0$ shaded) for 00Z 03 FEB 1993
slp (mb) wind barbs (kts) /d2/toga_coare/d2.gs

NOGAPS

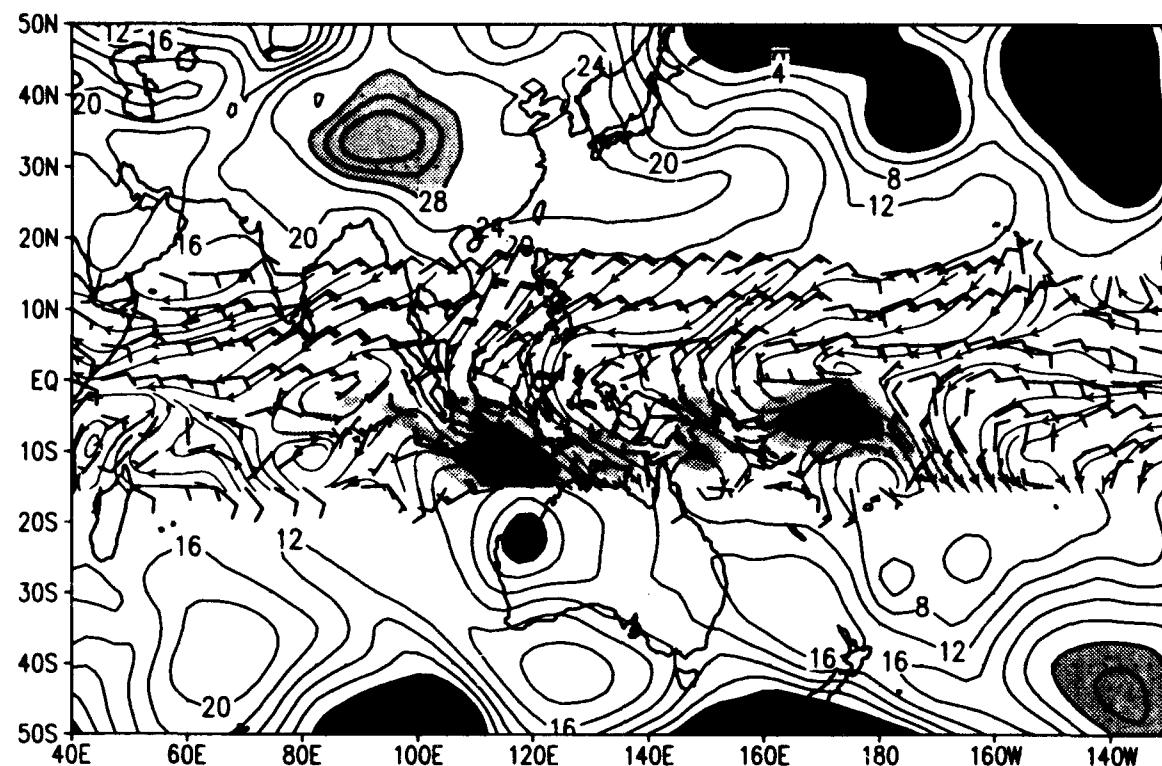


MRF

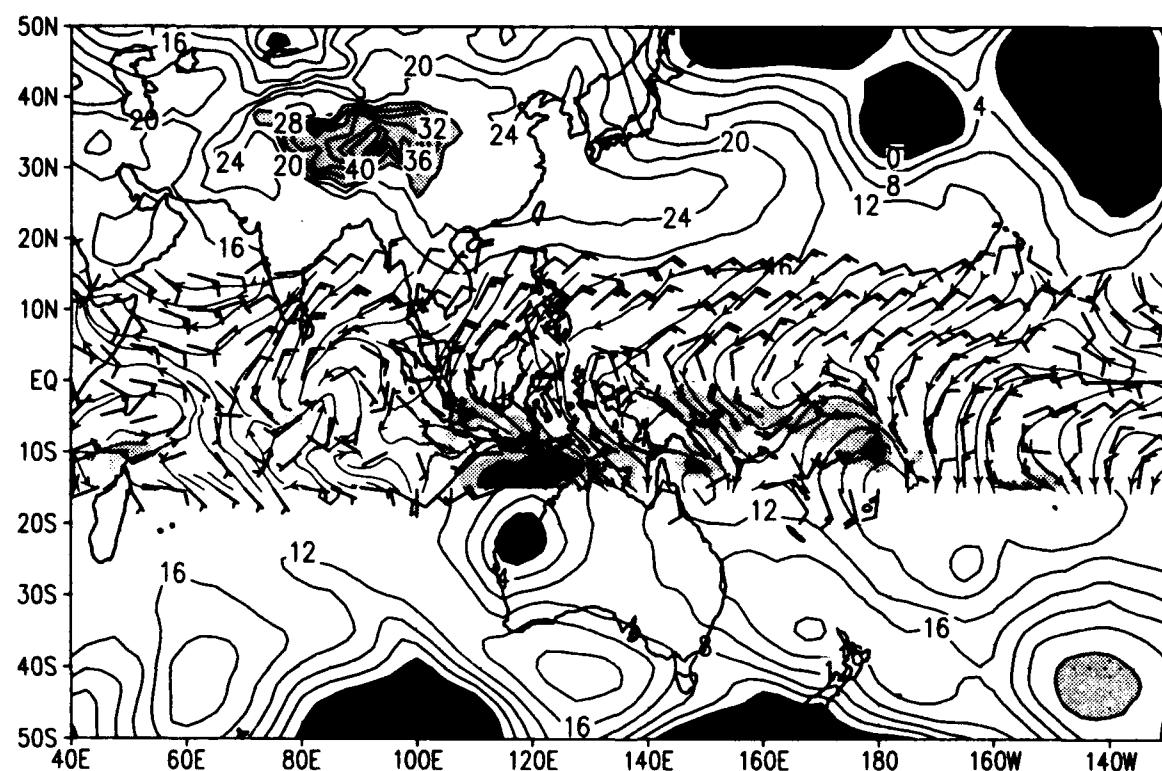


SLP and sfc winds ($u>0$ shaded) for 00Z 04 FEB 1993
slp (mb) wind barbs (kts) /d2/toga_coare/d2.gs

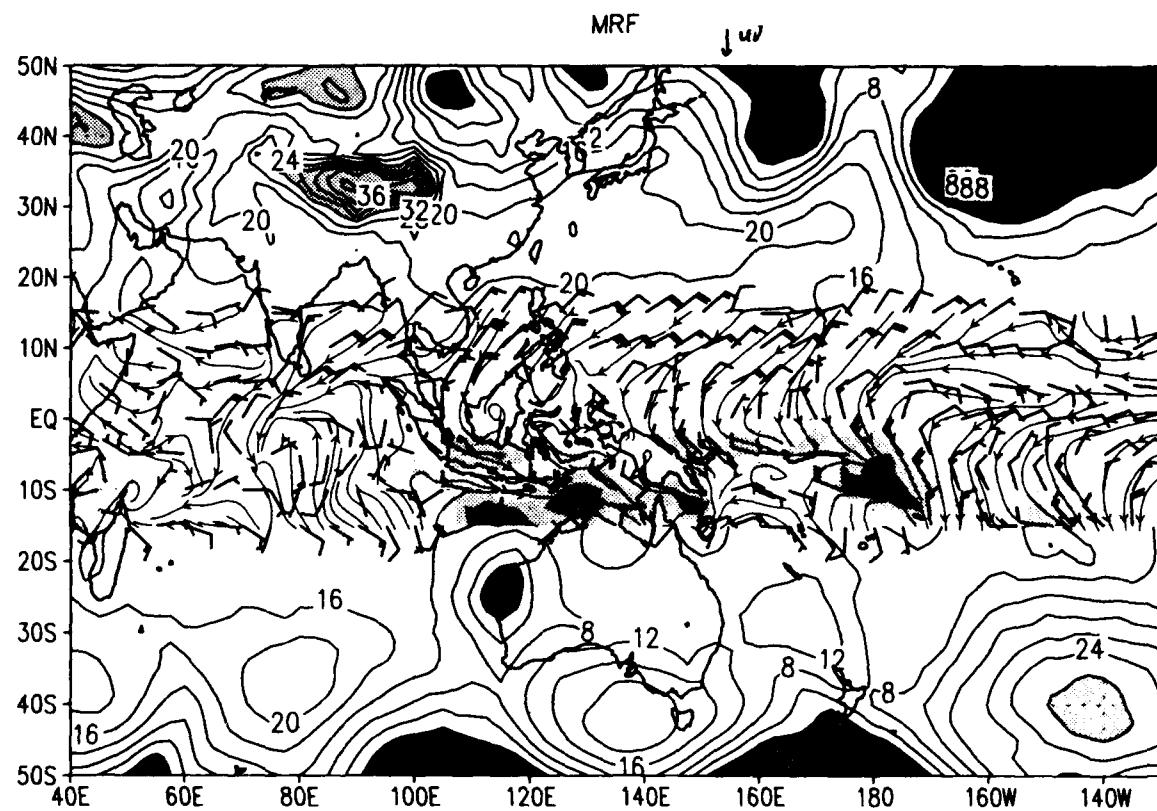
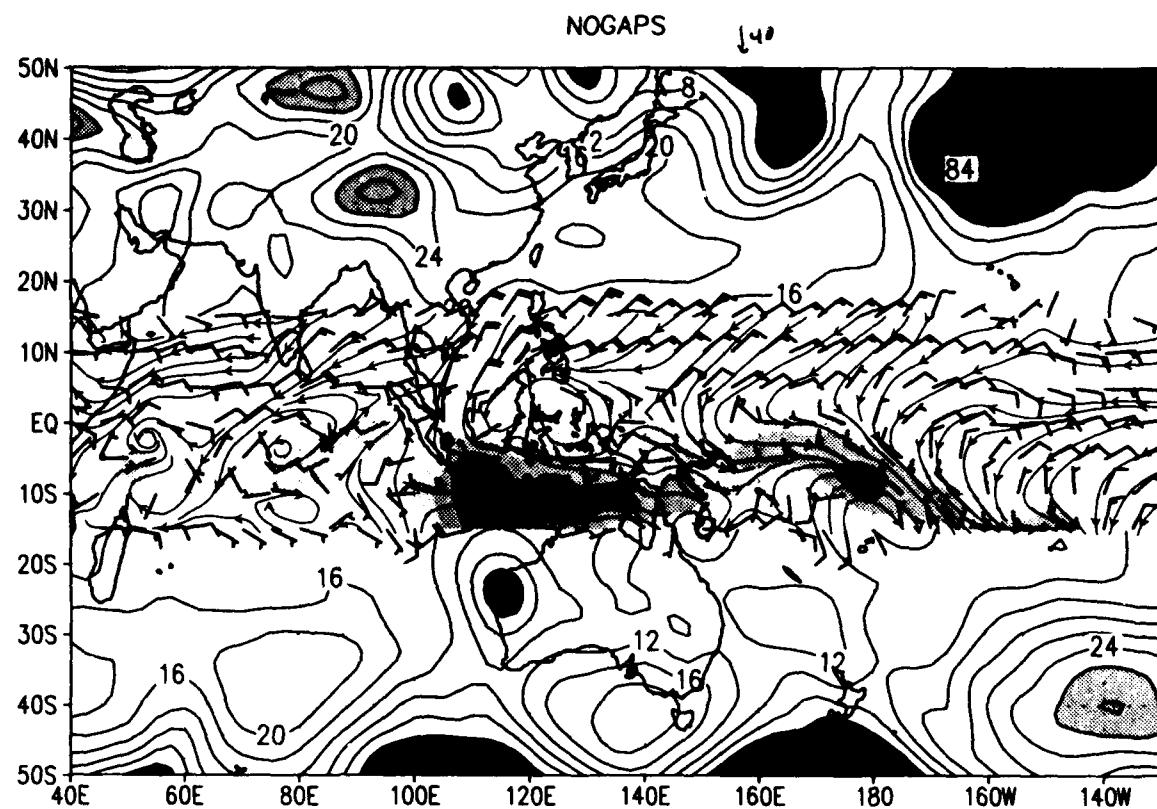
NOGAPS



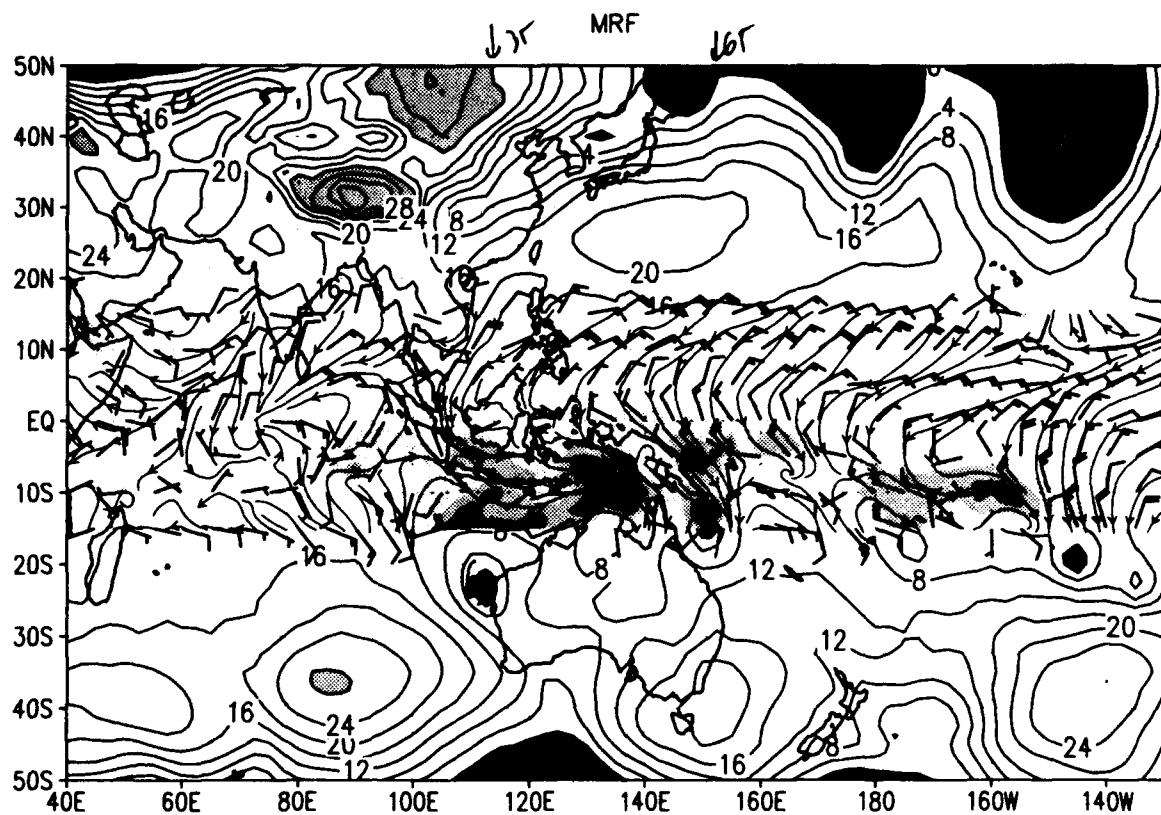
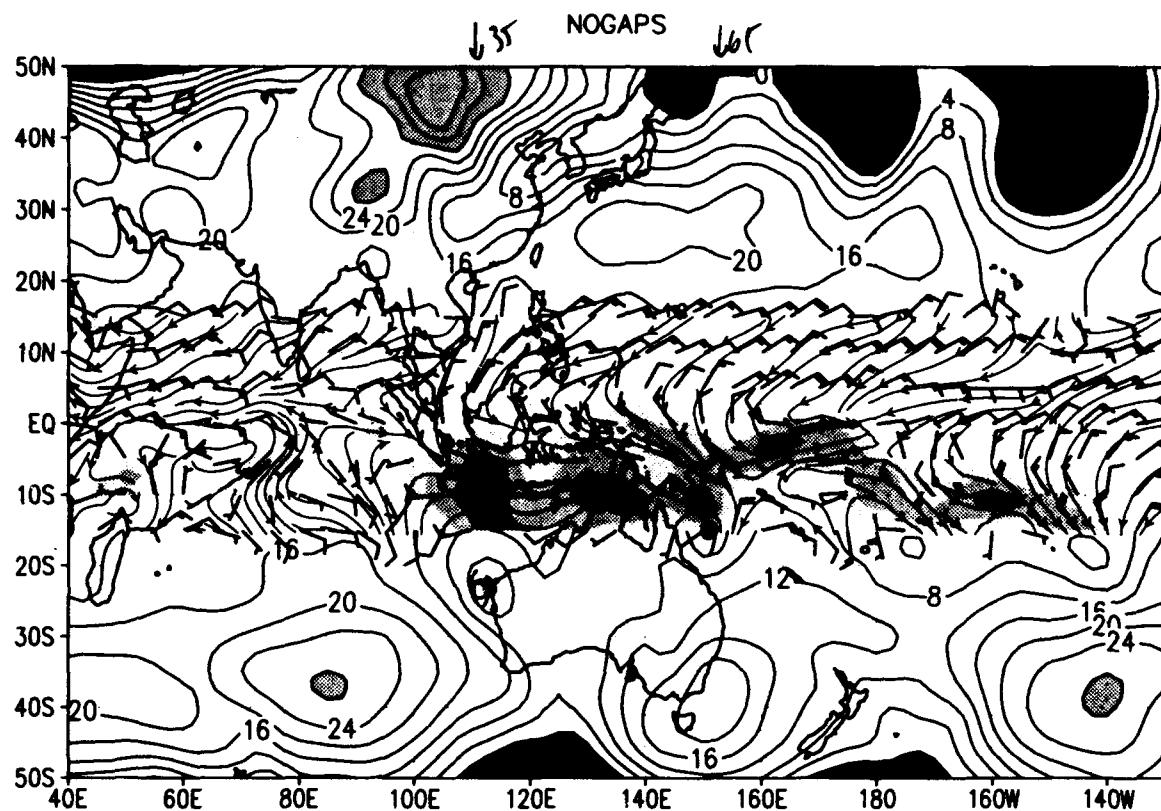
MRF



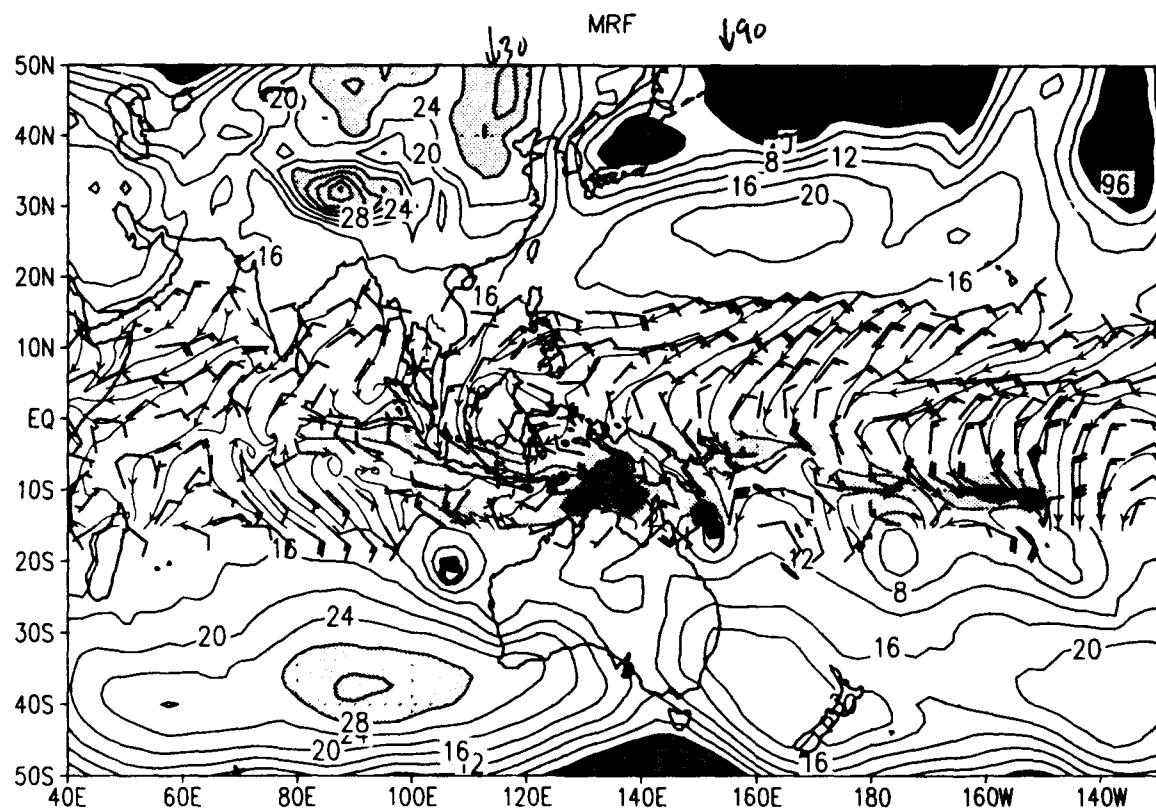
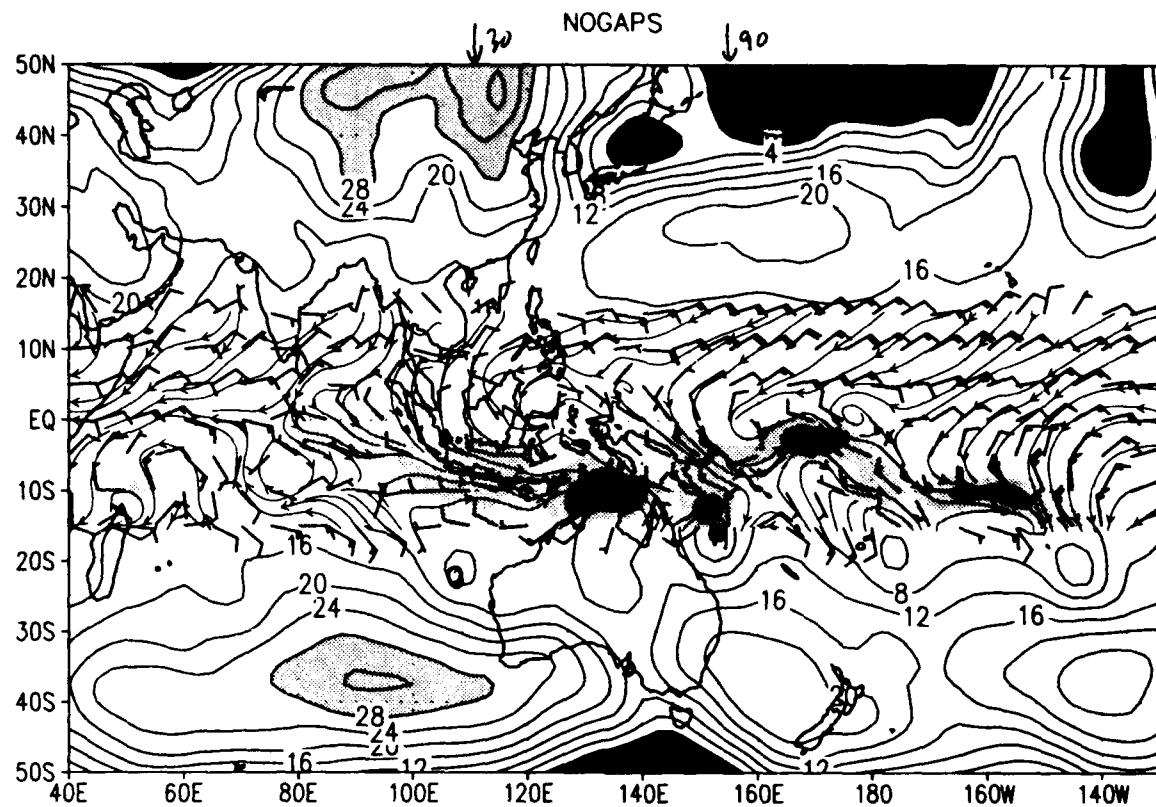
SLP and sfc winds ($u>0$ shaded) for 00Z 05 FEB 1993
slp (mb) wind barbs (kts) /d2/toga_coare/d2.gs



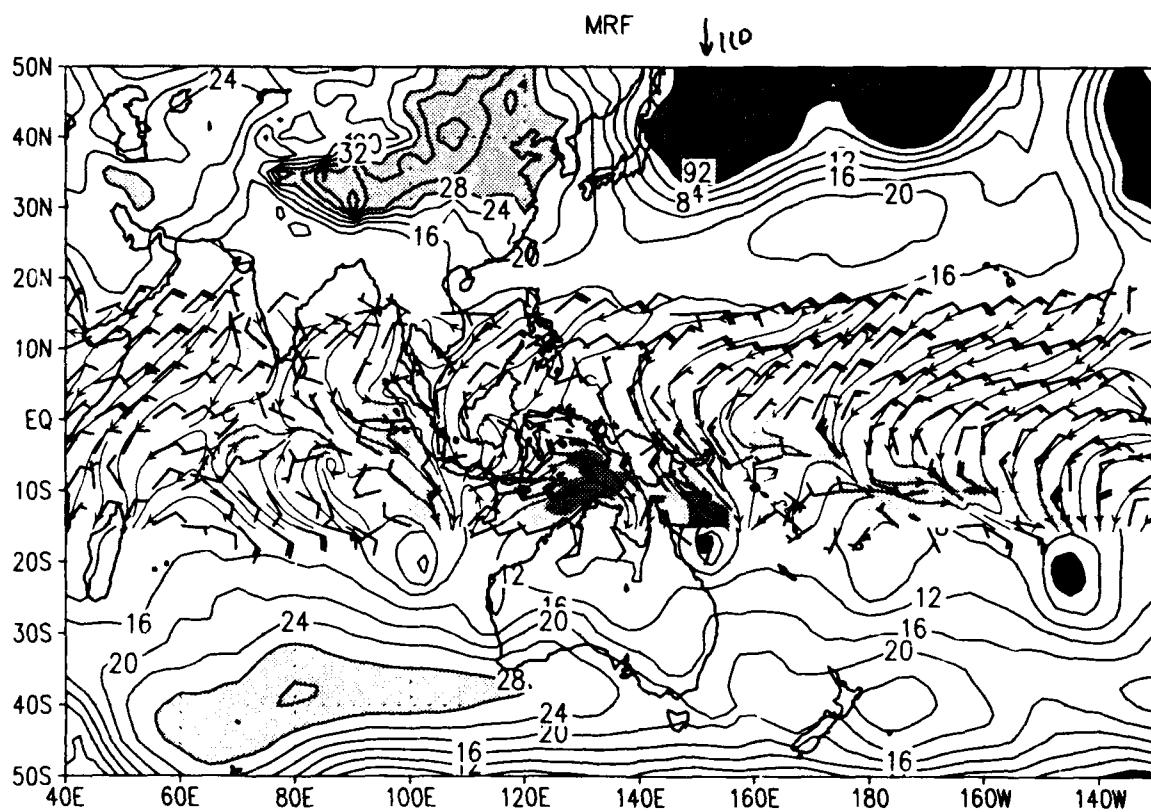
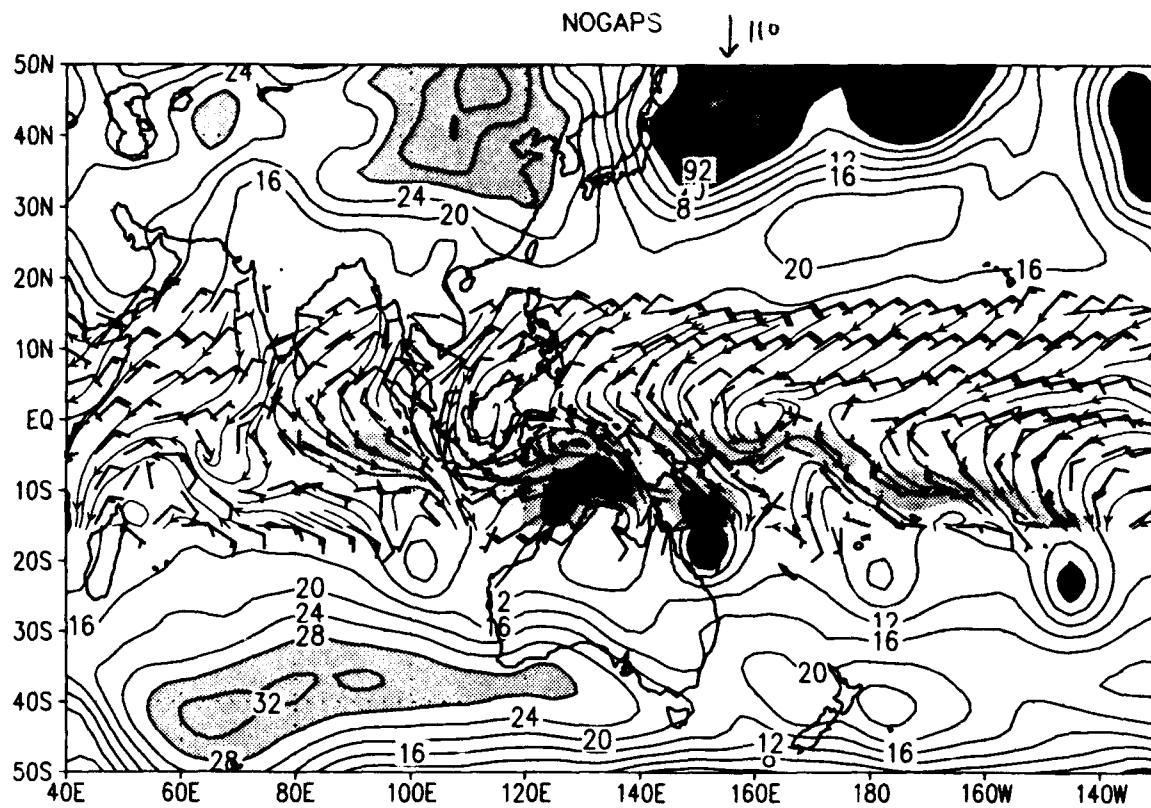
SLP and sfc winds ($u>0$ shaded) for 00Z 06 FEB 1993
slp (mb) wind barbs (kts) /d2/toga_coare/d2.gs



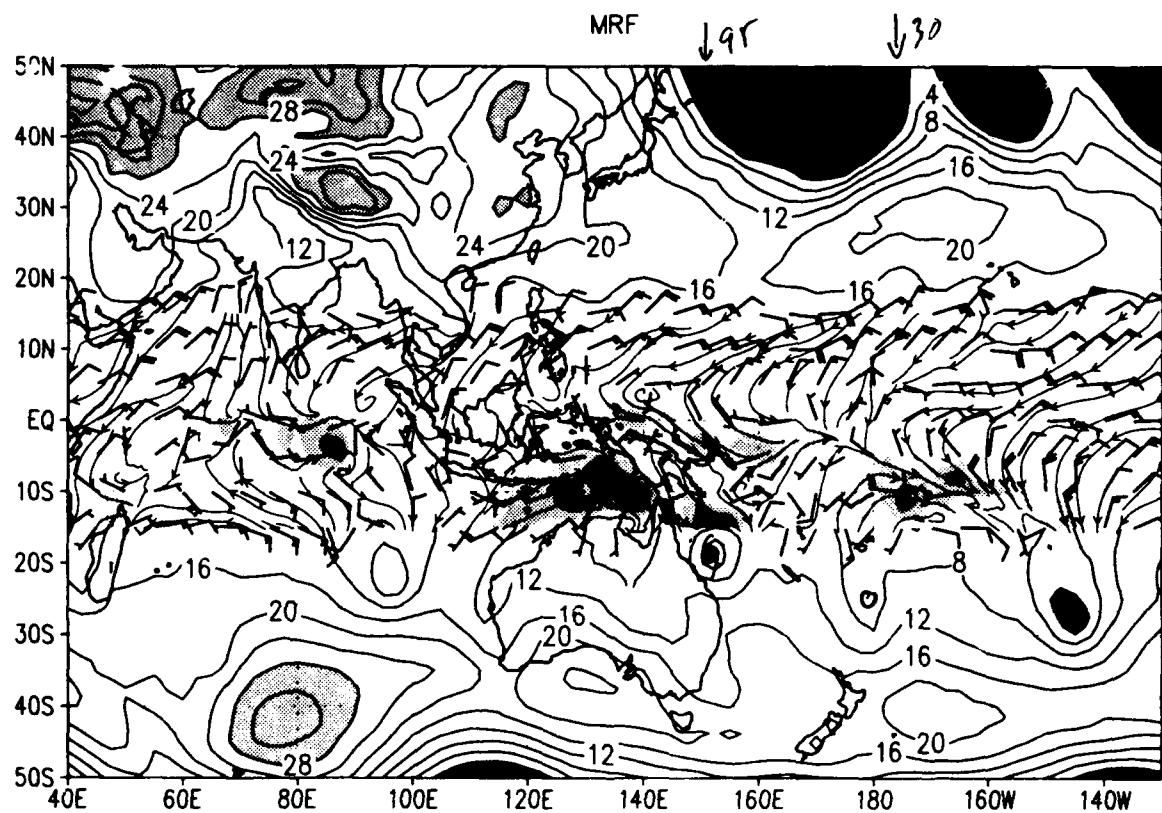
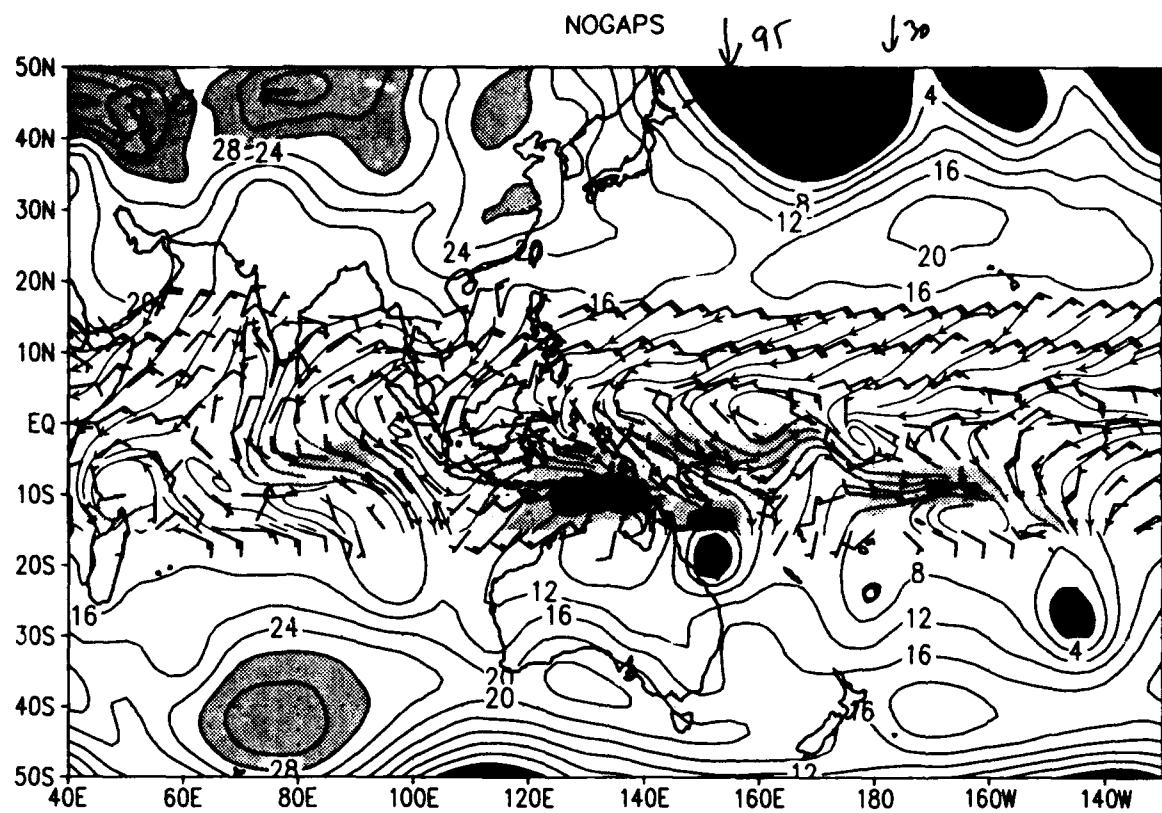
SLP and sfc winds ($u>0$ shaded) for 00Z 07 FEB 1993
slp (mb) wind barbs (kts) /d2/toga_coare/d2.gs



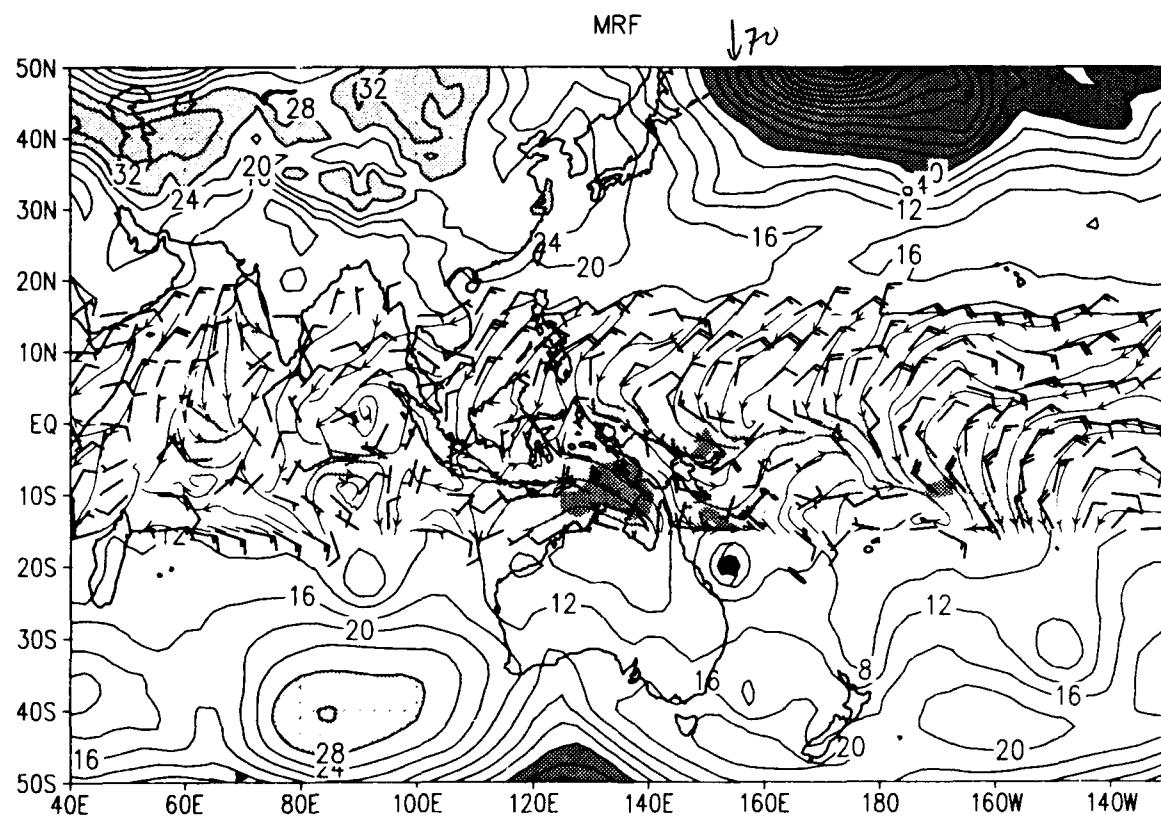
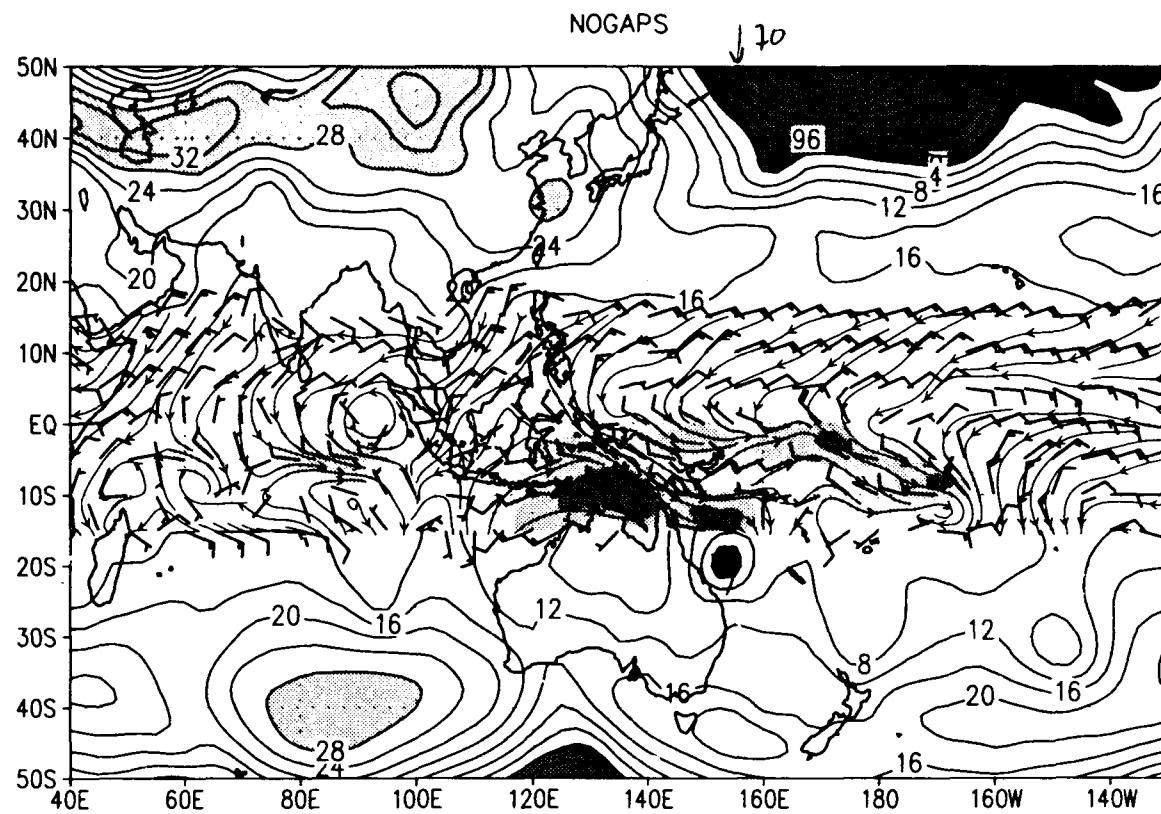
SLP and sfc winds ($u>0$ shaded) for 00Z 08 FEB 1993
slp (mb) wind barbs (kts) /d2/toga_coare/d2.gs



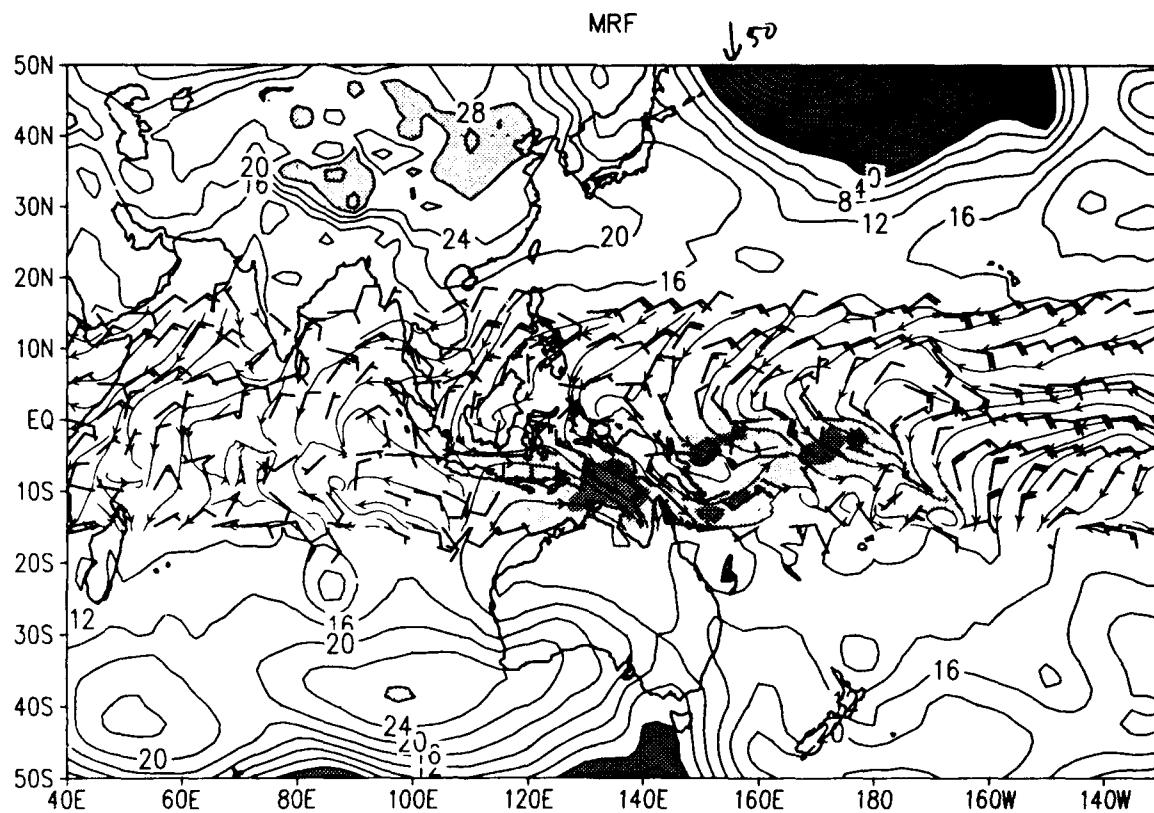
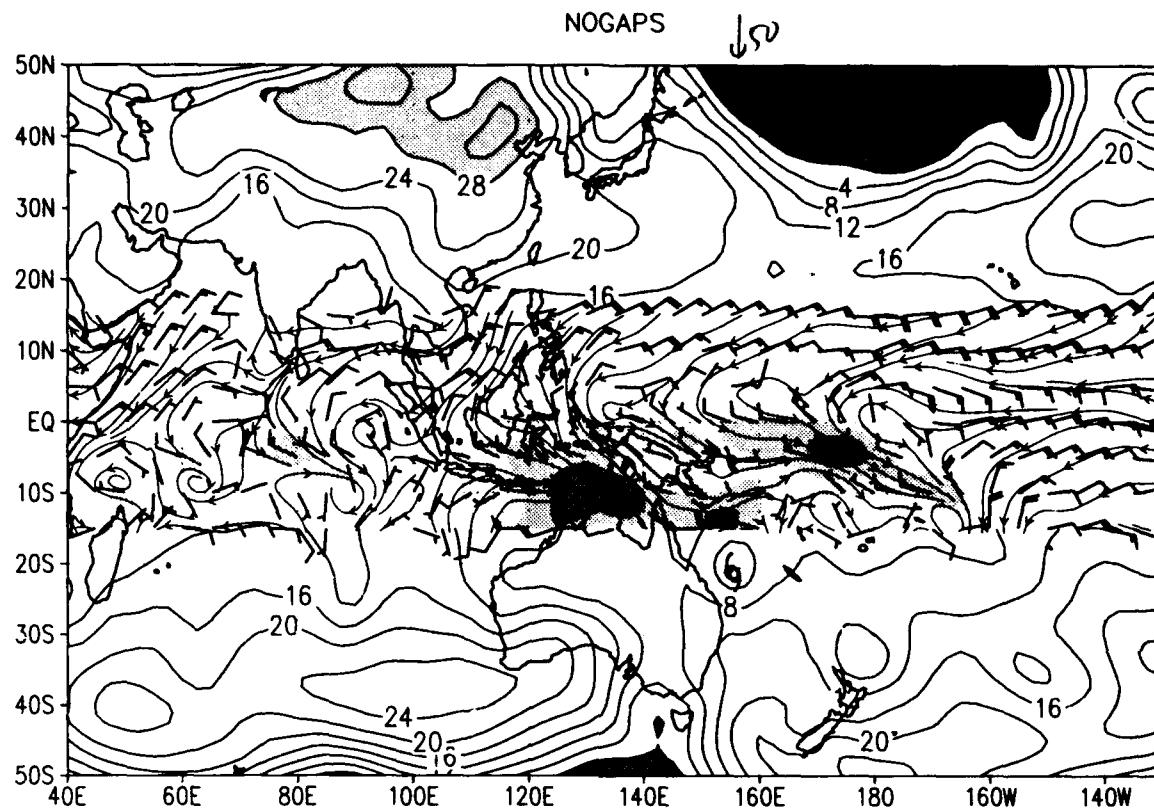
SLP and sfc winds ($u>0$ shaded) for 00Z 09 FEB 1993
slp (mb) wind barbs (kts) /d2/toga_coare/d2.gs



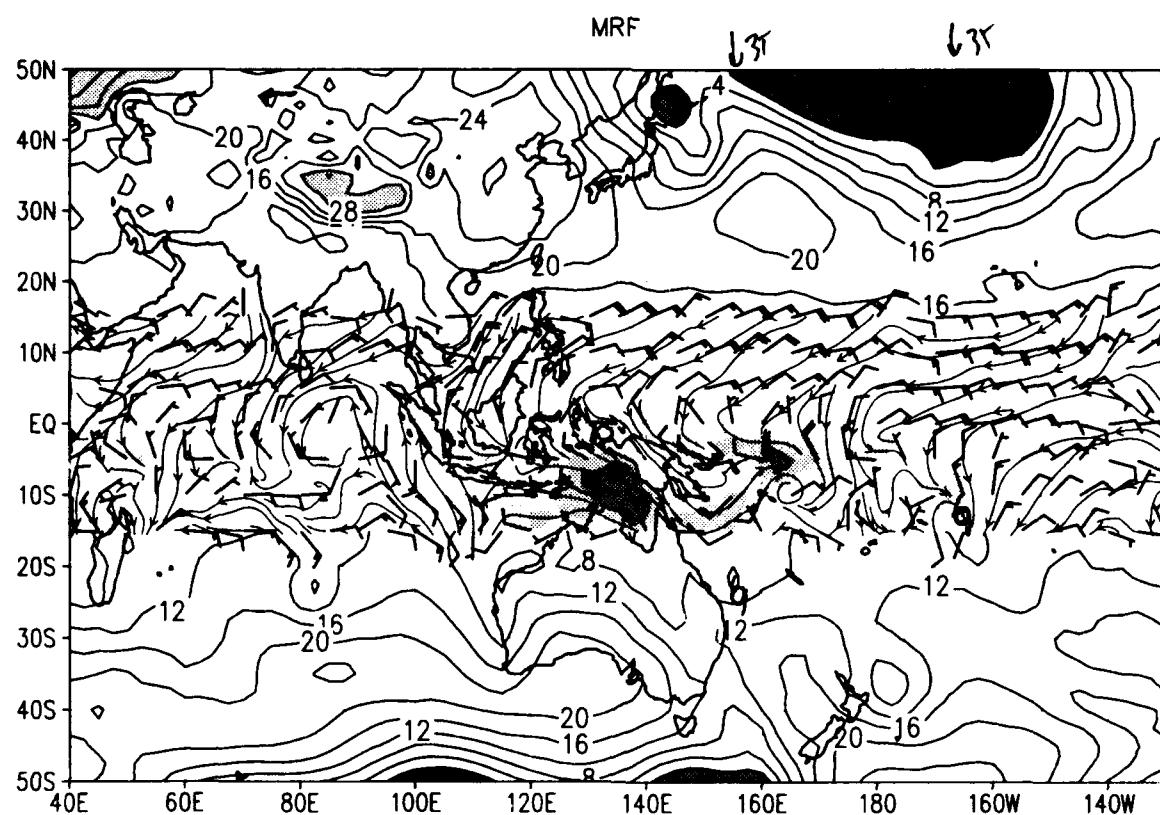
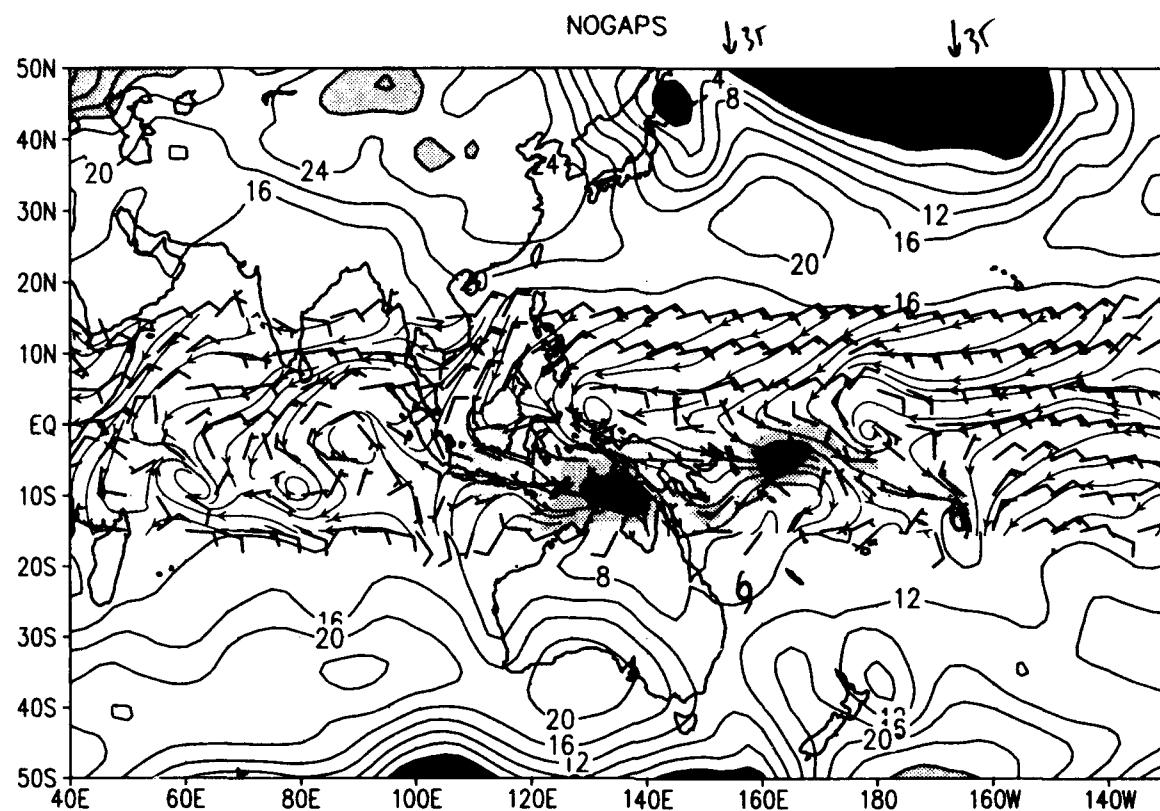
SLP and sfc winds ($u>0$ shaded) for 00Z 10 FEB 1993
slp (mb) wind barbs (kts) /d2/toga_coare/d2.gs



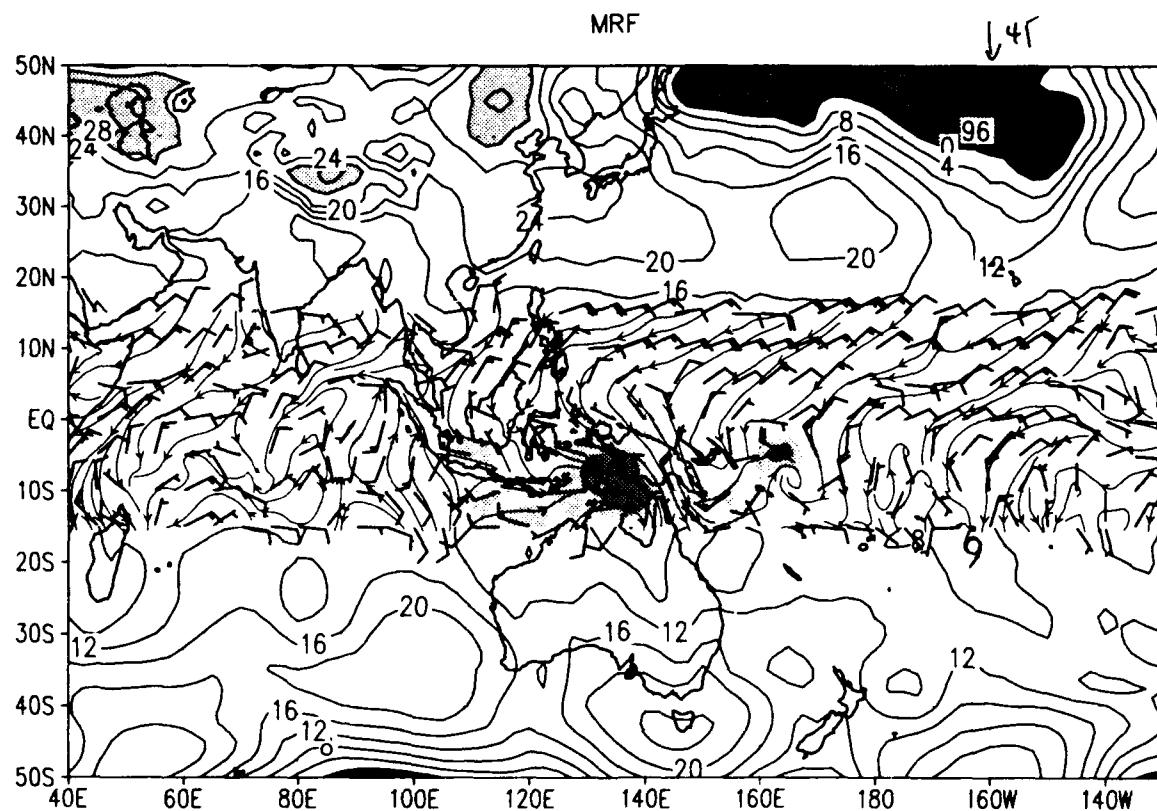
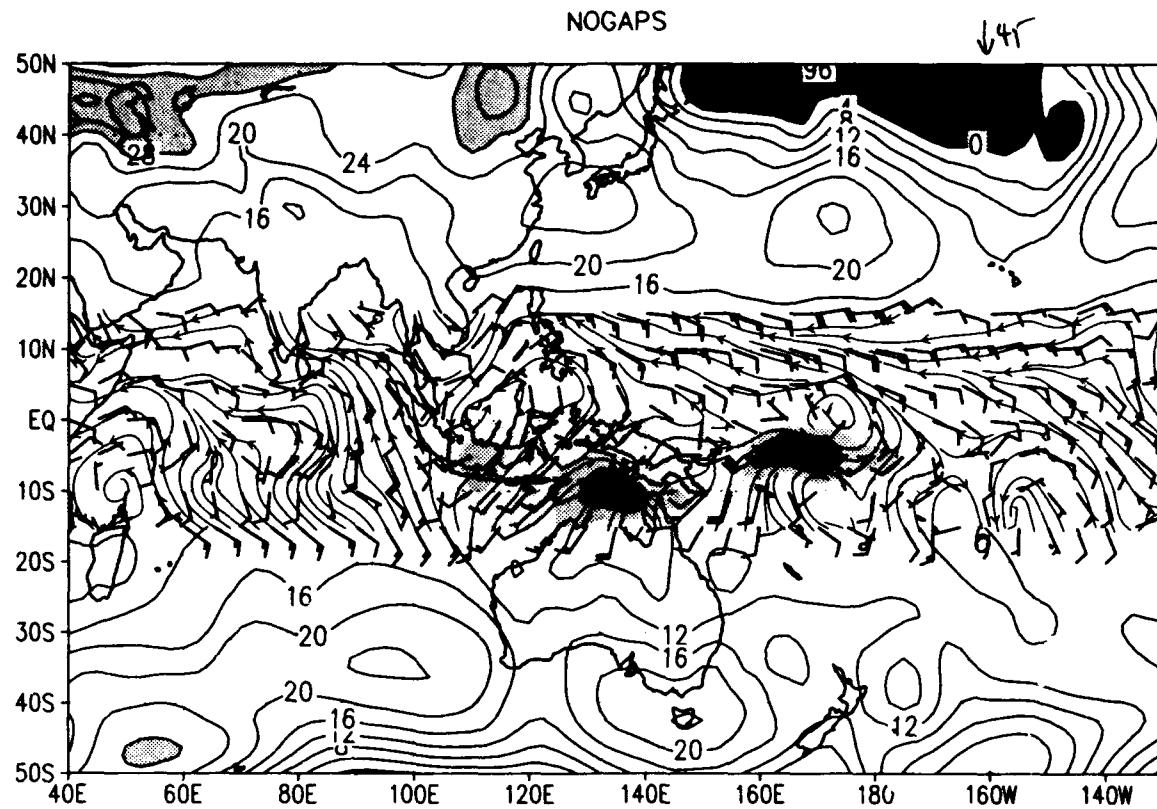
SLP and sfc winds ($u>0$ shaded) for 00Z 11 FEB 1993
slp (mb) wind barbs (kts) /d2/toga_coare/d2.gs



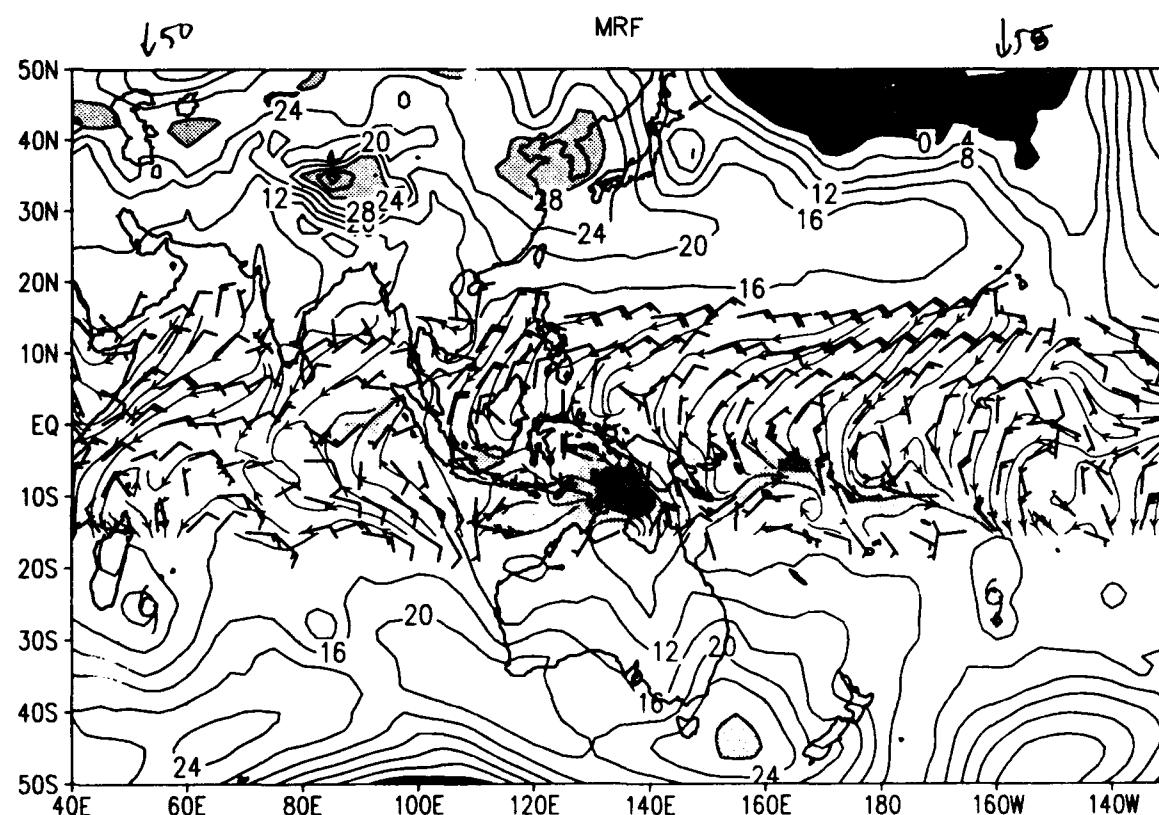
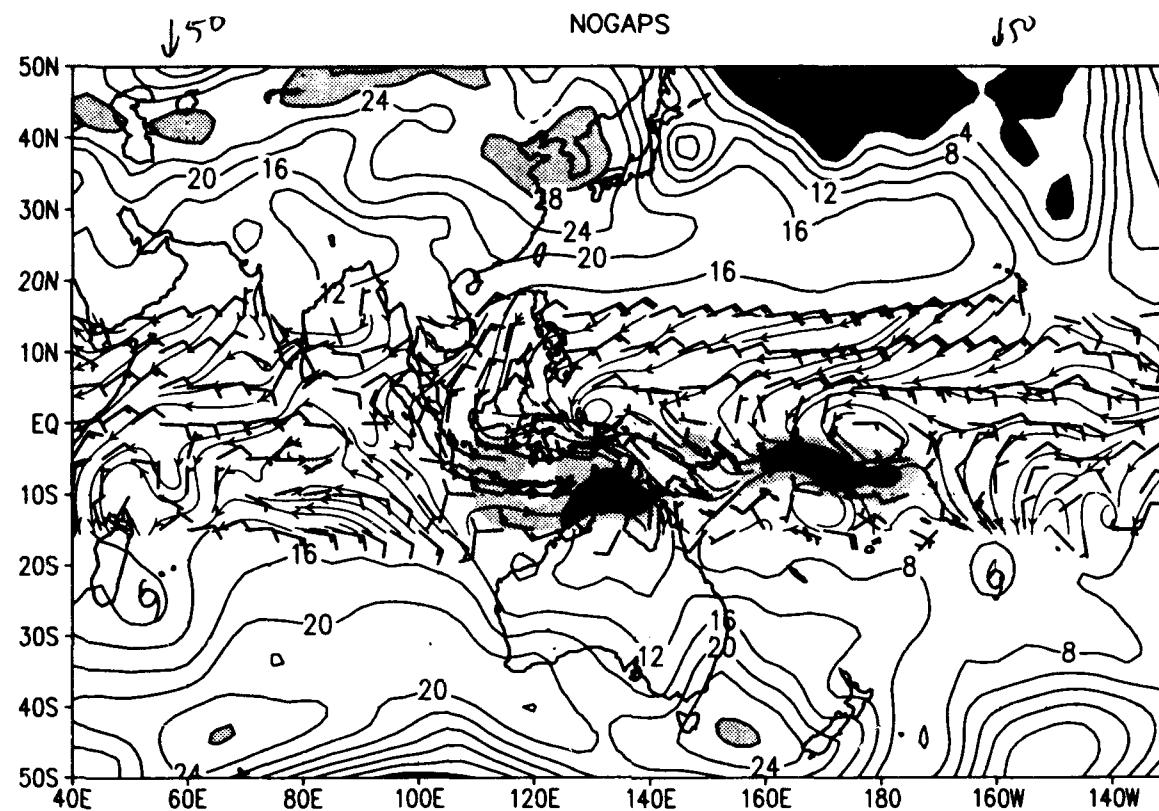
SLP and sfc winds ($u>0$ shaded) for 00Z 12 FEB 1993
slp (mb) wind barbs (kts) /d2/toga_coare/d2.gs



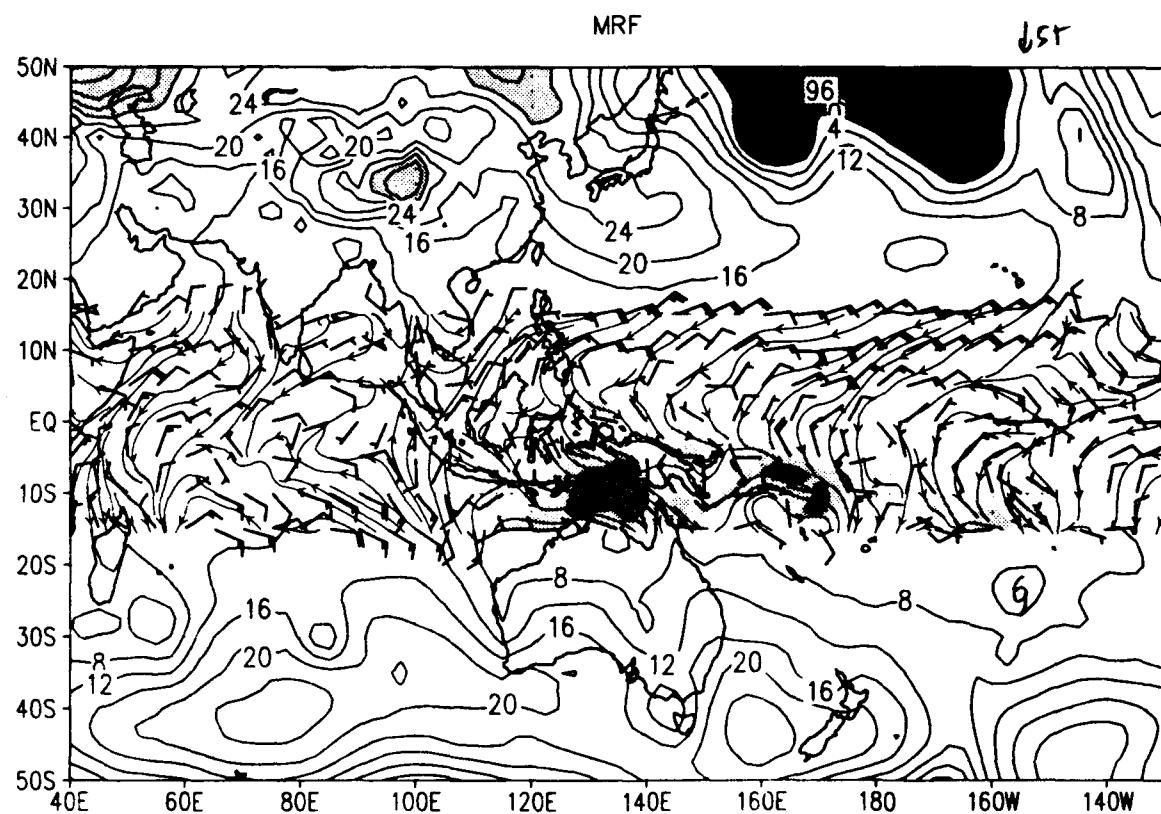
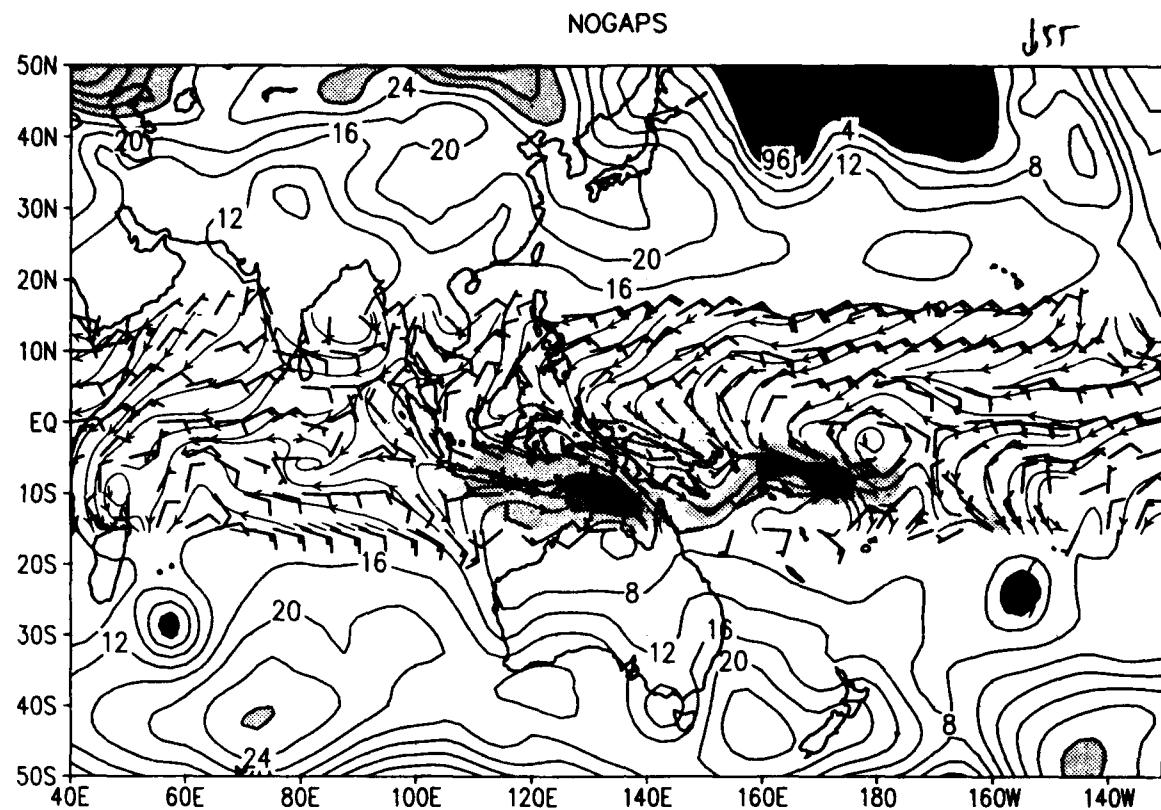
SLP and sfc winds ($u>0$ shaded) for 00Z 13 FEB 1993
slp (mb) wind barbs (kts) /d2/toga_coare/d2.gs



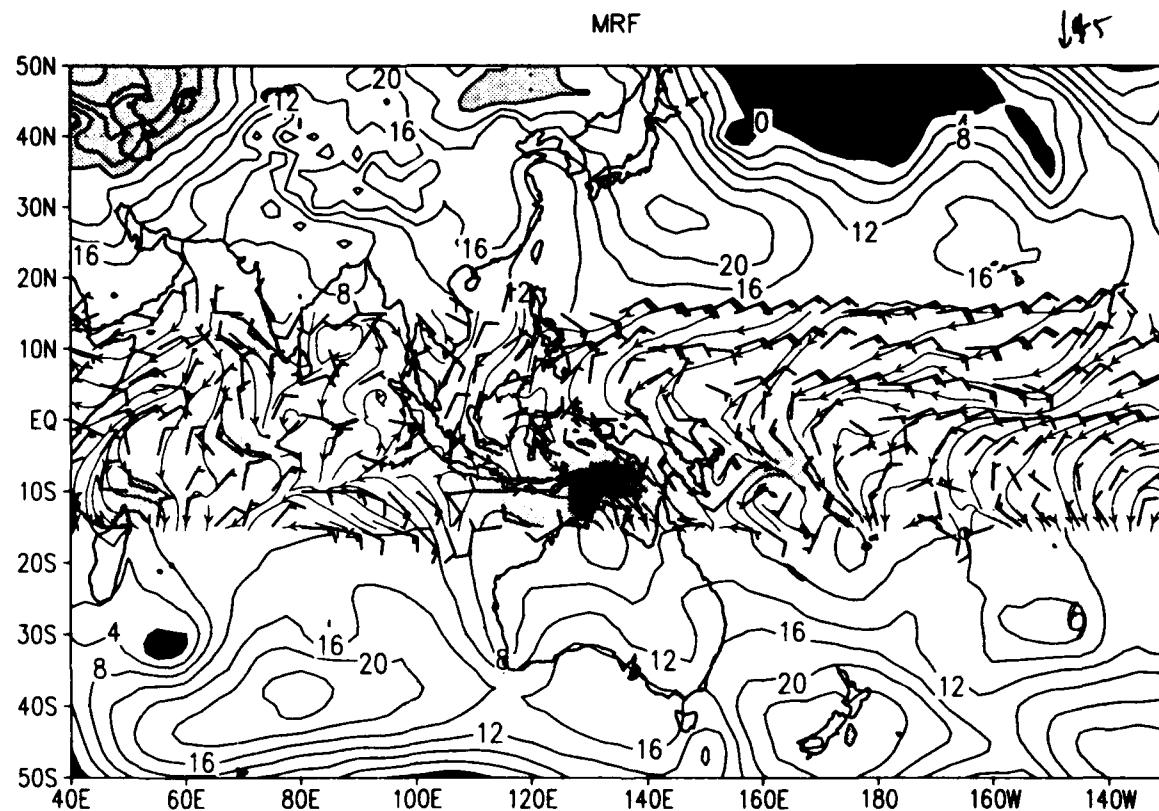
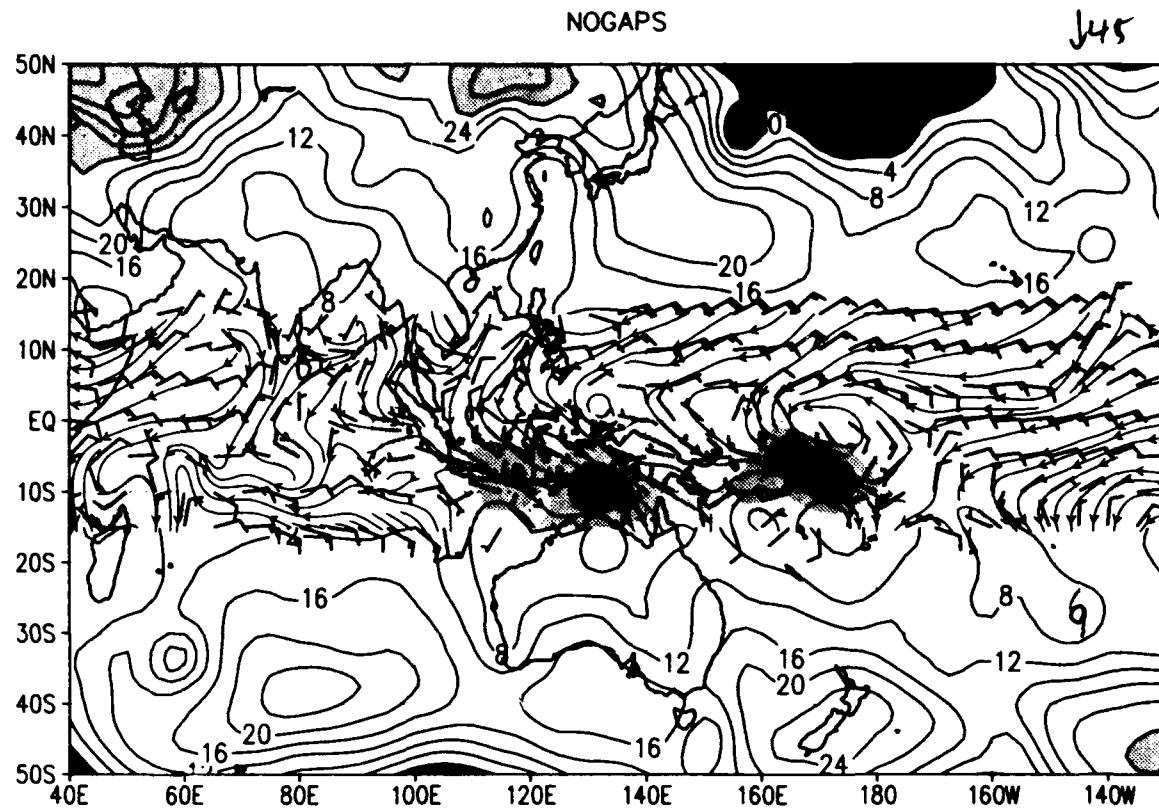
SLP and sfc winds ($u > 0$ shaded) for 00Z 14 FEB 1993
 slp (mb) wind barbs (kts) /d2/toga_coare/d2.gs



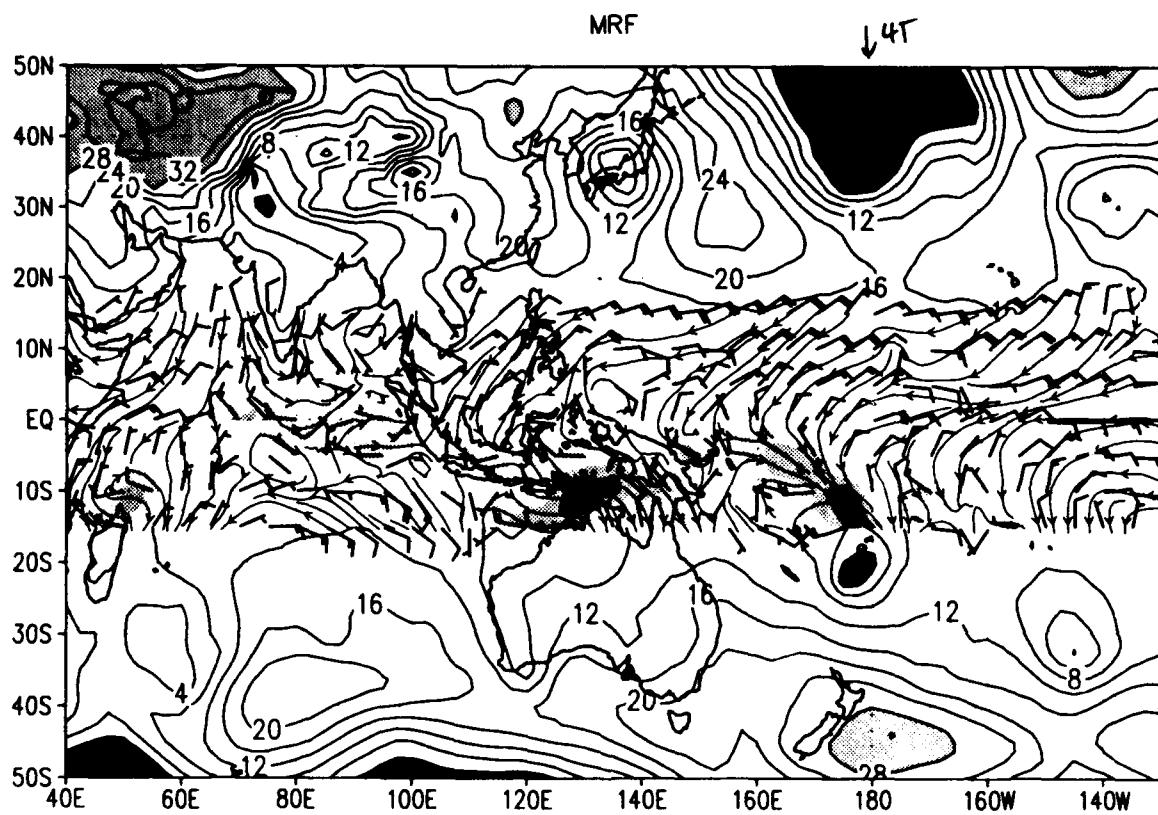
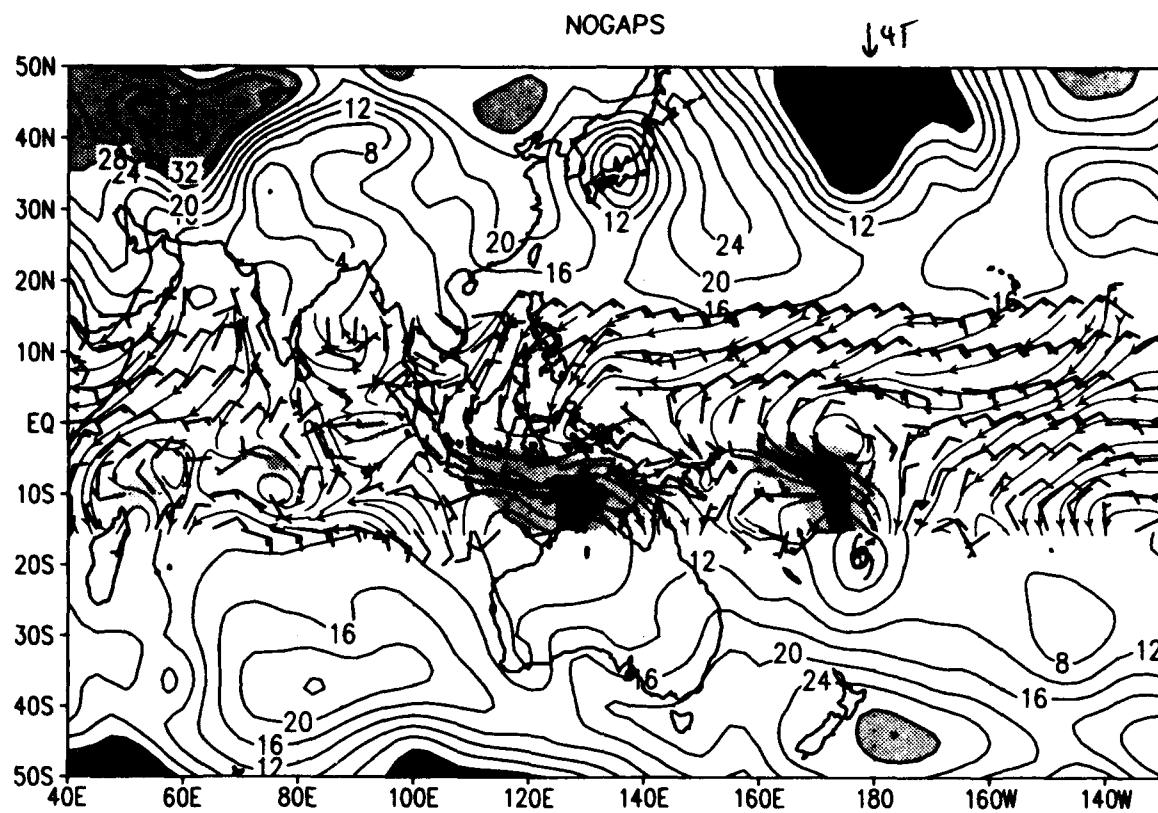
SLP and sfc winds ($u>0$ shaded) for 00Z 15 FEB 1993
slp (mb) wind barbs (kts) /d2/toga_coare/d2.gs



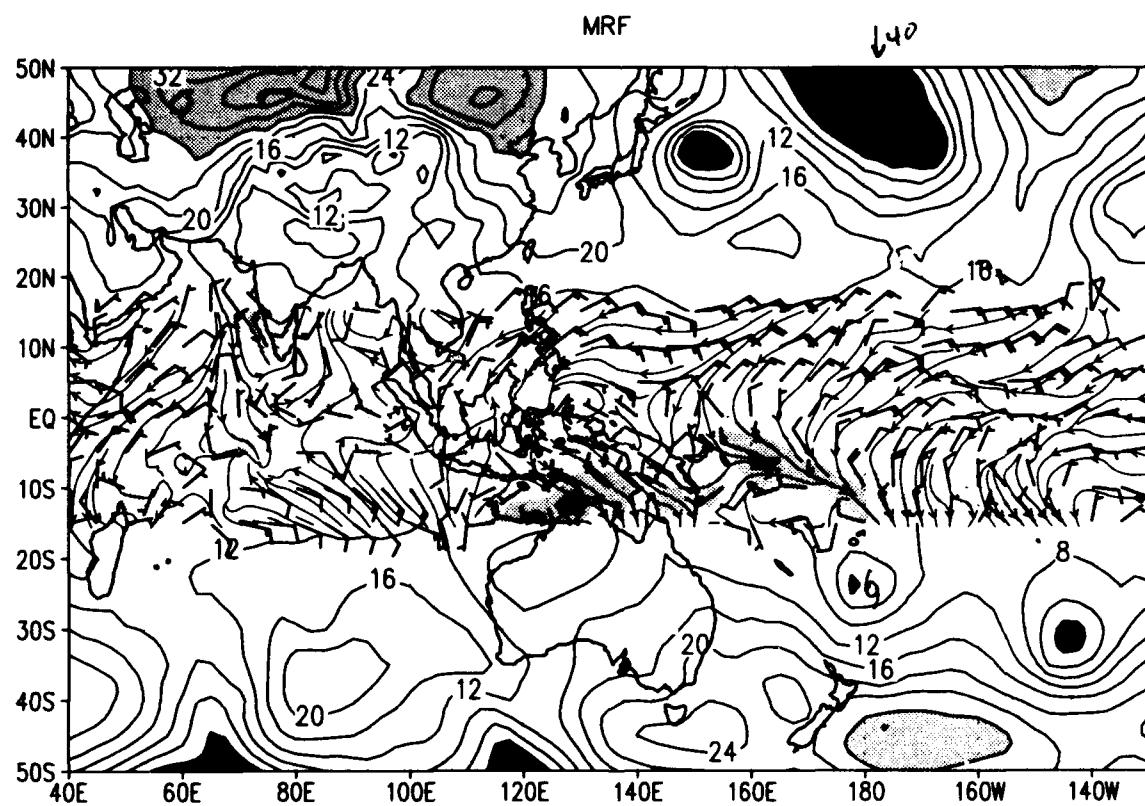
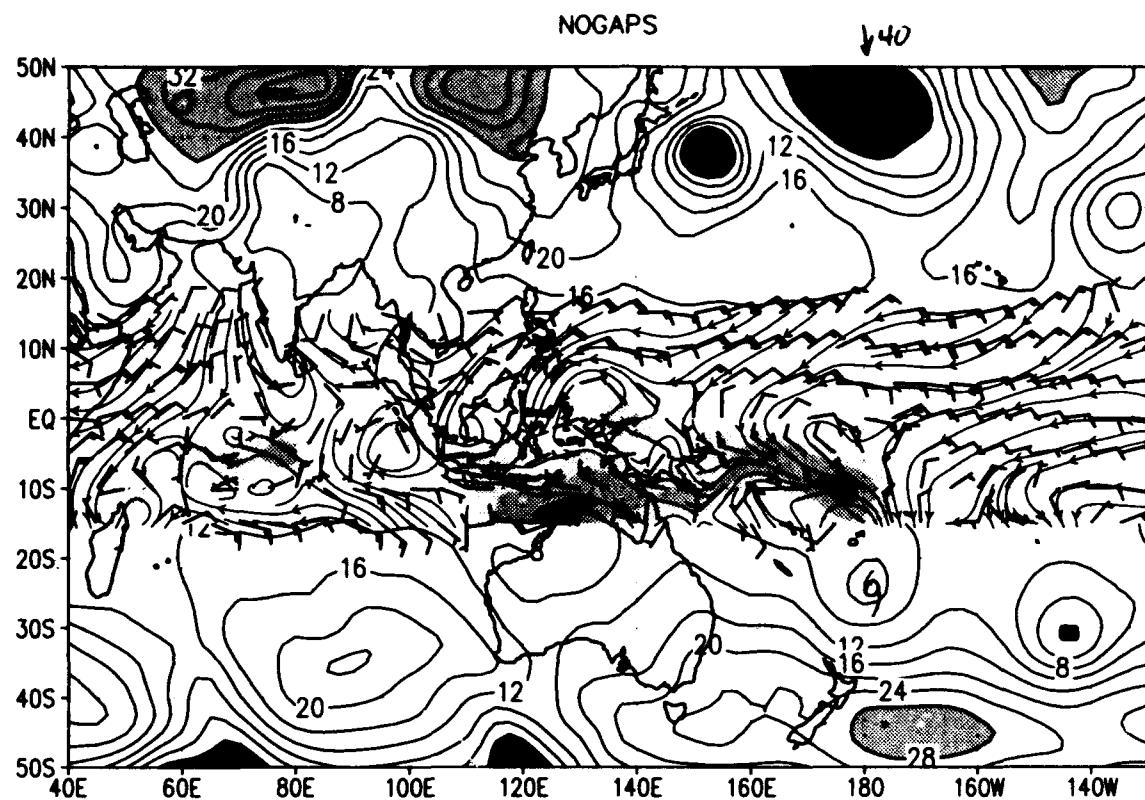
SLP and sfc winds ($u>0$ shaded) for 00Z 16 FEB 1993
slp (mb) wind barbs (kts) /d2/toga_coare/d2.gs



SLP and sfc winds ($u>0$ shaded) for 00Z 17 FEB 1993
slp (mb) wind barbs (kts) /d2/toga_coare/d2.gs

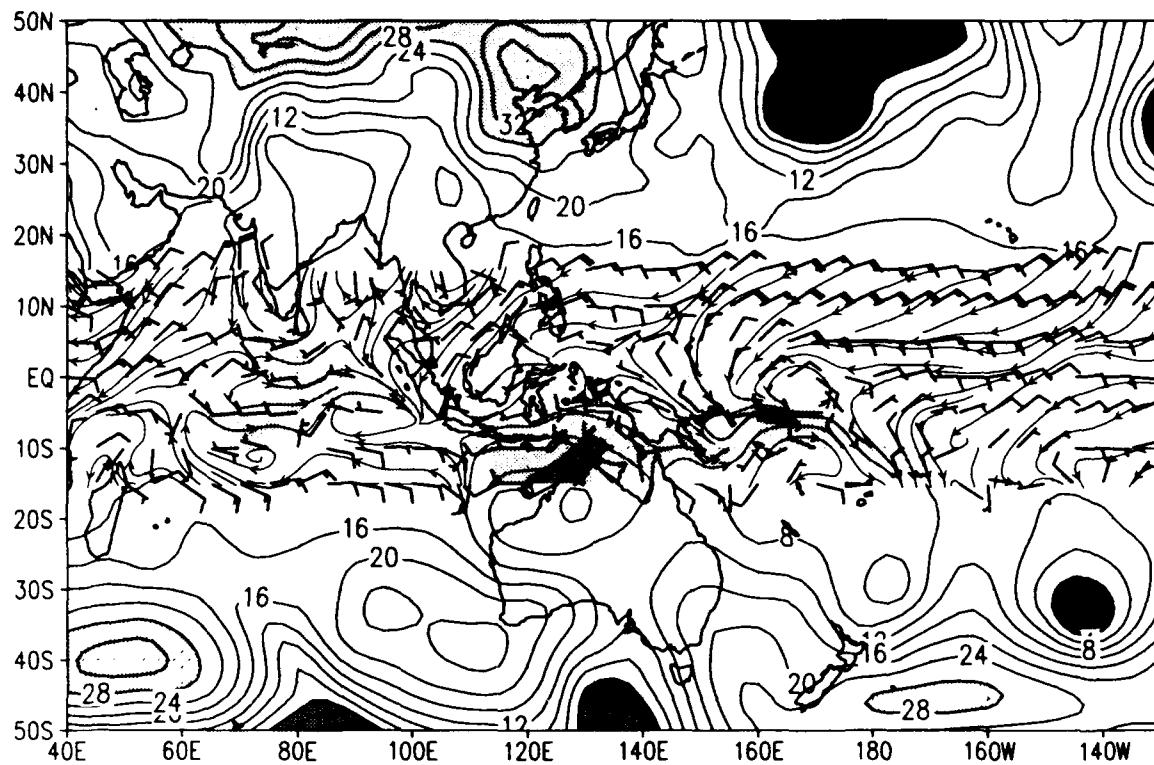


SLP and sfc winds ($u>0$ shaded) for 00Z 18 FEB 1993
slp (mb) wind barbs (kts) /d2/toga_coare/d2.gs

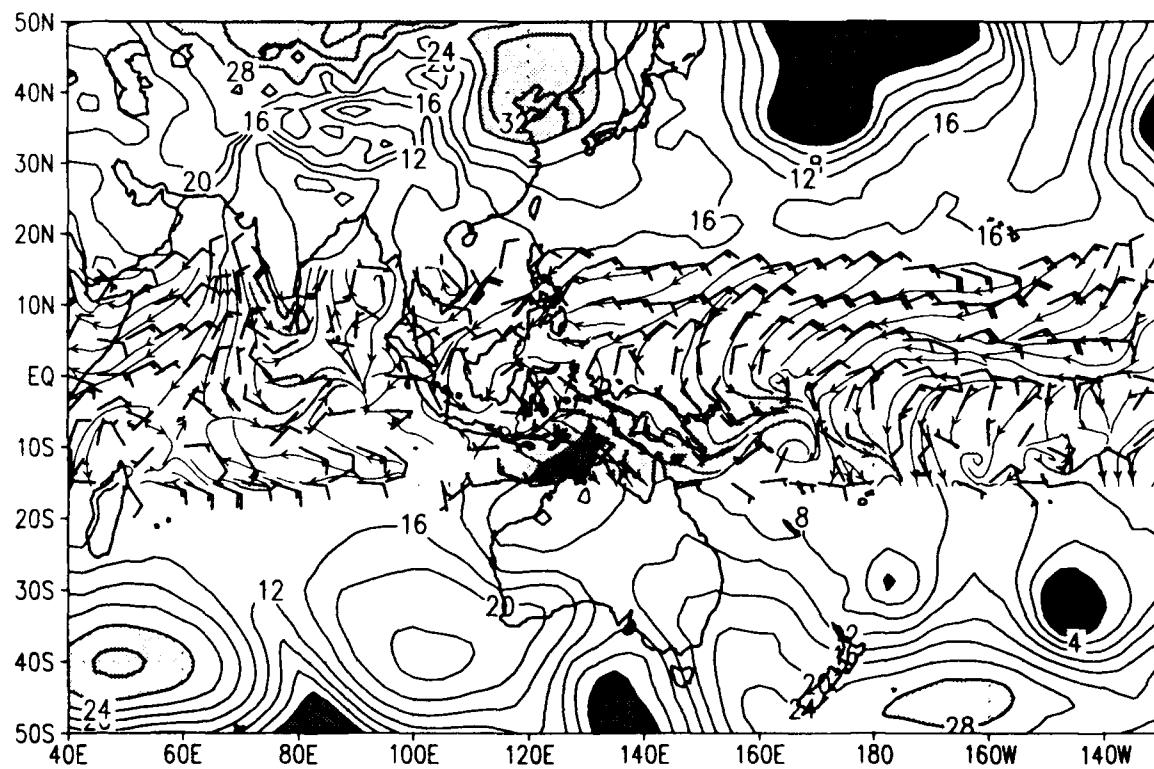


SLP and sfc winds ($u>0$ shaded) for 00Z 19 FEB 1993
slp (mb) wind barbs (kts) /d2/toga_coare/d2.gs

NOGAPS

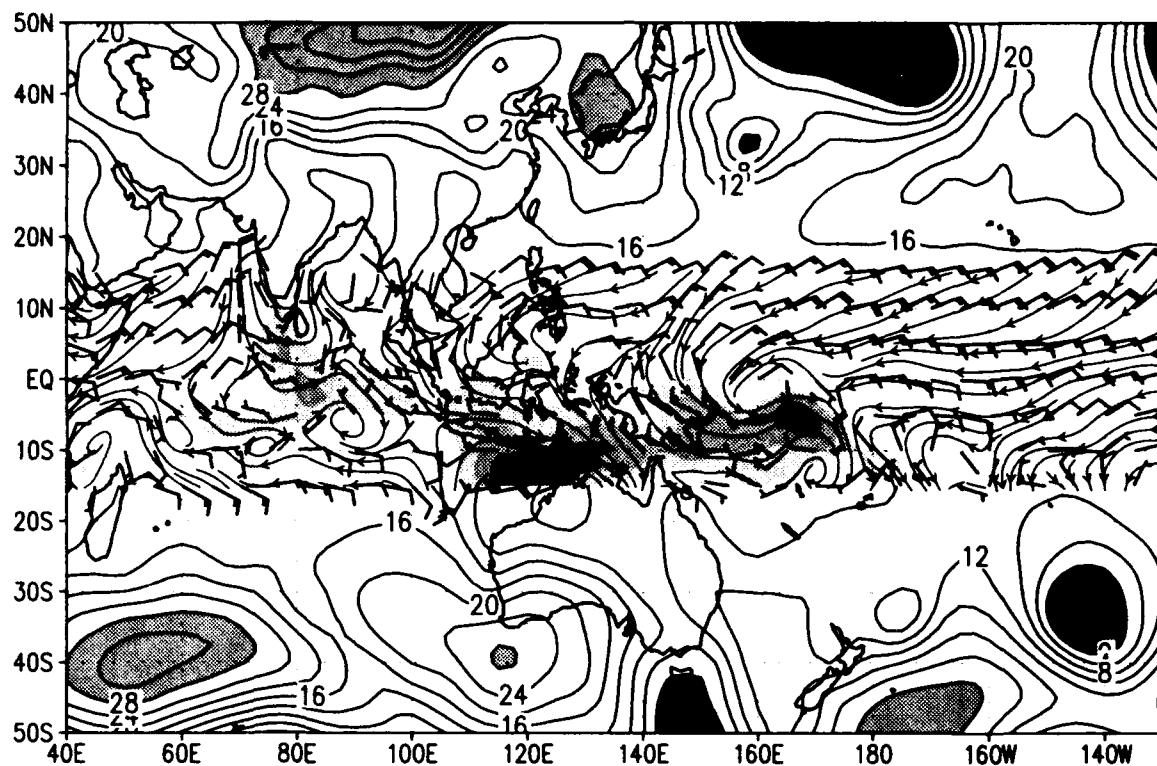


MRF

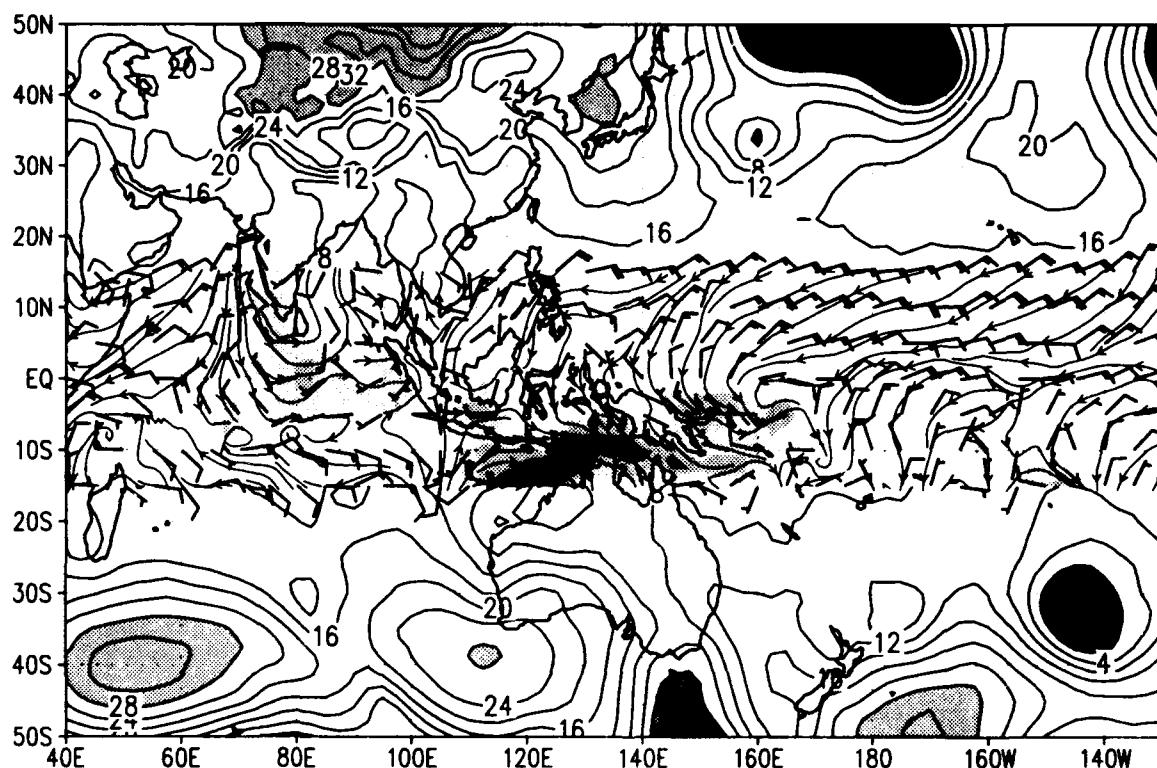


SLP and sfc winds ($u > 0$ shaded) for 00Z 20 FEB 1993
slp (mb) wind barbs (kts) /d2/toga_coare/d2.gs

NOGAPS

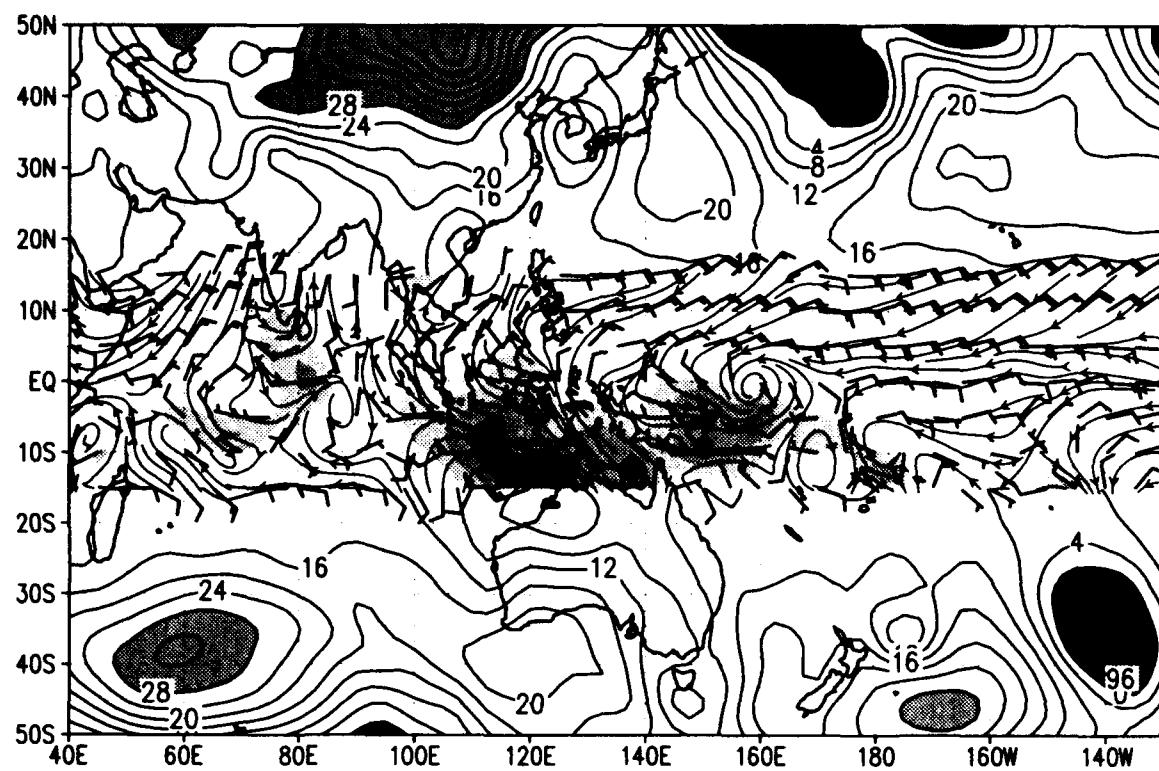


MRF

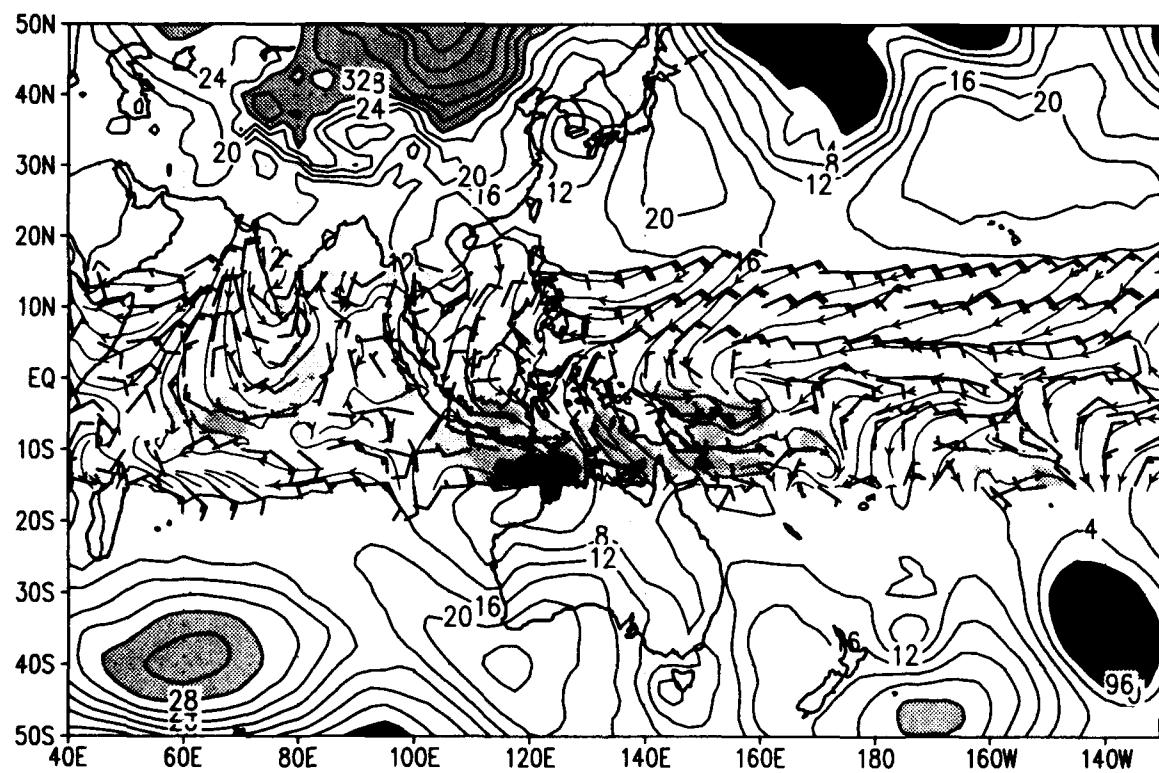


SLP and sfc winds ($u>0$ shaded) for 00Z 21 FEB 1993
slp (mb) wind barbs (kts) /d2/toga_coare/d2.gs

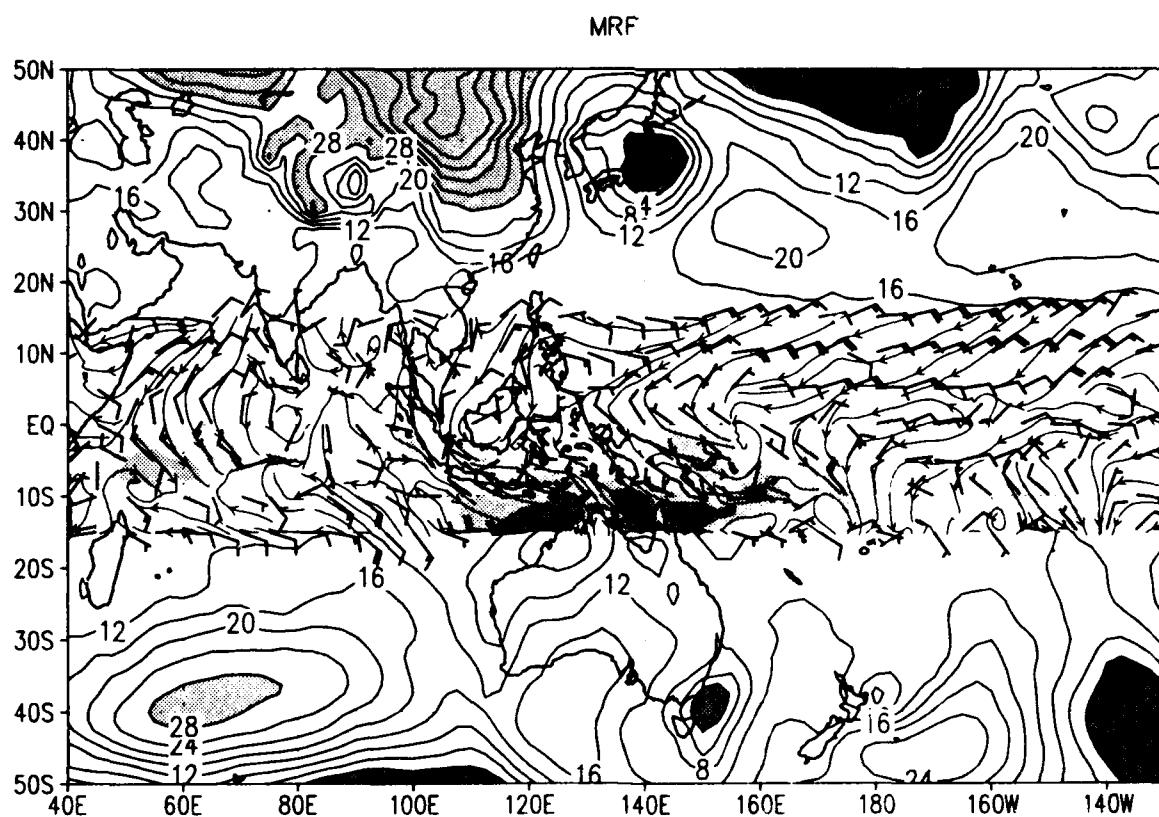
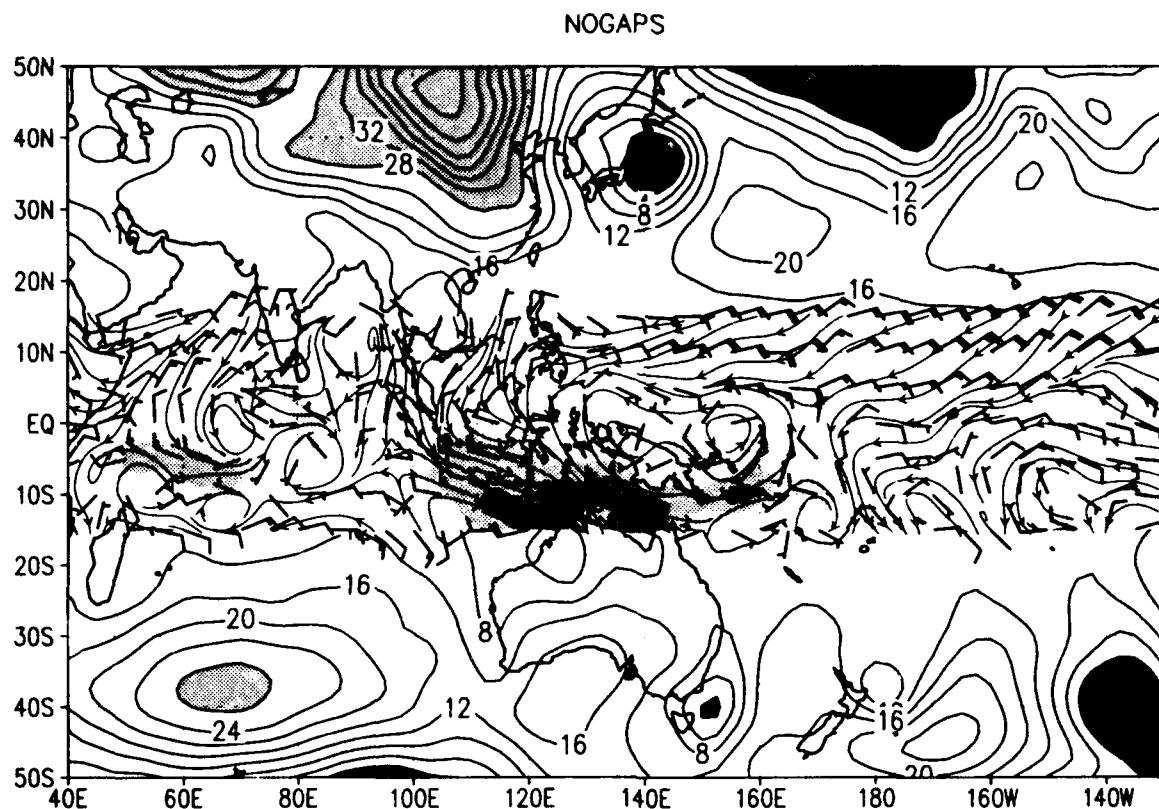
NOGAPS



MRF

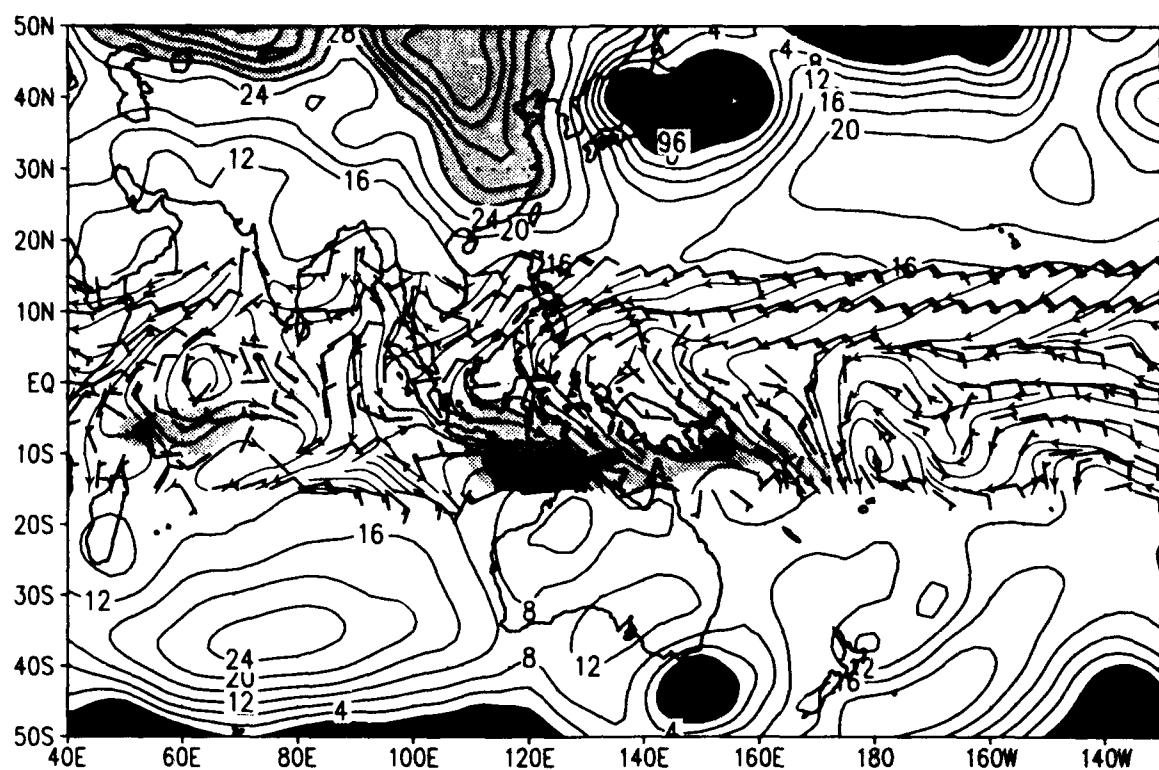


SLP and sfc winds ($u>0$ shaded) for 00Z 22 FEB 1993
slp (mb) wind barbs (kts) /d2/toga_coare/d2.gs

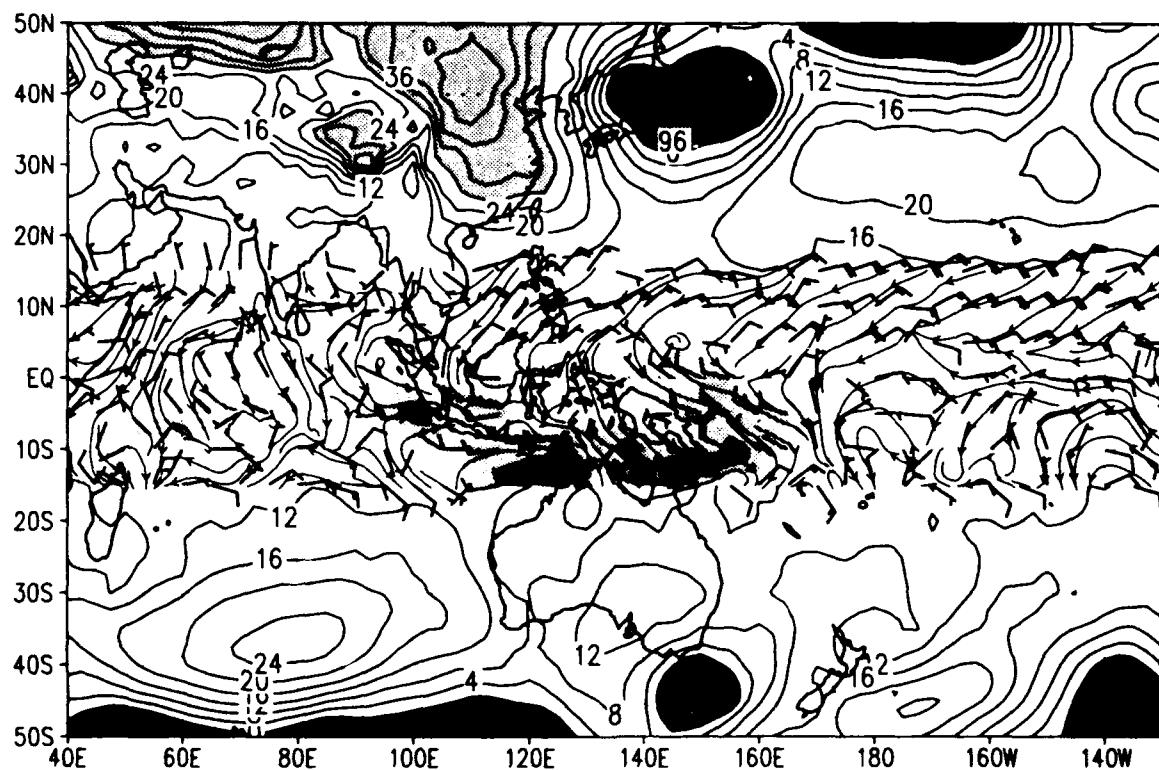


SLP and sfc winds ($u>0$ shaded) for 00Z 23 FEB 1993
slp (mb) wind barbs (kts) /d2/toga_coare/d2.gs

NOGAPS

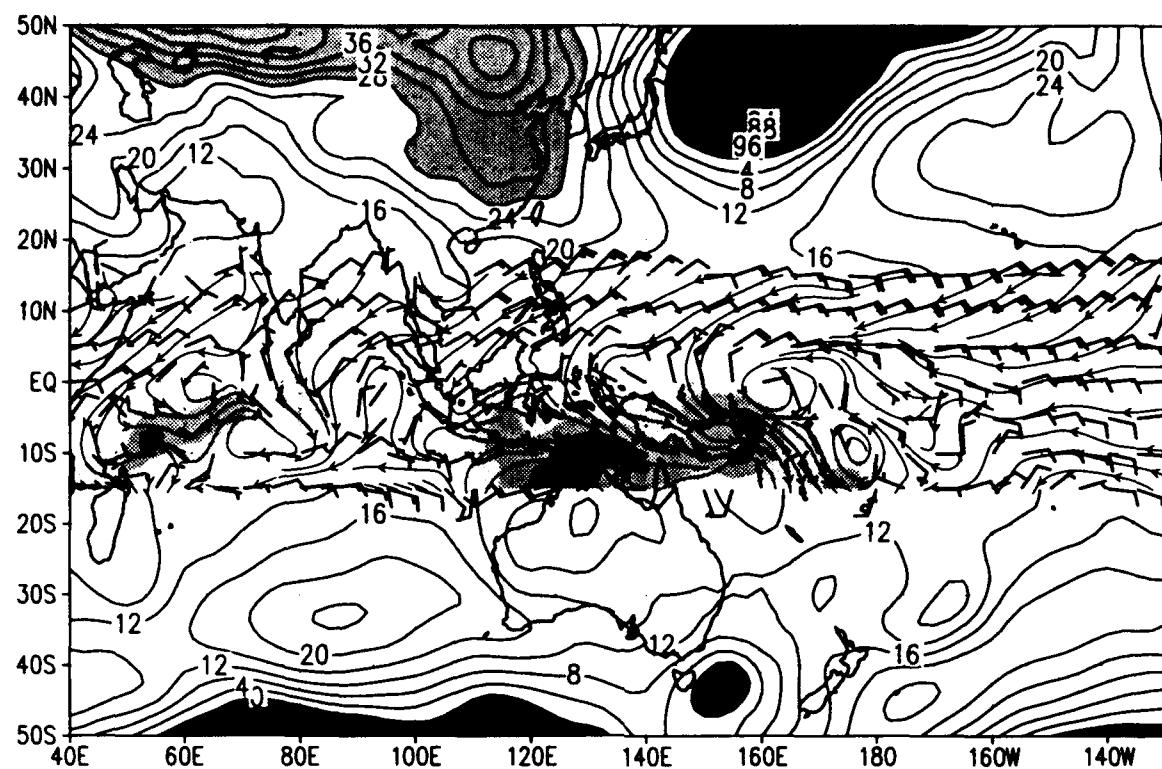


MRF

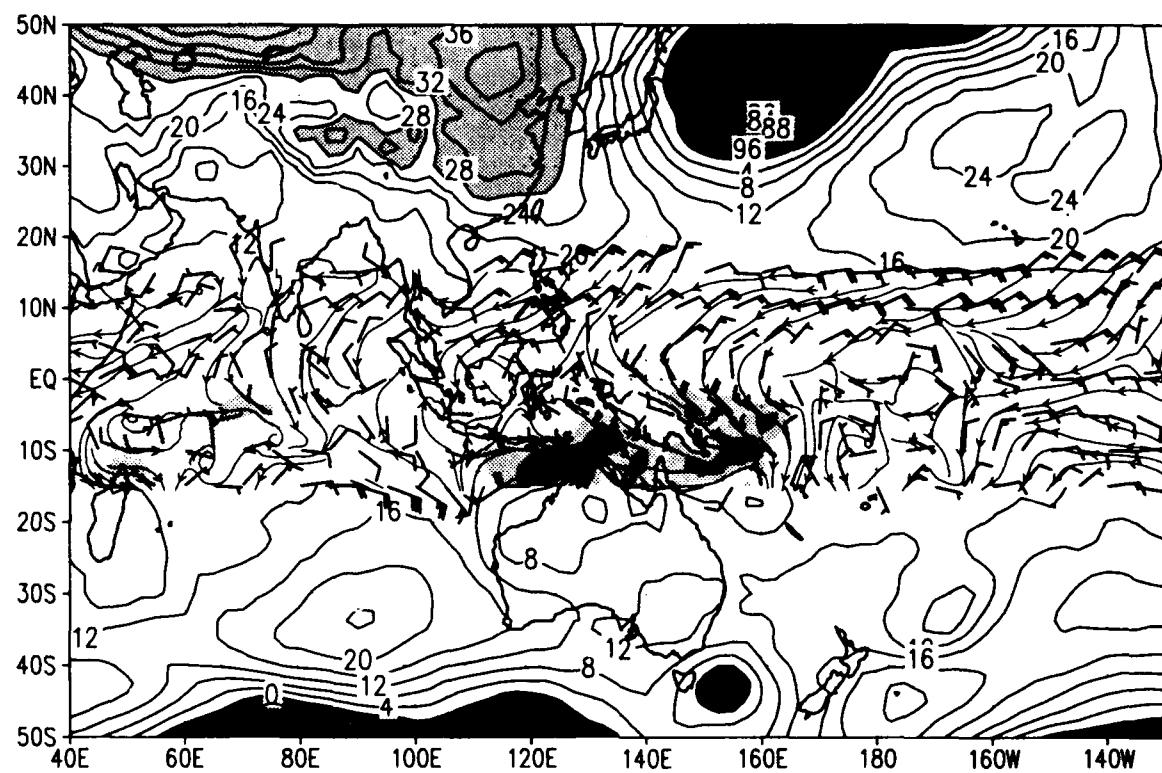


SLP and sfc winds ($u>0$ shaded) for 00Z 24 FEB 1993
slp (mb) wind barbs (kts) /d2/toga_coare/d2.gs

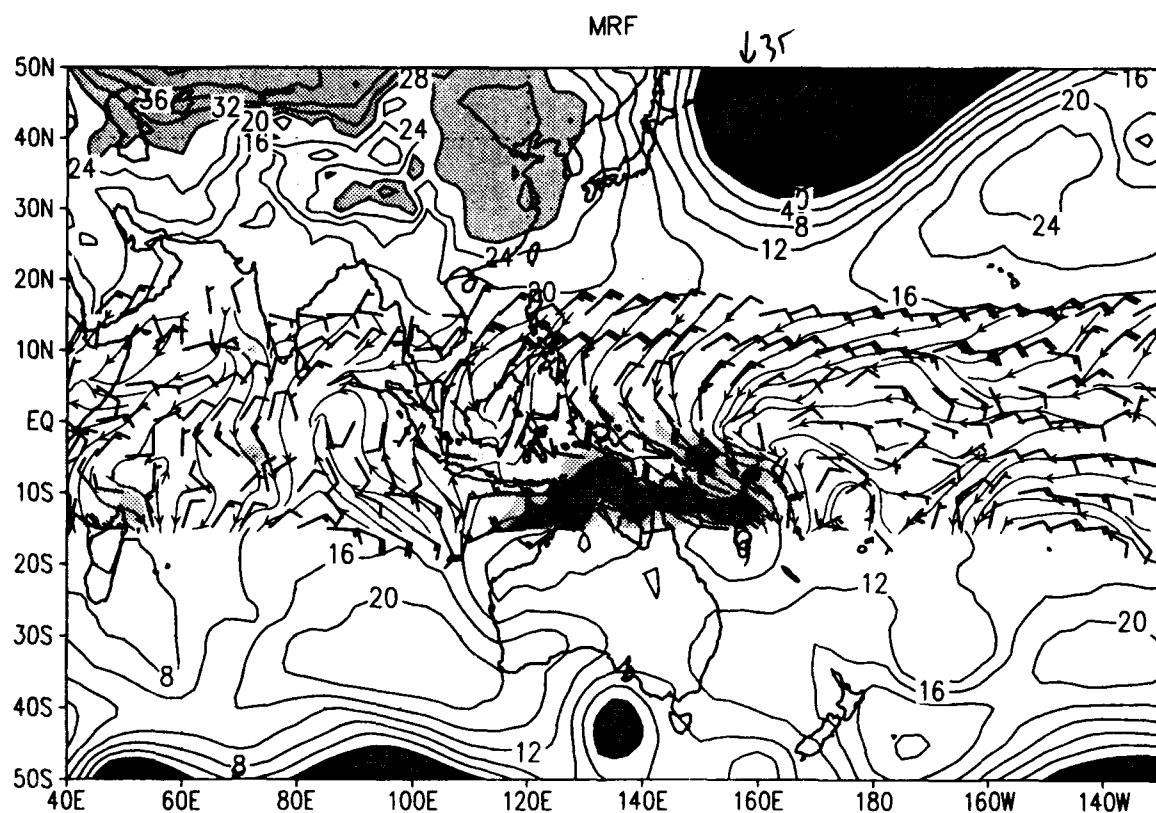
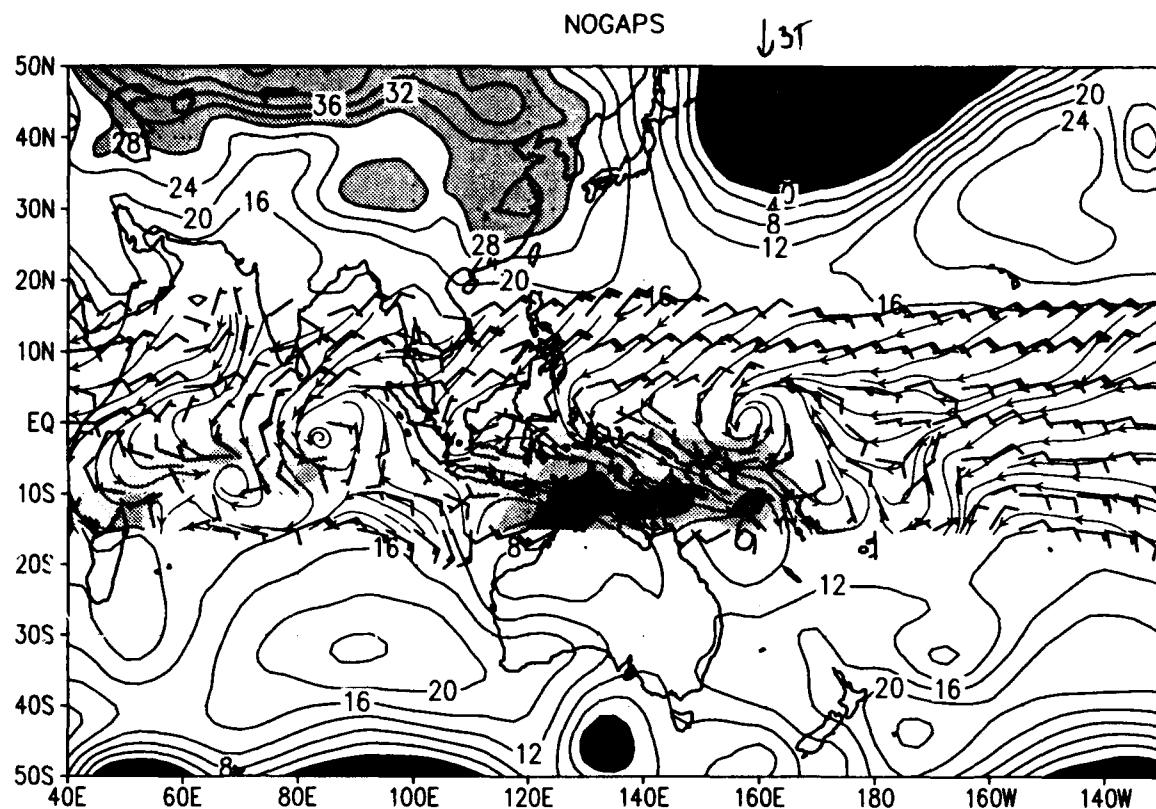
NOGAPS



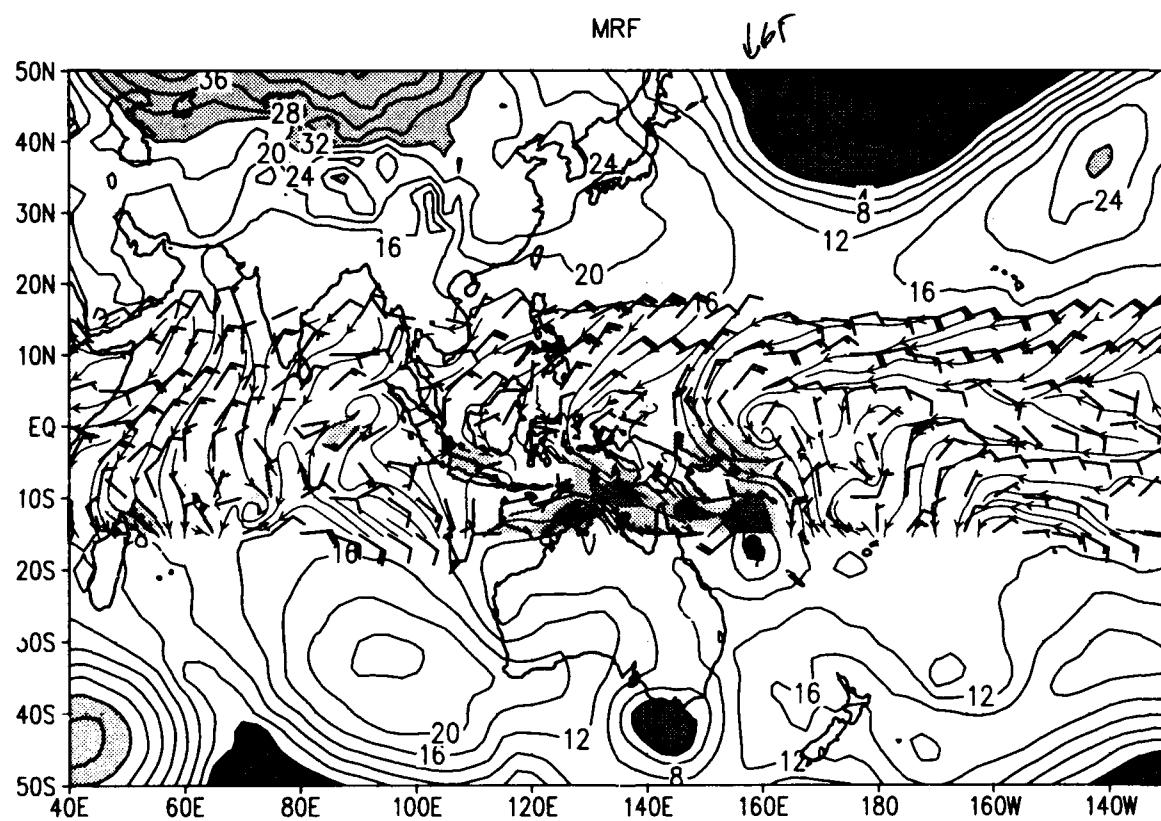
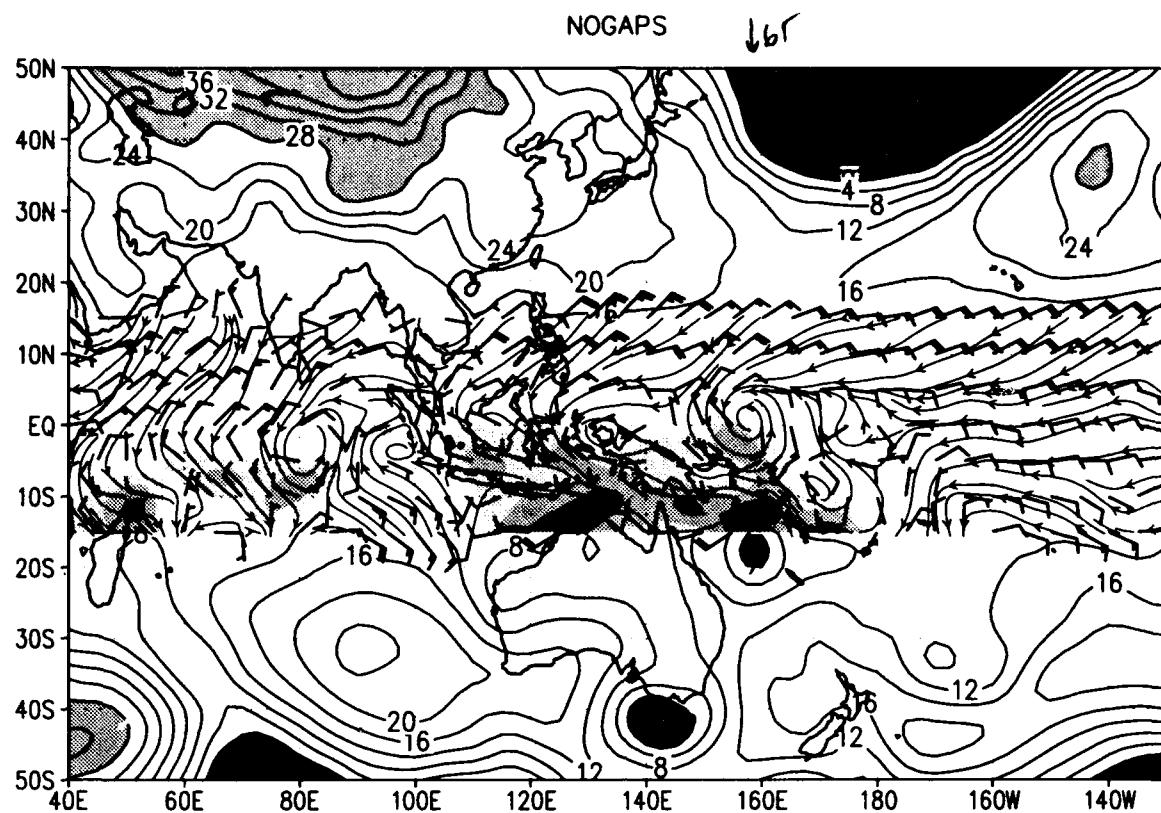
MRF



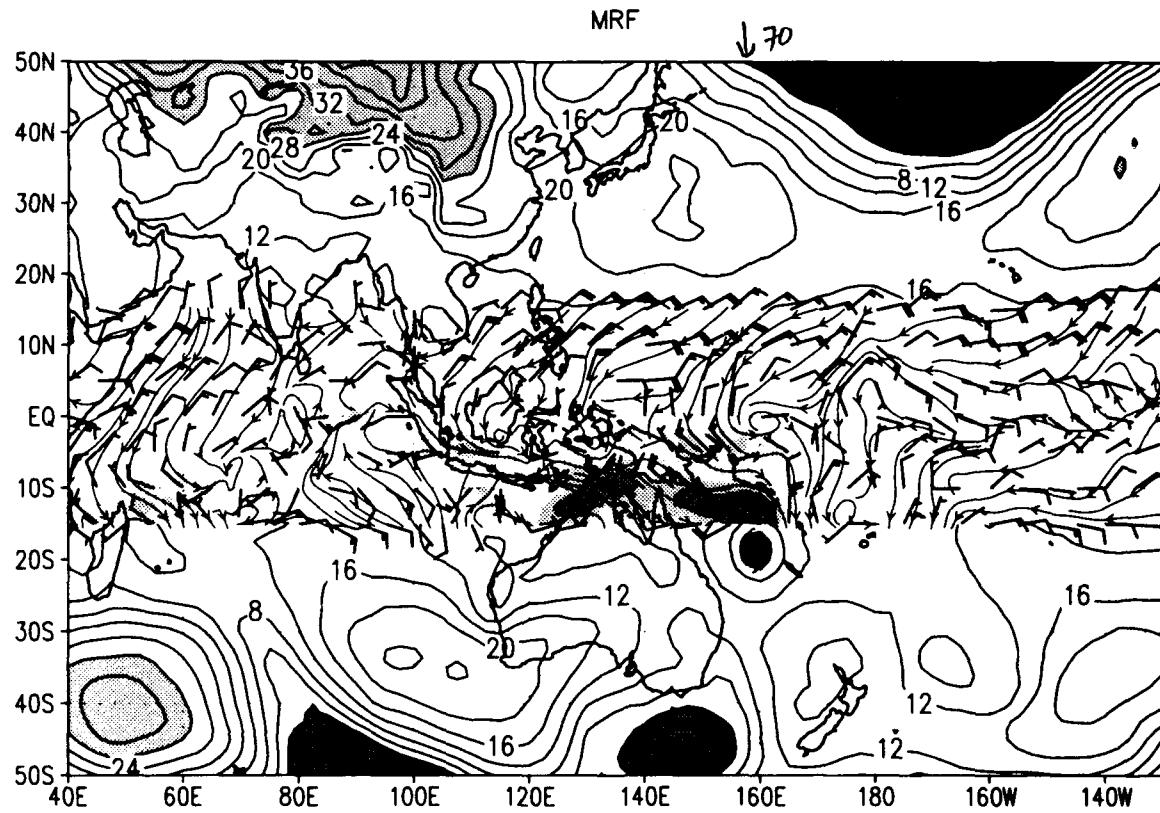
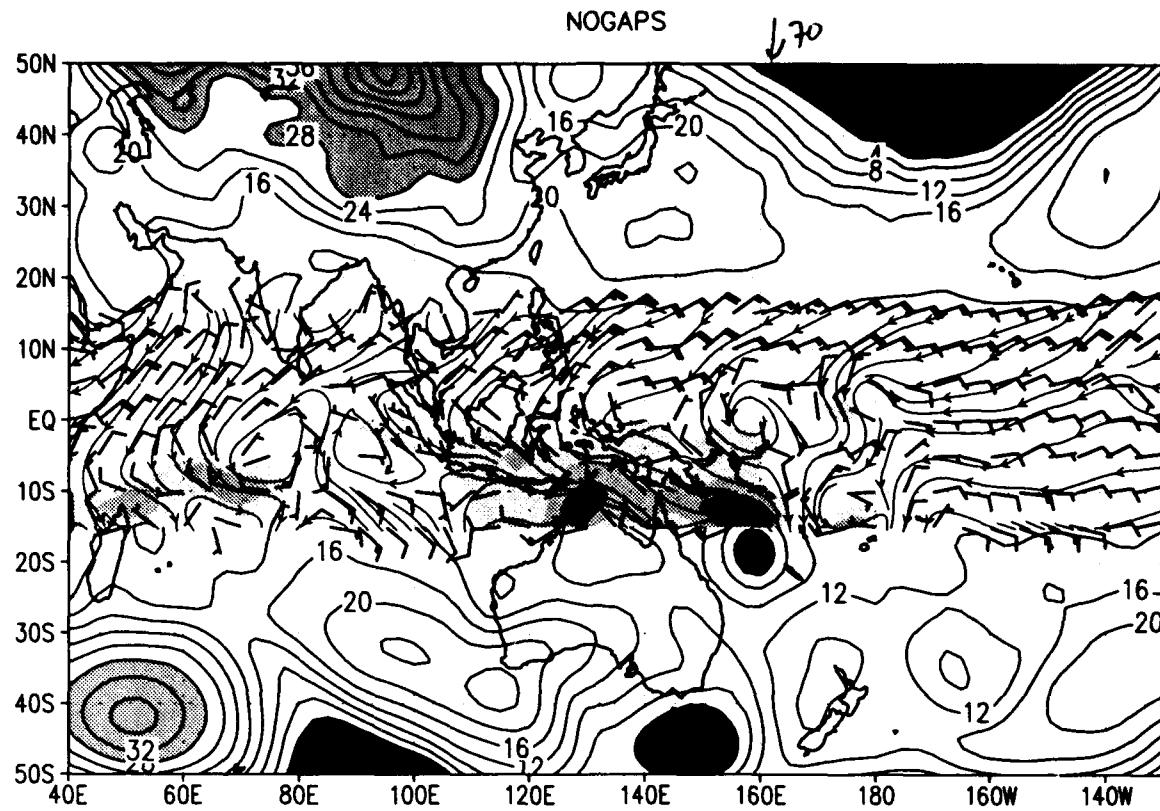
SLP and sfc winds ($u>0$ shaded) for 00Z 25 FEB 1993
slp (mb) wind barbs (kts) /d2/toga_coarse/d2.gs



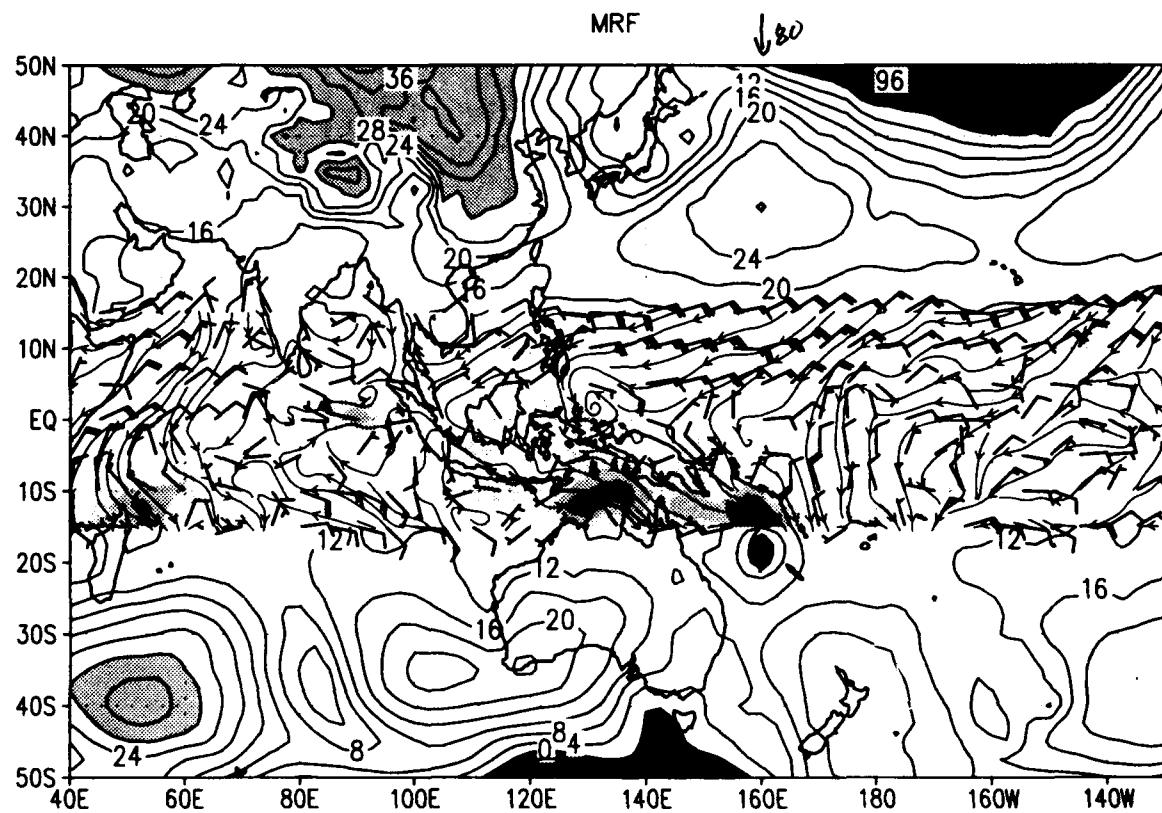
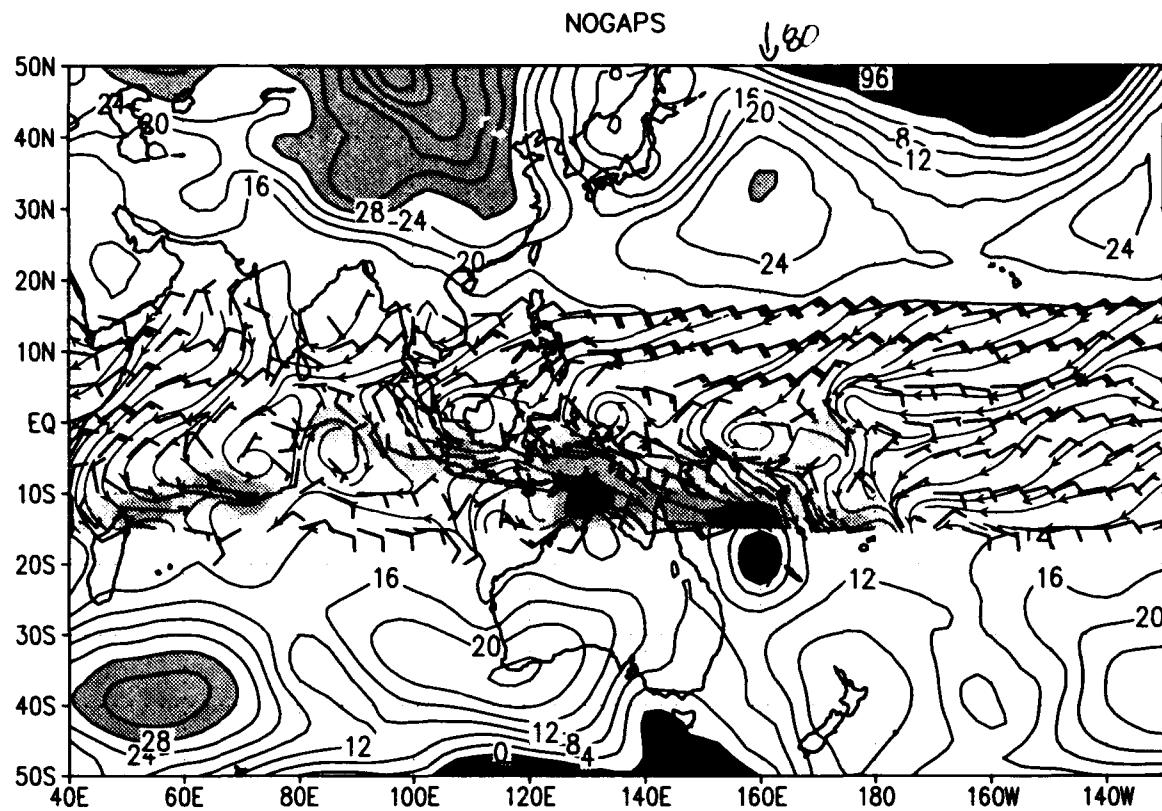
SLP and sfc winds ($u>0$ shaded) for 00Z 26 FEB 1993
slp (mb) wind barbs (kts) /d2/toga_coare/d2.gs



SLP and sfc winds ($u>0$ shaded) for 00Z 27 FEB 1993
slp (mb) wind barbs (kts) /d2/toga_coare/d2.gs



SLP and sfc winds ($u>0$ shaded) for 00Z 28 FEB 1993
slp (mb) wind barbs (kts) /d2/toga_coare/d2.gs



REPORT DOCUMENTATION PAGE			Form Approved OMB No. 0704-0188
<p>Public reporting burden for this collection of information is estimated to average 1 hour per response, including the time for reviewing instructions, searching existing data sources, gathering and maintaining the data needed, and completing and reviewing the collection of information. Send comments regarding this burden estimate or any other aspect of this collection of information, including suggestions for reducing this burden, to Washington Headquarters Services, Directorate for Information Operations and Reports, 1215 Jefferson Davis Highway, Suite 1204, Arlington, VA 22202-4302, and to the Office of Management and Budget, Paperwork Reduction Project (0704-0188), Washington, DC 20503.</p>			
1. AGENCY USE ONLY (Leave blank)	2. REPORT DATE	3. REPORT TYPE AND DATES COVERED	
	November 1993	Technical Memorandum	
4. TITLE AND SUBTITLE	5. FUNDING NUMBERS		
A Synoptic-Scale Overview of the TOGA COARE Intensive Observing Period November 1992 - February 1993 Based on Analyses From U. S. Operational Global Data Assimilation Systems	910		
6. AUTHOR(S)			
M. Fiorino, S. J. Lord, W. K.-M. Lau, P. A. Phoebeus, and C. G. Strey			
7. PERFORMING ORGANIZATION NAME(S) AND ADDRESS (ES)	8. PERFORMING ORGANIZATION REPORT NUMBER		
Goddard Space Flight Center Greenbelt, Maryland 20771	94B00015		
9. SPONSORING / MONITORING AGENCY NAME(S) AND ADDRESS (ES)	10. SPONSORING / MONITORING AGENCY REPORT NUMBER		
National Aeronautics and Space Administration Washington, DC 20546-0001	NASA TM-104593		
11. SUPPLEMENTARY NOTES			
Fiorino: Universities Space Research Assn., Columbia, MD; Lord: National Meteorological Center, Greenbelt, MD; Lau: Goddard Space Flight Center, Greenbelt, MD; Phoebeus: Naval Research Laboratory, Monterey, CA; Strey: Fleet Numerical Oceanography Center, Monterey, CA.			
12a. DISTRIBUTION / AVAILABILITY STATEMENT	12b. DISTRIBUTION CODE		
Unclassified - Unlimited Subject Category 47			
13. ABSTRACT (Maximum 200 words)			
<p>The operational global analyses from the two major U.S. numerical weather prediction centers, the Navy's Fleet Numerical Oceanography Center and the National Meteorological Center, are used to describe the synoptic-scale features of the 1 November 1992 to 28 February, 1993 TOGA COARE intensive observing period (IOP). TOGA COARE is an international field experiment in which a large number of research scientists from the Goddard Laboratory for Atmospheres (Code 910) and the Laboratory for Hydrospheres (Code 970) participated.</p> <p>Two high-amplitude intraseasonal (30-60 day) oscillations passed through the TOGA COARE observational network located in the equatorial western Pacific. Associated with the oscillations were two 6-10 day periods of persistent westerly surface winds at the equator or "westerly wind bursts." These events are depicted through time series and time-longitude cross sections of divergence/velocity potential, surface winds, precipitation, ocean mixed-layer depth and sea surface temperature. The high and low frequency components of the flow in which the intraseasonal oscillations were embedded are shown using seasonal, monthly, and 5-day averages of the surface, 850 and 200 mb winds, precipitation, and sea-level pressure, and a time-longitude cross section of tropical cyclone activity. Independent verification of precipitation comes from near real-time satellite estimates, and a reference climatology is given based on 9 years of ECMWF analyses. Daily 00 UTC analyses of surface winds and sea-level pressure for the entire western Pacific and Indian Ocean are provided to trace the evolution of individual synoptic events.</p>			
14. SUBJECT TERMS	15. NUMBER OF PAGES		
TOGA COARE, Intraseasonal Oscillation, Westerly Wind Bursts, Tropical Variability	294		
16. PRICE CODE			
17. SECURITY CLASSIFICATION OF REPORT	18. SECURITY CLASSIFICATION OF THIS PAGE	19. SECURITY CLASSIFICATION OF ABSTRACT	20. LIMITATION OF ABSTRACT
Unclassified	Unclassified	Unclassified	UL